UNIVERSITY OF SOUTHAMPTON

FACULTY OF MEDICINE, HEALTH AND LIFE SCIENCES

School of Medicine

GENETIC CHANGES IN THE DEVELOPMENT OF MULTIPLE MYELOMA

by

Laura Chiecchio

Thesis for the degree of Doctor of Philosophy

July 2010

UNIVERSITY OF SOUTHAMPTON

ABSTRACT

FACULTY OF MEDICINE, HEALTH AND LIFE SCIENCES
SCHOOL OF MEDICINE
Doctor of Philosophy

GENETIC CHANGES IN THE DEVELOPMENT OF MULTIPLE MYELOMA

by Laura Chiecchio

Multiple myeloma (MM) is a malignancy of clonal plasma cells (PC) which develops as a consequence of a multistep process of transformation from a normal PC to an asymptomatic stage known as monoclonal gammopathy of undetermined significance (MGUS) to MM to the more aggressive plasma cell leukaemia (PCL). MGUS is the most common PC disorder and the majority of cases never progress to MM requiring treatment, as progression only occurs in ~1% of patients per year. From a genetic point of view, specific abnormalities represent initiating events (i.e. *IgH* translocations or hyperdiploidy) of this multistep process while others occur at later stages. In this study, interphase-FISH showed that initiating events are present in MGUS (n=187) and asymptomatic MM (SMM, n=128) at similar frequencies as found in MM (n=400) (the only exception was t(4;14)) and showed that these abnormalities alone, regardless of their biological impact in MM, cannot drive progression to overt disease. The time of occurrence of deletion/monosomy of chromosome 13 (Δ13) was found to depend on the presence of specific concurrent abnormalities. Δ13 was extremely rare in MGUS and SMM with translocations directly involving *CCND1* and *CCND3* suggesting a possible role of Δ13 in the progression of disease specifically in these genetic sub-groups. However, it was clear that, excluding Δ13 in these sub-groups, standard interphase-FISH abnormalities are insufficient to predict progression of MGUS and SMM.

High resolution array CGH showed an increasing level of genomic complexity from MGUS (n=25) to SMM (n=15) to MM (n=47) to PCL (n=11). In MGUS, the number of copy number changes per case was highly associated with progression (P=0.003). The simplest profiles belonged to MGUS cases with t(11;14) and t(14;20); surprisingly, none of these patients had progressed to MM by the end of this study (median follow-up=72 months).

The integration of results from interphase-FISH, array CGH and metaphase analysis suggested that there were various abnormalities (corresponding to distinct molecular pathways) responsible for disease progression. A number of chromosomal changes were found to be strongly associated with progression (del(1)(p22.3-p23); del(6)(q25), *MYC* changes, del(12)(p13), Δ13 in t(11;14), abnormalities involving members of the NF-κB pathway, del(17)(p13)). Such associations were not only suggested by the fact that these abnormalities were rare in MGUS/SMM compared to MM, but also by the observation that all pre-malignant patients positive for these changes progressed to overt disease. However, among patients who did progress and carried the same abnormalities, time to progression was found to be highly variable from case to case. This suggested that other factors (genetic or otherwise) must be interacting with chromosomal abnormalities in order to lead to progression. Other changes, e.g. 1q21 gain, despite being rare in pre-malignant cases compared to MM and despite some being associated with a dismal prognosis in MM, did not appear to be linked to rapid progression.

This study has made significant progress towards understanding the progression from pre-malignant disease to MM, which will provide information towards potential novel targets for therapy to prevent progression or prolong the pre-malignant phase of a highly aggressive disease.

LIST OF CONTENTS

LIST OF TABLES

LIST OF FIGURES

DECLARATION OF AUTHORSHIP

I, Laura Chiecchio,
declare that the thesis entitled 'Genetic changes in the development of multiple myeloma' and the work presented in it are both my own, and have been generated by me as the result of my own original research. I confirm that:

- this work was done wholly or mainly while in candidature for a research degree at this University;
- no part of this thesis has previously been submitted for a degree or any other qualification at this University or any other institution;
- where I have consulted the published work of others, this is always clearly attributed;
- where I have quoted from the work of others, the source is always given. With the exception of such quotations, this thesis is entirely my own work;
- I have acknowledged all main sources of help;
- where the thesis is based on work done by myself jointly with others, I have made clear exactly what was done by others and what I have contributed myself;
- parts of this work have been published as:

Ross FM, **Chiecchio L**, Dagrada GP, Protheroe RKM, Stockley DM, Harrison CJ, Cross NCP, Szubert AJ, Drayson MT, Morgan GJ on behalf of the UK Myeloma Forum (2010). **The t(14;20) is a poor prognostic factor in myeloma but is associated with long term stable disease in MGUS**. *Haematologica. 95(7):1221-5.*

Chiecchio L, Dagrada GP, Ibrahim AH, Dachs Cabanas E, Protheroe RKM, Stockley DM, Orchard KH, Cross NCP, Harrison CJ, Ross FM on behalf of the UK Myeloma Forum (2009). **Timing of acquisition of deletion 13 in plasma cell dyscrasias is dependent on genetic context.** *Haematologica. 94(12):1708-13.*

Chiecchio L, Dagrada GP, Protheroe RKM, Stockley DM, Smith AG, Orchard KH, Cross NC, Harrison CJ, Ross FM; UK Myeloma Forum (2009). **Loss of 1p and rearrangement of *MYC***

are associated with progression of smouldering myeloma to myeloma: sequential analysis of a single case. *Haematologica. 94(7):1024-8.*

Chiecchio L, Dagrada GP, White HE, Towsend MR, Protheroe RKM, Cheung KL, Stockley DM, Orchard KH, Cross NC, Harrison CJ, Ross FM; UK Myeloma Forum (2009). **Frequent upregulation of *MYC* in plasma cell leukemia**. *Genes, Chromosomes and Cancer. 48(7):624-36*.

Leone PE, Walker BA, Jenner MW, **Chiecchio L**, Dagrada G, Protheroe RKM, Johnson DC, Dickens NJ, Brito JL, Else M, Gonzalez D, Ross FM, Chen-Kiang S, Davies FE, Morgan GJ. (2008). **Deletions of *CDKN2C* in multiple myeloma: biological and clinical implications**. *Clinical Cancer Research. 1;14(19):6033-41*.

CONTRIBUTION OF THE AUTHOR TO THE WORK PRESENTED IN THIS THESIS

The work presented in this thesis was conducted at the Leukaemia Research Fund UK Myeloma Forum Cytogenetic Database, which is part of the Wessex Regional Genetics Laboratory (WRGL) of the Salisbury District Hospital.

- The preparation of probe DNA for FISH, including bacterial growth, DNA extraction and labelling were carried out by the author, David Stockley and Rebecca Protheroe from the Myeloma Cytogenetic Database. Metaphase and FISH analyses were conducted by the author and by colleagues of the Database. The FISH analyses described in Sections 3.3 and 3.4 were exclusively performed by the author.

- Array CGH for all patients was performed by the author including DNA extraction, amplification, labelling and analysis (Sections 3.3, 3.4, 3.6).

- The collection of clinical information of the study patients was carried out by the author, Dr Fiona Ross, leader of the Myeloma Cytogenetic Database and Claire Smith, research nurse of the Database.

- Overall survival in MM described in Section 3.2 was calculated by Dr Fiona Ross.

- Statistical analyses of the data described in Sections 3.1, 3.3, 3.5 and 3.6 were performed by the author.

- DNA and RNA extraction as well as cDNA synthesis were performed by the author.

- MLPA (Section 3.6) was performed by Dr. Dave Bunyan (WRGL) and Mark Townsend from the Myeloma Database.

- Mutational analysis of the genes *FBXO38* and *TP53* was performed by the author; mutational analysis of the genes *CDCA2* and *PPP2R2A* was performed by Mark Townsend (Section 3.6).

- Quantitative RT-PCR (Section 3.6) was performed by Dr Helen White from the National Genetics Reference Laboratory (WRGL).

ACKNOWLEDGEMENTS

I am truly indebted to my main supervisors, Professor Christine Harrison and Professor Nick Cross for their help, guidance and support throughout this project. I would also like to thank Dr Kim Orchard from the Department of Haematology of the Southampton General Hospital for his advice regarding the clinical aspects of this project.

Very special thanks to Dr Fiona Ross, whose enthusiasm, dedication and knowledge of myeloma constantly encouraged me during this project.

Thanks to all patients; they were the reason for this project in the first place.

Thanks to all colleagues at the UK Myeloma Forum Cytogenetic Database who have actively contributed to this project. Particular thanks to Gian Paolo Dagrada for sharing ideas and discussing results and to Claire Smith for collecting precious clinical information from many different hospitals.

Thanks to my colleagues at the Wessex Regional Genetics Laboratory who shared their expertise, gave me advice and the training I needed in the past years; in particular I would like to acknowledge Sarah Beal, Viv Maloney and Derek Richardson for their advice regarding FISH and Shuwen Huang for her advice regarding array CGH.

Thanks to Helen Parker and John Strefford for training me in array CGH techniques and to Vikki Rand for helping me in analyzing the array CGH results.

Finally, thanks to my family in Italy and to my husband, Carl, for always supporting me, in many special ways.

ABBREVIATIONS

β2M	β2-microglobulin
Δ13	monosomy/deletion 13
ADM-2	Aberration Detection Method-2
ALL	acute lymphoblastic leukaemia
ASH	American Society of Haematology
BAC	bacterial artificial chromosome
BM	bone marrow
BSA	bovine serum albumin
CA	chromosomal abnormality
cDNA	complementary DNA
CEP	centromere
CGH	comparative genomic hybridization
CNV	copy number variation
CHORI	Children's Hospital Oakland Research Institute
CRAB	myeloma related organ or tissue impairment
dATP	deoxyadenosine triphosphate
dCTP	deoxycytidine triphosphate
ddNTP	dideoxynucleotides
der(14)	derivative of chromosome 14
dGTP	deoxyguanosine triphosphate
DM	double minute(s)
DNA	deoxyribonucleic acid
dNTP	deoxyribonucleotide triphosphate
dTTP	deoxythymidine triphosphate
dUTP	deoxyuridine triphosphate
EFS	event free survival
EMN	European Myeloma Network
FCS	fetal calf serum
FISH	fluorescence *in situ* hybridization
G-banding	Giemsa banding
HD	homozygous deletion
HDT	high-dose therapy
HMCL	human myeloma cell line
HRD	hyperdiploidy
HSC	hematopoietic stem cell
HSR	homogeneously staining region(s)
iFISH	interphase FISH
IFM	Intergroupe Francophone du Myelome
Ig	immunoglobulin
IgH	immunoglobulin heavy chain
IgHt	IgH translocation
IL	interleukin
IMS	industrial methylated spirit

ISCN	International System for Human Cytogenetic Nomenclature
ISS	International Staging System
kb	kilobase
LB	Luria-Bertani
LRF	Leukaemia Research Fund
M-	monoclonal
Mb	megabase
MDA	multiple displacement amplification
MGUS	monoclonal gammopathy of undetermined significance
Min	minute(s)
MLPA	multiplex ligation-dependent probe amplification
MM	multiple myeloma
MRC	Medical Research Council
MRI	magnetic resonance imaging
mRNA	messenger ribonucleic acid
nonHRD	non hyperdiploidy
OS	overall survival
PAC	P1-derived artificial chromosomes
PBS^{+}	phosphate buffered $saline^{+}$
PC	plasma cell
PCL	plasma cell leukaemia
POEMS	polyneuropathy, organomegaly, endocrinopathy, monoclonal gammopathy and skin changes
pPCL	primary plasma cell leukaemia
qRT-PCR	quantitative RT-PCR
RCL	red cell lysis
RPMI	Roswell Park Memorial Institute
RSS	recombination signal sequences
RT-PCR	reverse transcriptase polymerase chain reaction
SAP	shrimp alkaline phosphatase
SMM	smouldering/asymptomatic myeloma
SNP	single nucleotide polymorphism
Sp	spectrum
sPCL	secondary plasma cell leukaemia
S-phase	synthesis phase
TC	translocation and cyclin
U	Unit
UAMS	University of Arkansas for Medical Science
UCSC	University of California Santa Cruz
UIP	*IgH* translocation with unidentified partner
WBC	white blood cell
WHO	World Health Organization
WGA	whole genome amplification
WRGL	Wessex Regional Genetics Laboratory
YAC	yeast artificial chromosome

1 INTRODUCTION

1.1 Cancer

Cancer is the final stage of a multi-step process characterized by a number of somatic mutations that allow a normal cell to originate a population of proliferating and invasive cells [1].
Mammalian cells have multiple measures of defence to protect them against the effects of cancer gene mutations and only when several genes are defective does an invasive cancer develop [2]. Some mutations enhance cell proliferation, creating an expanded target population of cells; other mutations affect the stability of the entire genome, at either the chromosomal or the deoxyribonucleic acid (DNA) level, increasing the overall mutation rate.
Three types of genes have been recognized to be the main targets of mutations promoting tumourigenesis: oncogenes, tumour suppressor genes and stability genes. Proto-oncogenes promote cell proliferation through gain of function mutations which lead to forms that are excessively or inappropriately active; a single mutant allele may affect the phenotype of the cell. Among the tumour suppressor genes some prevent inappropriate cell cycle progression, while others push deviant cells into apoptosis. Mutations in both the maternal and the paternal alleles of a tumour suppressor gene are generally required to confer a selective advantage to a cell [3]. However, some tumour suppressor genes have been reported to exert a selective advantage on a cell when only one allele is inactivated while the other remains functional. This is known as haploinsufficiency [4]. Stability genes monitor genome integrity and coordinate cell cycle progression with DNA repair. When stability genes are mutated they promote tumourigenesis by loss of control of the incidence of genetic alterations. Other stability genes control mitotic recombination and chromosomal segregation [3].
Many different mechanisms can lead to aberrant functions of these genes and include polymorphisms, changes in genome copy number and structure, point mutations and epigenetic modifications.

1.2 Cancer cytogenetics

In 1960, Nowell and Hungerford discovered the first chromosomal abnormality associated with cancer using cytogenetics [5]. Specifically, they identified an abnormal minute chromosome that was present in cultured bone marrow (BM) cells of patients with chronic myeloid leukaemia, a form of cancer that causes unrestricted growth of myeloid cells in the BM. This minute chromosome was named the Philadelphia chromosome; later Rowley, using new cytogenetic

techniques namely quinacrine fluorescence and G-banding, discovered that the Philadelphia chromosome was formed from a specific translocation between chromosomes 9 and 22 [6]. In 1985, Heisterkamp *et al.* showed that the translocation led to the formation of an abnormal, fused gene called *bcr-abl* (breakpoint cluster region and V-abl Abelson murine leukemia oncogene homolog 1) [7]; this gene codes for an aberrant tyrosine kinase protein which is constitutively activated, interfering with normal cell regulation and allowing cells that express the aberrant protein to divide more rapidly [8].

Since the discovery of this chromosomal aberration, many abnormalities have been demonstrated to be associated with cancer as shown by the catalogue of recurrent abnormalities in a wide range of cancers compiled by Mitelman and colleagues (Mitelman Database of Chromosome Aberrations in Cancer, see URL in **Appendix 1**). These findings established the clinical associations of cytogenetics and malignancies.

1.2.1 Types of chromosomal changes

Chromosomal changes are highly variable and include altered ploidy, gain or loss of individual chromosomes or portions of them and structural rearrangements (**Figure 1-1**). The structural changes may involve balanced exchange of material between two chromosomal regions (i.e. Philadelphia chromosome) or may be non-reciprocal, such that portions of the genome are lost or gained. Restricted regions of the genome may be amplified and the amplified sequences may present in small acentric fragments (double minutes, DM), incorporated into chromosomes in nearly contiguous homogeneously staining regions (HSR) or spread throughout the genome [1]. There is considerable variability in the degree to which tumour genomes are aberrant at the chromosomal level; some tumours have few chromosomal aberrations whereas others may contain dozens [9]. Moreover, cancer cells generally gain multiple types of chromosomal aberrations during tumour progression; as a result, the genome becomes progressively more unstable.

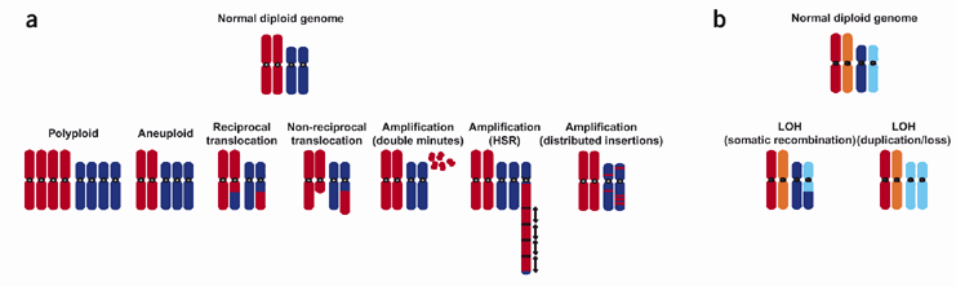

Figure 1- 1 Schematic illustration of mechanisms by which chromosomal aberrations arise leading to aneuploidy (a) or leaving the chromosome apparently intact (b)

Modified from Albertson et al., 2003 [1]

1.3 Haematopoiesis

The process of blood cell production and homeostasis is termed haematopoiesis. All mature blood cells are generated from a relatively small number of hematopoietic stem cells (HSC) [10,11]. HSC generate the multiple hematopoietic lineages through a successive series of intermediate progenitors. These include common lymphoid progenitors, which generate lymphocytes B, T and Natural Killer cells, and common myeloid progenitors, which generate red cells, platelets, granulocytes and monocytes (**Figure 1-2**) [12,13].

Downstream of the common lymphoid and myeloid progenitors are more mature progenitors that are further restricted in the number and type of lineages they generate [13]. Terminally differentiated cells cannot divide and undergo apoptosis after a period of time ranging from hours (for neutrophils) to decades (for some lymphocytes).

A complex interaction between the genetic processes of blood cells and their microenvironment determines whether HSC, progenitors and mature blood cells remain quiescent, proliferate, differentiate, self-renew or undergo apoptosis [14]. Cytokines, extracellular matrix components and chemokines are important environmental regulators of haematopoiesis.

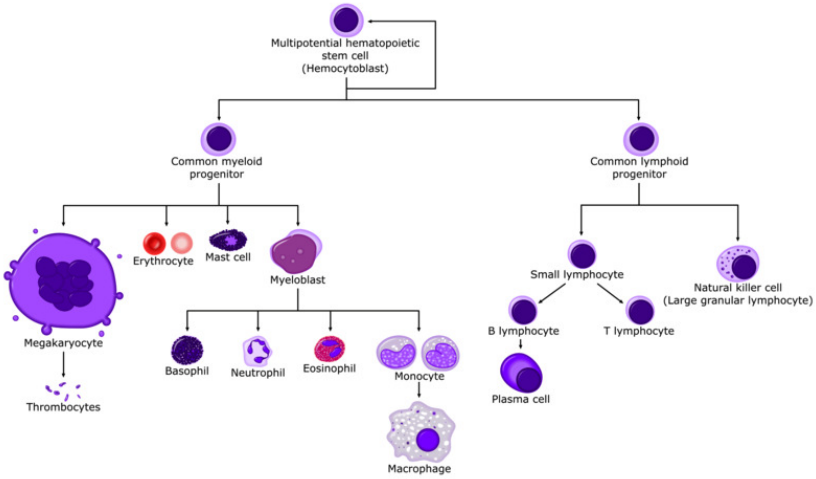

Figure 1- 2 The developmental stages of haematopoiesis

1.3.1 Lymphopoiesis

B cell development is a highly regulated process of ordered events; mature B cells, as well as mature T cells, express antigen receptors, each with different antigen specificity. B cells primarily originate and differentiate in the BM where the 'pre B cell' arises from the progenitor '(Pro) B cell' following rearrangement of the immunoglobulin (*Ig*) heavy chain (*IgH*) gene, resulting in cytoplasmic expression of the μ heavy chain. Subsequently, rearrangement of the light chain genes occurs. This results in the expression of a complete IgM molecule on the cell surface, consisting of two μ chains and two light chains. During this progression a pool of B cells is generated in which each B cell expresses one specific Ig with an appropriate affinity to a particular antigen. This 'immature B cell' is unable to initiate an immune response, but acquires this ability on leaving the BM and entering the peripheral lymphoid tissue. Here B cells migrate to the outer region of the lymph node within the primary follicles and later to the follicle mantles. This differentiation step is associated with the additional expression of IgD, as a result of an alternative splicing of *IgH* messenger ribonucleic acid (mRNA). These IgM+/IgD+ B cells, known as 'naive mature B cells', populate the blood and the peripheral lymphoid organs, where in response to the binding of foreign antigens, they transform into proliferating extra-follicular B blasts. The daughter cells either differentiate into short-lived, IgM-producing plasma cells (PC) or B cells that acquire the capacity to initiate a germinal centre reaction. These so-called 'primed B cells' proliferate and differentiate into centroblasts forming an early germinal centre [15,16]. During the mitotic proliferation and differentiation of centroblasts into

centrocytes, a randomized introduction of mutations in the variable region of the *Ig* genes (somatic hypermutation) leads to the production of *Ig* with high affinity for the antigens. Those centrocytes with advantageous mutations are positively selected and undergo several rounds of proliferation, mutation and selection before they finally differentiate into 'memory' B cells or long-lived PC. The presence of mutations in the variable (V) region of the *Ig* is considered to be a reliable marker for cells that have been exposed to the germinal centre. The affinity maturation process is associated with a switch in the IgH chain class from IgM to IgG, IgA or less commonly to IgE. The post-germinal centre B cells generate plasmablasts, which typically migrate to the BM microenvironment where they interact with stromal cells and differentiate into long-lived PC that survive for about 30 days [17].

1.4 The *Ig* loci

Immunoglobulins are either produced at the membrane of the B cell or they are secreted. They consist of two identical light chains (L) and two identical heavy chains (H). At the three-dimensional level, an Ig consists of one N-terminal variable domain and one (for an L) or several (for an H chain) C-terminal constant domain(s) (**Figure 1-3**).

The heavy chain variable region gene, located at chromosome 14q32.32, is split into arrays of gene segments, the V (variable), D (diversity), and J (junctional) segments. Light chain genes are similarly organised on different chromosomes (*Igκ* genes at chromosome band 2p11; *Igλ* on chromosome band 22q11) although they have no D gene segments. To express functional Ig, B cells undergo extensive genomic rearrangements within their *Ig* loci [18]: V(D)J recombination, somatic hyper mutation and class switch recombination.

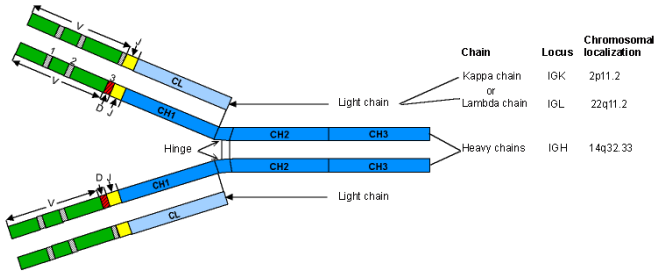

Figure 1- 3 Structure of the immunoglobulin molecule

(http://imgt.cines.fr/textes/IMGTeducation/Tutorials/IGandBcells/_UK/MolecularGenetics/angfig1.html)

i. V(D)J recombination

There are 87 V_H segments, of which at least 32 are pseudogenes and, so far, 30 germline D_H and six J_H segments have been identified. In order to increase diversity, the D region may be read in three different reading frames without generating stop codons and more than one D segment may join to form an enlarged D region.

Of the 76 V_k genes, 16 have minor defects and 25 are pseudogenes, leaving 35 potentially functional genes. While there are 5 J_k segments, there is only one constant-region gene. The number of possible κ chain variable regions that may be produced in this way is approximately 150. The *Igλ* gene contains a set of V genes, and each of the seven C genes is accompanied by one J gene [19].

The recombination of gene segments is a key feature in the generation of a functional immunoglobulin, for both light and heavy chain variable regions (**Figure 1-4**). Specific base sequences that act as recombination signal sequences have been identified. A signal sequence is found downstream (3') of each V and D segment, and immediately upstream (5') of all germ line D and J segments. The recombination signal sequences (RSS) following a V_k, V_λ, V_H or D segment are complementary to those preceding the J_k, J_λ, D or J_H segments with which they recombine. The recombination process is controlled at least in part by two lymphocyte-specific endonucleases, the recombination-activating genes (RAG-1 and RAG-2). These proteins cut the rearranging gene segments at RSS.

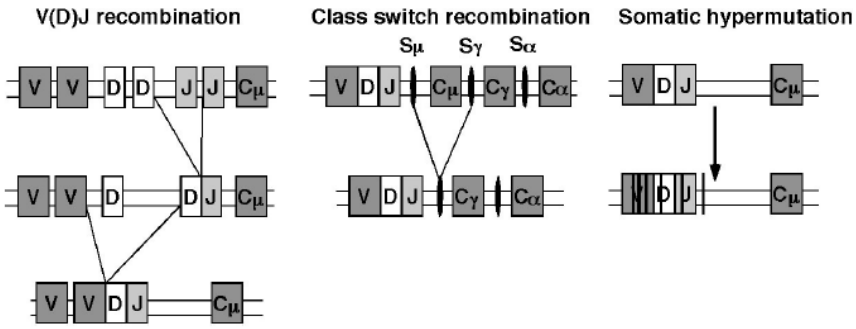

Figure 1- 4 Molecular processes modifying Ig genes

At the DNA level during the V(D)J recombination of the heavy chains, one of the D_H segments is joined to one of the J_H segments, with deletion of the intermediary DNA, to create a rearranged D_H-J_H segment. The rearranged D_H-J_H segment is then joined to one of the V_H segments. Small variations in the positions at which recombination takes place can generate additional diversity. Also, nucleotides of variable length and composition are randomly inserted between the rearranged V, D and J segments.

In the pre-B lymphocyte, the μ chain is synthesized first because the constant *IgH*M gene segment is located close to the V_H-D_H-J_H rearrangement. This μ chain is associated with the pseudo-light chain. The first kappa, if productive, leads to inhibition of the other allele of *Igκ* and *Igλ* genes. If kappa is unproductive, or cannot pair with the heavy chain, the lambda combines to constitute the pre-B receptor.

ii. Somatic hypermutation

The process of somatic hypermutation introduces mainly nucleotide substitutions; deletions and duplications account for only about 5% of the mutation events. Although the mechanism is still obscure, it has been demonstrated that hypermutation is associated with double-strand DNA breaks and that an error-prone DNA polymerase is involved in the introduction of mutations in the proximity of the DNA breaks [20,21].

iii. Class switch recombination

During class switch recombination, DNA strand breaks are introduced into both the switch μ region and the switch region associated with one of the downstream C_H genes. The DNA fragment between the switch regions is removed from the chromosome and the gene segments surrounding the deleted portion are rejoined to retain a functional antibody gene that produces an antibody of a different isotype [19,22].

All cells which arise from progenitor B cells possess two *Ig* gene rearrangement products, V_H-D_H-J_H and V_L-J_L, which are unique to that cell. Given the number of possible combinations in originating an Ig product, individual B cells differ from each other in their differently rearranged *IgH* and *IgL* genes; this diversity is termed 'polyclonality'. In contrast, tumour cells of B cell neoplasms possess identical V_H-D_H-J_H and V_L-J_L sequences, indicating that they have arisen from the same transformed B cell and, thereby, have formed a clone. This is termed 'monoclonality' [23].

1.4.1 Activation of proto-oncogenes by chromosomal translocation in B cell malignancies

Chromosomal translocations represent one of the main mechanisms of proto-oncogene activation in B cell malignancies [24]. In neoplasms originating from precursor lymphoid or myeloid cells, these translocations generally lead to the fusion of two genes originating a new

transcript with acquired oncogenic potential. One example is the translocation t(1;19)(q23;p13) found in childhood B cell acute lymphoblastic leukaemia (ALL) which gives rise to the *E2A/PBX1* fusion gene [25]; the product of the chimaeric gene can drive cell division, inhibit DNA repair and cause genomic instability.

In mature B and T cell malignancies, chromosomal translocations usually juxtapose the proto-oncogene to heterologous regulatory sequences of genes which are expressed at sustained levels in normal cells [23]; as a consequence of such translocations the oncogene expression is constitutively upregulated. Most of these translocations have one of the breakpoints involving either the *Ig* (B cells) or the T cell receptor (*Tcr;* T cells) loci. The specific location of these breakpoints indicates that double –stranded breaks naturally occurring during V(D)J recombination (*Ig* or *Tcr* loci), class-switch recombination (*IgH* locus) or somatic hypermutation (*Ig* loci) are implicated in the generation of these chromosomal rearrangements [26]. For example in lymphomas, errors in the V(D)J recombination result in the translocations t(11;14)(q13;q32) *CCND1-IgH*, in mantle cell lymphoma and t(14;18)(q32;q21) *BCL2-IgH*, in follicular lymphoma [27,28].
Somatic hypermutation is probably involved in the translocation t(8;14)(q24;q32) *MYC-IgH* in Burkitt's lymphoma: in fact *MYC* is often joined to the *IgH* locus within a rearranged and somatically mutated *IgH* variable region [29,30].
Chromosomal translocations originating from errors in class-switch recombination have been detected mainly in multiple myeloma (MM) and in sporadic Burkitt's lymphoma [31]. In such cases, the location of the breakpoints on chromosome 14 is within the switch regions [32]. It is thought that during the switch–region remodelling process, DNA double strand breaks are introduced into the switch regions of the recombining C_H genes and switch-like regions on other chromosomes, sometimes resulting in the translocation of oncogenes to the derivative chromosome 14 (der(14)) [33]. These oncogenes are juxtaposed to the potent *IgH* enhancers, resulting in their dysregulated expression.

1.5 Plasma cell neoplasms

PC neoplasms result from the expansion of a clone of Ig-secreting, heavy-chain class-switched, terminally differentiated B cells (**Figure 1-5A**). These cells are phenotypically similar to long-lived PC, including a strong dependence on the BM microenvironment for survival and growth [34]. They typically secrete a single electrophoretically homogeneous Ig product, known as the monoclonal (M) component (**Figure 1-5B**) [35].

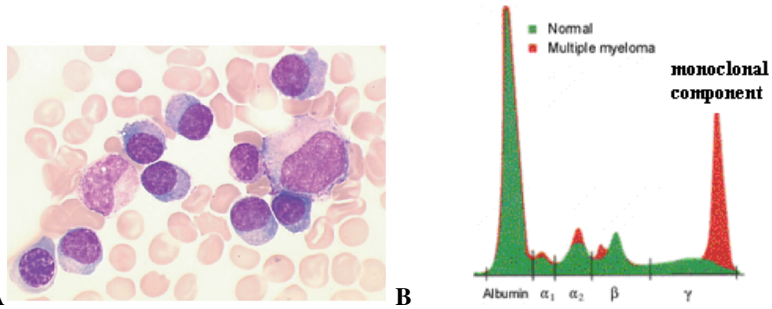

Figure 1- 5 A) Giemsa-stained BM smear of a MM case; B) Electrophoretic pattern of a normal person (green) and of a MM patient (red)

1.5.1 Classification of PC neoplasms

PC neoplasms have been classified into distinct groups by the World Health Organization (WHO) [36]. The WHO recognizes monoclonal gammopathy of undetermined significance (MGUS), MM, plasmacytoma (solitary plasmacytoma of the bone and extraosseous/extramedullary plasmacytoma), immunoglobulin deposition diseases (primary amyloidosis; systemic light and heavy chain deposition diseases) and osteosclerotic MM (POEMS syndrome). The diagnostic criteria of the PC neoplasms are summarized in **Table 1-1**. MGUS and MM are the two most common PC disorders. Within the MM group, three variants are also defined: asymptomatic/smouldering MM (SMM); non-secretory MM (affecting 3% of MM patients) characterized by no detectable M-protein in the serum or in the urine but only in the BM PC; and plasma cell leukemia (PCL). The diagnosis of the specific entities within this group of conditions is clinically challenging, as they often have overlapping features.

Table 1- 1 Diagnostic criteria for PC neoplasms [35]

MGUS
- M-protein in serum <30 g/L
- BM clonal PC <10% and low level of PC infiltration in the trephine biopsy (if done)
- No evidence of other B cell proliferative disorders
- No MM-related organ or tissue impairment (no end organ damage, including bone lesions)

SMM
- M-protein in serum ≥30 g/L **and/or** BM clonal PC ≥10%
- No evidence of other B cell proliferative disorders
- No MM-related organ or tissue impairment (no end organ damage) or symptoms

MM
- M-protein in serum and/or urine*
- BM clonal PC or plasmacytoma#
- No evidence of other B-cell proliferative disorders
- Related organ or tissue impairment (no end organ damage, including bone lesions)

* M-protein in most cases is >30 g/L (>25g/L sometimes used for IgA) and >1g/24 hr of urine light chain but some patients with symptomatic MM have levels lower than these

Monoclonal PC usually exceed 10% of nucleated cells in the BM but no minimal level is designated because about 5% of patients with symptomatic MM have <10% BM PC

Plamacytoma

• Solitary plasmacytoma of the bone
- No M-protein in the serum and/or urine (a small M-component may sometimes be present)
- Single area of bone destruction due to clonal PC
- BM not consistent with MM
- Normal skeletal survey (and magnetic resonance imaging (MRI) of spine and pelvis if done)
- No MM-related organ or tissue impairment (no end organ damage other than solitary bone lesions)

• Extramedullary plasmacytoma
- No M-protein in serum and/or urine (a small M-component may sometimes be present)
- Extramedullary tumour of clonal PC
- Normal BM
- Normal skeletal survey
- No MM-related organ or tissue impairment (no end organ damage other than solitary bone lesions)

Non-secretory MM
- No M-protein in serum and/or urine with immunofixation
- BM clonal plasmacytosis ≥10% or plasmacytoma
- Related organ or tissue impairment (end organ damage, including bone lesions)

Plasma cell leukaemia
- Absolute PC count in peripheral blood ≥2.0 x 10^9/l
- Peripheral blood differential white cell count with >20% PC

Amyloidosis
- Presence of an amyloid-related systemic syndrome
- Positive amyloid staining by Congo red in any tissue (e.g. fat aspirate, BM, organ biopsy)
- Evidence that amyloid is light chain-related established by direct examination of the amyloid
- Presence of a monoclonal PC disorder

Myeloma related organ or tissue impairment (CRAB)

Hypercalcemia (serum calcium >11.5mg/dl) (**C**), renal insufficiency (serum creatinine >177µmol/L) (**R**), anaemia (haemoglobin <10g/dl) (**A**); bone lesions: lytic lesions or oteoporosis with compression fractures (MRI may clarify) (**B**). Other: symptomatic hyperviscosity, amyloidosis, recurrent bacterial infections (> two episodes in 12 months) [37].

1.5.2 Pre-malignant conditions

MGUS and SMM are asymptomatic, pre-malignant disorders. They are characterized by clonal expansion of PC within the BM, which is responsible for the presence of an M-protein in the serum, but with no evidence of end-organ impairment [35]. Patients with MGUS and SMM are often diagnosed by chance, as M-proteins are frequently identified during investigation of unrelated symptoms or during health screening. These patients are associated with an increased risk of developing MM or related malignancy and require lifelong observation in order to detect signs of transformation. The purpose of monitoring is to try to identify transformation to a malignant disorder at an early stage, when there is no significant irreversible lytic bone disease, renal failure or other disabling symptoms and at a stage when the patient is fit enough to benefit from increasingly effective treatments. In line with the British Committee for Standards in Haematology Guidelines on the Diagnosis and Management of Multiple Myeloma 2005 [38], patients with MGUS or SMM are not treated unless progression occurs.
SMM needs to be differentiated from MGUS in the clinical setting as its rate of transformation is markedly higher (**Figure 1-6**).

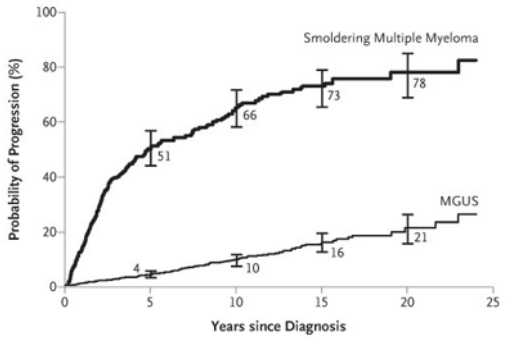

From Kyle et al.(2007) [39]

Figure 1- 6 Probability of progression to active MM or primary amyloidosis in patients with SMM or MGUS

Vertical bars denote 95% confidence intervals

The rate of progression of MGUS is ~1% per year *vs* 10% per year for SMM [40,41]. Moreover, while in MGUS this risk of progression remains constant over time [40], in SMM it is influenced by the time elapsed since diagnosis, being approximately 10% per year in the first 5 years, 3% in the next 5 years with a decrease to 1% per year thereafter [39]. Since the risk of progression to

MM is much higher in SMM compared to MGUS, SMM patients should be managed differently in terms of frequency of follow-up.

1.5.2.1 Monoclonal gammopathy of undetermined significance (MGUS)

MGUS is the most common PC disorder; its incidence increases with age, affecting approximately 3.2% and 5.3% of adults older than 50 and 70 years, respectively [42]. The median age at diagnosis is around 70 years; less than 2% of patients with MGUS are under 40 years of age [42]. For MGUS as well as for SMM and MM, the incidence is two fold higher in American blacks than whites and significantly higher in males [43].

Diagnostic criteria for MGUS are listed in **Table 1-1**. It has been suggested that the best test for an accurate diagnosis of MGUS (as compared with MM) is disease stability over a period of time of 6 to 12 months after diagnosis [40,44,45]. By applying this criterion, only a very small percentage of true MGUS with progression to MM would be missed, but most cases of early MM would be identified [46]; the problem is that this approach can only be applied retrospectively.

Different studies have followed the clinical course of MGUS patients. The original Mayo Clinic series of 241 MGUS patients was followed for more than 35 years. The study showed that the interval from the time of diagnosis of MGUS to the detection of a neoplastic condition ranged from 2 to 29 years (median, 10 years) [47], indicating that MGUS patients are biologically very heterogeneous and also that they must be monitored throughout their lives for evidence of progressive disease.

The constant rate of progression suggests a minimal two-hit genetic model of malignancy and, given that the risk of progression does not depend on the known duration of the antecedent MGUS phase, the second-hit responsible for progression appears to be a random event and not cumulative damage [40].

Risk factors for transformation of MGUS to a malignant condition have been addressed in several studies. A major shortcoming of most of these studies has been their relative small size. Kyle and colleagues studied a large group of MGUS patients in order to investigate whether specific clinical parameters were predictive of progressive disease [40]. Results showed that, although none of the markers could conclusively identify those patients who evolved, the presence of three adverse risk factors, namely a high serum M-protein level ($\geq$15 g/L), an abnormal serum free light chain ratio and non-IgG MGUS was associated with a risk of progression at 20 years of 58% (high-risk MGUS). Any two of these factors present together (high-intermediate-risk MGUS) were associated with a risk of 37%; the risk was 21% with one

of the factors (low-intermediate risk MGUS) and 5% when none of the risk factors were present [40,48]. The type and level of M-protein as risk factors for transformation have consistently been confirmed by a number of other studies [49-52].

1.5.2.2 Smouldering myeloma (SMM)

SMM is an uncommon form of MM accounting for slightly less than 10% of patients with this disease [53,54]. Diagnostic criteria of SMM are listed in **Table 1-1**. The distinction between SMM and MM cannot be made by histopathologic examination of the BM, but is determined by those clinical findings indicative of end-organ damage (CRAB), which are absent from SMM patients. The combination of serum M-protein level and the extent of BM involvement emerged as the most important independent risk factor of disease progression. The presence of IgA M-protein, urinary light chain, reduction in the levels of polyclonal Ig and the pattern of PC involvement in BM (sheets of cells *vs* singly distributed cells or small clusters) also emerged as significant markers of progression on univariate analysis [39]. Most patients with SMM eventually progress to symptomatic disease; however, some patients can remain progression free for a number of years. The median time to progression to symptomatic disease is approximately 3 to 4 years [53].

The pattern of disease progression seems to be variable. Rosinol *et al.* recognized two types of SMM: 'evolving' and 'non-evolving' [54]. The evolving variant was characterized by a progressive increase in the serum M-protein level until the development of symptomatic MM, a shorter time to progression and a previously recognized MGUS phase in most patients. The non-evolving type was characterized by a long-lasting stable M-protein until the onset of symptomatic disease, longer time to progression and no previous MGUS. Interestingly, the evolving type could be identified after the first two follow-up assessments, as most patients with evolving SMM had an increase in M-protein of $\geq$10% during the first 6 months of follow-up. The same evolution patterns recognized in SMM were identified in MGUS. Blade and colleagues found that the behaviour of about 10% of MGUS patients resembled that of the 'evolving variant', defined by a slow but progressive increase in the M-protein size during the first 3 years of follow-up [55]. The 'evolving MGUS' may be considered as an early MM, whereas the non-evolving type might be considered a true stable MGUS, requiring a second hit for malignant transformation.

1.5.3 Symptomatic multiple myeloma (MM)

MM is a devastating incurable malignancy which constitutes 1% of all cancers. It represents the second most common blood cancer after lymphomas accounting for 10% of all haematological malignancies [56]. The median age at diagnosis is 60-65 years, with fewer than 2% of patients younger than 40 years.

The malignant PC are located at multiple sites within the BM, in close association with stromal cells. The interaction between tumour and stromal cells, through cytokines and adhesion molecules, activates the stromal cells that further support the growth and survival of the MM cells, which leads to the complications associated with the condition [57].

MM PC have a minimal proliferative activity, their labelling index is very low with less than 1% of tumour cells synthesizing DNA until late disease. At this time MM cells are found outside the BM, including blood, pleural fluid and skin [58].

Diagnostic criteria for MM are shown in **Table 1-1**. The minimal level of clonal BM PC has been indicated to be 10%. However, approximately 5% of patients with symptomatic MM have a PC content <10%. This is usually due to an inadequate specimen or to the possibility of unevenly distributed PC within the BM. An IgG M-protein is found in about half of patients, one fifth have an IgA and monoclonal light chain only is found in almost 20% [35].

The outcome for MM patients is highly variable. Although the median overall survival (OS) is 3 to 4 years, the range is from less than 6 months to greater than 10 years. This variability is thought to derive from heterogeneity in both MM cell biology and multiple host factors [59].

Several prognostic factors have been used over the years in order to stratify patients into prognostic sub-groups (i.e. age, β2-microglobulin (β2M), albumin, lactate dehydrogenase, C-reactive protein, platelet count, abnormal karyotype and PC labelling index) [60-62]. More recently a worldwide collaboration defined an International Staging System (ISS), which is based on two readily available variables: β2M and albumin. These two parameters can separate patients into three stages with different outcome [59].

1.5.4 Plasma cell leukemia (PCL)

Primary or de novo plasma cell leukemia (pPCL) arises from the expansion of a clonal population of PC, diagnosed during the leukemic phase without a preceding diagnosis of MM. Secondary PCL (sPCL) arises from leukemic transformation of MM [35,63-65]. Approximately 60% of patients with PCL have the primary type. Diagnostic criteria are listed in **Table 1-1** [63]. PCL is a rare disorder, representing less than 5% of malignant PC neoplasia. Most patients have a poor

prognosis with a reported median survival of 6 to 8 months [66,67]. Compared to MM, pPCL shows more extensive disease [67].

Despite showing some degree of overlap in the antigenic expression of CD38 and CD138, PC from PCL appear to have a more immature phenotype than PC from MM. This is suggested by the expression of CD20 antigen, usually absent in MM [68]. Moreover PC from PCL frequently lack the antigens CD9, CD117, HLA-DR (Human leukocyte antigen DR-1) and CD56. The latter is considered to be important in anchoring PC to the BM stroma [69,70]. However, these phenotypic differences do not provide a complete discrimination between PCL and MM [71].

1.5.5 Plasmacytoma

Solitary plasmacytoma of the bone is a localized bone tumour consisting of monoclonal PC and represents 3%-5% of PC neoplasms. Complete skeletal radiographs show no other lesions; there are no clinical features of MM and no evidence of BM plasmacytosis, except for the solitary lesion. This lesion is usually found in BM sites where haematopoiesis is most active, such as the vertebrae, ribs, skull, pelvis, femur, clavicle and scapula. An M-protein is found in the serum or urine in 24%-72% of patients. Local control is achieved by radiotherapy in most cases, but up to two thirds of patients eventually evolve to MM or additional solitary or multiple plasmacytomas.

Extraosseous/extramedullary plasmacytomas are localized PC tumours that arise in tissues other than bone. They have a similar frequency to the solitary plasmacytomas of the bone. The majority (80%) occur in the upper respiratory tract but they may be found in the gastrointestinal tract, lymph nodes, bladder, breast, thyroid, testis, parotid and skin. In most cases these lesions are eradicated with localized radiation therapy. Progression to MM is infrequent, although 25% of patients develop new lesions in the same region with occasional metastasis to distant extraosseous sites [72,73].

1.5.6 Multistep transformation process

Until recently it was not clear whether all MM were preceded by an MGUS phase. Two studies published at the beginning of 2009 offered important clues about MGUS and its relationship to MM [74,75]. (**i**) Landgren and colleagues reported that among 77476 healthy adults enrolled in a prospective Cancer Screening Trial, 71 individuals developed MM. For all 71 patients there were stored serum samples obtained from 2 to 10 years prior to the diagnosis of MM. All MM

patients showed evidence of having gone through a preceding MGUS, with 75% of them showing a detectable M-protein 8 or more years prior to transformation to MM. In about half of the patients, the serum M-protein showed a year-by-year increase before the diagnosis of MM [74]. (**ii**) Weiss and colleagues reported on the prevalence of MGUS in 30 MM patients for whom there was available serum stored by the US department of Defence Serum Repository and collected 2 to 15 years prior to the diagnosis of MM. A preceding MGUS was detected in 27 of the 30 patients [75]. These two studies indicated that virtually all MM cases were preceded by an MGUS phase. They also showed that in 30%-50% of MGUS patients who evolved to MM, the M-protein remained stable until progression occurred, while in 50%-70% of patients the M-protein showed a gradual and progressive increase.

These with other studies led to the generation of disease models of MM based on the multistep progression of normal to MGUS through to myelomatous PC. In these models, the initiating event is thought to be an immortalization episode in PC, which initiates the formation of a clone. It has been suggested that such clones may remain quiescent and non-accumulating without producing end organ damage (MGUS/SMM stage). If transformation occurs, and so far the mechanisms leading to progression remain unknown, PC accumulate within the BM leading to organ and tissue impairment. This disease usually enters a quiescent phase of variable duration, followed by a late stage of drug resistance with resistance to apoptosis and independence from the BM microenvironment [76].

1.6 Genetic abnormalities in MM and related disorders

The acquisition of recurrent chromosomal abnormalities is an early event in MM development, as many of the genetic changes identified in the PC of MM patients have also been found in MGUS and SMM. Although the mechanisms responsible for the acquisition of these changes is not well understood, current evidence suggests that in many cases an abnormal response to antigenic stimulation may be a key factor [77-79].

Although several genetic abnormalities found in the neoplastic clone have been suggested to be associated with the transition from MGUS/SMM to MM, no definite genetic markers of progression have been identified. Specific genetic abnormalities are probably 'driver' events contributing critically to clonal selection and disease evolution. However, because of the asymptomatic nature of MGUS and SMM, at the time of MM diagnosis the developmental timing of these changes is buried in the MM's covert natural history. Furthermore, it remains unclear how much the genetic or epigenetic changes within the clonal PC affect disease progression compared to extrinsic changes in the non-tumour cells of the BM microenvironment. The BM microenvironment has been shown to undergo marked modifications during progression, including induction of angiogenesis and abnormal paracrine loops involving cytokines such as interleukin-6 (IL-6), which serves as a major growth factor for PC [80].

1.6.1 Methodological approaches: cytogenetic analysis and fluorescence *in situ* hybridization (FISH)

The initial approach to study genetic abnormalities of PC disorders has been cytogenetic analysis of metaphases. As previously mentioned, although MM is more proliferative than MGUS or SMM, all conditions are characterized by an extremely low proliferation rate. This aspect, together with the often poor quality of the BM samples due to the scattered and variable degree of BM infiltration, has made cytogenetic studies difficult. When cytogenetic analysis reveals only normal metaphases, they usually originate from the myeloid elements and not from the clonal PC [46]. For these reasons, metaphase analysis grossly underestimates the incidence of chromosomal changes in these conditions. Clonal abnormalities are almost never found in MGUS and SMM, while they are found in ~40% of MM cases, 20%-35% at diagnosis and about 60%-80% of patients in stage III (ISS staging system) or with an extramedullary tumour

(PCL) [81,82]. As a consequence most changes described by metaphase analysis mostly relate to the late stages of the disease, relapsing cases or PCL.
Culture parameters, such as addition of IL-6 or granulocyte colony stimulating factor and length of time in culture, appeared to increase the detection rate of chromosomal abnormalities [83,84].
Other aspects of cytogenetic analysis which make the interpretation of the karyotype difficult and often inaccurate include: the telomeric location of some translocation partners and the high level of complexity of most abnormal cases. In most patients, the karyotype resembles that of solid tumours: a multitude of complex chromosomal aberrations where it is difficult to understand which ones are responsible for tumour initiation and which for tumour progression. Despite these problems, metaphase analysis has identified a number of structural and numerical abnormalities. The latter, in particular, have subdivided patients into specific ploidy categories.

A technique that to a certain extent has overcome the limitations of metaphase analysis is interphase FISH (iFISH). The basis of this technique is the detection of specific sequences of genomic DNA in cytological material fixed to a microscope slide through the hybridization of a labelled DNA or RNA probe.
The development of FISH has permitted the study of chromosomal rearrangements at a resolution significantly higher than that of conventional cytogenetics. Furthermore, because iFISH does not need dividing cells, it has provided the opportunity of studying numerical and structural abnormalities in all patients at all disease stages [85]. Given the low PC infiltration characterizing most BM samples from cases with PC disorders, iFISH is preferentially done on purified cells (e.g. $CD138^+$ microbead selection, see **Section 2.2.5**) or using simultaneous immunofluorescence to identify the PC [46].
Interphase-FISH studies have shown that using probes for five to ten different chromosomes, more than 90% of cases (including both MM and MGUS) had at least one abnormality and confirmed that most MGUS PC were aneuploid [45,86].
A major limitation of this technique is that it is highly specific, requiring prior knowledge of the type and location of the genetic abnormality under investigation with no possibility to detect other changes.

Metaphase analysis, although uninformative in many cases, seems to have the advantage over iFISH of playing a major role in the prediction of outcome in MM (see **Section 1.6.4**). The detection of an abnormal clone, at any time in the disease or treatment course, is associated with an inferior outcome. The detection of chromosomal abnormalities in metaphase not only seems to reflect high proliferative activity, but also stroma-cell independence of *in vitro* cell division of malignant PC [87,88].

1.6.2 Disease stages and timing of oncogenic events

In MM two distinct pathways of pathogenesis have been recognized (**Figure 1-7**): a non-hyperdiploid (nonHRD) pathway (black triangle) that usually includes one of seven recurrent *IgH* translocations as an early event and a hyperdiploid (HRD) pathway (white triangle) which is associated with multiple trisomies of odd numbered chromosomes.

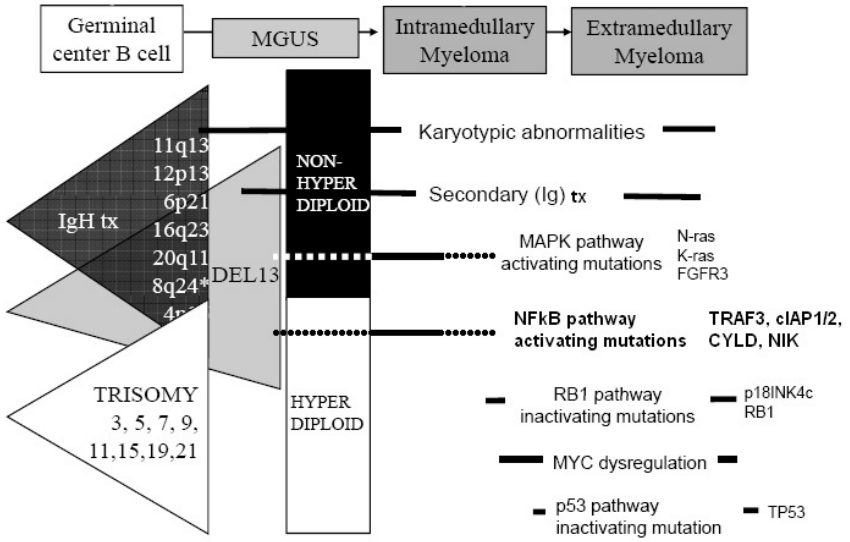

Adapted from Chng et al., 2007 [89]

Figure 1- 7 Disease stages and timing of oncogenic events

IgH tx, primary *Ig* translocations; DEL13, monosomy/deletion 13; * the partner at 8q24 refers here to *MAFA* as *MYC* is also located on 8q24; *MYC*-translocations are usually secondary events

Monosomy/deletion of chromosome 13 (Δ13) (grey triangle) has also been suggested to be an early abnormality shared by MGUS and MM tumours. *IgH* translocations, HRD and Δ13 are all early and partially overlapping events; however, the relative timing of their occurrence is not yet completely understood. Secondary chromosomal rearrangements and other abnormalities can occur at any time during tumourigenesis. Mutually exclusive activating mutations of *K*- or *N-RAS* (rat sarcoma viral oncogene homolog) or *FGFR3* (fibroblast growth factor receptor 3), when there is a t(4;14) translocation are rare in MGUS. Their prevalence is 30% to 40% in early MM with a small increase during tumour progression.

Late oncogenic events that occur at a time when tumours are becoming more aggressive include *MYC* (*v-MYC* avian myelocytomatosis viral oncogene homologue) dysregulation, promiscuous

mutations that constitutively activate the NF-κB (nuclear factor kappa-light-chain enhancer of activated B cells) pathway, additional inactivation of the retinoblastoma pathway, such as bi-allelic deletion of *p18/CDKN2C* (cyclin-dependent kinase inhibitor 2C), loss or mutation of *TP53* (tumour protein 53) and methylation of the *p16INK4A/CDKN2A* (cyclin-dependent kinase inhibitor 2A) promoter [89,90].

1.6.3 Aneuploidy

Numerical chromosomal abnormalities are present in virtually all MM and in most, if not all, cases of MGUS and SMM [85,91]. There is non random involvement of different chromosomes: the most common trisomies are 3, 5, 7, 9, 11, 15, 19 and 21, while the most common monosomies are 13, 14, 16, and 22. No specific numerical chromosomal change is constant or predictive of disease progression. In cases showing multiple gains, it is unknown if the extra chromosomes are accumulated one at a time, in sequential steps or as a single event.
Global aneuploidy analysis segregates patients into four sub-categories: hypodiploid (≤45 chromosomes), pseudodiploid (46 - 47 chromosomes), HRD (≥48 chromosomes), and near-tetraploid (≥75 chromosomes). Near-tetraploidy usually represents the doubling of hypodiploid or pseudodiploid chromosomal complements, as the majority of the cases with a near-tetraploid population also have cells with a pseudodiploid or hypodiploid karyotype [92-94].
It is agreed that there are specific patterns of association among these four classes: hypodiploid cases are classified with pseudodiploid and near-tetraploid as nonHRD [92-94]; half of MM cases fall in this ploidy category. Compared to the HRD group, nonHRD MM is characterized by a higher prevalence of *IgH* translocations, Δ13 and structural chromosomal abnormalities. Two studies have shown that HRD and nonHRD are not only established early in disease development but are maintained over time or during progression from pre-malignant stages to MM, although the relative percentages of cells carrying different chromosomal abnormalities may change [95,96]. As extramedullary MM and human myeloma cell lines (HMCL) almost always have nonHRD karyotypes, it is thought that HRD tumours are more stromal-cell-dependent than nonHRD tumours [97].

1.6.4 Chromosome 13 abnormalities (Δ13)

Δ13 is highly prevalent in PC disorders. In most cases, Δ13 represents a whole-chromosome monosomy [46,85,98]; only a subset of tumours show interstitial deletions, with a common deleted

region located at 13q14 [99,100]. Although the genes targeted by this abnormality remain unclear, the retinoblastoma (*RB1*) gene falls within the minimal common deleted region. *RB1* was the first tumour suppressor gene to be cloned. It is a negative regulator of the cell cycle through its ability to bind the transcription factor E2F and repress the transcription of genes required for entry to the synthesis (S) phase of the cell cycle [101]. Studies on other types of cancer showed that both copies of *RB1* must be inactivated to eliminate its tumour-suppressor function [34]. In MM, apart from rare cases of biallelic deletion, inactivating mutations of the remaining allele are not commonly seen. RB protein levels correlate with mRNA levels and DNA copy number, suggesting that mono-allelic loss of *RB1* might be tumourigenic through a haploinsufficiency mechanism. However, currently the role of *RB1* remains unclear [34,102].

Δ13 was originally detected in ~50% of patients with abnormal karyotypes, equivalent to 10-20% of all patients. Initially it was not described in MGUS or SMM, probably due to the difficulty in obtaining metaphases in these disease types [46]. Since the use of iFISH, it became clear that Δ13 occurred at all stages of PC neoplasms. However, conflicting reports have been published on the actual prevalence of this abnormality in MGUS and MM. Some studies reported a substantially lower incidence in MGUS (~25%) as compared to MM (50%–60%) [85], whereas others showed an almost identical prevalence [44,103]. The lower incidence in MGUS implied that Δ13 may be involved in the transition from pre-malignant conditions to MM, whereas the latter suggested that Δ13 was associated with initiation of the disease and was not an event linked to progression. A recent study suggested that, while in MM Δ13 is the hallmark of hypodiploidy, in MGUS the abnormality is associated with HRD. Therefore discrepancies in the incidence of Δ13 found in different series might be related to the relative proportions of HRD and hypodiploid patients tested [104]. Further studies are needed to resolve these discrepancies.

The presence of Δ13 has been associated with an adverse prognosis, but its clinical relevance appears to depend on the detection method used [46]. Metaphase analysis detects the abnormality in considerably fewer patients than iFISH (~20% *vs* ~50%), but when Δ13 is detected in metaphase it has been shown to confer a significantly shorter OS than when detected by iFISH. These findings indicated that Δ13 detected by iFISH is an inadequate independent prognostic marker and that the prognostic value of Δ13 depends on the ability of the PC clone to divide in vitro. As a confirmation of these results, PC with Δ13 in metaphase have been shown to have a distinct gene expression profile [102]. By iFISH, Δ13 was found to be predictive of inferior survival only when associated with other poor prognostic markers (i.e. t(4;14), 17p13 deletion).

In patients with Δ13 in the absence of other poor prognostic markers, Δ13 by iFISH was not significantly associated with an inferior survival [87,102,105].

1.6.5 *Ig* translocations are present in a majority of PC tumours

Like other post-germinal centre B cell tumours, translocations involving the *IgH* locus (14q32) or one of the *IgL* loci (κ, 2p12 or λ, 22q11) are common in PC neoplasms [22]. These translocations may be primary/initiating events during tumour pathogenesis or secondary, occurring during disease progression.

As previously described, primary translocations seem to originate from errors in one of the three B cell specific DNA modification mechanisms, specifically class switch recombination and somatic hypermutation. These translocations usually juxtapose an oncogene close to one or more of the potent Ig enhancers (Eμ, Eα1, Eα2) on the der(14) originated from the translocation [106]. Since there is no evidence that somatic hypermutation and class switch recombination are active in normal or neoplastic PC, presumably these translocations represent very early if not initiating oncogenic events arising as normal B cells pass through the germinal centre.
Studies from different groups have shown that the prevalence of primary *IgH* translocations increases with disease stage: about 50% in MGUS or SMM, 55%-70% in intramedullary MM, 85% in PCL, and >90% in HMCL [107-109]. Limited studies indicated that *Igλ* translocations are present in about 10% of MGUS/SMM and 15%-20% of intramedullary MM. Translocations involving an *Igκ* locus are rare, occurring in only 1%-2% of MM [34].
Secondary translocations appear to be very late events which do not always involve *Ig* loci and usually do not arise from B cell specific recombination mechanisms [110]. Typical examples of secondary translocations are those involving *MYC*. The breakpoints on both chromosomes 8 and 14 can be highly variable and therefore it is unlikely that *Ig* remodelling events are responsible for these translocations [111,112]. All of these translocations are readily detected by iFISH analysis in the majority of cases.

1.6.5.1 Seven recurrent *IgH* translocations represent primary oncogenic events

The seven recurrent chromosomal partners (oncogenes) involved in primary *IgH* translocations (listed in **Figure 1-7**) represent three recurrent *IgH* translocation groups [113-118]:

- ***Cyclin D***: 11q13 (Cyclin D1, *CCND1*), 15%; 12p13 (Cyclin D2, *CCND2*), <1%; 6p21 (Cyclin D3, *CCND3*), 2%
- ***MAF*** (*v-MAF* avian musculoaponeurotic fibrosarcoma oncogene): 16q23 (*c-MAF*), 5%; 20q12 (*MAFB*), 2%; 8q24.3 (*MAFA*), <1%
- ***MMSET/FGFR3*** (multiple myeloma SET domain/ fibroblast growth factor receptor 3): 4p16 (*MMSET* and usually *FGFR3*), 15%

IgH translocations involving *CCND2* and *MAFA* have recently been reported [89] and are extremely rare. The combined prevalence of these seven rearrangements is about 40% and they occur predominantly in nonHRD tumours; less than 10% of HRD cases have one of these rearrangements [34]. One of the striking features of *IgH* translocations in MM is the fact that some oncogenes are dysregulated even when they are located more than 1 Mb from the breakpoint on the der(14).

i. t(4;14)(p16.3;q32)

The translocation t(4;14) is cytogenetically cryptic and was first identified from cloning experiments in HMCL. It can be detected by iFISH or by reverse transcriptase polymerase chain reaction (RT-PCR) specific for the *IgH-MMSET* hybrid transcript. The translocation is seen in 15-20% of primary MM samples and in 25% of HMCL [46]. It is the second most common *IgH* translocation after t(11;14) [119]. Patients with t(4;14) often have an IgA isotype.
In the majority of cases, t(4;14) originates from illegitimate switch recombination. As a consequence of the translocation, *FGFR3* becomes associated with the 3'α enhancer(s) on the der(14). The 4p16 breakpoints cluster within a 60 kb region, within the 5' exons of the *MMSET* gene, 50-100 kb centromeric of *FGFR3.* FGFR3 is one of the four high-affinity tyrosine kinase receptors for the fibroblast growth factor (FGF) family of ligands. It is normally expressed in lung, kidney and at high levels in the developing central nervous system and cartilage. Its level of expression in mononuclear cells isolated from the BM is almost undetectable. On ligand stimulation, FGFR3 undergoes dimerization and tyrosine autophosphorylation resulting in cell proliferation or differentiation, depending on the cell context, through the mitogen-activated protein kinase (MAPK) and phospholipase Cγ signal transduction pathways [120,121].
The *MMSET* gene encodes four different protein products originating from two alternative splicing events and an alternative transcription site. Very little is known about the function of the various protein isoforms. Based on homology to other SET domain containing proteins, the full length isoform, MMSET II, is predicted to act as regulator of gene expression by methylating specific lysine residues on histones H3 and H4 [119]. *MMSET* is dysregulated in all cases by its association with the intronic enhancer (Eμ) on the der(4). Nearly one third of

patients with the translocation do not express *FGFR3*; *FGFR3* lack of expression is mainly due to the loss of the der(14). In some cases the der(14) is present, thus other mechanisms must be responsible for the loss of gene expression.

It is unclear whether loss of *FGFR3* expression is a primary or a secondary event and whether *FGFR3* dysregulation is critical for MM pathogenesis. Kinase-activating mutations of the dysregulated *FGFR3* are seen late in tumourigenesis, and it seems that the proliferation of these MM tumours is dependent on the mutated *FGFR3* [116]. Other t(4;14) tumours acquire *K*- or *N-RAS* mutations that appear to be mutually exclusive of *FGFR3* mutations [122]. The consistent persistence of *MMSET* dysregulation suggests that this gene might be the critical oncogene in the initiation of these tumours. However, it remains unclear how *MMSET* contributes to the pathogenesis of MM. The t(4;14) almost always coexists with Δ13 and is highly associated with nonHRD in both MM and MGUS.

The t(4;14) is associated with an unfavourable prognosis in MM patients treated with either conventional or high-dose therapy (HDT) with stem cell transplantion. The adverse outcome manifests as early relapse; the presence or absence of the der(14) does not appear to have an influence on survival [123]. FGFR3 inhibitors are available: PD173074 is a compound that has been shown to block proliferation and induce apoptosis in some HMCL with the translocation [49]. Recently, several studies have suggested that treatment with bortezomib overcomes the poor prognosis associated with t(4;14) in both newly diagnosed and relapsed patients [124-126].

ii. t(11;14)(q13;q32), t(6;14)(p21;q32) & t(12;14)(p13;q32)

The t(11;14) is easily detectable by metaphase analysis. It is found in 15-20% of MM patients, with approximately the same prevalence in MGUS and SMM [44,109,127], although its frequency is higher in primary amyloidosis (50%) [44,85,128].

The translocation results in ectopic expression of *CCND1*, which promotes the progression of cells from G1 growth arrest phase into the S phase. CCND1 is the regulatory subunit of a holoenzyme that phosphorylates and inactivates the RB1 protein and promotes progression through the G1-S phase of the cell cycle in a manner dependent on cyclin-dependent kinases (*CDK*). In addition, CCND1 has a number of cell cycle- and CDK-independent functions. It associates with and regulates transcription factors, co-activators and co-repressors that govern histone acetylation and chromatin remodelling proteins. Amplification or overexpression of *CCND1* play pivotal roles in the development of several human cancers, including parathyroid adenoma, breast cancer, colon cancer, lymphoma, melanoma, and prostate cancer [129-131]. Normal B cells express *CCND2* and *CCND3* but not *CCND1*.

The breakpoints in 14q32 are within either the J_H region or the switch regions, while the breakpoints at 11q13 are dispersed over 300 kb centromeric of *CCND1* [106,107]. Following the

translocation, *IgH* enhancers become located to the der(11). This may lead to dysregulation of the myeloma overexpressed (*MYEOV*) gene, which was found to be upregulated in three of seven HMCL with t(11;14) [132].

This translocation is usually associated with a diploid or pseudodiploid karyotype and it appears to have an intermediate prognosis. However, its overrepresentation in HMCL and PCL suggests that, at least in some cases, the t(11;14) results in aggressive clonal growth which might be due to the coexistence or acquisition of secondary genetic changes [113].

The t(6;14) and t(12;14) lead to dysregulation of *CCND3* and *CCND2,* respectively. The frequency of t(6;14) is ~3% in MM, although the frequency in pre-malignant conditions is unclear [117]; the t(12;14) is rare. Patients with t(6;14) or t(11;14) seem to follow a similar clinical course.

iii. t(14;16)(q32;q23)

The t(14;16) translocation has been identified in 5% of MM patients and leads to dysregulation of the c-*MAF* proto-oncogene. Despite the large distance between the translocated *IgH* enhancers and the c-*MAF* locus, the gene is highly up-regulated in these tumours, indicating that c-*MAF* is the targeted gene. Interestingly, a recent study using immunohistochemistry reported that in MM c-MAF protein is exclusively expressed in cases positive for c-*MAF* rearrangements [133].

Five of the breakpoints cloned on 16q23 occur over a region 550-1350 kb centromeric of c-*MAF* and all but one are located within the 800 kb intron of the *WWOX* (WW domain-containing oxidoreductase) gene. This region is a common fragile site, FRA16D. Deletions of this region have been found in adenocarcinoma of the stomach, lung, colon and ovary, suggesting a possible role of *WWOX* as a tumour suppressor gene [134,135]. c-MAF is a leucine-zipper transcription factor that heterodimerizes with jun (v-jun avian sarcoma virus 17 oncogene homolog) and fos (Finkel-Biskis-Jinkins (FBJ) murine osteosarcoma virus). It has been proposed that c-MAF transforms PC by stimulating cell cycle progression and altering BM stromal interactions [136]. From gene expression profiling, three c-MAF target genes have been identified which were all shown to be over-expressed: *CCND2*, *integrin β7* and *CCR1* (chemokine CC motif receptor 1).

The translocation is readily detected by iFISH, while its detection by metaphase analysis can be challenging, depending on the quality of the metaphase preparations. The prognostic significance of t(14;16) is less well established than t(4;14) as numbers are small. However, there is a suggestion that t(14;16) is associated with poor prognosis [108]. As seen with t(4;14), 80-90% of tumours with this translocation have Δ13.

Avet-Loiseau and colleagues found a decreased prevalence of *IgH* translocations involving 4p16 and 16q23 in MGUS as compared to MM [109]. Similar data were reported in two other studies [44,137]. Collectively, these findings suggested that these translocations may be associated with rapid progression from MGUS to MM, so that the pre-malignant stages are rarely recognized. However, in a number of MGUS or SMM cases positive for one of these two translocations, it appeared that the presence of the abnormality alone was insufficient to lead to progression to MM, with some patients remaining stable for years [44,137,138]. Given the overall low incidence of the t(14;16), such observations need to be confirmed in larger patient series.

iv. t(14;20)(q32;q12)

The translocation t(14;20) has been reported in 1-2% of primary MM. It leads to ectopic expression of *MAFB* (v-maf avian musculoaponeurotic fibrosarcoma oncogene homolog B). On chromosome 20, the breakpoint is located within a gene sparse region, with the closest oncogene, *MAFB*, located 1100 kb telomeric of the breakpoint [139].

The *MAFB* gene belongs to the MAF family of basic region/leucine zipper transcription factors [140]. Like other large MAF proteins, such as c-MAF, it has both a carboxy-terminal region/leucin zipper domain, which mediates DNA binding and dimer formation, and an amino-terminal acidic domain associated with transactivating capability. MAFB proteins have dual functions in the transcription of downstream genes and whether they function as transactivators or transrepressors depends on the target sequences and the interacting proteins. In hematopoietic cells, *MAFB* expression appears to be restricted to the myelomonocytic lineage and macrophages. *MAFB* plays a role in the proliferation of myelomonocytic progenitors, their differentiation into the monocytic lineage and in the prevention of erythroid differentiation [118].

This translocation seems to have a very poor prognosis in MM, although the information on its clinical associations is very limited. The prevalence of the translocation in MGUS/SMM has not been fully investigated [46].

1.6.5.2 Secondary *Ig* translocations

Among the secondary translocations, approximately 10-20% in MGUS and MM do not involve one of the seven recurrent partners or *MYC*. The partner loci have rarely been identified and many of those have been found in single cases only. These *IgH* translocations share many similarities with *MYC* translocations with breakpoints outside or close to *IgH* switch or VDJ regions, the presence of unbalanced or complex structural rearrangements and a similar prevalence in HRD and nonHRD tumours.

1.6.5.2.1 MYC rearrangements

The MYC transcription factor has been implicated in the control of many aspects of tumour cell biology. It promotes cell proliferation and restrains differentiation controlling the transcription of multiple genes involved in cell growth and metabolism, vasculogenesis, cell adhesion and genomic stability[141]. MYC is a basic helix-loop-helix-leucine zipper transcription factor that dimerizes with the related protein MAX. MYC/MAX heterodimers bind to specific DNA elements, designated as E-boxes, located in the promoter regions of target genes mediating either activation or repression of transcription [142]. In MM, rearrangements that involve the *MYC* proto-oncogenes are thought to represent a very late event, occurring at the time when MM tumours are becoming less stromal-cell-dependent and more proliferative. These rearrangements have been reported to be rare or absent in MGUS/SMM, while they have been found in 15% of primary MM tumours, 44% of advanced tumours and nearly 90% of HMCL [111]. *MYC,* located at the chromosomal band 8q24.21, is the gene most frequently involved. However, 2% of primary tumours ectopically express *N-MYC* and an *L-MYC* translocation has been identified in one cell-line (U-266 cell line, *L-MYC*, translocation and inversion). These rearrangements are usually complex translocations or insertions, sometimes involving three different chromosomes [34,109,110] and an *Ig* locus is involved in 25%-60% of cases [89]. Given the complexity and the multiple breakpoints identified in *MYC* rearrangements, FISH tests which only map some of the breakpoints, using relatively large bacterial artificial chromosome (BAC) probes cannot provide a full picture of *MYC* abnormalities. Therefore, survival analyses based on FISH results are not fully reliable. In support of this, Avet-Loiseau *et al.* found no difference in prognosis between patients with and without *MYC* abnormalities tested by FISH [143]. In contrast, an analysis of 596 patients based on gene expression profiling showed that patients with *N-MYC* expression, or very high levels of *MYC* expression had a significantly poorer survival (unpublished data revised by Chng *et al.* [89]).

1.6.6 Deletions of 17p13

Deletions of 17p13 detected by iFISH have been found in ~10% of MM patients and approximately 40% of PCL and HMCL [144,145]. The abnormality occurs with a similar prevalence in HRD and nonHRD tumours and has been associated with a poor prognosis (on uni- and multivariate analysis) in different studies [87,105,143]. Despite the often small size of these deletions, there is no definitive evidence to prove which is the critical gene targeted by the abnormality. Certainly, *TP53* is contained within the minimal deleted region reported by different groups and probes targeting this gene are the ones used to assess 17p status by iFISH. Almost all 17p13

deletions are mono-allelic. Chng *et al*. performed mutational analysis of *TP53* on 268 newly diagnosed MM patients and detected 3% of patients with mutations [146]. The spectrum of these mutations was broad and not typical of other malignancies, in fact two mutations were found in exons 4 and 11 which are rarely involved in mutations. The presence of *TP53* mutations was significantly associated with the presence of *TP53* deletions as five of the nine patients with mutation also had 17p13.1 hemizygous loss [146]. However, only five of 31 (16%) patients with 17p13 deletion had mutation of the remaining *TP53* allele. Also, the use of whole BM DNA may have resulted in a markedly reduced sensitivity of the study. In a smaller study (24 newly diagnosed MM patients) using $CD138^+$ PC, no *TP53* mutations were detected, but it is unclear whether these samples also had 17p13 deletion [147]. Although current evidence does not exclude *TP53* as the critical gene deleted on 17p13, more studies are needed. The p53 protein is a DNA binding protein, which acts as a tumour suppressor in response to DNA damage. It is part of the complex pathways which ensure the maintenance of the genome, allowing DNA repair or alternatively activating cellular apoptosis. The expression of p53 was found to correlate with 17p13 status defined by FISH and low expression of p53 was an independent factor associated with poor prognosis [147]. The frequency of *TP53* mutations appears to increase with disease stage and is about 3%-5% at MM diagnosis, 20%-40% in advanced MM or PCL and 65% in HMCL [146,148-150]. Deletions of *TP53* in MGUS or SMM are rare [46].

1.6.7 Gain of chromosome 1q21

Gain of the long arm of chromosome 1 (1q) is one of the most common genetic abnormalities in MM [151]. Although in most cases it is the whole arm that is gained, the band 1q21 seems to be consistently involved. The term 'amplification' has been widely used to indicate the presence of extra copies of this region without discriminating between amplification defined by $\geq$6 copies and low or high level gain (four-five copies).

By cytogenetic analysis it was noted that extra copies of 1q resulted from a number of different chromosomal rearrangements, such as unbalanced translocations, duplications and triplications, isochromosomes and 'jumping translocations' involving all or part of the chromosome arm [152]. Gene expression profiling studies found elevated expression levels of genes mapping to 1q21 in cases with gain of this region [151,153,154]. Among the genes found to be over-expressed, *MUC1* (Mucin-1 Precursor), *MCL1*(Induced myeloid leukaemia cell differentiation protein), *PDZK1* (PDZ domain containing 1), *IL6R* (Interleukin 6 receptor), *BCL9* (B cell CLL/lymphoma 9), *CKS1B* (CDC28 protein kinase regulatory subunit 1B), *PSMD4* (26S Proteaosomenon-ATPase regulatory subunit 4) and *RAB25* (member *RAS* oncogene family) have been suggested as

possible targets of the abnormality [155-158]. Different studies focused on *CKS1B* as the targeted gene and *CKS1B* probes are usually used to assess 1q status by iFISH [157,159]. *CKS1B* is a member of the highly conserved CKS1 protein family that interacts with CDK, playing a critical role in cell cycle progression while regulating the proteolysis of CDKN1B (cyclin-dependent kinase inhibitor B). If *CKS1B* is responsible for increased proliferation, it might be expected that other mechanisms involved in the dysregulation of this gene would be found, such as translocations. However, there has been no evidence of other mechanisms.
Gain of 1q21 is rare or absent in pre-malignant conditions and a few studies performed showed that when present in SMM it seems to be associated with progressive disease [160-164]. However, such findings were based on limited patient numbers and relatively short follow-up, therefore larger studies are needed in order to assess whether 1q gain is a reliable marker of disease progression in MGUS and SMM.

1q abnormalities are found at a higher incidence in cases with dysregulated expression of c-*MAF* or *FGFR3/MMSET* and those with a high proliferation expression index [162]. Hanamura and colleagues showed for the first time that 1q21 gain detected by FISH is a significant and independent poor prognostic factor [162]. However, another study from the Mayo Clinic showed that, while significantly associated with poor prognosis on univariate analysis, 1q21 gain was not an independent prognostic factor on multivariate analysis when PC labelling index and t(4;14) were included [165]. To confirm these findings, the French Intergroupe Francophone du Myelome (IFM) trials investigated 1q21 copy number by FISH on 365 patients and did not find 1q gain to be an independent marker of adverse prognosis [166]. The same group recently published a single-nucleotide polymorphism (SNP) array study of 192 newly diagnosed and uniformly treated MM patients younger than 66 years. Using uni- and multivariate analysis, they found three independent markers of prognosis: two associated with a poor prognosis: 1q23.3 gain and 12p13.31 loss; and one with a favourable prognosis: 5q31.3 gain. However, when these markers were adjusted to the established prognostic variables (i.e., t(4;14), loss of 17p13, β2M), 1q gain lost its significance [167].

1.7 Gene expression profiling in PC disorders

Different technological approaches have resulted in the ability to assess genomic aberrations at both the DNA and RNA levels in a global fashion.

1.7.1 Use of gene expression profiling to classify MM

1.7.1.1 Translocation and cyclin D (TC) classification

Cyclin D genes are expressed at low levels in quiescent cells, while in response to growth factors they are transcriptionally up-regulated and expressed in all proliferating cells. Despite the very low proliferative activity observed in PC from MGUS/SMM and MM patients, the level of *CCND1*, *CCND2* or *CCND3* mRNA in all these tumours was found to be relatively high compared with the level of *CCND2* mRNA expression in healthy proliferating PC [168]. This upregulation of *Cyclin D* genes is caused by either *IgH* translocations or other, unknown mechanisms.

Gene expression profiling can detect the expression levels of *CCND1*, *CCND2*, and *CCND3* and simultaneously identify spiked expression of genes deregulated by primary *IgH* translocations. Supervised analysis of gene expression profiles provided the basis for a molecular classification of MM: the translocation and cyclin D (TC) classification (**Figure 1-8**).

Eight groups of tumours were identified: (**1**) 4p16 tumours (15%) expressing high levels of *CCND2* and *MMS*ET (and in most cases *FGFR3*) as a result of the translocation t(4;14); (**2**) *MAF* tumours (7%) expressing the highest levels of *CCND2* and showing high levels of either c-*MAF* or *MAFB*, consistent with the possibility that both MAF transcription factors upregulate the expression of *CCND2*; (**3**) 11q13 (16%) and (**4**) 6p21 (3%) tumours expressing high levels of either *CCND1* or *CCND3* as a result of an *IgH* translocation; (**5**) D1 tumours (34%) ectopically expressing low to moderate levels of *CCND1* despite the absence of a t(11;14) translocation; (**6**) D1+D2 (6%) expressing both *CCND1* and *CCND2*. (**7**) D2 tumours (17%) were a mixture of tumours expressing *CCND2*; (**8**) none (1%) expressed no D-type cyclins. The TC classification did not clearly identify patients with HRD MM. HRD tumours were mainly found in the D1 and D1+D2 groups. D1 and D2 HRD MM appeared to have a higher incidence of proliferative disease compared to D1 HRD MM characterized by a low proliferative index. However, no differences in survival were noted between the two groups [168].

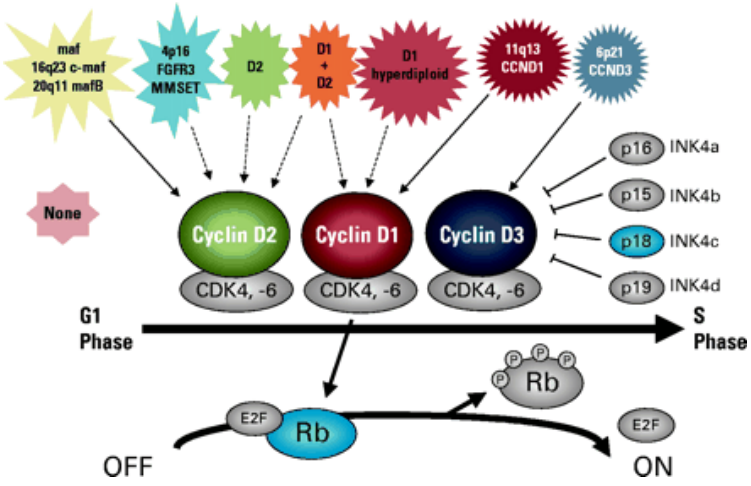

Adapted from Bergsagel et al., 2005 [90]

Figure 1- 8 Translocation and cyclin D (TC) classification

Dysregulation of one of the three cyclin D can be a consequence of an *Ig* translocations (solid arrow) or by an unknown mechanism (dashed arrow)

1.7.1.2 UAMS (University of Arkansas for Medical Science) molecular classification of MM

An alternative molecular classification was based on unsupervised clustering of tumours by gene expression profiling. This identified seven molecular groups, which were similar although not identical to the TC groups. These clusters identified tumours with t(4;14), *MAF* translocations, t(11;14) and t(6;14), corresponding to MS (MMSET), MF (MAF/MAFB) and CD (CCND) -1 or CD-2 groups, respectively. According to this classification, the t(11;14) and t(6;14) might belong to either the CD-1 or CD-2 group, depending on expression of CD20 and other B-related genes. In contrast to the TC classification, the UAMS identified HRD MM as a distinct HY (HYperdiploid) group. This group, however, included only about 60% of HRD tumours. The remaining HRD tumours were distributed between the other six groups. The PR (PRoliferation) group included MM with increased expression of proliferation-related genes, while the LB (Low Bone disease) group defined tumours with low bone disease and lower expression of genes associated with bone disease.

The PR, MS, and MF groups identified patients with a poor prognosis. The PR group comprised patients with t(4;14), t(11;14) and HRD with more proliferative disease and an associated inferior outcome.

The advantage of the UAMS classification is its close clinical relevance. It is also interesting that an unsupervised analysis of gene expression profiling data essentially identified the main genetic subtypes of MM, suggesting that the predominant transcriptional heterogeneity seen in MM is driven by these pivotal primary genetic events [124].

1.7.2 Use of gene expression profiling to define a high-risk molecular signature

Although many of the genetic and molecular lesions associated with disease initiation are known, those lesions that promote an aggressive clinical course among MM patients have remained unclear. Gene expression profiling has been used to define the molecular signature for high-risk disease. Shaughnessy and colleagues found 70 genes to be linked to early disease-related death (51 up-regulated and 19 down-regulated) [154]. Interestingly, 30% of these genes mapped to chromosome 1, with the majority of those up-regulated mapping to 1q and the down-regulated ones to 1p. The up-regulated genes were highly enriched for proliferation-related genes. Multivariate discriminant analysis revealed that a 17-gene subset (12 up-regulated) could predict outcome as efficiently as the 70-gene model. This 17-gene signature was validated in two additional datasets of newly diagnosed and relapsed patients. In both settings it was significantly associated with inferior outcome. It was also found that the presence of t(4;14) further dissected the high-risk group, with those having both t(4;14) and the high-risk 17-gene score displaying shorter survival.
The IFM group also used gene expression profiling to identify a 15-gene signature defining a high-risk group of patients. This group was significantly associated with Δ13, deletion of 17p, gain of 1q and t(4;14). The IFM 15-gene model also improved the ISS prognostication [169].

1.7.3 Use of gene expression profiling to differentiate MGUS from MM

Microarray studies have been applied to define global patterns of gene expression relevant to the biology of normal PC and PC from MGUS and MM patients. In initial studies, normal PC were differentiated from PC of MGUS and MM, but PC from MGUS could not be distinguished from PC from MM [170]. The main feature separating normal and malignant PC was the decreased level of expression of a large number of genes, while the list of up-regulated genes was more limited.

The similarity of the transcriptome between PC from MGUS patients and PC from MM was surprising, given the very different clinical behaviour of the two entities [171].
Using a third-generation microarray on a greater number of samples, Zhan *et al*. identified 52 genes to be differentially expressed in PC of healthy individuals, those with MGUS and patients with MM. In contrast to previous reports, among the 52 genes, 41 exhibited a progressive increase in expression levels along the transition from normal PC to MGUS to MM, while only four genes exhibited a progressive reduction in expression. Among the MM patients, they detected a group of MM (MGUS-like MM) with more benign clinical features and longer survival who showed a gene expression signature similar to the one characterizing MGUS patients. However, the existence of an MGUS-like MM is still unclear as, when the MGUS signature was applied to an independent cohort of MM patients from the Mayo Clinic none of them expressed the signature (unpublished data revised by Chng *et al.* [89]); furthermore Zhan and colleagues did not specify how they excluded from their analysis the effect of contamination from non-malignant cells in cases with minimal plasmacytosis such as MGUS. Within the MGUS group no significant differences were noted, making it impossible to distinguish between cases more likely to progress and those which would remain completely stable [172].
As previously mentioned, more recent gene expression profiling studies have suggested that *MYC* activation, as the result of different mechanisms, might be a unifying pathological event in the transition from MGUS to MM [173,174].

1.8 Whole-genome approaches for the analysis of copy number changes

The application of DNA probes to microarrays has emerged as a powerful technology in genetic studies. Microarray based comparative genomic hybridisation (CGH) enables the detection of copy number changes by competitively hybridising differentially labelled test and reference DNA to arrays of spotted and mapped clones. Thus, the technique allows the rapid screening of the whole genome at a resolution determined by the density of the markers spotted onto the array. This technique evolved from metaphase CGH [175] with the replacement of metaphase chromosomes by spotted clones as the hybridisation target [176,177].
Different studies have used CGH, array CGH or SNP GeneChip mapping arrays to characterize MM patients, in order to find distinct biological patterns of genomic alterations [155,178-182]. The results have revealed a high level of molecular heterogeneity not previously appreciated. In the paper by Carrasco and colleagues, unsupervised clustering of array CGH results allowed the

identification of two distinct groups of HRD patients, while FISH can only define HRD as a single group [178]. These two groups displayed a significantly different event free survival (EFS) and minor differences in their OS. The group with improved survival was characterized by the presence of 11q gain and the absence of 1q gain and Δ13. This classification was further confirmed by gene expression profiling of the same patients, analysed with gene set enrichment analysis of the transcriptomes, which revealed perturbation of distinct cancer-relevant pathways in each subclass. While *TP53* and *K-RAS* were altered in both subgroups, dysregulation of additional cancer-relevant pathways was observed in only one group. Particular attention was given to homozygously deleted and amplified chromosomal regions because they were more likely to involve those genes critical to the pathogenesis of the disease.

Two different studies using array CGH found a number of abnormalities involving genes coding for proteins belonging to the NF-κB pathway, confirming the presence of heterogeneous genetic abnormalities leading to the dysregulation of a common pathway [181,182].
Few studies have been performed on MGUS or SMM, the main reason being the limited number of PC that can be isolated from BM samples of these patients. One study used CGH on MGUS and MM patients and identified loss of 6q and gains of 3p and 1p to be associated with progression from MGUS to MM [183].

1.9 Aims of the study

A review of the literature, as presented in the preceding sections, shows that multiple and complex chromosomal and genetic abnormalities characterize PC of MGUS, SMM, MM and PCL patients. Some of these abnormalities are thought to be important in disease initiation while others seem to be responsible for disease progression. With the recent recognition that essentially all MM cases have a pre-existing asymptomatic phase, it becomes even more important to recognize those abnormalities that are associated with progression. The identification of these markers may allow for early detection of high-risk patients and for the development of primary prevention strategies in the future.
A number of disease models have been generated. These models attempted to correlate the multistep process of transformation from a normal PC to MGUS to MM to PCL with the progressive acquisition of genetic abnormalities. However, because karyotypes are almost impossible to obtain at the MGUS/SMM stage, most of our understanding of this process is derived from iFISH studies focused on relatively few, specific loci reported to be frequently abnormal in MM. From these studies, alterations found to be rare or absent in MGUS/SMM

were thought to be associated with disease progression while changes found with a similar frequency at all stages were thought to be initiating events.

The specific aim of this project is to identify molecular cytogenetic markers responsible for disease evolution from MGUS and SMM to MM and PCL. The study will initially focus on the genetic characterization of MGUS, SMM, MM and PCL using an extended panel of iFISH tests specific for baseline chromosomal abnormalities performed on large groups of patients with these diagnoses (also at the time of disease progression, whenever possible). This part of the study is intended to clarify the time of appearance of individual abnormalities and to identify whether specific changes are associated with evolving disease. Towards this aim, the availability of a detailed clinical history of the patients tested will be crucial for the interpretation of the findings.
The second phase of the study will involve the assembly of a comprehensive genome-wide profile of regional gains and losses in MGUS, SMM, MM and PCL in order to identify candidate loci relevant to genesis and progression. For this purpose high-density oligonucleotide array CGH will be undertaken. As it has been hypothesized that distinct mechanisms might be responsible for disease progression depending on the nature of the primary initiating events (i.e. presence/type of *IgH* translocations), all the patients selected for array analysis will be previously tested by FISH for the baseline genetic abnormalities. The array CGH data will then be correlated with the patients' clinical annotations. The incidence and clinical relevance of potential candidate genes or chromosomal regions, identified by array, will be validated by iFISH on a larger cohort of patients.

2 MATERIALS AND METHODS

2.1 Patient samples

This study includes diagnostic BM samples from patients sent to the Leukaemia Research Fund UK Myeloma Forum Cytogenetic Database at the Wessex Regional Genetics Laboratory (WRGL) with a known or suspected diagnosis of a monoclonal gammopathy; samples were sent from more than 30 different centres throughout the UK with informed consent for cytogenetic/FISH analysis. The diagnoses included: MGUS, SMM, MM and PCL; patients were classified according to standard criteria [35,184,185] and patients with MGUS or SMM were required to have no evidence of organ damage indicative of MM.
Almost half of the MM samples received were from patients entered into the Medical Research Council (MRC) Myeloma IX Trial. This Trial, whose main purpose was to investigate the impact of thalidomide, was structured into two main treatment pathways: intensive for younger/fitter patients and non-intensive for those older and less fit. Non-trial MM patients were treated with a number of different therapies. However, almost all of them received thalidomide at one point of their treatment.
As previously mentioned, most of the BM samples from patients with PC neoplasms (excluding PCL) are characterized by a low degree of plasmocytosis which hampers the interpretation of FISH and array CGH results. For this reason, PC were routinely purified in order to perform the various analyses on highly enriched material; for those samples where the proportion of PC, assessed at the beginning of the process, was greater than 50%, purification was not carried out. A poor PC recovery almost always limited the experiments to a minimum number of FISH tests (presence of Δ13, any *IgH* rearrangement, 17p13.1 deletion (*TP53*) and ploidy status).

Reagents marked with an asterix are described in **Appendix 2**.

2.2 Processing of BM samples

2.2.1 Cell count

The number of cells in the BM samples was counted at the beginning of the process.

2.2.1.1 Automatic count

The count was performed on 0.25ml of BM, using the Sysmex cell counter according to the machine instructions.

2.2.1.2 Manual count

A manual count was performed on very particulate samples, because of the risk of blocking the Sysmex counter.

1. A same amount of cell suspension and Zap-o-globin* (Beckman Coulter, UK) were mixed; the appropriate quantity was placed under a haemocytometer (BDH, UK) coverslip.
2. At least 100 cells were counted from the central square (defined by 3 perimeter lines). If more than 250 cells were counted in the top row, the specimen needed to be diluted appropriately. The number of cells in the central square was then multiplied by two, to allow for the dilution with Zap-o-globin and by 10^4 to give the number of cells/ml.

2.2.2 Red cell lysis

If the sample had a high red blood count, red cell lysis (RCL) was conducted.

1. The sample was spun at 1500 rpm for 10 minutes (min) and the supernatant was removed; a volume of pre-warmed RCL buffer* (37˚C) equal to 10-15 times the volume of the cell pellet was added, and the tube incubated for 10 min at 37ºC.
2. The tube was spun at 1400 rpm for 10 min and the supernatant was carefully removed. PC collect at the interface just above the white cell pellet, so it was important to retain this layer. After adding 5-10ml of wash medium*, the cell suspension was spun at 1400 rpm for 10 min and resuspended in 6ml of wash medium.

2.2.3 Lymphoprep method

Density gradient centrifugation was carried out on all samples after their count (or after RCL, if performed). This procedure separates the red cells and neutrophils from the remainder of the

mononuclear cells, removing cells incapable of dividing and increasing the mitotic index; it also improves the quality of the mitoses by removing the neutrophil granules from the cultures. No more than $5x10^7$ cells were usually placed in any one tube.

1. After transferring 3ml Lymphoprep (Nycomed, UK) into an appropriate tube, 6ml of marrow resuspended in wash medium was gently layered on the top and spun at 2000 rpm for 20 min without breaking (red cells, because enucleated, have the greatest density and fall to the bottom of the tube; mononucleated cells remain suspended in a layer between the lymphoprep and the plasma).
2. The interface and the wash medium above it were carefully transferred into a new tube. When particles were present, they were transferred into a separate bijou, mixed with ~1ml of wash medium and disaggregated using a 2ml syringe with a blunt-end needle; these smaller particles were then added to the remainder of the cells from the interface.
3. The recovered cells were washed twice with 10ml of wash medium and the final cell pellet was resuspended in 5ml of medium.

2.2.4 Assessment of the PC percentage

The separated sample was counted for the second time. On average, half of the total number of white cells was lost.

1. A statspin slide was made with $4x10^4$ cells using a cytofuge machine. The cells, resuspended in 200µl of wash medium, were concentrated into a 13mm spot on an X-tra slide (Surgipath, UK) coated on one side to allow the cells to stick; the medium was dried onto a filter paper placed on the top of the slide. The cytofuge was set for 6 min at 7000 rpm.
2. The slide was left to dry, and then stained with Leishman's stain (Sigma-Aldrich, UK): 1ml stain was dropped onto the slide and left for 1.5 min; then 2ml of Sorensen's phosphate buffer (Mercia Diagnostics, UK) was added for further 1.5 min. The slide was then rinsed with buffer and dried.
3. At least 300 cells were counted under the microscope in order to assess the PC percentage and the proportion of PC in the sample. Based on the total cell count and the PC percentage, it was decided whether there were enough cells for cytogenetic analysis and/or purification. Priority was given to the purification because purified cells can be used for techniques which don't rely on the capacity of the PC to divide *in vitro*.

Therefore, purification was carried out on almost all the samples, while only a proportion of them was set up for chromosomal analysis. The estimated 50% PC recovery after purification was then calculated. If the recovery was greater then $5x10^5$ cells, cultures for cytogenetic analysis were also set up. If the PC percentage was <20%, a 3DIS (3 day culture with IL-6; the letter 'S' indicates separated sample) and a 6 day (6DIS) cultures were set up; if the PC percentage was >20%, a 24 hour syncronized culture with IL-6 (F1IS) was also set up.

2.2.5 PC purification with $CD138^+$ magnetic micro-beads (Miltenyi Biotec, CA, USA)

CD138 or syndecan-1 is a cell surface glycoprotein constitutively expressed by epithelial cells and human PC, either normal or malignant. The protein is therefore a good marker for the identification and isolation of PC from BM samples. Magnetic microbeads are conjugated with a monoclonal antiboby specific for CD138 to which cells bind; when cells are passed through a magnetic column, the PC conjugated to the beads are retained, while the non-PC fraction is eluted. Limitations of this strategy are: (**i**) the method does not distinguish between normal and tumour PC; (**ii**) in a very small percentage of cases, PC subpopulations may be negative for the surface marker (i.e. its expression is lost on PC which undergo apoptosis) and therefore eluted with the non-PC fraction. However, the positive sort fraction is usually highly representative of the clone.
For each purification, no more than $2x10^8$ cells could be process through each individual column if the PC percentage was <50%; $1x10^8$ if the PC percentage was >50%.
All solutions were maintained at low temperature.

1. Cells were centrifuged at 1400 rpm for 10 min; the supernatant was removed completely and the tube was flicked to resuspend the pellet in phosphate buffered saline$^+$ (PBS^+) buffer* (ice-cold and de-gassed throughout the entire process). The volume of PBS^+ used was 80µl for every 10^7 cells if the PC percentage was <25%; 60µl for every 10^7 cells if PC percentage was >25% (if the PBS^+ volume was >900µl, it was evenly divided between two or more tubes).
2. The MACS CD138 microbeads were then added (bead volume = 20µl for every 10^7 cells, if PC percentage <25%, 40µl for every 10^7 cells, if PC percentage >25%; minimum volume=10µl). After gentle mixing, the tube was incubated at 4°C for 15 min.

3. A volume of PBS^+, 10 to 15 times the volume of the cellular suspension, was added and the tube was spun at 1400 rpm for 10 min. After completely removing the supernatant, the pellet was resuspended in PBS^+ (100µl for every 10^7 cells).
4. After washing the column in the magnetic field with 3ml PBS^+, the cells were applied to the column and washed three times with 3ml PBS^+ in order to elute the non-PC fraction. PC were eluted with 5ml PBS^+ in the absence of the magnetic field.
5. The tube was centrifuged at 1400 rpm for 10 min and the pellet resuspended in 1-2ml of wash medium; a new count was performed and a new statspin was made with $1x10^4$ cells; the final PC percentage was then calculated.
6. The allocation of the PC depended on both the purity and total cell number as shown in **Table 2-1**.

Number of cells recovered after purification, % PC	**Use of the cells**
$0\text{-}8x10^5$, PC%: 0%-100%	Fixed cells for FISH
$8x10^5 – 2.9x10^6$, PC%: 0%-80%	Fixed cells for FISH (~$1x10^6$) and dry pellet for DNA extraction
$>8x10^5$, PC%: 80%-100%	Fixed cells for FISH ($1x10^6$), dry pellet for DNA extraction, Trizol pellet for RNA extraction

Table 2- 1 Use of the isolated PC based on their number and purity

7. PC selected for FISH analysis were spun for 10 min at 1400 rpm and, after removing the supernatant, incubated for 10 min at 37˚C with 5ml of warm hypotonic solution*. PC were then spun for 10 min at 1400 rpm and, after removing the hypotonic, 5ml of Carnoy's fixative* was added dropwise until the cells were fully resuspended; PC were then kept at -20˚C. Fixed PC stored at -20˚C were primarily used for iFISH. For a number of samples, where no PC were stored as a dry pellet for DNA extraction, fixed cells were used to extract DNA for array CGH.
8. For dry pellets, PC were placed in a screw cap eppendorf and centrifuged in a microfuge for 12 min at 3000 rpm. The supernatant was removed carefully. Dry pellets for DNA extraction were stored at -80˚C.
9. For RNA extraction, every $1x10^6$ cells were resuspended in 200µl Trizol (Invitrogen, UK) by pipetting up and down, under a ventilated hood. The tube was left at room temperature for 10 min and then transferred to -80°C.

2.3 Metaphase analysis

2.3.1 Cytogenetic cultures of fresh BM samples

RPMI-1640 medium, developed at the Roswell Park Memorial Institute (hence the acronym RPMI), is used as a basal medium for culturing BM samples. Such medium is a buffered salt solution containing amino acids, sugars, polysaccharides and nutrients. Basal medium alone cannot support optimal cell growth. Fetal calf serum (FCS) made up to 5-30% of the complete medium contains proteins including growth factors essential for cellular proliferation. It also helps to maintain an optimum pH (7.2-7.4). L-Glutamine provides an essential amino acid. IL-6 is a cytokine which encourages the proliferation of PC within the marrow; *in vivo* it is released by the stromal cells [17,186]. IL-6* (First Link, UK) was added to cytogenetic cultures to promote PC division *in vitro*.

All culturing was carried out in a laminar flow hood using aseptic techniques. A standard culture was made of ~$5x10^6$ cells per 5ml of RPMI culture medium*. However cultures of smaller samples, for example of $2.5x10^6$ cells, were regularly set up with 1ml of medium per $1x10^6$ cells (this being considered the optimum cell density for BM culture). Cultures were set up in Nunclon polystyrene flat-sided tubes (Scientific Laboratory Supplies Ltd, UK) which provide a larger surface area for the cells to grow. Cells were incubated at 37˚C for 24 hours, 3 or 6 days; only the 24 hour cultures were synchronized.
Cell division can be blocked at various points in the cell cycle and subsequently released at a controlled time, producing synchronization of cell division. This enables colcemid exposure to be greatly reduced, consequently producing longer chromosomes. Fluorodeoxyuridine* (FdU; Sigma-Aldrich, UK) is an effective blocking agent as it integrates into the DNA and blocks DNA synthesis. Uridine* (Sigma-Aldrich, UK) is added at the same time to prevent blockage of RNA synthesis. Release of the block is achieved by adding excess thymidine* (Sigma-Aldrich, UK). Optimal harvest time for BM samples is about 6 hours after release.

1. 0.05ml FdU and 0.05ml uridine were added to cultures between 2 and 6pm on the day prior to the one of the harvest; cultures were then returned to 37^{o}C.
2. At 9am of the following day, 0.05ml thymidine was added to each culture; cultures were returned to the incubator for 5 hours and 45 min before starting the standard harvest procedure.

2.3.2 Tissue cultures from cryopreserved cells

Tissue culturing is a technique to promote the *in vitro* proliferation of animal cells in a nutrient medium for extended periods of time. It provides an inexhaustible supply of heterogeneous material such as DNA, RNA and proteins and the cells can easily be manipulated, i.e. by adding drugs to the media.

1. RPMI-1640 culture medium, supplemented with filtered FCS (20%), L-glutamine and penicillin/streptomycin, was warmed to 37˚C.
2. Liquid nitrogen stored cell pellet was defrosted at room temperature and 5ml medium was added (the first 3ml dropwise). The cell suspension was then transferred to a 15ml Falcon tube which was spun for 5 min at 4000 rpm.
3. After being washed twice, the pellet was resuspended in 10ml of fresh medium, which was transferred to a 10ml tissue culture flask. The flask was placed, with the lid loosely fastened, in the incubator at 37˚C with CO_2 levels at 5%.
4. According to the specific requirements of different cell lines, cells were supplemented with appropriate volumes of fresh medium at approximately 3 day intervals. The cell cultures were split and transferred into larger flasks as the volume increased. Cells were counted manually with Zap-o-globin, while trypan blue (Sigma-Aldrich, UK) was used to differentiate live from dead cells. Trypan blue is a negatively charged chromopore which interacts with damaged cell membranes: viable cells will exclude the dye while dead cells are stained blue.
5. Cultured cells were harvested to obtain metaphases for conventional analysis, and/or processed for DNA extraction.
6. For long term storage of cell pellets, cells were counted and resuspended in a universal container (Sterilin Ltd., UK) in complete medium at a concentration of 2–6x10^7/ml.
7. In a separate universal container, the cryopreserving solution was prepared: complete medium (20%), FCS (60%), dimethyl-sulfoxide (DMSO, Koch Light Ltd., UK) (20%). DMSO is an organic solvent that maintains the cells intact as they freeze.
8. Both containers were placed in the refrigerator for approximately 30 min. During this interval, 2ml plastic ampoules, screw top, for liquid nitrogen (Sterilin Ltd., UK) were labelled and placed in a rubber rack, which was then stored at -20˚C, until required.
9. The containers were removed from the refrigerator and put into an ice bath. The cryopreserving solution was added dropwise unto the container with the cell suspension which was agitated continuously.
10. The mixture of cell suspension and cryopreserving solution was aliquoted into the pre-cooled plastic ampoules which were then tightly capped and slowly cooled: 40 min at -

20˚C inside the rubber rack; 30 min at -80˚C inside the rubber rack; overnight at -80˚C inside metal-trays; -180˚C in liquid nitrogen.

2.3.3 Harvesting

1. 15 min before the end of the culture period, 0.05ml of colcemid* (Sigma-Aldrich, UK) was added to each culture; cultures were then returned to the incubator for 15 min. Colcemid is a colchicine-analogue which inhibits the formation of the mitotic spindle. The mitotic index is proportional to the length of exposure to colcemid. However, prolonged exposures result in condensed chromosomes.
2. The cultures were centrifuged for 5 min at 1600 rpm. After removing the supernatant, the cells were resuspended in 6ml of hypotonic solution* at 37^{o}C. The hypotonic solution has a lower salt concentration than the cell cytoplasm, allowing water to move into the cell by osmosis. This swells the cells and is critical for adequate spreading of the chromosomes on the slide. Timing is crucial, as too long an exposure will cause the cells to burst, while too short an exposure will not swell the cells sufficiently, resulting in poor spreading.
3. The tubes were then spun for 5 min at 1600 rpm and the supernatant was removed; after flicking the tube to disaggregate the pellet, 5ml of Carnoy's fixative was added with the first ml in a dropwise manner, while flicking the tube. Fixation kills the cells and preserves chromosomal morphology while removing nuclear and cytoplasmic proteins. Methanol fixes the chromosomes by replacing the water; acetic acid softens the cell membrane.
4. 6ml fixative was added to each tube; the tubes were stored at –20^{o}C for a minimum of 1 hour, but usually overnight.

2.3.4 Slide preparation for metaphase analysis

During slide preparation, the fixed cells are dropped onto glass slides for subsequent staining and analysis. In optimal preparations for cytogenetic analysis, metaphases must be well spread without any random chromosomal loss and with minimal overlapping of the chromosomes.

1. The fixed suspensions were removed from the freezer and spun at 1400 rpm for 10 min; the supernatant was removed and the pellet resuspended in fresh fixative; this stage was repeated four times. The pellet was then resuspended into a small quantity of fixative, to

provide the optimum cell density for slide making. The fixed cell suspension was usually dropped on dry slides at room temperature and slides were checked with a phase contrast microscope for metaphase quality and number.

2. Slides were aged by placing them in a 60°C oven for 1 hour in order to enhance chromosome banding.

2.3.5 Banding

In this study, chromosome preparations were stained using the Giemsa banding (G-banding) method. These banding patterns are thought to reflect both the structural and functional composition of the chromosomes. Dark bands replicate their DNA late in S-phase, contain A+T-rich DNA, appear to include relatively few active genes and may differ from light bands in protein composition.

1. After being aged under a UV source for 30 seconds, slides were treated with H_2O_2 for 1 min and 30 seconds, washed under tap water and shaken to dry.
2. 3ml Wright's buffer* (Mercia Diagnostics, UK) and 1ml Wright's stain* (Sigma-Aldrich, UK) were mixed rapidly and used to treat the slides for 2 - 5 min.
3. The slides were rinsed in gently running tap water for 5 seconds and shaken to dry. The quality of the banding was examined under a dry lens; the staining was adjusted if necessary by rinsing again or destaining in methanol and restaining for a shorter time.

2.3.6 Cytogenetic analysis

Slides were analyzed under a bright-field microscope. As in PC disorders the detection of an abnormal clone is rare, the analysis was carried out on 1 to 200 metaphases, depending on the cell availability.

A clone is defined as a cell population derived from a single progenitor. The general rule in tumour cytogenetics is that only the clonal chromosomal abnormalities found in a tumour should be reported [187]. This means two or more cells having the same structural abnormality, or having gained the same chromosome; if the abnormality is loss of chromosome, the same change must be present in at least three cells to be accepted as clonal. In this study a single abnormal metaphase with typical myeloma abnormalities was considered to be representative of

the abnormal clone when supported by the iFISH results. Karyotypes were described using the International System for Human Cytogenetic Nomenclature (ISCN) [187].

2.4 Fluorescence in situ hybridization (FISH) analysis

As discussed in **Section 1.6.1**, chromosomal analysis in cancer cytogenetics is sometimes hampered by failure in culture, paucity or complete absence of abnormal metaphases and by the presence of cryptic abnormalities not visible under the microscope. As FISH is applicable to non-dividing cells, it overcame many of the limitations intrinsic to conventional cytogenetics. The principle of FISH is the hybridization of a fluorochrome-labelled DNA 'probe' with a complementary target DNA sequence in nuclei, tissue sections or metaphase spreads. Radioactive isotopic labels were used initially, but were later replaced with fluorochromes, rendering the technique safer and easier to use [188-190]. Fluorochromes can be used to label the DNA directly; alternatively, the DNA can be labelled indirectly with haptens (digoxigenin and biotin are widely used) which are then detected by antibodies (anti-digoxigenin to detect digoxigenin and avidin for detection of biotin) conjugated to fluorochromes. The availability of a range of fluorochromes of different colours also gave the possibility of testing more than one probe simultaneously.
In this study, FISH analysis was performed on interphase cells (usually purified PC) and on metaphases from cytogenetic cultures.

2.4.1 Slide preparation for metaphase analysis

Slides with visible metaphases were first stained for G-banding analysis. After capturing the metaphases and recording the coordinates of their specific locations, the slides were then distained (10 min in Carnoy's fixative) and used for FISH analysis.

2.4.2 Slide preparation for interphase FISH

In order to maximize the number of tests for each sample, Dr. A. Vilain-Holmes developed a simple yet effective micro-technique in this laboratory that allowed multiple FISH tests to be

carried out even when as few as $2x10^5$ PC were recovered. This technique permitted the analysis of eight different patients on the same slide [191].
Slides were prepared in a temperature and humidity controlled 'harvester' room.

1. Fixed suspensions of purified PC were stored at -20˚C for at least 16 hours before being centrifuged for 10 min at 1400 rpm and resuspended in fresh fixative for slide making. The cell density was adjusted to approximately 2500 cell/µl by making a trial 0.2µl spot and concentrating or diluting as necessary.
2. While adjusting the PC density, prewashed slides (stored in fixative at -20˚C overnight) were removed from the fixative and left to drain.
3. The slide was positioned on a template (**Figure 2-1**) indicating the exact position of nine spots located under a 22x22 mm coverslip. The nine spots corresponded to eight patients and one control (PC from normal bone marrow donors or peripheral blood lymphocytes).
4. 0.2µl spots containing 100-500 cells were placed on the slide. This cell density ensured wide separation between each spot, preventing cross contamination.
5. Slides were checked under a phase contrast microscope. If the density was too low, multiple ejections were done onto the same spot, allowing each time the slide to dry before adding new cells.
6. When the slides were fully dry, they were washed with fixative and left at room temperature for several hours; they were then stored vertically at -20˚C, until required.

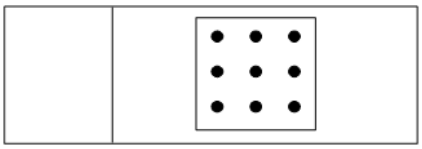

Figure 2- 1 Nine spot template for iFISH slides

2.4.3 Probes

The probes used in this study were commercial probes from Vysis (Abbott Diagnostic, UK) and those grown and labelled in the laboratory.

2.4.3.1 The Human Genome Project: resources for molecular cytogenetics

The hierarchical shotgun sequencing approach adopted by the International Human Genome Sequencing Consortium involved in initially fragmenting the genome into large segments which were subsequently cloned into various types of vectors for downstream applications. Different cloning vectors have been developed for cloning different DNA inserts. Cosmids were one of the first types of vectors available which are suitable to clone inserts of up to 45 kb [192]. However, the resulting clones may become unstable, with loss of inserts during replication. Yeast artificial chromosomes (YAC) [193] can support inserts of up to 1 Mb. However, YAC clones are difficult to construct and tend to undergo rearrangements leading to chimaerism. P1-derived artificial chromosomes (PAC; artificial chromosome based on bacteriophage P1), bacterial artificial chromosomes (BAC; artificial chromosome based on *E.coli* F factor) and fosmids (plasmid-phage hybrid based on *E.coli* F factor) are more efficient vectors. The average insert size cloned into a PAC is 120 kb and the resulting clones proved easy to purify. They presented low or non existent chimaerism and insert instability [194]. These same advantages were shared by BAC, which accept an insert with an average size of 170 kb [195] and fosmids, with an average insert size of 40 kb [196]. As a result of these developments, libraries of BAC, PAC and fosmids covering the entire human genome have been created. These individual clones can be utilised as DNA probes for FISH studies.

However, the major contribution of the Human Genome Project has been the assembly of the sequence of the human genome and the mapping and identification of human genes. These have been deposited in publicly available databases and can be accessed via human genome browsers. Ensembl, hosted by the Welcome Trust Sanger Institute, and the University of California Santa Cruz (UCSC) browser, are two of the main browsers available (URL in **Appendix 1**). These browsers integrate sequence data from the reference human genome and provide annotation for known and predicted genes alongside numerous other features, e.g. expression data, comparative genomics, human variation and repeat elements. They are invaluable data for the study of chromosome rearrangements.

In this study, home-made BAC/PAC clones mapping in the regions of interest were selected mainly from the Ensembl browser. Fosmid clones were used to detect deletions that array CGH results showed to be too small to be detected by BAC/PAC clones. They were selected from the UCSC browser and provided by the Children's Hospital Oakland Research Institute (CHORI, Oakland, California, USA; see URL in **Appendix 1**). BAC/PAC clones from the Ensembl clone sets were grown from glycerol stocks stored at the WRGL, which were originally kindly provided by the Welcome Trust Sanger Institute. The probe mapping of the *RB1* gene was kindly supplied by Prof. Mariano Rocchi from the Department of Genetics and Microbiology, University of Bari. Details of all probes used in this study are listed in **Appendix 3**.

2.4.3.2 Processing of in-house probes

2.4.3.2.1 Growing the probes

Bacteria were grown in Luria-Bertani (LB) broth* (Gibco, UK) overnight, prior to DNA extraction.

1. Bacteria were inoculated into 30ml of fresh LB broth in a sterile 30ml cell culture flask with the appropriate antibiotic*; the flask was incubated overnight at 37˚C with vigorous shaking (i.e. a 37˚C shaking incubator at ~220 rpm).
2. The freshly grown culture was used to inoculate LB agar (Dibco, UK) plates*. The culture was spread over the plate with an inoculation loop gradually reducing the concentration of the culture to obtain well spread colonies. The plate was incubated overnight at 37˚C.
3. Individual colonies were isolated and used to inoculate fresh LB broth of 30ml or 100ml with the appropriate antibiotic to obtain a purified colony culture. Thus culture was placed overnight in a 37ºC shaking incubator.
4. The culture was decanted into 30 ml centrifugation tubes and spun at 4ºC for 10 min at 3000rpm. The pellet was stored at -20ºC until required.

2.4.3.2.2 Extraction protocol (Rapid Alkaline Lysis)

1. 1.5ml eppendorf tubes were filled with 800µl ice-cold isopropanol (Sigma-Aldrich, UK) and stored at -20˚C until required.
2. 1.8ml P1 solution* was added to each 30ml pellet and the tubes were vortexed thoroughly to resuspend. Suspensions were then transferred to new centrifuge tubes.
3. 1.8ml P2 solution* was added to each tube and tubes were gently shaken and left at room temperature for 5 min (the suspension changed from very turbid to almost translucent).
4. 1.8ml P3 solution* was slowly added and the suspension was gently shaken. The tubes were placed on ice for 5 min (a thick white precipitate formed).
5. The tubes were spun at 10,000 rpm for 10 min (4˚C); the supernatant was transferred (avoiding the white precipitate) to the pre-prepared eppendorf tubes containing 800µl ice-cold isopropanol (Sigma-Aldrich, UK).
6. The tubes were left overnight at -20ºC (or for a minimum of 2 hours at -70ºC) and then spun at 14,000 rpm for 15 min. After discarding the supernatant, the pellets were washed twice with 500µl of 70% ethanol (BDH, UK).

7. After removing the ethanol, pellets were dried in a centrifuge dryer and after they turned from white to translucent in appearance (most of the ethanol had evaporated), they were resupended in 10µl TE* (Tris-EDTA) and left at room temperature overnight.

2.4.3.2.3 DNA quantification

DNA was then quantified using a Dyna Quant 200 Fluorometer (Hoefer Scientific Instruments, UK) which measures the amounts of DNA bound to a DNA-specific dye, compared with known standards.

1. For the Standard Assay*, the reference standard was prepared as follows: 10ml 10x TNE buffer*, 90ml dH_20 and 10µl Hoechst Buffer (Hoefer Scientific Instruments, UK).
2. 2ml Assay solution was transferred into the G cuvette (assay blank).
3. 2µl of the appropriate DNA reference standard (i.e. low range calf thymus DNA, 1 mg/ml) (Pharmacia Biotec, UK) was added to the 2ml assay solution. After calibration, 2ml of fresh Standard Assay were dispensed into a clean cuvette and placed in the well; 2µl of test sample were added to the Assay.

2.4.3.2.4 Agarose gel electrophoresis

Gel electrophoresis allows separation of DNA molecules by differential migration through the agarose according to their size. It was routinely used to assess the size and quantity of DNA. The agarose gel is a semi-permeable gel; if placed in a tank of buffer, it provides the ions to carry a current. DNA has a negative charge imparted by the phosphate backbone, therefore when applied at the cathode it migrates through the gel toward the anode. The smaller molecules are able to move more quickly through the polymer than the larger molecules. Ethidium bromide is added to the gel to visualise the DNA, as the positively charged ethidium ion intercalates between the bases of the DNA and fluoresces under ultra violet (UV) light.

1. Agarose gels used in this study ranged from 0.8%* to 3% agarose, and were prepared by dissolving the agarose (Bioline, UK) in 1x tris-borate (TBE) Buffer*. The gel was prepared by heating the suspension in a microwave for 1 min and 35 seconds twice, until the agarose had dissolved; the solution was cooled under running tap water until reaching ~50˚C. 0.4µg/ml ethidium bromide (Sigma-Aldrich, UK) was added.
2. The solution was poured into a tank with an appropriately sized comb and left for 30 min to set. When solid, the gel was transferred to the tank, which was then filled with 1x TBE.

Although 1.5% gels were used most often, smaller polymerase chain reaction (PCR) products were resolved on 2% to 3% gels. Typically, 5 to 10µl of a PCR reaction was mixed with 2µl of 6x loading buffer* before loading onto the gel, as this makes the PCR solution more visible and sink into the well. Gels were run at 80V for approximately 30 min, and viewed over a UV transilluminator. A 1 kb plus Ladder (100bp to 12 kb, Invitrogen, UK) was run alongside samples.

2.4.3.2.5 Restriction digestion

Running a restriction digest is a good indicator of the purity of the DNA: if it fails to cut on a restriction digest the probe should be re-purified. Restriction enzymes recognise specific nucleotide sequences that are usually 4bp to 8bp long; they then cleave the DNA at these sites. Eco RI with Buffer H, Bam HI or Hind III with Buffer B (Roche, UK) were used to obtain a digestion picture.

1. A total of 20µl reaction was prepared: 2µl enzyme (enzyme concentration: 10 units (U)/ µl; one U of enzyme is defined as the amount required to digest 1µg of wild-type bacteriophage DNA in 1 hour), 5µl DNA (~ 500-1000ng), 2µl of appropriate Buffer, 1µl Spermidine and 10µl dH_2O. The reaction was vortex gently, pulsed (<4000 rpm) and incubated at 37˚C for 1 hour.
2. The digested sample was then loaded on the gel; 18µl dH_2O was mixed with 2µl lambda HindIII marker (Invitrogen, UK) in the track adjacent to the cut DNA as a size marker. The gel was run at 112V for ~ 1 hour and then placed on the UV transilluminator to observe the restriction pattern.

2.4.3.2.6 Direct labelling of DNA probes - Nick translation

The purified DNA is labelled by using a suitable enzyme to incorporate labelled nucleotides. Nick translation was the labelling method used for labelling FISH probes. This procedure involves the random nicking of single-strand DNA by DNase I generating a 5' phosphate group and a 3' hydroxyl terminus. The Kornberg DNA polymerase I holoenzyme contributes two enzyme activities: (**i**) a 5'→3' exonuclease attacks the exposed 5' termini of a nick and sequentially removes nucleotides in the 5'→3' direction; (**ii**) a DNA polymerase adds new nucleotides to the exposed 3' hydroxyl group, continuing in the 5'→3' direction, thereby

replacing nucleotides removed by the exonuclease and causing lateral displacement of the nick. The length of the labelled fragments is proportional to the concentration of DNase I.

1. For approximately 1µg of DNA probe, 25µl of labelling reaction was set up. The following reagents were added to a dark brown tube on ice in this order: 2.5µl 10x nick translation buffer*, 1.9µl of deoxyribonucleotide triphosphate (dNTPs, Pharmacia, UK) *, 0.7µl Cy3-dUTP (deoxyuridine triphosphate, Amersham Biosciences, UK), or 1.4µl Spectrum Green dUTP* (Vysis, Abbott Laboratories, UK) or DEAC-dUTP (NEN Life Science NEL 455, UK), 0.5µl DNase I working solution (Sigma-Aldrich, UK)* (the volume was determined by titration), 0.5µl DNA polymerase (5 units) (Gibco, UK), 1µg of DNA, and sterile dH_2O to a volume of 25µl.
2. The tube was flicked, pulse centrifuged at 3500 rpm, and incubated at 15˚C for the time previously determined by titration (usually 1 hour and 30 min – 1 hour and 50 min); the tube was then transferred to ice to pause the reaction.
3. 8µl sterile dH_2O was mixed with 2µl of labelled sample and the size of the smear was checked on a 0.8% agarose gel. If the fragment sizes were around 500bp, the reaction could be stopped (if not the reaction was replaced at 15˚C for a longer time).
4. 1/10th of the volume (2.5µl) of 0.5M EDTA (ethylenediaminetetraacetic acid) was added to the reaction to inactivate the enzymes; 1/10th of the new volume (2.75µl) of 3M sodium acetate* (pH 7), and 2x the new volume (61µl) of ice-cold 100% ethanol were added to precipitate the DNA; the tube was incubated overnight at -20˚C (or for a minimum of 2 hours at -70˚C).
5. The tube was centrifuged at 14000 rpm for 10 min and the supernatant discarded.
6. 61µl ice-cold 80% ethanol was added without disturbing the pellet and the tube was centrifuged at 14000 rpm for 10 min. The supernatant was discarded, leaving the pellet as dry as possible; the pellet was dried at 37˚C, taking care not to over-dry.
7. The pellet was resuspended in 10µl/µg TE buffer (pH 7.5) for 1 hour minimum at 37˚C.
8. The probe was stored at -20˚C, until required.

2.4.3.2.7 Preparation of home-made probes

1. The tube of labelled DNA was thawed at 37˚C for 5 to 10 min. In general approximately 200-500ng of individual probe DNA was required for one slide, depending on the fluorochrome used and the probe combination.
2. The following reagents were required for preparing the amount of probe for 1 slide: 200–500ng of probe DNA, 4µl Cot 1 DNA* (working concentration 0.1µg/µl, GibcoBRL, UK), 4µl Carrier DNA (herring sperm DNA, working concentration 10mg/ml, Sigma-

Aldrich, UK). To this reaction, a quantity of 100% ethanol equal to 2 x the volume of the reaction was added.

3. The above reagents were vortexed and pulsed down; then the probe mixture was dried down in a speed Vacuum (temperature: 43˚C).
4. If the probe was not to be mixed with a commercial probe, after drying down, the DNA mixture was resuspended in 11µl complete hybridization mix*; the mixture was vortexed and pulsed down and incubated for 1 hour at 74˚C.
5. When probe preparations included an array of probes (*CCND3*, *MAFB*, etc), Cot-1 and carrier DNA volumes remained 4µl each per slide, but the ethanol was increased in proportion to the volume of DNA.

2.4.4 Preparation of commercial probes

1. Both the probe and the complete hybridization buffer (Vysis, Abbott Laboratories, UK) were thawed at 37˚C for approximately 5 to 10 min before mixing and pulsing down.
2. 1µl Vysis probe DNA, 8µl complete hybridization buffer and 2µl dH_2O were mixed in a dark brown PCR tube to constitute the working probe stock.
3. In a clear PCR tube, for each slide, 2.5µl working probe stock was mixed with 8µl complete hybridization buffer.

2.4.5 Slide pre-treatment

Slides of both metaphase and interphase preparations were pre-treated in order to remove proteinaceous material which might interfere with the hybridization.

1. The eight spot slides were removed from the freezer and immersed in fixative as soon as possible for 30 min; the slides were left to air dry. Metaphase slides were usually freshly made and kept for few days at room temperature; for these slides no treatment with fixative was required.
2. 900µl 2x SSC* was pre-warmed to 37˚C; 50µl aliquots of RNase* (working concentration 1mg/ml, Sigma-Aldrich, UK) and pepsin* (working concentration 50mg/ml, Sigma-Aldrich, UK) were defrosted, vortexed, pulsed down and added to the 2x SSC. The total mix was incubated at 37˚C for 10 min.

3. Each slide was treated with 200µl RNase/pepsin/2x SSC and covered with a parafilm coverslip for 3 min; the slides were then immersed in 2x SSC for 2 min, dehydrated for 2 min each in 70%, 90% and 100% industrial methylated spirit (IMS) (Genetics Store, UK), and left to dry.

2.4.6 Slide denaturation and hybridization

1. 10µl probe was placed onto a 22x22 mm coverslip and the slide was inverted over the coverslip. Air-bubbles were removed and the coverslip was sealed with vulcanising rubber solution (Weldtite, UK) and left to dry.
2. Slides were incubated in the Hybrite machine (Thermobrite, Abbott Diagnostic, UK). In the Hybrite chamber, tissues were moistened with water in order to ensure a high humidity. The metal slide surface was wiped with a damp tissue to create complete contact between the metal surface and the slides.
3. After having positioned all the slides and having lowered the cover, the Hybrite was set to reach a temperature of 75˚C for 5 min, followed by an overnight incubation at 37˚C.

2.4.7 Hybridization washes

Washes remove excess and loosely bound probe. The counterstain is used to provide overall staining of the chromosomes or cells.

1. A slide holder with 0.4x SSC/0.3% NP40* (Sigma-Aldrich, UK) was preheated to 74˚C, in a water-bath.
2. The glue sealant from the glass coverslip was removed and the slide was placed in a coplin jar with 4x SSC/0.05% NP40* at room temperature. The slide was agitated in order to gently release the coverslip from the slide without scratching the surface.
3. The slide was immersed for 1 min in 2x SSC/0.1% NP40* and then transferred to the 0.4x SSC/0.3% NP40 stringent wash at 74˚C for: 1 x 3 min for the Vysis probe 5/9/15; 2x 2 min for the Vysis probe *TP53* and *MYC*; 1 x 2 min for all other probes.
4. After immersing the slide in fresh 2x SSC/0.1% NP40 for 1 min, the excess solution was drained, without allowing the slide to dry, it was mounted with Vectorshield containing full strength 4′,6-diamidino-2-phenylindol (DAPI) (Vector Laboratories Inc, California,

USA) or half strength when probes were labelled with DEAC-dUTP. The coverslip was sealed with nail varnish.

2.4.8 Re-hybridization of FISH slides

A number of slides were re-hybridized when no further cell suspension was available to make new slides for additional tests. The slides previously hybridized were treated to remove the original probe, following the method described above.

1. After removing the coverslip, the slide was immersed in 4x SSC for 3 min, followed by 2 min in 2x SSC. The excess solution was then drained.
2. The slide was incubated with 10µl of complete hybridization buffer on a hot plate at 75˚C for 5 min and then immersed in fresh 2x SSC/0.1% NP40 for 2 min, followed by 2 min in 2x SSC. The slide was dehydrated for 2 min each in 70%, 90% and 100% IMS.

2.4.9 FISH scoring

A minimum of 100 nuclei were analyzed for each probe, for each patient. Knowing the proportion of PC present in the cell suspension, the percentage of abnormal PC carrying a specific abnormality was then calculated.

2.5 DNA extraction

The genomic DNA used in this study was derived from: purified PC stored at -80˚C as a dried pellet; purified PC stored in fixative; non-purified fixed cells after lymphoprep separation (when the sample percentage of PC was > 70%) and non-purified cells derived from 24 hour and 3 day cytogenetic cultures (all fixed suspensions were stored at -20˚C).
In order to extract DNA from fixed cells, cell suspensions were centrifuged at 4000 rpm for 12 min, the supernatant removed and the pellet washed four times with 1x PBS. The pellet was then re-suspended in 200µl 1x PBS.

2.5.1 Salt extraction (> 1.5 x 10^6 cells)

1. Cells were centrifuged for 12 min at 4000 rpm and the supernatant discarded.
2. After washing the cells with 500µl resuspension buffer (RSB*), the pellet was re-suspended and incubated overnight at 37˚C in 500µl RBS, 10µl sodium dodecyl sulphate (Sigma-Aldrich, UK) and 3µl proteinase K solution* (100mg/ml, Roche, UK) to remove cell lipids and digest cell proteins.
3. After checking that the cells were properly digested (if not 2µl proteinase K were added and left for as long as necessary), 150µl 6M NaCl (Sigma-Aldrich, UK) was added to precipitate the non-DNA components; the tube was shaken vigorously for 20 seconds and centrifuged at room temperature at 14000 rpm for 20 min.
4. The supernatant was transferred to a small sterilin tube (Sarstedt, UK) and approximately 1.5x volume of 100% ethanol was added to precipitate the DNA. The sterilin tube was inverted until the DNA visibly collected as a 'hair ball'. This DNA was removed using a sterile needle. (If no hairball was visible, the ethanol was frozen for at least 2 hours at -20˚C and then centrifuged for 20 min at 14000rpm. The supernatant was removed and the pellet resupended in 50µl of dH_2O).
5. The DNA was taken with the tip of a needle, washed in 70% ethanol in order to remove residual salts which might affect future manipulations and resupended in dH_2O. DNA samples were stored at 4˚C whilst being studied.

2.5.2 DNA extraction using DNeasy blood and tissue kit (Qiagen, UK) (<1.5 x 10^6 cells)

1. The AW1 and AW2 concentrates were made up with 25ml and 30ml 100% ethanol, respectively.
2. Cells for DNA extraction (maximum of $5x10^6$ cells per column) were resuspended in 200µl PBS, 20µl proteinase K and 200µl buffer AL. Tubes were then mixed by vortexing and incubated at 56˚C for 10 min. 200µl of 100% ethanol was then added and mixed.
3. The reaction mixture was pipetted into a DNeasy mini spin column placed in a 2ml collection tube and centrifuged for 1 min at 6000g. The flow through was discharged and the column was placed in a new collection tube.
4. 500µl buffer AW1 was added and the column was centrifuged as above. The flow through was discharged and the column was placed in a new collection tube.

Formatted: Bullets and Numbering

5. 500µl buffer AW2 was added and the column was centrifuged for 3 min at 20000 g to dry the membrane. The column was carefully removed from the collection tube to prevent any ethanol carryover and placed in a new one; 35-50µl dH_2O was added directly to the membrane, left to incubate for 1 min at room temperature and then centrifuged for 1 min at 6000 g.

2.5.3 DNA quantification using the NanoDrop ND-1000 (Thermo Scientific, UK)

NanoDrop-1000 is a spectrophotometer which determines the concentration and purity of DNA by measuring the amount of light that a sample absorbs. The sample is pipetted onto the end of a fiber optic surface (the receiving cable). An upper second fiber optic surface (the source cable) automatically engages the sample, using surface tension to form a liquid bridge that bridges the gap between the two fiber optic ends. A pulse of light originating in the source cable is passed through the sample. When a photon encounters a DNA molecule it is absorbed and the intensity of light reaching the receiving cable is reduced and measured. DNA absorbs UV light at a wavelength of 260nm, proteins absorb light at 280nm and 230nm. Other contaminates such as carbohydrates also absorb at 230nm. Absorbance is measured at these three wavelengths allowing the concentration and purity of the DNA sample to be determined.

1. With the sampling arm in the down position, the NanoDrop-1000 software was started and the 'nucleic acid application' was selected.
2. To calibrate NanoDrop-1000, the sampling arm was lifted and 1.5µl dH_2O was pipetted onto the lower measurement pedestal. The arm was lowered and 'blank' was selected.
3. The sampling arm was lifted and the water was wiped from both pedestals. 1.5µl dH_2O or TE was pipetted onto the lower measurement pedestal, the arm was lowered and 'measure' was selected. A flat base-line was returned. Both pedestals were wiped.
4. This last step was repeated for each DNA sample to be measured. The software provided a concentration in ng/µl which was calculated in the following way:

   Optical density (absorbance reading at 260nm) x 50 (1 absorbance unit at 260 nm = 50 µg/µl DNA)

5. To calculate DNA purity the absorbance at 260nm was divided by the absorbance at 280nm and at 230nm. This ratio should fall between 1.5 and 2.0. A ratio below 1.5 indicated a high level of contamination.

2.5.4 DNA quality assessment

The DNA quality was assessed by agarose gel electrophoresis (1%) as previously described. Genomic DNA comprises large molecules that do not migrate far along the gel, creating a discrete band. A smear indicates DNA degradation.
In case of contamination, two methods were attempted to clean the DNA: ethanol precipitation (for small quantities of DNA) or the 'Cleanup of genomic DNA' protocol from the QIAmp DNA Qiagen kit (for larger amounts of DNA).

2.5.5 Ethanol precipitation

1. A volume of 100% ice cold ethanol corresponding to 2-3x the volume of the sample and a volume of Na-Acetate corresponding to 1/10 the volume of the sample were added to the sample. The tube was stored at -20˚C for at least 2 hours (but usually overnight) and then centrifuged for 30 min at 13500 rpm at 4˚C.
2. The pellet was washed with 80% ice cold ethanol and centrifuged for 10 min at 13000 rpm, at 4˚C. This step was repeated twice.
3. The pellet was air dried and resuspended in an appropriate volume of nuclease-free water.

2.5.6 Clean-up of genomic DNA from the QIAmp DNA Micro Kit (Qiagen, UK)

1. The AW1 and AW2 concentrates were made up with 25ml and 30ml 100% ethanol, respectively.
2. The DNA was made up to 100µl with dH_2O into a 1.5 ml micro-centrifuge tube; 10µl buffer AW1 and 250µl buffer AW2 were added; the cell suspension was mixed by pulse-vortexing for 10 seconds and the sample was transferred to the QIAmp MinElute

Column. The column was centrifuged at 6000 g for 1 min and placed into a new collection tube.

3. 500µl buffer AW2 was added to the column. The column was then centrifuged at 6000g for 1 min and placed in a clean 2ml collection tube which was then centrifuged at 14000rpm for 3 min to dry the membrane completely.
4. The DNA was eluted with 35-50µl dH_2O applied to the centre of the membrane and left to incubate at room temperature for 1 min; the column was centrifuged at 14000rpm for 1 min.
5. The DNA quantity and purity were re-assessed.

Formatted: Bullets and Numbering

2.5.7 DNA amplification using REPLI-g kit (Qiagen, UK)

A number of genetic analyses, including array CGH, require large quantities of template for testing and much effort has been invested in developing methods for whole genome amplification. The rolling circle amplification [197] method was developed for amplifying large circular DNA templates such as plasmid and bacteriophage DNA [198] using ϕ29 DNA polymerase and random exonuclease-resistant primers. The kit from Qiagen uses the bacteriophage ϕ29 DNA polymerase and random hexamer primers to exponentially amplify genomic DNA in a cascading, strand displacement reaction termed multiple displacement amplification (MDA). This method should provide a highly uniform representation across the genome. The ϕ29 enzyme has strand displacement activity, which displaces the 5' end of each strand by another upstream strand growing in the same direction. Displaced strands, which are single-stranded, are now targeted by new random priming events and these new strands are elongated in the opposite direction. Such a mechanism produces microgram amounts of DNA from nanogram amounts of initial template. The template DNA had to be >2 kb in length with some fragments > 10 kb.

1. DLB Buffer was prepared by adding 500µl nuclease-free water to the tube. Buffer D1 (denaturation buffer) was prepared by mixing 35µl nuclease-free water with 5µl DLB Buffer; Buffer N1 (neutralization buffer) was prepared by mixing 72µl nuclease-free water with 8µl 'stop solution'.
2. Equal amounts of patient and control DNA (100ng) were adjusted to 2.5µl with nuclease-free water.
3. 2.5µl Buffer D1 was added to the DNA, mixed by vortexing, centrifuged briefly and left at room temperature for 3 min.

4. 5µl Buffer N1 was added to each sample and mixed.
5. The REPLI-g Polymerase was thawed on ice; a 40µl mix reaction was prepared with 10µl nuclease-free water, 29µl Reaction Buffer and1µl DNA Polymerase, this was mixed with the denatured DNA.
6. The reaction mix was incubated at 30˚C for 2-4-6-8-16 hours then the enzyme was heat inactivated at 65˚C for 3 min.
7. After cooling on ice the samples were stored at 4˚C until required.
8. The QIAprep Spin Miniprep Kit was used for the clean-up of amplified-digested DNA (Buffer PE was prepared adding 100% ethanol to the Buffer PE bottle).
9. 500µl Buffer PB was added to each 100µl sample which was then applied to a QIAprep Spin Miniprep column and spinned for 60 seconds at 17900 g.
10. After discarding the flow-through, 750µl Buffer PE was added and the column was spinned for 60 seconds at 17900 g. The flow-through was discarded and the column was spinned at the same conditions.
11. The DNA was eluted in 50µl Buffer EB and incubated for 60 seconds. The purified DNA was collected spinning the column for 60 seconds at 17900 g.
12. 5µg of amplified DNA from the patient and the control samples were used to set up the array.

2.6 Array-based Comparative Genomic Hybridisation

Array-based comparative genomic hybridization is a sophisticated molecular technique that is used to identify and characterize DNA copy number alterations at the genomic level. Genomic DNA from two cell populations, test and reference, are differentially labelled with fluorescent dyes and competitively hybridised to a glass slide spotted with short sequences of DNA complementary to sequences which represent a normal genome [199,200]. Lasers scan the surface of the slide, exciting the dyes to fluorescence. The intensity of the different fluorochromes is measured and an array CGH profile of each chromosome generated from the $\log_2$ fluorescent ratios. Regions in which there is no deviation from the normal will have a ratio of 0, whilst those regions with duplications will have positive ratio values, conversely those with deletions will have negative ratio values (**Figure 2-2**).

Prior to analysis, the data is normalized. This compensates for systematic experimental variation, such as unequal dye incorporation, detection inefficiencies and background fluorescence. The signal intensities are not a direct measure of copy number, rather an arbitrary

value, thus an alternative method (e.g. FISH) is required to confirm the actual DNA copy number. Copy number alterations are mapped directly onto the human genome sequence.
The resolution of the array platform is variable depending upon the design. Array-based CGH platforms have been produced using large-insert DNA clones, such as BAC, complementary DNA (cDNA) [201] and oligonucleotides as probe templates. Initial designs were based on BAC clones. These clones are approximately 200 kb long and usually each platform contains on average 3000 clones, spaced approximately 1Mb apart. Although they provide precise identification of the chromosome regions involved in the copy number change, their resolution is insufficient to identify specific gene aberrations; furthermore BAC clones are difficult to propagate [202]. BAC arrays have the advantages of providing more intense signals than arrays made from shorter sequences of DNA, and the clones can be used as FISH probes for confirmation of results. The optimization of oligonucleotide array CGH (oligo array CGH) has dramatically superseded the resolution of BAC approaches, providing a resolution to the magnitude of 6 kb.
Limitations of array CGH include: inability to identify balanced structural rearrangements that do not result in copy number alterations; inability to identify the nature of unbalanced structural rearrangements; difficulties in detecting ploidy changes.
When array CGH is applied to neoplastic samples or constitutional mosaic samples, the contamination with non-tumour cells, or the presence of different clones, can make the array CGH analysis difficult to analyze as the final result is an average of the specific abnormalities present in each clone [203]. Another problem is the presence of copy number variations/polymorphisms (CNV), which are abundant in the human genome, and have the potential to confound the identification of genuine somatic alterations. This problem can be solved by normalizing the DNA derived from the patient tumour with the patient's normal germline DNA [204]; unfortunately both DNA samples are not always available.
The Human Genome CGH 244k Microarray platform (Agilent Technologies, Palo Alto, USA) was used in this study. The platform consists of more than 236,000 60-mer oligonucleotide probes that span the human genome covering coding and non-coding sequences with emphasis on well-known genes, promoters, miRNAs and telomeric regions. It provides an average resolution of less than 6.5 kb. Patient DNA was hybridised against a sex-matched reference DNA extracted from peripheral blood of ten healthy donors (Promega, UK). Normal germline DNA from patients was not available in this study.

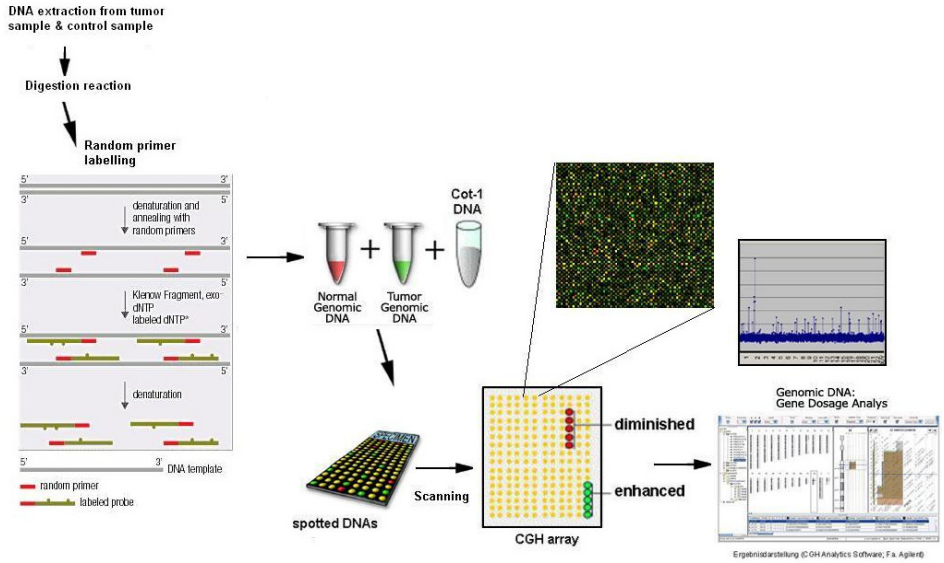

Figure 2- 2 Representation of array CGH technique

2.6.1 Restriction digestion of genomic DNA

1. The same amount (0.3-1.5µg) of genomic test DNA and reference DNA were made up to 20.2µl with nuclease free water in separate tubes.
2. 2µl nuclease free water, 2.6µl 10x Buffer C (Promega, UK), 0.2µl acetylated bovine serum albumin (BSA, Promega, UK) and 0.2µl of the restriction enzymes Alu I and Rsa I (Promega, UK) (digestion master mix) were added to both tubes, on ice. Samples were incubated in a water-bath at 37˚C for 2 hours. The enzymes were then inactivated by incubation at 65˚C for 20 min.

2.6.2 DNA labelling

1. 5µl 10x Random Primers (Agilent, USA) was added to each sample. The tubes were transferred to a hot plate at 95˚C for 3 min, and then transferred to ice for 5 min.
2. 10µl 5x buffer, 5µl 10x dNTP, 3µl Cy3-dUTP or Cy5-dUTP and 1µl exo-klenov (a genetically engineered enzyme in which the 3′ to 5′ exonuclease activity has been removed) (Agilent, USA) were added to each sample. They were incubated in a water-

bath at 37˚C for 2 hours. The enzyme was then inactivated by incubation at 65˚C for 10 min. Following incubation samples were transferred to ice.

2.6.3 Clean-up of labelled DNA

1. 430µl 1x TE buffer was added to each sample. A Microcon YM-3- filter (Millipore, Chemicon/ Upstate/ Linco, UK) was placed in a 1.5ml microfuge tube and the sample loaded onto the filter. It was centrifuged for 10 min at 8000 g. The flow-through was discarded.
2. 480µl 1x TE was applied to the filter. The tube was centrifuged as before and the flow-through was discarded; the filter was then inverted into a fresh collection tube which was centrifuged for 1 min at 8000 g.
3. If the sample volume exceeded 80.5µl, the sample was returned to its filter and centrifuged for 1 min at 8000 g, as previously described. The flow-through was discarded. The filter was inverted into a fresh collection tube and it was centrifuged for 1 min at 8000 g.
4. The labelling index of each DNA sample was evaluated with the NanoDrop-1000. From the main menu, 'Microarray Measurement' was selected; 1.5µl 1x TE was used to blank the instrument. 1.5µl purified labelled genomic DNA was used to measure the absorbance at A260nm (DNA), A550nm (cyanine 3), and A650nm (cyanine 5). The specific activity of the labelled genomic DNA was obtained by dividing 'pmol per µl dye/µg per µl genomic DNA'. The expected specific activity of cyanine-3 labelled samples was 25 to 40; of cyanine-5, 35 to 55. If the values were within the acceptable range, the test and reference DNA were combined and the volume was brought to 157µl with nuclease-free water.

2.6.4 Hybridisation

1. 1350µl nuclease-free water was added to the lyophilized 10x blocking agent (Agilent, USA) and incubated for 60 min at room temperature to reconstitute it.
2. 50µl Human Cot-1 DNA (Invitrogen, UK), 52µl 10x blocking agent and 260µl 2x hybridisation buffer (Agilent, USA) were added to the 157µl of combined sample. It was pipette mixed and centrifuged briefly to collect. The sample was incubated in a heat block at 95˚C for 3 min, then immediately transferred to a water bath at 37˚C for 30 min.

3. The sample was centrifuged for 1 min at 17900 g to collect.
4. A clean gasket slide was loaded into the Agilent SureHyb chamber base with the label facing up and aligned with the rectangular section of the chamber base.
5. 490µl hybridisation sample was slowly dispensed into the gasket well. An array was placed onto the gasket slide, so the numeric barcode side was facing up and the 'Agilent' barcode was facing down; the chamber cover was placed onto the sandwiched slides and the clamp was hand-tightened.
6. The assembled chamber was vertically rotated to wet the slides and assess the mobility of the bubbles. The assembly was tapped on a hard surface to move stationary bubbles; it was then placed into the hybridisation oven at 65˚C and rotated at 20 rpm for 40 hours.

2.6.5 Washes and drying

Excess unbound test and reference genomic DNA was removed by post hybridisation washes. At the same time it was important to stabilise and dry the hybridised array slide. As Cyanine 5 is sensitive to ozone degradation, stabilisation and drying solutions have been designed to minimize ozone induced degradation.

1. The required volume of Wash buffer 2 (Agilent, USA) was pre warmed in a 37˚C water bath, overnight. If the stabilization and drying solution showed a visible precipitation, this too required pre warming at 37˚C overnight.
2. Five slide staining tanks were filled with the following solutions: wash buffer 1 (Agilent, USA) (tank 1); wash buffer 1 filled to a sufficient level to cover a slide rack (tank 2); wash buffer 2 at 37˚C (tank 3); Acetonitrile (Sigma-Aldrich, UK) (tank 4); Stabilization and Drying solution (Agilent, USA) (tank 5). In addition to the solutions tank 2-5 contained a magnetic flea and all four tanks were placed on a magnetic stir plate which was set at speed level 3.
3. The slide was removed from the hybchamber and placed in tank 1. Whilst submerged in the wash, the slides forming the 'sandwich' were gently prised apart, and placed into the slide rack and quickly transferred to tank 2. The slides were left for 5 min before being transferred to tank 3, where they were left for 1 min. The rack was transferred to tank 4 and left for 1 min.
4. Finally the rack was transferred to tank 5 for 30 seconds. Very slowly the slides were removed from the tank, taking care to ensure that no droplets remained on the slide.

5. The slides were then scanned on an Agilent scanner using the default scan setting. The scan resolution was set to 5µm as recommended for 244k density array.

2.6.6 Data extraction

The feature extraction software version 9.5.3.1 (Agilent, USA) converts the TIF images obtained from the scanner into a reduced representative set of features, which are required to describe a large set of data accurately. The arrays were then analyzed using the Agilent CGH Analytics 3.5.40 and 4.0 softwares, which is based on the UCSC March 2006 assembly (Hg18). The ratio of the fluorescent intensity of the test gDNA compared to the reference gDNA was calculated and averaged for each replicate before being converted to a $\log_2$ ratio, which was then normalized using z-scoring or Aberration Detection Method-2 (ADM-2). Aberrant regions were identified for each point in the data by calculating the moving average within 0.5 Mb window. Outliers were classified using a cut off +/- 0.25. Five consecutive aberrant spots were required for an aberrant call.

2.7 RNA extraction (Qiagen RNEasy method) and cDNA synthesis

RNA was extracted using the Qiagen RNeasy kit (Qiagen, UK). At the beginning, four volumes of 100% ethanol were added to buffer RPE (included in the kit) to obtain the working concentration.

1. Equal amounts of Trizol (Invitrogen, UK) sample and chloroform (Sigma-Aldrich, UK) were combined (usually 350-500µl of each). The tube was shaken vigorously for 15 seconds and centrifuged at 14000 rpm for 5 min.
2. After centrifugation, the RNA remained in the upper colourless aqueous phase. This layer was transferred to a new eppendorf, being careful not to aspirate the interface.
3. The same amount of chloroform used in step 1 was added to the eppendorf; the tube was vortexed for 15 seconds and centrifuged for 5 min at 14000 rpm, at room temperature.
4. The top layer was carefully transferred into a new eppendorf and 70% ethanol was added in the same amount used for the chloroform.

5. At this point, because of the low number of cells usually present in the sample, 20ng carrier RNA (Polyadenylic acid, Amersham, UK; working concentration of 10ng/µl) was added to the cell lysate before loading it onto the RNeasy membrane. The carrier RNA was co-purified with the cellular RNA, as the small amount used for each extraction did not interfere with subsequent PCR reactions.
6. The cellular lysate and the RNA carrier were applied to the RNeasy column which was then centrifuged for 15 seconds at 10000 rpm and the flow through was discarded.
7. 650µl RW1 was added to the column and the tube was centrifuged for 15 seconds at 10000 rpm; the flow through was discarded. 500µl RPE was added to the column and the tube was centrifuged for 15 seconds at 10000 rpm; the flow through was discarded.
8. 500µl RPE was added to the column, and the column centrifuged for 2 min at 14000 rpm; the flow through was discarded and the column placed into a new 1.5ml eppendorf.
9. The cap of the column was left open for 3-5 min under the hood and then 25µl RNeasy free water was added at the centre of the filter, in the column.
10. The column was centrifuged for 1 min at 14000 rpm to elute the RNA and immediately placed on ice. After elution, the RNA was heated to 65˚C for 5 min and placed on ice, then immediately reverse transcribed into cDNA.
11. 1-5µg RNA was incubated for 2 hours at 37˚C in a final reaction volume of 40µl containing 50mM Tris (pH 8.3), 75mM KCl, 3mM MgCl2, 1mM dithiothreitol (DTT, Sigma-Aldrich, UK), 1mM deoxyadenosine triphosphate (dATP), 1mM deoxycytidine triphosphate (dCTP), 1mM deoxythymidine triphosphate (dTTP), and 1mM deoxyguanosine triphosphate (dGTP), together with 100µg/µl of random pd(N)6 hexamers (Amersham Pharmacia, Amersham, UK), 14,000U of Murine Molony Leukaemia Virus (MMLV) reverse transcriptase (Invitrogen, UK) and 1400U/ml RNase inhibitor (Promega, UK). Enzyme denaturation by heating to 65˚C for 10 min terminated cDNA synthesis. The cDNA was stored at -20˚C.

2.7.1 cDNA quality assessment

The quality of the cDNA was assessed by PCR with the BCR-ABL1 multiplex mix, used for detection of the translocation t(9;22)(q34;q11), which leads to fusion of the genes *BCR* and *ABL1* [205]. The PCR is a technique for the in vitro amplification of specific DNA sequences by the simultaneous primer extension of complementary strands of DNA [206]. A thermostable DNA polymerase synthesizes a DNA sequence using two primers, each complementary to opposite stands of the region of DNA, which has been denaturated by heating. This results in the de novo

synthesis of the region of DNA flanked by the two primers. The reaction requires deoxynucleotides, DNA polymerase, primers, template and buffer containing magnesium. A typical PCR programme of heating and cooling facilitates the exponential accumulation of DNA product which can be visualized by staining with ethidium bromide and electrophoresis on an agarose gel. The PCR programme used was as follow:

initial denaturation	95˚C for 10 min	
denaturation phase	95˚C for 1 min	29 cycles
primer annealing	60˚C for 1 min	
synthesis phase	72˚C for 1 min	
extension phase	72˚C for 10 min	
hold	15˚C	

PCR were performed in a volume of 21µl. All amplification reactions were performed in a MJ Research Tetrad thermocycler with heated lid, in sterile 200µl microtubes. The multiplex PCR mix contained 0.2µM primers (0,5µM for single PCR reactions), 0.2mM each of dCTP, dTTP, dATP, and dGTP, 1.5mM MgCl2, 1x buffer (10mM Tris-HCl (pH 8.3), 50mM KCl, 0.1% gelatine), 0.05 U/µl HotStar Taq polymerase (Qiagen, UK). The primer mix included: one reverse primer for exon 11 of the ABL gene (CA3-: tgt tga ctg gcg tga tgt agt tgc ttg g); one reverse primer for exon 21 of the BCR gene (C5e-: ata gga tcc ttt gca acc ggg tct gaa); one forward primer for exon 13 of the BCR gene (B2B: aca gaa ttc cgc tga cca tca ata ag); one forward primer for exon 1 for the BCR gene (BCR-C: acc gca tgt tcc ggg aca aaa g).
As positive control, 1µl of cDNA from one of the two cell-lines (SD1 or K562) was used.

2.8 Quantitative reverse transcription PCR (qRT-PCR)

This technique is used for RNA quantitation or determination of gene expression levels. It can also be used for DNA and cDNA quantitation. Real-Time PCR is identical to a simple PCR except that the progress of the reaction is monitored by a camera in ‘real-time’.
The taqman system uses a primer and a probe complementary to the gene of interest. The probe is labelled with a fluorescent reporter dye on the 5' end and a quencher molecule (capable of quenching the fluorescence of the reporter) on the 3' end. While the probe is intact, the proximity of the quencher molecule greatly reduces the fluorescence emitted by the reporter dye. The probe anneals to a target sequence downstream of the primer site and as the primer is extended by Taq DNA polymerase its 5' nuclease activity cleaves the reporter dye from the

quencher, which allows the fluorescence of the reporter to increase. Each cycle of denaturation, primer annealing and primer extension cleaves another probe. Reactions are characterized by the point in time during cycling when the fluorescence exceeds the threshold. The more RNA present the sooner this happens. The Taqman software generates a Ct value for each of the reactions. These refer to the cycle number needed to generate a defined amount of fluorescence when the PCR is in its linear phase. Therefore the higher the Ct value the less RNA is present in the sample. The comparative Ct method is used for quantitation of gene expression relative to an endogenous control gene. A housekeeping gene such as *GAPDH* (glyceraldehyde-3-phosphate dehydrogenase) is typically used as the reference gene.
In this study *MYC* mRNA expression levels were investigated in a number of patients. RNA was obtained from purified PC of PCL and MM patients. Normal PC are characterized by a low level of *MYC* expression, as the gene is silenced during PC differentiation [207]; therefore RNA from purified BM PC (85%) from a patient with myelodysplasia was used in this study as calibrator sample. The RNA from the human promyelocytic leukemia cell line, HL-60, was used as positive control for *MYC* overexpression [208].

Real-time quantitative PCR was performed with the Corbett Rotor Gene 6000 (Corbett Life Science, Sydney, Australia). The 10µL qRT-PCR contained 2µL cDNA, 1x TaqMan Universal PCR Master Mix (Applied Biosystems, UK), 300nM forward and reverse primers and 200nM probe. Cycling conditions were 50˚C for 2 min, 95˚C for 10 min followed by 45 cycles of 95˚C for 15 seconds and 60˚C for 1 min. Probes and primers used for *MYC* were: sense primer, 5'-ACCACCAGCAGCGACTCTGA-3'; antisense primer, 5'-TCCAGCAGAAGGTGATCCAGACT-3'; probe 5'FAM-ACCTTTTGCCAGGAGCCTGCCTCT-BHQ1 3' [209].

The level of *MYC* mRNA was determined by normalization to the level of the *GUSB* (beta-glucuronidase) and *BCR* genes, used as endogenous controls, which showed little variability in expression across the patient samples. Probes and primers for *GUSB* were as described by the European against Cancer group [210], and probes and primers for *BCR* were as described by Branford et al. [211]. The relative expression of *MYC*, compared to *GUSB* and *BCR*, was calculated using the Pfaffl method [212]. The myelodysplastic sample was measured in the same analytical run to exclude between-run variation.

2.9 Sequencing by dideoxynucleotide chain termination

The dideoxynucleotide chain termination is a PCR based technique for sequencing that utilises the addition of all four fluorescently labelled dideoxynucleotides (ddNTP) to homogeneous, single stranded template DNA with the correct primer, DNA polymerase and dNTP. The ddNTP lack the 3' hydroxyl group, necessary for the formation of 3' - 5' phosphodiester bond and therefore halts chain elongation at random when incorporated into the synthesised template DNA. The resultant mixture is a series of DNA molecules at different lengths which, when run through the capillary gel electrophoresis separate on the basis of size and are detected when a laser excites the fluorescent dye attached to the ddNTP.

2.9.1 ExoSAP

For fluorescent-based sequencing of PCR products, removal of unused primers was performed by incubating 3µl of the PCR product with 2µl of exonuclease I (New England Biolabs, UK) and shrimp alkaline phosphatase (SAP, Roche Diagnostics Ltd, UK) mix at 37˚C for 15 min and then denatured by heating to 80˚C for 15 min. Exonuclease I degrades any residual single stranded primers and extragenous single-stranded DNA, whilst the SAP hydrolyses the remaining dNTPs from the PCR reaction. The exonuclease I/ SAP mix was prepared combining the enzymes in a ratio 1:4, respectively. The PCR product was then diluted in 5µl of water.

2.9.2 Sequencing reaction

Exonuclease I/ SAP purified PCR products were sequenced in a reaction containing 1µl PCR product, 0.5µl of a single primer (either forward or reverse), 0.5µl of v1.1 or 3.1 Big Dye Terminator, 1.5µl of 5x sequencing buffer and made up to 10µl with deionised water (Applied Biosystems, Foster City, CA, USA). The sequencing reaction was made up on ice and the sequencing programme was as follows:

96°C	30 sec	25 cycles
50°C	15 sec	
60°C	2 min	
4°C	hold	

2.9.3 Removal of unincorporated dye terminators

Unincorporated dye terminators were removed from the sequencing reaction using the montage SEQ96 sequencing reaction clean up kits (Millipore, UK). 25µl of Injection Solution was added to every tube with the sequencing products and the entire mix was transferred into the wells. At this point the vacuum was activated (for 3-4 min) until the wells were empty in order to filter the small contaminants present in the mix. After adding 25µl of Injection Solution, the vacuum was re-activated for a second time until the wells were dried. Deionised formamide (Sigma-Aldrich, UK) or deionised water (20µl) was added to each well and used to resuspend the cleaned sequencing reactions, which were then loaded onto an Applied Biosystem 3100 or 3130 sequencing machine.

2.10 Multiplex Ligation-dependent Probe Amplification (MLPA)

MLPA is a method to establish the copy number of multiple nucleic acid sequences in one single reaction by yielding amplification products of unique size per target [213]. Products are separated by automated fluorescence-based sequence electrophoresis and the copy number of each target is determined from the relative intensities of the products compared to those obtained from controls. Genomic deletions and amplifications of a gene (or part of) will usually not be detected by sequence analysis of PCR amplified gene fragments if a normal copy is still present. With MLPA, only one pair of PCR primers is used and therefore MLPA reactions result in a very reproducible gel pattern with fragments ranging from 130 to 490bp (**Figure 2-3**). Each MLPA probe consists of a target-specific sequence and one phage M13 derived sequence. Two such probes are designed to hybridize immediately adjacent to each other and are joined by the action of a thermostable ligase. The outer phage-derived portions of the primer pair allow simultaneous amplification of all sequences in the reaction by FAM-labelled M13 primers, and contain a random ‘stuffer’ sequence designed to vary in length to aid separation of the individual targets. Each probe pair therefore gives rise to an amplification product of unique size, which can be quantified by capillary electrophoresis. The relative amounts of the probe amplification products reflect the relative copy number of the target sequences.

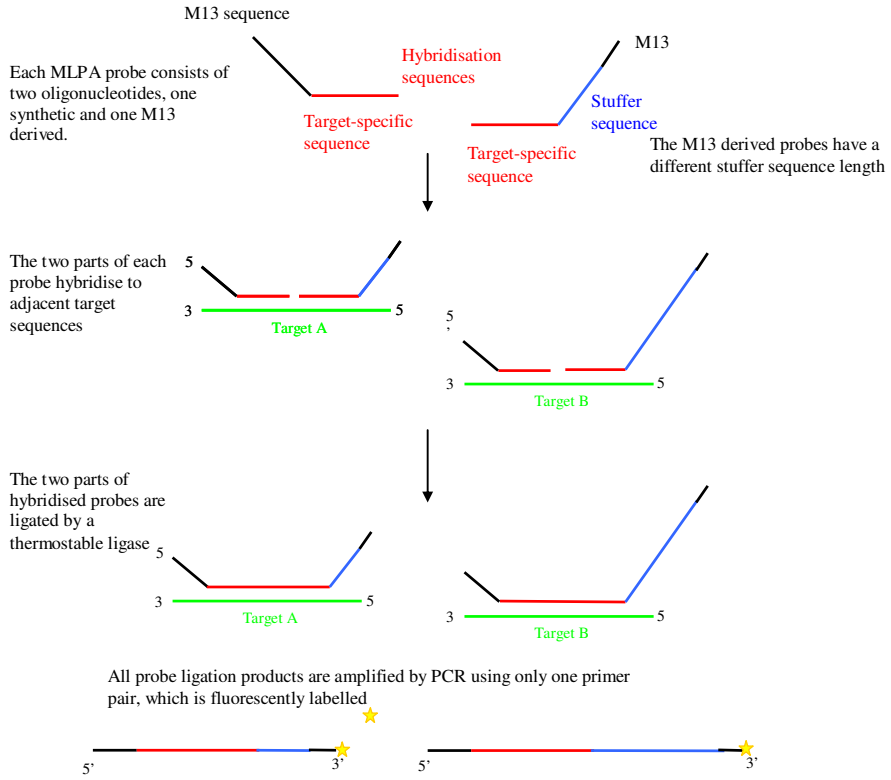

Figure 2- 3 Outline of the MLPA reaction

Genomic DNA is denatured and hybridised with a probe mixture. For MLPA on mRNA, an initial cDNA synthesis step using reverse transcriptase and target specific probes is required. From then on the DNA and mRNA MLPA strategies are the same. Adapted from Schouten *et al.* [213]

The amplification product of each probe has a unique length to allow amplified products to be separated by capillary electrophoresis. For MLPA on genomic DNA, relative amounts of probe amplification products reflect the relative copy number of target sequences. For MLPA performed on cDNA (RT-MLPA) the amounts of probe amplification product reflect the level of mRNA expression.

2.10.1 Methodology (MRC Holland, the Netherlands)

1. 1µl (50ng) DNA was added to 4µl of Tris-EDTA buffer in a 0.2ml PCR tube and overlaid with oil (to prevent evaporation overnight) before running on a MJ thermocycler tetrad 'Denature' programme (heat at 98˚C for 7 min; cool to 25˚C).

2. To each denatured sample was then added a mixture of 1.5µl relevant probe mix and 1.5µl MLPA buffer.
3. After mixing gently, samples were incubated for 1 min at 95˚C and then the probes were let to bound overnight at 60˚C.
4. The following morning, 3µl of Ligase buffer A, 3µl of Ligase buffer B, 25µl of water and 1µl of Ligase were combined (Ligase mix) for each sample less than one hour before use and stored in ice.
5. After stopping the 60˚C overnight run, samples were held at 54˚C for at least 2 min before adding 32µl of the above Ligase mix. Samples were then incubated for 15 min at 54˚C and at 98˚C for 5 min.
6. After the ligation was completed 1µl SALSA PCR-primers, 2µl SALSA Enzyme Dilution buffer, 15.75µl water, 0.25µl SALSA Polymerase and 5µl of Polymerase were added to each sample and the PCR reaction was started (PCR conditions, 35 cycles: 30 seconds 95˚C; 30 seconds 60˚C; 60 seconds 72˚C. The reaction was ended with 20 min incubation at 72˚C.
7. The PCR samples were then analyzed on an ABI3130 by mixing 1µl PCR product to 9µl of formamide and 0.1µl of ROX500 size standard (Applied Biosystems, USA).

Analysis of the samples was performed using Applied Biosystems Genescan software using a GS500 size standard. Following this, Applied Biosystem Genotyper software was used. Based on the number of probes in the MLPA kit the software can be manipulated. MLPA analysis sheets for each MLPA probe kit were set up in Microsoft Excel. The data from the genotyper table was imported into the Excel sheet and samples were compared to controls (genomic DNA from two healthy individuals). The peak height of each probe is compared against every other probe and against the control. This gives a data sheet of numbers (peak ratios) where 1 is normal, a horizontal row of 0.5 indicates a deletion and horizontal row of 1.5 a duplication.
A variety of MLPA probemixes are available from MRC-Holland. Alternatively, it is now possible to add some probes of specific interest to a commercial kit or to have purchased a completely new and personal MLPA kit. For this study, Mark Townsend with the help of Dr Dave Bunyan, enriched the commercial kit 'SALSA MLPA kit P088 Glioma 1' with six new probes mapping at 1p32.3 the genes *CDKN2C/p18* (Cyclin-dependent kinase 4 inhibitor C) and *FAF1* (Fas (TNFRSF6) associated factor 1) (description and location of the probes included in the commercial kit can be found on the MRC-Holland Website, see URL in **Appendix 1**; sequence, size and location of the six customized probes are described in **Appendix 4**). MLPA was used to detect the exact breakpoint of deletions occurring at this chromosomal band.

2.11 Statistical analysis

The frequencies of chromosomal abnormalities in different patient groups were compared by Fishers' exact test or Kruskall-Wallis test as appropriate.
Differences between survival curves in MM and differences between progression curves in MGUS were analysed using the Log-rank test. Kaplan-Meier curves were calculated using MINITAB 14.
Fishers' exact test was used to compare the frequencies of chromosomal abnormalities in PCL and MM patients (**Section 3.6.4.9**). The Mann-Whitney test was used to evaluate differences in *MYC* expression levels in MM and PCL between cases with and without evidence of 8q24 abnormalities.

3 RESULTS

3.1 Characterization of MGUS and SMM by iFISH

3.1.1 Introduction

The paucity of PC within the bone marrow of MGUS and SMM patients, associated with the low proliferative capacity of these cells, has precluded meaningful karyotypic studies in these patients. Interphase-FISH provides an alternative approach to investigate chromosomal abnormalities (CA) in tumour cells from which metaphases are difficult to obtain. In MGUS, the interpretation of CA detected by iFISH has been complicated by the inferior PC purity due to a lower level of BM plasmocytosis [85]. However, CA have been consistently detected by iFISH in a high proportion of patients, with roughly 50% of them carrying one of the primary *IgH* translocations (IgHt) and the remaining patients displaying an HRD karyotype. These findings suggested that ploidy status and *IgH* rearrangements were early events delineating different pathogenetic pathways [44,214,215].

Conflicting results have been reported on the prevalence of Δ13 in MGUS. Avet-Loiseau *et al.* reported a substantially lower frequency (~25%) compared to MM (~50%) [85,109] while others reported a similar incidence in both conditions [44,103]. Fonseca *et al.* also indicated that when Δ13 was detected in MGUS it occurred in the majority of clonal PC [44], consistent with that normally observed in MM [98,99], while others reported a greater heterogeneity in MGUS [98].

Here iFISH was used (**i**) to assess the incidence and the association of Δ13 with *IgH* translocations, ploidy status, deletions of 16q23 and *TP53* in a large series of MGUS and SMM patients; (**ii**) to compare these frequencies with those found in a group of newly diagnosed MM patients in order to determine whether the patterns of CA differ within the different diagnostic groups; (**iii**) to explore the reported clonal heterogeneity of MGUS by comparing the frequencies of the different CA detected in individual patients [85].

3.1.2 Patients

A consecutive series of 715 patients with PC disorders sent to the Myeloma Cytogenetic Database were evaluated. The cohort consisted of 187 MGUS (median age: 69 years, range 36-92 years) and 128 SMM patients (median age: 69 years, range 31-89 years) not requiring therapy, and 400 newly diagnosed MM patients entered into the MRC Myeloma IX Trial (median age: 64 years, range 30-89 years). Patients with an IgM heavy chain subtype were not eligible for this study, given their different biology [46]. Age was statistically similarly distributed within the patient groups. All but four SMM and eight MGUS patients were studied at the time of diagnosis.

3.1.3 Cytogenetic testing

Mononuclear cells were separated after density gradient centrifugation of BM aspirates over Lymphoprep (**Section 2.2.3**) and $CD138^+$ PC were isolated by magnetic-activated cell sorting (**Section 2.2.5**). Interphase-FISH was performed on PC using a panel of commercial and in-house probes (**Appendix 3**) as described in **Sections 2.4.6** to **2.4.9**. Results were available for Δ13 (two probes in 13q14: *RB1* and D13S319), *IgH* break-apart (14q32.33) (**Figure 3-1**), t(4;14)(p16;q32), *CCND3* break-apart (6p21), t(11;14)(q13;q32), t(14;16)(q32;q23), *MAFB* break-apart (20q11), deletion of 16q23, interstitial deletion of *TP53* (17p13) or monosomy 17 (centromere 17) and ploidy status. The multi-colour probe set from Abbott, specific for the locus 5p15.2 and centromeres (CEP) 9 and 15, was used to assess ploidy. Break-apart patterns for the *CCND3* or the *MAFB* probes, in cases with a concomitant break-apart of the *IgH* probe, were suggestive of t(6;14)(p21;q32) and t(14;20)(q32;q11), respectively. In these cases the presence of the suspected translocation was confirmed by re-hybridizing the same cells with the t(4;14)(p16;q32) probe (already found to be negative) with single colour probes for *CCND3* or *MAFB*; the finding of fusion signals proved the suspected translocation.
A FISH result was considered to be abnormal when above the cut-off levels recommended by the European Myeloma Network (EMN) FISH workshop: a level of 10% for fusion and break-apart probes, 20% for numerical abnormalities.

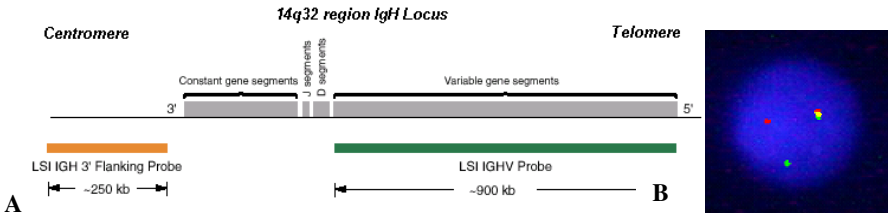

Figure 3- 1 Vysis IgH Dual Colour, break-apart probe

A) Map of the probe; B) *IgH* probe hybridized to a nucleus exhibiting a split at 14q32 corresponding to the signal pattern: 1G1R1F; this pattern is indicative of an *IgH* rearrangement. (G, green signal; R, red signal; F, fusion signal)

3.1.4 Results

3.1.4.1 Ploidy classification

Only conventional cytogenetics can provide an accurate ploidy classification because all chromosomes can be visualized and counted at the same time. Given the lack of availability of abnormal metaphases in most MM or related monoclonal gammopathies the estimation of ploidy was attempted using a panel of FISH probes mapping multiple loci on different chromosomes. The FISH method used here to assess ploidy was designed and validated on MM patients, using a modification of the method of Wuilleme *et al.* [216]. According to this system, all patients with gain of signals for any two of the chromosomes 5, 9 or 15 were defined as HRD. Cases not meeting these criteria, and showing only loss of signals were defined as nonHRD, along with those having >four copies of >four probes (near-tetraploidy, these were considered as nonHRD) [92]. All other cases, in particular those with gain of a single probe, had their full iFISH pattern compared with the hypothetical result that would have been obtained for the same probes on all complete myeloma karyotypes in the Mitelman Database of Chromosomes in Cancer (URL in **Appendix 1**) and our own cytogenetic results. Where the majority (>75%) of comparable cases were HRD or nonHRD, then the appropriate category was assigned. If no clear pattern emerged or the comparable cases were equally divided between HRD and nonHRD, the case remained unassigned for ploidy [87].

Patients with MGUS and SMM were classified as being HRD or nonHRD using this method. In this series of pre-malignant patients, seven MGUS and 17 SMM patients had abnormal cytogenetics. For these cases the ploidy status defined by iFISH was compared with the actual karyotype (karyotypes and ploidy defined by iFISH are listed in **Appendix 5**): all but two cases

(one MGUS and one SMM) were correctly classified by iFISH. The first discrepant case (MGUS) had 47 chromosomes and the karyotype showed: one extra copy of chromosome X, trisomies of chromosomes 9 and 11 (detected by iFISH), trisomy 19 and losses of chromosomes 13, 14 and 16 (detected by iFISH). Since trisomies of chromosomes 9 and 11 are usually associated with HRD and deletions of 14q32 and 16q23 detected by iFISH usually represent interstitial deletions the case was classified as HRD. The karyotype of the second discrepant case (SMM) had 48 chromosomes with a missing Y, one extra copy of chromosome 9 (detected by iFISH) and two extra copies of differently rearranged chromosomes 1. This is a very unusual karyotype and because iFISH only detected trisomy 9 with no other CA, the case has been classified as nonHRD.

3.1.4.2 Frequencies of chromosomal abnormalities

FISH analysis was performed according to availability of patient material: a minimum of eight loci were tested on all patients (4p16, 5p15.2, CEP 9, 11q13, 13q14 (two loci), 14q32 and CEP 15). In more than 80% of patients, 13 different loci were analysed. Copy number changes or structural alterations were observed for at least one of the chromosomal regions tested in 168/187 (90%) MGUS, 125/128 (98%) SMM and 396/400 (99%) MM.

Table 3-1 summarizes the frequencies of the specific CA within each diagnostic group. The incidence of Δ13 was substantially lower in MGUS (25%) and SMM (35%) than in MM (47%); the difference across the three groups was statistically highly significant (Kruskall-Wallis test, MGUS *vs* SMM *vs* MM, $P < 0.001$).
Rearrangements involving the *IgH* heavy chain locus located at 14q32 were detected with similar frequencies in MGUS and MM (41% *vs* 46%, respectively); the incidence in SMM (36%) was lower, but this difference was not statistically significant. When the individual chromosomal partners of the primary translocations were considered, similar frequencies of t(6;14), t(11;14) and t(14;16) were observed among the three groups; t(4;14) was rare in MGUS (3%), while SMM and MM showed almost the same incidence (13% *vs* 12%, respectively) (MGUS *vs* MM, $P<0.001$). The frequency of t(14;20) was higher in MGUS (5%) than in either SMM (<1%) or MM (2%). The difference in the incidence of this translocation was not statistically significant in this analysis, but it reached significance when the same MGUS group was compared to a larger population of MM patients (MM, n=1830; frequency of the translocation, 1.5%). Deletion of 16q23 was found to have a lower incidence in MGUS (6%)

and SMM (8%) than in MM (21%) (MGUS *vs* MM, *P*<0.001). Deletion of *TP53* was also very rare in MGUS (3%) and SMM (~1%).

CA	MGUS n=189	SMM n=127	MM n=400	*P*-value MGUS *vs* SMM	*P*-value MGUS *vs* MM	*P*-value SMM *vs* MM
	Number of patients (%)	*Number of patients (%)*	*Number of patients (%)*			
Δ13[†]	45/183 (25%)	43/124 (35%)	186/395 (47%)	0.07	**<0.001**	**0.017**
***IgH* rearrangement**	76/187 (41%)	45/126 (36%)	183/398 (46%)	0.41	0.25	**0.05**
t(4;14)	6/182 (3%)	16/123 (13%)	49/400 (12%)	**0.003**	**<0.001**	0.87
t(6;14)	2/174 (1%)	1[††]/119 (~1%)	6/393 (2%)	1	1	1
t(11;14)	29/184 (16%)	13/123 (11%)	55/399 (14%)[§]	0.24	0.53	0.44
t(14;16)	6/178 (3%)	4/120 (3%)	15/396 (4%)	1	1	1
Deletion 16q23	8/139 (6%)	7/84 (8%)	75/365 (21%)	0.58	**<0.001**	**0.008**
t(14;20)	8/176 (5%)	1/119 (~1%)	9/394 (2%)	0.09	0.18[#]	0.47
Deletion *TP53*	5/175 (3%)	1/117 (~1%)	38/388 (10%)	0.41	**0.003**	**<0.001**
HRD	72/171 (42%)	70/113 (62%)	223/388 (57%)	**0.002**	**<0.001**	0.45
nonHRD	99/171 (58%)*	43/113 (38%)**	165/388 (43%)			

Table 3- 1 Incidence of specific chromosomal abnormalities (CA) in the three diagnostic groups (statistically significant *P* values are in red)

[†] Near-tetraploid cases with only two copies of 13q14 were counted as Δ13.
[††] The locus 6p21 was involved in a t(6;22)(p21;q11) with the *IgL* locus.
*** 19/171 patients (11%) belonging to the nonHRD group were found to be normal for all the iFISH tests performed and were classified as diploid (nonHRD).**
**** 2/113 patients (~2%) were found to be normal for all the iFISH tests performed.**
[§] 2/55 (4%) patients showed amplification of *CCND1*, in absence of t(11;14); given that both abnormalities result in over-expression of *CCND1*, they were analysed as a single group.
 # When the frequency of t(14;20) in MGUS was compared to that found in a larger group of MM (1830 patients; frequency of 1.5%), the difference was highly significant.

The patient distribution in the two ploidy classes differed between the diagnostic groups. While a HRD karyotype was indicated in 62% of SMM and 57% of MM patients, only 42% of MGUS cases were assigned to this category. The nonHRD MGUS group also included those patients found to be negative for all the interphase FISH markers; in MGUS, 19 of 171 patients with ploidy results belonged to this group and accounted for most of the difference between the

groups. This result was not surprising as there probably are MGUS cases who are genuinely normal from a cytogenetic point of view.

IgH rearrangements involving the five recurrent loci (4p16, 6p21, 11q13, 16q23 and 20q11) were highly associated with a nonHRD karyotype in all three diagnostic groups: 93% of MGUS cases, 82% of SMM cases and 73% of MM cases with one of these *IgH* translocations were found in the context of nonHRD (P<0.001 for all groups). In contrast 35 of 49 MM cases with an *IgH* rearrangement not involving one of these loci were found in association with HRD (P=0.043). In the SMM group the six unidentified *IgH* rearrangements were equally distributed between the two ploidy groups. In MGUS, twelve of 16 unidentified *IgH* rearrangements were found in the context of a nonHRD karyotype but the association was not statistically significant.

3.1.4.3 Percentage of PC in patients with Δ13

When present, Δ13 showed a variable degree of PC involvement (**Figure 3-2**).

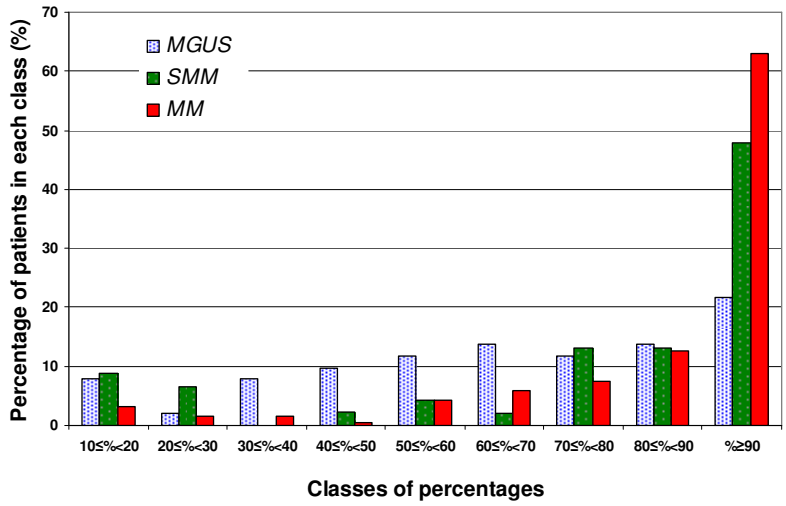

Figure 3- 2 Distribution of the percentages of abnormal PC with Δ13 in patients found positive for the abnormality, among the three groups of patients

As an exception, cases showing Δ13 in 10% to 20% PC were included in the assessment of the distribution of the percentages of abnormal PC with Δ13 in patients positive for the abnormality. Despite the fact that such cases were considered to be normal using the EMN criteria, some demonstrated a progressive increase in the percentage of Δ13 cells on sequential analysis,

indicating that, they did not represent technical artefacts (see patient 949, **Section 3.2.4** and patient 259, **Section 3.5.4.2**).

The median percentage of abnormal PC carrying the abnormality was 65% in MGUS, 88.5% in SMM and 95% in MM. Illegitimate *IgH* rearrangements showed no variation between disease types: in MGUS the median percentage of cells displaying a 14q32 translocation was 91.5% (range, 24%-100%).
The level of PC involvement of different CA was compared for all MGUS patients who exhibited Δ13 with at least one other abnormality (**Table 3-2**). Because of the differences in false positive rates between probes (fusion probes *vs* break-apart probes *vs* probes used to detect deletions), unequivocal evidence of heterogeneity within the neoplastic clone was only accepted when the difference in the proportions of cells affected by distinct CA was $\geq$30%. In 15 of 45 patients with Δ13, the abnormality was present in $\leq$60% PC (highlighted area of **Table 3-2**); of these 15 cases, 12 had other CA for comparison. All but four of these 12 showed the non-Δ13 abnormality to have a PC involvement at least 30% greater than the one shown by Δ13.

Interestingly four of five (80%) MGUS cases positive for both t(4;14) and Δ13 showed the same proportion (± 5%) of PC with the two abnormalities. In contrast, three of four (75%) t(14;20) MGUS with Δ13, showed at least 30% fewer Δ13-positive PC (median, 45%) compared with those with t(14;20) (median, 100%) (Δ13 *vs* t(14;20) for the four cases: 30% *vs* 100%; 45% *vs* 90%; 56% *vs* 100%). The only t(14;20) SMM case of this cohort also showed Δ13; while the translocation was present in 90% of PC, Δ13 was present in 60%. In MM seven of nine (78%) t(14;20) cases were associated with Δ13 and the median difference in PC involvement of Δ13 and the translocation was 10% (range, 0-27%).

In MGUS, 16q23 deletions were often present in a sub-clone of the PC population (median, 63%; range, 23%-100%), while in MM the median percentage of PC with the abnormality was 87% (range, 21%-100%). Those MGUS cases showing low level PC involvement of 16q deletion displayed at least one of the other CA in the majority of clonal PC (deletion 16q23 *vs* other CA: 23% *vs* 82% *IgH* split; 33% *vs* 93% deletion of 14q32; 44% *vs* 92% *IgH* split; 47% *vs* 99% *IgH* split).

Case	% of PC with Δ13	Other abnormalities (%)	Case	% of PC with Δ13	Other abnormalities (%)
1	20%	3 x '*CCND3*' (36%); *IgH* split (32%) (UIP)	**24**	75%	Trisomies 5, 9 & 15 (99%); *c-MYC* split (47%)
2	30%	**t(14;20) (100%)**	**25**	76%	**t(14;16) (96%)**
3	36%	*IgH* split (30%) (UIP)	**26**	77%	**t(6;14) (100%)**; trisomy 9 (35%); 3 x '*CCND1*' (55%)
4	38%	Trisomy & tetrasomy 9 (80%)	**27**	79%	Trisomy 5 (79%)
5	40%		**28**	80%	Unbalanced *IgH* split (80%) (UIP)
6	41%		**29**	81%	Unbalanced *IgH* split (100%) (UIP); deletion 16q23 (97%); deletion *TP53* (50%)
7	45%		**30**	82%	
8	45%	**t(14;20) (90%)**	**31**	83%	Trisomies 5, 11 & 15 (98%)
9	48%	**t(11;14) (100%)**	**32**	83%	Deletion 14q32 (79%)
10	52%	Trisomies 5, 6, 9 & 15 (>90%)	**33**	84%	**t(4;14) (85%)**
11	53%	Trisomies 5, 15 (>90%); deletion 16q (95%)	**34**	88%	3 x '*CCND3*' (75%); trisomy & tetrasomy 9 (100%); trisomy 15 (75%)
12	56%	**t(14;20) (100%)**	**35**	90%	Deletion 14q32 (79%)
13	56%	*IgH* split (89%) (UIP); deletion 16q (23%)	**36**	90%	Trisomies 5 & 9 (99%); tetrasomy 15 (88%); 3 x '*CCND1*' (76%); 3 x '*IgH*' (94%)
14	58%	Deletion 14q (67%)	**37**	94%	**t(4;14) (89%)**
15	58%	3 x '*CCND3*' (85%); trisomy 9 (89%); *IgH* split (76%) (UIP)	**38**	95%	**t (14;16) (100%)**
16	61%	**t(14;20) (75%)**	**39**	96%	Trisomies 5 & 15 (95%)
17	62%	**t(14;16) (60%)**	**40**	97%	Deletion 14q32 (93%); deletion 16q23 (33%)
18	62%	Trisomies 9 (52%) & 15 (60%)	**41**	97%	**t(4;14) (94%)**
19	63%	Trisomies & tetrasomies 5, 9 & 15 (79%)	**42**	100%	
20	65%	**t(4;14) (70%)**	**43**	100%	Trisomy 5 (94%); tetrasomy 9 & 15 (96%); 3 x '*CCND1*' (60%)
21	72%	**t(14;16) (95%)**	**44**	100%	Deletion 14q32 (88%)
22	72%	Unbalanced *IgH* split (96%) (UIP)	**45**	100%	*IgH* split (100%) (UIP)
23	74%	**t(4;14) (100%)**			

Table 3- 2 List of 45 MGUS patients with Δ13 ordered on the basis of the percentage of PC involvement of the abnormality

For each case, concomitant numerical or structural CA are specified with the percentage of PC involvement; blank cells represent cases with Δ13 only with no other CA among the ones tested. Highlighted cells represent cases where Δ13 was present in ≤60% PC. (UIP, unidentified partner)

3.1.4.4 Association of Δ13 with other abnormalities

Table 3-3 shows the association between Δ13 and other CA.

	Δ13			Significant *P* values
CA	**MGUS**	**SMM**	**MM**	
IgHr	24/74 (32%)	23/44 (52%)	110/182 (60%)	MGUS *vs* SMM, *P*=0.05 MGUS *vs* MM *P*<0.001
t(4;14)	5/6 (83%)	13/16 (81%)	45/48 (94%)	
t(6;14)	1/2 (50%)	0/1	4/6 (67%)	
t(11;14)	1/28 (3.6%)	2/13 (15%)	21/53 (40%)	MGUS *vs* MM, *P*<0.001
t(14;16)	4/6 (67%)	3/4 (75%)	11/15 (73%)	
t(14;20)	4/8 (50%)	1/1	7/9 (78%)	
HRD	11/71 (15%)	14/68 (21%)	74/219 (34%)	MGUS *vs* MM, *P*=0.003 SMM *vs* MM, *P*=0.05
nonHRD	30/99 (30%)	23/43 (53%)	109/164 (66%)	MGUS *vs* MM, *P*<0.001 MGUS *vs* SMM, *P*=0.01

Table 3- 3 Association between Δ13 and the different CA (IgHr, *IgH* rearrangements)

The Δ13 was less frequently associated with any of the *IgH* rearrangements in MGUS than in MM (MGUS *vs* MM, 32% *vs* 60%; *P*<0.001). However, when the individual translocations were examined, no significant differences were found in the frequencies of association of t(4;14), t(14;16), or t(14;20) with Δ13, among the three diagnostic groups.

In MM, Δ13 was found in 40% of t(11;14) cases with a very high PC involvement (>85%) while only one of 28 (3.6%) MGUS cases with t(11;14) had Δ13 (*P*<0.001). In this case, only 48% PC had Δ13 while the translocation was present in all cells. In SMM only two of t(11;14) cases had Δ13 (15%), but this was not significantly different from the percentage found in MM. Both SMM patients had Δ13 in 70% PC and the translocation in 100% PC.

In this study, the presence of t(6;14) was detected in only 1-2% of patients, in agreement with other reported series [46]. Despite the small number of cases, it was notable that Δ13 was present in four of the six (67%) MM cases; in MGUS one of the two t(6;14) cases was negative for the abnormality (12% PC were found with the deletion), the other (patient 355) was positive for Δ13. In this patient (M-protein type, IgGk; M-protein level, 26 g/L) iFISH analysis showed the presence of a t(6;14) in all PC, Δ13 in 77% of PC and three copies of chromosomes 9 centromere and *CCND1* in 35% and 55% of PC, respectively. Cytogenetic analysis done at the time of MGUS diagnosis revealed one abnormal metaphase out of 48; the karyotype confirmed

the t(6;14), the monosomy 13 and the trisomies 9 and 11 detected by iFISH as well as showing additional abnormalities (one extra copy of chromosome X, trisomy 19 and monosomies 14 and 16). A second BM sample was received 21 months later; at this time the patient progressed to SMM (M-protein level, 40.9 g/L; array CGH done on this sample, see **Section 3.3**) and Δ13 was found to be present in 90% PC. The patient transformed to MM 20 months after the second sample. Interestingly, the array CGH profile obtained at the stage of SMM not only confirmed the presence of all the CA detected by iFISH and by conventional cytogenetics but also showed no additional changes. All together these findings suggest that, despite the relatively slow progression, the genetic background characterizing the PC at the MGUS stage was probably able to drive the evolution to overt disease without the need of further events. Of note was that cytogenetic analysis performed on the sample taken during the MGUS stage, revealed the presence of one abnormal metaphase. This in itself was an interesting finding, indicative of an already acquired capacity of the malignant clone to divide *in vitro*.
Among the other three pre-malignant patients with either t(11;14) or t(6;14) and Δ13 (**Table 3-3**), the only MGUS case (999) was still stable after 75 months from diagnosis. However, it has to be noted that Δ13 was only present in 48% of his PC. One SMM patient (805) died within 2 years from diagnosis and no detailed information about his follow-up was available; the second SMM patient (2906), who had a recognized MGUS phase for more than 10 years prior to evolution to SMM, rapidly progressed to MM within 5 months from SMM diagnosis. In this patient, at the time of progression to SMM, Δ13 was present in 70% of PC while, at the time of MM diagnosis, the abnormality was present in all cells. Unfortunately, no material was available from the period corresponding to the MGUS stage, therefore it is impossible to know when Δ13 was acquired by the neoplastic clone.

Interestingly, the Δ13 was found to be less frequent in MGUS and SMM with an HRD karyotype compared with MM HRD (MGUS *vs* MM, P=0.003; SMM *vs* MM, P=0.05). The lower incidence of this CA in nonHRD MGUS and SMM patients compared with MM patients reflects the fact that almost all t(11;14) patients belong to this ploidy group.

3.1.5 Overall summary of the results and discussion

The examination of a range of numerical and structural chromosomal changes in MGUS, SMM and MM patients showed that none of the CA tested were exclusive to any one diagnostic group. However, statistically significant differences were observed in the incidence of specific abnormalities between the three conditions. A significantly lower frequency of Δ13 was found

in MGUS and SMM as compared with MM. This is in accordance with the findings reported by Avet-Loiseau *et al.* [85]. The frequency of Δ13 progressively increased from MGUS to SMM to MM, suggesting a possible role of this abnormality in disease progression. The incidence of 16q23 and *TP53* deletions also showed a progressive increase from MGUS to MM ($P<0.001$ and $P=0.003$, respectively). In contrast, a similar frequency of *IgH* rearrangements was observed in the three groups. When the individual incidences of the specific translocations were compared, only t(4;14) was significantly less frequent in MGUS, in agreement with other reports [44,85]. The t(14;20) showed a higher incidence in MGUS compared to SMM and MM; Chng *et al.* [89] reported a high prevalence of this translocation in MGUS (7%) compared to MM (2%), although the number of cases studied was not documented.

Interphase FISH was used to classify patients according to their ploidy status in HRD and nonHRD. The Δ13 was found more frequently in nonHRD patients than in HRD in all three groups (MGUS, 15% *vs* 30%; SMM, 21% *vs* 53%; MM, 34% *vs* 66%), suggesting that the specific association between Δ13 and nonHRD, extensively reported in MM [46,89], is already established at the MGUS stage. These findings differ from those reported by Brousseau *et al.* [104]. In MGUS, they found Δ13 more frequently in HRD patients (11/29, 38%) than in nonHRD (3/27, 11%), although the reverse association was seen in MM. They defined ploidy by measuring the PC DNA content using Feulgen reaction and image cytometry, they detected Δ13 by iFISH and observed a nonHRD DNA content (composed by hypodiploid and diploid cases) in 46% of their MGUS patients (34.5% were diploid). It is impossible to explain this discrepancy. However, the fact that ploidy was evaluated by two different methods may be partially responsible. Pseudodiploidy and low chromosome count HRD (48 – 49 chromosomes) are potentially difficult to identify by iFISH, compared to true hypodiploidy or high chromosome count HRD. However, comparison of ploidy determined by iFISH with the actual karyotypes for those patients with abnormal cytogenetics showed that all cases but two were accurately classified. Thus iFISH misclassification of ploidy is unlikely to account for the significant difference in results between the two series.

Abnormalities of 14q32 were observed in the majority of clonal PC, independently of the stage of the disease, whereas the percentage of PC carrying Δ13 or 16q23 deletion varied significantly between MGUS, SMM and MM, with MGUS patients showing the greatest heterogeneity. In MGUS, Δ13 was often present in a sub-clone of the abnormal PC. Although low level clones in MGUS may be due to only a small proportion of the CD138 positive PC being part of the neoplastic clone, the results of this study indicate that, in these cases, the Δ13 is a later change following *IgH* translocations or multiple trisomies. Similar findings were observed for most low level 16q23 deletions in which the cells were found to be 100% positive for other CA.

The results reported here clearly show that the time of occurrence of specific abnormalities is crucially dependent on genetic context. The t(4;14), t(14;16) and t(14;20) are highly associated with Δ13 in MM [46,87,89]. The same association was observed in MGUS and SMM patients. Moreover in t(4;14) and t(14;16) cases, *IgH* rearrangement and Δ13 were found in a similar proportion of abnormal cells in the three diagnostic groups, suggesting that Δ13 occurred early in their pathogenesis. However, a different time of occurrence of Δ13 was observed in relation to t(14;20). In MGUS, four of eight cases with t(14;20) also had Δ13. In three of four cases, the proportion of cells with Δ13 was at least 30% lower than those with the translocation. The only SMM case with t(14;20) showed the *IgH* translocation in all PC and the Δ13 in only 60% of cells. In MM, seven of nine t(14;20) had Δ13, and the deletion was present in the same proportion of cells carrying the translocation. In MGUS, Δ13 appeared to originate later than t(14;20).

A striking difference between MGUS and MM was seen regarding the association of Δ13 with t(11;14). While in MM 21/53 t(11;14) cases also showed Δ13, in MGUS only 1/28 cases with the translocation were associated with Δ13 ($P<0.001$). In MM the median percentage of PC with Δ13 in t(11;14) patients was 98% while the only MGUS with both t(11;14) and Δ13 showed all PC positive for t(11;14) but only 48% PC with Δ13. The Δ13 occurred less frequently also in SMM cases with t(11;14) (two of 13); one of them progressed to MM within 5 months from the diagnosis of SMM.

The translocation t(11;14) has been related to t(6;14) on the basis of a similar biological and clinical behaviour [90]. Both translocations activate a cyclin D family member (*CCND1* and *CCND3*, respectively) and gene expression profiling studies demonstrated that cases carrying either one or the other translocation exhibited dysregulation of similar transcriptional programmes showing overlapping gene expression profiles [90,124]. The Δ13 was found in 67% of MM cases with t(6;14); interestingly in MGUS, Δ13 was present in one of the two cases with this translocation and the patient evolved to MM after 41 months from the initial diagnosis. These findings are consistent with those reported by Bochtler *et al.* [217], who used clustering analysis on patients with amyloid light chain amyloidosis, MGUS and MM, in order to detect clustering of the chromosomal abnormalities t(11;14), t(4;14), gains of 11q23 and 1q21, and Δ13. Patients with amyloidosis and MGUS showed the t(11;14) branch independent of Δ13, while t(4;14), and gain of 1q21 were grouped together with Δ13.

It is clear that MM includes a number of conditions which, despite being morphologically similar, have different underlying genetic backgrounds which are thought to dictate the clinical heterogeneity of MM. The increasing understanding of how the different CA relate to each other can contribute to explain the unique pathogenesis of the different subtypes and their dissimilar outcome.

3.2 Biological significance of *IgH* translocations associated with a poor prognosis in MM and *TP53* deletion in the context of pre-malignant conditions

3.2.1 Introduction

In MM, genetic testing has become important in diagnostic evaluation to identify patient subgroups with different prognoses. Among the five recurrent chromosomal partners involved in primary *IgH* translocations, rearrangements involving the loci 4p16 (*FGFR3/MMSET*), 16q23 (*c-MAF*) and 20q12 (*MAFB*) have been associated with a poor prognosis, while rearrangements involving the loci 11q13 (*CCND1*) and 6p21 (*CCND3*) have been associated with an intermediate risk [46,218].

As shown in **Section 3.1.4.2** (**Table 3-1**), overall, *IgH* rearrangements have been identified at similar incidences in MGUS, SMM and MM, with the only exception being t(4;14) found less frequently in MGUS. These findings support the hypothesis that *IgH* translocations represent early cytogenetic events in PC dyscrasias. The rarity of t(4;14) in MGUS suggests that it might result in a more aggressive disease characterized by a very short MGUS stage (hardly ever detectable), rapidly evolving to overt MM. However, different groups have reported long periods of stability after diagnosis (with translocation present) in patients with t(4;14) and t(14;16), suggesting that these abnormalities alone, at least in some cases, were not sufficient for progression from MGUS/SMM to MM [44,109,137,138].

Deletions of 17p13 are rare in MM and even rarer in MGUS or SMM, as shown in **Section 3.1.4.2** (**Table 3-1**). This CA has been associated with shorter survival in MM by different groups [87,108,143,145,218].

In this section the outcome of the individual MGUS and SMM patients with t(4;14), t(14;16), t(14;20) and 17p13 deletion was followed in order to better understand the clinical significance of these CA associated with a poor outcome in MM, in the context of the pre-malignant conditions.

3.2.2 Outcome of t(4;14), t(14;16) and t(14;20) in MM

The MM Cytogenetics Database investigated the outcome of the three poor prognosis *IgH* rearrangements in a large group of MM patients (n=1830, 1695 were diagnostic samples) ranging in age from 27 to 93 years (median 65, with 33% over the age of 70 and 18% over the age of 75 years). These patients were treated with a variety of standard therapies within UK hospitals; 1020 patients were entered into the MRC Myeloma IX Trial and the majority of the remaining younger patients received at least one autologous transplant.
The median follow-up was 31.7 months. As it is accepted that primary *IgH* translocations are early events occurring at the beginning of the neoplastic transformation, survival (in MM) or follow-up time (in pre-malignant cases) were calculated from the time of diagnosis, regardless of the time of FISH analysis.
The incidence of t(4;14) and t(14;16) were 11% and 3%, respectively. The t(14;20) was confirmed to be rare, with an incidence of 1.5%. All three translocations resulted in short OS in MM patients (**Figure 3-3**) and among the three translocations, patients with t(14;20) showed the shortest median OS of only 14 months.

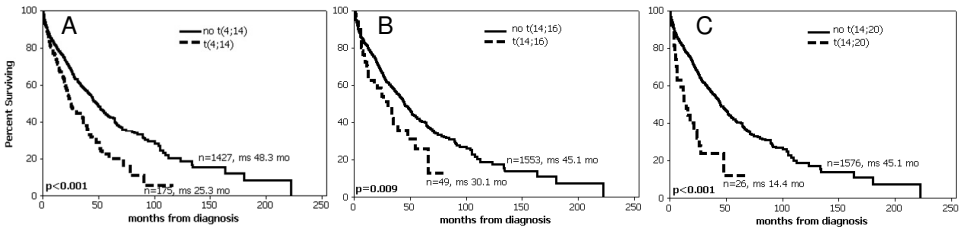

Figure 3- 3 Kaplan Meier survival curves of OS for patients with t(4;14) (A), t(14;16) (B) and t(14;20) (C)

3.2.3 Results

3.2.3.1 Characteristics of MGUS and SMM patients with the poor prognosis translocations

The outcome of 21 MGUS patients (age range: 39-84 years; median, 58 years) and 24 SMM (age range: 30-78 years; median, 60 years) positive for one of the poor prognosis translocations was examined. **Table 3-4** shows the genetic characteristics (*IgH* rearrangements, Δ13 and ploidy status) and the outcome of each patient.

Pt	Age	PP	Diagnosis	IgHt	Δ13	HRD	Stable	Time to progression/length of FU (months)
1230	56	IgAκ	MGUS	t(4;14)	√	-	**Lost**	-
2715	65	IgGκ	MGUS	t(4;14)	√	-	√	39
2664	42	IgGκ	MGUS	t(4;14)	√	-	√	44
1390	39	IgGλ	MGUS	t(4;14)	√	-	√	57
58	62	IgGλ	MGUS	t(4;14)	√	-	√	98
1275	58	IgAκ	MGUS	t(4;14)	-	√	**No**	**36 (SMM), 44 (MM)**
1494	39	IgGλ	MGUS	t(14;16)	√	-	√	17
2941	53	IgAλ	MGUS	t(14;16)	-	-	√	23
2190	66	IgGκ	MGUS	t(14;16)	√	-	√	45
1189	63	IgGκ	MGUS	t(14;16)	-	-	√	120*
837	47	IgGλ	MGUS	t(14;16)	√	-	**No**	**44 (MM)**
551	57	IgGλ	MGUS	t(14;16)	√	-	**No**	**76* (MM)**
2285	69	IgGκ	MGUS	t(14;20)	√	-	√	43
1862	43	IgGλ	MGUS	t(14;20)	-	-	√	53
1655	50	IgG	MGUS	t(14;20)	-	-	√	46
823	74	Free λ	MGUS	t(14;20)	-	-	√	54
976	78	IgGκ	MGUS	t(14;20)	√	-	√**	67
842	75	IgGλ	MGUS	t(14;20)	-	-	√	60
367	46	IgGλ	MGUS	t(14;20)	√	-	√	77
630	58	IgGκ	MGUS	t(14;20)	-	-	√	78
417	84	IgGλ	MGUS	t(14;20)	√	-	√	74
1252	56	IgGκ	SMM	t(4;14)	√	-	√	24
1342	65	IgGλ	SMM	t(4;14)	√	-	√**	9
508	61	IgGκ	SMM	t(4;14)	√	√	√	14
2849	69	IgGκ	SMM	t(4;14)	√	-	**No**	**21**
1516	77	IgGκ	SMM	t(4;14)	√	√	√	32
1925	60	IgG	SMM	t(4;14)	√	-	**No**	**33**
1107	50	IgGκ	SMM	t(4;14)	√	√	√	67
1134	37	IgGκ	SMM	t(4;14)	√	-	√	60
1385	63	IgAκ	SMM	t(4;14)	√	-	√	60
1509	46	IgAλ	SMM	t(4;14)	√	-	**No**	**6**[§]
105	68	IgGκ	SMM	t(4;14)	√	-	**No**	**7**
2295	42	IgAκ	SMM	t(4;14)	√	√	**No**	**8**
1597	63	IgGκ	SMM	t(4;14)	√	√	**No**	**11**[§]
2543	58	IgGλ	SMM	t(4;14)	√	-	**No**	**15**
1836	60	IgAκ	SMM	t(4;14)[¤]	√	-	**No**	**16**
3269	36	IgGλ	SMM	t(4;14)	√	-	**No**	**34**
331	71	IgGκ	SMM	t(4;14)	√	√	**No**	**33**
259	30	IgAκ	SMM	t(4;14)	-	-	**No**	**53**
579	78	IgGκ	SMM	t(4;14)	√	-	**No**	**78***
1073	67	IgG	SMM	t(14;16)	√	-	√	55
2198	60	IgGλ	SMM	t(14;16)	√	-	**No**	**124***
582	56	IgAκ	SMM	t(14;16)	-	√	**No**	**15**
1315	60	IgGλ	SMM	t(14;16)	√	-	**No**	**49**
866	44	IgG	SMM	t(14;20)	√	-	√	71

Table 3- 4 Disease course of MGUS (area in gray) and SMM patients with t(4;14), t(14;16) and t(14;20) (The outcome of patients who progressed is in bold)

(Pt, patient; PP, paraprotein; IgHt, *IgH* translocation; HRD, Hyperdiploid; FU, follow-up; √, presence of CA and disease stability; -, absence of CA).

Previous page, **Table 3-4**

*** Patients 1189, 2198, 551 and 579 studied at 86, 74, 66 and 27 months after diagnosis, respectively.**
§ Patients 1509 and 1597 also had deletion of 17p. ¤ Patient 1836 also had a t(8;14)(q24;q32).
**** Patients 1342 and 976 died of unrelated causes.**

3.2.3.2 Outcome of MGUS and SMM patients with t(4;14), t(14;16) and t(14;20)

The majority of MGUS patients (17 of 20, 85%) had stable disease throughout the study, with a median follow-up of 54 months (range, 17–120 months). Three MGUS patients (one with t(4;14) and two with t(14;16)) progressed to MM after 44, 44 and 142 months from diagnosis, respectively. None of the nine MGUS patients with t(14;20) progressed to MM, showing what appeared to be truly stable disease with no rise in paraprotein level after a period ranging from 43 to 78 months (median follow-up, 60 months). The presence of Δ13 in association with any of these translocations did not appear to have an effect on progression (P=1).

As expected, SMM cases showed a higher rate of progression [39], with 15 of 24 (63%) evolving to MM within a median period of 21 months (range, 6–124 months); the median follow-up for those nine patients who did not progress was 55 months (range, 9–71 months). Twelve of the 15 cases who progressed had t(4;14) and three had t(14;16); four patients (all t(4;14)) progressed within one year from initial presentation; four within the second year (three t(4;14) and one t(14;16)), while seven patients evolved to overt MM after a longer period of indolent disease, ranging from 33 to 124 months. As observed in MGUS, in SMM Δ13 did not appear to be a factor associated with progressive disease (P=0.51).

A sample from patient 2198 was received by the Database (August 2005) and tested by FISH after 74 months from initial diagnosis of SMM. After 50 months from the time of analysis (124 months from diagnosis), he progressed to MM. His serum paraprotein level did not show a constant increase but fluctuated substantially during the follow-up period (June 2002, 24 g/L; June 2005, 50 g/L; April 2007, 36 g/L). FISH results showed an *IgH* rearrangement involving *c-MAF* and loss of one copy of 22q11.22 in all cells, suggesting an early acquisition of these CA; Δ13 was also detected but only in 50% of PC, indicative of a later event. Moreover, a proportion of PC (~30%) was clearly near-tetraploid as in these cells all the CA detected in the hypodiploid state were found to be doubled-up. In this patient, the presence of the t(14;16) clearly did not lead to a more aggressive disease course as the patient experienced a period of stability with no MM-related symptoms for longer than 10 years.

The only SMM case with t(14;20) (866) retained a stable disease state until the end of this study, 71 months after diagnosis. This female patient was diagnosed with SMM at the age of 44 years, in May 2003. At that time, her IgG paraprotein level was 44.3 g/L; her BM aspirate showed a high level of infiltration with ~45% PC, while a 'squashed' trephine preparation

showed 7% PC. No Bence-Jones protein was detected and white blood cell (WBC) count, β2M and creatinin levels were normal. The magnetic resonance imaging (MRI) scan was also normal and the patient was totally asymptomatic. FISH results showed a t(14;20) in all PC and Δ13 in only a proportion of them (60%). Multiple CA were tested by iFISH (gain of 1q, deletion of 1p32.3, numerical abnormalities of chromosomes 3, 5, 7, 9, 15, *MYC* abnormalities and 17p13 deletion; probes are described in **Appendix 3**); they were all found to be negative. Conventional cytogenetics was also attempted but only 18 normal metaphases were found. At the last follow-up visit (April 2009) the patient was still totally asymptomatic: the PC percentage within the BM remained constant reaching 50% (5% greater compared with the time of diagnosis) at the last examination, by this time the paraprotein level, which fluctuated slightly during the follow-up time, lowered down to 34 g/L.

3.2.3.3 Outcome of MGUS patients with 17p13 deletion

Five MGUS patients showed deletion of 17p13. Among the four patients with available follow-up information, three progressed to MM; the fourth patient (684) died of an unrelated cause 2 months after diagnosis (**Table 3-5**).

Pt	Age	PP	Diagnosis	IgHt	Δ13	HRD	Stable	Time to progression/length of FU (months)
684¤	84	IgGκ	MGUS	-	-	yes	√	2*
2683§	54	IgG	MGUS	-	-	yes	**No**	**24**
949	75	IgAλ	MGUS	t(11;14)	-†	no	**No**	**32**
1960§	72	IgG	MGUS	UIP	√	no	**No**	**15**

Table 3- 5 Disease course of MGUS with 17p13 deletion

(Pt, patient; UIP, IgHt with unidentified partner; PP, paraprotein; HRD, Hyperdiploid; FU, follow-up; -, absence of CA)
***Patient 684 died for MM-unrelated causes (age 84 years) 2 months after MGUS diagnosis;**
¤ Patient 684 was found with ~60% PC carrying a bi-allelic 17p13 deletion.
† patient 949 showed Δ13 in 9% PC at time of presentation and 15% in a sample analyzed a year later; *TP53* deletion was present in 86% PC of the diagnostic sample.
§ Patients 2683 and 1960 had 17p13 deletion in only a sub-population of PC: 42% and 50%, respectively.

Two SMM patients had 17p13 loss (1509 and 1597) in association with t(4;14) and Δ13. Both patients evolved to MM 6 and 12 months after diagnosis, respectively. In both patients, the 17p deletion was detected in the majority of PC. However, it has to be noted that the initial diagnosis of the SMM case 1509 can be debated as he progressed to MM after only 6 months, suggesting

that the disease was fully unstable and probably more likely to be an early-MM instead of a SMM.

3.2.4 Overall summary of the results and discussion

Translocations associated with a poor prognosis in MM do not inevitably lead to aggressive disease when present in pre-malignant conditions. This is particularly true in the context of MGUS and of t(14;20) cases. In MGUS, not only a very small proportion of patients (15%) progressed, but in these patients progression occurred after more than 3 years from diagnosis. A higher proportion (63%) of SMM patients progressed to MM as compared with MGUS patients. However, those SMM cases who did not progress showed a median follow-up period almost three times longer than the median time to progression of those SMM patients who progressed. Moreover, among those SMM patients who progressed, the time to progression varied considerably. All together these observations suggest that the effect of these translocations is modulated by other factors and that these translocations alone cannot cause the establishment of a malignant phenotype.

Deletion of 17p13 is a high-risk feature in MM and presumably leads to loss of heterozygosity of *TP53* [146]. The rarity of 17p13 deletions in pre-malignant conditions is suggestive that this change is associated with the clinical manifestation of the disease. Ignoring MGUS patient 684 who died after 2 months from diagnosis from MM-unrelated causes, all MGUS and SMM cases positive for this abnormality progressed to MM. This strongly reinforces the role of 17p13 loss in the progression of these patients. However, progression was not rapid in all cases (patient 949 progressed after 32 months) and variations in time to progression were not dependent on the percentage of PC carrying the abnormality. Patient 949 had 17p13 loss in 86% of PC, while patient 1960, who progressed after 15 months, had 17p13 deletion in only 50% of PC. Interestingly, patient 949 was found with a 17p13 deletion in 86% of PC, t(11;14) in all cells and Δ13 in 9% of PC (reported as negative based on the EMN cut-off levels). A second sample sent to the Database a year later (when the patient was still MGUS) was found with 17p13.1 deletion in all cells and Δ13 in 15% of PC. This finding confirmed that Δ13 was not a technical artefact in the first sample and reinforces the idea that, in t(11;14) cases, Δ13 is a late event (in this case also slowly spreading within the neoplastic clone) and that its acquisition might be associated with disease progression.

3.3 Array CGH analysis of PC neoplasms

3.3.1 Introduction

The primary IgHt observed in MGUS and SMM seem to be in themselves insufficient to initiate overt MM, suggesting a minimal two 'hit' model for molecular pathogenesis and aetiology. Data initially derived from conventional cytogenetics [81,107,219,220] and later from high resolution SNP array and array CGH experiments [155,167,178,181,182] showed that MM cases usually have, in addition to the IgHt or HRD, multiple DNA aberrations or copy number abnormalities (CNA). It is very important to understand when, in relation to *IgH* rearrangements or HRD, these multiple CNA arise in the multi-step molecular pathogenesis and how they affect the course of the disease.
Interphase FISH, while useful to compare the frequencies of specific CA between different diagnostic groups, requires prior knowledge of the relevant abnormalities and can only test a few markers simultaneously. Whole genome approaches of investigations can overcome the limitations of FISH. However, the small amounts of material available from MGUS and SMM patients have restricted the number of meaningful studies. There are only a small number of reports using metaphase CGH to detect CA in these diagnostic groups [164,183], thus the global picture of the PC genome in MGUS and SMM remains almost unexplored.

Here, high-resolution array CGH has been used to identify the genetic changes associated with progression of MGUS and SMM to MM. Given the high genetic heterogeneity of PC neoplasms it is unclear whether different mechanisms are responsible for disease evolution dependent on the nature of the primary initiating events. To address this question within each diagnostic group, patients with different primary changes identified by iFISH were selected. Subsequently the CNA in MGUS, SMM and MM were compared and the minimally deleted/gained regions were mapped to localize potential genes involved in MM tumourigenesis.

3.3.2 Patients

Array CGH was performed on 87 samples (25 MGUS, 15 SMM and 47 MM) from 85 patients acquired through the Myeloma Cytogenetic Database (the characteristics of the patients are described in **Appendices 6** and **7**). Few patients within the Database had sequential BM samples taken at the time of MGUS or SMM diagnosis and at the time of progression to MM; patients 989 and 1581 were the only ones with enough material to perform array CGH at both time points. Patients were selected on the basis of material availability and their genetic profile previously defined by iFISH for a number of CA, including the presence of an *IgH* rearrangement and ploidy status. For each genetic group, patients at different stages of the disease were selected as shown in **Table 3-6**.
Array CGH was also used to characterize the MM cell line KMS-11.

	Cytogenetic groups							
Stage	***t(4;14)***	***t(6;14) & t(11;14)***	***t(14;16)***	***t(14;20)***	***HRD no IgHr or with t(8;14)***	***HRD Unid IgHr***	***nonHRD no IgHr***	***nonHRD unid IgHr or with t(8;14)***
MGUS	3	6	3	3	8*	0	2	0[§]
SMM	7	1	3	1	2	0	0	1
MM	11	8	8	2	12*	1	1	4[§]

Table 3- 6 Distribution of patients from the three diagnostic groups divided into different genetic classes on the basis of their iFISH profile

Patients 989 (*) and 1581 ([§]) are included in the table twice as different BM specimens were analyzed at different stages of the disease.
(Unid, unidentified; HRD, hyperdiploid; IgHr, *IgH* rearrangement).

Follow-up data was available for all MGUS and SMM and for 46 of the 47 MM patients; three MGUS, four SMM and five MM were not studied at diagnosis, for these patients follow-up was calculated from the time of analysis as it was impossible to know the exact time of acquisition of the different CNA detected by array CGH. Eight of 25 (32%) MGUS patients progressed to MM with a median follow-up of 60 months; the follow-up period for those patients who did not progress ranged between 17 and 84 months (median, 67 months). Nine of 15 (60%) SMM patients progressed to MM (time to progression: range, 7–50 months; median, 20 months); the follow-up period for those who did not progress ranged between 14 and 74 months (median, 55.5 months). For MM patients the median follow-up was 28 months; 29 of 46 (64%) died (median time, 18.5 months).

An independent group of consecutive patients (n=233) was tested by iFISH in order to define the frequencies and the eventual prognostic significance of five loci which were highlighted by array CGH analysis. The patient cohort consisted of 37 MGUS (median age: 73 years, range 50-90 years), 13 SMM patients (median age: 65 years, range 30-85 years) and 183 MM patients (median age: 64 years, range 35-88 years). Of the 183 MM patients, 135 (74%) were studied at diagnosis. In MM, median survival was 34 months (range, 0-84 months) when calculated from the time of cytogenetic analysis and 46 months (range, 0-136 months) when calculated from time of diagnosis.

3.3.3 Methods

3.3.3.1 Conventional cytogenetics

Cytogenetic studies were performed after density gradient separation of BM samples and PC percentage assessment as described in **Sections 2.2.3** and **2.2.4**. Cytogenetic cultures were set up on samples from 15 MGUS, 11 SMM and 39 MM patients as described in **Section 2.3**.

3.3.3.2 Array CGH

3.3.3.2.1 Genomic DNA

Patient genomic DNA. Genomic DNA was extracted from purified PC stored as a dried pellet (seven patients), purified PC stored in Carnoy's fixative (78 patients) and non-purified fixed cells derived from cytogenetic cultures of 24 hours (patient 2314) or 3 days (patient 1890) as described in **Section 2.5**. For the two latter MM patients, the PC percentage was deduced by testing the cell suspension by iFISH for a marker known to be abnormal in these cases; both patients were tested for the t(14;20). The percentage of PC carrying the translocation was 35% in patient 2314 and 38% in patient 1890. For the other cases tested, the percentage of PC after purification was >80%. DNA from the MM cell line was extracted from a dried pellet.

Control genomic DNA. Pooled DNA extracted from the peripheral blood of ten healthy donors, sex-matched to the test sample, was used as a reference (Promega, UK).

3.3.3.2.2 Array CGH platform

Human genome CGH 244k microarrays (Agilent Technologies, USA) were used as described in **Section 2.6**. A minimum quantity of DNA recommended for each test is 500ng.

3.3.3.2.3 Strategies for handling samples with small amount of DNA

For some MGUS and SMM patients, the amount of DNA recovered after purification ranged from 150ng to 500ng, which is below the minimum recommended amount. In order to be able to use the material from these patients, array CGH of amplified-DNA was attempted. To assess this approach, whole-genome amplification (WGA) was performed on good quality DNA extracted from a MM patient (342) previously tested by array CGH on non-amplified material.

Whole-genome amplification. WGA non-PCR-based, using ϕ29 DNA polymerase and random hexamer primers, was performed on DNA from patient 342 and a sex-matched control following the protocol described in **Section 2.5.7**; this method suggested amplification of the DNA for 16 hours in order to obtain maximum yields.
After the amplification reaction and before DNA labelling, 100ng of amplified DNA, measured by optical density at 260/280 nm, was analysed by multiplex PCR. The PCR reaction was performed with five primer sets which produce 100, 200, 300, 400 and 600 bp fragments from non overlapping target sites in the genes *TBXAS1* (exon 9; chr 7q33-34), *RAG1* (exon 2; chr 11q13), *PLZF* (exon 1; chr 11q23) and *AF4* (exons 3 and 11; chr 4q21) (primers are described in **Appendix 2**) [221]. Reagents were added to a 50µl total reaction with final concentrations: 1x Buffer II (Applied Biosystems, UK), 0.2mM dNTPs (Pharmacia, UK), 2.0mM MgCl2 (Applied Biosystems, UK), 1U AmpliTaq Gold (Applied Biosystems, UK), 2.5pmol each primer of primer mix A, 5pmol each primer of primer mix B, 100ng DNA. The cycling conditions were: 7 min 94˚C, 35 cycles each of 1 min 94˚C, 1 min 60˚C and 1 min 72˚C, followed by 7 min 72˚C ending at 4˚C. 10µl of each sample was analyzed on 1.5% TBE agarose ethidium bromide-stained gel, as described in **Section 2.4.3.2.4**.

Array CGH using <500ng non-amplified DNA. 200ng non-amplified DNA from patient 342 was used to set up array CGH; the same amount of control DNA was used. The array profile was compared with those obtained using 1.5µg non-amplified DNA and 2µg amplified DNA.

3.3.3.2.4 Array CGH analysis

The quality of the array hybridizations was expressed as a derivative log ratio spread (DLRS) calculated by the Agilent CGH Analytics software; this parameter reflects the spread of $\log_2$ ratio differences between consecutive probes along all chromosomes. The analysis of the array CGH data was performed as described in **Section 2.6.6**. Gains and losses were defined using a 500 kb weighted moving-average window and the ADM-2 algorithm of the CGH Analytics software with a threshold of 6.0. An abnormality was defined as recurrent when detected in more than three patients. CNV were identified with a database integrated into the Agilent CGH Analytic software, with the Database of the Genomic Variants and with Ensembl (URL in **Appendix 1**) and excluded from further analysis.

3.3.3.3 FISH

In order to confirm the presence of selected CNA detected by array CGH, FISH was performed on interphase or metaphase preparations using specific commercial and home-made probes. Interphase-FISH was also performed on a large and independent patient cohort, as described in **Sections 2.4.4** to **2.4.9**, in order to define the frequencies and prognostic significance of five loci highlighted by array CGH. Three loci encompassed genes involved in the NF-κB pathway: *BIRC2/3* (11q22.1), *TRAF3* (14q32.32) and *NIK* (17q21.31); the other two loci encompassed *CDKN2A/2B* (9p21.3) and *CDKN1B* (12p13.1). For 9p deletions, a BAC for *CDKN2A/2B* was combined with a BAC mapping *PAX5* at 9p13.2. The detection of *BIRC2/3* and *TRAF3* deletions was performed with a combination of BAC and fosmid clones selected in order to distinguish small and larger deletions. *NIK* abnormalities were detected using a fusion strategy involving four different BAC clones mapping 17q21.31. *CDKN1B* abnormalities were detected with the use of a single fosmid (all probes are described in **Appendix 3**).

3.3.4 Results

3.3.4.1 Array CGH Comparison between non-amplified DNA (standard *vs* small quantity) and amplified DNA

100ng DNA at high integrity from the patient and the control were amplified for 2, 4, 6, 8, 16 hours and purified. The amplified genomic DNA was analysed by 2% agarose gel

electrophoresis to visualize the DNA size distribution; the majority of fragments showed a size ranging between 200bp and 500bp, as recommended by the company.
The DNA quantification using the NanoDrop ND-1000 UV-VIS Spectrophotometer (see **Section 2.5.3**) showed a progressive increase in the amount of amplified DNA corresponding to longer incubation reactions. The amplification yields for the patient and the control were respectively: 0.5µg and 2.6µg at 2 hours, 1.2µg and 4.6µg at 4 hours, 2.7µg and 5.3µg at 6 hours, 2.3µg and 6.3µg at 8 hours, 4.9 and 7.4 at 16 hours.
Multiplex-PCR was used to test the quality of the amplified DNA. All DNA except the 600bp fragment from the 16-hour reaction of the patient showed all five PCR products (**Figure 3-4**). After 8 hours, more than 2µg amplified-purified DNA was generated for both the patient and the control. In order to minimize amplification bias, the 8-hour-amplified DNA samples from the patient and the control but not the 16-hour ones (recommended by Agilent) were used.

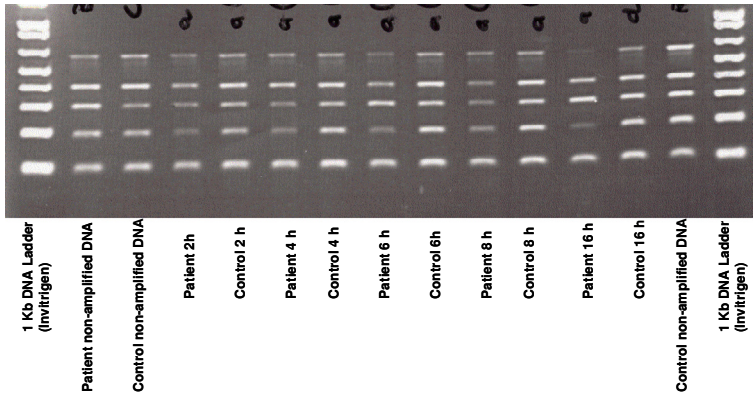

Figure 3- 4 Multiplex-PCR reveals whether the 100, 200, 300, 400 or 600bp fragments were amplified from 100 ng total genomic DNA (patient and control); for the 16-hour patient sample, the 600bp fragment was not visible

The array-profile obtained using 200ng non-amplified DNA was highly comparable to the one set up with 1.5µg non-amplified DNA (**Figure 3-5**). The two array CGH experiments were analyzed independently: an identical number of CNA and breakpoints were detected. In contrast, the array profile obtained using 8-hour amplified DNA was of poor quality (DLRS: 0.9), characterized by a high level of noise which made the accurate detection of CNA almost impossible. This was probably due to a large variation in the extent of amplification occurring between different genomic regions [222]; this amplification bias seemed to totally alter the information content of the DNA.

As a consequence of these findings, for all samples with <500ng DNA, array CGH was set up using non-amplified material.

CNA, detected by array CGH, were compared with the karyotype (if informative) or with the FISH results obtained using an extensive panel of probes. No discrepancies were found when array CGH was compared with FISH. Apparent discrepancies found when comparing array CGH and karyotype appeared to arise from misinterpretation of the conventional cytogenetics analysis due to the high complexity of the karyotypes.

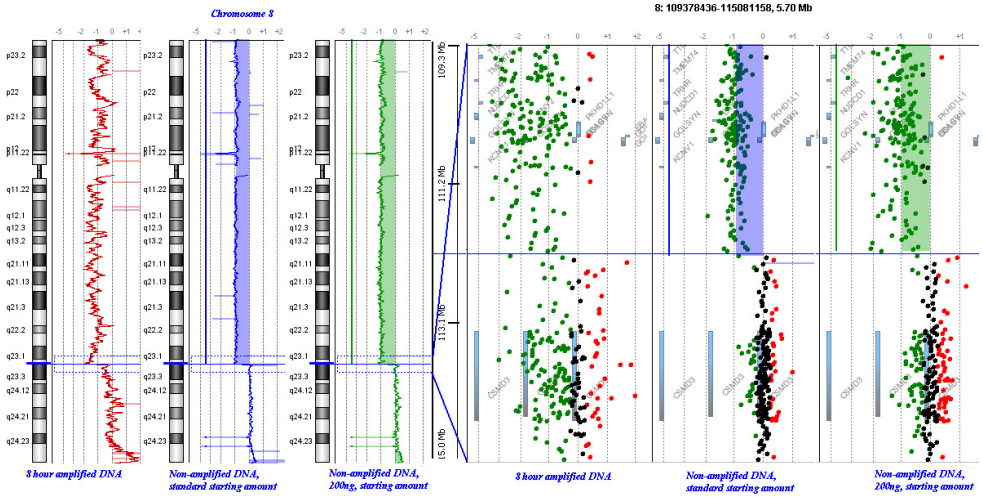

Figure 3- 5 G-banded idiogram and array CGH profiles of chromosome 8 obtained from hybridization of amplified and non-amplified DNA (standard amount *vs* 200ng) of patient 342. The plot of calls for every nucleotide of the region 8q23.2-q23.3 is shown for each array experiment; note the 'noisy' profile of amplified compared to non-amplified DNA

3.3.4.2 Conventional cytogenetics

Conventional cytogenetics revealed an abnormal karyotype in two of 15 MGUS, two of 11 SMM and 31 of 39 MM patients (karyotypes are described in **Appendices 6** and **7**); one MM case failed to show metaphases and the remaining cases had a normal karyotype.

Formatted: Bullets and Numbering

3.3.4.3 Array CGH

3.3.4.3.1 Overall abnormalities

Array CGH detected CNA in all but one MM sample (patient 1890); metaphase analysis for this patient showed the presence of two balanced rearrangements and no CNA (see karyotype in **Appendix 7**). Overall a total of 1327 CNA, defined as discrete segments showing copy number variation consistent with loss or gain, were detected with a median of 8 per case (range, 1-24) in MGUS, 11 per case in SMM (range, 5-19) and 19 per case in MM (range, 0-63) (array CGH results for each patient are described in **Appendix 8**; a graphical representation of CNA of all chromosomes for all patients is shown in **Appendix 9**).

Diagnostic group	Genetic group	Number of patients	Total number of gains (Average)	Total number of losses (Average)
MGUS	t(4;14), t(14;16) & nonHRD	8	31 (3.9)	52 (6.5)
	t(14;20)	3	1 (0.3)	13 (4.3)
	t(6;14) & t(11;14)	6	5 (0.8)	6 (1)
	HRD	8	71 (8.9)	26 (3.3)
SMM	t(4;14), t(14;16) & nonHRD	11	58 (5.3)	60 (5.5)
	t(14;20)	1	1	4
	t(6;14) & t(11;14)	1	3	3
	HRD	2	17 (8.5)	5 (2.5)
MM	t(4;14), t(14;16) & nonHRD	24	143 (6)	373 (15.6)
	t(14;20)	2	5 (2.5)	6 (3)
	t(6;14) & t(11;14)	8	83 (10.4)	85 (10.6)
	HRD	13	178 (13.7)	93 (7.2)

Table 3- 7 Number of CNA found in MGUS, SMM and MM by array CGH

Table 3-7 shows that, for all diagnostic groups the number of CNA progressively increased from MGUS to MM. The greatest difference was noted in patients with t(6;14) and t(11;14): in MGUS they showed an average of gains and losses of 0.8 and 1, respectively, while in MM these averages increased to 10.4 and 10.6, respectively. MGUS and SMM patients with t(14;20) also showed a relatively low number of CNA. One (1890) of the two MM patients with this translocation showed no CNA (confirmed by metaphase analysis); the second case showed six losses and five gains. Unfortunately no material from other MM cases with this translocation was available. However, within the Database 16 other MM patients with t(14;20) and abnormal

cytogenetics were found: the majority of them showed complex karyotypes with multiple structural and numerical changes (karyotypes are described in **Appendix 10**); therefore it is possible that the number of CNA detected by array CGH for these two patients was not entirely representative of MM patients with this translocation.
In all diagnostic groups, patients characterized by one of the poor prognosis *IgH* translocations or by a hypodiploid karyotype showed a higher average number of losses compared to gains, while in the HRD groups the opposite was true. Patients with t(11;14) showed a similar average of gains and losses in the three diagnostic groups.

In MGUS, there was a clear association between a high number of CNA (defined as >5) and disease progression to MM (**Figure 3-6**): none of the 11 MGUS patients with ≤5 CNA, regardless of the genetic group, progressed to MM while eight of 14 patients with >5 CNA evolved. The only SMM case (866) with ≤5 CNA (with t(14;20)) also showed no evidence of disease evolution after 71 months, as described in **Section 3.2.3.2**.

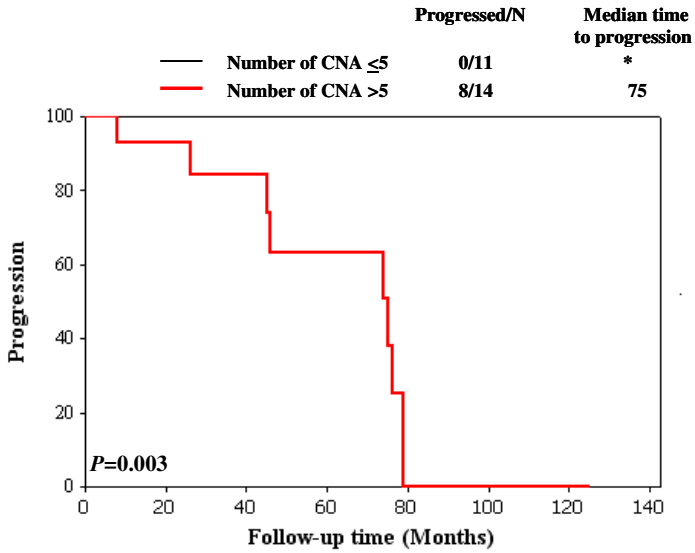

Figure 3- 6 Kaplan-Meier analysis of progression in MGUS displayed in relation to the number of CNA (≤5 or >5) per case detected by array CGH (Follow-up was calculated from the time of analysis)

Homozygous deletions (HD) and amplifications (defined as ≥6 copies) were very rare in pre-malignant patients. One HD but no amplified regions were detected in MGUS; one HD and one amplification were found in two SMM patients, while 25 HD and 19 amplifications were found in 20 MM patients; two HD were detected in the cell-line KMS-11. Five HD were found in more than one patient, while the only recurrent amplified region was located at 8q24.21 and

involved the *MYC* gene (**Table 3-8**). As HD and amplifications may be secondary events, they often involve only a sub-clone of the tumour population. In these cases, it may be difficult to detect them by array CGH as the $\log_2$ ratio for each locus represents the average of the number of copies for all cells, resulting in an overall dilution of the chromosome aberration calls. Therefore it is important to verify cases with suspicious high level gains or borderline HD by iFISH as they may hide sub-clonal amplifications or HD. One example was the amplification found at 22q13.1 in the SMM patient 1252. This CNA was initially interpreted as high level gain but iFISH showed amplification of this region in less than 50% of PC, with four to six copies of the cosmid probe for *PDGFβ* and >seven copies of the BAC probe centromeric to *PDGFβ* (probes are described in **Appendix 3**).

Patient	HD		Amplification	
	Chromosomal region	Mb position	Chromosomal region	Mb position
2715 (MGUS)	13q21.32	66239860 -66369533	-	-
1252 (SMM)	-	-	22q12.3-q13.2§	35160638 - 38954220
582 (SMM)	14q32.32§	102295758 - 102628399	-	-
375 (MM)	-	-	16q11.2 16q22.1 16q22.1-q22.2 16q22.2	45018886 – 46076516 66562569 – 68358572 69016058 – 69409552 69753919 - 70471343
665 (MM)	1p33-32.3§ 1p22.2	50131470 -51875603 89279518 - 90847519	-	-
719 (MM)	13q14.2 Xp22.11 Xq21.32	47791842 – 47995068 21341117 – 21372735 91645681 - 91688206	-	-
1875 (MM)	13q21.1	54752753 – 55074025*	-	-
342 (MM)	20q11.23 Xq21.32	34837268 – 34974263 91404795 - 91632202	-	-
374 (MM)	1p32.3§	51121283 - 51254925	-	-
1148 (MM)	13q34	63162766 – 63242385 *	17p13.2§	4735005 - 5683523
1336 (MM)	1p33-p32.3§ 11q22.3§	49905463 - 51755900 101061854 - 103024486	-	-
282 (MM)	16q23.1	77227769 - 77263523	17p12-p11.2§	15796976 - 17105002
309 (MM)	11q22.3§	97013770-103605664	-	-
619 (MM)	13q14.2 16q12.2 22q13.1	47817280 – 47928395 52181870 – 52500340 37683612 - 37709985	-	-
2906 (MM)	9p13.2	21998596 - 22007894	-	-
666 (MM)	-	-	20q13.33§	60474168 - 61929664
3325 (MM)	-	-	**8q24.21§**	**128132928 - 130339406**
1524 (MM)	-	-	**8q24.21§**	**127508344 - 128892972**
1213 (MM)	3q26.32 6q22.1 13q21.1 Xp11.3 Xq21.1	177442074 – 179423743 116673147 – 116710377 55200444 – 55365810 * 44678212 – 44827435 79721622 - 79876033	-	-
1776 (MM)	-	-	7p15.2	26931500 - 26987201
1512 (MM)	-	-	8q21.11 8q21.12-q21.13 8q21.3 **8q24.21§** 11q12.2-q12.3 11q13.2-q13.4§ 15q22.31 21q11.2	75628165 - 76191463 79745146 – 81155223 87369697 - 87865857 **128767860 - 129988129** 60447455 – 61203003 68972488 – 70439619 62778502 - 64490079 14294323 – 14489561
491 (MM)	14q32.32§	102408026 - 102592287	-	-
932 (MM)	16q12.1	49297007 - 49428333	-	-
KMS-11 (cell line)	1p33-p32.3§ 16q23.1	47928974 – 51949445 76737934 - 77794243	-	-

Table 3- 8 List of all HD and amplifications detected by array CGH

Recurrent HD are highlighted using the same colour. The only recurrent amplified region at 8q24.21 is indicated in red

*** no genes involved in the CNA. § CNA validated by FISH.**

Comparing the array CGH profiles among the three diagnostic groups, significantly higher frequencies of loss of 1p, 6q, 8p, 9p, 12p, 16q, 17p, 18p and gains/rearrangements of 8q24.21 were found in MM compared with MGUS and SMM. In **Table 3-9**, for each pre-malignant patient, the presence or absence of specific CNA is shown. CNA that were found to be totally absent in MGUS/SMM (i.e. 9p21.3 and 12p13.1 deletions) were not considered in this table.

CA	RegID	Diag	Progr	Age	Time to progr/ FU from diagnosis (months)	Time to progr/FU from analysis (months)	1q21 gain	1p21-p22 loss	6q25 loss	8p22-p21 loss	8q24 changes	16q23.1 loss	17p13 loss	TRAF3 HD
4;14	2715	MGUS	No	65	39	39	√							
4;14	2664	MGUS	No	42	44	44	√							
4;14	3318"	MGUS	No	85	17	17	√	√	√	√			√	
4;14	105	SMM	Yes	68	7	7	√							
4;14	1252#	SMM	No	56	24	24		√		√*				
4;14	259	SMM	Yes	30	53	31						√		
4;14	331	SMM	Yes	71	33	33	√							
4;14	508	SMM	No	61	14	14								
4;14	2849	SMM	Yes	69	21	21	√			√*				
4;14	1836	SMM	Yes	60	16	16	√		√		√			
14;16	837	MGUS	Yes	47	46	46	√							
14;16	1494	MGUS	No	39	17	17								
14;16	1189	MGUS	No	63	125	35								
14;16	582	SMM	Yes	56	15	15						√		√
14;16	2198	SMM	Yes	60	124	50						√		
14;16	1073	SMM	No	67	55	55	√			√*		√		
14;20	417	MGUS	No	84	74	74								
14;20	976	MGUS	No	78	67	67								
14;20	367	MGUS	No	46	78	78	√					√*		
14;20	866	SMM	No	44	71	71								
11;14	844	MGUS	No	57	67	67								
11;14	999	MGUS	No	77	74	74								
11;14	855	MGUS	No	83	17	17								
11;14	795	MGUS	No	76	69	69								
11;14	610	MGUS	No	59	84	84								
11;14	695	MGUS	No	71	156	72						√		
11;14	355	SMM	Yes	66	41	20						√*		
nonHRD	698	MGUS	Yes	74	75	75	√	√						
nonHRD	2326	MGUS	No	72	47	47								
nonHRD	1581	SMM	Yes	55	29	15	√		√			√		
HRD	2879	MGUS	No	83	26	26								
HRD	865	MGUS	No	51	71	71								
HRD	528	MGUS	Yes	75	45	45	√				√			
HRD	911	MGUS	Yes	61	8	8								
HRD	1473	MGUS	Yes	45	249	26								
HRD	121	MGUS	Yes	69	79	79								
HRD	396	MGUS	Yes	77	76	76								
HRD	989	MGUS	Yes	67	74	74		√	√	√				
HRD	1822	SMM	No	36	56	56								
HRD	403	SMM	No	57	74	74								

Table 3- 9 For each pre-malignant patient the disease course, follow-up time and presence of specific CNA is shown (patients who progressed are highlighted in blue)

Previous page, **Table 3-9**

(√, presence of CNA; blank cell, absence of CNA; Progr, progressed; FU, follow-up; Diagn, diagnosis; HRD, hyperdiploid; nonHRD, non-hyperdiploid). CNA that were not detected in any of the MGUS/SMM have not been included in the table. * The CNA was present in a sub-population of PC. ¤Patient 3318 died after 17 months from diagnosis for MM-unrelated causes. However, her paraprotein was beginning to rise and atypical PC were detected in her BM. # Patient 1252 moved to USA 24 months after diagnosis; although he remained asymptomatic, his paraprotein was rising considerably.

3.3.4.3.2 Chromosome 1 abnormalities

Chromosome 1 was one of the most highly rearranged chromosomes, usually characterized by gain of 1q and loss of 1p (**Figure 3-7**). On 1q, a minimal region of gain was identified at 1q12-q23.2 (141465960Mb – 157108464Mb). Gains of this region were detected in seven of 25 (28%) MGUS, six of 15 (40%) SMM and 21 of 47 (45%) MM.

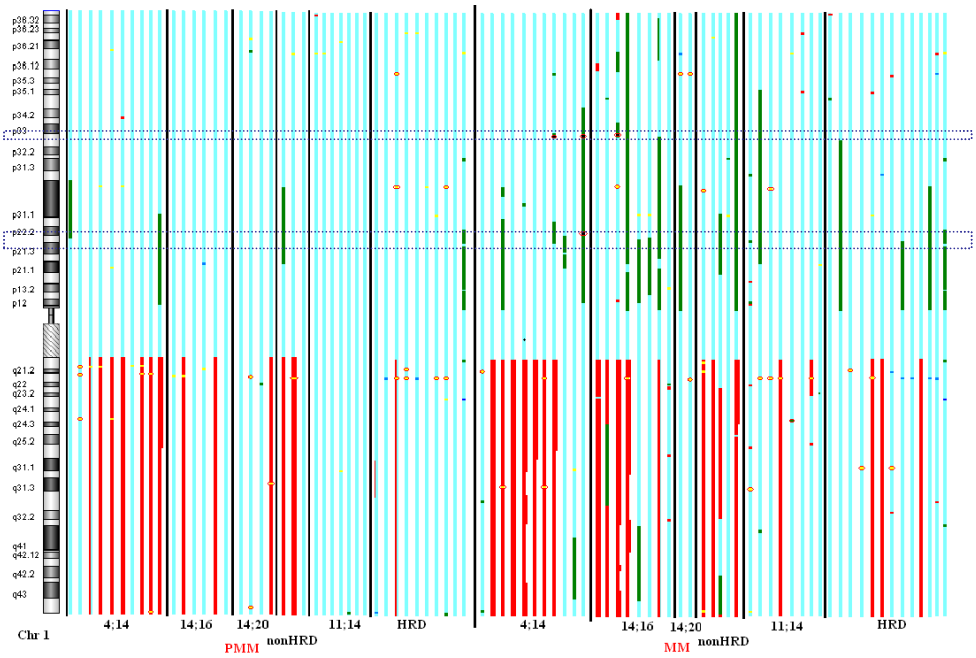

Figure 3- 7 Graphical representation of CNA of chromosome 1 for all patient groups

The 850-band idiogram of the G-banding pattern of the chromosome is shown on the left. Vertical blue lines correspond to each patient; red bars = gains; thicker red bars = gains of two extra copies; green bars = mono-allelic losses; black areas circled in red = HD; yellow and light blue areas = CNV, respectively losses and gains. Black bars divide the different genetic groups. Black vertical lines separate the different genetic groups. Two common minimally deleted regions on 1p are defined by grey dotted rectangles.

Even though the frequency of 1q21-q23.2 gain increased from MGUS to MM, this difference was not statistically significant (MGUS *vs* MM, *P*=0.21). In MGUS/SMM, 1q21-q23.2 gain was rare in HRD (1/10, 10%), while it was frequently detected in the t(4;14) group (7/10, 70%). The same association was found in MM patients with t(4;14) (7/11, 64%), with five patients showing two extra copies of the whole arm or part of it.
No statistically significant correlation was found between gain of 1q21-q23.2 and progression to MM, either in MGUS or in SMM. Three of the eight MGUS patients who progressed and four of the 17 patients who did not progress showed gain of 1q21-q23.2 (*P*=0.64). Within the SMM group, five of the nine patients who progressed and one of the six who did not progress had the abnormality (*P*=0.29). Among the five patients with 1q21-q23.2 gain and no evidence of progression, four had a follow-up of more than 3 years.

Deletions of 1p were highly complex in this patient cohort with some patients showing multiple interstitial losses. Eighteen of 47 (38%) MM patients were found with 1p deletions compared to three of 25 (12%) MGUS and one of 15 (7%) SMM patients (MGUS *vs* MM, *P*=0.028). These deletions were variable in size and had different breakpoints; in only one MM case was the whole arm deleted. In MM, three HD encompassed the same chromosomal region at 1p32.3-p33 (highlighted by the upper blue rectangle in **Figure 3-7** and in more detail in **Figure 3-8**): patient 374 (51121283Mb – 51254925Mb), patient 665 (50131470Mb – 51875603Mb) and patient 1336 (49905463Mb – 51755900Mb). All three HD encompassed the genes *CDKN2C/p18* and *FAF1*. The cell line KMS-11 also showed HD at this locus (47928974Mb – 51949445Mb). Three MM patients had hemizygous deletions involving this region, while no deletions were found in the pre-malignant cases.

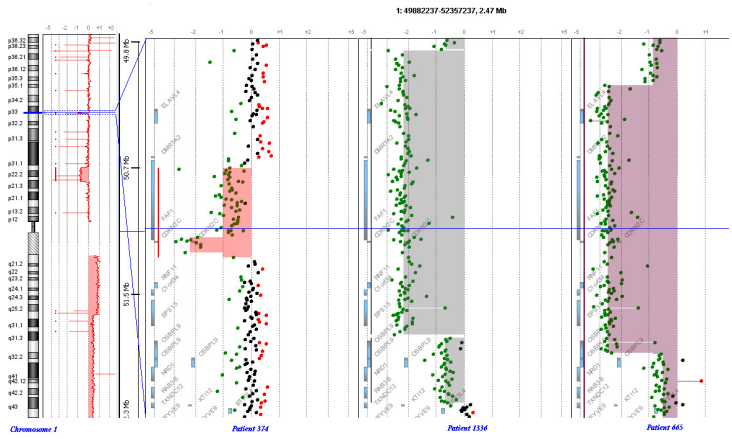

Figure 3- 8 Array CGH profile of the chromosomal region 1p32.3-p33 of patients 374, 665 and 1336

Previous page, **Figure 3-8**

The G-banded idiogram of chromosome 1 (on the left) and the plot of 'calls' for every oligonucleotide (on the right) of the selected chromosomal region are shown for the three patients

A second region of 1p was found to be deleted in 16 of 47 (34%) MM cases. It involved the chromosomal bands 1p21.3-p22.1 (93524365Mb – 95160822Mb) (highlighted by the bottom blue rectangle in **Figure 3-7**) and included the genes: *DR1, FNBP1L, BCAR3, DNTTIP2, GCLM, ABCA4, ARHGAP29, ABCD3, F3*, *SLC44A3, CNN3* and has-mir-760. No HD were detected. Within the pre-malignant group, all four cases (MGUS patients: 698, 989, 3318; SMM patient: 1252) with 1p losses encompassed this region. Two MGUS patients progressed to MM after 74 (989) and 75 (698) months; the MGUS patient 3318 died of MM-unrelated causes 17 months after diagnosis; however, her paraprotein level was steadily increasing. Patient 1252, despite lacking any clinical manifestation after 24 months (at this time he moved to the USA), showed a notable rise in paraprotein: in January 2004 (time of diagnosis), 16g/L; in January 2006, 25g/L (**Table 3-9**).

3.3.4.3.3 Chromosome 6 abnormalities

Chromosome 6 abnormalities were mainly characterized by gains of the short arm and deletions of the long arm (**Figure 3-9**). Deletions of 6q were observed in 20 of 47 (43%) MM patients; no specific association was seen between this abnormality and the genetic groups. Most deletions were large, with different break-points. Four common minimally deleted regions were found (highlighted by blue rectangles in **Figure 3-9**): 6q16.1 (97117200Mb – 97207730Mb, n=10); 6q16.3 (102293569Mb – 102493547Mb, n=10); 6q22.31 (124201765Mb – 124957157Mb, n=11); and 6q25.1-q25.2 (151458397Mb – 154443800Mb; n=16). The latter region contained 15 genes between *MTHFD1L* and *OPRM1*, including *MYCT1, FBXO5* and *MTRF1L*.
Deletions of 6q were detected in two MGUS (3318 and 989) and two SMM (1836 and 1581) patients and involved either both or only one (6q25.1-q25.2) of the two most telomeric common minimally deleted regions identified in MM. For the region 6q25.1-q25.2, the difference in frequency between MGUS and MM was statistically significant (P=0.020). Patients 989, 1836 and 1581 progressed to MM after 74, 16 and 15 months, respectively; patient 3318 (MGUS; 85 years old), as stated in **Table 3-9**, died of MM-unrelated causes 17 months after diagnosis although her paraprotein level had been rapidly rising and atypical PC were already present in her BM.

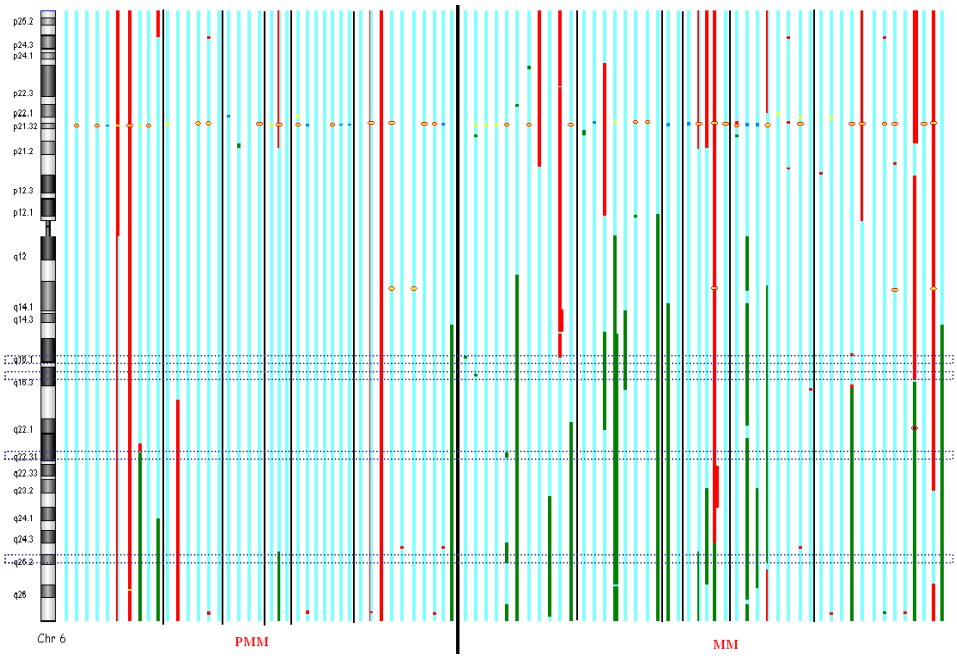

Figure 3- 9 Graphical representation of CNA for chromosome 6 for all patient groups

The 850-band idiogram of the G-banding pattern of the chromosome is shown on the left. Vertical blue lines correspond to each patient; red bars = gains; thicker red bars = gains of two extra copies; green bars = mono-allelic losses; black areas circled in red = HD; yellow and light blue areas = CNV, respectively losses and gains. Common minimally deleted chromosomal regions on 6q are defined by grey dotted rectangles. Black vertical lines separate the different genetic groups.

3.3.4.3.4 Chromosome 8 abnormalities

Deletions on 8p were large and shared a common minimally deleted region defined by the chromosomal bands 8p22-p21.2 (17652178Mb – 26788320Mb). Losses of this region were detected in two MGUS (8%), three SMM (20%) and 15 MM (32%) patients (MGUS *vs* MM, *P*=0.022). The three SMM patients showed this CNA to be present in only a sub-population of PC. One of the two MGUS patients with this CNA progressed to MM after 74 months, while the other (3318, see **Table 3-9**) died of MM-unrelated causes after only 17 months. Among the three SMM patients: one progressed to MM after 21 months, one remained stable after 55 months and the third (1252) despite lacking any clinical manifestation after 24 months (at this time he moved to the USA), showed a notable rise in paraprotein (**Table 3-9**).

CNA involving 8q were mainly represented by abnormalities involving the band 8q24.21 where the *MYC* gene is located. In the MM group a total of 12 CNA involved this locus (**Figure 3-10A**): small interstitial duplications were found in five patients (**Figure 3-10 B-C-D**) (minimally gained region, 128822396Mb – 128847262Mb; all were confirmed by FISH with the BAC RPI-80K22 described in **Appendix 3**). FISH using the *MYC* break-apart and the LSI IgH/MYC probes was carried out on all samples; one of the patients with small interstitial gains was also found to be positive for a t(8;14)(q24;q32); another patient gave a positive result with the *MYC* break-apart . Larger gains involving this region were found in three cases (297, 756, 2458) and amplifications in another three cases (1524, 3325, 1512). Patient 1037 was found to have a large deletion involving almost the entire chromosome 8 (8pter-q24.21; 61327Mb – 128470644Mb) terminating just proximal of the *MYC* locus. FISH confirmed the presence of a structural rearrangement at 8q24.21, resulting in an unbalanced t(8;14) translocation. Patient 314 was found to be positive for a *MYC* rearrangement by iFISH in the absence of CNA involving its locus. In total, 13 MM patients (28%) displayed *MYC* abnormalities either by FISH and/or array CGH; interestingly seven of these 13 (54%) cases were HRD (*P*=0.026). Only one MGUS patient was found with *MYC* abnormalities (MGUS *vs* MM, *P*=0.003). This MGUS case (528) showed an interstitial deletion involving the bands 8q24.13-q24.21 (125794416Mb – 128611131Mb) in a sub-population of PC. The deletion was immediately proximal of *MYC* and a *MYC* break-apart was confirmed by iFISH in 40% of PC. This case was HRD and had no *IgH* rearrangements; he progressed to MM after 45 months. The SMM patient 1836 (with a t(4;14)) was found to be positive for a t(8;14) by iFISH in all PC, with no CNA involving 8q24; the patient progressed to MM after 16 months.

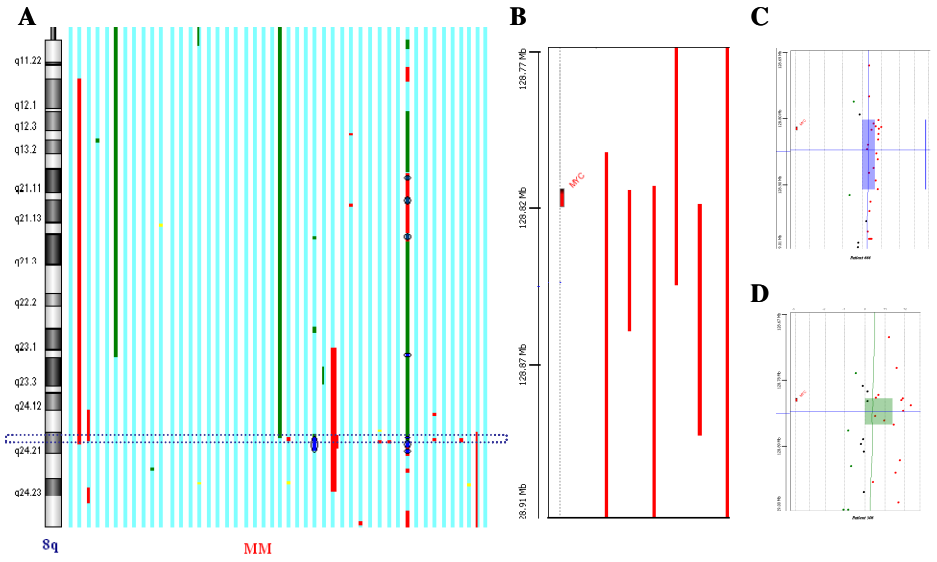

Figure 3- 10 Graphical representation of CNA for chromosome 8q for all MM patients (A); diagram showing the megabase positions of copy number gains involving *MYC* at 8q24.21, identified in six MM patients by array CGH (patients from left to right: 666, 506, 375, 756, 830, 1213) (B); Patient 666 in detail (C); Patient 506 in detail (D)

In Figure 3-10 (A) Vertical blue lines correspond to each patient; red bars = gains; thicker red bars = gains of two or more extra copies; green bars = mono-allelic losses; bright blue areas circled in black = amplifications. Yellow areas = CNV, losses. The common minimally gained region at 8q24 is indicated by the blue dotted rectangle.

Two of the three MM cases with amplification at 8q24.21 had t(11;14) (1524 and 3325); the third (1512) was HRD with no *IgH* rearrangements but with multiple other amplified regions including 11q13, where the *CCND1* gene is located. Both the t(11;14) and the 11q13 amplification resulted in *CCND1* overexpression; therefore in this patient cohort all cases with *MYC* amplification were associated with *CCND1* overexpression.

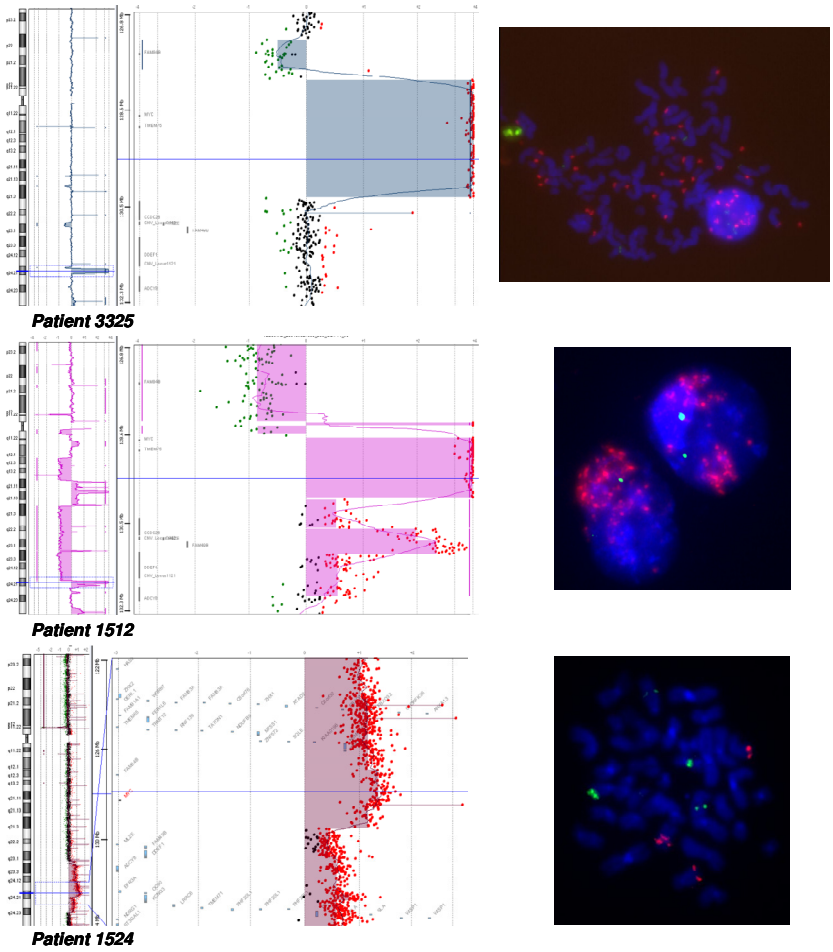

Figure 3- 11 Array CGH profile of the chromosomal region 8q24 in three patients carrying the amplification

The G-banded idiogram of chromosome 8 and the plot of 'calls' for each oligonucleotide of the selected chromosomal region are shown for the three patients on the left. On the right, images of metaphase and iFISH *MYC* amplification detected using the LSI IgH/MYC probe combination (*MYC* in sp red, *IgH* in sp green).

In the three cases, the level of *MYC* amplification by array CGH was remarkably different, as shown in **Figure 3-11**. Patient 3325 was found to have a 2.2 Mb amplicon containing only *MYC* and *TMEM75* (the smallest amplicon); the level of amplification was represented by a $\log_2$ ratio = +4. FISH showed typical amplification in the form of DM with 2 to ~100 copies of *MYC* in 80–100% of PC. Patient 1512 showed a complex pattern of gains and losses along 8q, with two main areas of amplification at 8q21.1 and 8q24 (128767860Mb – 129988129Mb); the level of amplification was represented by a $\log_2$ ratio = +4; iFISH showed 80% of PC with multiple

signals localized in two main clusters of amplification, suggestive of HSR; in this case iFISH and array CGH showed a similar level and pattern of amplification for *CCND1*. In patient 1524, array CGH showed a large region (8q23.2-q24.23) of variable high level gain, with part of 8q24.21 (127408340Mb – 128892972Mb) showing the highest level of gain represented by a $\log_2$ ratio = +1.5. The level of gain detected by array CGH was not suggestive of amplification; however, FISH for *MYC* detected the presence of seven - ten DM in 32% of PC. The presence of DM in a minority of PC resulted in an overall dilution of the chromosome aberration calls.

3.3.4.3.5 Chromosome 9 abnormalities

Eight MM patients showed deletions of 9p (with one showing entire monosomy 9): in seven, the commonly deleted region encompassed 9p21.3 (21853204Mb – 22018332Mb) and included the genes *CDKN2A* (cyclin-dependent kinase inhibitor 2A) and *CDKN2B*. Interestingly four of these seven cases had t(14;16), resulting in 50% of t(14;16) cases having this CNA; the other three cases were one each of: t(4;14), t(11;14) and HRD. The latter case, despite being classified as HRD, showed an *IgH* rearrangement with an unidentified partner, confirming that *CDKN2A/2B* loss preferentially arises in *IgH*-translocated MM. No chromosomal losses involving chromosome 9 were found in pre-malignant cases (MGUS/SMM *vs* MM, P=0.007).

iFISH was performed on the independent patient cohort for the genes *CDKN2A/2B* and *PAX5* (paired box gene 5; 9p13.2). Deletions of *CDKN2A/2B* were detected in four of 34 MGUS (12%) and ten of 174 MM (6%); none of the SMM patients showed deletions of this locus. In MGUS, the median percentage of PC with the deletion was 57% (range, 25%–64%); in MM, 65% (range, 24%-100%). These findings indicated that the deletion was as a secondary/later event. No deletions of *PAX5* were detected, confirming the interstitial nature of *CDKN2A/2B* deletions. In three MGUS and four MM, the FISH signal pattern for *CDKN2A/2B* included one signal of normal size (non-deleted allele) and one diminished signal (deleted allele) suggesting a partial deletion of the locus with one of the break-points falling within the gene.
In MM, *CDKN2A/2B* deletion was associated with nonHRD (*P*=0.04) (**Table 3-10**).

			t(4;14)		t(6;14) & t(11;14)		Deletion 13		t(14;16)		TP53 deletion		t(14;20)		Ploidy		1q gain		p18 deletion	
			N	T	N	T	N	Del	N	T	N	Del	N	T	HRD	nonHRD	N	Gain	N	Del
CDKN2A/2B deletion	MGUS	Absent	30	0	24	6	25	5	30	0	27	3	29	1	10	14	20	6	28	2
		Hemizygous	4	0	4	0	3	1	4	0	4	0	3	1	0	3	1	2	3	1
	MM	Absent	143	21	139	25	93	71	161	3	146	17	159	5	92	69	101	54	140	21
		Hemizygous	8	2	6	4	3	7	9	1	10	0	10	0	2	8	6	4	6	4

Table 3- 10 Table of associations between *CDKN2A/2B* deletion and other CA in MGUS and MM (statistically significant associations are highlighted in blue)

N, normal; T, translocated; Del, deletion

Array CGH showed that in MM this deletion was particularly frequent in patients with t(14;16); in this cohort no such association was found but it must be noted that only four t(14;16) cases were included. More cases, particularly those with t(14;16), need to be tested in order to investigate this possible association.

MM patients with *CDKN2A/2B* deletion showed significantly inferior OS compared to patients with normal 9p (11 months *vs* 41 months, *P*=0.006). This significance was found when survival was calculated from the time of analysis but not when the initial time point was time of diagnosis (26 months *vs* 53 months, *P*=0.07).

In MGUS, among the four patients positive for the deletion, two evolved to MM after 40 and 75 months from diagnosis; the other two patients were stable after 38 and 79 months.

3.3.4.3.6 Chromosome 12 abnormalities

Chromosome 12 was mainly characterized by deletions, with only one MM case showing entire monosomy. Deletions of 12p were found only in MM patients (n=11) and two distinct common minimally deleted regions were defined: 12p13.1 (12720245Mb – 12778201Mb; n=9) and 12p13.1-p12.3 (12904980Mb – 17188748Mb; n=9). The first region included only three genes: *GPR19*, *CDKN1B* (cyclin-dependent kinase inhibitor 1B, also known as *p27* or *Kip1*) and *APOLD1*. This deletion was confirmed by FISH using a fosmid probe for *CDKN1B* (**Appendix 3**). Decreased CDKN1B levels are a poor prognostic factor in many malignancies [223,224] and it has been proposed that *CKS1B* gain on 1q21 enhances CDKN1B degradation [157]. Thus the *CDKN1B* probe was used to test the independent cohort of patients: one of 34 (3%) MGUS, two of 13 SMM (15%) and 29 of 171 (17%) MM patients were found to be positive for this deletion (MGUS *vs* MM, *P*=0.033); all deletions were hemizygous. The relatively high frequency of this CA in MM, considering the genetic heterogeneity of the disease, was surprising. No significant associations were found between *CDKN1B* deletions and any of the other CA tested; there was only a non significant enrichment in t(4;14) (*P*=0.076) and nonHRD (*P* =0.061) noted (**Table 3-11**).

		t(4;14)		t(6;14) & t(11;14)		Deletion 13		t(14;16)		TP53 deletion		t(14;20)		Ploidy		1q gain		p18 deletion	
		N	T	N	T	N	Del	N	T	N	Del	N	T	HRD	nonHRD	N	Gain	N	Del
CDKN1B deletion	Absent	126	16	117	25	80	62	139	3	128	12	139	3	83	57	85	49	121	18
	Present	22	7	25	4	11	18	28	1	23	6	28	1	11	17	17	11	22	7

Table 3- 11 Table of associations between *CDKN1B* deletion and other CA in MM

N, normal; T, translocated; Del, deletion

In order to improve the definition of the size of these deletions, iFISH was performed on those cases found to be deleted with the fosmid probe, using BAC probes located 0.5Mb proximally and distally of *CDKN1B* (bA515B12 at 12p13.1 and bA388F6 at 12p13.32, **Appendix 3**). One case showed a diminished FISH signal for the *CDKN1B* probe suggesting that the breakpoint of the deletion was located within *CDKN1B*. In the remaining cases, at least one of the flanking markers was lost, indicating that the deletions were variable in size and rather large, suggesting the possible importance of other genes within the deleted region.

The Kaplan-Meier curve for OS showed no difference between MM patients with and without the deletion, either calculating the survival time from the time of analysis (39 months *vs* 39 months; *P*=0.754) or from the time of diagnosis (41 months *vs* 56 months; *P*=0.632).
The only MGUS patient (871) found to be positive for the deletion showed a HRD karyotype and normal *IgH;* the *CDKN1B* deletion was present in all PC. The patient was 85 years old when diagnosed with MGUS and died 9 months later for MM-unrelated causes. In both SMM patients (651 and 925), the *CDKN1B* deletion was detected in only a sub-population of PC (39% and 26%), while other CA detected by iFISH showed complete PC involvement. This suggested that, in these patients, this CNA represented a later event. Both patients had a HRD karyotype with no *IgH* rearrangements. Patient 651 was tested after 4.5 years from the initial diagnosis of SMM. Interestingly, at this time, Δ13 was also found in 19% PC, suggesting that, as for 12p deletion, some CA originated later when compared to trisomies 9 and 15 which were found in the majority of PC (76%). Both patients progressed to MM: patient 925, after 2 years from diagnosis and patient 651 after a period ranging between 6 and 30 months from cytogenetic analysis (uncertain follow-up information).

3.3.4.3.7 Chromosome 16 abnormalities

Chromosome 16 was mainly characterized by losses of chromosomal material. Deletions of 16p were detected in eight MM patients; they shared a common minimally deleted region at 16p13.3 defined by the positions 3603589Mb – 3883030Mb and encompassing the genes *DNASE1, TRAP1* and *CREBBP*. One MGUS (695) and one SMM (259) had loss of 16p (16p13.13-pter); the MGUS patient remained stable after 6 years from the detection of the CNA, the SMM patient progressed to MM after 53 months.

Deletions of 16q were found in 14 of 47 (30%) MM patients; eight were whole arm losses. Four deletions were found in t(14;16) patients, while there were none found in the t(4;14) group. The two most commonly deleted chromosomal regions were located at 16q12.1 (47178411Mb - 51135038Mb) (n=12) and 16q23.1 (n=12). The first region encompassed many genes including

the tumour suppressor gene, *CYLD* (Cylindromatosis); patient 932 had entire loss of 16q and HD at 16q12.1, only involving *CYLD* and *CARD15* (see **Section 3.3.4.4**). The second region of common loss encompassed the *WWOX* (WW domain containing oxidoreductase) gene; patient 282 had a HD involving only this gene (77227769Mb – 77263523Mb) (**Figure 3-12**) as the cell-line KMS-11 (76737934Mb – 77794243Mb). Among the pre-malignant patients, two MGUS and six SMM showed loss of 16q23.1; five patients showed loss of the entire 16q and in two of them the CNA appeared to be present in only a sub-population of PC. The three SMM patients (582, 1073 and 2198) with interstitial deletions encompassing 16q23.1 were positive for the t(14;16), and the common minimally deleted region involved only *WWOX* (77343069Mb – 77515188Mb).

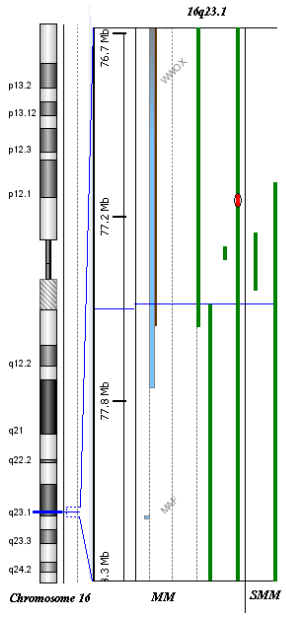

Figure 3- 12 Diagram showing the megabase positions of copy number losses involving *WWOX* at 16q23.1 in six patients (four MM and two SMM) (patients from left to right: 551, 309, 2068, 282, 582 and 2198)

Patient 282 showed the presence of a hemizygous deletion involving the whole 16q and a HD at 16q23.1 (red bar with black circle) involving *WWOX*.

Interestingly five of the six SMM with loss of 16q23.1 progressed to MM after 15, 15, 20, 31 and 50 months from the time of analysis; the sixth SMM case (1073) remained stable after 55 months. None of the two MGUS had shown evidence of disease evolution by the end of the study, after 72 and 78 months.

3.3.4.3.8 Chromosome 17 abnormalities

Ten MM cases showed 17p deletions, of which nine encompassed the *TP53* gene at 17p13.1. The common minimally deleted region at 17p13.1 was defined by the positions 7290085Mb and 7495207Mb. There was no specific association of this CNA with any particular genetic groups.

Five patients also shared a common minimally deleted region at 17p11.2 (19378373Mb – 20160056Mb). Only one MGUS patient (3318) showed loss of almost the entire chromosome including the 17p13.1 region. As previously stated in **Table 3-9**, despite the fact that the patient did not receive treatment for MM before her death (17 months after diagnosis), her paraprotein was steadily rising at that time.

3.3.4.3.9 Chromosome 18 abnormalities

Loss of 18p was found in six MM patients (one of them showed entire monosomy). Interestingly the five cases with interstitial losses were t(4;14) cases (*P*=0.002). The common minimally deleted region was defined by the chromosomal bands 18p11.2 and 18p11.32. Among the pre-malignant cases, one MGUS (3318) and one SMM (1252), both had t(4;14), as well as loss of 18p. Both patients were stable at 17 and 24 months, respectively; however, the second patient was lost to follow-up after this time.

3.3.4.4 CNA encompassing genes involved in the NF-κB pathway

3.3.4.4.1 Array CGH

Five of 27 (18%) HD identified in this patient cohort contained potential target genes associated with the regulation of the NF-κB signalling pathway (**Table 3-8**). Two recurrent HD were found at 11q22.1 (MM patients 309 and 1336, both with t(14;16)) and at 14q32.32 (SMM patient 582, with t(14;16); HRD MM patient 491). One HD was found at 16q12.1 (MM patient 932, with t(11;14)). The common minimally deleted region at 14q32.32 contains the genes *TRAF3* (TNF-receptor-associated factor 3), *AMN* (amnioless homolog, mouse) and *CDC42BPB* (CDC42-binding protein kinase beta) (**Figure 3-13A**). The HD found at 11q22.1 was relatively large in patient 1336. However, in patient 309 the HD involved only *BIRC2/cIAP1* (baculoviral IAP (inhibitor of apoptosis protein) repeat-containing protein 2) and *BIRC3/cIAP2* genes (**Figure 3-14**). Both CNA were confirmed by FISH. Given their small size, a combination of differently labelled fosmid and BAC probes was developed for their detection. The smallest HD were found in patient 582 for 14q32.32 and in patient 309 for 11q22.1; therefore the breakpoint positions characterizing these cases were used to design the probe combinations for iFISH. **Figure 3-13B** shows in detail the probe combination for the 14q32.32 deletion. The HD at 16q12.1 involved the genes *CYLD* (cylindromatosis) and *CARD15* (caspase recruitment domain-containing protein 15), as previously stated in **Section 3.3.4.3.7**.

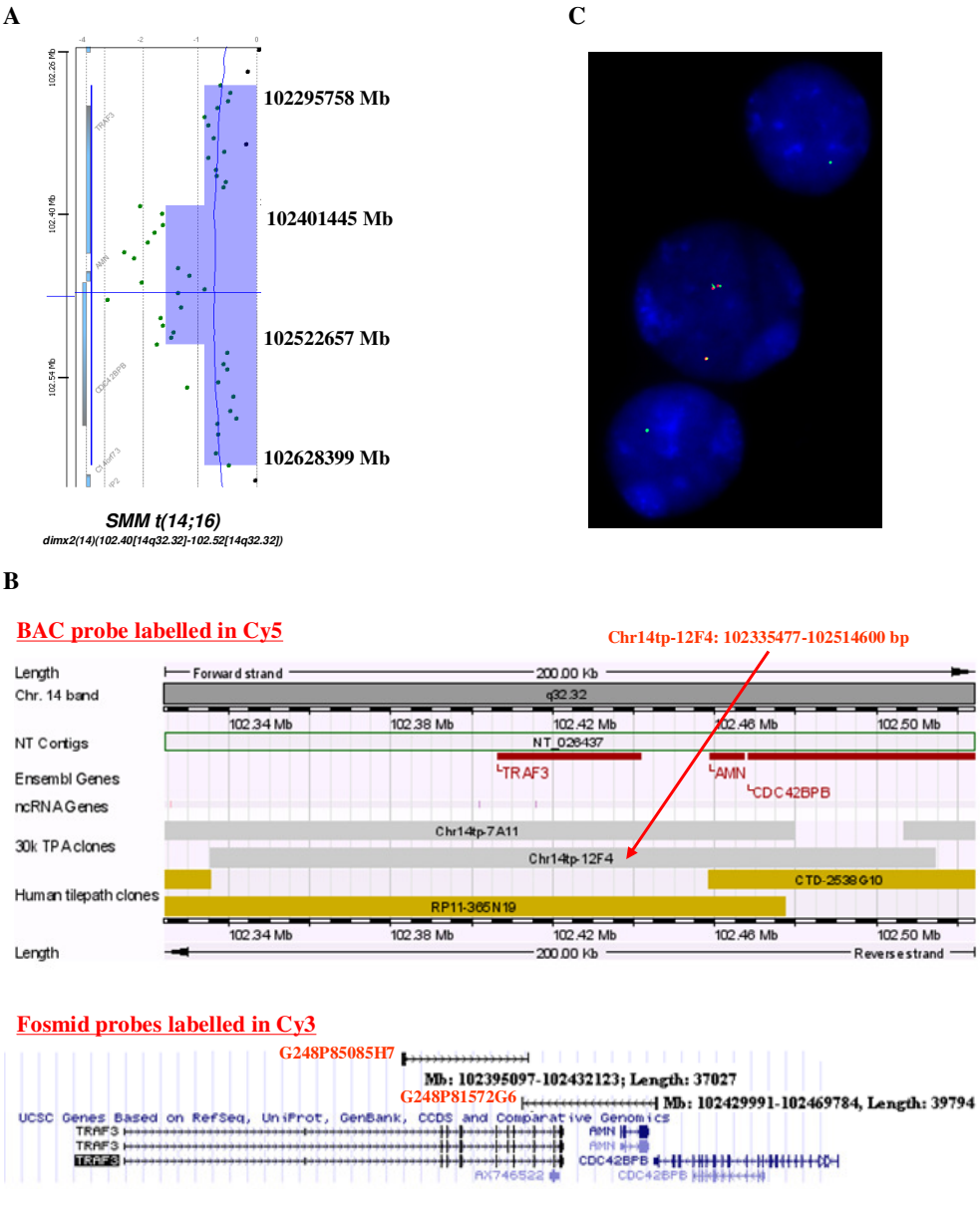

Figure 3- 13 **A) Patient 582: plot of calls for every oligonucleotide for the deleted region at 14q32.32; B) Screen shots from the Ensembl and UCSC browsers showing the locations of the BAC and fosmid probes selected for the 14q32.32 deletion; C) FISH confirmation of the deletion in patient 582: one nucleus with normal copy number for 14q32.32 (two red/green signals) and two nuclei with complete loss of the red signals and a diminished green signal consistent with HD of this region**

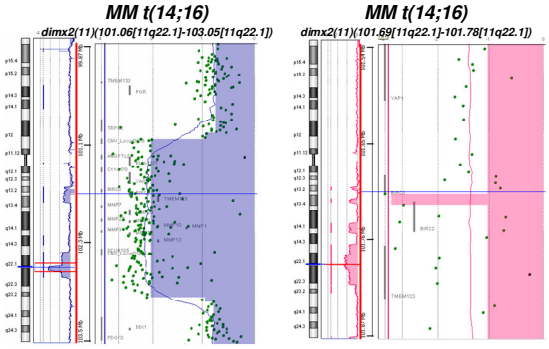

Figure 3- 14 G-banded idiograms of chromosomes 11 and the plot of 'calls' for every oligonucleotide for the selected chromosomal region are shown for patients 309 (on the left) and 1336 (on the right)

TRAF3, *BIRC2/3* and *CYLD* are negative regulators of the NF-κB signalling pathway and dysregulated expression of these genes has been detected in MM and HMCL carrying HD of these same chromosomal regions [181,182].

In the current study, hemizygous deletions encompassing these three regions were also found: 14q32.32, MM (n=9), pre-malignant conditions (n=3); 11q22.1, MM (n=4), pre-malignant conditions (n=0); 16q12.1, MM (n=8), pre-malignant conditions (n=4).

The array CGH profile of MM patient 2068 (t(14;16)) showed what appeared to be a hemizygous deletion at 14q32.32 including *TRAF3* involving only a sub-clone of the PC population. iFISH revealed instead the presence of a HD involving this chromosomal region in 25% of PC.

The array CGH profile of MM patient 551 (t(14;16)) showed a deletion at 14q32.32 involving *TRAF3* whose $\log_2$ ratio was intermediate between one indicating a hemizygous deletion and one indicating a HD. iFISH for this locus showed 30% of PC hemizygously deleted and 10% of PC carrying a HD, consistent with the array CGH results. This patient was initially diagnosed with MGUS and progressed to MM after a period of 76 months. Unfortunately the Database did not receive the BM sample taken at the time of MGUS diagnosis. However, a sample taken 6 months before the time of MM diagnosis was available for FISH analysis. This showed 37% of PC to have a hemizygous deletion with no cells having HD at this locus. This result clearly indicates that the loss of the second allele was a very late event, possibly involved in the clinical manifestation of the disease. These two last cases confirm the importance of using iFISH to confirm ambiguous array CGH results as the biological significance of hemizygous or HD is very different.

Three other genes coding for members of the NF-κB pathway were found to be involved in CNA:

1) *LTBR* (lymphotoxin-beta receptor) at 12p13; CNA involving this gene were seen in two patients:

i. HRD MM patient (314) with interstitial gain (size of CNA: 0.9Mb).

ii. MM patient with a t(4;14) (665) showing hemizygous deletion immediately centromeric of the *LTBR* gene suggesting the presence of a translocation at this locus leading to overexpression of this gene.

2) *TACI* (transmembrane activator and CAML interactor/TNFRSF13B) at 17p11.2-p12; CNA involving this gene were seen in two patients. This chromosomal region is characterized by a large number of low-copy repeats which are responsible for its instability. Fabris and colleagues firstly described an approximately 5Mb amplification at 17p11.2-p12 in the KMS-26 myeloma cell line by SNP microarray analysis and 12 genes included in this region were found to be significantly overexpressed, including *TNFRSF13B/TACI, COPS3* and *NCOR1* [225]. FISH analyses of 141 primary MM patients identified one MM carrying a 3.8 Mb amplified region at 17p11.2 and two MM with gains specifically involving the *TACI* locus.

i. MM patient with t(14;16) (282) with amplification at 17p11.2-p12 (size of the CNA: 1.3Mb) **(Figure 3-15)**. The gene was located within the chromosomal region showing the highest level of amplification.

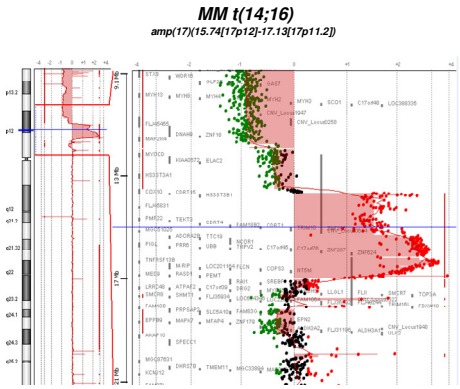

Figure 3- 15 G-banded idiogram (on the left) of chromosome 17 and the plot of 'calls' for every oligonucleotide for the selected chromosomal region (on the right) are shown for patient 282

ii. MM patient with an unidentified *IgH* rearrangement (1581) with interstitial gain at 17p11.2 (size of the CNA: 1.4Mb). In this patient, the same CNA was found by array CGH in the sample collected when the patient was a SMM.

3) NF-κB-inducing kinase (*MAP3K14/NIK*) at 17q21.31; CNA involving this gene were seen in two patients:

i. MM case with a t(11;14) (504) with interstitial gain (size of the CNA: 0.17Mb).

ii. MM case with t(11;14) (2993) with hemizygous deletion immediately proximal to *NIK* gene (end position of the CNA: 41031250) suggestive of a translocation. This latter abnormality was confirmed by iFISH using a fusion probe strategy combining four different BAC probes labelled in Cy3 and Spectrum Green (see **Appendix 3**); break-apart of the fusion probe was indicative of a structural rearrangement at this locus.

All these abnormalities involving members of the NF-κB pathway were mutually exclusive and seemed to preferentially involve MM cases with a rearranged *IgH* (11/13). However, it has to be noted that the *IgH* rearrangements present in these patients not only included those associated with a poor prognosis in MM, but also t(11;14). Two of these CNA were found in pre-malignant patients: case 582 (SMM) positive for a HD at 14q32.32 and case 1581 (SMM) positive for an interstitial duplication at 17p11.2 and involving the *TACI* gene; both patients evolved to MM within 15 months.

Interphase FISH was performed on the independent group of consecutive patients to search for abnormalities involving three of the NF-κB markers found to be recurrently involved in CNA by array CGH.

1) *BIRK2/3* (11q22.1). Homozygous and hemizygous deletions of *BIRC2/3* were detected in seven (4%) and two (1%) of 163 MM patients, respectively. No abnormalities involving these genes were found in MGUS or SMM.
In four of seven MM patients the HD was observed in the entire PC population; in the remaining three patients the HD was seen in a sub-clone of PC (14%;18%; 22%) with the remaining PC carrying hemizygous deletions.

		t(4;14)		t(6;14) & t(11;14)		Deletion 13		t(14;16)		TP53 deletion		t(14;20)		Ploidy		1q gain		p18 deletion	
		N	T	N	T	N	Del	N	T	N	Del	N	T	HRD	nonHRD	N	Gain	N	Del
BIRC2/3 deletion	Absent	137	17	129	25	87	67	152	3	138	15	150	5	87	65	96	51	131	21
	Hemizygous	2	0	2	0	1	1	1	1	2	0	2	0	0	2	0	1	0	2
	HD	3	4	5	2	0	7	7	0	5	2	7	0	1	6	1	6	5	2

Table 3- 12 Table of associations between *BIRC2/3* deletions and other CA in MM (statistically significant associations are highlighted in blue)

N, normal; T, translocated; Del, deletion; HD, homozygous deletion

BIRC2/3 HD was associated with Δ13 (*P*=0.004), t(4;14) (*P*=0.006), ploidy (*P*=0.045), gain of 1q (*P*=0.010) and 1p32.3 loss (*P*=0.03) (**Table 3-12**).

2) *TRAF3* (14q32.32). In MGUS and SMM, no HD at 14.32.32 were detected; five of 35 MGUS and 3 of 11 SMM showed hemizygous deletions at this locus. In MM (n=168) 27 hemizygous deletions (16%) and six HD (~4%) were detected; the HD involved the majority of PC in three cases; in the remaining cases, they were detected in 26%, 35% and 37% of PC with the rest of PD carrying hemizygous deletions.

		t(4;14)		t(6;14) & t(11;14)		Deletion 13		t(14;16)		TP53 deletion		t(14;20)		Ploidy		1q gain		p18 deletion	
		N	T	N	T	N	Del	N	T	N	Del	N	T	HRD	nonHRD	N	Gain	N	Del
TRAF3 deletion	Absent	118	17	110	25	78	57	133	2	121	12	130	5	79	54	85	44	116	16
	Hemizygous	23	4	24	3	9	18	26	1	23	4	28	0	10	16	13	12	20	7
	HD	4	2	6	0	1	5	5	1	4	2	6	0	2	4	1	4	5	1

Table 3- 13 Table of associations between *TRAF3* deletions and other CA in MM (statistically significant associations are highlighted in blue)

N, normal; T, translocated; Del, deletion; HD, homozygous deletion

TRAF3 loss (including both hemizygous and homozygous deletions) was significantly associated with Δ13 (*P*=0.006) and nonHRD (*P*=0.03). HD, despite being more frequent in cases with Δ13 and 1q gain, did not show any significant association (**Table 3-13**).

The effect of *TRAF3* loss on OS was calculated using both the time of diagnosis and the time of analysis (**Figure 3-16**). Patients with *TRAF3* HD showed inferior OS compared with those with normal 14q32.32 and those with hemizygous deletions of this chromosomal region (*P*=0.012 when survival time was calculated from time of diagnosis; *P*=0.002, when survival time was calculated from time of analysis). Interestingly, no difference was found between patients with normal 14q32.32 and patients with hemizygous deletions at this locus.

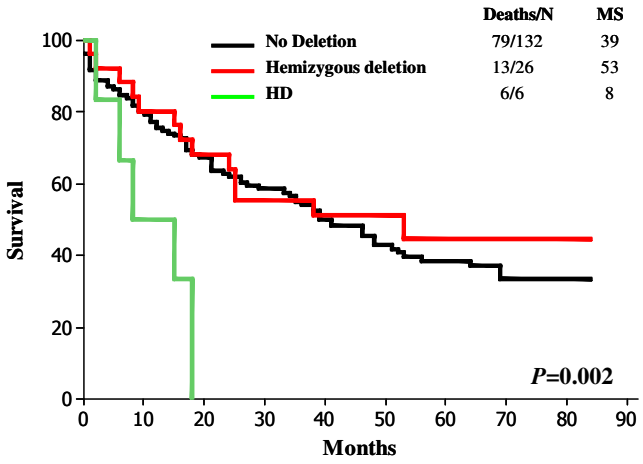

Figure 3- 16 Kaplan-Meir curve for OS of MM patients calculated from time of cytogenetic analysis; patients were stratified for *TRAF3* hemizygous and homozygous deletions

3) *MAP3K14/NIK* (17q21.31). Abnormalities involving *NIK* were absent in MGUS and SMM, while they were found in three of 164 MM patients (~2%); all three patients were HRD. One MM patient (1192) showed amplification (≥6 copies) of this locus: the number of signals was highly variable from cell to cell. Patient 1044 showed three fusion signals corresponding to non-rearranged copies of the gene, but two of these signals appeared to be tandemly duplicated. Patient 963 was found with a break-apart of the fusion probe associated with deletion of the probe centromeric to *NIK* and duplication of *NIK* itself. This FISH pattern was indicative of an unbalanced structural rearrangement of the gene in 81% of PC. This patient was also positive for an *IgH* rearrangement whose partner gene was not one of the five primary ones discussed in **Section 3.1**. Translocations t(14;17)(q32;q21), involving *IgH* and *NIK* loci have been previously reported [181,182]; co-hybridization of probes for *IgH* and *NIK*, each labelled using a single fluorochrome, confirmed the presence of t(14;17) in this patient. The same patient also showed HD of *TRAF3* in 26% of PC, indicating that the *TRAF3* abnormalities followed the *NIK* rearrangement. In these three cases the CA involving *NIK* was present in the majority of PC. Two further MM patients showed a small percentage of PC (<10%) with what appeared to be a structural balanced rearrangement involving *NIK*; because of the low percentage of positive cells these cases were considered to be normal. No specific associations were found between *NIK* abnormalities and any other CA tested.

The presence of any one of the three abnormalities (*TRAF3* HD, *BIRC2/3* HD and *NIK* rearrangements) was found to have an impact on OS calculated for MM patients from the

independent cohort (median survival: 18 months *vs* 41 months, *P*=0.057). Although ten of the 15 changes were found in nonHRD patients, this difference was not statistically significant (*P*=0.10).

3.3.4.5 CNA involved in MGUS/SMM-MM transition of patients with t(11;14)

Patient	Diagn	Losses	Gains	Amp	HD	Total	Specific CNA
844	MGUS	0	1	0	0	**1**	
695	MGUS	3	0	0	0	**3**	
855	MGUS	1	1	0	0	**2**	
999	MGUS	1	1	0	0	**2**	
610	MGUS	1	1	0	0	**2**	
795	MGUS	0	1	0	0	**1**	
355	SMM	3	3	0	0	**6**	
						Average=2.1	
2906	MM	9	15	0	1	**25**	HD: 9p21.3, *CDKN2A/2B*
3325	MM	15	15	1	0	**31**	Amp: 8q24, *MYC*
932	MM	4	9	0	1	**14**	HD: 16q12, *CYLD* Hemizygous loss: 14q32.32, *TRAF3*
1524	MM	22	10	1	0	**33**	Amp: 8q24, *MYC*
504	MM	0	18	0	0	**18**	*NIK* duplication (17q21.31)
1300	MM	6	1	0	0	**7**	
308	MM	10	8	0	0	**18**	
2993	MM	17	5	0	0	**22**	*NIK* rearr (17q21.31)
						Average=21	

Table 3- 14 CNA in patients with t(6;14) or t(11;14)

(Diagn, diagnosis; Amp, amplification; HD, homozygous deletion ; rearr, rearrangement)

Table 3-14 and **Figure 3-17** show that pre-malignant patients with t(11;14) had a relatively simple genome with an average of 2.1 CNA per case compared with 21 CNA observed in MM patients with the same translocation. In MM, recurrent CNA involved *MYC* and members of the NF-κB pathway, while in MGUS CNA were mainly represented by gains or losses of entire chromosomes. Such differences in the number of CNA between MGUS and MM was not seen in patients with t(4;16), t(14;16) or HRD (**Table 3.7**), in which the genome of the pre-malignant cases showed a relatively high level of complexity which often was not anticipated from the iFISH results. This observation might suggest that the acquisition of new CNA, associated with disease evolution, is a slower process in t(11;14) patients. Interestingly, none of the MGUS patients progressed to MM by the end of the study (follow-up range: 17-84 months; median, 72

months). However, it has to be noted that within the Database many MM cases with t(11;14) and abnormal karyotype appeared to be very simple, with few CNA (data not shown). This observation suggested that, within the array CGH patient cohort, MM cases with t(11;14) were biased towards more complex cases.

Figure 3- 17 Graphical representation of CNA in t(11;14) patients using snpview

The bar at the top indicates the starting and the finishing positions of each chromosome. Every horizontal line corresponds to a patient: in black are regions with no CNA, in red regions of loss, in green regions of gain. Regions where the red/green colour is less intense describe CNA only present in a sub-clone of PC.

In patients with t(11;14), the CNA most common to all diagnostic groups was the duplication of 11q13-qter with the breakpoint in 11q13 identical to the one characterizing the t(11;14). Loss of chromosome 13 was found in only one MGUS patient (999) in a sub-population of PC (48% of PC by iFISH, as described in **Section 3.1**), compared with six of eight MM cases. Array CGH confirmed that MGUS negative for Δ13 by iFISH, did not have other CNA of this chromosome, notably not involving the band 13q14 (where the iFISH probes map).

By chance all patients with t(11;14) and array CGH results were female and loss of one copy of chromosome X was found in one of seven pre-malignant cases and in six of eight MM patients (P=0.040).

The only SMM patient with t(6;14) (described in **Section 3.1.4.4**) progressed to MM after 20 months from analysis and, compared with the MGUS group, had a higher number of CNA (n=7), including monosomy 13**.**

3.3.4.6 Patients with array CGH on paired samples

Within the Database, two patients had paired samples taken at the time of MGUS or SMM diagnosis and at the time of progression to MM, with good PC recovery at both stages. Array CGH was performed on both samples in order to determine whether disease evolution was associated with the acquisition of new CNA.

3.3.4.6.1 MGUS-MM transition of a HRD patient

Clinical data. Patient 989, a 67 year old caucasian male, was diagnosed with MGUS in July 2003 due to the finding of an IgG paraprotein level of 18.81g/L. At this time his WBC, haemoglobin, calcium and β_2M levels were normal. The BM aspirate showed BM elements to be adequately represented with a percentage of PC equal to 3%. His trephine was normal and no lytic lesions were observed by skeletal survey. The patient evolved to MM after a period of ~6.5 years. During this follow-up period his paraprotein level showed a small but steady increase for the first 5 years, while it rapidly rose to 54 g/L in the last year and a half, as shown in **Figure 3-18**. During his last year of follow-up the patient refused MRI, but in September 2009 he attended hospital with back pain. At this time his skeletal survey revealed multiple lesions in his long bones, a crushed vertebrae and the right hip at risk of fracture. At this time BM examination revealed 65% of PC.

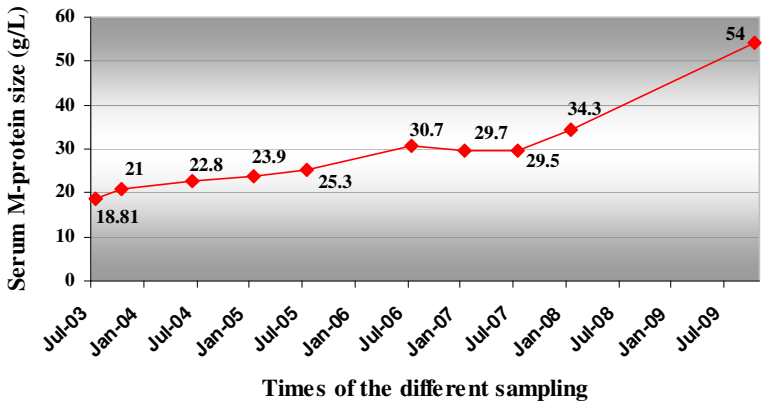

Figure 3- 18 Chart showing the variation of the serum M-protein (IgG) from the diagnosis of MGUS to diagnosis of symptomatic MM

Genetic results. Two BM samples were sent to the Database: one taken when MGUS was diagnosed (sample 1) and one from the time of the MM diagnosis (sample 2). Sample 1 was

tested by iFISH for the presence of *IgH* and *MYC* rearrangements, Δ13 and ploidy status. Cytogenetic cultures were also set up. While metaphase analysis revealed only 33 normal metaphases (46,XY), iFISH showed the presence of multiple trisomies (chromosomes 3, 7, 9, 11 and 15) in the absence of IgHt or Δ13, consistent with a relatively 'simple' HRD karyotype. On sample 2, iFISH was performed to test for IgHt and *MYC* rearrangements: no abnormalities were found.

Array CGH was performed on purified PC from both samples (PC purity: 96% in sample 1; 100% in sample 2). The array CGH profile of sample 1 showed a highly rearranged genome with 12 gains and 11 losses; most of the interstitial CNA detected could not be identified by routine iFISH tests. Sample 2 showed 20 regions of loss and 17 regions of gain; no HD or amplifications were detected in any of the samples (CNA of samples 1 and 2 are described in **Table 3-15**). Sample 1 showed the highest number of CNA when compared with the number of CNA of other HRD MGUS patients tested by array CGH and the second highest number of the entire MGUS group. All the CNA detected in sample 1 were confirmed in sample 2; the only exception was 8p loss: sample 1 showed loss of the entire arm, while sample 2 showed a smaller deletion (8p11.1-p22) where the degree of loss varied from region to region. Both CNA appeared to be present in a sub-clone of the PC population, while other changes involved all cells. Two alternative mechanisms may explain these findings: (**i**) within the sub-clone with 8p loss seen in sample 1, the remained allele further rearranged and partially duplicated; (**ii**) the CNA involving 8p in sample 2 arose in a distinct sub-clone with no 8p loss, while the clone with the 8p loss seen in sample 1 progressively disappeared during disease evolution. In sample 2, most of the 8p loss showed a $\log_2$ ratio = -0.3 indicating a hemizygous deletion in a sub-clone of PC; within this region, two interstitial regions at 8p21.3 and 8p22 showed a $\log_2$ ratio = -1 suggesting that, within the sub-clone, these two regions were homozygously deleted.

Most interesting was the acquisition of monosomy 13 in sample 2 in almost all PC (this CA was completely absent in sample 1) (**Figure 3-19 A**), confirming that in HRD cases this CA may be a later event (see **Table 3-4**) and a possible driver of disease evolution.

Following page

Table 3- 15 Presence and megabase position of CNA in paired samples of patient 989 and associated genes

*** Loss of 8p was smaller in the second sample: 8p22-8p11.1 (17,652,178Mb- 41,739,024Mb)**
¤ This CNA appeared only subclonal in sample 1

Abnormality				Sample 1 (MGUS)	Sample 2 (MM)	Gene(s) in region
Type	**Cytoband**	**Megabase position**				
		Start	***End***			
Loss	1p36.13	16884678	17130584	√	√	
Loss	1p32.1-p31.3	59838544	62700901	√	√	
Loss	1p22.2-p22.1	88594706	94289803	√	√	
Loss	1p21.3-p13.2	95525023	113437396	√	√	
Loss	1p13.2-p11.1	114054012	120474160	√	√	
Loss	1q32.3	210638344	211099834	—	√	*HHAT, KCNH1*
Trisomy	3	39066	198858311	√	√	
Loss	4p16.1-p14	5237776	37140498	√	√	
Gain	4q24	103284326	103736367	—	√	*NFKB1, MANB, UBE2D3*
Gain	4q28.2	130561729	130984065	—	√	*No genes*
Trisomy	5	601072	180588699	√	√	
Loss	6q15-qter	88906931	170469193	√	√	
Gain	7pter-q21.13	140213	89079942	√	√	
Loss	7q21.13-q21.2	89110055	91396559	√	√	
Gain	7q21.2-q22.1	91403435	100536696	√	√	
Loss	7q22.1-q22.2	100549092	104379552	√	√	
Gain	7q22.2-qter	104399350	158568421	√	√	
Loss	8pter-p11.1	63810	47062180	√¤	√*	*Many*
Gain	9pter-p11.1	153131	44167323	√	√	
Gain	9q11-qter	44167323	140036287	—	√	*Many*
Loss	10p12.32	20205581	21727776	—	√	*PLXDC2, TEM7R, NEBL, C10orf113*
Loss	10q25.3	115517085	115677160	—	√	*DCLRE1A, NHLRC2, C10orf81, AK027190, AK000154*
Gain	11pter-11q14.2	182372	87080566	√	√	
Gain	11q14.3-qter	90041154	134352297	√	√	
Loss	12q23.1	98580482	98617562	√	√	
Monosomy	13	18065953	113562984	—	√	*Many*
Loss	14q13.1-q21.1	31820354	40521910	—	√	*Many*
Gain	14q31.1	78503451	80349809	—	√	*KIAA074, NRXN3*
Trisomy/ Tetrasomy	15	18362555	100123384	√	√	
Loss	16q12.1	47178411	51135038	—	√	*Many including CYLD*
Loss	17q21.2-21.31	36541969	38054342	—	√	*Many*
Loss	17q23.3-q24.2	59484545	61567907	—	√	*Many*
Trisomy/ Tetrasomy	19	64418	63603518	√	√	
Loss	20q11.22-q13.2	31804568	50177871	√¤	√	
Trisomy	21	13334960	46846246	√	√	
Gain (x2)	Xq21.32-qter	92358622	154143903	√	√	

Interesting changes acquired in sample 2 were: gain of 4q24, which includes the *NFKB1* gene and loss of 16q12.1, which includes *CYLD* (**Figure 3-19 B**). Both genes encode for members of the NF-κB pathway and CA involving these chromosomal regions have been reported to be altered in primary MM patients and cell-lines [181,182] but not in stable MGUS (see **Section 3.3.4.4**).

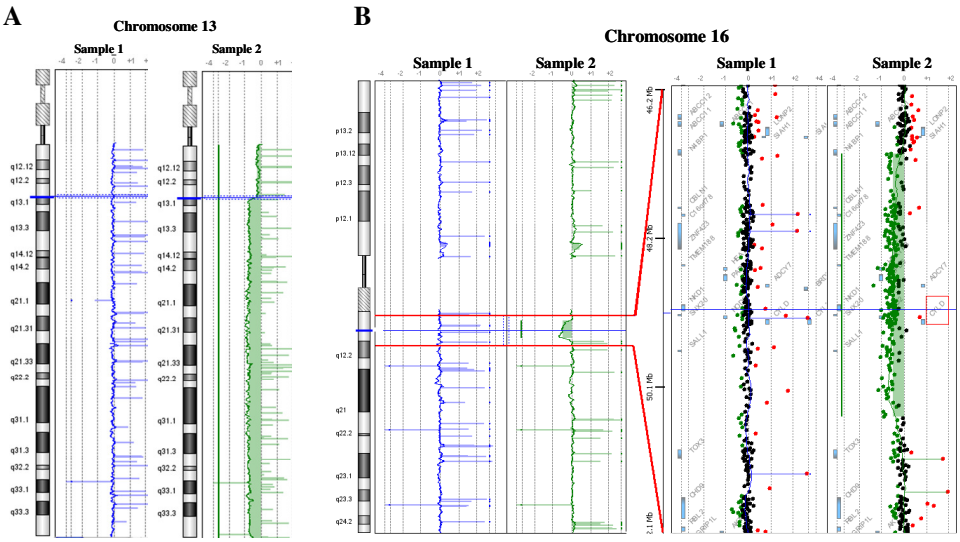

Figure 3- 19 G-banded idiograms (on the left) and array CGH profiles (on the right) obtained with the Agilent software of chromosomes 13 (A) and 16 (B), for samples 1 and 2 of patient 989. For chromosome 16 the plot of 'calls' for every oligonucleotide for 16q12.1 (on the right) is shown

3.3.4.6.2 SMM-MM transition of a nonHRD patient with unidentified IgH rearrangement

Clinical data. The BM sample of patient 1581, a 55 year old caucasian male, was received in August 2004 (sample 1), 14 months after he was diagnosed with SMM. In November 2005 (15 months after sample 1 and 29 months after diagnosis) a second BM sample (sample 2) was received; at this time the patient was diagnosed with MM and was entered into the Myeloma IX Trial. His paraprotein (IgAλ) level was: 19.35 g/L in July 2004; 21.7 g/L in May 2005; 26.4 g/L in August 2005; 27.1 g/L in October 2005; 41.04 g/L November 2005. At this time his WBC, calcium and β_2M levels were normal, while the haemoglobin level was 117 g/L (reference range, 120 – 150 g/L).

Abnormality				Sample 1 (SMM)	Sample 2 (MM)	Gene(s) in region
Type	**Cytoband**	**Megabase position**				
		Start	***End***			
Gain (x2)	1q12-qter	141465960	245433898	√	√	*Many*
Gain	3q26.2	170637939	171652421	√	√	*Many including MDS1, ARPM1, MYNN*
Gain	6pter-p21.2	97634	39021664	√	√	*Many*
Loss	6q25.1-qter	151508818	170943147	√	√	*Many*
Loss	7pter-p21.1	140213	16917680	√	√	*Many*
Monosomy	13	18065953	114123908	√	√	*Many*
Loss	14q24.1-q32.33	68331511	105760541	√	√	*Many*
Gain (sub-clonal)	16p13.13	10614700	11953884	√	√	
Loss	16q12.1-qter	45018886	88690615	√	√	*Many*
Gain	17p12-p11.2	16117789	17556868	√	√	*Many including TACI (**see** Section 3.3.4.4)*
Gain	19p13.12	15790620	16485583	√	√	
Gain	Xq27.1-qter	137568878	154492983	√	√	*Many*

Table 3- 16 Presence and megabase position of CNA in paired samples of patient 1581 and associated genes

Genetic results. Both samples 1 and 2 were tested by iFISH for the presence of *IgH* and *MYC* rearrangements, Δ13 and ploidy status; cytogenetic cultures were also set up on sample 2 but only two normal metaphases (46,XY) were detected. iFISH showed the presence of Δ13, deletion of 16q23 and the presence of an unbalanced *IgH* rearrangement with an unidentified partner associated with loss of the der(14). All CA were found to be present in both samples; Δ13 and the *IgH* rearrangement were found in the majority of PC in both samples; 16q23 deletion was found in 79% of PC in sample 1 and in 96% of PC in sample 2. Array CGH was performed on purified PC from both samples (PC purity: 98% in sample 1; 92% in sample 2) and showed the same profile of losses (n=5) and gains (n=8), with no acquisition of new CNA within the 15 months follow-up (**Table 3-16**). All the CNA detected by array CGH confirmed the iFISH results. Interestingly the patient showed tetrasomy of chromosome 1q, loss of 6q25.1-qter, loss of 16q and gain of 17p12-p11.2 (including the *TACI* gene); the latter three CNA were found to be significantly more frequent in MM as compared with pre-malignant conditions (see **Sections 3.3.4.3** and **3.3.4.4**). As no new CNA were acquired after the first sample was taken, it can be hypothesised that the genetic changes characterizing the PC at the SMM stage were able to promote disease evolution; the SMM represented what may be called an 'early MM'.

3.3.5 Overall summary of the results and discussion

This study has shown that evolution of the genetic profiles from MGUS to SMM to MM is characterized by increasing complexity, which is evident from the significant increase in the mean number of CNA from asymptomatic conditions to overt disease. CNA were detected in all but one patient. In this MM case, characterized by t(14;20), the karyotype confirmed the presence of balanced structural rearrangements but no apparent copy-number changes.
A number of CNA were detected in MGUS, SMM and MM at similar frequencies indicating that they are probably not involved in the transition from asymptomatic to overt disease (i.e trisomies of odd chromosomes, gain of Xq, gain of 11q). Other CNA were detected at a higher frequency in MM compared to MGUS/SMM, suggesting that these changes may be positively associated with disease progression (del(1p), del(6q), del(8p), 8q24 abnormalities, del(12p), del(16q), del(17p)).
Interestingly, none of the MGUS patients with a low level of CNA (≤ 5) progressed to MM within the end of this study (P=0.003) (follow-up time: range, 17-125 months; median, 69 months). The majority of cases with a low number of CNA had t(11;14) and t(14;20). However, patient 1189 (with t(14;16)) and patient 2326 (with deletion of 14q and no IgHt) also showed <5 CNA with complete disease stability after 125 and 47 months from diagnosis, respectively. These observations suggested that the association between the level of CNA and disease evolution is independent of the specific primary translocation.
As the difference in the number of CNA between MGUS and MM was much higher in t(11;14) cases compared to those with t(4;14), t(14;16) and HRD, it can be hypothesised that the genetic background associated with t(11;14) has reduced potential for rapid acquisition of new abnormalities and further complexity may only be acquired when specific secondary changes arise. In this study, the comparison between MGUS and MM with t(14;20) was less clear, as only two MM cases with this translocation had available material for array CGH of which one had no CNA, only balanced translocations. However, the second t(14;20) patient showed a total of 11 CNA and metaphase analysis of 18 MM patients with t(14;20) and abnormal cytogenetics showed highly complex karyotypes with multiple gains and losses of chromosomal material in the majority of cases which would correspond to high number of CNA.

Among the abnormalities found to be rare in MGUS/SMM and more frequent in MM, some appeared to be exclusive to pre-malignant patients who then evolved to symptomatic disease. The same abnormalities were found in patients who, despite showing a continuous and rapid rise in their paraprotein level, either were never treated for MM because of premature death from MM-unrelated causes or no further follow-up was available. Examples of such abnormalities are 1p21-p22 loss, 6q25 loss, 8q24 abnormalities, 12p13.1 loss and *TRAF3* HD

(**Table 3-17**) which are strongly associated with evolving disease. Other abnormalities, despite being less frequent in MGUS/SMM and detected in patients who eventually progressed, were also found in patients characterized by long-term stability and who remained completely asymptomatic at the end of the study (8p22-p21 loss, 9p21 loss and 16q23 loss; **Table 3-17**). Understanding the biological effect of these CNA is challenging.

Gain of 1q has been reported to be absent from MGUS and has been associated with evolving disease by different groups [162-164]. However, in this patient cohort its frequency was not significantly different between diagnostic groups and its association with t(4;14), previously reported in MM [162,165], was found to be already established in pre-malignant conditions. Moreover, no significant association was found between 1q gain and evolving disease either in MGUS or in SMM. As a result of these observations, the impact of this abnormality on progression has to be further investigated in a larger patient series (**Section 3.4**).
Loss of 1p32.3, involving the *CDKN2C/p18* and *FAF1* genes, was found in MM but not in pre-malignant disease. HD involving this locus was detected in three MM patients and in the KMS-11 cell line, indicating that the presence of this CNA is associated with the clinical manifestation of MM. Deletions of this locus have been previously reported in MM using 50K SNP-based mapping and array CGH [155,178]. As all CNA involved both genes, it was impossible to ascertain which one was the target of this abnormality. However, HD affecting only *CDKN2C/p18* have been detected in three MM cell lines. This gene has been associated with tumour progression, an increased proliferative index [226] and its ectopic expression was found to inhibit growth and induce apoptosis [227]. Bergsagel and colleagues suggested that *p18* dysregulation is a late oncogenic event in MM, which occurs at a time when tumours become more proliferative and consequently more aggressive [90]. According to this model, the abnormality would not be associated with evolution from MGUS to MM.
On chromosome 1p a second region of loss has been identified (1p21.3-p22.1), which appeared to be associated with progression to MM although progression was not immediate (74 and 75 months in two MGUS patients). Interestingly, Chang *et al.* investigated the prevalence and prognostic significance of 1p21.2 loss in MM and MGUS by iFISH using a BAC probe immediately centromeric of the common minimally deleted region defined in the current study. The abnormality was detected in 18% of MM patients and those with 1p21 deletions were found to have significantly shorter progression-free survival and OS than those without such deletions. Of note was that the abnormality was absent from MGUS patients in support of the findings of the current study [228].

Combining array CGH and FISH, abnormalities involving the chromosomal band 8q24.21 (where *MYC* is located) were found in 13 of 47 (28%) MM patients, with increased incidence in

HRD cases (*P*=0.025). This incidence was higher than that reported by Avet-Loiseau *et al.* (13%) [111,143]. The *MYC* abnormalities detected in the present study were highly variable and included small interstitial duplications, amplifications, deletions within the proximity of the gene, balanced and unbalanced rearrangements. The small duplications identified by array CGH were too small to be detected by the commercially available FISH probes or by the in-house probes described by Avet-Loiseau and colleagues. These observations suggested that a proportion of *MYC* abnormalities remain undetected when screened by FISH. This may explain why the frequency of *MYC* abnormalities varies between series, as it is dependent on the detection method used. All CNA involving *MYC* identified in the present study were confirmed using an in-house BAC probe for *MYC,* specifically grown and labelled for this purpose. However, given the multiple break-points and the variable nature of *MYC* abnormalities, an improved approach either using individual techniques (i.e. multiple iFISH probes, MLPA) or a combination needs to be developed in order to detect the majority of changes. *MYC* abnormalities were rare in pre-malignant conditions: only one MGUS and one SMM were found to be positive for abnormalities at 8q24.21. The rarity of these abnormalities in pre-malignant conditions and the fact that both cases progressed to MM (at 16 and 45 months) are strongly suggestive that *MYC* aberrations are involved in disease evolution of these cases. Interestingly, the patient who progressed after 45 months had the abnormality in only a sub-population of cells.

In MM, array CGH defined two common minimally deleted regions on 12p. The most telomeric one, at 12p13.1, involved only three genes including *CDKN1B*. However, apart from two cases with small localized deletions which defined the two minimally deleted regions, 12p deletions were large with no common break-points, involving both common regions of loss. In the array CGH group, 12p deletions were absent from MGUS and SMM. In the iFISH group, 12p13.1 deletions were found to be very rare in pre-malignant cases and, when present, they appeared to be associated with progression to MM. *CDKN1B* is a critical cell-cycle regulator which arrests cell division and inhibits G_1-S transition. In MM, immunohistochemical studies have shown that patients with low *CDKN1B* expression had a significantly shorter OS, while patients with high *CDKN1B* expression experienced prolonged survival [229]. However, mutation or silencing of *CDKN1B* in human cancer is extremely rare [230] while loss of CDKN1B protein is a common event resulting from enhanced proteolysis. This probably explains why, in the current study, 12p13.1 deletion by iFISH was not associated with inferior OS in MM patients. As previously stated, the majority of 12p deletions were large, thus other genes within this chromosomal region may be associated with disease progression. In contrast, Avet-Loiseau and colleagues recently published a SNP array study in which they concluded that 12p13.31 loss represented a very powerful marker of inferior prognosis in MM [167]. However, preliminary FISH results

collected by the UK Myeloma Database on a similar number of patients did not confirm this finding (unpublished data).

The initial array CGH results suggested a possible role of *CDKN2A/2B* loss at 9p21.3 in disease progression, in particular in t(14;16) cases. Surprisingly iFISH on the independent cohort showed a higher prevalence of this abnormality in MGUS as compared to MM (12% *vs* 6%). No 9p21.3 losses were detected in SMM patients. In MM, the presence of this abnormality was associated with shorter OS (*P*=0.006). In MGUS, the biological effect of the abnormality was unclear as two patients progressed to MM, while another two remained stable after 38 and 79 months. *CDKN2A* and *CDKN2B* encode for cell cycle regulators ($p16^{INK4a}$, $p14^{ARF}$ and $p15^{INK4B}$) involved in the inhibition of G_1 phase progression. Mutant or absent *CDKN2A* is a critical oncogenic factor in prestine-induced murine plasmacytomas, but the role of this gene in MM is less clear [231]. Surprisingly, Uchida *et al.* [232] found no mutations or deletions of *CDKN2A/2B* in MM, but promoter methylation was reported at an incidence of 58%. Similarly, Gonzales-Paz *et al.* showed that methylation of *CDKN2A* was a common event in all PC disorders (including MGUS and SMM) and that its frequency increased with disease progression, although only in a modest fashion. In the same study gene methylation did not appear to affect gene expression levels; in addition no difference in OS was seen between patients with or without *CDKN2A* methylation, suggesting that the methylation of this gene may be a marker for overall epigenetic changes associated with disease progression with no obvious direct biological or clinical consequences [233]. However, a recent quantitative real-time PCR study by Sarasquete *et al.* showed that p15 expression was lower in symptomatic MM than in SMM with similar results for p14/p16. MM patients whose PC displayed high p15 and/or p14/p16 expression had a lower percentage of S-phase PC than the remaining cases, favourable prognostic factors and longer survival (*P*=0.007) [234]. These findings are in agreement with those reported in the current study.

In this study a number of CNA were found to involve genes encoding for regulators of the NF-κB pathway. Is has been suggested that activation of this pathway is important for the survival of healthy PC [235] as well as MM tumours [236-238]. The NF-κB family of transcription factors consists of NFKB1 (p50 and its precursor p105), NFKB2 (p52 and its precursor p100), RelA (p65), RelB and c-Rel [239]. There are two general pathways of activation: classical and alternative (**Figure 3-20**). In the classical pathway activated IKKβ, which is part of an IKKα-IKKβ-IKKγ complex, phosphorylates the inhibitory subunits IkBα, IκBβ or IκBε leading to their proteasomal degradation. As a result, NFKB homodimers and heterodimers comprised mainly of RelA, RelC and p50, accumulate in the nucleus. Many different stimuli activate the classical pathway [239] which is required for a successful immune response and to amplify the

survival and proliferation of cells. In the alternative pathway, NIK activates IKKα, which phosphorylates NFKB2 resulting in proteasomal removal of an inhibitory C-terminal domain, generating the p52 subunit. This leads to accumulation of p52/RelB heterodimers in the nucleus. The alternative pathway, which is important in lymphoid development, is activated in response to a small subset of tumour necrosis factor (TNF) family members, including CD40L, LTαβ (lymphotoxin α or β), BAFF (B-cell-activating factor), RANKL (receptor activator of NF-κB ligand) and TWEAK (THF-related weak inducer of apoptosis). Several recent reports have indicated that the alternative NF-κB signalling is regulated mainly through the control of NIK turnover with TRAF3, TRAF2 and BIRC2/3 critically involved in this process [240,241].

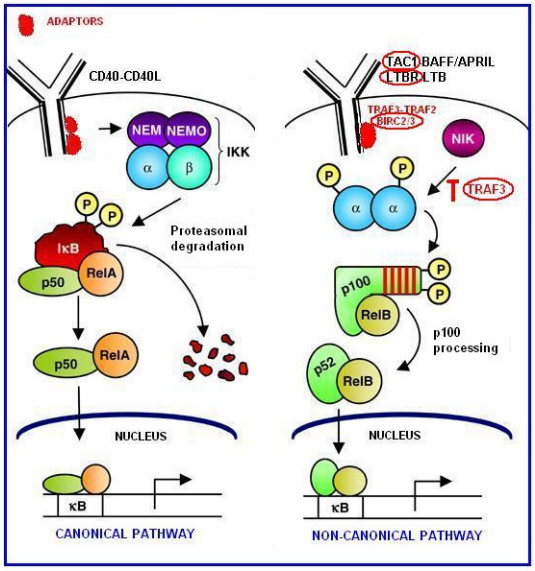

Figure 3- 20 NF-κB signal transduction pathways

Modified from Gilmore, 2006 [242]

Various cancer types utilize constitutive NF-κB signalling to block apoptosis [243] and it has been shown that 50% of HMCL and most primary MM samples have a high level of NF-κB activity, which was based on a transcription signature of 11 genes [182]. It has also been reported that approximately 40% of HMCL and at least 17% of primary MM tumours have mutations in components of this pathway, and that the presence of these mutations is associated with a high level of NF-κB activity and possibly stromal cell independence [181,182,244]. Overall, these abnormalities involved loss of function of *TRAF2, TRAF3, CYLD, BIRC2/3* and gain of function of *NFKB1, NFKB2, CD40, LTBR, TACI* and *NIK*. Some of these changes appear mainly to activate the classical pathway (*CYLD, NFKB1, TACI*) and one mainly the alternative pathway

(*NFKB2*), but most activate the alternative and to a lesser extend the classical pathway (*BIRC2/3, NIK, TRAF2, TRAF3, CD40*) [245].

In this array CGH study, 13% (2/15) of SMM and 26% (12/47) of MM patients, were found to have CNA involving members of this signalling pathway (one CNA was found in paired samples of the same patient at different stages of the disease). iFISH on the independent cohort of MM patients detected an overall incidence of abnormalities involving *BIRC2/3*, *TRAF3* or *NIK* of 9%. In both patient cohorts, cases with hemizygous deletions of *TRAF3, BIRC2/3* and *CYLD* were considered inconclusive, as no information was available on the status of the other allele. Inactivating mutations of *TRAF3* and *CYLD* were found in 50% (8/16) and 20% (1/5) of MM patients with hemizygous deletions of these loci [181]. The lower frequency of NF-κB abnormalities in the independent cohort tested by iFISH may be explained by the fact that most MM patients from the array CGH cohort had a more aggressive disease. This hypothesis is in line with the fact that, because array CGH requires a relatively high quantity of good quality DNA, samples with high PC infiltration (often associated with high grade disease) are more likely to have been selected for this type of analysis. This observation also concurs with the hypothesis that changes involving this pathway are secondary events that occur late in the development of the disease. In agreement with this hypothesis, iFISH showed that in MM, these CA often involved only a proportion of neoplastic PC while other abnormalities, within the same patient, were found to be present in the entire PC population. Furthermore, a number of cases with HD of *TRAF3* or *BIRC2/3* showed that the loss of the second allele only involved a subclone of the population with the hemizygous deletion, indicating that the loss of the second allele occurred later on in tumour progression.

In MM, the presence of *TRAF3* HD was found to be significantly associated with an inferior outcome (P=0.002), while patients with hemizygous deletion showed a clinical course almost identical to patients with no abnormalities at this locus. This suggested that inactivation of both alleles is necessary to exert a biological effect.

In the array CGH patient cohort, one SMM with t(14;16) was found to have a HD involving *TRAF3;* another SMM was found with an interstitial duplication at 17p12-p11.2 including *TACI*. Both evolved to MM within 15 months. Interestingly, the MGUS patient (989) with array CGH performed at the time of MGUS diagnosis and at the time of MM evolution showed acquisition of 4q24 gain (where *NFKB1* is located) and 16q12.1 hemizygous deletion (where *CYLD* is located) only at the time of the second sample. In the iFISH patient cohort no HD of *TRAF3*, *BIRC2/3* or *NIK* abnormalities (translocations or amplifications) were detected in MGUS or SMM patients. Overall, these findings suggested that abnormalities involving members of this pathway may play a role in the transition from MGUS/SMM to MM. Hemizygous deletions of *TRAF3* were found in 14% and 27% of MGUS and SMM, respectively. It would have been interesting to perform mutational analysis on MGUS, SMM

and MM with *TRAF3* hemizygous deletions in order to determine whether complete abrogation of the gene function was present in pre-malignant conditions or restricted to MM. Unfortunately the lack of material made this impossible.
Interestingly, Annunziata *et al.* [182] showed that not all molecular sub-groups of MM had equivalent expression of the NF-κB signature. It was high in tumours with *c-MAF* or *MAFB* dysregulation and those with low levels of bone disease. Expression was low in tumours with t(4;14) and MM with increased expression of proliferation-related genes. In our iFISH patient cohort, there was a significant association between these abnormalities and *IgH* rearranged cases, including tumours with t(4;14).

Table 3-17 summarizes the various CNA found to be more frequent in MM than in MGUS and SMM. In MGUS and SMM, the presence of these CNA was correlated with the clinical course of the disease. Some of these CNA appeared strongly associated with progression to overt MM, while others were also found in cases characterized by long-term stability throughout the study.

CNA	CNA frequencies among diagnostic groups	Association with progression
1q21-q23.2 gain	Increasing frequency from MGUS to SMM to MM However, difference not significant	No[§]
1p32.3 loss	Absent in MGUS/SMM; present in MM (also in form of HD)	Unclear whether CNA involved in MGUS to MM progression or only associated with late stage MM [§]
1p21.3-p22.1 loss	Increasing frequency from MGUS to SMM to MM	High
6q25.1-q25.2 loss	Increasing frequency from MGUS to SMM to MM	High
8p22-p21.2 loss	Increasing frequency from MGUS to SMM to MM	Ambiguous
***MYC a*bnormalities (8q24)**	Increasing frequency from MGUS to SMM to MM	High
9p21.3 loss	• Array CGH cohort: absent in MGUS/SMM; present in MM (also in form of HD) • iFISH cohort: higher frequency in MGUS than in MM	Ambiguous
12p13.1-p12.3 loss	• Array CGH cohort: absent in MGUS/SMM; present in MM • iFISH cohort: higher frequency in MGUS than in MM	High
13q loss	Increasing frequency from MGUS to SMM to MM in t(11;14) patients	High
16q23.1 loss	Increasing frequency from MGUS to SMM to MM	Ambiguous
17p13.1 loss	Increasing frequency from MGUS to SMM to MM	High
NF-κB abnormalities	Absent in MGUS; increasing frequency from SMM to MM in both the array CGH and iFISH patient cohort	High

Table 3- 17 Summary of the CNA with increasing frequency from MGUS to SMM to MM and their association with disease progression

[§] Confirmation of these findings was obtained on a larger patient cohort using array CGH and iFISH reported in Section 3.4.

3.4 Chromosome 1 abnormalities

3.4.1 Introduction

The array CGH results, described in **Section 3.3.4.3.2,** showed that 1q gain is present in the context of MGUS and SMM as well as in MM. The frequency of 1q gain was found to increase from MGUS to MM; however, the differences among the diagnostic groups were not statistically significant. More importantly, 1q gain did not appear to be significantly associated with disease evolution of pre-malignant patients.
These results are in contrast with data that has been previously published. Hanamura and colleagues compared the frequency of 1q21 gain in different diagnostic groups. Such frequencies were 0% in MGUS (n=14), 45% in SMM (n=31), 43% in overt MM (n=479) and 72% in relapsed cases (n=45) [162]. The same frequency of 1q21 gain in MGUS was reported by Chang *et al.* (n=23) [163]. In the paper by Hanamura *et al.*, the abnormality was associated with a higher risk of transition of SMM to active MM, as 1q21 gain was detected in ten of 12 patients who evolved to MM compared to four of 19 patients who remained stable (P=0.001). In another study including 15 SMM patients studied by metaphase CGH, gain of 1q was also identified as one of the abnormalities which characterized the evolving-type of SMM (**Section 1.5.2.2**), together with Δ13 and deletions of 8p, 13q, 14q and 16q [164]. The pitfall of these studies was the fact that they all included relatively limited numbers of patients. Moreover, because of the high quantity of DNA required for metaphase- and array CGH, patient cohorts tested with these techniques may be biased towards patients with a higher degree of BM plasmacytosis. This is confirmed by the fact that abnormal metaphases were detected in 31 of the 39 (79%) MM patients tested by array CGH in **Section 3.3,** while the overall rate of MM patients with abnormal cytogenetics is ~38% [87] (P=6.42 e-8).

Array CGH showed that deletions of 1p are rare in pre-malignant conditions (**Section 3.3.4.3.2**). Within this chromosomal arm, two recurrently deleted regions were detected in the MM group. One was located at 1p32.3, where the common minimally deleted region encompassed the genes *FAF1* and *CDKN2C*. No MGUS/SMM cases were found to be positive for this abnormality in line with the suggestion that it is predominantly a late change present in advanced MM [90]. However, the number of pre-malignant cases tested by array CGH was too small to conclude that 1p32.3 is exclusively associated with overt MM.

Here iFISH was used (**i**) to assess the incidence of 1q21 gain and 1p32.3 loss in a large cohort of patients with PC disorders; (**ii**) to look at the possible associations of these abnormalities with other changes tested by FISH; (**iii**) to clarify their prognostic significance in newly diagnosed MM patients; (**iv**) to assess whether 1q gain or 1p32.3 loss might be associated with disease progression.

3.4.2 Patients

A series of 924 patients with samples sent to the Myeloma Cytogenetic Database from multiple centres throughout the UK were evaluated. They comprised MGUS (n=100) (median age, 70 years; range, 39-91 years), SMM (n=57) (median age, 65 years; range, 37-86 years) and MM patients (n=767) (median age, 65 years; range, 30-93 years).
In the MGUS group, 16 patients had an IgA paraprotein isotype, 69 an IgG and two an IgM; for 13 patients this information was not available. The paraprotein level at diagnosis was accessible for 75 cases: in 38 patients this was <15 g/L. Among the MM group, 445 patients were entered into the Myeloma IX Trial (median age, 64 years; range, 30-89 months); of the 322 non-trial patients, 82% were studied at diagnosis. OS was calculated for MM patients studied at diagnosis (trial patients: median follow-up, 21 months; range, 0-63 months; non-trial patients: median follow-up, 20 months; range, 0-78 months). In the MGUS series, follow-up data was available on 96 patients (median follow-up, 41 months; range, 3-86 months). Seven MGUS patients were not studied at diagnosis (the interval between diagnosis and cytogenetic analysis ranged from 8 to 223 months); in these cases the follow-up was calculated from the time of analysis given the impossibility of knowing the time of acquisition of chromosome 1 abnormalities. In SMM, follow-up information was available for 47 patients (median follow-up, 35 months; range, 6-99 months); in this group, one patient was not studied at diagnosis (patient 1581) and the only information available was that he had a long history of SMM.

3.4.3 Methods

3.4.3.1 Fluorescence *in situ* hybridization and array CGH

Interphase FISH was performed on $CD138^+$ purified PC as described in **Section 3.1.3.1**.
Patients were characterized for the presence of *IgH* rearrangements, ploidy status, Δ13 and deletions of *TP53*. To assess 1q status additional in-house probes were used: all patients were

tested for *CKS1B* (1q21.3); a proportion of patients were also tested for *PDZK1* (1q21.1) (78% of MGUS, 54% of SMM and 28% of MM) and *ASPM* (1q31.3) (48% of MGUS, 26% of SMM and 28% of MM) (probes are described in **Appendix 3**). PDZK1 has been reported to be involved in organizing proteins at the cell membrane [246] and in linking transmembrane proteins to the actin cytoskeleton [247]; the gene has been suggested to be one of the potential targets for 1q gain and its product has been associated with drug resistance [156]. The *ASPM* locus was tested in order to assess whether the abnormality involved only the proximal region of 1q or a more extended area.

Deletions of 1p32.3 were assessed using a BAC mapping to the *CDKN2C/p18* and *FAF1* genes. Deletions of this locus can be particularly challenging to detect as they may be very small. Different probes were validated on cases known to be positive for a deletion at this locus by array CGH. The BAC clone RP11-116M11 (51364760Mb-51437772Mb; size: 73013bp) was the only one small enough to detect all deletions and was therefore applied to interphase cells of all samples. For 12 MGUS patients, 1q and 1p32.3 status was deduced from the array CGH results described in **Section 3.3**.

3.4.4 Results

3.4.4.1 Frequency and associations of 1q21 gain

Within the MGUS group, 1q21 gain was found in 26 of 100 (26%) patients (detailed copy numbers for 1q21 are shown in **Figure 3-21**). In all positive cases detected by array CGH (five of 12), the gain involved the entire arm; in those tested by iFISH, when the three 1q probes were tested, all loci showed the same copy number in all but one patient (this case showed 5 copies of *CKS1B/ASPM* but normal *PDZK1*). By iFISH, 1q21 gain was found in a sub-population of PC in two patients (21% and 26%); in the remainder of cases the abnormality was present in all PC.

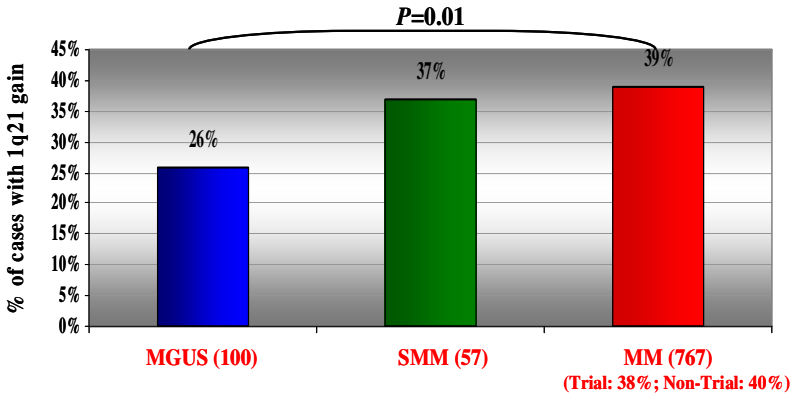

	MGUS	SMM	MM
Median % of PC with 1q21 gain	87% *range*, 21-100% [§]	93% *range*, 39-100%	94% *range*, 28-100%
3 copies of 1q21	19%	28%	30%
4 copies of 1q21	4%	9%	7%
5 copies of 1q21	3%	0%	1%
Amplification (≥ 6 copies)	0%	0%	<1%

Figure 3- 21 Detailed copy number of 1q21 in MGUS, SMM and MM

[§] The MGUS cases assessed by array CGH showed 1q gain to be present in the majority of PC

In SMM and MM, the frequency of 1q21 gain was found to be significantly higher compared to MGUS (MGUS *vs* MM, *P*=0.01): 21 of 57 (36.8%) SMM patients and 297 of 767 (38.7%) MM patients were positive for the abnormality. True amplification, defined as ≥6 copies, was absent in MGUS/SMM and rare in MM (n=6). In MGUS and MM, 1q21 gain was significantly associated with t(4;14), Δ13, and inversely associated with t(11;14) and t(6;14); in MM 1q21 gain was also associated with t(14;16), t(14;20) and nonHRD; in SMM, 1q21 gain was associated with Δ13 (**Table 3-18**).

			t(4;14)		t(6;14) & t(11;14)		Δ13		t(14;16)		*TP53* Del		t(14;20)		Ploidy		*p18* Del	
			N	*T*	*N*	*T*	*N*	*Del*	*N*	*T*	*N*	*Del*	*N*	*T*	*HRD*	*nonHRD*	*N*	*Del*
1q21 status	MGUS	*N*	71	2	56	18	57	17	72	2	70	4	71	3	29	44	66	2
		Gain	22	4	26	0	12	14	23	3	22	2	23	2	8	16	21	2
	SMM	*N*	33	3	31	5	27	9	35	1	36	0	35	1	22	13	30	3
		Gain	15	6	18	2	8	13	18	3	20	1	21	0	8	13	16	1
	MM	*N*	447	26	379	94	297	176	465	7	429	39	470	2	286	165	373	47
		Gain	239	56	266	28	114	181	280	14	265	26	283	10	152	127	223	41

Table 3- 18 Associations between 1q21 gain and other chromosomal abnormalities in the three diagnostic groups

(Δ13, deletion/monosomy 13; N, normal; T, translocated; Del, deleted; HRD, hyperdiploid; nonHRD, non-hyperdiploid)
Positive associations are highlighted in blue, negative ones in yellow

Statistically significant associations:

- t(4;14) in MM (P<0.001) and MGUS (P=0.039)
- inverse association with t(6;14) and t(11;14) in MM (P<0.001) and MGUS (P=0.003)
- Δ13 in MM (P<0.001), SMM (P=0.010) and MGUS (P=0.006)
- t(14;16), t(14;20) and ploidy in MM (P<0.001, P=0.002 & P=0.019, respectively)

3.4.4.2 Prognostic relevance of 1q21 gain in newly diagnosed MM and impact of this abnormality on the transition from MGUS and SMM to MM

3.4.4.2.1 MM

Among the MM patients studied at diagnosis (n=691), those with 1q21 gain showed significantly inferior OS compared with those with normal 1q (27 months *vs* 51 months, *P*=7.6e-6). Inferior OS was found for both trial and non-trial patients when analyzed separately (**Figure 3-22**).

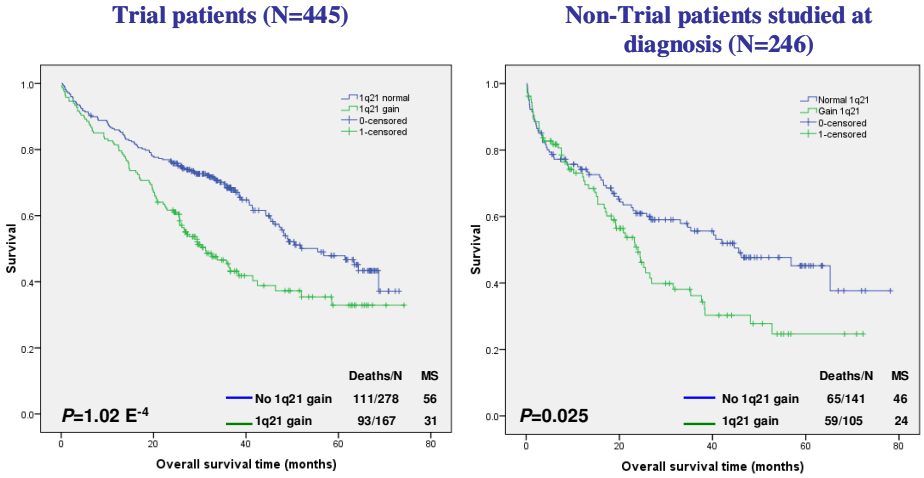

Figure 3- 22 Kaplan-Meier analysis of OS in MM displayed in relation to the presence or absence of 1q21 gain; trial (on the left) and non-trial (on the right) patients were considered separately

When MM patients with 1q21 gain were stratified on the basis of the presence or absence of other genetic markers of poor prognosis, gain of 1q21 remained an independent poor prognostic factor for OS (*P*=0.019) (**Figure 3-23**).

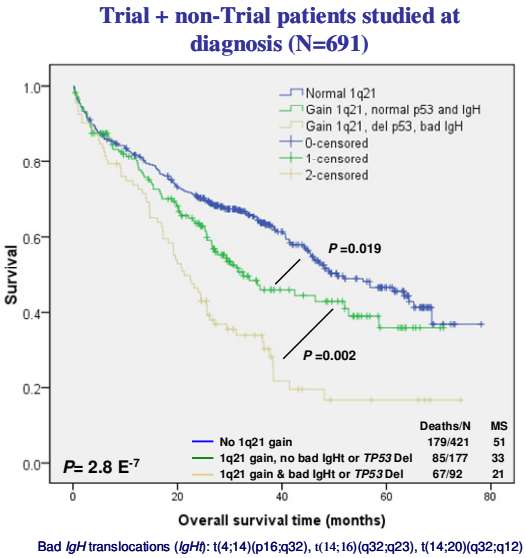

Figure 3- 23 Kaplan-Meier analysis of OS in MM displayed in relation to the presence or absence of 1q21 gain and other chromosomal markers of inferior prognosis

3.4.4.2.2 MGUS

Within the MGUS group, follow-up information was available for 96 of 100 patients. Twenty-four patients (25%) progressed to MM with a median time to progression of 33.5 months (range, 4-79 months) (**Table 3-19**). In this study, there was no significant difference in the rate of progression between patients with a paraprotein level below or equal/greater than 15 g/L. Six of 16 (38%) patients with an IgA subtype progressed to MM, compared with 16 of 66 (24%) patients with IgG. However, this difference was not statistically significant.

Only five of 25 (20%) patients positive for 1q21 gain evolved to MM (median time to progression, 45 months) compared with 19 of 71 (27%) cases negative for the abnormality (median time to progression, 32 months) (*P*=0.60) (**Table 3-19**).

P=0.60		Patient follow-up		
		Stable	*Progressed*	*Total*
1q21 status	*Normal*	52	19 (27%)	71
	Gain	20	5 (20%)	25

Table 3- 19 Association between progression and 1q21 gain in MGUS patients

The median follow-up of the 20 patients with 1q21 gain and no evidence of progression was 42 months (range, 3-78 months); six of these patients were completely stable after 5 years (**Figure 3-24**) and their paraprotein level hardly changed from diagnosis. Interestingly two cases, stable after 57 and 74 months, had five copies of 1q21.

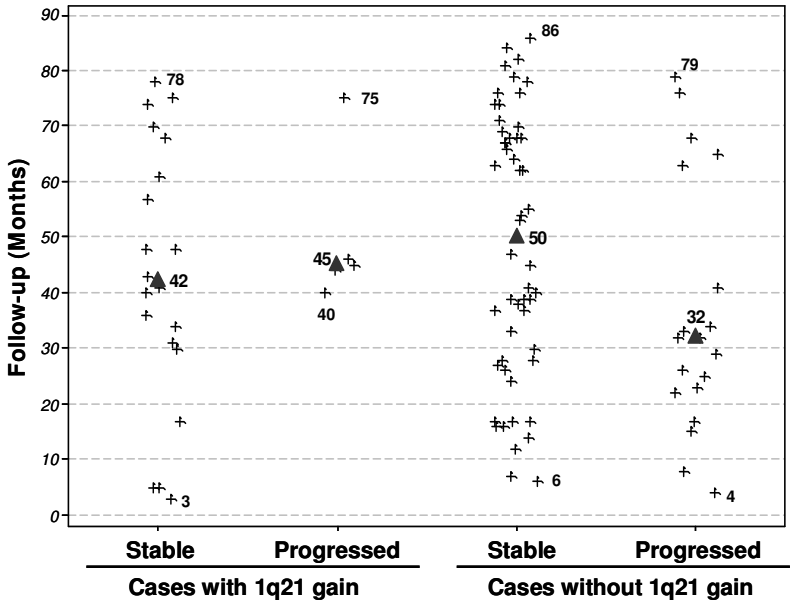

Figure 3- 24 Plot of MGUS patient follow-up versus progression and 1q21 status

Median follow-up values for the different groups are indicated by black triangles (stable MGUS cases with 1q21 gain, 42 months; progressed MGUS cases with 1q21 gain, 45 months; stable MGUS cases with no 1q21 gain, 50 months; progressed MGUS cases with no 1q21 gain, 32 months). The three stable MGUS patients with 1q21 gain and less than 6 month follow-up died of MM-unrelated causes.

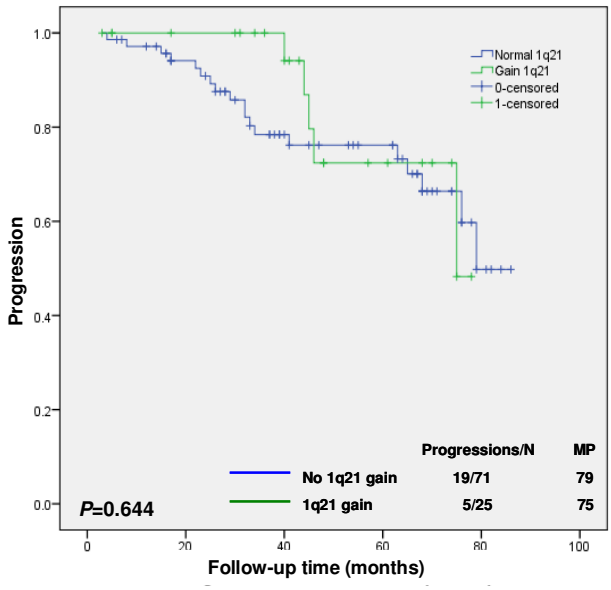

Figure 3- 25 Kaplan-Meier analysis of progression in MGUS displayed in relation to the presence or absence of 1q21 gain

As shown in **Figure 3-25,** there was no evidence that the presence of 1q21 gain in MGUS results in a more rapid progression to MM (*P*=0.644).

The five MGUS patients with 1q gain who progressed to MM were found to be positive for other abnormalities associated with a dismal prognosis in MM: t(4;14), t(14;16), Δ13, nonHRD and loss of *p18*. However, among the MGUS patients with 1q gain and stable disease for more than four years, similar abnormalities were detected: t(4;14), t(14;20), nonHRD, Δ13, deletions of chromosome 16, which have also been linked to an inferior prognosis [248].

3.4.4.2.3 SMM

Within the SMM group, follow-up information was available for 47 of 57 patients. Eighteen patients (38%) progressed to MM with a median time to progression of 22 months (range, 11-56 months). Eight of 18 (44%) patients positive for 1q21 gain evolved to MM (median time to progression, 22.5 months) compared with ten of 29 (34.5%) cases negative for the abnormality (median time to progression, 22 months) (*P*=0.55) (**Table 3-20** and **Figure 3-26**).

P=0.55		Patient follow-up		
		Stable	*Progressed*	*Total*
1q21 status	*Normal*	19	10 (34.5%)	29
	Gain	10	8 (44.4%)	18

Table 3- 20 Association between progression and 1q21 gain in SMM patients

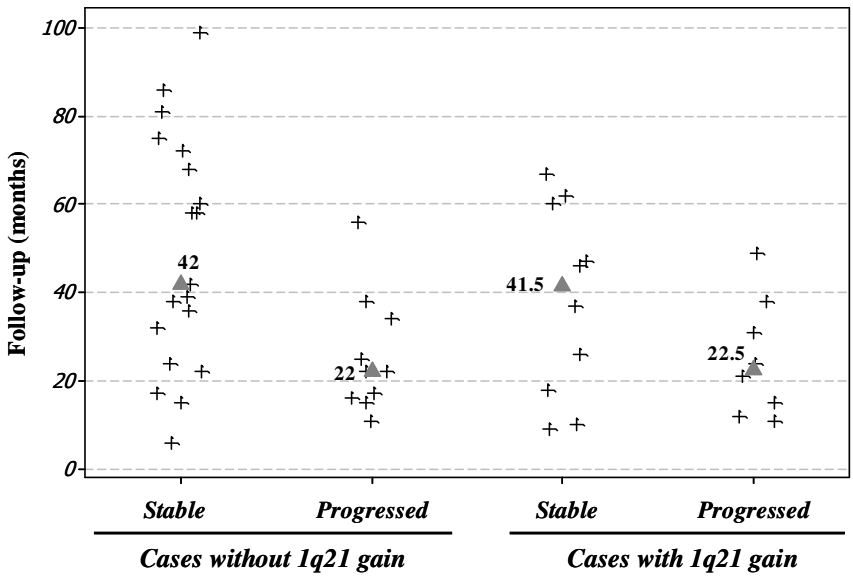

Figure 3- 26 Plot of SMM patient follow-up versus progression and 1q21 status

Median follow-up values for the different groups are indicated by black triangles (stable SMM cases with 1q21 gain, 41.5 months; progressed SMM cases with 1q21 gain, 22.5 months; stable SMM cases with no 1q21 gain, 42 months; progressed SMM cases with no 1q21 gain, 22 months)

Interestingly none of the stable cases with the abnormality had more than one extra copy of 1q21; in contrast four of the eight cases who progressed had two extra copies of 1q21 in all PC or in more than half of the PC population, with the remaining PC carrying three copies.
As already observed in MGUS, 1q21 gain was found in association with other poor prognostic markers in both SMM cases who progressed and cases who remained stable.

3.4.4.3 Frequency and associations of 1p32.3 loss

Loss of 1p32.3 was found in four of 95 (4%) of MGUS, 4 of 50 (8%) of SMM and in 94 of 709 (13%) of MM patients (MGUS *vs* MM, *P*=0.01). HD of this locus were only found in MM (9/709, 1%). One MGUS patient showed the deletion in 18% of PC and was considered negative for the abnormality (cut-off level: 20%). In two MGUS cases the abnormality was found in less than 50% of PC (40% and 45%); in the other two cases 1p32.3 loss was present in the majority of PC. All four positive SMM cases showed the abnormality to be present in less than 50% of PC; in MM the median percentage of PC with the deletion was 92% (range, 21-100%).

Within the MM group, 1p32.3 loss was positively associated with 17p13 deletions (*P*=0.045) and nonHRD (*P*=0.003) and inversely associated with the translocations t(6;14) and t(11;14) (*P*=0.01) (**Table 3-21**). No specific association was found between 1p32.3 loss and any of the other CA tested in both MGUS and SMM; this was probably due to the small number of patients in these diagnostic groups who were positive for the abnormality.

			t(4;14)		t(6;14) & t(11;14)		Δ13		t(14;16)		*TP53* Del		t(14;20)		Ploidy		1q21 gain	
			N	*T*	*N*	*T*	*N*	*Del*	*N*	*T*	*N*	*Del*	*N*	*T*	*HRD*	*nonHRD*	*N*	*Gain*
1p32.3 status	MGUS	*N*	84	6	74	17	65	26	87	4	84	4	84	6	33	56	66	21
		Del	4	0	3	1	3	1	4	0	3	1	4	0	3	1	2	2
	SMM	*N*	40	6	38	7	29	17	42	4	46	0	45	1	24	20	30	16
		Del	3	1	4	0	3	1	4	0	4	0	4	0	1	3	3	1
	MM	*N*	550	65	506	108	337	278	599	14	562	48	605	7	358	215	373	223
		Del	85	9	87	7	49	45	89	5	77	13	91	3	42	50	47	41

Table 3- 21 Associations between 1p32.3 loss and other chromosomal abnormalities in the three diagnostic groups

(Δ13, deletion/monosomy 13; N, normal; T, translocated; Del, deleted; HRD, hyperdiploid; nonHRD, non-hyperdiploid)
Positive associations are highlighted in blue, negative ones in yellow

Statistically significant associations:

- *TP53* deletion in MM (*P*=0.045)
- nonHRD in MM (*P*=0.003)
- inverse association with t(6;14) and t(11;14) in MM (*P*=0.01)

3.4.4.4 Prognostic relevance of 1p32.3 loss in newly diagnosed MM and impact of this abnormality on the transition from MGUS and SMM to MM

Among the four MGUS patients with the deletion: for one case, the follow-up was lost immediately after diagnosis; one patient died of MM-unrelated causes 3 months after diagnosis, while the remaining two patients progressed to MM after 40 and 68 months.
Among the four SMM patients: two patients remained stable after 9 and 81 months; one patient progressed to MM after 22 months and subsequently died of refractory disease; whilst the last fourth case was lost to follow-up soon after diagnosis.

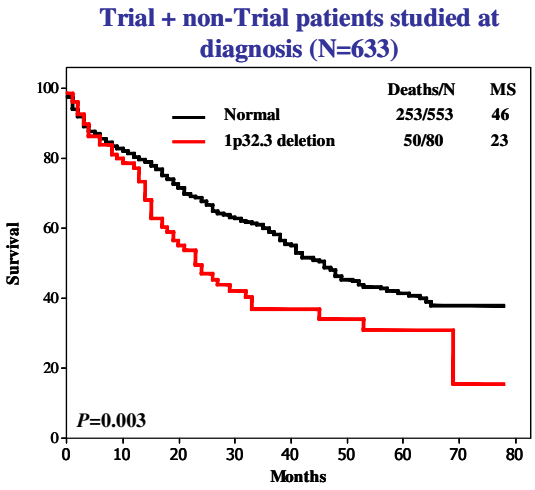

Figure 3- 27 Kaplan-Meier curve for OS in newly diagnosed MM patients for 1p32.3 deletions

In newly diagnosed MM, patients with 1p32.3 loss (either loss of one or two copies) showed a significantly inferior OS compared to patients without the abnormality (median survival, 23 months *vs* 46 months, *P*=0.003) (**Figure 3-27**). Among the nine patients with HD at this locus, seven (78%) died (median time to death = 17 months). When MM patients with 1p32.3 loss were stratified on the basis of the presence or absence of *TP53* deletion (given the association between the two abnormalities), 1p32.3 loss remained an independent poor prognostic factor of OS (*P*=0.019).

3.4.5 Overall summary of the results and discussion

This study shows for the first time that 1q21 gain may be present in MGUS (26%); disagreement with other reports is probably due to the limited number of cases enrolled in those studies [162,163]. The frequencies of 1q21 gain in SMM and MM were in agreement with published data [162,163,165]. However, when the specific copy number of *CKS1B* was considered in cases positive for the abnormality, MM patients from our cohort only showed ~9% of cases with more/equal four copies, while Hanamura and colleagues [162] reported 18% of their MM patients with high level gains.
Despite being considered as a secondary change, only two of 26 (8%) MGUS cases with the abnormality showed 1q21 in a PC sub-clone, suggesting that the acquisition of this CA is often an early event.
The same associations as found in MM between 1q21 gain and other CA were confirmed in MGUS and SMM; lack of significant associations for some of the markers in SMM was probably a consequence of the fact that fewer patients were included in this group. In MM, 1q21 gain was associated with inferior OS in both the trial and the non-trial groups (P=1.02e-4 and P=0.025, respectively) and despite its coexistance with other markers of poor prognosis (i.e. adverse *IgH* translocations), 1q21 gain appeared to be independent of these factors.

In MGUS, 1q21 status was correlated with time to progression using the Kaplan-Meier analysis: no evidence was found that the presence of 1q21 gain was responsible for very rapid progression, as there was no difference in the time to progression between patients with and without 1q gain. Interestingly, six patients with the abnormality were completely stable for more than 5 years and two patients, stable at 57 and 74 months, clearly showed five copies of 1q21 in their clonal PC. It was hypothesized that the specific association with other chromosomal abnormalities might modulate the biological effect of 1q21 gain in MGUS. In this study, no difference in the association of 1q21 with other chromosomal markers was detected between patients with 1q21 gain who progressed and patients with 1q21 gain whose disease remained stable. However, this needs to be explored further in a larger series as the disease is genetically highly heterogeneous and some changes are relatively rare.

A risk stratification system for MGUS patients based on clinical parameters was defined by the Mayo Clinic; this combines paraprotein isotype, paraprotein level and free light chain ratio [48]. Unfortunately MGUS patients from this cohort were not assessed for free light chain ratio. However, both the paraprotein isotype and the paraprotein level could be correlated with time to progression: no significant association between these markers and progression was found. Interestingly, similar results have been reported by Weiss *et al.* [75]: in their patient cohort there

were no patients who satisfied the criteria for high-risk MGUS defined by the Mayo clinic model, in fact patients who rapidly progressed were classified as low risk by this same model. In SMM the effect of 1q21 gain on progression was more difficult to assess as the follow-up was only available on 47 patients: 44% of patients with 1q21 gain progressed to MM compared with 35% without the abnormality. This difference was not statistically significant (P=0.55) and no difference in median follow-up time was found between stable cases with and without the abnormality (41.5 months *vs* 42 months, respectively). However, it should be noted that none of the stable patients with 1q21 gain had more than three copies of 1q while half of the patients who progressed had at least two extra copies of the chromosomal arm. This observation may suggest that, in SMM, either acquisition of extra copies of 1q affects disease evolution or it might be that those cases (with more than one extra copy of 1q) achieved a high level of genomic complexity. Maybe this complexity was responsible for their evolution, with tetrasomy 1q being only a manifestation of this complexity and not the cause of progression.

Loss of 1p32.3 was found to be rare in MGUS (4%) confirming the array CGH results. In six of eight pre-malignant cases positive for the abnormality, this was found to involve only a sub-clone of PC suggesting that the abnormality is a secondary event in most cases.
In MM loss of 1p32.3 was associated with an inferior OS (P=0.003). In MGUS and SMM a clear understanding of the effect of 1p32.3 loss was hampered by the limited number of patients with the abnormality and by the lack of follow-up information for three of the eight. However, it is of interest that of the five patients with this information, two MGUS and one SMM patient progressed to MM after 40, 68 and 22 months, respectively. As noticed for other abnormalities, in those patients with 1p32.3 loss who progressed to MM time to progression was variable suggesting that other factors might have played a role in their transformation.

3.5 Sequential analysis of a SMM case

3.5.1 Introduction

The course of MGUS and SMM patients is usually monitored by the continuous observation of clinical parameters, while BM samples are only taken at diagnosis or when progression is suspected. This practice makes it difficult to perform longitudinal genetic studies on those rare cases who transform to frank MM.

Patient 259 was initially diagnosed as SMM and was followed for a period of 4.5 years until progression to symptomatic MM. Five serial BM samples, taken every year following diagnosis of SMM, were sent to the Myeloma Cytogenetic Database with detailed information of the BM morphology and the clinical parameters. Conventional cytogenetics, iFISH and array CGH were carried out on the five serial samples in order to associate the time of appearance of the different abnormalities detected in the neoplastic clone with the clinical course of the disease.

3.5.2 Case Report

Patient 259, a 30 year old caucasian woman, was incidentally found to have protein in her urine in September 2001, in the absence of urinary symptoms or infections of the urinary tract. Laboratory findings included WBC count of 6.4 x 10^9/L (reference range, 4.0–11.0 x 10^9/L); haemoglobin level of 125 g/L (reference range, 120–150 g/L); calcium corrected of 2.32nmol/L (reference range, 2.15–2.55 nmol/L). Her BM aspirate (sample 1) showed BM elements adequately represented, with normal differentiation and maturation; 9% PC with atypical morphology was observed (**Figure 3-28A**). The trephine displayed a degree of architectural disorganization, with low level increase in the number of PC, and occasional focal aggregations. There was an IgAk paraprotein of 32.4 g/L (reference range, 0.8–2.8 g/L) and kappa light chain in the urine, with no evidence of end organ damage, although β_2M was 3.4 mg/L (reference range, 1.2–2.4 mg/L) and renal function was slightly impaired (creatinine 132 µmol/L; reference range, 60–125 µmol/L). A renal biopsy showed minor glomerular abnormalities, but no changes that are typically associated with MM related renal damage. She was diagnosed with SMM and

no treatment was given. Laboratory examination in 2002 indicated stable disease, with no raise in paraprotein or in creatinine levels; WBC count, haemoglobin, electrolytes and calcium levels were also normal. Subsequent BM investigations were performed in June 2003 (sample 2), June 2004 (sample 3) and May 2005 (sample 4). PC levels were 13%, 3% (haemodilute) and 28%, respectively, with trephines indicating low level PC infiltration in normocellular marrows. Paraprotein levels fluctuated between 25.5 and 33.2 (**Figure 3-29**). Creatinine did not increase, and was 113 μmol/L in 2005, but β_2M increased to 5.6 mg/L at that time. Repeat MRI scans showed no change from diagnosis.

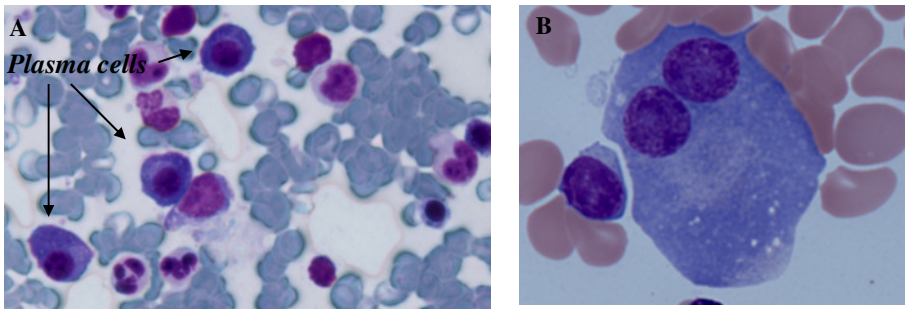

Figure 3- 28 A) Bone marrow aspirate (2001 sample); B) Binucleated PC in 2006 sample (Hematoxylin and eosin stain)

In January 2006 the patient remained asymptomatic, despite a slight increase in paraprotein (35.7 g/L) and a marginal decrease in platelet count (116 x 10^9/L). In March 2006 she was urgently re-assessed and treated, due to bone pain in her left clavicle, subsequently shown to be due to a lytic lesion. The BM aspirate (sample 5) showed ~30% PC with binucleated forms present (**Figure 3-28B**), while the biopsy revealed sheets of atypical PC in some areas. The patient was found to be anemic and trombocytopenic with a haemoglobin level of 106 g/L and platelet count of 97 x 10^9/L. She was entered into the MRC Myeloma IX Trial and treated with cyclophosphamide, thalidomide, and dexamethasone, followed by autologous stem cell transplantation in September 2006. She had an initial good response achieving partial remission, but relapsed with rising paraprotein in September 2008.

3.5.3 Methods

PC were isolated from all five samples described above as described in **Section 2.2.6**. All samples were tested by iFISH (probes are described in **Appendix 3**), with samples 2 and 5 also

adequate for cytogenetic analysis (**Section 2.3**). Sample 2 had sufficient material to extract DNA for array CGH analysis. For array CGH, genomic DNA (1.9µg) was extracted from purified PC stored in Carnoy's fixative and hybridized to the 244k microarray and processed as described in **Section 2.6**. Duplicated, amplified and deleted regions were defined using a 500 kb weighted moving-average window and the ADM-2 algorithm of the CGH Analytics software with a threshold of 6.0 (**Section 2.6.6**).

3.5.4 Results

3.5.4.1 Clinical data

The paraprotein level, monitored for the 4.5 years, did not show a progressive increase as depicted in **Figure 3.29**.

The pattern of BM infiltration by PC, except for a slight increase, did not change significantly until the clinical diagnosis of MM. At this time, sheets of atypical PC were present in the marrow.

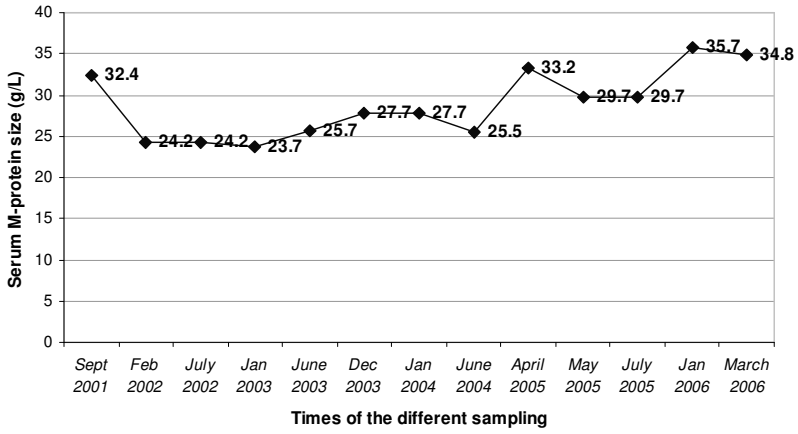

Figure 3- 29 Chart showing the variation of the serum M-protein (IgA) from the diagnosis of asymptomatic SMM to diagnosis of symptomatic MM

3.5.4.2 Genetic data

The main iFISH results are shown in **Table 3-22**. FISH indicated a hypodiploid karyotype for all samples (confirmed in sample 2 by array CGH and in sample 5 by cytogenetic analysis). At presentation all PC had a t(4;14) with loss of the der(14). It is not clear whether loss of der(14) occurred at the time of t(4;14) formation or was a secondary change, although no FISH signal patterns indicative of the balanced form were observed. No other abnormalities were detected by iFISH at this time apart from Δ13 in 18% PC. This is below the European Myeloma Network–agreed cut-off of 20%, but well above our laboratory false positive rate, indicating the presence of a low level population with this abnormality. As a confirmation, the proportion of PC with this abnormality progressively increased throughout the years: sample 2, <20%; sample 3, 40%; sample 4, 74%; sample 5 (diagnosis of MM), 100%. Conventional cytogenetic analysis of the second sample revealed only 26 normal metaphases. The 16q23 status was tested for the first time on the second sample; at this time a deletion of this locus was found in 69% of PC; similar to Δ13, the proportion of PC with this CA increased to 97% in the 2005 sample.

Sample number (date) diagnosis	*Test*	*Δ13 (%PC)*	*IgHr (%PC)*	*t(4;14) Form (%PC)*	*CCND1*	*16q status*	*ΔTP53*	*1q status*	*1p32.3 status*	*t(8;14) & MYC split*	*CC*
1 (09/2001) SMM	iFISH	(18%)	(98%)	Unbalanced (100%)	N	nt	N	N	N	N	Not set up
2 (06/2003) SMM	Metaphase analysis; iFISH, array CGH	(<20%)	(100%)	Unbalanced* (100%)	N	16q23 deletion* (69%)	N	N *	N *	N	Normal: 46,XX[26]
3 (06/2004) SMM	iFISH	(40%)	(100%)	Unbalanced (100%)	N	16q23 deletion (89%)	N	nt	N	N	Not set up
4 (05/2005) SMM	iFISH	(74%)	(100%)	Unbalanced (100%)	N	16q23 deletion (97%)	N	N	deletion (**42%**)	*MYC* split (**40%**)†; t(8;14) negative	Not set up
5 (03/2006) MM	Metaphase analysis; iFISH	(100%)	(100%)	Unbalanced (100%)	N	nt	N	N	deletion (**82%**)	*MYC* split (**100%**)	**Abnormal**

Table 3- 22 Summary of the critical iFISH results for the five samples

N indicates normal/negative result; IgHr, IgH rearrangement; unb, unbalanced; der(14), derivative (14) from an IgHt; nt, not tested

16q status was deduced from loss of the *c-MAF* part of the Abbott IgH/MAF probe combination

*** Result confirmed by array CGH**

† The *MYC* split was detected with the Abbott MYC break apart probe combination; the t(8;14)(q24;32) was tested with the IgH/MYC, CEP 8 probe combination

The array performed on sample 2 (2003) showed several CNA. All were losses, involving chromosomal regions 2p, 4p, 12q, 16p, 16q, 19q and monosomies of chromosomes 13 and 14; all chromosomal regions apart from chromosome 13 ($\log_2$ ratio = –0.18) (**Figure 3-30**) showed loss of one copy in the majority of tumour cells, consistent with the iFISH results exhibiting Δ13 in only a minor population of cells.

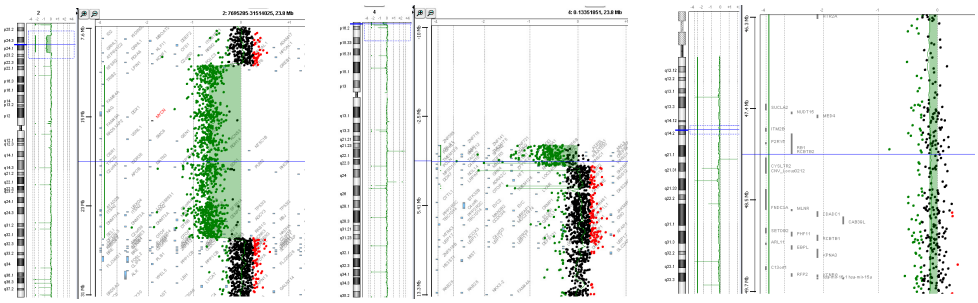

Dim (2)(11.19[2p25.1]-26.43[2p23.3]) **Dim (4)(0.04[4pter]-1.85[4p16.3])** **Monosomy(13)(18.07-114.12)**

Figure 3- 30 Array CGH analysis for chromosomes 2, 4 and 13 with the G-banded idiograms

G-banded idiograms (on the left) with the size of the abnormalities are shown for every chromosome; for the chromosomal regions 2p23-p25, 4p16 and 13q14 the plot of 'calls' for every nucleotide is shown in detail. Gains are labelled in red, losses in green

Array results: Dim*(1)(145.82[1q21.1/.2]-146.47[1q21.1/.2]); DimX2(1)(165.96[1q24.2]-165.99[1q24.2]);* Dim (2)(11.19[2p25.1]-26.43[2p23.3*]); Dim(2)(89.0[2p11.2]-89.31[2p11.2]);* Dim (4)(0.04[4pter]-1.85[4p16.3]); Enh(5)(37.49[5p13.2]-37.5[5p13.2]); *Dim (5)(172.59[5q35.1/.2]-172.6[5q35.1/.2]); Dim (6)(32.57[6p21.32]-32.63[6p21.32]); Dim (8)(6.93[8p23.1]-7.79[8p23.1]); Enh (8)(39.36[8p11.23]-39.51[8p11.23]);* Dim (12)(34.42[12CEP]-132.39[12qter]); Dim(13)(18.07-114.12); Dim(14)(18.15-105.99); *Enh(15)(18.68[15q11.2]-20.25[15q11.2]);* Dim(16)(0.03[16pter]-10.97[16p13.13]); *Dim(16)(34.06[16p11.2]-34.61[16p11.2]);* Dim(16)(45.03[16q12.1]-88.69[16qter]); Dim(19)(47.99[19q13.13]-48.45[19q13.13]); *Enh(22)(22.69[22q11.23]-22.73[22q11.23]); Dim(22)(37.68[22q13.1]-37.71[22q13.1])* (CNV are written in italics).

FISH for the three markers on 1q showed no numerical changes in any of the samples; array CGH on sample 2 did not show CNA involving any region of chromosome 1.
However, the abnormal karyotype found at the time of diagnosis of MM showed an interstitial deletion on 1p, defined as 1p13 to 1p3?2 (**Figure 3-31**). FISH analysis performed with probes in 1p12 and 1p32.2 confirmed the involvement of 1p32.3 within the deletion, encompassing the *CDKN2C/p18* and *FAF1* genes. The preceding samples were then retrospectively tested for this CA. As shown in **Table 3-21**, the first three were negative as confirmed by array CGH on sample 2, but samples 4 and 5 showed 42% and 82% of PC, respectively, with the deletion. The

deletion observed in this patient appeared to be larger than this specific locus, therefore the possible importance of other genes within this chromosomal region cannot be ruled out.

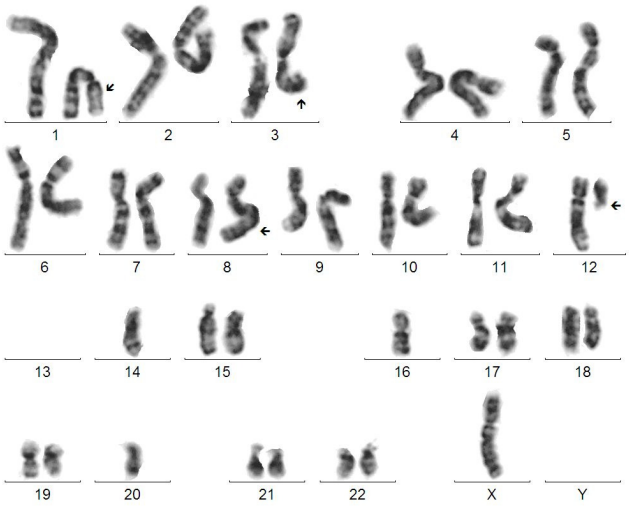

Figure 3- 31 Karyotype description

40~41,X,-X,del(1)(p13p3?2),add(3)(q2?6),der(8)t(8;13)(q24;q12),del(12)(q11),-13,-13,-14, -16,-20[cp2]

The karyotype also showed a rearrangement involving 8q24, as an unbalanced translocation t(8;13). FISH confirmed that this rearrangement involved *MYC*, as shown in **Figure 3-32,** but not the *IgH* locus. Although the *IgLλ* locus was not tested in this case, it has been reported that in the majority of MM patients *MYC* rearrangements occur through translocations with other, unknown partner regions [111].

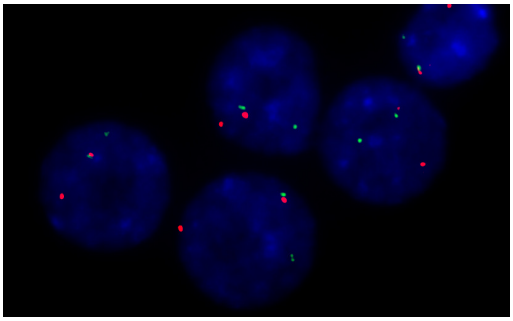

Figure 3- 32 Interphase FISH patterns from sample 5 (2006) hybridized with LSI *MYC* dual colour break-apart *MYC* probe (Vysis)

The one orange (119kb upstream of the 5′ end of *MYC*), one green (1.5Mb 3′ of *MYC*), and one fusion pattern represents a breakpoint within the gap between the hybridization targets of the probe combination resulting in a *MYC* rearrangement

Similar to the 1p deletion, the *MYC* rearrangement was observed for the first time in sample 4 and at this time it involved only a sub-population of cells (40%). This rapidly increased to 100% in sample 5.

3.5.5 Overall summary of the results and discussion

This female patient was incidentally diagnosed with SMM at the unusually young age of 30 years; less than 3% of SMM patients are younger than 40 years of age [39]. Serial annual genetic analyses were carried out over a period of 4.5 years, at which time evolution to symptomatic MM had occurred. This gave a rare opportunity to compare the clinical course of the disease at the same time points as the characterization of the genetic profile of her clonal PC at different stages of her follow-up.

As described in **Section 1.5.2.2**, a number of diagnostic clinical parameters have been defined as predictive for disease progression to MM in patients with SMM. Despite having evidence of an IgA paraprotein, the patient had <10% PC in the BM and a paraprotein level >30g/L. These parameters have been associated with the lowest median rate and longest median time to progression [39]. According to the definition of 'evolving' and 'non-evolving' type of SMM defined by Rosinol *et al.*[54] and described in **Section 1.5.2.2**, this patient conformed to the 'non-evolving' type as her paraprotein did not show a progressive increase during the follow-up time.

An unbalanced t(4;14) was found in all PC from the time of the first sample. The balanced and the unbalanced forms of this translocation are associated with a poor outcome in MM [123,218] but, as shown in **Section 3.2** and in agreement with other reports [44,138], its presence does not necessarily lead to disease evolution in the context of pre-malignant cases. In this patient at diagnosis the translocation was not associated with an aggressive phenotype. The appearance of Δ13 was clearly secondary to the *IgH* translocation and the increase in proportion of cells with this abnormality was slow, particularly in the first three years. Array CGH suggested that monosomy 13 was the latest numerical change to have been acquired by the time of the second sample. Although the abnormality might have conferred a proliferative advantage to the cell, it did not represent the cause of malignant transformation.

As described in **Sections 3.3.4.3.4** and **3.4.4.3**, chromosomal rearrangements involving *MYC* and loss of 1p32.3 are very rare in MGUS and SMM; in MM they have been associated with advance stage disease [90]. However, in this patient, both abnormalities seemed to be associated with the establishment of symptomatic MM.

3.6 Comparison between genetic abnormalities detected in MM and those detected in PCL

3.6.1 Introduction

Due to the rarity of PCL, only sporadic cytogenetic studies have been published; these have shown complex karyotypes, mainly hypodiploid, with multiple marker chromosomes involving unidentified chromosomal regions. Although unable to detect cryptic and balanced alterations, metaphase CGH has provided additional information [151,153] while FISH revealed the presence of specific changes in patients with failed, normal and highly rearranged karyotypes [97,151,153,249-252]. Many of the chromosomal abnormalities reported in PCL have also been described in MM and the other plasma cell dyscrasias. However, the incidence of such abnormalities appeared to differ between the specific disease subtypes. The translocation t(11;14)(q13;q32), involving the *CCND1* and *IgH* genes, is such an example. Although not exclusive to pPCL, it represents the most frequent *IgH* translocation, suggesting a potential role of this rearrangement in the etiology of this disease [97,252].

In this section, array CGH was used to define the genomic profile of 12 PCL patients in combination with conventional cytogenetic and FISH. These results were then compared with those obtained from MM patients described in **Sections 3.1** and **3.3**.

3.6.2 Patients

BM samples from 12 PCL patients were evaluated using multiple techniques; ten were classified as pPCL, the remaining two were sPCL. Their median age was 72.5 years (range: 23-83 years). The most relevant clinical features of the 12 patients are presented in **Appendix 11**. OS was extremely poor (median: 3 months; range: 1–20 months) following heterogeneous treatment regimens. Five of 11 patients died within the first month from diagnosis and four within the first year. FISH data from these patients were compared with those from the cohort of 400 newly diagnosed MM patients described in **Section 3.1.2**. Array CGH profiles of PCL

patients were compared with those obtained from the group of 47 MM patients described in **Section 3.3**.

3.6.3 Methods

3.6.3.1 Metaphase analysis

Cytogenetic studies were performed on BM from all PCL patients following density gradient separation (**Section 2.2.3**). PC percentage was assessed on Leishman's-stained slides from cytospin preparations (**Section 2.2.4**). Cells were cultured for 24 hours, 3 days and/or 6 days, depending on the quantity of cells available as described in **Section 2.3**.

3.6.3.2 iFISH studies

All samples were tested by iFISH as described in **Section 2.4**. The probes used were those described in **Section 3.1.3.1**. Additional probes were used for *MYC* status (the t(8;14)(q24;q32) fusion probe combination, *MYC* break apart probe combination; PAC RP1-80K22 covering only *MYC*). BAC RP11-473K22 was used to test for deletion at 5q32; BAC probes RP11-142D17 and RP11-395I14 were used to confirm deletion at 8p21.2 (probes are listed in **Appendix 3**).

3.6.3.3 Array CGH studies

Eleven of the 12 PCL patients were tested by array CGH. Genomic DNA was extracted from purified PC stored as a dried pellet (patients 325, 3210 and 3342), purified PC stored in Carnoy's fixative (patients 3272, 3125, 3343, 2359 and165) or non-purified fixed cells derived from 24 hour (patients 742 and 1188) and 3 day (patient 1576) cytogenetic cultures with a percentage of abnormal cells (tested by iFISH for known abnormalities) greater than 70% (**Section 2.5**). Genomic DNA was hybridized to the 244k microarray and processed as described in **Section 2.6**. Duplicated, amplified and deleted regions were defined using a 500 kb weighted moving-average window and the ADM-2 algorithm of the CGH Analytics software with a threshold of 6.0 (**Section 2.6.6**).

3.6.3.4 mRNA identification of genes mapping at 5q33.1

At 5q33.1, a common minimally deleted region was identified and included eight genes: *SPINK5L2* (Kazal type serine protease inhibitor 5-like 2), *SPINK6* (serine peptidase inhibitor, Kazal type 6) *SPINKL5L3*, *SPINK7, SPINK9, FBXO38* (F-BOX only protein 38), *HTR4* (5-ydroxytryptamine (serotonin) receptor 4) and *ADRB2* (β-2-adrenergic receptor). Based on the NCBI Unigene EST Profile Viewer (URL in **Appendix 1**), only *FBXO38* is expressed in the BM, lymph nodes and also in BM samples from patients with leukaemia. However, despite being ubiquitously expressed, no certain information was available on its expression in PC. In order to ascertain that only *FBXO38* is expressed in PC, total RNA was extracted from purified PC from four randomly selected MM patients (374, 665, 1037, 1148) and two patients with myelodysplastic syndrome whose PC were isolated from total BM as described in **Section 2.2.5** (final PC purity: 70% and 80%). The total RNA was converted into cDNA (**Section 2.7**) and checked for quality (**Section 2.7.1**). Specific sequences covering two or more exons were selected for each gene product (primers are listed in **Appendix 12**). The PCR mix contained: 5µl of 10x Buffer, 2µl $MgCl_2$, 1µl dNTP mix (25 nM each nucleotide), 2µl primer (forward and reverse), 0.5µl HotStar Taq polymerase (Qiagen, UK), 1µl of template and 37.5µl of water. PCR was performed with an initial denaturation at 95˚C for 15 min, followed by 30 cycles of 95˚C for 30 seconds, the annealing temperature for 30 seconds and 72˚C for 30 seconds. A final extension of 72˚C for 10 min concluded the PCR. PCR products were run for 40 min on a 1.2% Agarose gel.

3.6.3.5 Mutational analysis of *TP53*, *CDCA2*, *PPP2R2A* and *FBXO38*

Exons 5 to10 of the *TP53* gene were amplified from genomic DNA of nine PCL patients (325, 3210, 3342, 1188, 3272, 742, 1576, 165, 3343): exons 5-6 (with 5F, 5'-CTTTGCCGTCTTCCAGTTG-3'; 6R, 5'-ACGCCATTCTCCTTCCTCAGC-3'), exons 7-10 (with 7F, 5'GCCTCATCTTGGGCCTGTGT-3'; 10R, 5'-GCAGGCTAGGCTAAGCTATGAT-3'; 8F, 5'-CTGATTTCCTTACTGCCTCTTG-3'); alternative (a) exon 10 (with 10aF, 5'-CAGCCAAGATTGCACCATTGC-3'; 10aR, 5'-TTGACCATGAAGGCAGGATGA-3').
All exons (n=22) of the *FBXO38* (F-box only protein 38) gene also known as *MoKA* were amplified from genomic DNA of four MM patients (282, 665, 1776, 2993) and the KMS-11 cell line (primers are listed in **Appendix 13**).
All exons (n=10) of the gene *PPP2R2A* (protein phosphatase 2 (formerly 2A) regulatory subunit B, alpha isoform) were amplified from genomic DNA of three PCL (165, 3210, 3343) and seven MM (309, 1798, 1037, 1776, 342, 374, 114, 2993) patients; all exons (n=15) of the gene

CDCA2 (cell division cycle associated 2) were amplified from four patients (two PCL; 165, 3210) and two MM (1798, 1037) (primers for the two genes are described in **Appendix 14**). The PCR mix contained: 5µl of 10x Buffer, 2µl MgCl2, 1µl dNTP mix (25 nM each nucleotide), 2µl primer (forward and reverse), 0.5µl HotStar Taq polymerase (Qiagen, UK), 1µl of template and 37.5µl of water. PCR was performed with an initial denaturation at 94˚C for 15 min, followed by 30 cycles of 94˚C for 30 seconds, the primer specific annealing temperature for 30 seconds and 72˚C for 30 seconds. A final extension of 72˚C for 10 min concluded the PCR. The PCR products were purified using Exo-SAP reaction (**Section 2.9.1**). Products were sequenced directly using BigDye v1.1 or v3.1 (Applied Biosystems, UK) as described in **Section 2.9.2** and purified using the montage SEQ96 sequencing reaction clean up kit (**Section 2.9.3**). DNA from the purified sequencing reaction was resuspended in deionised formamide and loaded onto an ABI 3100 sequencer Genetic Analyser (Applied Biosystems, UK).

3.6.3.6 Quantitative reverse transcription polymerase chain reaction (qRT-PCR)

RNA was extracted from purified PC from seven PCL (325, 3210, 1576, 742, 2359, 1188 and 3342) and 19 randomly selected MM patients as described in **Section 2.7**. The qRT-PCR was performed as described in **Section 2.8**.

3.6.3.7 MLPA

MLPA, using the modified MRC-Holland kit 'SALSA MLPA kit P088 Glioma 1'**,** was performed on genomic DNA of the PCL patient 3210 as described in **Section 2.10.1**; genomic DNA from two healthy individuals was used as control.

3.6.4 Results

3.6.4.1 Metaphase analysis and iFISH results

Eleven of 12 patients (92%) showed an abnormal karyotype and eight were classified as highly complex (**Table 3-21**). Five were hypodiploid ($\leq$45 or $\geq$75 chromosomes in tetraploid cases), two were pseudodiploid (46-47 chromosomes) and four were HRD ($\geq$48 and <75

chromosomes). The case without cytogenetic information appeared to have a nonHRD karyotype by iFISH and array CGH.

Specific IgHt at 14q32 were detected in nine cases (75%) (**Table 3-23**): five (four pPCL and one sPCL) had t(11;14)(q13;q32), three had t(14;16)(q32;q23), the remaining sPCL case had t(4;14)(p16.3;q32). Eight of the nine (89%) 14q32 translocations were found in nonHRD karyotypes. Interestingly three of the four pPCL patients with t(11;14) translocation showed a duplication of the LSI *IgH* 3' flanking probe, corresponding to a duplication of the fusion signal with *CCND1* on the der(14). In these cases, array CGH showed gain of part of 11q, commencing at the chromosomal position corresponding to the breakpoint involved in the translocation and including *CCND1*, confirming the iFISH results.

Δ13 was found in seven patients (58%), involving the majority of the cells (range: 85%-100% PC). Deletions of chromosome 16 at 16q23 were found in six patients (50%). A deletion at 17p13.1 was detected in three of 12 (25%) tumours, two pPCL and one sPCL. Compared with the MM group, several abnormalities were more frequent in PCL: deletion of 16q (50% *vs* 21%; *P*=0.025), deletion of *TP53* (25% *vs* 10%) although non statistically significant (*P*=0.114), t(11;14) (41.7% *vs* 14%; *P*=0.020), t(14;16) (25% *vs* 4%; *P*=0.015) and nonHRD (75% *vs* 43%; *P*=0.036) (**Table 3-24**). FISH for the t(8;14) showed only one case (3343) with an unbalanced translocation involving *MYC*.

Following page

Table 3- 23 iFISH and metaphase analysis results for the twelve PCL: pPCL were ordered by the *IgH* translocation partner; the last two patients correspond to the two sPCL

(Del, deletion; der, derivative chromosome; Unb, unbalanced; N, normal; ps, pseudodiploid; HOD, hypodiploid; DM, double minutes)

In the description of the karyotype, the karyotype of the normal cell population has been omitted. Abnormal FISH signal patterns for *MYC* status have been described. For t(8;14) probe, B = 8CEP, R = 8q24, G = *IgH*; for *MYC* break apart probe, F = fusion signal, R = centromeric probe at 8q24, G = telomeric probe at 8q24

[a] Patients with interstitial abnormalities involving or in close proximity to *MYC* detected by array CGH. [b] *MYC* duplication confirmed with PAC RP1-80K22. [c] FISH showed three copies of *MYC* due to an extra-copy of 8q, array CGH showed a further extra-copy of *MYC*, not detectable by FISH.

	iFISH results					Metaphase analysis	iFISH for 8q24
Pt	**Δ13 %PC**	***IgH* Locus (%PC)**	**IgHt**	***TP53* (%PC)**	**Ploidy**	**Karyotype**	***MYC* status**
325[a]	N	Split (100%), +der(14) (30%)	Unb t(11;14)	N	Ps	46,XX,der(7)t(X;7)(q23;p21),der(14)t(11;14)(q13;q32),add(19)(q13)[12]	t(8;14): 2B-3G-3R (90%); 2B-3G-[2-100]R (10%) ***Amp MYC in form of DM***
3210[a]	Del (87%)	Split +der(14) (100%)	Unb t(11;14)	Del (86%)	HOD	40,X,-X,del(1)(p12p3?3),add(3)(q1?),add(4)(q2),add(6)(q2),add(8)(p1),-9, -10,der(11)t(11;14)(q13;q32),add(11)(q2?3),-12,der(12)t(12;14)(p1;q1)t(11;14)(q13;q32),-13,-14,-14, -22,+mar1,+mar2[4]/40,idem,+3,-add(3),add(4)(p1),+del(6)(q1),-dd(6),+der(8)?add(8)(p1)add(8)(q24), -add(8),+11,-add(11),der(12)t(12;14)(p1;q1)t(11;14)(q13;q32)t(?;11)(?;q2?4),del(16)(q),-17,+mar[3]	t(8;14): negative *MYC* break apart: 1G-1R-1F (90%) ***8q24 split (90%)***
1576[a]	Del (85%)	Split +der(14) (100%), +der(14) (18%)	Unb t(11;14)	N	Ps	48,XY,add(1)(q1), -2,+4,add(4)(q2?5)?x2,add(6)(p1?1),+9,**t**(11;14)(q13;q32)?t(6;11)(p?21;q21),der(12)t(2;12)(q11;q24), del(13)(q?),-16,add(16)(p13),dic(20;22)(q11;p11),+21,+der(?)t(?;1)(?;q21),+mar[9]	t(8;14): 2B-(3-4)G-2R (1R signal of bigger size, shown to be doubled up by smaller probe [b]) ***MYC duplication at 8q24***
128	N	Split (100%)	t(11;14)	N	Ps	46,XY,t(6;20)(q21;p11),der(9)t(9;16)(p11;q13)del(16)(q13q24),der(14)t(11;14)(q13;q32),add(22)(q13)	t(8;14): 2B-3G-2R (15%); 2B-3G-3R (85%) *MYC* break apart: 2R-1F (90%) ***MYC Split (88%)***
3272[a]	Del (95%)	N	--	N	HOD	44-45,XY,+7,-12,-13,-17,+add(19)(q1),-20,-22,+mar,inc[3]	t(8;14): negative *MYC* break apart: negative
742[a]	N	N	--	N	HRD	59,X,-X, del(1)(q12),+der(1;8)(q10;q10)x2,+der(1;9)(q10;q10),+2,+3,+add(6)(q1?1),+7,inv(10)(p1?3q2?4), +11, +11,+15,+15,+18,+19,+20,+21[18]	t(8;14): negative *MYC* break apart: 3 F (90%) [c]
165	Del (100%)	N	--	N	HRD	47-48,X,del(X)(p21p22),der(1)ins(1;5)dup(1)(1qter->1p22::1?::5q13->5q33::1?::1p13->1q32), +3,der(4)t(4;15)(q35;q15),+5,del(5)(q22q35),der(5)t(5;7)(q13;p1?3),+6,add(6)(q13), der(6)t(1;6)(q4?2;q13),der(7)t(1;7)(q4?2;p15),-13,-15,+16,der(16)t(8;16)(p11;q23),+19[10]	t(8;14): negative *MYC* break apart: negative
3125	N	Split (100%)	t(14;16)	N	HOD	45,XY,del(5)(q14.3q32),der(10)t(10;17)(p11;q21),t(14;16)(q32;q23),-18,add(21)(p1)[1]	t(8;14): negative
3343[a]	Del (100%)	Split (100%)	t(14;16)	N	HOD	41-43,X,-X,-1,del(6)(q2?1q2?3),add(7)(p2?1),-8,-10,rea(11),-13, der(13;14)(q10;q10),add(16)(q2?2),+2mar[cp5]	t(8;14): 2B 2G 2R (43%); 1B 3G 1F (57%) *MYC* break apart: 2F (60%); 1F (40%) ***Unbalanced t(8;14), insertion of IgH in 8q24***
2359	Del (100%)	Split (100%)	Unb t(14;16)	Del (95%)	HOD (iFISH)	Failed	t(8;14): 2B-3G-3R (88%) *MYC* break apart: 3F (83%); 4F (16%)
1188[a]	N	Split x 2 (98%)	t(11;14)	N	HRD	50,XX,add(8)(q11),+11,t(11;14)(q13;q32),+13,+18,+18[9]	t(8;14): negative
3342	Del (100%)	Split (90%)	t(4;14)	Del (70%)	HOD	45,XY,del(X)(q13),+1,+1,der(1;16)(q10;p10),der(1;17)(q10;q10),-13,add(18)(q23),del(20)(q13)[3]	t(8;14): negative *MYC* break apart: negative

CA	MM cases (%) n=400	PCL cases (%) n=12	*P-value*
Δ13	186/395 (47)	7/12 (58.3)	0.561
Deletion 16q23	75/365 (21)	6/12 (50)	**0.025**
Deletion *TP53*	38/388 (10)	3/12 (25)	0.114
Any IgHt	183/398 (46)	9/12 (75)	0.075
t(4;14)	49/400 (12)	1/12 (8.3)	1
t(6;14)	6/393 (2)	0/12	-
t(11;14)	55/399 (14)	5/12 (41.7)	**0.020**
t(14;16)	15/396 (4)	3/12 (25)	**0.015**
t(14;20)	9/394 (2)	0/12	-
nonHRD	165/388 (43)	9/12 (75)	**0.036**

Table 3- 24 Prevalence of CA detected by iFISH in MM and PCL (Statistically significant *P* values are in red)

3.6.4.2 Array CGH results: overall abnormalities

Good quality DNA for array CGH analysis was available from 11 PCL patients and CNA were detected in all samples. Overall, a total of 322 CNA, defined as discrete segments showing copy number variation consistent with loss or gain, were detected with a median of 26 per case (range, 15–48) (array CGH results for each patient are described in **Appendix 8**; a graphical representation of CNA for all chromosomes of all patients is shown in **Appendix 9**). Patients 3210 and 2359 harboured the highest number of CNA (48 and 42, respectively). Interestingly the three patients who remained alive throughout the study (at 3, 13 and 20 months from diagnosis) had fewer than the median value of CNA (23, 15 and 22). Ten HD were detected (**Table 3-25**) in five patients, with four of them occurring in the same patient, corresponding to the most complex karyotype in the series. Notably, all HD (apart from 13q14.2) were observed only once. The only amplified region (defined as more than/equal to six copies) was found at 8q24.13-q24.21 (124.98Mb - 129.42Mb) in one case (**Table 3-23**). Chromosomes 1, 8, 13 and 16 showed the highest number of CNA (**Figure 3-33**).

Patient	Chr	Chromosomal position	Start (Mb)	End (Mb)	Size of CNA (Mb)	Genes involved
3210	1	1p32.3	51,139,615	51,157,731	0.018	*CDKN2C*
2359	1	1q31.3-q32.1	194,597,222	196,876,612	2.279	*C1orf53, LHX9, NEK7, ATP6V1G3, DENND1B*
3125	5	5q32	146,702,762	148,211,914	1.509	*STK32A, DPYSL3, JAKMIP2, SPINK1, SCGB3A2, SPINK5, AC1163334.1, SPINK7, MGC23985, SPINK6, FBX038, SPINK9, HTR4, ADRB2*
3342	6	6q27	165,695,958	165,701,090	5.132	*PDE10A*
3210	8	8pter-p23.3	63,810	1,122,897	1.059	*OR4F21, AC131281.7, ZNF596, FAM87A, FBX025, C8orf42, AC090691.16, ERICH1*
742	8	8p21.2	25,205,684	26,224,281	1.018	*DOCK5, AC103779.5, GNRH1, KCTD9, CDCA2, EBF2, AC090103.4, PPP2R2A*
2359	13	13q14.2	47,797,577	47,896,834	0.099	*RB1, P2RY5*
3342	13	13q14.2	47,851,735	47,948,983	0.097	*RB1, P2RY5*
3210	14	14q22.1	51,967,480	52,064,804	0.097	*TXNDC16*
3210	14	14q22.3	54,932,376	54,960,676	0.028	*KIAA0831, TBPL2*

Table 3- 25 HD revealed by array CGH in PCL with their chromosomal location and genes involved (recurrent HD are highlighted in blue)

3.6.4.3 Chromosome 1 abnormalities

All patients showed abnormalities of chromosome 1. Deletions of 1p were detected in four patients: two had a single interstitial deletion while the other two had multiple interstitial deletions. In two patients the deletion included 1p32.3: the first (patient 3125) showed a mono-allelic deletion (50.64Mb - 51.18Mb, size of the CNA: 546kb) involving the genes *FAF1* and *CDKN2C* (confirmed by iFISH); the second (patient 3210) showed three different interstitial deletions on 1p, of which the largest (1p35.1-p21.3; 33.33Mb - 97.02Mb), had a small region deleted from both alleles, involving only *CDKN2C* (51.13Mb - 51.15Mb). This CNA was confirmed by MLPA which showed the two probe binding sites on *p18*, the one between *FAF1* and *p18* and the one centromeric of *p18* to be involved in the HD, while the two probe binding sites selected for the *FAF1* gene were found to be hemizygously deleted (**Appendix 15**).

Abnormalities involving 1q were highly complex: the region from 1q12 to 1q22 (141.52Mb - 145.64Mb) was gained in seven of the 11 patients; four patients had one extra copy of the region and three patients had two extra copies.

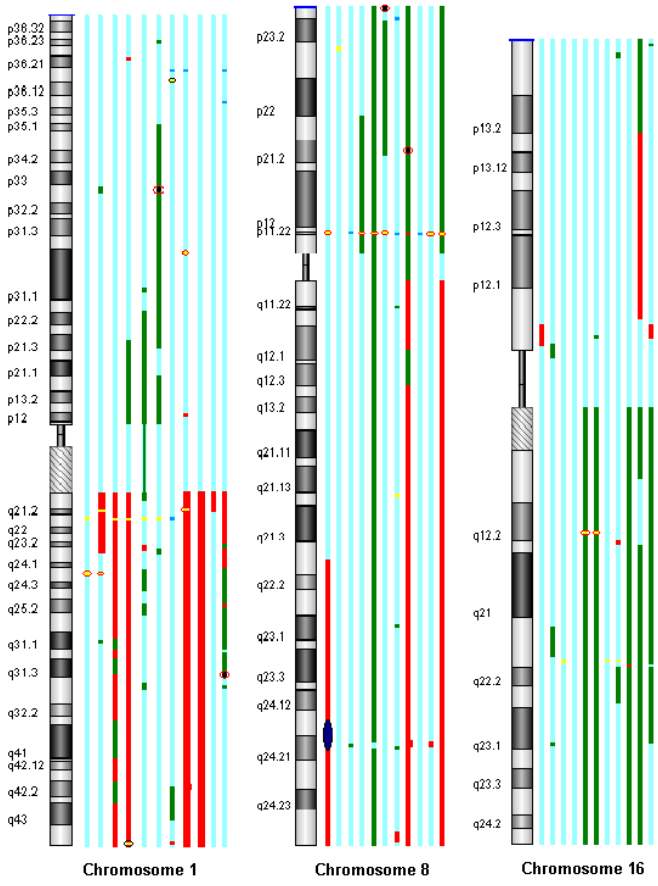

Figure 3- 33 Graphical representation of CNA for chromosomes 1, 8 and 16 in PCL

The 850-band idiograms of the G-banding patterns are shown on the left. Vertical blue lines correspond to each patient; red bars = gains, thicker red bars = gain of two extra copies; green bars = mono-allelic losses; black areas circled in red = HD; dark blue areas = amplifications; yellow and light blue areas = CNV, respectively losses and gains

3.6.4.4 Chromosome 8 abnormalities and mutational analysis of *CDCA2* and *PPP2R2A*

Combining array CGH and FISH, abnormalities of chromosome 8 were seen in eleven of the 12 patients (92%): five (45%) showed deletions of 8p, which were relatively large and involved the whole arm in three cases. The common minimally deleted region was defined by the bands 8p21.2 (26.06Mb) and 8p21.3 (19.02Mb). Within this region, one case (742) with hemizygous loss of the entire arm showed HD at 8p21.2 (25.20Mb - 26.22Mb) involving the genes *DOCK5, AC103779.5, GNRH1, KCTD9, CDCA2, EBF2, AC090103.4* and *PPP2R2A*. The deletion was confirmed by iFISH (probes for *PPP2R2A* are described in **Appendix 3**): a normal copy number was detected in cells other than PC and complete loss of the region was observed in the PC; this was proof that the deletions of both alleles were somatically acquired. This HD has not been previously reported in PC disorders. As described in **Section 3.3.4.3.4**, deletions of 8p were present in 32% of MM patients; in these patients the common minimally deleted region was defined as 8p22-p21.2, which included the HD found in the PCL patient. After investigating the literature for the possible functional importance of the genes included in this HD, mutational analysis of *PPP2R2A* (on ten patients) and *CDCA2* (on four patients) was carried out on cases found to be hemizygously deleted at 8p21. No mutations were found in any of the genes.

A number of abnormalities involving 8q were found, including gain of the whole arm in three cases (27%). One case (patient 325) showed a high level gain at 8q24.13-q24.21 (124.98Mb - 129.42Mb). The level of gain did not indicate a genomic amplification, while metaphase-FISH for *MYC* showed a highly variable degree of amplification in the form of DM (2 - 100 copies), which were present in only approximately 10% of the malignant clone. This finding clarified the apparent discrepancy between the level of amplification found by FISH and the level of gain by array CGH. Two cases (patients 3272 and 1188) showed two small deletions at 8q24.21 not directly involving *MYC*: the first (128.82Mb - 128.97Mb) between *MYC* and *TMEM75*; the second (129.09Mb - 129.21Mb) telomeric of *TMEM75*. Cytogenetic and FISH analysis failed to detect these small deletions. Patient 1576 displayed an interstitial duplication involving *MYC* and *TMEM75* (8q24.21; 128.45Mb - 129.38Mb) which corresponded to a tandem duplication of 8q as indicated by FISH. One case (patient 742) showed gain of the whole 8q and a further gain involving only *MYC* and *TMEM75* (128.64Mb - 129.13Mb). Patient 3343 with monosomy of the entire chromosome 8 showed a small region with a normal ratio by array CGH at 8q24.21 (128.81Mb - 129.7Mb), which iFISH showed to be involved in a t(8;14) translocation. Interphase FISH revealed a split of *MYC* arising from a translocation with an unknown partner other than *IgH* in patients 3210 and 128, who showed a normal copy number ratio at 8q24.21 by

array CGH. Interestingly patient 3210 also showed gain of the chromosomal region 2pter to 2p24.3 with the breakpoint at the position 15.95Mb, immediately distal to the *N-MYC* locus (15.99Mb – 16.00Mb).

3.6.4.5 Chromosome 13 abnormalities

Losses of chromosome 13 were detected in seven patients (64%) of which five showed complete monosomy, while the remaining two patients had large deletions. The common minimally deleted region was defined by the bands 13q13.1 (33.0Mb) and 13q31.1 (80.53Mb). Within this region of hemizygous loss, two patients showed a homozygous deletion at 13q14.2 including only the genes *RB1* and *P2RY5* (**Table 3-24**). Interestingly HD of the same chromosomal region was found in two MM patients (**Table 3-8**).

3.6.4.6 Chromosome 16 abnormalities

Seven (64%) patients showed loss of 16q with three areas most frequently affected: 16q22.1 (65.39Mb - 68.09Mb) in six patients (55%); 16q22.2 -q23.1 (69.76Mb - 73.52Mb) in six patients (55%), and 16q23.1 (77.64Mb - 77.84Mb) including only the *WWOX* gene in six patients (55%).

3.6.4.7 Chromosome 5 abnormalities and mutational analysis for *FBXO38*

The very young pPCL patient (3125; 23 years old) was found to have a HD at 5q33.1 (146702762Mb – 148240825Mb) (**Figure 3-34 A**) within a relatively simple karyotype. The HD was confirmed to be restricted to the neoplastic PC clone by iFISH (probe described in **Appendix 3**). The array CGH profiles for chromosome 5 in MM patients (**Section 3.3**) showed the presence of a number of losses on chromosome 5q in nonHRD cases; these losses were characterized by different break-points and shared two minimally deleted regions at 5q31.1 (132267368Mb – 132912148Mb; n=5) and 5q33.1-q33.2 (147507861Mb – 150556320Mb; n=5); the array CGH profile of the KMS-11 cell-line also showed a hemizygous deletion involving the most telomeric of these two regions (**Figure 3-34 B**).

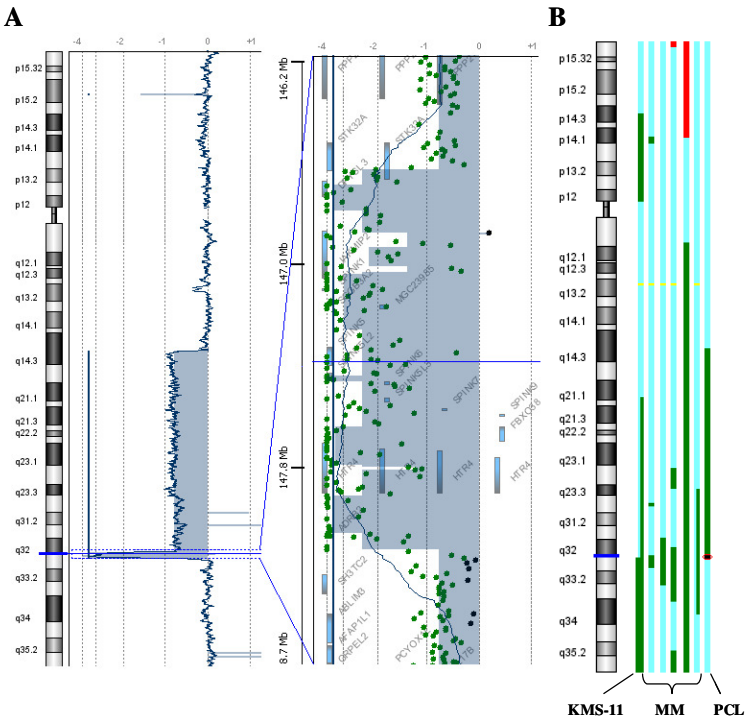

Figure 3- 34 A) Patient 3125: G-banded idiogram of chromosome 5 (on the left) with the CNA for the p and the q arms. For the chromosomal region 5q33.1, the plot of 'calls' for every nucleotide is shown in detail; B) Graphical representation of chromosome 5 losses in PCL (n=1, patient 3125), MM (n=5) and the cell line KMS-11 (light blue bars = individual patients; green bars = losses; red bars: gains; black areas circled in red = HD)

Among the genes included in the common minimal deleted region, mRNA identification of genes mapping to 5q33.1 showed a PCR product for mRNA only for *FBXO38* (two bands of 850bp and 150bp corresponding to two isoforms: variant 2 missed exon 15) and *ADRB2* (product of 380bp). However, *ADRB2* has only one exon therefore it is likely that the detected band was derived from contamination with genomic DNA. None of the other six genes showed a band suggesting that they are not expressed in PC. Mutational analysis of *FBXO38* in four MM patients and the KMS-11 cell line with hemizygous deletions of 5q33.1 detected by array CGH showed no mutations of the remaining allele.

3.6.4.8 Mutational analysis for *TP53*

Functionally relevant *TP53* coding mutations were found in three patients: two pPCL (patient 325 and 3210) and one sPCL (patient 3342). Patients 325 and 3210 (this patient was also positive for a hemizygous deletion) were both found to have a missense mutation in the DNA binding domain, in exon 8 (c.839G>A) and exon 6 (c.653T>A) (**Figure 3-35 A-B**), respectively, resulting in non-functional proteins. Patient 3342 had a hemizygous deletion at 17p13 and was found to be positive for a missense mutation in exon 5 (c.536A>C) also generating a non functional protein (data were obtained from the IARC p53 website, URL in **Appendix 1**).

A

B

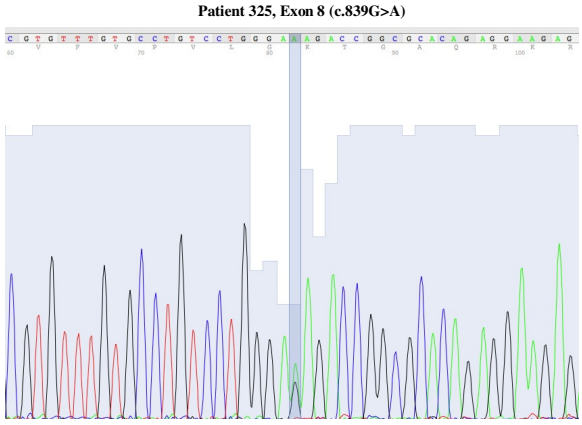

Figure 3- 35 DNA sequences showing the mutation at exon 6 (A) and exon 8 (B) of the *TP53* gene in patients 3210 and 325, respectively. Patient 3210 showed the presence of only one allele as the other was found to be deleted by iFISH

3.6.4.9 Correlation between CNA at 8q24 and *MYC* expression

Array CGH and iFISH detected a number of different CNA involving chromosomal band 8q24 (**Figure 3-36**). These different alterations directly involved *MYC* or were in close proximity (i.e. within 400kb) of the gene. *MYC* mRNA expression levels were analyzed in seven PCL and 19 randomly selected MM patients by qRT-PCR (the individual levels of *MYC* expression relative to *BCR* and *GUSB* and the FISH and/or array CGH results for 8q24 are described for every patient in **Appendix 16** and **Figures 3-37** and **3-38**). Five PCL (patients 325, 3210, 1576, 742 and 1188) and six MM patients had evidence of 8q24 rearrangements by array CGH (including small interstitial deletions within the proximity of *MYC*) or by iFISH. All patients with abnormalities at 8q24, including the one with the small interstitial deletion telomeric of *TMEM75* detected by array CGH, showed increased levels of *MYC* expression. Those cases with gain of the entire 8q arm were not considered to be abnormal for *MYC*. In fact one pPCL (2359) with gain of the entire 8q did not show increased level of *MYC* mRNA. The three MM cases with t(8;14) showed comparable levels of *MYC* expression; in these cases the level of expression was lower than those observed in cases with gene amplification in the form of DM, or with multiple copies of *MYC* in marker or ring chromosomes (patients 1247 and 1524). The two latter cases were also tested for *MYC/Igλ* rearrangements and were both found to be negative. The difference in *MYC* expression levels between cases (MM and PCL) with and without evidence of structural or numerical abnormalities at 8q24 was highly significant (Mann-Whitney test, $P<0.001$ for *BCR*; $P=0.005$ for *GUSB*) (**Figure 3-37**). When only MM patients were considered, the difference was significant for *BCR* but not for *GUSB* (Mann-Whitney test, $P=0.02$ for *BCR*; $P=0.10$ for *GUSB*). Four of 13 MM patients, with no apparent *MYC* abnormalities by iFISH, showed levels of *MYC* mRNA comparable to those detected in cases with t(8;14) (**Figure 3-38**). The sPCL patient 3342, also showed increased level of *MYC* mRNA in the absence of 8q24 abnormalities by FISH or by array CGH, resulting in both sPCL cases having *MYC* upregulation.

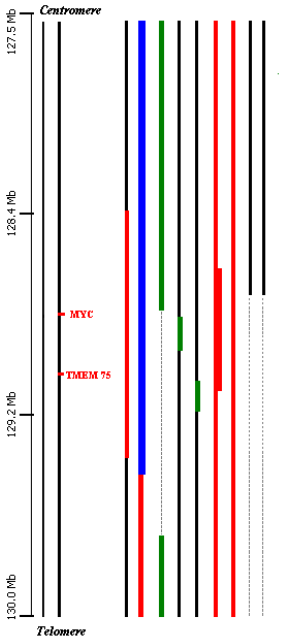

Figure 3- 36 Diagram showing the different CNA identified in nine PCL patients by iFISH and array CGH in a region of 2.5Mb centred on *MYC* at 8q24 (patient order from left to right: 1576, 325, 3343, 3272, 1188, 742, 2359, 128 and 3210)

Vertical black lines correspond to regions with no CNA or structural aberrations detected; red bars = gains; green bars = mono-allelic losses; blue bar = amplification; dotted lines = structural rearrangements detected with the *MYC* break apart probe

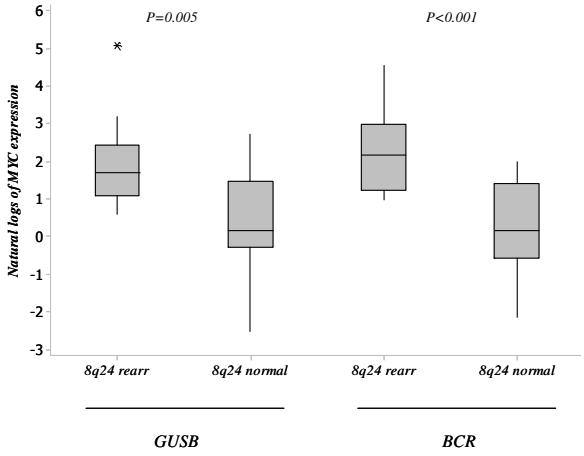

Figure 3- 37 Box plot of natural log values of *MYC* mRNA levels relative to *GUSB* and *BCR* as determined by qRT-PCR in 15 MM and PCL patients with no apparent rearrangements at 8q24 (8q24 normal) and 11 MM and PCL patients with different alterations at 8q24 (8q24 rearr) (Mann-Whitney test)

Asterisk symbol corresponds to outlier value, open boxes indicate the interquartile range, and the horizontal lines inside the boxes indicate median values

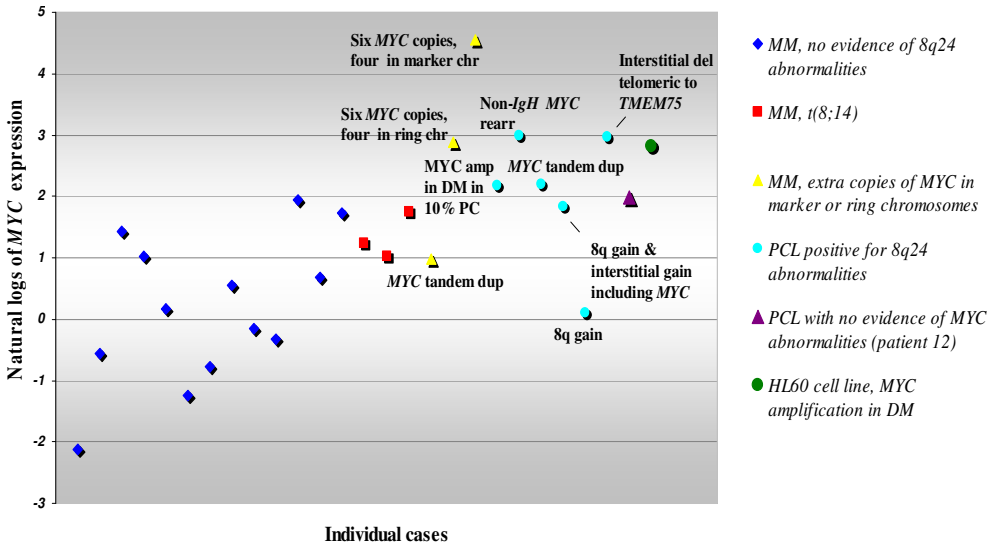

Figure 3- 38 Natural log values of *MYC* mRNA levels relative to *BCR* for all patients

The specific genetic abnormalities at 8q24 are described for the MM group with extra copies of *MYC* in marker or ring chromosomes and for PCL patients positive for 8q24 abnormalities (amp, amplification; chr, chromosome; del, deletion; DM, double minutes; dup, duplication; rear, rearrangement)

3.6.5 Overall summary of the results and discussion

In this study, a series of 12 PCL, ten primary and two secondary, were genetically characterized using cytogenetic analysis, iFISH, and array CGH. As previously reported in other series, the prognosis of these patients, particularly those with pPCL, was very poor: 50% of the pPCL patients died within the first month.

The percentage of PCL patients with an abnormal clone by cytogenetic analysis was 92%, significantly higher than MM (30%-50%) [83,87]. These data suggest that clonal PC from PCL display a higher proliferative capacity *in vitro* compared to PC from MM patients, characterized by a slow cell turnover comparable to non-malignant BM cells. The majority of pPCL (75%) were nonHRD, although two pPCL and one sPCL displayed a HRD karyotype. This contrasts with the recent series reported by Tiedeman *at al.* [252] in which all pPCL were exclusively nonHRD and HRD was found only in sPCL. However, it should be noted that patient 1188 (sPCL), despite having a karyotype with 50 chromosomes, also had a t(11;14) which is rarely associated with a HRD karyotype. Furthermore, of the extra chromosomes commonly acquired

in HRD cases, only chromosome 11 was gained in this patient. Therefore it is unclear whether, biologically, this patient should be considered as HRD or nonHRD.

Translocations of the *IgH* locus were present in 75% of cases (seven of ten pPCL and both sPCL), with t(11;14) (four cases) and t(14;16) (three cases) only being found in these pPCL, confirming the specific association of these two translocations with this disease [65,97]. The t(4;14) was not seen in this series of pPCL. The prevalence of t(11;14) in our cohort (41%) was similar to that reported by Avet-Loiseau *et al.* (33%) [97]. Interestingly, 80% of pPCL with t(11;14) showed duplication of the fusion signal on the der(14) with an associated interstitial gain of 11q (minimally gained region: 11q13.3-q13.4). This was shown to be a secondary event as it was found in only a subpopulation of the neoplastic cells. This same 11q duplication has been observed in MM and pre-malignant patients (**Figure 3-17**), thus it is not exclusive to PCL. However, in MGUS and MM no duplication of the fusion signal deriving from the translocation was observed, suggesting that the two mechanisms are different. Using a survival end-point of 12 months, t(11;14) has been associated with significantly longer OS [97]. This was not so in our series. However, an association between longer survival and low genomic complexity as assessed by array CGH was observed. Similar findings have been described in chronic lymphocytic leukemia, suggesting that this may be a widespread feature of mature lymphoid disorders [253].

Translocations t(11;14) and t(14;16), as well as 16q23 deletion and nonHRD, were significantly more common in PCL than in MM, suggesting that, despite the presence of overlapping chromosomal abnormalities, the two diseases involve different genetic pathways which may explain their different clinical behaviour. In this study Δ13 was more frequent in PCL than in MM (58% *vs* 47%). However, this difference was not statistically significant (*P*=0.561), which was in contrast to other reports [65,71,97,252]. A HD at 13q14.2 was found in 18% of PCL (one pPCL and one sPCL), involving only the genes *RB1* and *P2RY5*. These HD were too small to be detected by the probes routinely used to assess chromosome 13 status by iFISH. HD at the same chromosomal position were found in two of 47 MM patients (4%) (**Table 3-8**). These findings suggest that *RB1* is one of the targeted genes of Δ13. Deletions of 17p13.1 were found in only 20% of pPCL patients, at an incidence significantly lower than those reported in other series [71,97,252]. *TP53* loss was complemented by functionally relevant *TP53* coding mutations in two other pPCL cases (325 and 3210). Patient 3210 was also positive for the deletion, leading to a bi-allelic *TP53* inactivation.

Array CGH detected CNA in all cases tested. Cytogenetic analysis and array CGH showed that the karyotype and the genomic profile of the majority of these patients was complex. Other

studies had reported that cytogenetic changes were more frequent in PCL than in MM [153,254,255]. Our data confirms that although some PCL cases are extremely complex, others have relatively simple changes.

CNA on chromosome 1 were frequent. A recent iFISH study which included 41 cases of PCL found deletions of 1p21 in 37% of cases and the abnormality was associated with a shorter OS by univariate analysis [256]. Deletions of 1p were found in 36% of PCL in our series, including one heterozygous deletion and one HD both at 1p32.3. The heterozygous deletion involved the *FAF1* and *CDKN2C* genes, while the HD encompassed only *CDKN2C* suggesting that this gene is the target of deletions occurring at this locus. This HD was confirmed using MLPA as the CNA by array CGH included only three consecutive aberrant calls, while a called aberration requires a minimum of five consecutive aberrant oligonucleotides.

Gain of 1q was found in 39% of MM patients and in this group it was associated with an inferior prognosis (**Section 3.4.4.1**). The PCL patients showed multiple CNA of 1q, including interstitial gains and deletions, sometimes within the same patient. The region 1q12-q22 was gained in 64% of patients, with three patients having two extra copies. No amplifications of $\geq$6 copies were found.

Chromosome 5 is one of the chromosomes usually gained in MM, particularly in those cases with a HRD karyotype. The gain of this chromosome is routinely used with chromosomes 9 and 15 to define the ploidy status by iFISH [216]. In this PCL cohort, only one HRD case (patient 165), with no IgHt, had a partial gain of chromosome 5. One young pPCL patient (3125) with a relatively simple karyotype showed a large heterozygous deletion of 5q (5q14.3-q33.1) with an associated small HD at 5q33.1 (146702762Mb – 148240825Mb). FISH confirmed that the small HD was confined to the PC population. Fourteen genes were included in the HD. This novel deletion has not been previously reported although 5q deletions were observed in four of 24 cases (17%) [97] and eight of 27 cases (30%) [252]. In both series, these large deletions encompassed the whole or part of 5q and all included 5q33.1. Comparing array CGH results from PCL with those from MM described in **Section 3.3**, six further cases (including the KMS-11 cell line) were found to be hemizygously deleted at this locus. Among the genes included in the common minimal deleted region, *FBXO38* (*MoKA*) was found to be expressed in PC from both MM patients and individuals without PC dyscrasias, thus it was postulated to be involved in myelomagenesis. *FBXO38* codifies for an F-Box Protein that modulates and enhances the Krüppel-like transcription factor 7 (KLF7) activity [257,258]. KLF7 is a member of the mammalian Kruppel-like family of zinc finger proteins which can modulate cell cycle regulators. Its induced overexpression results in a decrease in DNA synthesis, induction of $p21^{WAF1/Cip1}$ (cyclin-

dependendent kinase inhibitor 1A) protein, inhibition of cyclin D1 and G1 arrest [259]. Despite representing a plausible target gene of these deletions, no mutations were detected in four patients with loss of one allele. However, it can be hypothesised that other mechanisms control *FBXO38* expression.

Loss of 8p was frequent in PCL. As mentioned above, few studies have reported the prognostic significance of this abnormality in MM. Bryant *et al.* [260] found 8p loss to be associated with shorter survival in MM, regardless of treatment. In MM patients, we found that 8p deletions were usually large; thus it was difficult to determine the targeted genes. Within the PCL cohort, array CGH defined a common minimally deleted region at 8p21.2-p21.3 (26.06Mb - 19.02Mb). Within this region a HD at 8p21.2 (25.20Mb - 26.22Mb) involving the genes *DOCK5, AC103779.5, GNRH1, KCTD9, CDCA2, EBF2, AC090103.4* and *PPP2R2A* was found. In the paper by Carrasco *et al.* [178] among the high-confidence minimal common regions of loss, they listed the region at 8p21.3-p12 including the genes *TNFRSF10B* and *PPP2R2A*. PPP2R2A belongs to the phosphatase 2 regulatory subunit B family. Protein phosphatase 2 is one of four major Ser/Thr phosphatases and is implicated in the negative control of cell growth and division. Studying the fusion of *CHEK2* and *PPP2R2A* in childhood teratoma, Jin *et al.* [261] reported that deregulation of *CHEK2* and/or *PPP2R2A* is of pathogenetic importance in at least a subset of germ cell tumors. HD of *PPP2R2A* have also been found in prostate cancer cell lines [262]. Interestingly, combined SNP array and GEP data on 259 newly diagnosed MM patients analyzed at the Section of Haemato-Oncology, The Institute of Cancer Research, London, Walker *et al.* found that among the 237 genes mapping within common 8p deletions the most under-expressed genes were *ZDHHC2*, *FDFT1*, *CNOT7*, *PPP2R2A* and *PPP2CB* (unpublished data). CDCA2 is a regulator of chromosome structure during mitosis, required for condensin-depleted chromosomes to retain their compact architecture through anaphase. The protein has been found to be overexpressed together with other cell cycle and proliferation-related genes [124]. Unfortunately in this study, sequencing analysis of both genes did not show the presence of mutations suggesting that if one of these genes is important in MM and PCL pathogenesis the mechanism leading to its dysregulation does not involve mutations at the genomic level.

Avet-Loiseau and colleagues showed that *MYC* translocations at 8q24 were rare in primary PCL. This was a surprising result given the high prevalence in advanced primary tumours and HMCL that are derived from primary and secondary PCL [111,263,264]. In a series of 43 HMCL, Dib *et al.* showed *MYC* overexpression in 93% of cases; two cell lines expressed *N-MYC* and one *L-MYC* [263]. Consistent with these results, *N-MYC* expression was found in eight of 559 primary MM tumours whereas none of these tumours expressed *L-MYC* [124]. In this study, the chromosomal region most frequently involved in structural and numerical abnormalities, apart

from 14q23, was 8q24 (including seven of ten pPCL and one of two sPCL); the other sPCL patient, despite lacking evidence of 8q24 abnormalities by iFISH or array CGH showed *MYC* upregulation by qRT-PCR. The nature of such abnormalities was highly variable (as previously observed in MM patients described in **Section 3.3.4.3.4**) including amplification, tandem duplication, small interstitial deletions, balanced and unbalanced translocations. The detection of these alterations could only be achieved combining FISH and array CGH. The *MYC* amplification in the form of DM, observed in patient 325, was present in only a subset of tumour cells, providing evidence for a secondary event in this case. Quantitative RT-PCR confirmed that these different alterations led to increased levels of *MYC* mRNA. The level of *MYC* overexpression seemed to vary depending on the type of genomic abnormality involved. Such variation was not dependent on the proportion of PC carrying the abnormality as, apart from the pPCL patient 325, all cases showed the *MYC* abnormality in all malignant cells. There was no evidence from array CGH or metaphase analysis of abnormalities specifically involving *L-* or *N-MYC* in any of the PCL patients. Among the PCL cases with *MYC* abnormalities, only patient 3343 showed involvement of the *IgH* locus. In newly diagnosed MM, the *IgH* and *Igλ* loci were found to be involved in 17% and 10%, respectively, of cases with a *MYC* rearrangement; *Igκ* was rarely involved [111]. In our series there was no indication from metaphase analysis of rearrangements involving *Igλ* or *Igκ*. However, because these loci were not tested by FISH, their involvement in cryptic rearrangements cannot be excluded (e.g. small insertion of *Igλ* enhancers in proximity to *MYC*). Potentially, cryptic alterations that are not detectable by FISH with commercial probes or by array CGH could account for cases such as patient 3342, who showed increased *MYC* expression in the absence of apparent *MYC* abnormalities. Alternatively, *MYC* may be upregulated by the activity of mutant, activated proteins (e.g. β-catenin) [265]. Overall, these findings confirm the complex and unpredictable nature of the mechanisms leading to *MYC* overexpression in PC disorders and suggest that *MYC* dysregulation is one of the major molecular events in the oncogenesis of PCL.

4 DISCUSSION

The PC dyscrasias, MGUS, SMM, MM and PCL, are conditions diagnosed on the basis of clinical parameters such as the M-protein level, the percentage of PC within the BM or the peripheral blood (for PCL) and the presence or absence of clinical manifestations. Biologically, these conditions likely represent a continuum with MGUS and SMM characterized by a limited clonal PC expansion, while MM and PCL are characterized by an increasing clonal PC expansion in the presence of symptoms. The gradual progression of the disease makes the distinction between the different entities very difficult, particularly between early MM and advanced stage SMM or MGUS. Moreover, the pattern and the timing of evolution of pre-malignant patients seem to differ between individuals. Some patients are in the process of evolution at the beginning of their follow-up and are characterized by constant and progressive increase of their paraprotein level and the level of BM plasmacytosis. Other pre-malignant patients, in particular within the MGUS group, may remain completely stable for long periods from their recognition and, if progression occurs, it seems to happen relatively rapidly.

This extensive overlap between the different conditions is also observed at a genetic level. In **Section 3.1**, using a panel of probes to investigate 13 different loci, iFISH showed that 90% of MGUS and 98% of SMM patients had cytogenetic changes which are usually found in MM. Furthermore, none of the chromosomal abnormalities tested were exclusive to a specific stage of the disease, confirming that common chromosomal markers, usually investigated in MM, cannot be used to discriminate between asymptomatic and symptomatic stages. However, statistically significant differences were observed in the incidence of specific abnormalities between the three conditions. In particular the incidences of Δ13, 16q23 deletion and *TP53* deletion were found to progressively increase from MGUS to SMM to MM. In MGUS, these abnormalities were often detected in a sub-clone of the malignant PC population while, in the same cases, other abnormalities were present in all PC. These observations confirm that the acquisition of these changes often represents a secondary event.

The rarity of Δ13 in MGUS, as compared to MM, was not common to all genetic groups. It applied to cases with t(11;14) (one of 28 MGUS patients; MGUS *vs* MM, $P<0.001$) and those with t(6;14) (although this translocation is too rare to draw significant conclusions). In SMM patients with t(11;14), Δ13 was also rare (two of 13). In contrast, the Δ13 was present in 40% of MM and in 60% of pPCL patients with this translocation. Such striking difference in the incidence of Δ13 in t(11;14) cases, depending on the diagnostic class, has not been previously described. However, other published studies reported lower overall incidences of Δ13 in MGUS as compared with MM [85,109]. These findings suggest that in patients with t(11;14) the Δ13 is a secondary event occurring a long time after the acquisition of the *IgH* translocation. In these patients Δ13 might be involved in driving disease evolution, as two of the three pre-malignant patients belonging to this genetic group with available follow-up information progressed to MM. Despite the fact that Δ13 was found to be highly associated with t(4;14), t(14;16) and

t(14;20) in all diagnostic groups, there was evidence that the temporal appearance of Δ13 is related to the presence of specific concomitant abnormalities: early when t(4;14) or t(14;16) is present, later with t(14;20), and even later with t(11;14) (and probably with t(6;14), although the incidence of this latter abnormality is too low to find significant associations). The Δ13 was tested for by iFISH with two probes located to 13q14, therefore there was concern that cases considered to be normal by iFISH may carry chromosome 13 deletions not involving this chromosomal region. However, array CGH profiles of patients from all diagnostic groups showed that only three of 67 (4%) cases with chromosome 13 deletions did not involve the loci investigated by iFISH. Moreover, the only recurrent HD detected on this chromosome involved the *RB1* gene, reinforcing its role as one of the targeted genes of Δ13.

Overall, the presence of *IgH* rearrangements was found at similar frequencies in the three diagnostic groups and, in cases positive for these translocations, the rearrangement involved the majority of cells in the PC clone. These findings confirm the theory that these translocations are early events in MM pathogenesis. These changes lead to the overexpression of a cyclin D gene which then enables PC to autonomously overcome the early G_0G_1 checkpoint, contributing to the limited clonal PC expansion characterizing the MGUS and the SMM stages.
However, a lower incidence of t(4;14) was observed in MGUS compared with SMM and MM patients (3% *vs* 13% *vs* 12%, respectively). The t(4;14), as well as t(14;16) and t(14;20), are associated with a very poor prognosis in MM [46,87,89,143] and the survival curves obtained from over 1800 MM patients studied at the Myeloma Database confirmed these findings (**Section 3.2.2**). The observation that t(4;14) was less frequent in MGUS has been previously demonstrated [40,44,109,137,138]. Reports have implied that, because of the biological impact of this translocation on PC, the MGUS phase quickly evolves to overt MM in those patients. However, the t(14;16) was found at similar frequencies in MGUS and MM, and t(14;20), which was associated with the worst outcome and the shortest median survival in MM, was present in 5% of MGUS but in only 2% of MM patients. Therefore, by comparing the incidence of the *IgH* translocations in MGUS, SMM and MM, the assumption that *IgH* translocations associated to a poor prognosis in MM induce MGUS patients to progress more rapidly applied only to t(4;14) MGUS patients. In order to evaluate the biological effect of these three translocations in pre-malignant cases, as described in detail in **Section 3.2**, the disease course of a total of 45 MGUS and SMM patients with one of these three rearrangements was followed until the end of this study. In MGUS, the presence of any one of these translocations, including t(4;14), was not found to be associated with immediate progression to MM, in fact long-term stability was experienced by many patients. This was particularly true for patients with t(14;20), as none of them became symptomatic within a median follow-up period of 5 years. Since the rate of progression of SMM patients is normally higher than that seen in MGUS, the effect of these

translocations on patients in the SMM group was more difficult to assess. Notably, some SMM patients remained completely stable up to 5 years from diagnosis. Interestingly, for both MGUS and SMM, the presence of Δ13 associated with any of these three translocations did not appear to influence the disease course.

The reasons why translocations that are high-risk features in MM are associated with long periods of stability in the absence of symptoms in pre-malignant conditions is not clear. One possible explanation is that, to exert the effect seen in MM, they have to be associated with other factors, genetic or otherwise. A similar explanation probably accounts for the high prevalence of t(11;14) in PCL (42%), as described in **Section 3.6** and previously reported in other studies [97,252]. In MM, this translocation is associated with an intermediate prognosis, while it is the most frequent *IgH* rearrangement in the most aggressive of the PC dyscrasias. However, PCL karyotypes were found to be extremely complex with multiple structural and numerical changes coexisting with the *IgH* translocation. Interestingly, all t(11;14) PCL included in the current study were found to have associated abnormalities involving *MYC* at 8q24 and *MYC* abnormalities appear to be ubiquitous molecular events in the pathogenesis of PCL.

Together with the translocations t(4;14), t(14;16) and t(14;20), deletion of 17p13.1, the location of the tumour suppressor gene *TP53*, is a high risk feature in MM and it is considered to be the most significant molecular cytogenetic factor for prognostication [266]. Unlike the translocations, this abnormality has been described as a secondary/late genetic event in MM and in fact, for accurate prognostic determination, testing for 17p13.1 loss should be repeated at later time-points after the initial diagnosis [266]. Deletions of 17p13.1 have been reported to be uncommon in pre-malignant conditions, in accordance with the findings described in **Section 3.1** (3% in MGUS; ~1% in SMM). The incidence of this abnormality was found to be higher in patients with extramedullary disease: Tiedeman *et al.* reported that most cases of PCL (primary and secondary) have abnormalities in the *TP53* gene [71,97,252]. In **Section 3.6**, combining FISH for 17p13.1 and mutational analysis of *TP53,* deletions and coding mutations were found in only 30% of pPCL cases with one patient being positive for both changes. However, as inactivation of p53 can also occur through overexpression of the regulatory protein Mdm2 or by p14ARF inactivation [267,268], it is possible that other mechanisms inhibiting p53 activity might be present in cases negative for *TP53* deletions or mutations.

All pre-malignant patients with 17p13.1 deletion progressed to MM suggesting that, unlike the *IgH* translocations, the presence of this abnormality is responsible for the more aggressive behaviour in these conditions. All patients except one progressed to MM within two years from diagnosis, with SMM patients showing the most rapid evolution. The variation in time to progression seen in these patients was not dependent on the percentage of PC positive for the abnormality, as the MGUS patient who progressed after 32 months had 17p13.1 deletion in 87%

of PC. These observations indicated that other factors must be modulating the biological effect of 17p13.1 loss in MGUS and SMM. It should be noted that, despite its strong association with progression, this abnormality is very rare in all diagnostic groups, including MM; thus 17p13.1 loss cannot represent a ubiquitous mechanism of disease evolution from MGUS to MM.

In contrast to 17p13.1 deletion, gain of 1q21 is a secondary change which is highly prevalent in MM as well as in SMM patients (40%-45%) [162,163,165,269]. In **Sections 3.3** and **3.4**, the incidence of this abnormality was evaluated by array CGH and iFISH (with the same BAC probe used in previously published studies) in a large patient cohort: the frequencies of 1q21 gain in MM and SMM were found to be similar to those reported by other groups (MM, 39%; SMM, 37%). In PCL (**Section 3.6**), 1q gain was detected in 58% of patients. In the literature 1q21 gain has been reported to be absent from MGUS [162,163], while in the present study (the largest so far) 26% of MGUS patients were found with extra copies of 1q21, indicating that although the abnormality is rarer in MGUS as compared with MM or SMM (MGUS *vs* MM, P=0.01), it does occur in all diagnostic groups. Among all three groups, the size and the chromosomal position of these gains appeared to be the same. Moreover, similar associations between 1q21 gain and other chromosomal abnormalities were found in MGUS, SMM and MM.
In MM, gain of 1q21 was found to be associated with a dismal prognosis in different studies [154,165]. This finding, together with the rarity of the abnormality in MGUS, highlighted 1q21 gain as a possible marker of progression [48,162,164]. The current study confirmed 1q21 gain as an independent marker of poor prognosis in MM. However, there was no evidence that the presence of the abnormality in MGUS resulted in rapid evolution to symptomatic disease, an effect that was observed in MGUS patients with 17p13.1 deletion. Within the MGUS group, 80% of patients with the 1q21 gain remained completely stable up to the end of the study within a maximum follow-up period of 78 months; 30% of patients with the abnormality were totally asymptomatic 5 years from diagnosis. It should be noted that in this study the number of transformations within the MGUS group was high (25% of patients transformed) compared to the rate of malignant progression of ~1% per year which has been reported for this condition [40,42]. There is no obvious explanation to account for this difference, particularly because samples were collected from many different centres. It may be hypothesized that the cohort was biased towards high-risk MGUS cases. However, if high-grade patients are defined by their M-protein level and paraprotein type, no over-representation of this patient category was found in this cohort. In relation to this bias, because the purpose of this study was to better understand the biological role of 1q21 gain in MGUS, having a representative number of transformations was highly informative. As MGUS, SMM patients with 1q21 gain did not seem to preferentially evolve to MM, as a similar proportion of patients with and without 1q21 gain progressed to MM with the same median time to progression. In addition, 30% of patients with the abnormality

remained totally stable 5 years from diagnosis. However, the number of patients within this group was relatively small.

One limitation of this analysis was that the median follow-up of the MGUS and the SMM groups were only 41 and 22 months, respectively. MGUS in particular is a slowly evolving disease and a longer follow-up is required to fully understand the effects of genetic changes in asymptomatic patients. Therefore the study remains as work in progress. Another aspect that needs to be considered is that, although there was no suggestion that the different effects of 1q21 gain might depend on its specific association with other genetic markers either in MGUS or in SMM, these diseases are genetically highly heterogeneous and some changes are relatively rare, thus larger sample sizes are required.

Regarding chromosome 1, it has been reported that in MM 1q gain is closely related to 1p loss [152,178,270]. Array CGH results for the total patient cohort, described in **Section 3.3**, showed that all the abnormalities involving 1p were chromosomal losses. However, there was no association between these abnormalities and 1q gain (P=0.76). These losses, which were highly variable in size and break-points, were rare in pre-malignant cases, while they accounted for 36% of MM cases. Two common minimal deleted regions were identified at 1p21.3-p22.1 and at 1p32.3. Loss of 1p21.3-p22.1 appeared to be strongly related to progression to MM in the array CGH group. However, this finding has to be confirmed on a larger patient cohort and genomic results have to be correlated with expression data in order to identify the possible gene(s) targeted by this deletion. The second region of loss on 1p was particularly interesting as it was hemizygously deleted in three MM and one PCL patients and homozygously deleted in another three MM, the cell-line KMS-11 and a second pPCL case. More importantly, within the array CGH patient cohort, no pre-malignant cases showed deletion of this region. In MM and in the cell-line, HD involved both the *CDKN2C/p18* and the *FAF1* genes as they are situated in close proximity to one another. However, in the PCL case only *CDKN2C/p18* seemed to be included in the HD, reinforcing the potential role of *CDKN2C* as the targeted gene of this abnormality. The analysis of this region was extended to a larger patient cohort by iFISH which confirmed that 1p32.3 is very rare in MGUS (4%) and that it occurred in 8% and 13% of SMM and MM patients, respectively. In MM, 1% of these deletions were HD while those found in pre-malignant cases were hemizygous. In MM, hemizygous and homozygous deletions of 1p32.3 were found to be associated with an inferior OS (P=0.003).

In the SMM case described in **Section 3.5**, a large deletion on chromosome 1p was detected by metaphase analysis at the time of progression to MM. FISH confirmed the involvement of 1p32.3 but not of 1p21.3-p22.1 in the deletion and revealed that while this change involved the entire PC population at the time of MM diagnosis, it was present in only a sub-clone of PC a year before progression and was completely absent in the three previous samples, taken each year during the follow-up period. This finding from the iFISH results confirms that 1p losses are

likely to be secondary changes associated with the clinical manifestation of MM and suggests that 1p loss may have been directly involved in disease transformation of this specific case. However, the karyotype showed a large deletion of 1p, therefore the importance of other genes within the region of loss cannot be excluded. Moreover, together with 1p loss the patient was found to have acquired a *MYC* rearrangement within the year prior to progression, making it difficult to decipher the effect of the individual abnormalities on progression. From examination of the disease course of those MGUS and SMM patients found to be positive for 1p32.3 loss within the large cohort tested by iFISH, no definite conclusions could be drawn. Among the four MGUS patients, two had informative follow-up information and both progressed to MM, although evolution was not immediate (at 40 and 68 months from diagnosis). Among the SMM patients with the abnormality, although one progressed to MM after 22 months, two remained stable until the end of the study, 9 and 81 months from diagnosis. Nine months represents a very short follow-up period, therefore the first of the two SMM cases who did not progress by the end of the study was not highly informative. However, in the other patient the abnormality clearly was not enough to promote disease evolution within a period of more than 6.5 years. These inconsistent results may reflect the data reported by Leone *et al*. [271]. In MM, *CDKN2C* losses were found to be rarely HD and frequently hemizygous. Leone and colleagues found no mutations or methylation within the locus involving the residual allele in hemizygously deleted cases, suggesting that the main mechanism of loss of function of *CDKN2C* is by deletion. Moreover, they demonstrated that cases with HD not only lacked *CDKN2C* expression but, using an expression-based proliferation index, they were the most proliferative MM, consistent with the biological function of the gene as a cyclin-dependent kinase inhibitor. However, in hemizygously deleted cases, no direct correlation was found between *CDKN2C* mRNA levels and DNA copy number of the locus and only 78% of these cases showed a high proliferation index [271]. Therefore it may be hypothesized that in cases with hemizygous loss of *CDKN2C* there is a gene dosage effect, but this needs the additive effect of other dysregulated elements involved in the G_1-S transition.

In addition to 1p loss, array CGH detected a number of other chromosomal regions which appeared to be more frequently involved in copy number abnormalities in MM compared to MGUS or SMM. As expected, the overall number of CNA increased from MGUS to SMM to MM in all genetic groups. However, apart from MGUS and SMM patients with t(11;14) and t(14;20), the other pre-malignant patients already showed a high level of genomic complexity. In MGUS, this level of genomic complexity, expressed as the number of CNA per case, was found to be associated with progression, independently from the primary *IgH* rearrangement or ploidy class (P=0.003). However, because the majority of cases with a low level of CNA were represented by MGUS patients with t(11;14) or t(14;20), it can be hypothesized that MGUS

cases in which these two *IgH* translocations represented the primary genetic events, are characterized by a genetic background which does not promote rapid acquisition of additional abnormalities. As progression seems to originate from the acquisition of specific secondary genetic events, in these pre-malignant cases the genetic hit leading to MM has a reduced chance of occurring. In contrast, in MGUS cases where the primary genetic event is represented for example by t(4;14) or t(14;16), the genetic background established by these initiating changes tends to promote a more rapid acquisition of secondary abnormalities with an associated higher probability that changes responsible for progression will occur. This model is in agreement with the observations regarding the timing of acquisition of Δ13 within the different genetic classes.
The integration of array CGH results with information about the disease course of pre-malignant cases has shown that the rarity of a specific abnormality in MGUS or SMM compared to MM is insufficient to consider that this abnormality is responsible for progression, as clearly shown for 1q21 gain. Changes such as losses of 1p32.3, 8p21-p22, 9p21 and 16q23 were also significantly more frequent in MM. However, they were also found in MGUS/SMM patients who experienced long periods of stability despite the presence of the abnormality. A detailed example is shown by the acquisition of 16q23 loss in the SMM patient described in **Section 3.5**. In MM, 16q23 loss is a secondary event whose presence has been associated with an inferior OS [248]. However, in the SMM patient with serial genetic analysis**,** the abnormality was detected in a high proportion of PC more than 3 years before progression to MM. This suggested that, although it's role in disease transformation cannot be excluded, 16q23 loss was not the critical factor responsible. The ambiguous role of these abnormalities can be explained through different mechanisms: (**i**) these changes do not affect progression but simply reflect a higher degree of genomic complexity established at the time of disease evolution; (**ii**) they have an impact on progression which can only be exerted in co-operation with other factors; (**iii**) they do influence disease evolution but act in a slow, gradual manner consistent with the fact that MGUS is a slowly evolving condition. Therefore for some patients within this study their effect has not become apparent.
Other abnormalities such as 1p22.3-p23 loss, 6q25 loss, 8q24 changes (where *MYC* is located), 12p13 loss, Δ13 in t(11;14)/t(6;14) patients, changes involving members of the NF-κB pathway and 17p13 loss were exclusively found in patients who had progressed before the end of this study. However, also among patients with these abnormalities, time to progression varied considerably, with some cases experiencing rapid evolution to MM and others only progressing after some years. Such variation in time to progression was observed among patients carrying the same abnormality, suggesting that these changes are probably not the only factors which determine disease progression.
Among the patients with multiple samples taken at different stages of their disease course two different patterns of evolution were noted. Two patients (MGUS patient 355, **Section 3.1.4.4**;

SMM 1581 patient, **Section 3.3.4.6.2**) showed no differences in the abnormalities of their clonal PC before and at the time of progression, suggesting that those abnormalities were sufficient to drive disease evolution in these patients. The PC of both patients had changes associated with progression: patient 355 (with t(6;14)) had loss of 16q, and monosomy 13; patient 1581 had loss of 6q25, loss of 16q and gain of 17p12-p11.2, where *TACI* is located. Interestingly, in both patients the paraprotein level did not remain stable but steadily increased from diagnosis. In another two patients, the CNA detected at the time of diagnosis did not appear to be sufficient to drive disease progression and these patients experienced long-term stability with no fluctuation in paraprotein level. Progression to symptomatic MM coincided with the acquisition of new abnormalities which seemed to be strongly associated with progression. Patient 989 (MGUS, **Section 3.3.4.6.1**) and patient 259 (SMM, **Section 3.5**) represent two examples of this pattern of evolution: the first patient (HRD) acquired monosomy 13 and abnormalities involving the NF-κB pathway; the second (t(4;14)) acquired loss of 1p (including 1p32.3) and a *MYC* rearrangement. However, it should be noted that in both samples at the time of MGUS or SMM diagnosis, FISH and array CGH had already detected a high number of abnormalities which were suggestive of a genetic background prone to acquiring new changes.

Increased levels of MYC protein are found in many types of human cancer because the control mechanisms of MYC are inactivated during malignant transformation [141,142,272]. *MYC* is the oncogene dysregulated by *Ig* translocations in Burkitt lymphoma [273], mouse plasmacytoma [274] and rat immunocytomas [275]. In these tumours *MYC* dysregulation represents the primary event driving malignant transformation. In MM, *MYC* abnormalities are not initiating events and can occur through a number of different mechanisms (i.e. reciprocal and non-reciprocal translocations, insertions, inversions, deletions, duplications or amplifications). In the present study, the only recurrent amplified chromosomal region identified among the different diagnostic groups was 8q24 and combination of array CGH and FISH detected *MYC* abnormalities in 23% of MM (**Section 3.3**) and 67% of PCL (**Section 3.6**). In PCL, *MYC* overexpression seemed to represent a preferred mechanism of oncogenesis. These incidences are considerably higher than those reported in other series [97,111,143], suggesting that more comprehensive and detailed analysis of the *MYC* locus can reveal a higher incidence of *MYC* abnormalities. Interestingly, *MYC* abnormalities appeared to occur in all genetic classes, with a particular association with HRD. However, in the present study qRT-PCR also detected *MYC* overexpression in cases with no apparent 8q24.21 abnormalities, suggesting that a variety of mechanisms give rise to *MYC* dysregulation. Some may occur by dysregulated trans-activation through the transcriptional activity of presently uncharacterized factors. Thus, gene expression studies are more accurate for the identification of *MYC*-related tumours.

In pre-malignant patients, *MYC* abnormalities were detected in only one MGUS and two SMM patients; all three progressed to MM. One of the two SMM patients was followed for 4.5 years before progression to MM (**Section 3.5**). She was found to have acquired a *MYC* rearrangement in 40% of PC 10 months prior to transformation. By the time of MM diagnosis, the aberration was present in all cells. It should be noted that, although in both SMM cases progression occurred relatively rapidly (10 and 16 months from the detection of the abnormality), in the MGUS patient, clinical symptoms did not appear until 45 months from diagnosis. This difference in time to progression indicates that, as in cases with 17p13.1 deletion, the biological effect exerted by abnormalities which are strongly associated with evolving disease varies in different individuals; probably highly dependent on the influence of other factors.

Chesi and colleagues reported the generation of a transgenic mouse model, Vk*MYC, from C57BL/6 oocytes [276]. In these mice, sporadic *MYC* activation in the germinal centre is Activation-Induced Deaminase (AID) [277] dependent and mediated by the process of somatic hypermutation. In this study, whereas C57BL/6 mice developed benign monoclonal gammopathy with age [278], all of Vk*MYC mice developed indolent MM associated with biological and clinical features highly characteristic of the human disease. The fact that in the Vk*MYC mice, *MYC* activation led to MM in a mouse prone to MGUS, suggested that *MYC* is capable of driving the same progression in man. Consistent with these findings, recent reports of differential gene expression in MGUS and MM suggested that *MYC* overexpression or alterations in the *MYC* pathway in MM are not as rare as initial iFISH studies suggested. Elevated levels of *MYC* mRNA and *MYC* target genes distinguished patients with MM from those with MGUS, implicating a causal role for *MYC* in the progression of MGUS to MM. A gene expression profiling study performed on MGUS and MM patients from the Mayo Clinic, using gene-set enrichment analysis, reported over 300 gene-sets significantly enriched for genes overexpressed in MM compared to MGUS, representing potential activated pathways mediating transformation [173,276,279,280]. Gene-set enrichment analysis is a method that determines whether an *a priori* defined set of genes (group of genes that share common biological function, pathway, chromosomal location or regulation; information, which is extracted from published experimental data or curated databases) shows statistically significant differences between two biological states (i.e. MGUS and MM). After the clustering of the 313 gene-sets, three groups emerged: one including cell cycle related gene-sets, one proliferation related gene-sets and one *MYC* activation related gene-sets. These findings were validated in an independent cohort of 50 MGUS and 351 MM patients [279,280]. From these findings, a *MYC*-signature was derived which included targets under the direct control of MYC in a B cell specific transcriptional network [281]. The highest *MYC* expression was seen in samples with a strong *MYC* signature. Both *MYC* signature and *MYC* expression were absent from normal PC, peripheral blood B cells, chronic

lymphocytic leukemia and Waldenstrom macroglobulinemia, rarely weakly present in MGUS, strongly expressed in Burkitt lymphoma and in the majority (60%) of MM. Similar results were described by Anguiano *et al.* using gene expression from 877 PC dyscrasia patients with differential diagnoses [174]. *RAS* mutations have been identified only rarely in MGUS, but are present in 30% of newly diagnosed MM, with an increasing frequency in advanced disease [282]. Interestingly, tumours with *RAS* mutations were found to consistently express the *MYC* signature and cases with *RAS* mutations together with samples with very high expression of *MYC* mRNA deriving from *MYC* translocations accounted for 67% of cases with *MYC* activation [280]. Overall, these results suggest that the *MYC* pathway is central in the evolution of MGUS to MM. However, other gene-sets not related to the *MYC* pathway were found to be differentially expressed between MGUS and MM, suggesting that *MYC* dysregulation is not the only mechanism responsible for MM development.

In many haematological malignancies such as Hodgkin lymphoma, mucosa-associated lymphatic tissue lymphoma and diffuse large B cell lymphoma, NF-κB is constitutively activated [283]. Most primary MM (80%) and nearly 50% of HMCL have been shown to have elevated NF-κB transcriptional index defined by the transcription signature of eleven genes [182]. High expression of this signature was also found in PC isolated from BM of MGUS patients (in virtually 100% of cases) and of healthy individuals [182]. Normal and most neoplastic PC are strongly dependent on the BM microenvironment and part of the increased NF-κB signature activation is likely to be related to signals that PC receive within this microenvironment. Given the multiple recurrent abnormalities involving various regulators of this signalling which have been reported in HMCL and primary MM tumours [181,182], it has been proposed that the acquisition of mutations in genes coding for these regulators result in constitutive and ligand-independent activation of the signalling. As a confirmation, it was observed that in virtually all HMCL their high NF-κB index was a consequence of inactivation of suppressors (by either HD or deletion/mutation combinations) or by hyperactivation of pathway inducers as a consequence of gain/amplification or chromosomal translocation.
The present study confirmed the presence of changes involving various members of the NF-κB pathway (*BIRC2/3, TRAF3, TACI, NKB1, LTBR, CYLD*) with *TRAF3* and *BIRC2/3* losses being the predominant ones. The high incidence of *TRAF3* loss might be partly explained by the fact that *TRAF3* deletion is significantly more frequent in nonHRD MM (P=0.03) and the gene is located on chromosome 14, which is frequently lost in tumours in this ploidy category. *BIRC2/3* loss was also found to be associated with nonHRD. However, the high frequency of this abnormality cannot be similarly explained, as chromosome 11 (where *BIRC2/3* are located) is rarely lost in MM. Interestingly, such abnormalities were only found in MM and in two SMM

patients who evolved to MM after 6 and 15 months, respectively. Moreover, in one MGUS case with available material from both the time of MGUS diagnosis and the time of progression to MM, CNA involving NF-κB members (gain of *NFKB1* and loss of *CYLD*) were found to be present only in the MM sample. These findings suggested that changes dysregulating members of this pathway are only associated with overt MM and that they may promote the evolution of pre-malignant conditions by the constitutive activation of the pathway.

Interestingly, none of the PCL patients showed HD or amplification of any of the genes encoding for members of the pathway. This is in line with the fact that, while more than 80% of MM patients were found to have high NF-κB expression, only half of HMCL showed over-activation of the pathway. In most of these HMCL, mutations involving the signalling members were detected [181]. The majority of HMCL are derived from BM PC of PCL patients; therefore it is possible that NF-κB dysregulation does not play a major role in the etiology of PCL.

A number of reports have shown that in MYC-driven lymphomas, NF-κB is not involved in tumour promotion. In the EμMyc-mouse model, which has a transgene expressing the *MYC* oncogene under the control of the enhancer (μ) in the *IgH* locus, NF-κB activity was found to be dispensable for lymphomagenesis [284]. Another two studies reported that low expression of NF-κB target genes were hallmarks of Burkitt lymphoma [285,286]. Klapport *et al.* [287], investigating the role of NF-κB in mouse and human *MYC*-transformed lymphomas, reported that the NF-κB canonical pathway is extinguished in murine lymphoma cells and that extrinsic stimuli, typically inducing NF-κB activity, failed to activate this pathway. In these cells, genetic activation of the NF-κB signalling induced apoptosis, whereas inhibition of NF-κB provided a selective advantage in vitro. The activation of NF-κB was also found to induce apoptosis in human Burkitt lymphoma cells.

In the present study, it was evident that the majority of PCL patients were characterized by *MYC* abnormalities (eight of 12 patients) associated with *MYC* overexpression. Moreover, of the patients tested by qRT-PCR, *MYC* overexpression was observed in one patient lacking any abnormality at 8q24, confirming that *MYC* overexpression can be activated by a number of different mechanisms. This finding together with the fact that no abnormalities involving NF-κB members were detected in PCL, may suggest that in these patients the NF-κB pathway is not essential. Interestingly, within the group of MGUS, SMM and MM patients analyzed by array CGH, abnormalities involving *MYC* and abnormalities involving members of the NF-κB pathway were found to be mutually exclusive. However, it has to be noted that in *MYC*-driven lymphomas, *MYC* dysregulation has been implicated as a primary event, while in MM it is responsible for progression, meaning that the biology of these tumours may be different with regard to the inter-relation between the *MYC* and the NF-κB pathways. Moreover, the comparison between *MYC* expression [263]and the NF-κB index [245] for a number of recently published HMCL showed that some cell lines with high *MYC* expression also have high NF-κB

index. However, these suggestions need to be investigated further as NF-κB inhibitors are widely used in the treatment of MM patients and such responses may have negative implications for therapy in *MYC*-positive tumours.

Concluding remarks

The main aim of this study was to identify molecular cytogenetic markers responsible for disease evolution from MGUS and SMM to MM and PCL. The findings presented in the preceding chapters have yielded novel insights into the role of different chromosomal abnormalities in the development of MM. Despite the high level of genetic complexity which characterizes PC disorders, it has been possible to discern an underlying order of events characterizing various abnormalities and to better understand their biological impact in the context of different stages of the disease.

The first main observation from this study was the increasing genomic complexity from MGUS to SMM to MM to PCL, a pattern which was common to all genetic groups. In MGUS, a high level of complexity, defined as the number of chromosomal gains and losses per case, was found to be associated with progression, independent of the underlying *IgH* translocation or ploidy category. None of the primary *IgH* translocations, regardless of their biological impact in MM, seemed to have an effect on progression in either MGUS or SMM patients. The comparison of copy number and structural aberrations among the different classes did not identify one common chromosomal aberration associated with progression but instead uncovered various secondary changes, which were rare or absent in pre-malignant cases and recurrent in MM and PCL. In addition, within the same genetic group, there did not appear to be a common event associated with progression, apart from possibly Δ13 in most pre-malignant cases with t(6;14) and t(11;14) and dysregulation of members of the NF-κB pathway in *IgH*-translocated cases. These findings suggested that either (**i**) many different mechanisms can induce MGUS or SMM patients towards progression or that (**ii**) there are common pathways which are crucial for progression to MM, but these same pathways can be dysregulated through a number of different members and mechanisms. In either scenario, identification of the mechanism is difficult when attempted exclusively from the genetic point of view, given the karyotypic chaos characterizing many cases. These observations strongly suggested that an approach where genomic studies are integrated with gene expression data is required. Another main finding of this study was that changes found to be significantly rare in MGUS and SMM compared to MM were not necessarily associated with disease progression. For some of these changes, it is unknown whether they are directly involved in disease progression or whether they simply reflect the increased genomic complexity typical of overt MM. This was also true in the context of those abnormalities which in MM have been confirmed to be associated with inferior prognosis. Thus, the biological significance of chromosomal changes in pre-malignant

conditions cannot be assumed from the effect they exert in patients receiving treatment. High-risk chromosomal changes do not automatically lead to overt disease when present in MGUS or SMM; gain of 1q21 is one such example. Other changes seem to be directly responsible for progression (i.e. 17p13.1 loss, 1p21.3-p22.1 loss and *MYC* abnormalities). However, time to progression in patients positive for these abnormalities seemed to vary considerably suggesting that other modulating factors, which might be represented by co-existent genetic abnormalities, may play a role. In order to investigate possible interactions between different chromosomal changes, studies must be conducted over long follow-up periods, given the slow disease evolution of most MGUS cases. In addition they have to involve large numbers of patients considering the high level of genetic heterogeneity (e.g. previous studies failed to detect 1q21 gain in MGUS because the number of cases investigated was too small [162,163]). For these reasons, this study should be continued by: (**i**) following the sample patients in order to re-evaluate the effect of the different abnormalities in the context of longer-term follow-up and (**ii**) studying increased numbers of new patients in order to confirm or disprove the role of those abnormalities found to be associated with disease progression in the current study. Particular effort should be made to collect and genetically characterize sequential patient samples at different stages of the disease, as these provide the unique opportunity to determine how and when specific abnormalities arise and how these changes correlate with the clinical evolution of the disease.

Although this study has advanced the understanding of the genetics of PC dyscrasia, much more work still needs to be done. In particular with consideration of novel technologies including deep sequencing and other complex technologies, such as chromatin immunoprecipitation and DNA methylation methodologies in order to identify epigenetic changes in addition to genomic abnormalities. These new approaches may uncover previously unidentified changes/mechanisms responsible for MGUS and SMM progression to MM, which may be applicable as potential novel molecular targets for therapy, either to prevent progression or, at least, to prolong the pre-malignant stage. In addition, the early detection of abnormalities known to drive disease evolution (i.e. changes of *MYC*, *TP53* and NF-κB) in MGUS and SMM patients may provide the opportunity to use increasingly effective treatments on patients fit enough to benefit from them as they do not suffer from irreversible lytic bone disease, renal failure or other disabling symptoms.

APPENDICES

Appendix 1: URL

- Children's Hospital Oakland Research Institute (BACPAC Resources): http://bacpac.chori.org/order.php
- Database of Genomic Variants: http://projects.tcag.ca/variation/
- Department of Genetics and Microbiology, University of Bari (Prof. Rocchi): http://www.biologia.uniba.it/rmc/
- Ensembl Human Genome Browser: http://www.ensembl.org/Homo_sapiens/
- GeneCards: http://www.genecards.org/
- OMIM: http://www.ncbi.nlm.nih.gov/Omin
- Primer3 program: http://primer3.sourceforge.net/
- University of California Santa Cruz Human Genome browser: http://genome.ucsc.edu/
- Mitelman Database of Chromosomes in Cancer: http://cgap.nci.nih.gov/Chromosomes/Mitelman/
- MRC-Holland biotechnology company: http://www.mrc-holland.com/
- IARC p53 website: http://www-p53.iarc.fr/index.html
- NCBI UniGene EST Profile Viewer: http://www.ncbi.nlm.nih.gov/Unigene/ESTProfileViewer.cgi?uglist=Hs.2936

Appendix 2: Buffers and Reagents

- **Zap-o-globin**

Stock solution was kept at 4˚C; working solution (1:1; Zap-o-globin:sterile water) was kept at room temperature

- Red Cell Lysis (RCL) buffer

155mM NH_4Cl
10mM $KHCO_3$
0.1mM EDTA

RCL buffer kept at room temperature; the dispenser bottle in use kept at 37°C

- **RPMI culture medium**

RPMI 1640 Dutch modification medium (Gibco)
20% Fetal calf serum (Sigma-Aldrich)
1% penicillin/streptomycin (Sigma-Aldrich)
2% L-Glutammine (Sigma-Aldrich)

The constituents were filtered using a syringe with attached a Sarsted filter. Culture medium was kept at 4˚C and warmed up at 37˚C before used

- **Wash medium**

This was either be outdated full RPMI culture medium or freshly made up RPMI culture medium but containing only 12.5% of fetal calf serum. Wash medium was kept at 4˚C and warmed up at 37˚C before used

- **Phosphate buffered saline$^+$ (PBS$^+$) buffer**

For 200ml solution: 1 tablet of PBS (Sigma-Aldrich)
0.5% BSA (albumin from bovin serum; Sigma-Aldrich)
2mM EDTA

The solution was filtered into sterile 100ml bottles and left 24 hours in the fridge at 4˚C with the lids partially unscrewed to allow the degassing

- **IL-6 (First Link)**

IL-6 stock solution: 1µg/ml (stored at -20˚C). For the working solution (100ng/ml), the stock solution was diluted in wash medium; this solution was viable for one week if kept at 4˚C. Concentration used for cytogenetic cultures: 10µl per ml of culture medium (1ml culture medium = $1x10^6$ cells)

- **FdU** (Sigma-Aldrich; working solution: $1x10^{-5}$M in PBS, kept at 4˚C)

- **Uridine** (Sigma-Aldrich; working solution: $4x10^{-4}$M in PBS, kept at 4˚C)

- **Thymidine** (Sigma-Aldrich; working solution: $1x10^{-3}$M in PBS, kept at 4˚C)

- **Colcemid** (Gibco; working solution: 10µg/ml, kept at 4˚C)

- **Hypotonic solution**: 0.075M KCl (Sigma-Aldrich; 5.56g KCl was added to a 1 litre of sterile water and kept at room temperature. The dispenser in use was kept at 37^{o}C)

- **Carnoy's fixative** (3:1; methanol:acetic acid; methanol and glacial acetic acid were dispensed immediately before use)

- **Wright's buffer** (10ml of commercial Sorensen's phosphate buffer (Mercia Diagnostics) were added to 100ml of sterile water)

- **Wright's stain** (1.5g of Wright's stain (Sigma-Aldrich) was dissolved in 500ml of methanol)

- **LB Broth (GibcoBRL)**

  20g per litre dH_20 (autoclaved and then stored at room temperature)

- **Agar (Dibco)**

  2g/100ml LB Broth (autoclaved and kept at 50˚C until ready)
  The desired concentration of antibiotic was added when cool
  Plates were poured and stored at 4˚C

- **Antibiotics**

Kanamycin Sulphate (GibcoBRL)	10mg/ml
Ampicillin (Hospital Pharmacy)	10mg/ml
Tetracycline (Hospital Pharmacy)	10mg/ml
Chloramphenicol (Sigma-Aldrich)	10mg/ml

- **P 1 solution**

15mM Tris Base pH8.0
10mM EDTA
100µg/ml RNase A (Sigma-Aldrich) added just before use

- **P 2 solution**

4ml NaOH (Sigma-Aldrich; 4g NaOH Anhydrous pellets in 100ml dH_20)
2ml 10% SDS (20% SDS + equal vol. dH_20)
14ml dH_20

- **P 3 solution**

60ml 5M KAC
11.5ml Glacial Acetic Acid
28.5ml dH_20

- **TE (pH8.0)**

10ml 1M Tris (pH8.0)
2ml 0.5M EDTA (pH 8.0)

- **0.8% Agarose Gel**

1.2g Agarose (Bioline)
150ml 1x TBE

- **5x TBE Buffer** (Sigma-Aldrich)

Contents of container dissolved in 4L of dH_20

- **Standard DNA Assay**

  100µl Calf Thymus DNA (1mg/ml, Pharmacia Biotec)
  100µl 10xTNE Buffer
  800µl dH_20 filtered

- **Loading Buffer (for gels)**

  8g Sucrose (Sigma-Aldrich)
  1ml 5% Orange G (Sigma-Aldrich)
  40µl 0.5M EDTA
  Made up to final volume of 20ml with dH_20

- **Stock DNase I** (1mg; Sigma-Aldrich)

Enzyme Diluent 400µl sterile dH_2o
100µl 10x Nick Translation Buffer
500µl Sterile Glycerol

DNase I Working Solution (1µg/ml): 1µl of Stock Dnase I in 1ml of Enzyme Diluent

- **10x Nick Translation Buffer**

  0.5M Tris.Cl pH7.5
  0.1M $MgS0_4$
  1mM Dithiothreitol (Mw 154.25)
  500µg/ml Bovine Serum Albumin
  All reagents stored at -20°C

- **0.5 mM dNTPs** (Pharmacia, 100mM)

  2µl each of dATP, dCTP, dGTP, and 1194µl of sterile dH_20

- **Spectrum Green dUTP** (Vysis)

  50µl TE (pH7.5) added to powder

- **3M Sodium Acetate** (pH 7.0)

  24.61g dissolved in 200ml sterile dH_20

- **Human Cot - 1 DNA** (500mg; GibcoBRL)

  50µl aliquots (2µl in 18µl dH_20)

- **Complete Hybridization Mix**

  5ml de-ionised formamide + dextron sulphate *

  2ml 10x SSC**

  3ml dH_20

* De- ionised formamide: 5g (monobed) resin in 150ml formamide, stirred for 45 min at room temperature and filtered. 20% dextron sulphate (Polysciences Inc.) and dissolve overnight.

** 10x SSCP - equal Vol. of 20x SSC and dH_20.

- **RNase A** (Sigma-Aldrich)

1mg/ml of RNase buffer (stored at -20˚C)
RNase buffer (10mM Tris; 15mM NaCl (pH 7.5))
Boiled for 30 minutes to destroy DNase and stored in 50µl aliquots at -20˚C

- **Pepsin** (Sigma-Aldrich)

  50mg/ml in 0.01M HCl

  Stored in 50µl aliquots at -20˚C

- **20x SSC**

175.3g NaCl (Sigma-Aldrich)
88.2g NaCit (Sigma-Aldrich)
Made up to 1 litre dH_20 (stirred for a couple of hours to ensure complete dissolvement)

- **2x SSC**

  450mls dH_20

  50mls 20 x SSC

- **0.4x SSC/0.3% NP40** (Igepal, Sigma-Aldrich)

  4ml 20xSSC

  196ml dH_2O

  600µl NP40

- **2x SSC/0.1%NP40**

  100ml 20xSSC
  900ml dH_2O
  1000µl NP40

- **4x SSC/0.05%NP40**

  100ml 20xSSC
  400ml dH_2O
  250µl NP40

- **RSB (Resuspension Buffer)**

  0.075M NaCl
  0.024M EDTA
  In 1L dH_2O (pH=8.0)

- **Proteinase K** (Sigma-Aldrich)

  50mg/ml in dH_2O

- **BCR-ABL Multiplex Mix**

2.4ml PCR buffer (Invitrogen)

0.9ml $MgCl_2$ (Invitrogen)

192µl dNTPs at 25 mM*

120µl of each of the primers (CA3-, C5e-, B2B, BCR-C)**

16ml dH_2O

* dNTPs was made by combining equal volumes of each of the 4 dNTPs

** All primers were at 100µM

250µl aliquots were stored at -70C

- **Control Gene Multiplex PCR Primers**

Frag.	Gene	Exon	Forward primer	Reverse primer
100 bp	TBXAS1	9	5′-GCC CGA CAT TCT GCA AGT CC-3′	5′-GGT GTT GCC GGG AAG GGT T-3′
200 bp	RAG1	2	5′-TGT TGA CTC GAT CCA CCC CA-3′	5′-TGA GCT GCA AGT TTG GCT GAA-3′
300 bp	PLZF	1	5′-TGC GAT GTG GTC ATC ATG GTG-3′	5′-CGT GTC ATT GTC GTC TGA GGC-3′
400 bp	AF4	11	5′-CCG CAG CAA GCA ACG AAC C-3′	5′-GCT TTC CTC TGG CGG CTC C-3′
600 bp	AF4	3	5′-GGA GCA GCA TTC CAT CCA GC-3′	5′-CAT CCA TGG GCC GGA CAT AA-3′

Primer mix A:

25µl of each 10pmol/µl stock: 100bpF, 100bpR

200bpF, 200bpR

300bpF, 300bpR

400bpF, 400bpR

Primer mix B:

50µl of each 10pmol/µl stock: 600bpF, 600bpR

Appendix 3: List of in-house FISH probes

Chr	p arm				q arm			
	Probe	Gene involved	position	Fluorochrome	Probe	Gene involved	position	Fluorochrome
1	bA418J17		1p12	Cy3	bA373C9	*PDZK1*	1q21.1	Cy3
	bA278J17	*p18 (CDKN2C)*	1p32.3	Sp Green	bA307C12	*CKS1B*	1q22	Sp Green
	bA296A18	*p18 (CDKN2C)*	1p33	Sp Green	bA32D17	*ASPM*	1q31.3	Sp Aqua
	bA116M11	*p18 (CDKN2C)*	1p33	Sp Green				
5					bA473K22	*MoKA (FBX038)*	5q32	Cy3
6	bA298J23	*CCND3*	6p21	Cy3				
	dJ973N23	*CCND3*	6p21	Cy3				
	bA7K24	*CCND3*	6p21	Sp Green				
	bA533O20	*CCND3*	6p21	Sp Green				
8	bA395I14	*PPP2R2A*	8p21.2	Sp Green	dJ80K22	*MYC*	8q24.21	Cy3
	bA142D17	*PPP2R2A*	8p21.2	Cy3				
9	bA469D03	*PAX5*	9p13.2	Sp Green				
	bA149I2	*p16 (CDKN2A)*	9p21.3	Cy3				
11					WI2-2395O14 *	*BIRC2*	11q22.2	Cy3
					WI2-1116O16 *	*BIRC3*	11q22.2	Cy3
					bA315O6	*BIRC2*	11q22.2	Sp Green
					bA177O8	*BIRC3*	11q22.2	Sp Green
12	bA388F6	*centromeric to CCND2*	12p13.32	Cy3				
	WI2-1673N13*	*CDKN1B*	12p13.2	Cy3				
	bA515B12		12p13.1	Sp Green				
13					bA305D15	*RB1*	13q14	Sp Green
					bA174I10	*RB1*	13q14	Sp Green
14					WI2-959M11 *	*TRAF3*	14q32.32	Cy3
					WI2-1602P13 *	*TRAF3*	14q32.32	Cy3
					bA347M8	*TRAF3*	14q32.32	Sp Green
17					dJ1169K15	*NIK (MAP3K14)*	17q21.31	Sp Green
					bA419E16	*NIK (MAP3K14)*	17q21.31	Cy3
					bA339E12	*NIK (MAP3K14)*	17q21.31	Sp Green
					bA403G3	*NIK (MAP3K14)*	17q21.31	Cy3
20					dJ54G6	*mafB*	20q12	Cy3
					dJ600E6	*mafB*	20q12	Cy3
					bA264H10	*mafB*	20q12	Sp Green
					dJ1123D4	*mafB*	20q12	Sp Green
					bA79G10	*mafB*	20q12	Sp Green
					bK3184A7	*RTEL1/STMN3*	20q13.33	Cy3
22					dJ1019H10	*IgL*	22q11.2	Sp Green
					dJ889J22	*CARD10*	22q13.1	Sp Green
					LL22NC03-10C3 **	*PDGFB*	22q13.1	Cy3

Fish probes are listed with their chromosomal position, name of the gene involved and fluorochrome used (Chr, chromosome; Sp, spectrum)

* **Fosmid probe**

** **Cosmid probe**

Source: Sanger Institute, Hinxton, UK (except for *RB1* which was sent by Prof. Rocchi, Resources for Molecular Cytogenetics, University of Bari, Italy)

List of commercial FISH probes from Vysis (Abbott)

Chromosome	Probe	Vysis code
3	CEP3 (D3Z1) Spectrum Orange	32-130003
4/14	LSI IGH/FGFR3 Dual Colour (Spectrum Orange & Green), Dual Fusion Translocation Probe	N/A
5/9/15	LSI D5S23/D5S721/CEP 9/ CEP 15 Multi-colour Probe Set § (Spectrum Aqua, Green & Orange)	32-231021
8	LSI MYC Dual Color (Spectrum Orange & Green), Break Apart Rearrangement Probe	32-191096
	LSI IGH/MYC, CEP 8 Tri-Colour Translocation Probe (Spectrum Aqua, Green & Orange)	32-191020
7	CEP7 (D7Z1) Spectrum Aqua	32-131007
9	CEP9 Spectrum Aqua	32-131009
11/14	LSI IGH/CCND1 XT Dual Colour (Spectrum Orange & Green), Dual Fusion Translocation Probe	N/A
13	LSI D13S319 (13q14.3) Spectrum Orange Probe	32-190045
14	LSI IGH Dual Color (Spectrum Orange & Green), Break Apart Rearrangement Probe	32-191019
16/14	LSI IGH/MAF t(14;16)(q32;q23) Dual Colour (Spectrum Orange & Green), Dual Fusion Translocation Probe	32-231014
17	CEP17 (D17Z1) Spectrum Green	32-132017
	LSI p53 (17p13.1) Spectrum Orange	32-190008
22	LSI 22 (BCR) Spectrum Green	32-192024

Appendix 4: Custom probes added to the 'Salsa MLPA kit P088 Glioma 1' (MRC-Holland) for the detection of copy number changes of the genes *FAF1* and *CDKN2C*

Probe	Chromosome band & Mb position	Gene involved	Probe sequence (in bold, 48bp) & stuffer sequence of variable length
120	**1p32.3** 51,096,722Mb-51,096,769Mb	***FAF1*, intron 8**	**GAGCCACATTTCAAGGACTCACTAGCCACA TGTGTCTAGCAGCTACCA**AGAGATAATCAA CGACAATGCGTGCGTGAT
117	**1p32.3** 51,197,762Mb-51,197,809Mb	***FAF1*, intron 1**	**GGATTGGAGGTATTAATGACTTGGGTTACA ATGTGTGTGGAATGTGTA**ACACCCTTCACGC CGCGCAAAAAAGTA
124	**1p32.3** 51,204,913Mb-51,204,960Mb	**Between *FAF1* & *CDKN2C***	**GACCCTAAGCTCTGCACTGCCAATTCTGGT TTACCCAACAGGCAGATG**GGATGCGCATCC TGAAATGTTGATGGGGTTGAGG
108	**1p32.3** 51,207,906Mb-51,207,953Mb	***CDKN2C*, exon 1**	**TCTGGAGAAGCCCAGAGCACTGGGCAATC GTTACGACCTGTAACTTGA**TTTAACAATCCA GTAGC
111	**1p32.3** 51,208,620Mb-51,208,667Mb	***CDKN2C*, exon 2**	**CCCTAAAGAATGGCCGAGCCTTGGGGGAA CGAGTTGGCGTCCGCAGCT**TAACTTTTTTCA AGCTCTACC
114	**1p32.3** 51,213,914Mb-51,213,961Mb	**Centromeric of *CDKN2C***	**GAAGGACATGGTTCTGATGCCTGACCTAAC AAGGATTGGAATGGCTGG**TGTTACTTACCTG TTGGGGACCGC

Appendix 5: Karyotype description of the cytogenetically abnormal MGUS and SMM cases studied in Section 3.1; for each patient the ploidy status determined by iFISH is shown

RegID	Diag	Ploidy	Karyotype
355	**MGUS**	**HRD**	**47,XX,+X,t(6;14)(p21;q32),+9,+11,-13,-14,-16,+19[1]/46,XX[47]**
551	MGUS	nonHRD	45,XX,t(3;12)(q27;q13),der(12)t(1;12)(q21;q22),-13,t(14;22)(q32;q11),der(16)t(1;16)?(q21;q22)[3]/45,idem,t(5;20)(q33;q13.3),t(3;14)(q13;q31)t(14;22)(q32;q11)[12][15]/46,XX[37]
911	MGUS	HRD	52,X,-X,+3,+5,+7,+add(9)(q22),-13,+15,+15,+19,+21[1]/46,XX[52]
949	MGUS	nonHRD	85<4n>XX,-Y,-Y,dic(8;15)(q24;p11)x2,t(11;14)x2,+15,-16,-16,-17,-19,-20,-22,+2mar[1]/46,XY[16]
1494	MGUS	nonHRD	46,XX,del(13)(q12q22),t(14;16)(q32;q24),add(16)(q24)[1]/46,XX[73]
1870	MGUS	HRD	52,X,-X,+5,+9,+11,+15,+18,+19,+19[1]/46,XX[76]
1889	MGUS	HRD	57,X,-X,+3,+4,+5,+7,+9,+9,+11,+15,+18,+19,+21,+21[1]/46,XX[131]
2136	SMM	nonHRD	46,XY,del(1)(p13p?31),del(14)(q22)[4]/46,idem,der(15)t(1;15)(q11;q26)[1]/46,XY[65]
2436	SMM	HRD	56,X,-Y,+3,der(3)t(1;3)(q12;p25),+6,+7,+9,+11,+14,+15,+15,+18,+19,+21[4]/56,idem,t(2;15)(q21;q22),t(6;22)(p21;q13)[2]/57,idem,+?del(1)(p12)[3]/57,sdl2,-der(3)(1;3),+3[1]/57,sdl3,add(1)(p36),add(6)(q13)x2,del(22)(q12),+mar[2]/58,sdl2,add(1)(p36),der(3)t(1;3)dup(1)(q21q42),+6,add(6)(q13)x2,del(22)(q12)[2]/46,XY[30]
1175	SMM	HRD	52,Y,-X,der(1;6)(p10;q10),del(1)(p36),+2,+3,+5,+6,der(8)t(1;8)(p22;p11),+9,+9,+11,+15,+19[2]/46,XY[36]
1516	SMM	HRD	50,X,-Y,t(1;8)(p13;q24),+3,+3,+7,+9,der(13)t(1;13)(q21;q12),+15[4]/46,XY[48]
1717	SMM	HRD	57,XY,+3,+8,+9,+9,+11,+add(14)(q32),+15,+15,?+19,+2mar[2]/46,XY[59]
2178	SMM	nonHRD	46,XY,t(11;14)(q13;q32)[1]/46,XY,der(16)t(1;16)(q11;q23)/46,XY[50]
276	SMM	HRD	50,X,-X,+3,+6,+7,der(7)t(1;7)(q12;p22),+9,-13,+15,+19[10]/46,XX[80]
2033	SMM	HRD	52,XY,del(1)(p?21p32),+3+5,+9,+11,add(12)(q24),+15,+19[2]/52,idem,add(18)(q23)[2]/46,XY[45]
616	SMM	HRD	48,X,-X,+3,+4,der(6)t(6;?7)(q2?3;q1?1),add(7)(p1),-8,+9,add(10)(q26),+11,add(12)(q24),-13,add(16)(p1),add(18)(p1),+20,add(20)(q11)x2,-22,+mar[1]/46,XX[49]
331	SMM	HRD	48,XX,+3,+del(6)(?q21q23),add(7)(p22),+8,+9,-13,-14,der(15)t(?3;15)(p11;p11),-16,+add(17)(p11),der(20)t(1;20)(q12;p13),inc[1]/46,XX[78]
2035	SMM	nonHRD	46,XX,t(11;14)(q13;q32)[cp2]/46,XX[177]
1441	SMM	HRD	52,X,-X,del(1)(p21p34),add(2)(q35),+3,+5,+9,add(10)(q22),+add(11)(p11),add(13)(p11),der(13)t(1;13)(p34;q32),+der(15)t(15;?;1)((p11;?;q12),-16,add(16)(q24),+19,+19,+mar[2]/46,XX[120]
1925	SMM	nonHRD	45,X,t(X;11)(q13;q23),der(11)t(1;11)(q12;p15),-13,?del(14)(q2?4q32),?rdel(20)(p11q12),del(20)(p1),+mar[3]/46,XX[168]
1873	**SMM**	**nonHRD**	**48,X,-Y,?dup(1)(q21q32),+?der(1)add(1)(p12)?dup(1)(q21q32),+9,+19[1]/46,XY[78]**
231	SMM	HRD	54,XY,+3,+5,+7,dic(8;12)(p23;p11),+9,+9,+11,?psudic(11;18)(q25;p11),+15,+15,+19,+20[3]/46,XY[50]
508	SMM	HRD	54,XX,+3,t(6;16)(p21;p13),+7,+9,+11,+15,+18,+19[1]/46,XX[14]
2213	SMM	HRD	57,XY,del(1)(p11),+t(1;3)(p3?6;p1?3),t(2;8)(p12;q24),+5,+5,+7,+7,+9,+9,+11,+15,+19[1]/57,idem,+2,+8,-t(2;8),add(14)(q32)[1]/46,XY[13]

Cases where FISH and karyotype were discrepant for ploidy status are in red

(Reg ID, patient ID; diagn, diagnosis)

Appendix 6: Characteristics of MGUS and SMM patients with array CGH results

Genetic group	RegID	Age	Gender	CC	Karyotype	Diagn	PP	Progr	Time to progression/FU from diagnosis (months)	Time to progression/FU from array CGH analysis (months)
4;14										
	2715	65	F	Normal	46,XX[38]	MGUS	IgGk	**No**	39	39
	105	68	M	Normal		SMM	IgGk	**Yes**	7	7
	1252	56	M	Normal	46,XX[33]	SMM	IgGk	**No**	24	24
	259*	30	F	Abnormal at the time MM diagnosis	40~41,X,-X,del(1)(p13p31),add(3)(q2?6),der(8)t(8;?13)(q24;q12),del(12)(q11),-13,-13,-16,-20[cp2]/46,XX[4]	SMM	IgAk	**Yes**	53	31
	331	71	F	Abnormal	48,XX,+3,+del(6)(?q21q23),add(7)(p22),+8,+9,-13,-14,der(15)t(?3;15)(p11;p11),-16,+add(17)(p11),der(20)t(1;20)(q12;p13),inc[1]/46,XX[78]	SMM	IgGk	**Yes**	33	33
	508	61	F	Abnormal in following sample (1 year later)	54,XX,+3,t(6;16)(p21;p13),+7,+9,+11,+15,+18,+19[1]/46,XX[14]	SMM	IgGk	**No**	14	14
	2849	69	F	NSU		SMM	IgGk	**Yes**	21	21
	1836	60	F	NSU		SMM	IgAk	**Yes**	16	16
	2664	42	M	Normal	46,XY[60]	MGUS	IgGk	**No**	44	44
	3318	85	M	NSU		MGUS	IgM1	**No**	17	17
t(6;14) & t(11;14)										
	844	57	F	NSU		MGUS	IgG	**No**	67	67
	355*	66	F	Abnormal in previous sample (MGUS stage)	47,XX,+X,t(6;14)(p21;q32),+9,+11,-13,-14,-16,+19[1]/46,XX[47]	SMM	IgGk	**Yes**	41	20
	999	77	F	NSU		MGUS	IgGk	**No**	74	74
	855	83	F	NSU		MGUS	IgG1	**No**	17	17
	795	76	F	NSU		MGUS	IgG1	**No**	69	69
	610	59	F	Normal	46,XX[38]	MGUS	IgG	**No**	84	84
	695*	71	F	NSU		MGUS	IgG1	**No**	156	72
t(14;16)										
	837	47	F	Normal	46,XX[74]	MGUS	IgG1	**Yes**	46	46
	582	56	F	NSU		SMM	IgAk	**Yes**	15	15
	2198*	60	F	Normal	46,XX[44]	SMM	IgG1	**Yes**	124	50
	1494	39	F	Abnormal	46,XX,+1,der(1;16)(q10;q10),?del(13)(q12q22),t(14;16)(q32;q24)[1]/46,XX[73]	MGUS	IgG1	**No**	17	17
	1189*	63	F	NSU		MGUS	IgGk	**No**	125	35
	1073	67	F	Normal	46,XX[29]	SMM	IgG	**No**	55	55
t(14;20)										
	417	84	F	Normal	46,XX[57]	MGUS	IgG1	**No**	74	74
	866	44	F	Normal	46,XX[18]	SMM	IgG	**No**	71	71
	976	78	M	Normal	46,XY[6]	MGUS	IgGk	**No**	67	67
	367	46	F	Normal	46,XX[71]	MGUS	IgG1	**No**	78	78
HRD										
	1822	36	F	Normal	46,XX[45]	SMM	IgAk	**No**	56	56
	865	51	F	Normal	46,XX[52]	MGUS	IgGk	**No**	71	71
	528	75	F	NSU		MGUS	IgAk	**Yes**	45	45
	911	61	F	Abnormal	52,X,-X,+3,+5,+7,+add(9)(q22),-13,+15,+15,+19,+21[1]/46,XX[52]	MGUS	IgG1	**Yes**	8	8
	403	57	M	Normal	46,XY[162]	SMM	IgG1	**No**	74	74
	1473*	45	M	Normal	46,XY[202]	MGUS	IgGk	**Yes**	249	26
	121	69	F	NSU		MGUS	IgG1	**Yes**	79	79
	396	77	F	Normal	46,XX[42]	MGUS	IgGk	**Yes**	76	76
	989	67	M	Normal	46,XX[33]	MGUS	IgG	**Yes**	74	74
	2879	83	F	Normal	46,XX[3]	MGUS	IgG	**No**	26	26
nonHRD										
	698	74	M	NSU		MGUS	IgGk	**Yes**	75	75
	1581*	55	M	NSU		SMM	IgA1	**Yes**	29	15
	2326	72	M	Normal	46,XY[37]	MGUS	IgA	**No**	47	47

(RegID, patient identification; CC, conventional cytogenetics; Diagn, diagnosis; PP, paraprotein type; Progr, progression; FU, follow-up time; F, female; M, male)

*** Patient not studied at diagnosis**

Appendix 7: Characteristics of MM patients with array CGH results

Genetic group	RegID	Age	Gender	CC	Karyotype	PP	Status	FU from analysis	FU from diagnosis
t(4;14)									
	719	77	M	Abnormal	44,X,-Y,der(3)t(1;3)(q12;q29),der(4)t(4;?7)(p16;q22),add(6)(q2?7),t(8;13)(q24;q14),-13,add(16)(p13)add(17)(p13)[13]/46,XY[4]	IgAk	Dead	4	4
	604	55	M	NSU		IgGl	Dead	21	21
	1148	40	M	Abnormal	49,XY,+3,t(5;7)(q15;q34),add(6)(p23),+del(6)(q22q26),add(10)(p11),-13,-14,der(15)t(15;17)(p11;q21),-17,-18,-18,+19,-22,+der(?)t(?;18)(;?q11),+3~4mar[7]/46,XY[88]	IgGl	Dead	40	40
	342	69	M	Abnormal	42~43,X,-Y,+dic(1;2)(p11;q15),t(2;3)(q21;p13),del(5(p14),der(6)del(6)(q13q25)t(6;8)(p25;q23),-8,-13,-14,dic(18;22)(p11;p11)[cp13]	k only	Dead	3	3
	374	51	F	Abnormal	44,X,-X,+dic(1;10)(p13;?;p11),der(2)t(2;6)(p23;p12),+7,+8,dic(8;10)(p11;p11),+9,dic(9;11)(q10;q25),+10,-13,-14,-22[2]/43,idem,-8[5]/42,idem,-7,-8[8]/46,XX[29]	IgGl	Dead	2	92
	1875	51	F	Abnormal	43,X,-X,+1,dic(1;19)(p10;q13.43),dic(8;20)(p10;q10),-13,rea(14)/46,XX[102]	IgAl	Alive	34	34
	52	66	M	Abnormal	>>46,XX,?del(13)(q14q22),?del(11)(q13),inc[3]/46,XX[87]	IgAk	Dead	3	3
	665	49	M	Abnormal	42,X,-Y,del(1)(p11p31),add(5)(q13),del(6)(q23q27),t(9;12)(q32;q1?5),dic(9;?)(q34;?),add(12)(p1?1),-13,t(13;20)(p11;q13),-14,add(16)(q24),add(17)(p12),del(18)(p11),-21,-22,add(22)(p11),+mar[4]/41,idem,-der(5),-del(18),+19[2]/46,XY[11]	IgG	Dead	15	15
	1172	67	M	Abnormal	42,X,-Y,add(5)(q1?3),der(7)t(7;12)(p22;q15),-12,-13,add(16)(p13),-18,-22,+mar[2]/42,idem,t(1;10)(p2;q24),del(8)(q21q24)[1]/46,XY[62]	IgAk	Dead	41	41
	2458	65	F	Abnormal	43~44,X,-X,add(5)(q31),der(5)t(1;5)(q12;q35),der(8;14)(q10;q10),add(8)(q24),+9[2],der(12)t(1;12)(q12;p13),-13,del(18)(q21)[cp32]	IgGk	Dead	4	4
	756	54	F	Abnormal	43,XX,+1,dic(1;11)(p13;p15),dic(1;19)(p?21;p13),add(5)(q15),?r(8)(p23q24),der(9)t(1;9)(p31;q12),-12,-13,-14,add(15)(q26),+mar[6]/42,XX,+1,dic(1;11)(p13;p15),+dic(1;21)(p11;p11),add(6)(q13),add(7)(q36),dicr(8;12)(p23q24;p1q24),der(9)t(1;9)(p31;q12),-13,-14,add(15)(q26)[4]/46,XX[31]	IgG	Dead	9	9

Genetic group	RegID	Age	Gender	CC	Karyotype	PP	Status	FU from analysis	FU from diagnosis
t(14;16)									
	551	57	F	Abnormal	45,XX,t(3;12)(q27;q13),der(12)t(1;12)(q21;q22),-13,t(14;22)(q32;q11),der(16)t(1;16)?(q21;q22)[3]/45,idem,t(5;20)(q33;q13.3),t(3;14)(q13;q31)t(14;22)(q32;q11)[12][14]/46,XX[2]	IgGk	Dead	19	19
	1336	58	M	Abnormal	43,X,-Y,trp(1)?(1pter->1q21::1q32->1q21::1q21->1q32::1q21->1qter),del(3)(p21.31-p24),der(6)del(6)(q15;q22.1)dup(6)(p11.2p23),t(6;19)(p21;p13),del(11)(q13.2q13.4),-13,t(14;16)(q32;q23),-22,der(22)t(1;22)(q12;p13)[43]/46,XY[2]	IgAl	Dead	6	6
	309	49	F	Normal		IgA	Dead	12	12
	2068	67	M	NSU		IgGl	Dead	25	25
	954	75	F	NSU		IgGl	Dead	6	67
	1798	70	F	NSU		Unknown	Unknown		
	2125	61	F	Abnormal	44,X,-X,del(1)(p13p22),-13,del(14)(q22q32),t(14;16)(q32;q23)[16]/44,idem,?t(15;16)(q22;p13)[2]/46,XX[55]	IgAl	Alive	37	37
	282	42	F	Abnormal	75~81,XX,-X,-X,dic(1;15)(q10;q10)x2,dupdic(1)(p11q21)x2,-2,del(5)(q22q33)x2,del(6)(q13q25),del(6)(q25q273),add(7)(p15)x2,-11,-11,-13,-13,add(13)(q32),t(14;16)(q32;q23)x2,-16,-16,-17,-21,add(21)(p11),-22,-22,+2~6mar[cp5]/46,XX[110]	l only	Alive	84	84
HRD									
	297	67	M	Normal		IgA	Alive	56	56
	506	59	F	Abnormal	55,XX,+5,+7,+7,+9,+9,+11,-13,+15,-16,+19,+21,+21,+mar[7][ab11]/46,XX[11]	IgG	Alive	59	59
	375	79	F	Abnormal	51~54,X,?add(X)(q22),der(1;11)(q10;q10),dic(3;?)(q13;?),add(4)(p15),add(4)(q21),?dup(5)(q31q35),+7,+9,add(10)(q22),+11,?del(12)(q24),+add(19)(p13),+21,+1~4mar[cp6]/46,XX[12]	IgGk	Dead	2	2
	824	80	M	Abnormal	55,XY,+3,+5,+7,+9,+11,+15,+15,dic(15;17)(q26;p11),dic(15;17)(q26;p11)del(17)(q12q21),+19,+19,+?21,+mar[cp3]/46,XY[7]	IgGk	Dead	21	21
	1512	74	F	NSU		k only	Dead	34	34
	491	48	M	NSU		IgGk	Dead	20	29
	314	74	M	Abnormal	52,XY,+1,der(1;16)(q10;q12),+5,+7,del(8)(q24),+9,+11,t(11;12)(q13;p13),-13,der(14)t(7;14)(q34;q32),+15,ins(15;14)(q26;q32),der(17)t(17;15;8)(q23;q?;q24),+18,+19,der(19)t(15;19)(q?;p13),+21,-22[27] /52,idem,der(12)t(7;12)(?q34;q15),der(14)t(7;14)t(7;12) [2]/46,XY[1]	IgA	Dead	18	18
	830	55	F	Normal		IgGk	Alive	63	63
	883	60	M	Normal		IgGk	Alive	61	61

Genetic group	RegID	Age	Gender	CC	Karyotype	PP	Status	FU from analysis	FU from diagnosis
	2218	44	M	Abnormal	55,XY,+3,+5,+7,+8,+9,+11,+15,+19,+21[4]/46,XY[123]	IgGl	Alive	36	36
	989	67	M	NSU		IgG	Alive	4	4
	1776	75	M	Abnormal	48~50,X,-Y,+3,del(5)(q2?3q2?5),del(8)(p1?2),del(9)(p13p21),+11,add(13)(p11),-14,+15,+18,+19[cp3]/46,XY[41]	IgAl	Dead	4	62
	1213	65	M	Abnormal	48,XY,der(2)t(2 ;6)(q3 ?3 ;?q25),+5,del(5)(q11q31),der(5)t(5 ;9)(q31 ;?),der(6)t(X ;6)(?q22 ;q ?15)x2,der(8)t(8 ;16)(q24 ;?p12),der(12)t(1 ;12)(q12 ;p13),-13,der(14)t(8 ;14)(q24 ;q32),+15,der(16)t(6 ;16)(?q11 ;p11),+19,der(21)t(6 ;21)(p21 ;q22)[44]/46,XY[43]	IgAk	Dead	0	0
t(11;14)									
	3325	82	F	Abnormal	46~48,XX,der(1)add(1)(q4?2)del(1)(p22p36),+dic(3;6)(p11;q11),-6,der(7)t(7;14)(p22;q1)t(11;14)(q13;q32),-14,-14,add(15)(p1),-16,+19,+mar1,+mar2,+mar3,+mar4,+dm[cp5]/87~95,idemx2,-13,-13,-18,-18,+dm[cp2]	Unknown	Dead	Unknown	Unknown
	1524	73	F	Abnormal	41,-X,der(X)t(X ;1)(q13 ;q12),+1,dic(1 ;13)(p12 ;p11), ?i(4)(p12) or add(4)(p ?),der(5 ;15)(p10 ;q10),der(6)t(6 ;11)(q12 ;q13),+der(6)t(6 ;17)(q13 ;q11),t(11 ;14)(q13 ;q32),-12,-13,add(16)(q12),-17,-22[9]/44,idem,+ ?20,+ ?21,+22[1] /46,XX[57]	IgAl	Dead	20	20
	1300	61	F	Normal			Dead	12	12
	504	47	F	NSU		IgGk + free k	Dead	6	6
	308	57	F	Abnormal	44,X,-X,add(1)(p13),der(5)t(5 ;12)(q31 ;q13),t(11 ;14)(q13 ;q32),-12, ?der(13)t(1 ;13)(p13 ;q14)[9]	k only	Alive	57	57
	2993	74	F	Abnormal	44~45,X,-X,add(3)(q2),del(5)(q3q3),add(6)(q2),del(8)(p1),add(9)(q3?4),t(11;14)(q13;q32),del(12)(p11p13),-13,+mar[cp6]/46,XX[31]	IgGl	Dead	13	
	932*	62	F	Normal		IgA	Alive	4	4
	2906	65	M	Failed		IgGk	Alive	26	26
t(14;20)									
	2314	52	F	Abnormal	87,XX,-X,-X,del(1)(p1p3?2)x2,t(1;8)(p1;q22)x2,del(2)(q3?1q3?3)x2,inv(2)(p1?3q3?7)x2,der(3;6)(q10;p10)x2,+3,+3,-13,-13,t(14;20)(q32;q11)x2,-16,-20,+mar[4]/46,XX[16]	IgGl	Dead	26	26
	1890	59	F	Abnormal	46,XX,t(2;8)(p11;q24),t(14;20)(q32;q12)[13]	IgGk	Dead	45	45

Genetic group	RegID	Age	Gender	CC	Karyotype	PP	Status	FU from analysis	FU from diagnosis
nonHRD unid IgHr/ no IgHr									
	3004	76	M	Abnormal	43~45,XY,t(2;16)(p13;q1),add(3)(p25),t(4;?10)(q3?1;q11),del(5)(q3?3;q3?5),der(12;17)(q10;q10),add(14)(q32),?del(14)(q1q2?4),del(20)(q11),-22,+mar[cp2]/46,XY[57]	IgAk	Alive	29	28
	1581	55	M	Normal		IgAl	Alive	43	43
	619	86	F	Abnormal	43,X,-X,+1,add(1)(q21),dic(1;21)(p13;p11),dic(1;22)(p13;p11),add(2)(q37),+9,-13,der(16)t(1;16)(q21;q13),add(17)(q25),-22[3]/46,XX[102]	IgGk	Dead	25	25
	1037	56	M	Abnormal	47,XY,dicdup(1;12)(1pter->q42::1q21->1q32::12q11->12qter),add(3)(q21),+7,add(7)(p22),der(7)t(7;15)(p11;q11),-8,add(10)(p11),+11,add(11)(p11),t(11;19)(q13;q13),-13,add(13)(p11),der(14)t(8;14)(q24;q32),-18,+19,add(20)(q13),?-22,+3mar[3]/46,XY[15]	IgGk	Alive	35	35
	666	68	M	Abnormal	47,XY,add(5)(q35),+6,?del(6)(q23q25),+9,+11,-13,idic(15)(p13),+19,-20,-22[cp6]/46,XY[53]	IgGl	Alive	43	43

(RegID, patient identification; CC, conventional cytogenetics; PP, paraprotein level; FU, follow-up; NSU, not set up; nonHRD, non-hyperdiploid; unid, unidentified partner; IgHr, *IgH* rearrangement)

Appendix 8: Description of array CGH results for all the patient groups

Patient ID	Diagnosis	Genetic group	CNA by array CGH 'Dim' and 'Enh' describe loss and gain respectively, with the genomic position of the abnormality shown in brackets after the chromosome; Dim X2 = HD. Trisomy, tetrasomy and monosomy have additional breakpoint information. CNV are in blue.
3318	**MGUS**	**t(4;14)**	Dim(1)(82.91[1p31.1]-142.72[1p11.1]); Enh(1)(142.72[1q12]-246.84[1qter]); Dim(2)(0.02[2pter]-13.86[2p24.3]); Dim(2)(14.98[2p24.3]-15.18[2p24.3]); Dim(2)(16.43[2p24.3]-20.15[2p24.1]); Enh(2)(20.71[2p24.1]-20.74[2p24.1]); Enh(2)(42.84[2p21]-42.87[2p21]); Dim X2(2)(88.93[2p11.2]-89.15[2p11.2]); Dim(2)(141.52[2q22.1]-141.91[2q22.1]); Dim(3)(23.31[3p24.3]-23.52[3p24.3]); Enh(3)(48.58[3p21.31]-48.68[3p21.31]); Dim(4)(0.04[4pter]-38.43[4p14]); Dim(4)(69.06[4q13.2]-69.17[4q13.2]); Dim(4)(124.96[4q28.1]-125.09[4q28.1]); Enh(5)(0.08[5pter]-24.27[5p14.2]); Enh(6)(0.1[6pter]-7.94[6p24.3]); Dim(6)(142.42[6q24.1]-170.17[6qter]); Dim(7)(38.28[7p14.1]-38.32[7p14.1]); Dim(8)(0.06[8pter]-34.8[8p12]); Enh(10)(0.12[10pter]-24.36[10p12.1]); Enh(10)(46.37[10q11.21]-46.57[10q11.22]); Dim X2(12)(9.53[12p13.31]-9.55[12p13.31]); Dim(12)(99.38[12q23.1]-132.13[12qter]); Monosomy(13)(18.07-113.58); Dim(14)(60.57[14q23.1]-81.18[14q31.1]); Enh(14)(105.08[14q32.33]-105.28[14q32.33]); Dim(14)(105.33[14q32.33]-106.16[41q32.33]); Dim(15)(54.18[15q21.3]-54.31[15q21.3]); Dim(15)(68.92[15q23]-68.97[15q23]); Dim(16)(33.88[16p11.2]-45.02[16p11.2]); Dim(17)(0.03[17pter]-40.53[17q21.31]); Dim(17)(54.65[17q22]-78.65[17qter]); Dim(18)(0.0[18pter]-10.69[18p11.22]); Dim(18)(62.7[18q22.1]-75.59[18qter]); Enh(19)(0.06[19pter]-19.72[19p12]); Dim X2(22)(21.39[22q11.22]-21.58[22q11.22]); Enh(22)(22.61[22q11.23]-22.73[22q11.23]); Enh(X)(127.81[Xq25]-154.49[Xqter])
2664	**MGUS**	**t(4;14)**	Enh(1)(142.72[1q12]-245.59[1qter]); Dim X2(1)(150.82[1q21.3]-150.85[1q21.3]); Dim X2(1)(246.79[1q44]-246.86[1q44]); Dim(2)(88.94[2p11.2]-89.03[2p11.2]); Dim(3)(164.0[3q26.1]-164.1[3q26.1]); Dim X2(4)(69.06[4q13.2]-69.17[4q13.2]); Dim X2(6)(32.6[6p21.32]-32.63[6p21.32]); Dim X2(8)(39.36[8p11.22]-39.51[8p11.22]); Enh(9)(70.17[9q12]-140.04[9qter]); Dim X2(12)(9.53[12p13.31]-9.55[12p13.31]); Monosomy(13)(18.07-113.96); Dim(14)(19.27[14q11.2]-19.49[14q11.2]); Dim(14)(105.31[14q32.33]-105.62[14q32.33]); Dim(18)(67.67[18q22.3]-75.9[18qter]); Enh(19)(0.06[19pter]-32.55[19p12])
2715	**MGUS**	**t(4;14)**	Dim(1)(16.77[1p36.13]-17.03[1p36.13]); Enh(1)(141.47[1q12]-245.43[1qter]); Dim(2)(89.0[2p11.2]-89.32[2p11.2]); Dim(4)(1.85[4p16.3]-1.87[4p16.3]); Dim(4)(70.35[4q13.2]-70.44[4q13.2]); Dim(5)(172.24[5q35.1]-172.42[5q35.2]); Dim(8)(7.04[8p23.1]-8.14[8p23.1]); Enh(8)(39.36[8p11.22]-39.5[8p11.22]); Dim(9)(79.37[9q21.13]-79.52[9q21.13]); Monosomy(13)(18.07-114.12); Dim X2(13)(66.24[13q21.32]-66.37[13q21.32]); Enh(14)(21.44[14q11.2]-22.03[14q11.2]); Dim(14)(105.34[14q32.33]-105.85[14q32.33]); Enh(15)(18.74[15q11.2]-20.22[15q11.2]); Dim(17)(41.55[17q21.31]-42.05[17q21.31]); Monosomy(21)(9.9-46.91); Monosomy(22)(14.5-49.51); Monosomy(X)(2.69-154.49)
2849	**SMM**	**t(4;14)**	Enh(1)(141.47[1q12]-245.43[1qter]); Dim(2)(89.01[2p11.2]-91.04[2p11.2]); Dim(6)(89.88[6q15]-89.93[6q15]); Dim(7)(3.03[7p22.2]-12.47[7p21.3]); Dim(8)(0.06[8pter]-39.33[8p11.22]); Monosomy(13)(18.07-114.12); Enh(14)(105.35[14q32.33]-105.42[14q32.33]); Monosomy(22)(14.5-48.91); Enh(X)(136.99[Xq26.3]-154.49[Xqter])
508	**SMM**	**t(4;14)**	Dim(1)(145.82[1q21.1]-146.01[1q21.1]); Dim(2)(88.99[2p11.2]-89.27[2p11.2]); Dim(2)(242.64[2q37.3]-242.74[2q37.3]); Trisomy(3)(0.04-199.38); Dim(4)(0.06[4pter]-1.85[4p16.3]); Enh(4)(1.9[4p16.3]-2.06[4p16.3]); Dim(4)(91.53[4q22.1]-91.62[4q22.1]); Dim(6)(162.67[6q26]-162.9[6q26]); Trisomy(6)(0.1-170.86); Trisomy(7)(0.14-158.62); Dim(8)(39.36[8p11.21]-39.51[8p11.21]); Trisomy(9)(0.15-138.4); Dim(9)(1.41[9p24.3]-1.56[9p24.3]); Dim(10)(67.77[10q21.3]-68.03[10q21.3]); Trisomy(11)(0.18-134.43); Enh(14)(105.57[14q32.33]-106.35[14q32.33]) Enh(15)(18.36-100.28); Trisomy(18)(0.0-76.11); Trisomy(19)(0.06-63.78); Enh(22)(22.65[22q11.23]-22.73[2q11.23])
259	**SMM**	**t(4;14)**	Dim(1)(145.82[1q21.1/.2]-146.47[1q21.1/.2]); Dim X2(1)(165.96[1q24.2]-165.99[1q24.2]); Dim(2)(11.19[2p25.1]-26.43[2p23.3]); Dim(2)(89.0[2p11.2]-89.31[2p11.2]); Dim(4)(0.04[4pter]-1.85[4p16.3]); Enh(5)(37.49[5p13.2]-37.5[5p13.2]); Dim(5)(172.59[5q35.1/.2]-172.6[5q35.1/.2]); Dim(6)(32.57[6p21.32]-32.63[6p21.32]); Dim(8)(6.93[8p23.1]-7.79[8p23.1]); Enh(8)(39.36[8p11.23]-39.51[8p11.23]); Dim

			X2(10)(134.26[10q26.3]-134.28[10q26.3]); Dim(12)(34.42[12CEP]-132.39[12qter]); Monosomy(13)(18.07-114.12); Monosomy(14)(18.15-105.99); Enh(15)(18.68[15q11.2]-20.25[15q11.2]); Dim(16)(0.03[16pter]-10.97[16p13.13]); Dim(16)(34.06[16p11.2]-34.61[16p11.2]); Dim(16)(45.03[16q12.1]-88.69[16qter]); Dim(19)(47.99[19q13.13]-48.45[19q13.13]); Enh(22)(22.69[22q11.23]-22.73[22q11.23]); Dim(22)(37.68[22q13.1]-37.71[22q13.1])
1836	**SMM**	**t(4;14)**	Enh(1)(141.47[1q12]-245.43[1qter]); Dim(1)(145.82[1q21.1]-146.47[1q21.2]); Dim X2(1)(149.37[1q21.3]-149.4[1q21.3]); DimX2(2)(89.0[2p11.2]-89.2[2p11.2]); Dim(3)(11.73[3p25.3]-12.18[3p25.2]); Enh(3)(164.0[3q26.1]-164.1[3q26.1]); Dim(4)(69.2[4q13.2]-69.31[4q13.2]); Dim(6)(32.56[6q21.32]-32.66[6p21.32]); Enh(6)(121.24[6q22.31]-123.33[6q22.31]); Dim(6)(123.33[6q22.31]-170.94[6qter;); Dim(8)(7.26[8p23.1]-8.12[8p23.1]); Dim X2(8)(39.36[8p11.23]-39.51[8p11.22]); Enh(12)(11.4[12p13.2]-11.44[12p13.2]); Enh(12)(19.27[12p12.3]-19.54[12p12.3]); Enh(12)(50.97[12q13.13]-51.07[12q13.13]); Monosomy(13)(18.07-114.12); Dim X2(14)(105.31[14q32.33]-106.11[14q32.33]); Trisomy(15)(18.36-100.28); Enh(16)(33.21[16p11.2]-33.54[16p11.2]); Dim(16)(54.35[16q12.2]-54.39[16q12.2]); Enh(17)(41.52[17q21.31]-41.71[17q21.31]); Enh(17)(77.42[17q25.3]-77.5[17q25.3]); Trisomy(19)(0.06-63.78); Trisomy(21)(13.33-46.91); Monosomy(22)(14.5-49.51); Monosomy(X)(2.69-154.49)
331	**SMM**	**t(4;14)**	Enh(1)(44.92[1p34.2]-45.0[1p34.2]); Enh(1)(141.47[1q12]-245.33[1qter]); Enh(2)(0.02[2pter]-91.23[2p11.2]); Dim(2)(88.99[2p11.2]-89.32[2p11.2]); Trisomy(3)(0.04[3pter]-199.21[3qter]); Dim(4)(0.06[4pter]-1.85[1p16.3]); Enh(4)(153.93[4q31.3]-153.99[4q31.3]); Dim(4)(91.68[4q22.1]-91.95[4q22.1]); Dim(4)(171.36[4q33]-171.48[4q33]); Dim(1)(39.36[8p11.2]-39.51[8p11.2]); Trisomy(9)(0.15-138.4); Trisomy(10)(0.12-135.4); Enh(11)(64.36[11q13.1]-64.46[11q13.1]); Enh(12)(101.34[12q23.2]-101.4[12q23.2]); Monosomy(13)(18.07-114.12); Monosomy(14)(18.15-106.35); Dim(15)(19.81[15q11.2]-20.08[15q11.2]); Enh(16)(69.41[16q22.2]-69.75[16q22.2]); Enh(17)(9.27[17p13.1]-78.65[17qter]); Enh(19)(2.02[19p13.3]-2.07[19p13.3]); Enh(22)(22.67[22q11.23]-22.72[22q11.23]); Dim(22)(44.87[22q13.31]-44.90[22q13.31])
105	**SMM**	**t(4;14)**	Dim(1)(16.99[1p36.13]-17.02[1p36.13]); Enh(1)(141.47[1q12]-146.01[1qter]); Dim(1)(145.82[1q21.1]-146.01[1q21.1]); Dim(2)(88.99[2p11.2]-89.2[2p11.2]); Dim(4)(91.75[4q22.1]-92.2[4q22.1]); Enh(5)(37.48[5p13.2]-37.52[5p13.2]); Dim(6)(32.56[6p21.32]-32.65[6p21.32]); Enh(7)(38.07[7p14.1]-38.08[7p14.1]); Dim X2(7)(141.41[7q34]-141.44[7q34]); Dim(8)(39.36[8p11.22]-39.49[8p11.22]); Dim(9)(8.99[9p24.1]-9.17[9p24.1]); Dim(11)(99.28[11q22.1]-99.52[11q22.1]); Monosomy(13)(18.07-114.12); Dim(14)(105.31[14q32.33]-105.93[14q32.33]); Dim(15)(32.51[15q14]-32.63[15q14]); Dim(16)(31.86[16p11.2]-34.1[16p11.2]); Enh(16)(69.41[16q22.1/.2]-69.74); Enh(17)(77.44[17q25.3]-77.52); Dim(19)(3.48[19p13.3]-3.49); Dim(19)(47.99[19q13.31]-48.24[19q13.31]); Dim(22)(39.27[22q13.2]-49.47[22qter]); Dim(X)(88.16[Xq21.31]-92.1[Xq21.31]); Enh(X)(141.59[Xq27.2]-154.49[Xqter])
1525	**SMM**	**t(4;14)**	Dim(1)(35.11[1p35.1]-35.48[1p35.1]); Dim(1)(70.29[1p31.1]-93.76[1p21.3]); Dim(2)(88.98[2p11.2]-89.31[2p11.2]); Dim(7)(106.53[7q22.3]-106.59[7q22.3]); Dim(8)(0.06[8pter]-32.99[8p12]); Dim(8)(39.36[8p11.22]-39.48[8p11.22]); Dim(12)(11.4[12p13.2]-11.4[12p13.2]); Dim(13)(18.07[13pter]-110.63[13q33.4]); Dim(14)(19.27[14q11.2]-19.49[14q11.2]); Dim(14)(56.74[14q23.1]-87.19[14q31.1]); Dim(14)(105.33[14q32.33]-106.14[14q32.33]); Enh(15)(19.82[15q11.2]-20.31[15q11.2]); Dim(15)(32.51[15q14]-32.61[15q14]); Dim(18)(0.0[18pter]-14.79[18p11.1]); Dimx2(22)(21.09[22q11.22]-21.57[22q11.22]); Enh(22)(22.68[22q11.23]-22.73[22q11.23]); Dim(22)(27.43[22q12.1]-28.01[22q12.2]); Ampl(22)(35.16[22q12.3]-38.95[22q13.2]); Enh(X)(71.27[Xq13.1]-154.49[Xqter])
837	**MGUS**	**t(14;16)**	Enh(1)(141.47[1q12]-245.33[1qter]); Dim(2)(88.98[2p11.2]-89.2[2p11.2]); Enh(2)(173.25[2q31.1]-173.48[2q31.1]); Enh(3)(164.0[3q26.1]-164.1[3q26.1]); Enh(4)(38.57[4p14]-38.78[4p14]); Enh(6)(7.84[6p24.3]-8.07[6p24.3]); Enh(6)(109.19[6q21]-109.3[6q21]); Enh(6)(168.16[6q27]-168.39[6q27]); Enh(8)(39.36[8p11.21]-39.51[8p11.21]); Dim(9)(0.15[9pter]-301.34[9p21.1]); Enh(9)(32.24[9p21.1]-38.61[9p13.2]); Dim(10)(45.49[10q11.21]-47.16[10q11.21]); Monosomy(13)(18.07-114.12); Trisomy(14)(18.15-106.35); Dim(14)(105.34[14q32.33]-105.43[14q32.33]); Enh(15)(18.66[15q11.2]-19.43[15q11.2]); Enh(15)(63.8[15q22.31]-64.01[15q22.31]); Enh(16)(55.43[16q12.2]-55.58[16q12.2]); Enh(17)(41.52[17q21.31]-41.71[17q21.31]); Dim(22)(15.43[22q11]-35.1[22q12.3]); Dim X2(22)(21.43[22q11.2]-21.57[22q11.2]); Dim X2(22)(23.99[22q11.23]-24.23[22q11.23]); Enh(X)(98.65[Xq22.1]-154.35[Xqter])
582	**SMM**	**t(14;16)**	Enh(1)(16.78[1p36.13]-17.02[1p36.13]); Dim(1)(149.37[1q21.3]-149.4[1q21.3]); Dim(2)(89.0[2p11.2]-89.15[2p11.2]); Trisomy(3)(0.04-199.38); Enh(4)(0.04-191.31); Enh(6)(32.56[6p21.32]-32.65[6p21.32]); Trisomy(7)(0.01-158.62); Enh(8)(39.36[8p11.22]-39.51[8p11.22]);

			Dim(8)(140.84[8q24.3]-141.02[8q24.3]); Trisomy(9)(0.15-138.4); Dim(10)(46.4[10q11.22]-47.74[10q11.22]); Trisomy(11)(0.18-134.43); Trisomy(13)(18.07-114.12); Enh(14)(18.54[14q11]-34.94[14q13.2]); Dim(14)(93.51[14q32.13]-94.26[14q32.13]); Dim(14)(102.3[14q32.32]-102.63[14q32.32]); Dim X2(14)(102.4[14q32.32]-102.52[14q32.32]); Dim(14)(1051.14[14q32.33]-105.46[14q32.33]); Enh(14)(105.97[14q32.33]-106.31[14q32.33]); Enh(15)(18.66[15q11.2]-20.22[15q11.2]); Dim(16)(0.51[16p13.3]-0.54[16p13.3]); Enh(16)(28.49[16p11.2]-30.85[16p11.2]); Enh(16)(32.11[16p11.2]-33.54[16p11.2]); Dim(16)(54.35[16q12.2]-54.39[16q12.2]); Dim(16)(77.34[16q23.1]-77.52[16q23.1]); Trisomy(17)(0.03-78.65); Trisomy(19)(0.06-63.78); Enh(22)(17.27[22q11.21]-17.33[22q11.21]); Dim(22)(20.6[22q11.22]-20.92[22q11.22]); Monosomy(X)(2.69-154.49)
2198	**SMM**	**t(14;16)**	Dim(2)(88.99[2p11.2]-89.14[2p11.2]); Enh(2)(96.35[2q11.2]-97.03[2q11.2]); Dim(4)(69.04[4q13.2]-70.53[4q13.2]); Enh(8)(39.36[8p11.21]-39.51[8p11.21]); Enh(9)(68.15[9q12]-138.4[9qter]); Monosomy(13)(18.07-114.12); Enh(14)(105.02[14q32.33]-105.33[14q32.33]); Dim(14)(105.34[14q32.33]-105.41[14q32.33]); Dim(14)(105.96[14q32.33]-106.0[14q32.33]); Enh(14)(106.13[14q32.33]-106.35[14q32.33]); Dim(16)(77.19[16q23.1]-86.1[16q24.2]); Enh(19)(0.06[19pter]-19.75[19p11]); Monosomy(22)(14.5-48.87); Monosomy(X)(2.69-154.49)
1494	**MGUS**	**t(14;16)**	Enh(1)(16.07[1p36.13]-16.14[1p36.13]); Enh(1)(103.82[1p21.1]-103.88[1p21.1]); Dim(2)(88.98[2p11.2]-89.31[2p11.2]); Dim(2)(230.92[2q37.1]-231.93[2q37.1]); Dim(3)(164.0[3q26.1]-164.1[3q26.1]); Dim(5)(44.22[5p12]-46.01[5p12]); Dim(5)(68.37[5q13.1]-70.78[5q13.1]); Dim(7)(75.86[7q11.23]-76.23[7q11.23]); Dim(7)(117.45[7q31.2]-147.29[7q36.1]); Enh(8)(142.3[8q24.3]-145.91[8q24.3]); Dim(12)(110.8[12q24.12]-111.04[12q24.12]); Monosomy(13)(18.07-114.12); Enh(14)(18.86[14q11.2]-19.49[14q11.2]); Enh(14)(21.53[14q11.2]-22.11[14q11.2]); Dim(14)(30.23[14q12]-31.15[14q12]); Enh(14)(100.07[14q32.13]-101.31[14q32.13]); Enh(14)(103.62[14q32.33]-105.31[14q32.33]); Dim(14)(105.34[14q32.33]-105.9[14q32.33]); Dim(15)(18.84[15q11.2]-20.08[15q11.2]); Enh(15)(76.84[15q25.1]-76.89[15q25.1]); Enh(16)(31.96[16p11.2]-33.54[16p11.2]); Enh(22)(18.08[22q11.21]-19.03[22q11.21]); Dim(22)(21.08[22q11.22]-21.56[22q11.22]); Enh(X)(6.31[Xp22.31]-7.95[Xp22.31]); Enh(X)(152.07[Xq28]-153.48[Xq28])
1189	**MGUS**	**t(14;16)**	Dim(2)(89.01[2p11.2]-89.2[2p11.2]); Enh(11)(99.39[11q22.1]-131.77[11q25]); Dim(14)(105.52[14q32.33]-106.28[14q32.33]); Monosomy(X)(3.26-154.49)
1073	**SMM**	**t(14;16)**	Enh(1)(142.61[1q12]-245.43[1qter]); Dim(2)(88.98[2p11.2]-89.11[2p11.2]); Enh(3)(185.44[3q27.2]-186.0[3q27.2]); Dim(5)(69.27[5q13.2]-70.72[5q13.2]); Dim(5)(171.28[5q35.1]-171.4[5q35.1]); Dim(6)(109.37[6q21]-170.94[6qter]); Dim(8)(0.06[8pter]-37.6[8p12]); Enh(8)(39.36[8p11.22]-39.5[8p11.22]); Dim(11)(132.82[11q25]-133.38[11q25]); Monosomy(13)(18.07-114.12); Enh(14)(18.54[14q11.2]-19.52[14q11.2]); Dim(14)(23.99[14q12]-91.7[14q32.12]); Dim(14)(105.35[14q32.33]-105.74[14q32.33]); Enh(15)(18.66[15q11.2]-20.06[15q11.2]); Dim(16)(69.74[16q22.2]-88.69[16qter]); Dim(17)(41.55[17q21.31]-41.98[17q21.31]); Trisomy(19)(0.06-63.78); Dim(22)(15.68[22q11.21]-35.88[22q13.1]); Dim X2(22)(22.7[22q11.23]-22.71[22q11.23]); Monosomy(X)(2.69-154.49)
417	**MGUS**	**t(14;20)**	Dim(1)(153.85[1q22]-153.99[1q22]); Enh(3)(164.05[3q26.1]-164.11[3q26.1]); Dim(8)(39.36[8p11.22]-39.51[8p11.22]); Monosomy(13)(18.07-114.12); Dim(14)(18.19[14q11.2]-19.5[14q11.2]); Dim(14)(105.35[14q32.33]-106.35[14qter]); DimX2(14)(105.54[14q32.33]-105.58[14q32.33]); Dim(15)(19.39[15q11.2]-20.25[15q11.2]); Dim(20)(0.01[20pter]-38.01[20q12]); Monosomy(22)(14.5-49.51)
866	**SMM**	**t(14;20)**	Dim(1)(12.8[1p36.21]-12.85[1p36.21]); Dim(1)(16.79[1p36.13]-17.02[1p36.13]); Dim(2)(88.99[2p11.2]-89.28[2p11.2]); Dim(2)(213.49[2q34]-213.56[2q34]); Dim(2)(242.64[2q37.3]-242.67[2q37.3]); Enh(4)(69.2[4q13.2]-69.31[4q13.2]); Dim X2(5)(140.2[5q31.2]-140.22[5q31.3]); Dim(6)(37.92[6p21.2]-38.56[6p21.2]); Dim(8)(7.26[8p23.1]-8.12[8p23.1]); Enh(8)(39.36[8p11.22]-39.51[8p11.22]); Enh(10)(1.16[10p15.3]-1.26[10p15.3]); Dim(10)(46.4[10q11.22]-47.13[10q11.22]); Monosomy(13)(18.07-114.12); Dim X2(14)(105.34[14q32.33]-105.79[14q32.33]); Enh(15)(18.43[15q11.2]-19.28[15q11.2]); Enh(16)(28.74[16p11.2]-29.5[16p11.2]); Monosomy(22)(14.5-18.08)
976	**MGUS**	**t(14;20)**	Dim(1)(193.44[1q31.3]-193.53[1q31.3]); Dim(2)(89.0[2p11.2]-89.15[2p11.2]); Dim(2)(242.44[2q37.3]-242.73[2q37.3]); Enh(3)(164.0[3q26.1]-164.1[3q26.1]); Dim(3)(193.48[3q29]-193.57[3q29]); Dim(4)(70.03[4q13.2]-70.38[4q13.2]); Enh(6)(29.96[6p21.33]-30.01[6p21.33]); Enh(7)(38.07[7p14.1]-38.08[7p14.1]); Dim(8)(39.36[8p11.22]-39.49[8p11.23]); Dim X2(12)(9.53[12p13.31]-9.59[12p13.31]); Monosomy(13)(18.07-114.12); Dim X2(14)(105.33[14q32.33]-106.12[14q32.33]); Dim(15)(18.72[15q11.2]-20.22[15q11.2]); Enh(22)(22.68[22q11.23]-22.72[22q11.23])
367	**MGUS**	**t(14;20)**	Enh(1)(142.72[1q12]-246.36[1qter]); Dim X2(1)(193.47[1q31.3]-193.53[1q31.3]); Dim(2)(88.96[2p11.2]-89.31[2p11.2]); Dim(4)(145.18[4q31.21]-

			145.42[4q31.21]); Enh(5)(0.74[5p15.33]-0.86[5p15.33]); Dim(6)(32.61[6p21.32]-32.63[6p21.32]); Dim(8)(7.04[8p23.1]-8.13[8p23.1]); Enh(8)(39.36[8p11.22]-39.51[8p11.22]); Dim(12)(82.97[12q21.31]-92.99[12q22]); Dim(12)(98.65[12q23.1]-100.93[12q23.2]); Dim(12)(105.02[12q23.3]-107.47[12q23.3]); Dim(12)(122.65[12q24.31]-123.23[12q24.31]); Dim(12)(126.64[12q24.32]-132.2[12q24.33]); Dim(13)(18.07[13q11]-110.27[13q34]); Enh(14)(21.5[14q11.2]-22.2[14q11.2]); Dim X2(14)(105.4[14q32.33]-106.12[14q32.33]); Dim(16)(45.06[16q11.2]-88.69[16qter]); Enh(20)(1.49[20p13]-1.59[20p13]); Dim(21)(13.38[21q11.2]-13.6[21q11.2]); Dim(22)(21.5[22q11.22]-21.57[22q11.22])
698	**MGUS**	**nonHRD**	Dim(1)(72.49[1p31.1]-102.25[1p21.1]); Enh(1)(141.47[1q12]-145.43[1qter]); Enh(2)(29.21[2p23.2]-81.69[2p12]); Dim(2)(89.01[2p11.2]-89.14[2p11.2]); Enh(3)(101.83[3q12.2]-101.92[3q12.2]); Enh(3)(102.08[3q12.2]-199.38[3qter]); Dim(3)(164.02[3q26.1]-164.11[3q26.1]); Enh(5)(172.97[5q35.1]-173.04[5q35.2]); Dim(6)(32.56[6p21.32]-32.74[6p21.32]); Dim(7)(141.22[7q34]-141.25[7q34]); Dim(7)(143.32[7q35]-143.51[7q35]); Dim(8)(6.93[8p23.1]-8.14[8p23.1]); Dim(8)(39.36[8p11.23]-39.51[8p11.22]); Dim(11)(7.77[11p15.4]-7.78[11p15.4]); Enh(12)(7.88[12p13.31]-8.06[12p13.31]); Monosomy(13)(18.07-114.12); Enh(14)(60.45[14q23.1]-64.26[14q23.2]); Dim(14)(64.27[14q23.3]-106.35[14qter]); Dim X2(14)(105.33[14q32.33]-105.63[14q32.33]); Dim(15)(18.81[15q11.2]-20.08[15q11.2]); Dim(20)(13.4[20p12.1]-13.54[20p12.1]); Dim(Y)(2.69-57.37)
1581	**SMM**	**nonHRD, unid *IgH* rearr**	Enh(1)(141.47[1q12]-245.43[1qter]); Dim X2(1)(149.37[1q21.3]-149.4[1q21.3]); Dim(2)(88.98[2p11.2]-89.11[2p11.2]); Enh(2)(91.06[2p11.2]-91.45[2p11.2]); Enh(3)(166.18[3q26.2]-167.91[3q26.2]); Enh(6)(0.1[6pter]-38.96[6p21.2]); Dim X2(6)(32.59[6p21.32]-32.73[6p21.32]); Dim(6)(151.52[6q25.1]-170.94[6qter]); Dim(7)(0.14[7pter]-16.94[7p21.1]); Dim(8)(7.04[8p23.1]-8.14[8p23.1]); Dim(8)(39.36[8p11.22]-39.51[8p11.22]); Dim X2(11)(5.74[11p15.4]-5.76[11p15.4]); Monosomy(13)(18.07[13pter]-114.12[13qter]); Dim(14)(68.33[14q24.1]-105.76[14q32.33]); Dim(15)(32.52[15q14]-32.65[15q14]); Enh(16)(10.61[16p13.13]-11.95[16p13.13]); Enh(16)(32.21[16p11.2]-33.53[16p11.2]); Dim(16)(45.02[16q11.2]-88.69[16qter]); Enh(16)(69.41[16q22.1]-69.75[16q22.2]); Enh(17)(16.12[17p12]-17.56[17p11.2]); Dim(17)(41.52[17q21.31]-41.84[17q21.31]); Enh(17)(41.84[17q21.31]-42.14[17q21.31]); Enh(19)(15.81[19p13.12]-16.89[19p13.11]); Dim(22)(21.06[22q11.22]-21.58[22q11.22]); Dim(22)(37.68[22q13.1]-37.71[22q13.1]); Enh(X)(137.57[Xq27.1]-154.49[Xqter]); Dim(Y)(2.69-57.37)
2326	**MGUS**	**nonHRD**	Dim(4)(69.07[4q13.2]-69.64[4q13.2]); Dim(9)(22.2[9p22.1]-22.42[9p22.1]); Dim(14)(77.62[14q24.3]-87.26[14q31.3]); Dim(14)(105.32[14q32.33]-105.32[14q32.33]); Enh(16)(55.22[16q13]-55.28[16q13])
844	**MGUS**	**t(11;14)**	Dim(1)(16.79[1p36.13]-17.0[1p36.13]); Dim X2(2)(34.61[2p22.3]-34.64[2p22.3]); Dim(2)(88.99[2p11.2]-89.11[2p11.2]); Enh(3)(35.78[3p22.3]-35.9[3p23]); Enh(5)(32.15[5p13.3]-32.2[5p13.3]); Enh(6)(32.56[6p21.32]-32.66[6p21.32]); Enh(6)(168.16[6q27]-168.4[6q27]); Dim X2(8)(39.36[8p11.22]-39.51[8p11.22]); Dim X2(13)(56.66[13q21.1]-56.67[13q21.1]); Dim(14)(73.08[14q24.3]-73.12[14q24.3]); Dim(14)(105.35[14q32.33]-105.42[14q32.33]); Dim X2(14)(105.6[14q32.33]-105.63[14q32.33])
355	**SMM**	**t(6;14)**	Enh(1)(1.14[1p36.33]-1.18[1p36.33]); Dim(1)(16.8[1p36.13]-16.99[1p36.13]); Dim(2)(34.61[2p22.3]-34.64[2p22.3]); Dim(2)(89.0[2p11.2]-89.2[2p11.2]); Enh(3)(164.0[3q26.1]-164.1[3q26.1]); Dim(4)(69.2[4q13.2]-69.31[4q13.2]); Enh(5)(0.74[5p15.33]-0.9[5p15.33]); Dim(6)(29.96[6p22.1]-30.01[6p21.33]); Dim X2(6)(32.57[6p21.32]-32.67[6p21.32]); Dim(8)(7.26[8p23.1]-7.79[8p23.1]); Enh(8)(39.36[8p11.22]-39.51[8p11.22]); Trisomy(9)(0.15-138.4); Trisomy(11)(0.18-134.43); Enh(12)(11.4[12p13.2]-11.43[12p13.2]); Monosomy(13)(18.07-114.12); Enh(14)(18.19[14q11.1]-19.4[14q11.2]); Monosomy(14)(18.15-106.35); Dim X2(14)(105.31[14q32.33]-106.16[14q32.33]); Enh(16)(31.86[16p11.2]-33.54[16p11.2]); Dim(16)(34.69[16q11.2]-88.09[16q24.3]); Dim X2(16)(54.35[16q12.2]-54.38[16q12.2]); Enh(17)(76.89[17q25.3]-76.95[17q25.3]); Enh(17)(77.42[17q25.3]-77.5[17q25.3]); Trisomy(X)(2.69-154.49)
999	**MGUS**	**t(11;14)**	Dim(1)(246.79[1q44]-246.88[1q44]); Dim(4)(69.06[4q13.2]-246.88[4q13.2]); Dim X2(6)(32.56[6p21.32]-32.61[6p21.32]); Dim X2(8)(39.36[8p11.22]-39.51[8p11.22]); Enh(11)(68.8[11q13.2]-133.98[11qter]); Dim X2(12)(9.53[12p13.31]-9.63[12p13.31]); Monosomy(13)(18.07-113.76); Enh(14)(18.62[14q11.1]-19.51[14q11.1]); Enh(15)(18.44[15q11.2]-19.99[15q11.2]) Enh(16)(31.84[16p11.2]-34.61[16p11.2]); Dim(17)(41.58[17q21.31]-41.71[17q21.31]); Enh(22)(22.68[22q11.23]-22.73[22q11.23])
855	**MGUS**	**t(11;14)**	Dim X2(1)(88.94[2p11.2]-89.22[2p11.2]); Enh(5)(0.74[5p15.33]-0.86[5p15.33]); Enh(6)(32.56[6p21.32]-32.66[6p21.32]); Enh(8)(39.37[8p11.22]-39.54[8p11.22]); Enh(10)(46.47[10q11.22]-46.57[10q11.22]); Enh(11)(68.91[11q13.2]-134.32[11qter]); Enh(14)(18.62[14q11.1]-19.54[14q11.2]);

			Dim X2(14)(105.33[14q32.33]-105.82[14q32.33]); Enh(15)(18.72[15q11.2]-20.08[15q11.2]); Dim(22)(20.85[22q11.22]-21.57[22q11.22]); Monosomy(X)(2.71-154.39)
795	**MGUS**	**t(11;14)**	Dim(1)(12.76[1p36.21]-12.84[1p36.21]); Dim(1)(187.6[1q31.1]-187.81[1q31.1]); Dim(2)(35.38[2p22.3]-35.54[2p22.3]); Dim(2)(88.93[2p11.2]-89.09[2p11.2]); Dim X2(3)(164.0[3q26.1]-164.1[3q26.1]); Dim(4)(69.06[4q13.2]-69.17[4q13.2]); Dim X2(7)(141.41[7q34]-141.45[7q34]); Enh(8)(39.36[8p11.22]-39.51[8p11.22]); Enh(11)(0.18[11pter]-77.82[11q14.1]); Dim X2(14)(73.07[14q24.3]-73.09[14q24.3]); Dim(14)(105.33[14q32.33]-105.41[14q32.33]); Enh(15)(18.66[15q11.2]-19.99[15q11.2]); Enh(16)(31.86[16p11.2]-34.06[16p11.2]); Dim X2(22)(22.68[22q11.23]-22.73[22q11.23]
610	**MGUS**	**t(11;14)**	Dim X2(2)(88.92[2p11.2]-89.1[2p11.2]); Enh(5)(32.15[5p13.3]-32.22[5p13.3]); Enh(11)(68.97[11q13.3]-134.2[11qter]); Dim(14)(105.28[14q32.33]-106.06[14q32.33]); Enh(22)(41.23[22q13.2]-41.28[22q13.2]); Monosomy(X)(2.71-154.39)
695	**MGUS**	**t(11;14)**	Dim(4)(69.06[4q13.2]-69.17[4q13.2]); Enh(6)(32.56[6p21.32]-32.67[6p21.32]); Enh(8)(39.36[8p11.22]-39.51[8p11.22]); Dim(11)(5.74[11p15.4]-5.76[11p15.4]); Dim(12)(10.46[12p13.31]-10.49[12p13.31]); Dim(14)(105.25[14q32.33]-105.9[14q32.33]); Dim(16)(0.03[16pter]-10.93[16p13.13]); Dim(16)(45.02[16q11.2]-88.67[16qter]); Dim(20)(19.71[20p11.23]-19.82[20p11.23]); Dim(22)(21.07[22q11.22]-21.58[22q11.22])
1822	**SMM**	**HRD**	Enh(1)(181.83[1q31.1]-195.8[1q32.1]); Enh(1)(245.05[1q44]-245.13[1q44]); Dim(2)(242.63[2q37.3]-242.68[2q37.3]); Trisomy(3)(0.04-199.38); Trisomy(5)(0.01-180.64); Dim(8)(0.53[8p23.3]-0.63[8p23.3]); Enh(8)(2.31[8p23.2]-2.6[8p23.3]); Enh(8)(39.36[8p11.23]-39.51[8p11.23]); Trisomy(9)(0.15-138.4); Dim(10)(46.4[10q11.22]-46.56[10q11.22]); Trisomy(11)(0.18-134.43); Monosomy(13)(18.07-114.12); Monosomy(14)(18.15-106.35); Dim X2(14)(105.34[14q32.33]-105.96[14q32.33]); Tetrasomy(15)(18.36-100.28); Trisomy(19)(0.06-63.78); Trisomy(21)(9.9-46.91); Dim X2(22)(22.68[22q11.23]-22.72[22q11.23]); Monosomy(X)(2.69-154.49)
865	**MGUS**	**HRD**	Enh(1)(149.37[1q21.3]-149.4[1q21.3]); Dim(2)(88.99[2p11.2]-89.27[2p11.2]); Trisomy(3)(0.04-199.29); Dim X2(3)(46.77[3p21.31]-46.83[3p21.31]); Dim X2(4)(69.2[4q13.2]-69.31[4q13.3]); Trisomy(5)(0.08-180.64); Trisomy(6)(0.1-170.94); Trisomy(7)(0.14-158.62); Enh(8)(39.36[8p11.22]-39.51[8p11.22]); Enh(9)(21.16[9p21.3]-21.21[9p21.3]); Trisomy(11)(0.18-134.43); Dim(11)(5.74[11p15.4]-5.76[11p15.4]); Dim(11)(7.77[11p15.4]-7.78[11p15.4]); Monosomy(13)(18.07-1141.12); Dim X2(13)(56.66[13q21.1]-56.67[13q21.1]); Dim(14)(105.34[14q32.33]-105.88[14q32.33]); Trisomy(15)(18.36-100.28); Trisomy(17)(0.03-78.65); Trisomy(19)(0.06-63.78); Enh(X)(152.21[Xq28]-152.62[Xq28])
528	**MGUS**	**HRD**	Dim X2(1)(25.35[1p36.11]-25.41[1p36.11]); Enh(1)(142.57[1q12]-245.43[1qter]); Dim(1)(149.37[1q21.3]-149.4[1q21.3]); Dim(1)(245.05[1q44]-245.13[1q44]); Dim(2)(89.0[2p11.2]-89.11[2p11.2]); Dim(4)(69.2[4q13.2]-69.82[4q13.2]); Dim(4)(70.33[4q13.2]-70.53[4q13.2]); Trisomy(5)(0.08-180.64); Trisomy(6)(0.1-170.94); Trisomy(7)(0.14-158.62); Enh(8)(39.36[8p11.22]-39.51[8p11.22]); Dim(8)(125.79[8q24.13]-128.61[8q24.13]); Trisomy(9)(0.15-138.4); Monosomy(13)(18.07-114.12); Dim(14)(18.54[14q11.1]-18.62[14q11.1]); Dim(14)(105.14[14q32.33]-105.58[14q32.33]); Trisomy(15)(20.31-100.28); Trisomy(19)(0.06-63.78); Trisomy(21)(14.31-46.91); Enh(22)(36.38[22q13.1]-36.43[22q13.1]); Monosomy(X)(2.69-154.49)
911	**MGUS**	**HRD**	Dim(1)(145.82[1q21.1]-145.99[1q21.1]); Dim(2)(88.99[2p11.2]-89.94[2p11.2]); Trisomy(3)(0.04-199.38); Dimx2(3)(164.0[3q26.1]-164.1[3q26.1]); Trisomy(5)(0.08-180.64); Dim(6)(32.6[6p21.32]-32.63[6p21.32]); Dim X2(6)(79.04[6q14.1]-79.08[6q14.1]); Trisomy(7)(0.14-158.62); Dim(8)(3.91[8p23.2]-6.66[8p23.1]); Dim(8)(39.36[8p11.23]-39.51[8p11.22]); Trisomy(9)(0.15-138.4); Monosomy(13)(18.07-114.12); Enh(14)(18.64[14q11.1]-19.48[14q11.1]); Dim(14)(73.08[14q24.3]-73.11[14q24.3]); Dim(14)(105.34[14q32.33]-105.42[14q32.33]); Dim(14)(105.6[14q32.33]-105.63[14q32.33]); Dim(14)(105.67[14q32.33]-106.35[14q32.33]); Tetrasomy(15)(18.36-100.28); Enh(16)(33.21[16p11.2]-33.54[16p11.2]); Dim(17)(41.53[17q21.31]-42.05[17q21.31]); Tetrasomy(19)(0.06-63.78); Trisomy(21)(14.49-46.91); Dim(22)(20.72[22q11.22]-21.56[22q11.22]); Dim(22)(22.67[22q11.23]-22.72[22q11.23]); Monosomy(X)(2.7-154.49)
403	**SMM**	**HRD**	Trisomy(3)(0.04-199.38); Trisomy(5)(0.08-180.64); Trisomy(7)(0.14-158.62); Trisomy(9)(0.15-138.4); Trisomy(11)(0.18-134.43); Dim(14)(19.27[14q11.2]-19.5[14q11.2]); Dim(14)(103.61[14q32.33]-105.33[14q32.33]); Trisomy(15)(18.36-100.28); Enh(17)(77.39[17q25.3]-77.61[17q25.3]); Trisomy(19)(0.21-63.78); Trisomy(21)(14.31-46.91); Enh(22)(17.27[22q11.21]-17.34[22q11.21]); Dim(22)(21.08[22q11.22]-21.58[22q11.22]); Enh(22)(44.82[22q13.31]-44.87[22q13.31]); Dim(X)(43.9[Xp11.3]-43.91[Xp11.3]); Enh(X)(151.82[Xq28]-153.47[Xq28])
1473	**MGUS**	**HRD**	Dim(2)(88.99[2p11.2]-89.14[2p11.2]); Trisomy(3)(0.04-199.38); Trisomy(5)(0.08-180.64); Dim(6)(79.04[6q14.1]-79.08[6q14.1]);

			Dim(8)(7.04[8p23.1]-8.15[8p23.1]); Dim(8)(39.36[8p11.23]-39.47[8p11.23]); Trisomy(9)(0.15-138.4); Trisomy(11)(0.18-134.43); Enh(12)(56.43[12q13.3]-56.46[12q13.3]); Dim(14)(105.34[14q32.33]-105.42[14q32.33]); Trisomy(15)(19.14-100.28); Dim(17)(41.53[17q21.31]-41.65[17q21.31]); Trisomy(19)(0.06-63.78); Enh(X)(3.31[Xp22.33]-3.59[Xp22.33]);
121	**MGUS**	**HRD**	Dim X2(1)(72.49[1p31.1]-72.51[1p31.1]); Dim X2(1)(149.37[1q21.3]-149.4[1q21.3]); Dim(1)(158.32[1q23.3]-158.37[1q23.3]); Dim(1)(244.97[1q44]-245.43[1qter]); Dim(2)(15.29[2p24.3]-15.43[2p24.3]); Dim(2)(88.98[2p11.2]-89.2[2p11.2]); Enh(3)(164.0[3q26.1]-164.1[3q26.1]); Trisomy(5)(0.08-180.64); Dim(5)(140.2[5q31.2]-140.22[5q31.3]); Dim(6)(32.6[6p21.32]-32.63[6p21.32]); Trisomy(7)(0.14-158.62); Enh(8)(39.36[8p11.22]-39.51[8p11.22]); Trisomy(9)(0.15-138.4); Dim(13)(73.26[13q22.1]-73.34[13q22.1]); Dim(14)(105.14[14q32.33]-105.45[14q32.33]); Trisomy(15)(18.36-100.28); Trisomy(18)(0.0-76.11); Trisomy(19)(0.06-63.78); Dim(22)(21.03[22q11.22]-21.58[22q11.22]); Monosomy(X)(2.7-154.49)
396	**MGUS**	**HRD**	Dim(1)(83.33[1p31.1]-83.58[1p31.1]); Dim(2)(89.01[2p11.2]-91.04[2p11.2]); Trisomy(3)(0.04-199.38); Trisomy(5)(0.08-180.64); Dim(5)(69.77[5q13.2]-70.7[5q13.2]); Dim(6)(29.96[6p22.1]-30.02[6p22.1]); Dim(6)(32.6[6p21.32]-32.63[6p21.32]); Dim(8)(7.26[8p23.1]-8.12[8p23.1]); Enh(8)(39.36[8p11.22]-39.51[8p11.22]); Trisomy(9)(0.15-138.4); Dim(10)(46.38[10q11.22]-47.03[10q11.22]); Trisomy(11)(0.18-134.43); Dim(12)(7.92[12p13.31]-8.01[12p13.31]); Dim X2(13)(56.66[13q21.1]-56.67[13q21.1]); Dim X2(14)(105.33[14q32.33]-105.42[14q32.33]); Enh(15)(20.8[15q11.2]-100.28[15qter]); Dim(17)(41.53[17q21.31]-41.71[17q21.31]); Enh(18)(0.32[18p11.32]-0.7[18p11.32]); Trisomy(19)(0.06-63.78); Dim(20)(30.39[20q11.21]-30.47[20q11.21]); Trisomy(21)(13.33-46.91); Dim(X)(88.11[Xq21.31]-91.69[Xq21.32])
989	**MGUS**	**HRD**	Dim(1)(16.88[1p36.13]-17.13[1p36.13]); Dim(1)(59.84[1p32.1]-62.70[1p31.3]); Dim(1)(88.59[1p22.2]-94.29[1p22.1]); Dim(1)(95.53[1p21.3]-113.44[1p13.2]); Dim(1)(114.05[1p13.2]-120.47[1p11.1]); Enh(1)(159.78[1q23.3]-159.91[1q23.3]); Dim(2)(88.96[2p11.2]-89.03[2p11.2]); Trisomy(3)(0.04-199.38); Dim(4)(5.24[4p16.1]-37.14[4p14]); Dim(4)(70.18[4q13.2]-70.30[4q13.3]); Trisomy(5)(0.08-180.64); Enh(6)(35.57[6p21.32]-32.67[6p21.32]); Dim(6)(88.91[6q15]-170.47[6qter]); Enh(7)(0.14[7pter]-89.08[7q21.13]); Dim(7)(89.11[7q21.13]-91.40[7q21.2]); Enh(7)(91.40[7q21.2]-100.54[7q22.1]); Dim(7)(100.55[7q22.1]-104.38[7q22.2]); Enh(7)(104.40[7q22.2]-158.57[7qter]); Dim(8)(0.63[8pter]-47.06[8p11.1]); Enh(8)(39.36[8p11.22]-39.51[8p11.22]); Enh(9)(0.15[9pter]-44.17[9p11.1]); Enh(10)(45.48[10q11.21]-46.57[10q11.21]); Enh(11)(0.18[11pter]-87.08[11q14.2]); Dim(11)(55.12[11q11.2]-55.20[11q11.1]); Enh(11)(90.04[11q14.3]-134.35[11qter]); Enh(12)(9.53[12p13.31]-9.63[12p13.31]); Dim(12)(18.36[12q23.1]-98.62[12q23.1]); Dim(14)(19.27[14q11.2]-19.48[14q11.2]); Dim(14)(105.35[14q32.33]-105.45[14q32.33]); Dim X2(14)(105.60[14q32.33]-105.63[14q32.33]); Dim X2(14)(105.96[14q32.33]-106.00[14q32.33]); Trisomy(15); Enh(16)(31.81[16p11.2]-32.75[16p11.2]); Enh(17)(77.41[17q25.3]-77.56[17q25.3]); Trisomy(19); Dim(20)(31.80[20q11.22]-50.18[20q13.2]); Trisomy(21); Enh X2(X)(92.36[Xq21.32]-154.14[Xqter])
2879	**MGUS**	**HRD**	Trisomy(3)(0.04-199.19); Dim(4)(69.07[4q13.2]-69.17[4q13.2]); Trisomy(5)(0.08-180.44); Enh(6)(32.56[6p21.32]-32.66[6p21.32]); Enh(6)(150.2[6q25.1]-150.39[6q25.1]); Trisomy(7)(0.14-158.81); Enh(8)(37.85[8p12]-38.28[8p12]); Dim X2(8)(39.36[8p11.22]-39.51[8p11.22]); Enh(8)(145.06[8q24.3]-145.09[8q24.3]); Tetrasomy(9)(0.15-140.02); Trisomy(11)(0.18-134.36); Enh(14)(42.8[14q21.3]-43.29[14q21.3]); Dim(14)(105.31[14q32.33]-105.43[14q32.33]); Tetrasomy(15)(18.36-100.16); Trisomy(17)(0.03-78.65); Tetrasomy(19)(0.06-63.78)
719	**MM**	**t(4;14)**	Enh (1)(141.47[1q12]-245.43[1qter]); Enh(1)(141.47[1q21]-181.76[1q31.3]); Enh(1)(197.82[1q32.1]-209.02[1q41]); Enh(1)(232.14[1q42.3]-245.43[1qter]); Dim(2)(89.0[2p11.2]-8.11[2p11.2]); Dim(4)(0.04[4pter]-37.68[4p14]); Dim(5)(68.85[5q13.2]-70.69[5q13.2]); Dim(5)(118.33[5q23.1]-118.63[5q23.1]); Dim(6)(32.56[6p21.32]-32.73[6p21.32]); Dim(6)(124.2[6q22.31]-124.96[6q22.31]); Dim(6)(149.16[6q25.1]-155.54[6q25.3]); Dim(6)(167.09[6q27]-170.94[6q27]); Enh(7)(81.85[7q21.11]-158.62[7qter]); Dim(8)(39.34[8p11.22]-39.48[8p11.22]); Dim(9)(8.71[9p23]-17.75[9p22.2]); Enh(10)(46.37[10q11.22]-47.99[10q11.22]); Dim(11)(79.86[11q14.1]-104.4[11q22.3]); Monosomy(13)(18.07-114.12); Dim X2(13)(47.79[13q14.2]-48.0[13q14.2]); Dim(14)(105.32[14q32.33]-105.95[14q32.33]); Dim(15)(18.86[15q11.2]-19.79[15q11.2]); Dim(15)(32.51[15q14]-32.59[15q14]); Dim(16)(3.18[16p13.3]-9.13[16p13.2]); Enh(17)(0.07[17pter]-10.04[17p13.1]); Enh(17)(14.94[17p12]-28.88[17q11.2]); Enh(17)(38.26[17q21.31]-78.65[17qtel]); Dim(20)(14.63[20p12.1]-14.71[20p12.1]); Dim X2(X)(21.34[Xp22.11]-21.37[Xp22.11]); Dim(X)(88.46[Xq21.31]-92.1[Xq21.32]); Dim(Y)(2.69-57.37)
604	**MM**	**t(4;14)**	Enh X2(1)(141.47[1q12.1]-245.43[1qter]); Dim(2)(88.98[2p11.2]-89.16[2p11.2]); Dim(2)(180.3[2q31.2]-180.35[2q31.2]); Dim(4)(69.2[4q13.2]-

			69.79[4q13.2]); Dim(4)(81.79[4q21.21]-81.91[4q21.21]); Dim(5)(163.28[5q34]-163.52[5q34]); Dim(6)(32.59[6p21.32]-32.72[6p21.32]); Dim(7)(138.83[7q34]-139.12[7q34]); Dim(8)(39.36[8p11.22]-39.51[8p11.22]); Dim(8)(67.65[8q13.1]-68.11[8q13.1]); Dim(9)(116.58[9q33.1]-116.68[9q33.1]); Enh(10)(46.37[10q11.22]-47.99[10q11.22]); Dim (10)(64.74[10q21.3]-64.83[10q21.3]); Monosomy(13)(18.07-114.12); Dim(14)(19.27[14q11.2]-19.49[14q11.2]); Enh(14)(21.53[14q11.2]-22.26[14q11.2]); Dim(14)(105.31[14q32.33]-106.28[14q32.33]); Dim(16)(5.35[16p13.3]-9.96[16p13.2]); Trisomy(19)(0.06-63.78); Dim(22)(21.38[22q11.22]-21.6[22q11.22]); Dim(X)(90.19[Xq21.31]-91.69[Xq21.31]); Dim(Y)(3.43[Yp11.31]-6.82[Yp11.2])
1148	**MM**	**t(4;14)**	Dim(1)(185.86[1q31.1]-186.57[1q31.1]); Dim(1)(215.11[1q41]-238.02[1q43]); Dim(2)(233.86[2q37.2]-234.0[2q37.2]); Enh(3)(0.04[3pter]-68.9[3p14.1]); Enh(3)(85.53[3p12.1]-199.38[3qter]); Dim(4)(26.26[4p15.2]-26.37[4p15.2]); Dim(4)(70.28[4q13.3]-70.5[4q13.3]); Dim(4)(103.15[4q24]-103.38[4q24]); Dim(4)(168.26[4q32.3]-168.95[4q32.3]); Dim(4)(175.67[4q34.1]-177.2[4q34.1]); Dim(4)(188.78[4q35.2]-188.88[4q35.2]); Dim(5)(90.6[5q14.3]-91.12[5q14.3]); Dim(5)(94.04[5q15]-94.07[5q15]); Dim(5)(94.35[5q15]-94.81[5q15]); Enh X2(6)(0.1[6pter]-90.01[6q15]); Enh X2(6)(91.13[6q15]-97.13[6q16.1]); Dim(7)(76.77[7q21.11]-76.94[7q21.11]); Dim(7)(109.96[7q31.1]-110.05[7q31.1]); Dim(8)(84.02[8q21.13]-84.16[8q21.13]); Dim(8)(134.48[8q24.22]-134.65[8q24.22]); Dim(10)(0.12[1opter]-7.81[10p14]); Dim(10)(20.36[10p12.31]-21.14[10p12.31]); Enh(12)(50.98[12q13.13]-51.09[12q13.13]); Dim(13)(18.07[13q12.11]-20.3[13q12.11]); Dim(13)(26.49[13q12.2]-33.95[13q13.2]); Dim(13)(51.06[13q14.3]-51.18[13q14.3]); Dim(13)(56.31[13q21.1]-76.92[13q22.3]); Dim X2(13)(63.16[13q21.31]-63.24[13q21.31]); Dim(13)(110.24[13q34]-110.58[13q34]); Dim(14)(49.28[14q21.3]-49.33[14q21.3]); Dim(14)(49.46[14q21.3]-99.33[14q32.2]); Dim(14)(105.31[14q32.33]-106.29[14q32.33]); Enh(15)(18.41[15q11.2]-33.31[15q14]); Enh(15)(39.2[15q15.1]-42.93[15q15.3]); Enh(15)(47.06[15q21.1]-50.96[15q21.3]); Enh(15)(85.81[15q25.3]-88.62[15q26.1]); Dim(15)(88.74[15q26.1]-88.8[15q26.1]); Enh(15)(95.37[15q25.2]-98.14[15q26.3]); Enh(16)(4.32[16p13.3]-4.38[16p13.3]); Dim(17)(0.12[17pter]-1.01[17p13.3]); Enh(17)(1.11[17p13.3]-2.08[17p13.3]); Dim(17)(2.09[17p13.3]-2.84[17p13.3]); Dim(17)(3.04[17p13.2]-3.07[17p13.2]); Enh(17)(3.14[17p13.2]-5.82[17p13.2]); Amplified(17)(4.74[17p13.2]-5.68[17p13.2]); Dim(17)(5.87[17p13.2]-9.17[17p13.1]); Enh(17)(9.17[17p13.1]-9.27[17p13.1]); Dim(17)(9.27[17p13.1]-9.42[17p13.1]); Enh(17)(9.42[17p13.1]-10.21[17p13.1]); Dim(17)(10.22[17p13.1]-13.04[17p12]); Enh(17)(13.55[17p12]-14.13[17p12]); Dim(17)(14.14[17p12]-15.28[17p12]); Dim(17)(19.65[17p11.2]-21.21[17p11.2]); Enh(17)(22.34[17p11.1]-24.41[17q11.2]); Dim(17)(24.45[17q11.2]-24.71[17q11.2]); Enh(17)(26.76[17q11.2]-26.93[17q11.2]); Dim(17)(27.55[17q11.2]-28.25[17q11.2]); Dim(18)(1.08[18p11.32]-6.36[18p11.31]); Dim(18)(6.4[18p11.31]-9.82[18p11.22]); Enh(18)(9.83[18p11.22]-20.5[18q11.2]); Dim(18)(20.52[18q11.2]-31.27[18q12.1]); Enh(18)(31.28[18q12.2]-32.06[18q12.2]); Dim(18)(32.07[18q12.2]-36.2[18q12.3]); Dim(18)(72.39[18q23]-72.52[18q23]); Trisomy(19)(0.06-63.78); Dim(22)(14.88[22q11.11]-30.19[22q12.3]); Enh(X)(113.86[Xq23]-115.42[Xq23]); Dim(X)(115.44[Xq23]-115.9[Xq23]); Enh(X)(115.94[Xq23]-154.49[Xqter]); Dim(Y)(2.77[Yp11.31]-6.78[Yp11.2]) ; Dim(Y)(2.69-57.37)
342	**MM**	**t(4;14)**	Dim(1)(77.99[1p31.1]-78.18[1p31.1]); Enh(1)(141.47[1q21.1]-245.43[1qter]); Enh(1)(141.47[1q21.1]-183.00[1q31.1]); Enh(2)(0.02[2pter]-91.57[2p11.1]); Dim(2)(89.0[2p11.2]-89.32[2p11.2]); Dim(2)(183.12[2q31.3]-183.22[2q32.1]); Enh(3)(48.55[3p21.31]-48.67[3p21.31]); Dim(3)(79.08[3p12.3]-79.15[3p12.3]); Dim(3)(85.71[3p12.1]-85.92[3p12.1]); Dim(3)(164.0[3q36.1]-164.1[3q36.1]); Dim(4)(40.81[4p13]-41.01[4p13]); Dim(4)(69.2[4q13.2]-69.82[4q13.2]); Dim(4)(190.86[4q35.2]-191.05[4q35.2]); Dim(5)(0.08[5pter]-33.32[5p13.2]); Dim(6)(26.26[6p22.1]-26.34[6p22.1]); Dim(6)(74.42[6q13]-170.74[6qter]); Dim(7)(3.61[7p22.2]-3.77[7p22.2]); Dim(7)(151.38[7q36.2]-151.55[7q36.2]); Dim(8)(0.06[8pter]-112.27[8q23.3]); Dim(11)(34.04[11p13]-34.17[11p13]); Dim(11)(72.44[11q13.4]-72.55[11q14.3]); Dim(11)(76.93[11q13.5]-77.7[11q13.5]); Dim(12)(12.72[12p13.1]-12.78[12p13.1]); Monosomy(13)(18.07-114.12); Monosomy(14)(18.15-106.35); Dim(15)(68.68[15q23]-68.88[15q23]); Dim(16)(10.69[16p13.3]-10.82[16p13.13]); Enh(16)(69.41[16q22.2]-69.74[16q22.2]); Dim(18)(0.0[18pter]-15.32[18p11]); Dim(20)(34.75[20q11.23]-35.58[20q11.23]); Dim X2(20)(34.84[20q11.23]-34.97[20q11.23]); Dim(20)(40.65[20q12]-40.65[20q12]); Dim(X)(87.81[Xq21.31]-92.1[Xq21.32]); Dim(Y)(2.69-57.37)
374	**MM**	**t(4;14)**	Dim(1)(25.52[1p36.11]-25.81[1p36.11]); Dim(1)(50.62[1p32.3]-51.3[1p32.3]); Dim X2(1)(51.12[1p32.3]-51.25[1p32.3]); Dim(1)(85.84[1p22.3]-95.16[1p21.3]); Enh(1)(141.47[1q21.1]-245.43[1qter]); Enh(1)(141.47[1q21.1]-179.25[1q25.3]); Dim(2)(88.99[2p11.2]-89.47[2p11.2]); Dim(2)(97.15[2q11.2]-97.71[2q11.2]); Dim(2)(108.66[2q13]-111.61[2q13]); Dim(2)(122.08[2q14.3]-122.7[2q14.3]); Dim(2)(123.41[2q14.3]-

			124.99[2q14.3]); Enh(2)(185.51[2q32.1]-198.45[2q33.1]); Dim(3)(75.47[3p12.3]-76.02[3p12.3]); Enh(3)(164.02[3q26.1]-164.11[3q26.1]); Dim(3)(173.33[3q26.31]-173.59[3q26.31]); Dim(4)(0.04[4pter]-1.24[4p16]); Enh(5)(1.05[5p15.33]-1.2[5p15.33]); Dim(5)(85.37[5q14.3]-85.63[5q14.3]); Enh(6)(0.33[6pter]-43.72[6p21.1]); Trisomy(7)(0.14-158.62); Dim(8)(0.06[8pter]-35.59[8p12]); Dim(8)(39.36[8p11.22]-39.54[8p11.22]); Dim(9)(9.68[9p23]-10.01[9p23]); Enh(9)(68.13[9q12]-138.40[9qter]); Dim(10)(0.12[10pter]-8.23[10p14]); Dim(10)(15.12[10p13]-18.77[10p12.31]); Dim(10)(22.99[10p12.2]-23.99[10p12.2]); Enh(10)(41.93[10q11.21]-135.4[10qter]); Monosomy(13)(18.07-114.12); Dim(14)(18.15[14pter]-105.99[14q32.33]); Dim (15)(18.45[15q11.2]-20.25[15q11.2]); Dim(18)(0.0[18pter]-15.32[18p11.21]); Monosomy(22)(14.5-49.51); Monosomy(X)(2.69-154.49)
1875	**MM**	**t(4;14)**	Enh(1)(141.47[1q12]-245.43[1qter]); Dim(2)(88.98[2p11.2]-89.11[2p11.2]); Enh(4)(40.54[4p14]-40.62[4p14]); Dim(4)(69.2[4q13.2]-69.31[4q13.2]); Dim(5)(69.74[5q13.2]-70.34[5q13.2]); Dim(6)(16.51[6p22.3]-17.01[6p22.3]); Dim(8)(0.06[8pter]-35.52[8p12]); Dim(8)(39.36[8p11.23]-39.51[8p11.22]); Dim(9)(11.81[9p23]-12.19[9p23]); Enh(10)(46.38[10q11.22]-47.74[10q11.22]); Dim(10)(116.86[10q25.3]-117.7[10q25.3]); Dim(11)(55.12[11q11]-55.21[11q11]); Monosomy(13)(18.07-114.12); Dim X2(13)(54.75[13q21.1]-55.07[13q21.1]); Enh(14)(18.86[14q11.2]-19.49[14q11.2]); Dim(14)(44.6[14q21.2]-44.77[14q21.2]); Dim(14)(4619[14q21.3]-46.27[14q21.3]); Dim(14)(57.54[14q23.1]-86.96[14q31.3]); Dim(14)(105.28[14q32.33]-1059.99[14q32.33]); Enh(15)(18.43[15q11]-20.08[15q11]); Dim(17)(42.86[17q21.32]-43.02[17q21.32]); Dim(20)(0.01[20pter]-26.16[20p11]); Dim X2(22)(20.88[22q11.22]-21.57[22q11.22]); Dim(22)(22.7[22q11.23]-22.71[22q11.23]); Monosomy(X)(2.69-154.49)
52	**MM**	**t(4;14)**	Dim(1)(91.68[1p22.1]-98.86[1p21.3]); Dim(1)(99.82[1p21.2]-105.54[1p21.1]); Dim(2)(88.99[2p11.2]-89.27[2p11.2]); Enh(3)(12.31[3p25.2]-19.01[3p24.3]); Enh(4)(1.83[4p16.3]-26.51[4p15.2]); Dim(4)(95.11[4q22.3]-124.36[4q28.1]); Dim(6)(136.12[6q23.3]-168.98[6q27]); Dim(8)(0.06[8pter]-43.65[8p11.1]); Dim(12)(0.03[12pter]-30.39[12p11.22]); Dim(12)(49.02[12q13.12]-49.1[12q13.12]); Monosomy(13)(18.07-114.12); Dim(14)(30.54[14q12]-105.42[14q32.3]); Enh(14)(105.42[14q32.33]-106.35[14qter]); Dim(15)(33.58[15q14]-38.39[15q14]); Dim(17)(0.03[17pter]-13.39[17p12]); Dim(17)(17.73[17p11.2]-22.32[17p11.2]); Dim(17)(77.42[17q25.3]-77.69[17q25.3]); Dim(20)(0.01[20pter]-25.47[20p11.1]); Dim(20)(596.55[20q13.33]-62.38[20qter]); Monosomy(22)(15.45-49.51); Dim(X)(2.72[Xpter]-125.55[Xq25]); Dim(Y)(2.69-57.37)
665	**MM**	**t(4;14)**	Dim(1)(45.89[1p34.1]-117.9[1p12]); Dim X2(1)(50.13[1p331]-51.88[1p32.3]); Dim X2(1)(89.28[1p22.2]-90.85[1p22.2]); Enh(2)(0.02[2pter]-81.03[2p12]); Dim(2)(81.15[2p12]-84.24[2p12]); Dim X2(2)(88.98[2p11.2]-89.33[2p11.2]); Enh(3)(0.04[3pter]-54.2[3p14.3]); Dim(3)(176.92[3q26.32]-177.29[3q26.32]); Enh(5)(0.08[5pter]-28.09[5p14.1]); Dim(5)(58.37[5q11.2]-180.64[5qter]); Dim X2(6)(32.56[6p21.32]-32.6[6p21.32]); Dim(6)(115.34[6q22.1]-170.94[6qter]); Enh(7)(69.51[7q11.22]-158.62[7qter]); Dim(8)(2.21[8p23.2]-5.97[8p23.2]); Dim(8)(85.39[8q21.2]-85.57[8q21.2]); Dim(9)(0.15[9pter]-32.16[9p21.1]); Enh(9)(32.93[9p13.3]-43.95[9p11.2]); Dim(10)(46.41[10q11.22]-46.57[10q11.22]); Enh(11)(88.05[11q14.3]-134.43[11qter]); Dim(12)(6.37[12p13.31]-20.57[12p12.1]); Monosomy(13)(18.07-114.12); Dim(14)(19.27[14q11.2]-19.5[14q11.2]); Dim(14)(28.13[14q12]-29.03[14q12]); Enh(14)(30.04[14q12]-31.57[14q12]); Dim(14)(31.59[14q12]-95.37[14q32.2]); Dim(14)(98.84[14q32.2]-106.35[14qter]); Dim X2(14)(105.41[14q32.33]-106.12[14q32.33]); Dim(17)(0.03[17pter]-22.13[17p11.2]); Dim(18)(0.0[18pter]-15.11[18p11.21]); Trisomy(19)(0.06-63.78); Dim(20)(0.01[20pter]-16.07[20p12.1]); Enh(20)(29.39[20q11.21]-63.03[20qter]); Monosomy(22); Dim X2(22)(21.43[22q11.22]-21.57[22q11.22])
1172	**MM**	**t(4;14)**	Dim X2(1)(145.82[1q21.1]-146.01[1q21.1]); Dim(1)(199.09[1q32.1]-199.29[1q32.1]); Dim(1)(245.05[1q44]-245.13[1q44]); Dim X2(2)(89.0[2p11.2]-89.34[2p11.2]); Dim(3)(59.61[3p14.2]-59.8[3p14.2]); Dim(3)(70.0[3p13]-78.56[3p12.3]); Dim(3)(133.82[3q22.1]-133.86[3q22.1]); Dim(3)(167.47[3q26.1]-168.5[3q26.2]); Dim(4)(108.1[4q24]-109.28[4q25]); Dim(4)(131.3[4q28.3]-132.24[4q28.3]); Enh(5)(32.09[5p13.3]-32.2[5p13.3]); Dim(5)(58.72[5q11.2]-58.93[5q11.2]); Dim(5)(98.04[5q21.1]-138.09[5q31.2]); Dim(6)(97.12[6q16.1]-97.21[6q16.1]); Dim(7)(0.14[7pter]-16.44[7p21.1]); Dim(12)(0.03[12pter]-56.43[12q14.1]); Monosomy(13)(18.07-114.12); Dim(16)(0.03[16pter]-8.52[16p13.12]); Enh(16)(27.2[16p11.2]-31.41[16p11.2]); Dim(18)(0.0[18pter]-18.86[18q11.2]); Dim(18)(20.21[18q11.2]-20.93[18q11.2]); Dim(22)(14.79[22q11.1]-34.36[22q12.3]); Dim X2(X)(75.92[Xq21.1]-75.99[Xq21.1]); Enh(X)(114.95[Xq23]-154.49[Xqter]); Dim(Y)(2.69-57.37)
2458	**MM**	**t(4;14)**	Enh X2(1)(141.47[1q12]-245.43[1qter]); Dim X2(2)(89.0[2p11.2]-89.27[2p11.2]); Dim(3)(85.91[3p12.1]-85.97[3p12.1]); Dim(4)(69.2[4q13.2]-69.79[4q13.2]); Dim(5)(21.85[5p14.3]-22.08[5p14.3]); Dim(5)(79.94[5q14.1]-80.01[5q14.1]); Dim(6)(32.57[6p21.32]-32.6[6p21.32]);

			Dim(6)(35.61[6p21.31]-35.78[6p21.31]); Dim(6)(102.29[6q16.3]-102.49[6q16.3]); Enh(7)(14.66[7p21.1]-15.39[7p21.1]); Enh(7)(128.03[7q31.32]-128.16[7q31.32]); Dim(7)(151.38[7q36.1]-151.55[7q36.2]); Dim(8)(0.06[8p23.3]-0.96[8p23.3]); Dim(8)(6.43[8p23.1]-41.8[8p11.21]); Enh(8)(39.36[8p11.22]-39.51[8p11.22]); Enh(8)(55.7[8q12.1]-129.55[8q24.21]); Enh(8)(142.08[8q24.3]-145.79[8q24.3]); Enh(12)(56.43[12q14.1]-56.47[12q14.1]); Monosomy(13)(18.07-114.12); Dim X2(14)(105.41[14q32.33]-106.23[14q32.33]); Enh(18)(37.32[18q12.3]-62.79[18q22.1]); Enh(22)(18.08[22q11.21]-19.11[22q11.21]); Monosomy(X)(2.69-154.49)
756	**MM**	**t(4;14)**	Dim(1)(72.84[1p31.1]-76.02[1p31.1]); Dim(1)(83.99[1p31.1]-14.47[1p11.1]); Enh(1)(141.47[1q12]-245.43[1qter]); Dim X2(1)(195.02[1q31.3]-195.06[1q31.3]); Dim(2)(88.99[2p11.2]-89.33[2p11.2]); Dim(3)(122.31[3q13.33]-122.4[3q13.33]); Enh(3)(164.0[3q26.1]-164.1[3q26.1]); Dim(4)(0.04[4pter]-1.83[4p16.3]); Enh(6)(32.56[6p21.32]-32.66[6p21.32]); Dim(8)(0.06[8pter]-39.64[8p11.22]); Enh(8)(39.36[8p11.22]-39.51[8p11.22]); Enh(8)(122.52[8q24.13]-128.84[8q24.21]); Enh(8)(138.31[8q24.23]-140.0[8q24.23]); Monosomy(12)(0.03-132.39); Monosomy(14)(18.15[14pter]-105.45[14q32.33]); Enh(15)(18.66[15q11.2]-20.08[15q11.2]); Enh(16)(31.96[16p11.2]-33.54[16p11.2]); Dim(17)(7.26[17p13.1]-7.75[17p13.1]); Dim(18)(25.63[18q12.1]-27.3[18q12.1]); Enh(19)(0.6[19p13.3]-0.63[19p13.3]); Dim(X)(2.69[Xp22.33]-127.44[Xq25]); Enh(X)(128.0[Xq25]-154.49[Xqter])
KMS-11	**Cell-line**	**t(4;14)**	Dim(1)(27.4[1p35.3]-47.31[1p33]); Dim X2(1)(47.93[1p33]-51.95[1p32.3]); Enh(1)(51.98[1p32.3]-52.64[1p32.3]); Dim(1)(54.88[1p32.2]-59.66[1p32.1]); Enh(1)(59.71[1p32.1]-60.15[1p32.1]); Dim(1)(60.15[1p32.1]-97.99[1p21.3]); Enh(1)(98.0[1p21.2]-98.73[1p21.2]); Dim(1)(98.73[1p21.2]-109.29[1p13.3]); Enh(1)(109.31[1p13.3]-110.41[1p13.3]); Dim(1)(110.42[1p13.2]-120.22[1p11.2]); Enh(1)(141.47[1q21.1]-164.81[1q24.2]); Enh(1)(171.5[1q24.2]-214.95[1q41]); Dim(2)(0.02[2pter]-28.96[2p23.2]); Dim(2)(52.4[2p16.3]-53.95[2p16.2]); Dim(2)(88.99[2p11.2]-91.12[2p11.2]); Enh(2)(91.18[2p11.2]-91.32[2p11.2]); Dim(2)(94.77[2q11.2]-151.8[2q23.3]); Enh(2)(151.8[2q23.3]-153.96[2q24.1]); Dim(2)(153.96[2q24.1]-154.34[2q24.1]); Enh(2)(154.36[2q24.1]-159.84[2q24.2]); Dim(2)(159.84[2q24.2]-171.7[2q31.1]); Dim(2)(187.8[2q32.1]-242.78[2qter]); Dim(3)(0.04[3pter]-113.32[3q13.2]); Dim(4)(0.04[4pter]-49.42[4p12]); Dim(4)(69.2[4q13.2]-69.79[4q13.2]); Dim(5)(21.07[5p14.3]-49.6[5p12]); Enh(5)(98.92[5q21.1]-102.11[5q21.1]); Dim(5)(102.21[5q21.1]-180.64[5qter]); Monosomy(6)(0.1-170.94); Dim(7)(17.57[7p21.1]-18.44[7p21.1]); Enh(7)(71.45[7q11.23]-71.74[7q11.23]); Enh(7)(111.98[7q31.1]-158.62[7qter]); Dim(8)(0.06[8pter]-59.58[8q12.1]); Enh(8)(73.54[8q13.3]-75.0[8q21.11]); Dim(8)(76.96[8q21.11]-87.64[8q21.3]); Enh(8)(91.39[8q21.3]-101.72[8q22.3]); Dim(8)(112.65[8q23.3]-116.44[8q23.3]); Dim(8)(129.62[8q24.21]-137.66[8q24.23]); Enh(8)(137.66[8q24.23]-138.59[8q24.23]); Dim(8)(138.61[8q24.23]-146.0[8qter]); Dim(9)(0.15[9pter]-64.14[9p11.1]); Dim(9)(123.98[9q33.3]-125.83[9q33.3]); Dim(10)(41.93[10q11.21]-135.4[10qter]); Dim(11)(0.18[11pter]-74.99[11q13.5]); Enh(11)(85.28[11q14.2]-86.53[11q14.2]); Dim(11)(86.56[11q14.3]-134.43[11qter]); Dim(12)(1.61[12p13.33]-29.72[12p11.22]); Enh(12)(51.8[12q13.13]-81.8[12q21.31]); Dim(12)(81.81[12q21.31]-132.39[12qter]); Dim X2(12)(117.07[12q24.23]-117.19[12q24.23]); Monosomy(13)(18.07-114.12); Dim(14)(18.15[14q11.2]-104.98[14q32.33]); Dim(14)(105.22[14q32.33]-106.35[14q32.33]); Monosomy(15)(19.81-100.28); Dim(16)(45.07[16q12.1]-88.69[16qter]); Enh(16)(69.41[16q22.1]-69.74[16q22.1]); Dim X2(16)(76.74[16q23.1]-77.79[16q23.1]); Dim(17)(0.03[17pter]-22.13[17p11.1]); Dim(17)(30.09[17q12]-32.43[17q12]); Dim(17)(38.33[17q21.31]-38.58[17q21.31]); Dim(17)(41.52[17q21.33]-44.06[17q22]); Dim(18)(0.0[18pter]-17.95[18q11.2]); Enh(18)(39.32[18q12.3]-76.11[18qter]); Dim(19)(0.06[19pter]-32.55[19p12]); Dim(19)(51.09[19q13.32]-63.78[19q13.43]); Dim(20)(0.01[20pter]-29.3[20q11.21]); Enh(20)(47.33[20q13.13]-62.38[20qter]); Monosomy(22)(14.5-49.51); Monosomy(X)(2.69-154.49)
551	**MM**	**t(14;16)**	Enh(1)(21.34[1p36.12]-22.9[1p36.12]); Enh(1) X2(141.47[1q12]-245.43[1qter]); Dim(2)(88.98[2p11.2]-89.34[2p11.2]); Dim(3)(163.98[3q26.1]-164.25[3q26.1]); Enh(3)(170.54[3q26.2]-172.25[3q26.2]); Dim(6)(34.56[6p21.31]-35.29[6p21.31]); Enh(8)(39.36[8p11.22]-39.5[8p11.22]); Dim(9)(21.85[9p21.3]-22.02[9p21.3]); Enh(12)(46.99[12q13.11]-48.59[12q13.11]); Dim(12)(48.65[12q13.12]-50.04[12q13.12]); Dim(12)(74.69[12q21.2]-132.26[12qter]); Monosomy(13)(18.07-114.12); Enh(14)(21.37[14q11.2]-22.02[14q11.2]); Dim(14)(22.15[14q11.2]-22.49[14q11.2]); Dim(14)(72.31[14q24.2]-74.96[14q24.2]); Dim(14)(90.28[14q32.12]-90.88[14q32.12]); Dim(14)(102.09[14q32.32]-102.86[14q32.32]); Dim(14)(105.34[14q32.33]-106.35[14q32.33]); Enh(15)(18.72[15q11.2]-20.22[15q11.2]); Dim(15)(91.31[15q26.1]-91.34[15q26.1]); Dim(16)(45.06[16q11.2]-77.62[16q23.1]); Enh(16)(69.41[16q22.1]-69.75[16q22.3]); Enh(19)(1.81[19p13.3]-2.77[19p13.3]); Dim(22)(16.0[22q11.1]-30.45[22q12.3])

1336	**MM**	**t(14;16)**	Dim(1)(16.99[1p36.13]-24.24[1p36.11]); Dim(1)(45.59[1p34.1]-52.2[1p32.3]); Dim X2(1)(49.91[1p33]-51.76[1p32.3]); Enh(1)(117.3[1p12]-117.69[1p12]); Enh(1) X2(141.47[1q12]-245.43[1qter]); Dim(2)(88.98[2p11.2]-89.32[2p11.2]); Dim(3)(25.93[3p24.2]-4.77[3p21.31]); Enh(5)(61.63[5q12.1]-70.34[5q13.2]); Dim(5)(70.69[5q13.2]-83.62[5q14.3]); Enh(6)(14.7[6p22.3]-57.13[6p12.1]); Dim(6)(90.07[6q15]-117.81[6q22.31]); Dim(8)(39.36[8p11.21]-39.51[8p11.21]); Dim(9)(20.92[9p21.3]-22.45[9p21.3]); Enh(11)(60.24[11q12.2]-65.87[11q13.2]); Dim(11)(65.88[11q13.2]-72.95[11q13.4]); Dim(11)(94.78[11q21]-106.14[11q22.3]); Dim X2(11)(101.06[11q22.1]-103.02[11q22.3]); Monosomy(13)(18.07-114.12); Dim(14)(19.27[14q11.2]-19.49[14q11.2]); Enh(14)(70.19[14q24.2]-70.24[14q24.2]); Dim(14)(105.34[14q32.33]-105.62[14q32.33]); Enh(16)(55.45[16q13]-55.52[16q13]); Enh(16)(69.41[16q22.1]-69.74[16q22.1]); Monosomy(22)(14.5-49.51); Dim X2(22)(21.09[22q11.22]-21.56[22q11.22]); Dim(X)(88.11[Xq21.31]-92.21[Xq21.31]); Dim(Y)(2.69-57.37)
309	**MM**	**t(14;16)**	Dim(1)(83.29[1p31.1]-83.38[1p31.1]); Dim(1)(93.28[1p22.1]-118.36[1p12]); Dim(1)(193.47[1q31.3]-193.56[1q31.3]); Dim(1)(210.93[1q41]-239.34[1q43]); Enh(3)(164.02[3q26.1]-164.10[3q26.1]); Dim(4)(5.95[4p16.2]-6.95[4p16.2]); Enh(4)(7.1[4p16.1]-7.2[4p16.1]); Enh(4)(7.5[4p16.1]-7.72[4p16.1]); Enh(4)(7.95[4p16.1]-8.37[4p16.1]); Dim(4)(8.38[4p16.1]-8.83[4p16.1]); Dim(4)(15.83[4p15.33]-15.89[4p15.33]); Dim(4)(16.72[4p15.32]-22.07[4p15.31]); Dim(4)(22.21[1p15.31]-25.64[1p15.2]); Dim(4)(33.02[4p15.1]-34.41[4p15.1]); Enh(4)(35.52[4p14]-37.63[4p14]); Dim(6)(84.01[6q14.2]-106.95[6q21]); Dim(8)(0.17[8pter]-41.03[8p11.21]); Dim(9)(0.15[9pter]-4.84[9p24.1]); Dim(9)(20.62[9p21.3]-30.96[9p21.1]); Dim(11)(66.28[11q13.2]-67.74[11q13.2]); Dim(11)(71.74[11q13.4]-73.71[11q13.4]); Dim(11)(82.83[11q14.1]-87.32[11q14.2]); Dim(11)(92.28[11q21]-110.37[11q23.1]); Dim X2(11)(97.01[11q22.1]-103.61[11q22.3]); Dim(11)(133.71[11q25]-134.43[11q25]); Dim(16)(2.42[16p13.3]-8.89[16p13.13]); Dim(16)(23.96[16p12.2]-26.58[16p12.1]); Dim(16)(34.13[16p11.2]-35.01[16p11.2]); Enh(16)(45.47[16q12.1]-62.07[16q21]); Dim(16)(77.55[16q23.1]-88.69[16qter]); Enh(17)(41.52[17q21.31]-41.7[17q21.31]); Dim(21)(13.46[21q11.2]-16.05[21q21.1]); Dim(22)(21.4[22q11.22]-21.55[22q11.22]); Monosomy(X)(2.69-154.49)
2068	**MM**	**t(14;16)**	Dim(1)(35.39[1p34.3]-35.43[1p34.3]); Enh(1)(141.47[1q12]-167.53[1q24.3]); Dim(1)(167.59[1q24.3]-200.42[1q32.1]); Enh(1)(200.45[1q32.1]-245.43[1qter]); Dim(2)(89.05[2p11.2]-89.94[2p11.2]); Dim(4)(70.33[4q13.2]-70.47[4q13.3]); Enh(6)(32.56[6p21.32]-32.66[6p21.32]); Enh(9)(68.15[9q13]-138.21[9qter]); Dim(12)(101.72[12q23.1]-104.29[12q23.1]); Monosomy(13)(18.07-114.03); Enh(14)(18.86[14q11.2]-19.48[14q11.2]); Enh(14)(105.02[14q32.33]-105.24[14q32.33]); Dim(14)(105.34[14q32.33]-105.95[41q32.33]); Dim(15)(19.54[15q11.2]-20.39[15q11.2]); Dim(16)(3.09[16p13.3]-10.23[16p13.12]); Enh(16)(31.96[16p11.2]-33.53[16p11.2]); Dim(16)(45.06[16q12.1]-64.72[16q22.1]); Enh(16)(69.42[16q22.2]-69.74[16q22.2]); Dim(16)(77.26[16q23.1]-77.48[16q23.1]); Dim(17)(41.53[17q21.31]-42.18[17q21.31]); Dim(22)(21.38[22q11.22]-21.51[22q11.22]); Dim(22)(27.43[22q12.1]-27.58[22q12.1])
954	**MM**	**t(14;16)**	Dim(1)(3.6[1p36.32]-19.88[1p36.12]); Dim(1)(51.41[1p32.3]-101.06[1p21.1]); Dim(1)(105.01[1p21.1]-141.47[1p11.2]); Enh(1)(141.47[1q12]-245.33[1qter]); Dim(2)(111.72[2q13]-126.6[2q14.3]); Dim(2)(143.48[2q22.3]-150.49[2q23.2]); Dim(2)(171.64[2q31.1]-175.87[2q31.1]); Dim(2)(178.5[2q31.2]-183.73[2q32.1]); Dim(2)(220.26[2q35]-225.54[2q36.3]); Enh(3)(164.0[3q26.1]-164.1[3q26.1]); Dim(3)(146.09[3q24]-149.68[3q24]); Dim(6)(32.59[6p21.32]-32.65[6p21.32]); Dim(7)(1.83[7p22.3]-1.91[7p22.3]); Dim(7)(21.16[7p15.3]-26.98[7p15.2]); Enh(8)(39.36[8p11.22]-39.51[8p11.22]); Enh(10)(134.9[10q26.3]-135.05[10q26.3]); Dim(11)(77.46[11q14.1]-107.56[11q22.3]); Dim(13)(18.69[13q11]-45.53[13q14.13]); Dim(13)(105.28[13q33.2]-107.26[13q33.3]); Dim(14)(105.34[14q32.33]-106.28[14q32.33]); Enh(16)(31.96[16p11.2]-33.76[16p11.2]); Dim(16)(77.21[16q23.1]-77.32[16q23.1]); Enh(17)(77.44[17q25.3]-77.5[17q25.3]); Dim(22)(21.0[22q11.22]-21.53[22q11.22]); Dim(X)(2.69[Xpter]-96.87[Xq21.33])
1798	**MM**	**t(14;16)**	Dim(1)(35.13[1p34.3]-36.16[1p34.3]); Dim(1)(91.02[1p22.2]-93.79[1p22.1]); Enh(1)(146.97[1q21.2]-148.25[1q21.2]); Enh(1)(149.99[1q21.3]-150.75[1q21.3]); Dim(1)(15.21[1q22]-152.4[1q22]); Enh(1)(152.75[1q22]-153.34[1q22]); Enh(1)(170.41[1q24.3]-171.32[1q25.1]); Enh(1)(180.02[1q25.3]-180.82[1q25.3]); Enh(1)(205.95[1q32.2]-206.72[1q32.2]); Dim(2)(32.03[2p22.3]-32.92[2p22.3]); Dim(2)(60.75[2p15]-62.32[2p15]); Dim(2)(88.98[2p11.2]-89.11[2p11.2]); Enh(2)(113.51[2q14.1]-113.88[2q14.1]); Dim(3)(47.07[3p21.31]-48.35[3p21.31]); Enh(4)(153.22[4q31.3]-154.33[4q31.3]); Dim(5)(133.98[5q31.1]-134.25[5q31.1]); Dim(5)(68.36[5q13.2]-70.86[5q13.2]); Dim(6)(62.04[6q11.2]-170.94[6qter]); Dim(7)(4.72[7p22.1]-5.03[7p22.1]); Dim(7)(5.53[7p22.1]-6.64[7p22.1]); Dim(8)(0.17[8pter]-43.52[8p11.21]); Enh(8)(39.36[8p11.22]-39.5[8p11.22]); Dim(9)(0.15[9pter]-14.77[9p22.3]); Dim(9)(20.14[9p21.3]-26.59[9p21.2]); Dim(9)(31.63[9p21.1]-32.61[9p21.1]);

			Dim(9)(129.74[9q34.11]-129.98[9q34.11]); Dim(12)(52.04[12q13.13]-52.12[12q13.13]); Dim(12)(78.54[12q21.31]-78.6[12q21.31]); Dim(12)(97.32[12q23.1]-97.55[12q23.1]); Enh(14)(21.53[14q11.2]-22.15[14q11.2]); Dim(15)(18.74[15q11.2]-20.08[15q11.2]); Dim(15)(56.8[15q21.3]-57.14[15q21.3]); Enh(19)(15.99[19p13.11]-16.66[19p13.11]); Dim(19)(19.6[19p12]-22.21[19p12]); Dim(19)(37.84[19q13.11]-38.31[19q13.11]); Dim(19)(39.28[19q13.11]-39.71[19q13.11]); Dim(19)(41.9[19q13.12]-42.21[19q13.12]); Enh(22)(24.8[22q12.1]-25.79[22q12.1]); Dim(X)(142.27[Xq27.2]-142.61[Xq27.2])
2125	**MM**	**t(14;16)**	Dim(1)(83.38[1p31.1]-83.57[1p31.1]); Dim(1)(91.42[1p22.1]-115.39[1p13.1]); Dim(2)(89.05[2p11.2]-89.32[2p11.2]); Dim(2)(230.93[2q37.1]-231.44[2q37.1]); Enh(3)(164.04[3q26.1]-164.11[3q26.1]); Dim(4)(69.2[4q13.2]-69.31[4q13.2]); Dim X2(4)(70.33[4q13.2]-70.53[4q13.2]); Dim(5)(68.84[5q13.2]-70.7[5q13.2]); Dim(6)(57.34[6p11.2]-57.6[6p11.2]); Enh(8)(39.36[8p11.22]-39.51[8p11.22]); Monosomy(13)(18.07-114.12); Dim(14)(29.87[14q12]-95.37[14q32.2]); Dim(14)(105.41[14q32.33]-105.9[14q32.33]); Enh(17)(77.27[17q25.3]-77.65[17q25.3]); Dim(22)(21.0[22q11.22]-21.54[22q11.22]); Monosomy(X)(2.69-154.49)
282	**MM**	**t(14;16)**	Dim(1)(0.6[1pter]-101.92[1p21.1]); Dim(1)(105.89[1p21.1]-120.96[1p11.1]); Enh(1) X2(141.47[1q12]-245.33[1qter]); Monosomy(2)(0.02-242.78); Deeper Dim(2)(0.02[2pter]-5.06[2p25.2]); Dim X2(2)(88.98[2p11.2]-89.95[2p11.2]); Enh(3)(164.0[3q26.1]-164.1[3q26.1]); Dim(3)(196.93[3q29]-196.97[3q29]); Dim(5)(142.99[5q31.3]-156.11[5q33.3]); Dim(6)(32.56[6p21.32]-32.74[6p21.32]); Dim(6)(62.04[6q11.1]-170.94[6qter]); Dim(7)(0.14[7pter]-16.37[7p21.1]); Enh(8)(39.36[8p11.22]-39.51[8p11.22]); Dim(8)(137.76[8q24.23]-137.92[8q24.23]); Dim(9)(92.09[9q22.31]-92.12[9q22.31]); Enh(10)(46.57[10q11.22]-47.17[10q11.22]); Monosomy(11)(0.18-134.43); Dim(12)(0.03[12pter]-25.63[12p12.1]); Dim(12)(26.65[12p12.1]-52.52[12q13.13]); Dim(12)(53.66[12q13.2]-54.07[12q13.2]); Dim(12)(56.61[12q13.2]-58.02[12q14.1]); Dim(12)(58.96[12q14.1]-132.39[12qter]); Dim(13)(18.07[13q11]-64.57[13q21.31]); Dim(13)(66.51[13q21.32]-66.86[13q21.32]); Enh(14)(21.37[14q11.2]-22.02[14q11.2]); Dim(14)(105.33[14q32.33]-105.96[14q32.33]); Enh(15)(18.68[15q11.2]-20.22[15q11.2]); Dim(15)(76.47[15q25.1]-100.28[15qter]); Dim(16)(0.03[16pter]-11.71[16p13.13]); Dim(16)(14.96[16p13.11]-15.02[16p13.11]); Dim(16)(32.38[16p11.2]-88.69[16qter]); Dim X2(16)(77.23[16q23.1]-77.26[16q23.1]); Dim(17)(0.03[17pter]-13.88[17p12]); Enh(17)(14.03[17p12]-17.45[17p11.2]); Amplified(17)(15.8[17p12]-17.11[17p11.2]); Dim(17)(18.7[17p11.2]-19.65[17p11.2]); Dim(21)(9.9[21p11.2]-32.74[21p22.11]); Dim(22)(14.5[22q11.1]-32.33[22q12.3]); Dim X2(22)(21.0[22q11.22]-21.56[22q11.22])
2314	**MM**	**t(14;20)**	Enh(1)(16.68[1p36.13]-16.98[1p36.13]); Dim(1)(25.32[1p36.11]-25.41[1p36.11]); Dim(1)(72.54[1p31.1]-120.23[1p11.2]); Enh(1)(158.27[1q23.3]-158.38[1q23.3]); Dim(1)(245.05[1q44]-245.13[1q44]); Dim(2)(88.99[2p11.2]-89.33[2p11.2]); Dim(3)(58.99[3p14.2]-119.55[3q13.32]); Enh(3)(120.09[3q13.33]-199.38[3qter]); Dim(4)(69.2[4q13.2]-69.79[4q13.2]); Enh(6)(32.57[6p21.32]-32.6[6p21.32]); Dim(6)(81.89[6q14.1]-170.94[6qter]); Dim X2(8)(39.36[8p11.23]-39.51[8p11.22]); Monosomy(13)(18.07-114.12); Dim(15)(19.79[15q11.2]-20.08[15q11.2]); Enh(16)(0.76[16p13.3]-0.83[16p13.3]); Dim(16)(45.02[16q11.2]-88.69[16qter]); Enh(17)(31.46[17q12]-31.5[17q12]); Dim(22)(21.38[22q11.22]-21.58[22q11.22]); Dim(X)(2.69[Xp22.33]-99.34[Xq22.1]); Enh(X)(138.76[Xq27.1]-139.03[Xq27.1])
1890	**MM**	**t(14;20)**	Dim(8)(7.26[8p23.1]-7.79[8p23.1]); Enh(8)(39.36[8p11.22]-39.51[8p11.22]); Dim(15)(32.54[15q14]-32.68[15q14])
3004	**MM**	**nonHRD, unid *IgH* rearr**	Dim(1)(108.73[1p13.3]-120.96[1p11.1]); Enh(1)(141.47[1q12]-245.43[1qter]); Dim(1)(142.47[1q21.1]-142.52[1q21.1]); Dim(1)(145.73[1q21.2]-146.51[1q21.2]); Dim(1)(245.08[1q44]-245.13[1q44]); Dim X2(2)(89.0[2p11.2]-91.06[2p11.2]); Enh(5)(0.73[5p15.33]-0.92[5p15.33]); Enh(6)(32.52[6p21.32]-32.74[6p21.32]); Dim(8)(7.26[8p23.1]-8.12[8p23.1]); Enh(8)(39.36[8p11.22]-39.51[8p11.22]); Dim(12)(59.75[12q14.1]-105.31[12q23.3]); Enh(12)(122.42[12q24.31]-122.58[12q24.31]); Dim(13)(18.07[13q12.11]-19.86[13q12.11]); Enh(13)(19.86[13q12.11]-20.2[13q12.11]); Dim(13)(20.2[13q12.11]-27.1[13q12.2]); Enh(13)(27.1[13q12.2]-28.06[13q12.3]); Dim(13)(28.06[13q12.3]-94.14[13q32.1]); Enh(13)(94.15[13q32.1]-101.41[13q33.1]); Dim(13)(101.42[13q33.1]-103.37[13q33.2]); Enh(13)(103.37[13q33.2]-103.73[13q33.2]); Dim(13)(103.77[13q33.2]-113.05[13q34]); Enh(13)(113.05[13q34]-113.66[13q34]); Dim(13)(113.77[13q34]-114.12[13q34]); Dim(14)(35.97[14q13.2]-38.12[14q13.3]); Dim(14)(60.05[14q23.1]-63.44[14q23.2]); Dim(14)(66.61[14q23.3]-96.32[14q32.2]); Dim(14)(105.33[14q32.33]-105.9[14q32.33]); Dim(16)(31.96[16p11.2]-34.1[16p11.2]); Dim(16)(71.02[16q22.2]-71.33[16q22.2]); Dim(16)(73.3[16q23.1]-74.02[16q23.1]); Dim(16)(74.17[16q23.1]-74.19[16q23.1]); Monosomy(22)(14.5-49.51)
1581	**MM**	**nonHRD,**	Enh(1)(141.47[1q12]-245.43[1qter]); Dim X2(1)(149.37[1q21.3]-149.4[1q21.3]); Dim(2)(88.98[2p11.2]-89.11[2p11.2]); Enh(2)(91.06[2p11.2]-

		unid *IgH* rearr	91.45[2p11.2]); Enh(3)(166.18[3q26.2]-167.91[3q26.2]); Enh(6)(0.1[6pter]-38.96[6p21.2]); Dim X2(6)(32.59[6p21.32]-32.73[6p21.32]); Dim(6)(151.52[6q25.1]-170.94[6qter]); Dim(7)(0.14[7pter]-16.94[7p21.1]); Dim(8)(7.04[8p23.1]-8.14[8p23.1]); Dim(8)(39.36[8p11.22]-39.51[8p11.22]); Dim X2(11)(5.74[11p15.4]-5.76[11p15.4]); Monosomy(13)(18.07[13pter]-114.12[13qter]); Dim(14)(68.33[14q24.1]-105.76[14q32.33]); Dim(15)(32.52[15q14]-32.65[15q14]); Enh(16)(10.61[16p13.13]-11.95[16p13.13]); Enh(16)(32.21[16p11.2]-33.53[16p11.2]); Dim(16)(45.02[16q11.2]-88.69[16qter]); Enh(16)(69.41[16q22.1]-69.75[16q22.2]); Enh(17)(16.12[17p12]-17.56[17p11.2]); Dim(17)(41.52[17q21.31]-41.84[17q21.31]); Enh(17)(41.84[17q21.31]-42.14[17q21.31]); Enh(19)(15.81[19p13.12]-16.89[19p13.11]); Dim(22)(21.06[22q11.22]-21.58[22q11.22]); Dim(22)(37.68[22q13.1]-37.71[22q13.1]); Enh(X)(137.57[Xq27.1]-154.49[Xqter]); Dim(Y)(2.69-57.37)
619	**MM**	**nonHRD, unid *IgH* rearr**	Dim(1)(0.6[1pter]-141.47[1p11.1]); Enh(1)(141.47[1q12]-245.43[1qter]); Dim X2(2)(89.0[2p11.2]-89.32[2p11.2]); Enh(2)(91.12[2p11.2]-91.45[2p11.2]); Dim(2)(225.23[2q36.2]-225.31[2q36.2]); Dim(2)(236.48[2q37.2]-242.78[2qter]); Dim(3)(77.74[3[12.3]-77.78[3p12.3]); Enh(3)(164.02[3q26.1]-164.11[3q26.1]); Dim X2(5)(68.87[5q13.2]-70.69[5q13.2]); Dim X2(6)(32.56[6p21.32]-32.73[6p21.32]); Dim(7)(69.28[7q11.22]-69.68[7q11.22]); Dim(7)(104.19[7q22.2]-104.27[7q22.2]); Dim(7)(110.57[7q31.1]-110.64[7q31.1]); Enh(8)(39.36[8p11.23]-39.51[8p11.22]); Trisomy(9)(0.15-138.4); Enh(12)(9.53[12p13.31]-9.63[12p13.31]); Monosomy(13)(18.07-114.12); Dim X2(13)(47.82[13q14.2]-47.93[13q14.2]); Dim(14)(93.97[14q32.13]-94.0[14q32.13]); Dim X2(14)(105.31[14q32.33]-105.9[14q32.33]); Enh(15)(18.66[15q11.2]-20.08[15q11.2]); Enh(15)(35.53[15q14]-100.28[15qter]); Dim(16)(3.6[16p13.3]-3.88[16p13.3]); Dim(16)(45.02[16q11.2]-88.69[16qter]); Dim X2(16)(52.18[16q12.2]-52.5[16q12.2]); Dim(17)(1.65[17p13.3]-1.75[17p13.3]); Monosomy(22)(14.5-49.51); Dim X2(22)(37.68[22q13.1]-37.71[22q13.1]); Dim(X)(2.69[Xp22.33]-138.72[Xq27.1]); Enh(X)(138.72[Xq27.1]-154.49[Xqter])
1037	**MM**	**t(8;14), nonHRD**	Dim(1)(81.28[1p31.1]-106.95[1p13.3]); Enh(1)(153.02[1q21.3]-212.5[1q41]); Dim(1)(230.39[1q42.3]-244.87[1q44]); Enh(1)(245.09[1q44]-245.43[1q44]); Dim(2)(89.0[2p11.2]-89.27[2p11.2]); Enh(3)(111.07[3q13.13]-128.23[3q21.3]); Dim(4)(69.2[4q13.2]-69.31[4q13.2]); Enh(5)(0.08[5pter]-64.32[5q12.3]); Enh(5)(142.34[5q31.3]-180.64[5q35.3]); Enh(6)(0.1[6pter]-38.92[6p21.2]); Dim(6)(138.23[6q24.1]-155.19[6q25.3]); Enh(7)(52.25[7p12.1]-131.85[7q33]); Dim(8)(0.06[8pter]-128.47[8q24.21]); Dim(10)(0.13[10pter]-9.35[10p14]); Dim(11)(35.33[11p15.4]-3.91[11p13]); Enh(11)(134.43[11q12.1]-59.32[11qter]); Dim(12)(8.13[12p13.31]-29.6[12p11.22]); Dim(12)(70.43[12q21.1]-101.18[12q23.2]); Dim(13)(18.07[13q11]-75.53[13q22.2]); Dim(14)(44.76[14q21.2]-44.89[14q21.2]); Trisomy(15)(18.36-100.28); Dim(17)(70.79[17q25.1]-70.89[17q25.1]); Monosomy(18)(0.0-76.11); Enh(X)(102.99[Xq22.2]-103.14[Xq22.2])
666	**MM**	**nonHRD**	Dim(1)(59.72[1p32.1]-59.77[1p32.1]); Dim(1)(83.36[1p31.1]-83.58[1p31.1]); Enh(2)(73.77[2p13.2]-73.87[2p13.1]); Dim X2(2)(88.99[2p11.2]-89.32[2p11.2]); Dim(2)(226.9[2q36.3]-242.78[2qter]); Enh(3)(48.58[3p21.31]-48.68[3p21.31]); Dim(3)(164.0[3q36.1]-164.11[3q36.1]); Dim(4)(69.2[4q13.2]-69.31[4q13.2]); Enh(5)(131.75[5q31.1]-180.64[5qter]); Dim X2(5)(180.34[5q35.3]-180.37[5q35.3]); Enh(6)(0.1[6pter]-149.34[6q25.1]); Dim X2(6)(32.56[6p21.32]-32.73[6p21.32]); Dim X2(6)(79.04[6q14.1]-79.08[6q14.1]); Dim(6)(149.34[6q25.1]-170.94[6qter]); Enh(7)(4.87[7p22.1]-4.97[7p22.1]); Enh(7)(7.92[7p21.3]-8.08[7p21.3]); Dim(7)(151.38[7q36.1]-151.58[7q36.1]); Enh(8)(39.37[8p11.22]-39.51[8p11.22]); Enh(8)(128.81[8q24.21]-128.92[8q24.21]); Dim(8)(137.8[8q24.23]-137.92[8q24.23]); Dim(9)(107.84[9q31.2]-108.42[9q31.2]); Trisomy(11)(0.18-134.43); Dim(12)(11.4[12p13.2]-11.44[12p13.2]); Monosomy(13)(18.07-114.12); Dim X2(14)(105.24[14q32.33]-106.23[14q32.33]); Enh(15)(19.81[15q11.2]-100.28[15qter]); Dim(15)(40.63[15q15.2]-40.71[15q15.2]); Dim(17)(41.53[17q21.31]-41.84[17q21.31]); Enh(17)(77.41[17q25.3]-77.52[17q25.3]); Enh(19)(0.06[19pter]-18.98[19p13.11]); Dim(20)(0.01[20pter]-59.39[20q13.33]); Enh(20)(59.43[20q13.33]-60.48[20q13.33]); Amplified(20)(60.49[29q13.33]-61.93[20q13.33]); Enh(20)(61.94[20q13.33]-62.06[20q13.33]); Dim(20)(62.07[20q13.33]-62.21[20q13.33]); Dim(22)(14.5[22q11.1]-16.42[22q11.1]); Dim(22)(21.5[22q11.22]-21.56[22q11.22]); Dim(22)(25.37[22q12.1]-30.31[22q12.2]); Enh(22)(49.0[22q13.33]-49.51[22q13.33])
1776	**MM**	**HRD, unid *IgH* rearr**	Dim(1)(71.04[1p31.1]-120.12[1p11.1]); Dim(2)(88.99[2p11.2]-89.28[2p11.2]); Trisomy(3)(0.04-199.38); Dim(5)(122.33[5q23.2]-128.06[5q23.3]); Dim(5)(145.27[5q32]-159.93[5q34]); Dim(5)(178.19[5q35.3]-178.47[5q35.3]); Enh(7)(26.93[7p15.2]-26.99[7p15.2]); Enh(7)(97.12[7q21.3]-102.06[7q22.1]); Dim(8)(0.98[8p23.3]-35.2[8p12]); Dim(8)(137.76[8q24.23]-137.92[8q24.23]); Dim(9)(15.75[9p22.3]-32.61[9p13.3]); Trisomy(11)(0.18-134.43); Dim(14)(24.4[14q12]-28.16[14q12]); Dim(14)(35.16[14q13.2]-48.7[14q21.3]); Dim(14)(55.12[14q22.3]-71.97[14q24.2]); Dim(14)(77.36[14q24.3]-90.58[14q23.12]); Dim(14)(96.51[14q32.2]-98.71[14q32.2]); Dim(14)(102.3[14q32.32]-102.43[14q32.32]);

			Enh(14)(102.44[14q32.33]-102.48[14q32.33]); Enh(14)(104.39[14q32.33]-105.31[1432.33]); Trisomy(15)(20.39-100.28); Trisomy(19)(0.06-63.78)
3325	**MM**	**t(11;14)**	Dim(1)(26.47[1p36.11]-102.18[1p21.1]); Dim X2(1)(45.91[1p34.1]-46.07[1p34.1]); Dim X2(1)(149.37[1q21.3]-149.4[1q21.3]); Dim(1)(210.75[1q32.3]-211.47[1q41]); Dim(2)(89.0[2p11.2]-89.11[2p11.2]); Enh(3)(0.04[3pter]-51.46[3p21.2]); Enh(3)(56.94[3p14.3]-66.4[3p14.1]); Dim(3)(77.71[3p12.3]-95.02[3p11.1]); Enh(3)(95.02[3q11.2]-199.38[3qter]); Dim X2(4)(69.2[4q13.2]-69.31[4q13.2]); Dim(5)(28.18[5p14.1]-29.8[5p13.3]); Dim(5)(132.29[5q23.3]-132.92[5q31.1]); Dim(5)(147.51[5q32]-150.55[5q33.1]); Enh(6)(32.56[6p21.32]-32.66[6p21.32]); Dim(6)(64.68[6q12]-78.57[6q14.1]); Dim(6)(82.06[6q14.1]-116.32[6q22.1]); Dim(6)(119.6[6q22.31]-164.88[6q27]); Dim(1)(166.48[6q27]-170.94[6q27]); Dim(7)(0.14[7pter]-10.45[7p21.3]); Dim(7)(108.27[7q31.1]-109.01[7q31.1]); Dim(8)(86.91[8q21.3]-87.49[8q21.3]); Dim(8)(105.21[8q22.3]-107.12[8q23.1]); Dim(8)(127.37[8q24.13]-127.95[8q24.13]); Amplified(8)(128.13[8q24.21]-130.34[8q24.21]); Enh(9)(0.15[9pter]-8.64[9p23]); Enh(9)(31.62[9p21.1]-138.4[9pter]); Enh(11)(0.18[11pter]-89.11[11q14.3]); Enh(11)(94.37[11q21]-95.8[11q22.1]); Enh(11)(102.66[11q22.3]-134.43[11qter]); Dim(12)(12.9[12p13.1]-17.19[12p12.3]); Dim(12)(128.23[12q24.32]-128.78[12q24.33]); Dim(13)(43.16[13q14.11]-76.65[13q31.1]); Enh(14)(75.93[14q24.3]-105.14[14q32.33]); Dim(14)(105.41[14q32.33]-105.88[14q32.33]); Enh(16)(31.96[16p11.2]-33.54[16p11.2]); Enh(18)(0.0[18pter]-27.4[18q12.1]); Enh(18)(58.06[18q21.33]-60.28[18q22.1]); Trisomy(19)(0.06-63.78); Enh(X)(123.77[Xq25]-154.49[Xqter])
1524	**MM**	**t(11;14)**	Enh(1)(141.47[1q21.1]-245.43[1qter]); Dim X2(1)(149.37[1q21.3]-149.4[1q21.3]); Dim(2)(88.98[2p11.2]-89.27[2p11.2]); Dim(2)(99.94[2q11.2]-100.01[2q11.2]); Dim(2)(111.62[2q13]-111.84[2q13]); Dim(2)(112.54[2q13]-112.72[2q13]); Dim(2)(112.98[2q13]-113.21[2q13]); Enh(3)(164.02[3q26.1]-164.1[3q26.1]); Dim(4)(0.04[4pter]-34.81[4p15.1]); Enh(4)(35.92[4p15.1]-42.89[4p13]); Enh(4)(47.6[4p12]-48.16[4p12]); Dim(4)(52.69[4q11]-71.66[4q13.3]); Dim X2(4)(69.2[4q13.2]-69.79[4q13.2]); Enh(4)(71.94[4q13.3]-190.29[4q35.2]); Enh(5)(0.08[5pter]-44.27[5p12]); Enh(5)(53.85[5q11.2]-55.54[5q11.2]); Dim(5)(55.97[5q11.2]-180.64[5q35.3]); Enh(6)(0.33[6p25.3]-28.65[6p22.1]); Dim(6)(77.53[6q14.1]-154.49[6q25.2]); Enh(6)(157.25[6q25.3]-170.94[6qter]); Dim(8)(0.06[8pter]-39.56[8p11.22]); Dim X2(8)(39.36[8p11.22]-39.51[8p11.22]); Enh(8)(110.93[8q23.2]-138.61[8q24.23]); Enh(11)(58.51[11q12.1]-133.96[11qter]); Dim(12)(0.03[12pter]-36.98[12q12]); Dim(12)(65.89[12q14.3]-88.41[12q21.33]); Dim(12)(89.13[12q21.33]-90.95[12q22]); Dim(12)(92.52[12q22]-94.13[12q22]); Dim(12)(95.27[12q23.1]-110.24[12q24.12]); Dim(12)(123.62[12q24.31]-132.39[12qter]); Monosomy(13)(18.07-114.12); Dim(14)(105.31[14q32.33]-105.59[14q32.33]); Enh(15)(18.81[15q11.2]-2.01[15q11.2]); Enh(15)(34.68[15q14]-100.28[15qter]); Dim(16)(0.03[16pter]-10.18[16p13.13]); Dim(16)(45.02[16q11.2]-88.69[16qter]); Dim(17)(0.03[17pter]-22.14[17p11.1]); Dim(18)(62.22[18q22.1]-76.11[18qter]); Dim(22)(20.72[22q11.22]-21.05[22q11.22]); Dim X2(22)(21.06[22q11.22]-21.56[22q11.22]); Enh(22)(22.67[22q11.23]-22.73[22q11.23]); Dim(22)(42.74[22q13.31]-42.86[22q13.31]); Monosomy(X)(2.69-154.49)
1300	**MM**	**t(11;14)**	Enh(1)(8.36[1p36.23]-9.09[1p36.23]); Enh(1)(32.14[1p35.1]-32.63[1p35.1]); Enh(3)(170.95[3q26.2]-171.56[3q26.2]); Enh(4)(153.89[4q31.3]-154.06[4q31.3]); Enh(6)(7.66[6p24.3]-8.24[6p24.3]); Enh(6)(31.62[6p21.33]-32.12[6p21.33]); Enh(6)(44.3[6p21.1]-44.34[6p21.1]); Enh(8)(33.26[8p12]-33.72[8p12]); Enh(8)(39.36[8p11.23]-39.51[8p11.22]); Enh(8)(66.81[8q13.1]-67.3[8q13.1]); Enh(8)(81.05[8q21.13]-81.56[8q21.13]); Enh(9)(123.85[9q33.3]-124.26[9q33.3]); Enh(10)(111.86[10q25.2]-112.35[10q25.2]); Enh(10)(125.77[10q26.13]-126.31[10q26.13]); Enh(11)(68.82[11q13.3]-134.43[11qter]); Enh(12)(11.69[12p13.2]-12.23[12p13.2]); Enh(12)(26.6[12p11.23]-27.15[12p11.23]); Enh(14)(104.99[14q32.33]-105.25[14q32.33]); Dim(14)(105.31[14q32.33]-105.63[14q32.33]); Enh(14)(105.71[14q32.33]-105.86[14q32.33]); Dim(14)(105.87[14q32.33]-106.35[14qter]); Enh(17)(18.81[17p11.2]-19.23[17p11.2]); Enh(17)(27.95[17q11.2]-28.49[17q11.2]); Enh(17)(40.55[17q21.31]-40.72[17q21.31]); Dim(22)(22.67[22q11.23]-22.73[22q11.23])
504	**MM**	**t(11;14)**	Dim(1)(16.79[1p36.13]-16.84[1p36.13]); Dim X2(2)(89.0[2p11.2]-89.33[2p11.2]); Dim X2(2)(242.64[2q37.3]-242.74[2q37.3]); Dim(5)(22.54[5p14.3]-22.6[5p14.3]); Dim(6)(29.96[6p22.1]-30.01[6p21.33]); Dim(8)(0.06[8pter]-26.79[8p21.2]); Enh(8)(39.36[8p11.22]-39.51[8p11.22]); Dim(9)(38.76[9p13.1]-43.09[9p13.1]); Enh(11)(69.13[11q13.3]-134.43[11qter]); Enh(12)(9.53[12p13.31]-9.61[12p13.31]); Enh(14)(21.56[14q11.2]-22.02[14q11.2]); Dim X2(14)(105.31[14q32.33]-105.93[14q32.33]); Dim(14)(105.95[14q32.33]-106.35[14qter]); Enh(15)(18.66[15q11.2]-20.08[15q11.2]); Dim(16)(58.03[16q21]-58.45[16q21]); Enh(17)(77.41[17q25.3]-77.5[17q25.3]); Dim X2(22)(22.67[22q11.23]-22.73[22q11.23]); Monosomy(X)(2.69-154.49)

308	**MM**	**t(11;14)**	Dim(1)(65.34[1p31.2]-66.72[1p31.2]); Dim(1)(93.11[1p22.1]-93.2[1p22.1]); Enh(1)(109.94[1p13.3]-109.97[1p13.3]); Dim(1)(117.73[1p12]-118.17[1p12]); Enh(1)(118.18[1p12]-118.34[1p12]); Enh(1)(176.82[1q25.2]-176.97[1q25.3]); Dim X2(1)(193.47[1q31.3]-193.53[1q31.3]); Dim(1)(244.95[1q44]-245.01[1q44]); Dim(2)(88.99[2p11.2]-89.08[2p11.2]); Enh(2)(130.63[2q21.1]-130.67[2q21.1]); Enh(2)(233.02[2q37.1]-233.13[2q37.1]); Enh(3)(170.95[3q26.2]-171.55[3q26.2]); Dim(4)(69.2[4q13.2]-69.31[4q13.2]); Dim(4)(109.31[4q25]-109.44[4q25]); Enh(4)(185.44[4q35.1]-186.14[4q35.1]); Dim X2(5)(69.74[5q13.2]-69.74[5q13.2]); Dim(5)(150.17[5q33.1]-180.64[5qter]); Enh(6)(32.03[6p21.32]-32.12[6p21.32]); Dim X2(6)(32.6[6p21.32]-32.63[6p21.32]); Dim(6)(35.61[6p21.31]-35.76[6p21.31]); Enh(7)(128.03[7q32.1]-128.15[7q32.1]); Dim(8)(7.26[8p23.1]-8.12[8p23.1]); Enh(8)(39.36[8p11.22]-39.51[8p11.22]); Enh(10)(134.89[10q26.3]-135.05[10q26.3]); Enh(11)(66.35[11q13.2]-66.99[11q13.2]); Dim(12)(41.63[12q12]-50.68[12q13.13]); Enh(12)(51.47[12q13.13]-51.99[12q13.13]); Dim(12)(52.01[12q13.13]-52.17[12q13.13]); Dim(13)(42.35[13q14.11]-114.12[13qter]); Dim X2(14)(105.31[14q32.33]-105.45[14q32.33]); Dim(14)(105.86[14q32.33]-106.24[14q32.33]); Enh(15)(22.96[15q11.2]-23.05[15q11.2]); Dim(15)(75.27[15q24.3]-75.41[15q24.3]); Enh(16)(28.48[16p11.2]-31.15[16p11.2]); Enh(16)(31.38[16p11.2]-31.41[16p11.2]); Enh(16)(31.96[16p11.2]-33.43[16p11.2]); Enh(17)(77.28[17q25.3]-77.65[17q25.3]); Enh(22)(22.58[22q11.23]-22.73[22q11.23]); Monosomy(X)(2.69-154.49)
2993	**MM**	**t(11;14)**	Dim(1)(149.37[1q21.3]-149.4[1q21.3]); Enh(2)(32.55[2p22.3]-33.23[2p22.3]); Dim(2)(88.99[2p11.2]-89.34[2p11.2]); Dim(3)(196.93[3q29]-196.97[3q29]); Dim(4)(17.95[4p15.32]-37.93[4p14]); Dim X2(4)(69.2[4q13.2]-69.31[4q13.2]); Dim(5)(27.73[5p14.1]-27.87[5p14.1]); Dim(5)(69.74[5q13.2]-70.62[5q13.2]); Dim(5)(128.32[5q23.3]-163.91[5q34]); Dim(5)(180.35[5q35.3]-180.36[5q35.3]); Dim(6)(134.17[6q23.2]-162.14[6q26]); Enh(8)(7.26[8p23.1]-7.79[8p23.1]); Dim(8)(12.63[8p22]-39.36[8p11.23]); Enh(8)(39.36[8p11.23]-39.51[8p11.23]); Dim(8)(113.96[8q23.3]-116.71[8q23.3]); Dim(9)(20.55[9p21.3]-23.56[9p21.3]); Enh(9)(127.23[9q34.11]-128.45[9q34.11]); Dim(11)(79.3[11q14.1]-104.33[11q22.3]); Enh(11)(110.02[11q23.1]-111.34[11q23.1]); Dim(12)(2.78[12p13.33]-22.22[12p12.1]); Dim(13)(18.07[13q11]-36.15[13q13.3]); Enh(14)(18.62[14q11.2]-19.5[14q11.2]); Dim(14)(105.33[14q32.33]-105.64[14q32.33]); Enh(15)(18.66[15q11.2]-20.08[15q11.2]); Dim(15)(32.52[15q14]-32.63[15q14]); Enh(16)(32.21[16p11.2]-33.54[16p11.2]); Dim(17)(40.74[17q21.31]-41.03[17q21.31]); Enh(17)(41.58[17q21.31]-41.84[17q21.31]); Dim(17)(56.75[17q23.2]-61.91[17q24.2]); Dim(19)(2.17[19p13.3]-2.21[19p13.3]); Enh(19)(15.3[19p13.12]-17.31[19p13.11]); Dim(19)(57.72[19q13.41]-63.78[19qter]); Dim(22)(21.37[22q11.22]-21.58[22q11.22]); Monosomy(X)(2.69-154.49)
932	**MM**	**t(11;14)**	Enh(1)(141.47[1q12]-157.11[1q23.2]); Dim X2(1)(149.37[1q21.3]-149.4[1q21.3]); Enh(1)(175.56[1q25.1]-175.81[1q25.1]); Dim X2(2)(88.99[2p11.2]-89.06[2p11.2]); Enh(3)(53.08[3p11]-53.25[3p11]); Enh(3)(164.0[3q26.1]-164.11[3q26.1]); Dim(4)(69.05[4q13.2]-69.84[4q13.2]); Dim(6)(29.96[6p22.1]-30.02[6p21.33]); Dim X2(6)(32.53[6p21.32]-32.73[6p21.32]); Enh(6)(150.25[6q25.1]-150.48[6q25.1]); Enh(7)(141.93[7q34]-141.98[7q34]); Enh(8)(39.51[8p11.23]-39.36[8p11.22]); Enh(8)(145.17[8q24.3]-145.77[8q24.3]); Enh(10)(7.44[10p14]-7.7[10p14]); Enh(12)(11.4[12p13.2]-11.44[12p13.2]); Monosomy(13)(18.07-114.12); Dim(14)(19.52[14q11.2]-106.35[14qter]); Dim X2(14)(105.34[14q32.33]-106.35[14q32.33]); Dim(15)(19.38[15q11.2]-20.08[15q11.2]); Dim(16)(45.02[16q11.2]-88.69[16qter]); Dim X2(16)(49.3[16q12.1]-49.43[16q12.1]); Enh(20)(3.0[20p13]-3.04[20p13]); Dim(22)(21.06[22q11.22]-21.54[22q11.22]); Monosomy(X)(2.69-154.49)
2906	**MM**	**t(11;14)**	Enh(1)(65.27[1p31.2]-67.22[1p31.2]); Dim(1)(83.45[1p31.1]-83.57[1p31.1]); Enh(1)(103.82[1p21.1]-103.88[1p21.1]); Dim(1)(151.8[1q22]-151.83[1q22]); Dim(1)(154.71[1q23.2]-155.25[1q23.2]); Dim(2)(89.0[2p11.2]-89.11[2p11.2]); Dim(2)(132.09[2q21.2]-132.23[2q21.2]); Enh(4)(69.22[4q13.2]-69.31[4q13.2]); Enh(6)(18.22[6p22.3]-19.0[6p22.3]); Dim(6)(32.52[6p21.32]-32.63[6p21.32]); Enh(6)(105.9[6q21]-106.79[6q21]); Enh(7)(24.66[7p15.2]-26.81[7p15.2]); Dim(7)(26.92[7p15.2]-26.99[7p15.2]); Enh(9)(36.81[9p13.2]-37.36[9p13.2]); Dim(9)(136.52[9p34.3]-136.54[9p34.3]); Dim(11)(65.07[11q13.2]-65.16[11q13.2]); Monosomy(13)(18.07-114.12); Dim(14)(19.27[14q11.2]-19.49[14q11.2]); Enh(14)(102.04[14q32.32]-102.82[14q32.32]); Dim(14)(105.33[14q32.33]-105.63[14q32.33]); Enh(17)(72.51[17q25.2]-72.81[17q25.2]); Enh(19)(10.18[19p13.2]-10.78[19p13.2]); Dim(21)(13.33[21q11.2]-14.44[21q11.2]); Enh(22)(17.26[22q11.21]-17.34[22q11.21]); Enh(22)(22.64[22q11.23]-23.63[22q11.23]); Enh(X)(48.43[Xp11.23]-48.51[Xp11.23]); Enh(X)(153.38[Xq28]-154.04[Xq28])
297	**MM**	**HRD**	Enh(1)(16.07[1p36.13]-16.13[1p36.13]); Enh(1)(149.36[1q21.3]-149.4[1q21.3]); Enh(1)(199.29[1q32.1]-199.35[1q32.1]); Trisomy(2)(0.02-242.78); Trisomy(3)(0.04-199.38); Dim(4)(135.3[4q28.3]-135.54[4q28.3]); Trisomy(5)(0.08-180.64); Enh(6)(0.1[6pter]-134.02[6q23.1]);

			Dim(6)(32.59[6p21.32]-32.63[6p21.32]); Enh(6)(161.56[6q26]-170.94[6qter]); Trisomy(7)(0.14-158.62); Dim(8)(7.04[8p23.1]-8.15[8p23.1]); Dim(8)(39.36[8p11.23]-39.48[8p11.23]); Enh(8)(126.97[8q24.13]-146.26[8qter]); Tetrasomy(9)(0.15-138.4); Trisomy(11)(0.18-134.43); Enh(12)(56.43[12q14.1]-56.46[12q14.1]); Dim(14)(105.34[14q32.33]-106.0[14q32.33]); Tetrasomy(15)(18.36-100.28); Enh(16)(29.06[16p11.2]-29.26[16p11.2]); Trisomy(19)(20.42-20.49); Enh(22)(17.04[22q11.21]-17.34[22q11.21]); Dim(22)(22.7[22q11.23]-22.72[22q11.23]); Enh(X)(52.78[Xp11.22]-52.83[Xp11.22])
506	**MM**	**HRD**	Enh(1)(0.97[1p36.33]-1.23[1p36.33]); Dim(1)(35.21[1p34.3]-35.69[1p34.3]); Dim(2)(233.36[2q37.1]-233.55[2q37.1]); Trisomy(5)(0.08-180.64); Enh(6)(45.63[6p21.1]-46.05[6p21.1]); Tetrasomy(7)(0.14-158.62); Dim(8)(7.04[8p23.1]-8.12[8p23.1]); Dim(8)(16.0[8p22]-16.06[8p22]); Enh(8)(126.62[8q24.13]-126.8[8q24.13]); Enh(8)(128.82[8q24.21]-128.87[8q24.21]); Tetrasomy(9)(0.15-138.4); Trisomy(11)(0.18-134.43); Monosomy(13)(18.07-114.12); Dim(14)(19.22[14q11.2]-19.5[14q11.2]); Dim X2(14)(105.32[14q32.33]-105.45[14q32.33]); Trisomy(15)(18.36-100.28); Dim(16)(45.02[16q11.1]-85.85[16qter]); Trisomy(19)(0.06-63.78); Trisomy(21)(13.33-46.91); Dim(22)(23.97[22q11.23]-24.47[22q12.1])
375	**MM**	**HRD**	Dim(1)(52.85[1p32.3]-141.47[1p11.1]); Enh(3)(164.0[3q26.1]-164.1[3q26.1]); Trisomy(4)(0.04-191.31); Dim(4)(69.2[4q13.2]-69.31[4q13.2]); Trisomy(5)(0.08-180.64); Enh(5)(76.12[5q13.3]-76.18[5q13.3]); Enh(5)(78.53[5q14.1]-112.51[5q22.2]); Dim(6)(29.96[6p21.33]-30.02[6p21.33]); Enh(6)(168.16[6q27]-168.39[6q27]); Trisomy(7)(0.14-158.62); Dim(8)(7.26[8p23.1]-7.79[8p23.1]); Enh(8)(39.36[8p11.22]-39.51[8p11.22]); Enh(8)(128.82[8q24.21]-128.92[8q24.21]); Trisomy(9)(0.15-138.4); Dim(10)(46.38[10q11.22]-47.01[10q11.22]); Enh(10)(105.99[10q25.1]-106.09[10q25.1]); Enh(11)(0.18[11pter]-34.89[11p13]); Enh(11)(54.79[11q11]-134.43[11qter]); Enh(12)(7.88[12p13.31]-8.01[12p13.31]); Dim(12)(26.6[12p11.23]-27.81[12p11.23]); Enh(14)(104.99[14q32.33]-105.28[14q32.33]); Dim(14)(105.33[14q32.33]-105.5[14q32.33]); Trisomy(15)(18.36-100.28); Amplified(16)(45.02[16q11.2]-46.08[16q12.1]); Enh(16)(50.65[16q12.1]-52.33[16q12.2]); Amplified(16)(65.24[16q22.1]-70.48[16q22.2]); Enh(16)(73.43[16q22.3]-79.37[16q23.2]); Enh(16)(46.08[16q12.1]-49.21[16q12.1]); Enh(17)(77.97[17q25.3]-78.11[17q25.3]); Trisomy(19)(0.06-63.78); Dim(20)(0.01[20pter]-19.63[20q11.23]); Enh(20)(19.63[20p11.23]-62.38[20qter]); Trisomy(21)(9.9-46.91); Enh(X)(96.39[Xq21.33]-154.49[Xqter])
824	**MM**	**HRD**	Dim(1)(30.85[1p35.2]-31.01[1p35.2]); Dim(1)(145.73[1q21.2]-146.53[1q21.2]); Dim(2)(45.08[2p21]-45.15[2p21]); Enh(2)(70.17[2p13.3]-70.38[2p13.3]); Dim(2)(89.0[2p11.2]-89.2[2p11.2]); Trisomy(3)(0.04-199.38); Enh(4)(185.56[4q35.1]-185.93[4q35.1]); Dim(4)(187.4[4q35.1]-187.46[4q35.1]); Trisomy(5)(1.93-180.64); Trisomy(7)(2.93-158.62); Enh(8)(7.04[8p23.1]-7.79[8p23.1]); Trisomy(9)(0.15-132.9); Enh(11)(3.32[11p15.5]-133.69[11qter]); Dim(14)(105.33[14q32.33]-105.43[14q32.33]); Trisomy(15)(19.82-100.2); Enh(15)(31.38[15q14]-73.29[15q23]); Dim(17)(0.03[17pter]-16.5[17p11.2]); Dim(17)(19.12[17p11.2]-20.55[17p11.2]); Enh(17)(20.57[17p11.2]-21.01[17p11.2]); Dim(17)(21.13[17p11.2]-21.72[17p11.2]); Enh(17)(21.84[17p11.2]-69.76[17q25.3]); Trisomy(19)(0.06-63.78); Dim(20)(59.18[20q13.33]-62.38[20q13.33]); Enh(22)(20.34[22q11.22]-21.73[22q11.22]); Dim(22)(21.88[22q11.23]-22.91[22q11.23])
1512	**MM**	**HRD**	Dim(1)(193.47[1q31.3]-193.53[1q31.1]); Dim(1)(199.09[1q32.1]-199.29[1q32.1]); Enh(2)(0.02[2pter]-15.29[2p24.3]); Dim(2)(15.29[2p24.3]-17.18[2p24.3]); Enh(2)(17.21[2p24.3]-44.52[2p21]); Enh(2)(45.85[2p21]-46.64[2p21]); Enh(2)(60.35[2p16.1]-62.42[2p15]); Enh(2)(64.15[2p14]-64.15[2p14]); Dim(2)(104.83[2q12.1]-107.4[2q12.3]); Enh(2)(111.21[2q13]-116.4[2q14.1]); Enh(2)(119.85[2q14.2]-123.31[2q14.3]); Enh(2)(126.35[2q14.3]-131.53[2q21.1]); Enh(2)(132.43[2q21.2]-132.86[2q21.2]); Dim(2)(133.54[2q21.2]-135.06[2q21.2]); Dim(2)(136.32[2q21.3]-137.44[2q21.3]); Enh(2)(137.86[2q22.1]-138.69[2q22.1]); Dim(2)(138.72[2q22.1]-139.09[2q22.1]); Enh(2)(139.1[2q22.1]-140.19[2q22.1]); Enh(2)(150.94[2q23.2]-242.78[2qter]); Trisomy(3)(0.04-199.38); Enh(4)(34.06[4p15.1]-34.44[4p15.1]); Enh(4)(43.2[4p13]-191.31[4qter]); Dim(4)(69.2[4q13.2]-69.79[4q13.2]); Enh(5)(0.08[5pter]-50.12[5q11.1]); Dim(6)(32.57[6p21.32]-32.63[6p21.32]); Enh(6)(95.64[6q16.1]-97.13[6q16.1]); Enh(6)(104.41[6q16.3]-106.5[6q21]); Dim(6)(106.6[6q21]-170.94[6qter]); Dim X2(8)(39.36[8p11.22]-39.51[8p11.22]); Dim(8)(47.58[8q11.21]-50.06[8q11.21]); Enh(8)(53.74[8q11.23]-56.46[8q12.1]); Dim(8)(62.7[8q12.3]-74.91[8q21.11]); Enh(8)(75.01[8q21.11]-87.87[8q21.3]); Amplified(8)(75.63[8q21.11]-76.19[8q21.11]); Amplified(8)(79.75[8q21.12]-81.16[8q21.13]); Amplified(8)(87.37[8q21.3]-87.87[8q21.3]); Dim(8)(88.08[8q21.3]-128.43[8q24.21]); Enh(8)(128.45[8q24.21]-128.5[8q24.21]); Dim(8)(128.51[8q24.21]-128.67[8q24.21]); Amplified(8)(128.77[8q24.21]-129.99[8q24.21]); Enh(8)(130.03[8q24.21]-132.04[8q24.22]); Enh(8)(134.42[8q24.22]-135.32[8q24.22]); Enh(8)(143.1[8q24.3]-146.09[8q24.3]); Trisomy(9)(0.15-138.4); Trisomy(11)(0.18-134.43); Amplified(11)(60.45[11q12.2]-61.2[11q12.3]);

			Amplified(11)(68.97[11q13.2]-70.44[11q13.4]); Dim(12)(61.14[12q14.1]-66.06[12q15]); Dim(12)(66.6[12q15]-82.48[12q21.31]); Monosomy(13)(18.07-114.12); Dim(14)(19.27[14q11.2]-19.5[14q11.2]); Dim(14)(105.34[14q32.33]-105.93[14q32.33]); Trisomy(15)(18.36-100.28); Enh(15)(33.58[15q14]-100.28[15qter]); Amplified(15)(62.78[15q22.31]-64.49[15q22.31]); Dim(17)(7.29[17p13.1]-8.76[17p13.1]); Dim(17)(19.38[17p11.2]-20.16[17p11.2]); Enh(17)(77.39[17q25.3]-77.65[17q25.3]); Enh(19)(0.06[19pter]-19.9[19p12]); Enh(19)(32.55[19q12]-63.78[19qter]); Trisomy(21)(9.9-46.91); Amplified(21)(14.29[21q11.2]-14.49[21q11.2]); Enh(21)(14.67[21q11.2]-14.7[21q11.2]); Enh(X)(94.02[Xq21.32]-154.49[Xqter])
491	**MM**	**HRD**	Enh(1)(28.71[1p35.3]-28.77[1p35.3]); Dim(1)(83.31[1p31.1]-83.58[1p31.1]); Enh(1)(141.47[1q12]-245.43[1qter]); Trisomy(2)(0.02-242.78); Dim(2)(89.0[2p11.2]-89.33[2p11.2]); Trisomy(3)(0.04-199.38); Dim(3)(164.0[3q26.1]-164.1[3q26.1]); Dim(4)(69.2[4q13.2]-69.31[4q13.2]); Enh(6)(0.1[6pter]-62.53[6p11.1]); Trisomy(7)(0.14-158.62); Dim(8)(7.04[8p23.1]-7.79[8p23.1]); Dim(8)(12.28[8p23.1]-12.51[8p23.1]); Dim(11)(49.11[11p11.12]-49.82[11p11.12]); Dim(11)(107.59[11q22.3]-107.92[11q22.3]); Monosomy(13)(18.07-114.12); Monosomy(14)(18.15-106.35); Dim X2(14)(19.27[14q11.2]-19.5[14q11.2]); Dim X2(14)(102.41[14q32.32]-102.59[14q32.32]); Dim X2(14)(105.31[14q32.33]-105.99[14q32.33]); Trisomy(15)(18.36-100.28); Trisomy(18)(0.0-76.11); Enh(19)(0.06[19pter]-32.55[19p12]); Enh(X)(52.78[Xp11.22]-52.84[Xp11.22]); Dim(Y)(2.69-57.37)
314	**MM**	**HRD**	Enh(1)(141.47[1q21.1]-181.66[1q25.3]); Enh(1)(194.46[1q31.3]-2455.43[1qter]); Dim(2)(89.0[2p11.2]-89.11[2p11.2]); Trisomy(5)(0.08-180.64); Trisomy(7)(0.14-158.62); Trisomy(9)(0.15-138.4); Trisomy(11)(0.18-134.43); Enh(12)(6.01[12p13.31]-6.94[12p13.31]); Monosomy(13)(18.07-114.12); Enh(14)(64.13[14q23.3]-65.17[14q23.3]); Enh(14)(104.21[14q32.33]-105.31[14q32.33]); Dim(14)(105.6[14q32.33]-106.17[14q32.33]); Trisomy(15)(18.36-100.28); Dim(16)(45.02[16q11.2]-88.69[16qter]); Trisomy(18)(0.0-76.11); Trisomy(19)(0.06-63.78); Enh(20)(31.63[20q11.21]-32.11[20q11.22]); Trisomy(21)(13.33-46.91); Monosomy(22)(14.5-49.51); Enh(X)(107.83[Xq23]-154.49[Xqter])
830	**MM**	**HRD**	Enh(1)(26.03[1p36.11]-26.25[1p36.11]); Enh(1)(116.86[1p12]-116.91[1p12]); Enh(1)(147.59[1q21.2]-147.69[1q21.2]); Dim(1)(193.47[1q31.3]-193.53[1q31.3]); Enh(1)(204.26[1q32.2]-204.35[1q32.2]); Dim(2)(34.61[2p22.3]-34.64[2p22.3]); Dim(2)(88.99[2p11.2]-89.44[2p11.2]); Enh(3)(13.38[3p25.2]-13.53[3p25.2]); Enh(3)(52.21[3p21.2]-52.28[3p21.2]); Enh(3)(164.04[3q26.1]-164.1[3q26.1]); Dim(3)(196.91[3q29]-196.95[3q29]); Trisomy(4)(0.04-191.31); Trisomy(5)(0.08-180.64); Enh(6)(7.82[6p24.3]-7.96[6p24.3]); Dim(6)(32.6[6p21.32]-32.66[6p21.32]); Enh(6)(167.58[6q27]-168.12[6q27]); Trisomy(7)(0.14-158.62); Enh(8)(39.36[8p11.22]-39.51[8p11.22]); Enh(8)(128.82[8q24.21]-128.91[8q24.21]); Trisomy(9)(0.15-138.4); Dim(11)(5.74[11p15.4]-5.77[11p15.4]); Enh(11)(66.04[11q13.2]-66.18[11q13.2]); Enh(12)(11.4[12p13.2]-11.43[12p13.2]); Monosomy(13)(18.07-114.12); Dim(14)(105.29[14q32.33]-105.58[14q32.33]); Dim(14)(105.99[14q32.33]-106.35[14qter]); Trisomy(15)(18.36-100.28); Enh(17)(41.55[17q21.31]-41.71[17q21.31]); Trisomy(19)(0.06-63.78); Enh(20)(31.88[20q11.22]-31.98[20q11.22]); Enh(22)(21.51[22q11.22]-21.7[22q11.22]); Dim(22)(37.68[22q13.1]-37.71[22q13.1]); Monosomy(X)(2.69-154.49)
883	**MM**	**HRD**	Dim(1)(93.52[1p22.1]-141.47[1p11.1]); Dim(2)(88.99[2p11.2]-89.91[2p11.2]); Enh(2)(233.06[2q37.1]-233.13[2q37.1]); Trisomy(3)(0.04-199.38); Trisomy(5)(0.08-180.64); Enh(6)(43.04[6p21.1]-43.11[6p21.1]); Dim(6)(79.04[6q14.1]-79.08[6q14.1]); Trisomy(7)(0.14-158.62); Trisomy(9)(0.15-138.4); Trisomy(11)(0.18-134.43); Dim(12)(31.66[12p11.21]-32.83[12p11.21]); Dim(12)(34.06[12p11.21]-34.32[12p11.21]); Enh(14)(103.61[14q32.33]-105.32[14q32.33]); Dim(14)(105.34[14q32.33]-105.38[14q32.33]); Trisomy(15)(18.36-100.28); Enh(16)(29.05[16p11.2]-29.26[16p11.2]); Dim(16)(45.02[16q11.2]-88.69[16qter]); Dim(17)(4.84[17p13.2]-5.39[17p13.2]); Dim(17)(7.5[17p13.1]-16.66[17p11.2]); Dim(17)(41.53[17q21.31]-42.14[17q21.31]); Trisomy(19)(0.06-63.78); Enh(X)(95.84[Xq21.33]-154.49[Xqter]); Enh(Y)(2.69-57.37)
2218	**MM**	**HRD**	Dim(2)(42.78[2p21]-44.76[2p21]); Trisomy(3)(0.04-199.38); Trisomy(5)(0.08-180.64); Enh(6)(168.16[6q27]-168.39[6q27]); Trisomy(7)(0.14-158.62); Dim(7)(153.37[7q36.2]-153.43[7q36.2]); Dim(8)(7.04[8p23.1]-8.12[8p23.1]); Dim(8)(39.36[8p11.22]-39.47[8p11.22]); Tetrasomy(9)(0.15-138.4); Trisomy(11)(0.18-134.43); Dim(11)(5.74[11p15.4]-5.76[11p15.4]); Dim(14)(105.34[14q32.33]-105.42[14q32.33]); Enh(14)(105.42[14q32.33]-105.47[14q32.33]); Dim(14)(105.48[14q32.33]-106.02[14q32.33]); Trisomy(15)(18.36-100.28); Trisomy(19)(0.06-63.78); Dim(22)(21.38[22q11.22]-21.54[22q11.22]); Enh(Y)(2.69-57.37)
989	**MM**	**HRD**	Dim(1)(16.88[1p36.13]-17.13[1p36.13]); Dim(1)(59.84[1p32.1]-62.70[1p31.3]); Dim(1)(88.59[1p22.2]-94.29[1p22.1]); Dim(1)(95.53[1p21.3]-113.44[1p13.2]); Dim(1)(114.05[1p13.2]-120.47[1p11.1]); Enh(1)(159.78[1q23.3]-159.91[1q23.3]); Dim(1)(210.64[1q32.3]-211.10[1q32.3]);

			Dim(2)(88.96[2p11.2]-89.03[2p11.2]); Trisomy(3)(0.04-199.38); Dim(4)(5.24[4p16.1]-37.14[4p14]); Dim(4)(70.18[4q13.2]-70.30[4q13.3]); Enh(4)(103.28[4q24]-103.74[4q24]); Enh(4)(130.56[4q28.2]-130.98[4q28.2]); Trisomy(5)(0.08-180.64); Enh(6)(35.57[6p21.32]-32.67[6p21.32]); Dim(6)(88.91[6q15]-170.47[6qter]); Enh(7)(0.14[7pter]-89.08[7q21.13]); Dim(7)(89.11[7q21.13]-91.40[7q21.2]); Enh(7)(91.40[7q21.2]-100.54[7q22.1]); Dim(7)(100.55[7q22.1]-104.38[7q22.2]); Enh(7)(104.40[7q22.2]-158.57[7qter]); Dim(8)(0.63[8pter]-47.06[8p11.1]); Enh(8)(39.36[8p11.22]-39.51[8p11.22]); Enh(9)(0.15[9pter]-44.17[9p11.1]); Enh(9)(44.17[9q11]-140.04[9qter]); Dim(10)(20.21[10p12.32]-21.73[10p12.32]); Enh(10)(45.48[10q11.21]-46.57[10q11.21]); Dim(10)(115.52[10q25.3]-115.68[10q25.3]); Enh(11)(0.18[11pter]-87.08[11q14.2]); Dim(11)(55.12[11q11.2]-55.20[11q11.1]); Enh(11)(90.04[11q14.3]-134.35[11qter]); Enh(12)(9.53[12p13.31]-9.63[12p13.31]); Dim(12)(18.36[12q23.1]-98.62[12q23.1]); Monosomy(13)(18.07-114.12); Dim(14)(31.82[14q13]-40.52[14q21.1]); Enh(14)(78.50[14q31.1]-80.35[14q31.1]); Dim(14)(19.27[14q11.2]-19.48[14q11.2]); Dim(14)(105.35[14q32.33]-105.45[14q32.33]); Dim X2(14)(105.60[14q32.33]-105.63[14q32.33]); Dim X2(14)(105.96[14q32.33]-106.00[14q32.33]); Trisomy(15); Enh(16)(31.81[16p11.2]-32.75[16p11.2]); Dim(16)(47.18[16q12.1]-51.13[16q12.1]); Dim(17)(36.54[17q21.2]-38.05[17q21.31]); Dim(17)(59.48[17q23.3]-61.57[17q24.2]); Enh(17)(77.41[17q25.3]-77.56[17q25.3]); Trisomy(19); Dim(20)(31.80[20q11.22]-50.18[20q13.2]); Trisomy(21); Enh X2(X)(92.36[Xq21.32]-154.14[Xqter])
1213	**MM**	**HRD**	Enh(1)(141.47[1q21.1]-245.43[1qter]); Dim(2)(224.44[2q36.2]-242.78[2qter]); Dim(3)(68.0[3p14.1]-68.64[3p14.1]); Dim(3)(177.44[3q26.32]-179.42[3q26.32]); Dim X2(3)(178.36[3q26.32]-178.40[3q26.32]); Enh(5)(0.08[5pter]-58.37[5q11.2]); Enh(5)(131.23[5q23.3]-142.17[5q31.3]); Enh X2(6)(0.1[6pter]-37.92[6p21.2]); Enh(6)(48.06[6p12.3]-103.2[6q16.3]); Dim(6)(103.63[6q16.3]-170.94[6qter]); Dim X2(6)(116.67[6q22.1]-116.71[6q22.1]); Dim(7)(32.44[7p14.3]-32.89[7p14.3]); Enh(8)(39.37[8p11.22]-39.51[8p11.22]); Enh(8)(128.27[8q24.21]-129.47[8q24.21]); Enh(9)(0.15[9pter]-15.56[9p22.3]); Dim(9)(120.57[9q33.2]-120.99[9q33.2]); Dim(12)(10.47[12p13.2]-10.49[12p13.2]); Dim(12)(85.45[12q21.32]-85.55[12q21.32]); Dim(13)(18.07[13CEP]-22.37[13q12.12]); Dim(13)(23.79[13q12.12]-114.12[13qter]); Dim X2(13)(55.20[13q21.1]-55.37[13q21.1]); Dim(14)(29.28[14q12]-29.46[14q12]); Dim(14)(38.78[14q21.1]-40.03[14q21.1]); Enh(14)(104.68[14q32.33]-105.31[14q32.33]); Dim X2(14)(105.33[14q32.33]-105.42[14q32.33]); Dim(14)(105.67[14q32.33]-106.35[14q32.33]); Trisomy(15)(18.36-100.28); Trisomy(19)(0.06-63.78); Dim(21)(20.82[21q21.1]-21.5[21q21.1]); Dim(21)(43.84[21q22.3]-46.91[21qter]); Dim(22)(41.56[22q13.2]-48.87[22q13.33]); Dim(X)(2.69[Xpter]-113.68[Xq23]); Dim X2(X)(44.68[Xp11.3]-44.83[Xp11.3]); Dim X2(X)(79.72[Xq21.1]-79.88[Xq21.1]); Enh(X)(113.69[Xq33]-154.49[Xqtel]); Dim(X)(122.16[Xq25]-122.96[Xq25])
325	**pPCL**	**t(11;14)**	Dim X2(1)(149.37[1q21.3]-149.4[1q21.3]); Dim X2(1)(165.96[1q24.2]-165.99[1q24.2]); Dim X2(1)(245.06[1q44]-245.13[1q44]); Dim(2)(89.0[2p11.2]-89.33[2p11.2]); Dim(3)(60.36[3p14.2]-60.56[3p14.2]); Dim(4)(69.2[4q13.2]-69.31[4q13.2]); Dim(5)(69.74[5q13.2]-70.62[5q13.2]); Dim(6); Dim(7)(0.14[7pter]-20.19[7p21.1]); Dim(8)(7.26[8p23.1]-8.12[8p23.1]); Dim X2(8)(39.36[8p11.22]-39.51[8p11.22]); Enh(8)(96.83[8q22.1]-146.26[8qter]); Amplified(8)(124.98[8q24.13]-129.42[8q24.21]); Dim(10)(46.37[10q11.22]-46.57[10q11.22]); Enh(11)(69.1[11q13.3]-134.43[11qter]); Enh(14)(104.39[14q32.33]-105.28[14q32.33]); Dim(14)(105.31[14q32.33]-106.35[14qter]); Enh(15)(64.66[15q23]-67.15[15q23]) ; Enh(16)(32.11[16p11.2]-33.76[16p11.2]); Dim(17)(41.71[17q21.31]-42.18[17q21.31]); Enh(19)(1.59[19p13.3]-2.35[19p13.3]); Enh(19)(63.06[19q13.43]-63.78[19q13.43]); Enh(20)(43.97[20q13.12]-46.79[20q13.13]); Dim(X)(76.61[Xq21.1]-76.81[Xq21.1]); Enh(X)(114.29[Xq23]-154.49[Xqter])
1576	**pPCL**	**t(11;14)**	Enh(1)(142.58[1q21.1]-148.1[1q21.3]); Dim(2)(88.98[2p11.2]-91.12[2p11.2]); Enh(2)(99.3[2q11.2]-99.38[2q11.2]); Enh(3)(14.85[3p25.1]-15.88[3p25.1]); Enh(4)(0.04[4pter]-154.56[4q31.3]); Dim(4)(69.2[4q13.2]-69.31[4q13.2]); Enh(6)(0.1[6pter]-31.71[6p21.32]); Dim X2(6)(32.57[6p21.32]-32.73[6p21.32]); Enh(6)(151.48[6q25.1]-152.74[6q25.2]); Dim X2(8)(39.36[8p11.22]-39.51[8p11.22]); Enh(8)(128.45[8q24.21]-129.38[8q24.21]); Trisomy(9)(0.15-138.4); Enh(10)(5.39[10p15.1]-6.38[10p15.1]); Enh(11)(68.74[11q13.3]-73.19[11q13.4]); Enh(11)(94.87[11q21]-134.18[11q25]); Dim X2(12)(11.4[12p13.2]-11.43[12p13.2]); Dim(13)(33.0[13q13.1]-114.12[13qter]); Enh(14)(22.1[14q11.2]-23.17[14q11.2]); Enh(14)(104.79[14q32.33]-105.18[14q32.33]); Dim(14)(105.29[14q32.33]-105.8[14q32.33]); Dim(16)(0.03[16pter]-10.3[16p13.2]); Enh(16)(10.33[16p13.13]-31.25[16p11.2]); Dim(16)(34.1[16p11]-34.63[16p11]); Dim(16)(46.11[16q12.1]-49.0[16q12.1]); Dim(16)(56.07[16q13]-88.69[16qter]); Enh(17)(41.52[17q21.31]-41.57[17q21.31]); Dim(20)(34.35[20q11.23]-62.38[20qter]);

			Trisomy(21)(9.9-46.91); Enh(22)(17.26[22q11.21]-17.39[22q11.21]); Dim(22)(23.06[22q11.23]-34.64[22q12.3])
3210	**pPCL**	**t(11;14)**	Dim(1)(8.41[1p36.23]-8.55[1p36.23]); Dim(1)(33.33[1p35.1]-97.02[1p21.3]); Dim X2(1)(51.14[1p32.3]-51.16[1p32.3]); Dim(1)(106.05[1p21.1]-141.47[1p11.1]); Dim(1)(149.37[1q21.3]-149.4[1q21.3]); Dim(1)(159.29[1q23.3]-159.46[1q23.3]); Enh(2)(0.02[2pter]-15.95[2p24.3]); Dim(2)(35.44[2p22.3]-35.53[2p22.3]); Dim(2)(89.0[2p11.2]-89.34[2p11.2]); Dim(2)(114.33[2q14.1]-114.37[2q14.1]); Dim(2)(127.35[2q14.3]-128.99[2q21.1]); Dim(2)(160.27[2q24.2]-163.04[2q24.2]); Dim(2)(196.31[2q32.3]-201.53[2q33.2]); Dim(3)(22.92[3p24.3]-23.36[3p24.3]); Dim(3)(161.42[3q25.33]-161.63[3q25.33]); Dim(4)(30.32[4p15.1]-30.54[4p15.1]); Dim(4)(43.81[4p13]-49.42[4p11]); Dim(4)(69.2[4q13.2]-69.31[4q13.2]); Enh(4)(102.98[4q24]-105.96[4q24]); Dim(4)(135.3[4q28.3]-135.54[4q28.3]); Dim(4)(162.23[4q32.2]-166.33[4q32.3]); Enh(6)(79.04[6q14.1]-79.08[6q14.1]); Dim(6)(79.75[6q14.1]-79.82[6q14.1]); Dim(6)(85.77[6q14.3]-86.42[6q14.3]); Dim(6)(90.11[6q15]-170.94[6qter]); Dim(7)(29.93[7p15.1]-30.57[7p14.3]); Dim(7)(110.16[7q31.1]-110.42[7q31.1]); Dim X2(8)(0.06[8pter]-1.12[8p23.3]); Dim(8)(3.05[8p23.2]-26.07[8p21.2]); Dim X2(8)(39.36[8p11.22]-39.51[8p11.22]); Dim(9)(0.15[9pter]-32.16[9p21.1]); Enh(9)(136.67[9q34.3]-136.7[9q34.3]); Monosomy(10)(0.12-135.4); Enh(11)(69.08[11q13.1]-99.58[11q22.1]); Dim(12)(0.03[12pter]-20.8[12p12.2]); Dim(12)(31.27[12p11.21]-46.89[12q13.12]); Dim X2(12)(36.98[12q12]-37.2[12q12]); Enh(12)(48.7[12q13.12]-51.67[12q13.13]); Dim(12)(57.97[12q14.1]-110.06[12q24.12]); Monosomy(13)(18.07-114.12); Enh(14)(18.5[14q11.1]-19.54[14q11.2]); Dim(14)(25.91[14q12]-27.99[14q12]); Dim X2(14)(51.97[14q22.1]-52.06[14q22.1]); Dim X2(14)(54.93[14q22.3]-54.96[14q22.3]); Enh(14)(86.41[14q31.3]-105.4[14q32.33]); Dim(14)(105.41[14q32.33]-106.11[14q32.33]); Dim(15)(18.72[15q11.2]-20.22[15q11.2]); Dim(16)(33.21[16p11.2]-33.4[16p11.2]); Dim(16)(45.06[16q12.1]-88.62[16qter]); Dim X2(16)(54.35[16q12.2]-54.38[16q12.2]); Dim(17)(0.03[17pter]-38.58[17q21.31]); Dim(18)(25.08[18q12.1]-25.46[18q12.1]); Enh(18)(47.96[18q21.1]-76.11[18qter]); Monosomy(22)(15.4-49.51); Dim X2(22)(21.49[22q11.22]-21.56[22q11.22]); Dim X2(22)(22.7[22q11.23]-22.71[22q11.23]); Monosomy(X)(2.69-154.49)
742	**pPCL**	**HRD**	Enh(1)(141.47[1q11]-245.43[1qter]); Dim(1)(145.82[1q21.1]-145.99[1q21.2]); Enh(1)(16.95[1p36.13]-1.7[1p36.13]); Enh(1)(117.41[1p12]-117.49[1p12]); Trisomy(2)(0.02-242.78); Trisomy(3)(2.16-199.38); Dim(3)(85.93[3p12.1]-86.1[3p12.1]); Dim(4)(69.2[4q13.2]-69.31[4q13.2]); Enh(5)(133.89[5q31.1]-134.03[5q31.1]); Enh(5)(156.75[5q33.3]-157.25[5q33.3]); Enh(6)(0.1[6pter]-63.69[6q12]); Trisomy(7)(0.14-158.62); Dim(8)(0.06[8pter]-48.07[8q11.21]); Dim X2(8)(25.21[8p12.2]-26.22[8p12.2]); Enh(8)(39.36[8p11.22]-39.51[8p11.22]); Enh(8)(48.12[8q11.21]-59.55[8q12.1]); Dim(8)(59.55[8q12.1]-65.84[8q12.3]); Enh(8)(65.85[8q12.3]-146.26[8qter]); Enh(9)(0.15[9pter]-94.03[9q22.31]); Enh(9)(94.84[9q22.32]-95.99[9q22.33]); Enh(9)(105.81[9q31.2]-106.88[9q31.2]); Enh(9)(113.62[9q32]-130.15[9q34.12]); Enh(9)(136.83[9q34.3]-138.4[9qter]); Dim(10)(42.15[10q11.21]-69.39[10q21.3]); Enh(10)(70.82[10q22.1]-70.95[10q22.1]); Dim(10)(97.67[10q24.1]-97.91[10q24.1]); Dim X2(10)(100.68[10q24.2]-100.69[10q24.2]); Tetrasomy(11)(0.18-134.43); Dim(12)(81.94[12q21.31]-83.82[12q21.31]); Dim(14)(73.07[14q24.3]-73.1[14q24.3]); Tetrasomy(15)(18.36[15pter]-100.28[15qter]); Enh(16)(55.26[16q131]-55.7[6q13]); Dim(16)(68.71[16q22.1]-68.75[16q22.1]); Dim(16)(69.76[16q22.2]-73.52[16q23.1]); Enh(17)(22.32[17q11.2]-25.61[17q11.2]); Enh(17)(37.83[17q21.2]-78.65[17qter]); Trisomy(18)(0.0-76.11); Trisomy(19)(0.06-63.78); Trisomy(20)(0.01-62.38); Trisomy(21)(9.9-46.91); Enh(22)(21.57[22q11.22]-22.13[22q11.23]); Enh(22)(22.61[22q11.23]-22.67[22q11.23]); Monosomy(X)(2.69-154.49)
165	**pPCL**	**HRD**	Enh(1)(12.79[1p36.21]-12.85[1p36.21]); Dim(1)(25.35[1p36.11]-25.41[1p36.11]); Dim(1)(97.55[1p21.3]-119.47[1p12]); Enh(1)(141.47[1q12]-245.43[1qter]); Dim(1)(193.47[1q31.3]-193.56[1q31.3]); Dim X2(1)(245.05[1q44]-245.12[1q44]); Enh(2)(233.07[2q27.1]-233.13[2q27.1]); Trisomy(3)(0.04-199.38); Dim(4)(53.18[4q12]-54.45[4q12]); Dim X2(4)(69.2[4q13.2]-69.31[4q13.2]); Enh(4)(69.84[4q13.2]-70.9[4q13.3]); Dim(4)(189.59[4q35.2]-190.86[4q35.2]); Enh(5)(0.08[5pter]-103.98[5q21.3]); Enh(5)(161.34[5q34]-180.64[5qter]); Enh(6)(0.1[6pter]-66.67[6q12]); Dim(6)(52.78[6p12.2]-52.88[6p12.2]); Dim(6)(56.35[6p12.1]-56.43[6p12.1]); Dim(6)(66.67[6q12]-170.94[6qter]); Dim(7)(0.14[7pter]-18.97[7p21.1]); Enh(7)(18.97[7p21.1]-140.37[7q34]); Enh(7)(142.42[7q35]-145.39[7q35]); Enh(7)(152.92[7q36.2]-157.93[7q36.3]); Dim(8)(19.02[8p21.3]-43.65[8p11.1]); Dim X2(8)(39.36[8p11.22]-39.51[8p11.22]); Dim(9)(132.97[9q34.2]-132.99[9q34.2]); Dim(10)(96.5[10q23.33]-96.56[10q23.33]); Dim(11)(5.74[11p15.4]-5.76[11p15.4]); Enh(12)(6.34[12p13.31]-7.13[12p13.31]); Dim(12)(126.9[12q24.32]-128.09[12q24.32]); Monosomy(13)(18.07-114.12); Dim(14)(19.27[14q11.2]-19.49[14q11.2]); Enh(14)(104.21[14q32.33]-105.31[14q32.33]); Dim(14)(105.41[14q32.33]-105.63[14q32.33]); Enh(14)(105.71[14q32.33]-105.9[14q32.33]); Dim(14)(105.96[14q32.33]-

			106.06[14q32.33]); Dim(15)(18.36[15q11.2]-32.46[15q14]); Dim(15)(77.0[15q25.1]-77.52[15q25.1]); Dim(15)(77.95[15q25.1]-78.31[15q25.1]); Dim(15)(81.5[15q25.2]-100.28[15qter]); Dim(18)(10.58[18p11.22]-10.82[18p11.22]); Dim(18)(35.13[18p12.2]-35.45[18p12.2]); Trisomy(19)(0.06-63.78); Dim(19)(23.42[19p12]-23.83[19p12]); Dim X2(20)(1.52[20p13]-1.53[20p13]); Dim(22)(21.37[22q11.22]-21.51[22q11.22]); Enh(22)(22.61[22q11.23]-22.75[22q11.23]); Enh(22)(41.22[22q13.2]-41.27[22q13.2]); Enh(X)(2.69[Xpter]-11.42[Xq22.2]); Enh(X)(140.46[Xq27.2]-154.49[Xqter])
2359	**pPCL**	**t(14;16)**	Enh(1)(16.95[1p36.13]-17.02[1p36.13]); Enh(1)(25.36[1p36.11]-25.41[1p36.11]); Enh(1)(141.47[1q12]-156.56[1q23.2]); Dim(1)(156.57[1q23.2]-158.29[1q23.3]); Enh(1)(158.31[1q23.3]-164.67[1q24.2]); Dim(1)(164.67[1q24.2]-196.88[1q25.2]); Enh(1)(175.52[1q25.2]-175.62[1q25.2]); Dim(1)(175.62[1q25.2]-187.41[1q31.2]); Dim(1)(188.03[1q31.2]-194.6[1q31.3]); Dim X2(1)(194.6[1q31.3]-196.88[1q32.1]); Dim(1)(199.19[1q32.1]-199.22[1q32.1]); Dim X2(2)(34.61[2p22.3]-34.67[2p22.3]); Dim(2)(88.98[2p11.2]-89.2[2p11.2]); Dim(3)(164.05[3q36.1]-164.1[3q36.1]); Dim(3)(184.92[3q27.1]-199.38[3qter]); Dim(5)(119.26[5q23.1]-119.62[5q23.1]); Enh(5)(180.03[5q35.3]-180.15[5q35.3]); Dim X2(5)(180.35[5q35.3]-180.36[5q35.3]); Dim X2(6)(32.56[6p21.32]-32.75[6p21.32]); Dim(8)(0.06[8pter]-47.06[8p11.1]); Dim X2(8)(39.36[8p11.23]-39.51[8p11.22]); Enh(8)(47.06[8q11.1]-146.26[8qter]); Dim(9)(136.9[9q34.3]-137.09[9q34.3]); Enh(10)(56.12[10q21.1]-56.16[10q21.1]); Enh(11)(72.02[11q13.4]-134.43[11qter]); Dim(12)(0.02[12pter]-4.41[12p13.32]); Dim(12)(5.19[12p13.32]-16.31[12p12.3]); Dim(12)(17.87[12p12.3]-25.61[12p12.1]); Dim(12)(27.17[12p11.23]-28.47[12p11.22]); Dim(12)(32.84[12p11.1]-33.4[12p11.1]); Enh(12)(8.6[12q21.32]-126.61[12q24.32]); Dim(12)(126.64[12q24.32]-132.39[12qter]); Dim(13)(22.02[13q12.11]-80.53[13q31.1]); Dim X2(13)(47.8[13q14.2]-47.9[13q14.2]); Enh(13)(85.05[13q31.1]-114.12[13qter]); Dim(14)(19.27[14q11.2]-19.48[14q11.2]); Dim(14)(105.18[14q32.33]-106.35[14qter]); Enh(15)(18.66[15q11.2]-19.81[15q11.2]); Dim(15)(19.81[15q11.2]-20.22[15q11.2]); Dim(16)(0.51[16p13.3]-0.05[16p13.3]); Enh(16)(32.11[16p11.2]-33.53[16p11.2]); Dim(16)(45.02[16q11.2]-77.46[16q23.1]); Dim(17)(0.03[17pter]-1.63[17p13.3]); Dim(17)(7.19[17p13.1]-7.22[17p13.1]); Dim(17)(7.33[17p13.1]-15.42[17p12]); Dim(17)(21.09[17p11.2]-21.63[17p11.2]); Enh(18)(0.0[18pter]-61.37[18q22.1]); Dim(18)(61.4[18q22.1]-76.11[18qter]); Enh(22)(17.04[22q11.21]-17.39[22q11.21]); Dim(22)(20.24[22q11.21]-32.79[22q12.3]); Dim(X)(90.84[Xq21.31]-92.1[Xq21.31]); Enh(X)(97.65[Xq21.33]-154.49[Xqter])
3125	**pPCL**	**t(14;16)**	Dim(1)(50.64[1p32.3]-51.19[1p32.3]); Dim(1)(83.33[1p31.1]-83.58[1p31.1]); Enh(1)(141.52[1q12]-145.65[1q23.3]); Dim(1)(145.65[1q21.2]-146.01[1q21.2]); Dim(1)(193.49[1q31.1]-193.56[1q31.1]); Dim(2)(88.99[2p11.2]-8.91[2p11.2]); Enh(3)(185.32[3q27.2]-185.56[3q27.2]); Dim(4)(70.33[4q13.3]-70.41[4q13.3]); Dim(5)(87.79[5q14.3]-148.72[5q32]); Dim X2(5)(146.7[5q32]-148.21[5q32]); Dim(6)(32.56[6p21.32]-32.73[6p21.32]); Dim(8)(7.36[8p23.1]-8.12[8p23.1]); Dim(10)(0.12[10p15.3]-38.6[10p11.1]); Dim(11)(111.42[11q23.1]-111.49[11q23.1]); Enh(12)(9.53[12p13.31]-9.61[12p13.31]); Dim(14)(19.27[14q11.2]-19.5[14q11.2]); Enh(14)(21.72[14q11.2]-22.02[14q11.2]); Dim(14)(105.31[14q32.33]-105.99[14q32.33]); Dim(16)(34.06[16p11.2]-45.02[16p11.2]); Dim(16)(65.39[16q22.1]-68.09[16q22.1]); Dim(16)(77.64[16q23.1]-77.84[16q23.1]); Enh(17)(44.02[17q21.32]-78.65[17qter]); Dim(X)(88.16[Xq21.31]-90.84[Xq21.31])
3343	**pPCL**	**t(14;16)** **t(8;14)**	Dim(1)(82.13[1p31.1]-82.62[1p31.1]); Dim(1)(88.33[1p22.2]-144.83[1q21.1]); Dim(1)(149.37[1q21.3]-149.4[1q21.3]); Enh(1)(158.3[1q23.3]-158.38[1q23.3]); Dim(1)(165.1[1q24.2]-168.72[1q25.1]); Dim(1)(173.88[1q25.2]-176.71[1q25.3]); Dim(1)(199.09[1q32.1]-199.25[1q32.1]); Dim(2)(89.0[2p11.2]-89.33[2p11.2]); Dim(4)(91.48[4q22.1]-91.65[4q22.1]); Dim(5q13.2); Dim(7)(0.14[7pter]-13.01[7p21.3]); Enh(7)(127.69[7q32.1]-158.62[7qter]); Monosomy(8)(0.06-146.26); Dim X2(8)(39.36[8p11.22]-39.51[8p11.22]); Normal(8)(128.81[8q24.21]-129.7[8q24.21]); Enh(10)(46.37[10q11.22]-47.74[10q11.22]); Dim(12)(11.4[12p13.2]-11.44[12p13.2]); Monosomy(13)(18.07-114.12); Enh(14)(18.5[14q11.2]-19.49[14q11.2]); Dim(14)(42.54[14q21.2]-42.8[14q21.2]); Enh(14)(104.95[14q32.33]-105.29[14q32.33]); Dim(14)(105.41[14q32.33]-106.17[14q32.33]); Dim(15)(19.41[15q11.2]-20.08[15q11.2]); Enh(15)(75.28[15q24.3]-77.09[15q25.1]); Dim(16)(27.42[16p12.1]-27.55[16p12.1]); Dim(16)(45.06[16q11.2]-88.69[16qter]); Normal(16)(77.15[16q23.1]-77.37[16q23.1]); Enh(17)(21.25[17p11.2]-21.47[17p11.2]); Dim X2(22)(22.67[22q11.23]-22.71[22q11.23])
3272	**pPCL**	**nonHRD**	Enh(1)(141.47[1q12]-182.87[1q31.1]); Dim X2(1)(149.37[1q21.3]-149.4[1q21.3]); Dim(1)(182.89[1q31.1]-186.42[1q31.1]); Enh(1)(186.59[1q31.1]-188.86[1q31.2]); Dim(1)(188.96[1q31.2]-195.14[1q31.3]); Enh(1)(195.17[1q32.1]-208.32[1q32.3]); Dim(1)(208.34[1q32.3]-218.0[1q41]); Enh(1)(218.17[1q41]-227.09[1q42.2]); Dim(1)(227.12[1q42.2]-232.13[1q43]); Enh(1)(232.25[1q42.3]-245.43[1qter]); Dim X2(2)(88.98[2p11.2]-

			89.33[2p11.2]); Dim(2)(116.05[2q14.1]-116.18[2q14.1]); Enh(3)(0.04[3pter]-83.81[3p12.1]); Dim(3)(164.04[3q26.1]-164.11[3q26.1]); Dim(3)(178.21[3q26.32]-178.41[3q26.32]); Dim(3)(181.62[3q26.33]-199.38[3qter]); Dim(4)(70.33[4q13.3]-70.41[4q13.3]); Dim(5)(140.2[5q31.2]-140.21[5q31.2]); Trisomy(7)(0.14-158.62); Dim(8)(128.83[8q24.21]-128.97[8q24.21]); Dim(11)(83.76[11q14.1]-84.25[11q14.1]); Monosomy(12)(0.03-132.39); Monosomy(13)(18.07-114.12); Enh(14)(21.5[14q11.2]-22.07[14q11.2]); Dim(14)(105.28[14q32.33]-105.79[14q32.33]); Dim(15)(18.75[15q11.2]-19.87[15q11.2]); Dim(16)(68.73[16q22.1]-68.75[16q22.1]); Dim(16)(72.93[16q22.3]-73.01[16q22.3]); Enh(19)(0.06[19pter]-23.4[19p12]); Dim(19)(52.33[19q13.32]-63.78[19qter]); Dim(20)(0.01[20pter]-13.75[20p12.1]); Dim(22)(20.88[22q11.22]-21.57[22q11.22]); Dim(22)(37.68[22q13.1]-37.71[22q13.1])
3342	**pPCL**	**t(4;14)**	Enh(1)(141.47[1q12]-245.43[1qter]); Dim X2(2)(89.0[2p11.2]-89.16[2p11.2]); Dim(3)(196.91[3q29]-196.97[3q29]); Dim X2(4)(69.2[4q13.2]-69.79[4q13.2]); Dim(4)(181.46[4q34.3]-181.72[4q34.3]); Enh(6)(32.57[6p21.32]-32.67[6p21.32]); Dim X2(6)(165.7[6q27]-165.7[6q27]); Dim(7)(41.78[7p14.1]-41.87[7p14.1]); Dim X2(7)(141.22[7q34]-141.25[7q34]); Dim(7)(151.56[7q36.1]-151.88[7q36.2]); Enh(8)(39.36[8p11.22]-39.51[8p11.22]); Dim(9)(9.3[9p23]-9.47[9p23]); Dim X2(12)(9.53[12p13.31]-9.59[12p13.31]); Dim(12)(19.5[12p12.3]-19.54[12p12.3]); Dim(12)(95.14[12q23.1]-95.28[12q23.1]); Dim(12)(113.41[12q24.21]-132.39[12qter]); Monosomy(13)(18.07-114.12); Dim X2(13)(47.85[13q14.2]-47.95[13q14.2]); Enh(14)(18.64[14q11.2]-19.5[14q11.2]); Dim(14)(105.31[14q32.33]-105.85[14q32.33]); Enh(15)(18.72[15q11.2]-20.08[15q11.2]); Enh(15)(54.5[15q21.3]-54.54[15q21.3]); Dim(16)(45.02[16q11.2]-88.69[16qter]); Enh(16)(69.41[16q22.2]-69.75[16q22.2]); Dim(17)(0.03[17pter]-21.74[17p11.1]); Dim X2(19)(56.83[19q13.41]-56.84[19q13.41]); Enh(20)(48.72[20q13.13]-62.38[20qter]); Enh(22)(22.67[22q11.23]-22.73[2q11.23]); Enh(22)(23.98[22q11.23]-24.23[22q11.23]); Dim(X)(81.84[Xq21.1]-124.15[Xq25]); Enh(X)(152.0[Xq28]-154.49[Xq28])
1188	**sPCL**	**t(11;14)**	Dim(1)(16.79[1p36.13]-16.84[1p36.13]); Enh(1)(16.95[1p36.13]-17.0[1p36.13]); Dim X2(1)(19.35[1p36.13]-19.36[1p36.13]); Enh(1)(149.37[1q21.3]-149.4[1q21.3]); Dim(1)(229.37[1q42.2]-237.78[1q43]); Enh(1)(244.16[1q44]-244.63[1q44]); Enh(2)(74.58[2p13.1]-74.67[2p13.1]); Dim X2(2)(89.0[2p11.2]-89.11[2p11.2]); Dim X2(3)(164.0[3q26.1]-164.1[3q26.1]); Dim X2(4)(13.24[4p15.33]-13.26[4p15.33]); Dim(4)(145.2[3q31.21]-145.34[3q31.21]); Enh(6)(27.87[6p22.1]-27.98[6p22.1]); Enh(6)(30.63[6p22.1]-30.65[6p21.33]); Enh(6)(33.49[6p21.32]-33.5[6p21.32]); Dim(7)(3.85[7p22.2]-3.86[7p22.2]); Enh(8)(2.34[8p23.2]-2.9[8p23.2]); Enh(8)(39.36[8p11.22]-39.51[8p11.22]); Dim(8)(52.77[8q11.22]-53.13[8q11.22]); Dim(8)(84.6[8q21.13]-85.33[8q21.2]); Dim(8)(108.35[8q23.1]-108.81[8q23.1]); Dim(8)(129.09[8q24.21]-129.22[8q24.21]); Trisomy(11)(0.18-134.43); Trisomy(13)(18.07-114.12); Dim(14)(105.34[14q32.33]-106.22[14q32.33]); Enh(15)(19.81[15q11.2]-20.08[15q11.2]); Dim(16)(68.73[16q22.1]-68.75[16q22.1]); Enh(17)(31.44[17q12]-31.5[17q12]); Dim(17)(36.76[17q21.2]-36.78[17q21.2]); Tetrasomy(18)(0.0-76.11); Dim(22)(21.47[22q11.22]-21.58[22q11.22]); Enh(22)(22.61[22q11.22]-22.73[22q11.22]); Enh(X)(134.53[Xq26.3]-134.64[Xq26.3])

Appendix 9: Graphical representation of array CGH results for all patient groups

The 850-band idiogram of the G-banding pattern of the chromosome is shown on the left. Vertical light-blue lines correspond to each patient; red bars = gains; thicker red bars = gains of two extra copies or more; green bars = mono-allelic losses; black areas circled in red = HD; yellow and light blue areas = CNV, respectively losses and gains; dark blue areas circled in black = amplifications. Black vertical lines separate the different genetic groups. From left to right: pre-malignant patients, MM and PCL. Patients from the MGUS/SMM and MM groups were ordered as follow (from left to right): t(4;14), t(14;16), t(14;20), IgHt with unidentified partner, t(6;14)/t(11;14) and HRD.

Chromosome 1

Chromosome 2

Chromosome 3

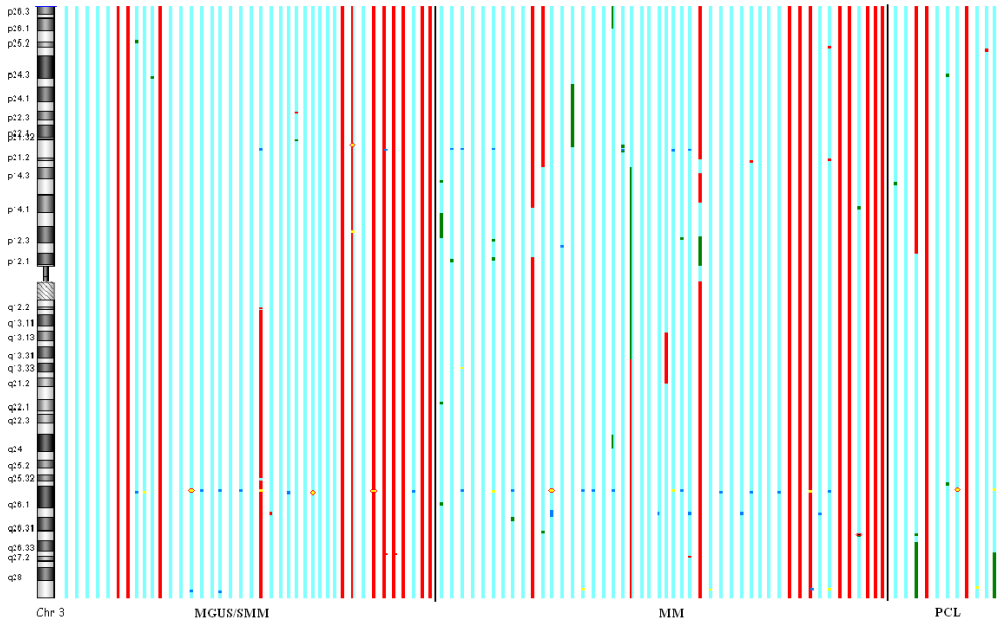

Chromosome 4

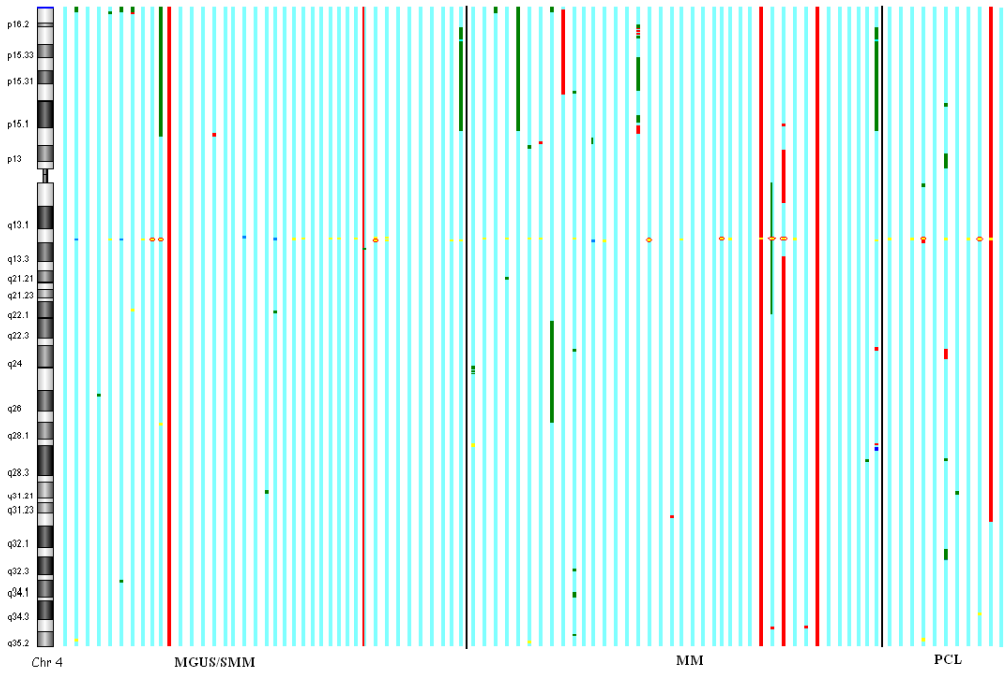

Chromosome 5

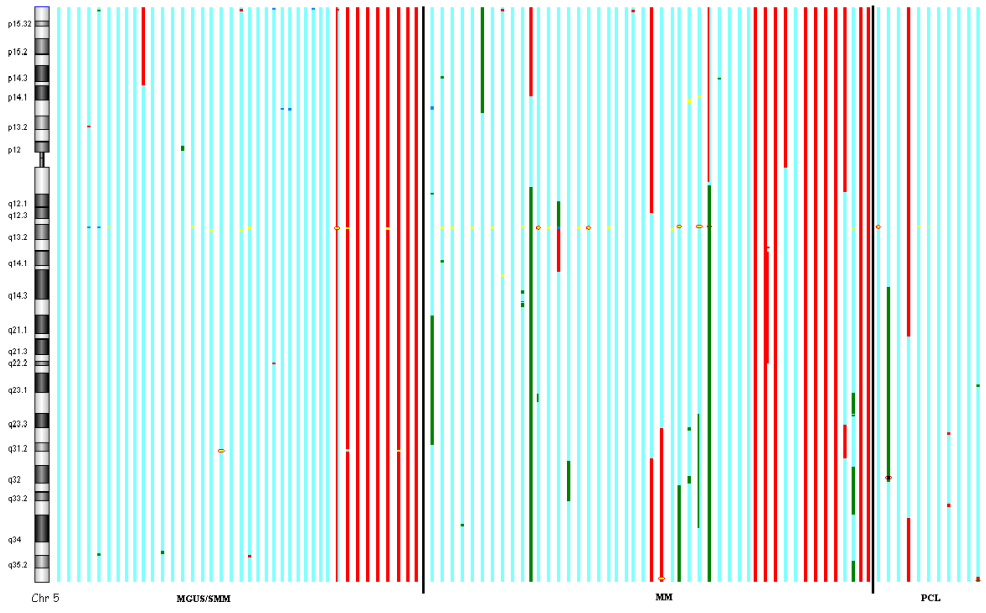

Chromosome 6

Chromosome 7

Chromosome 8

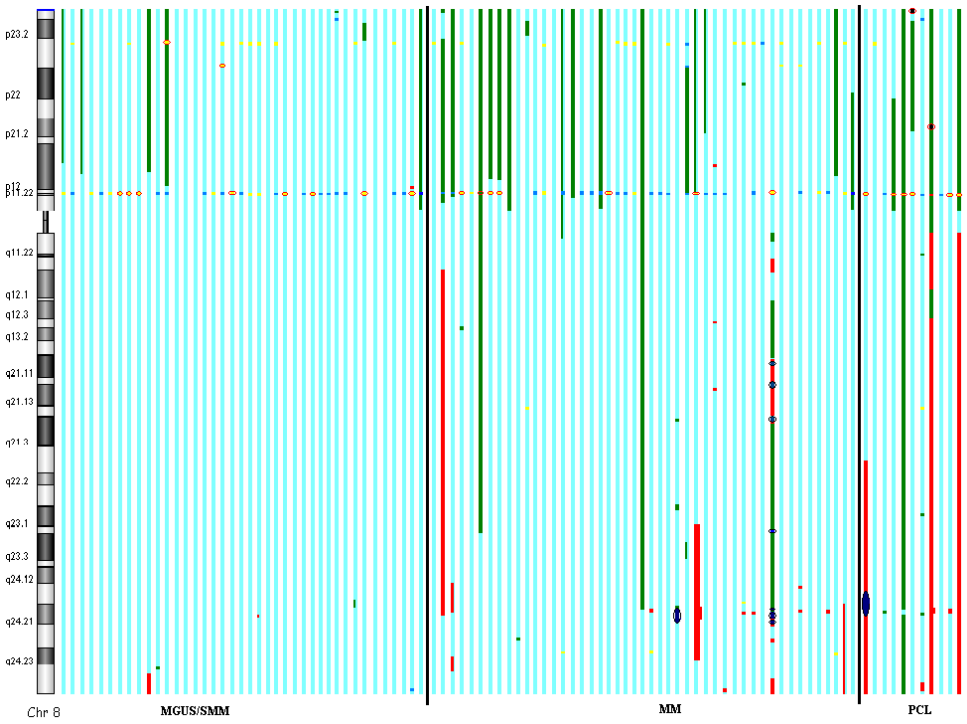

Chromosome 9

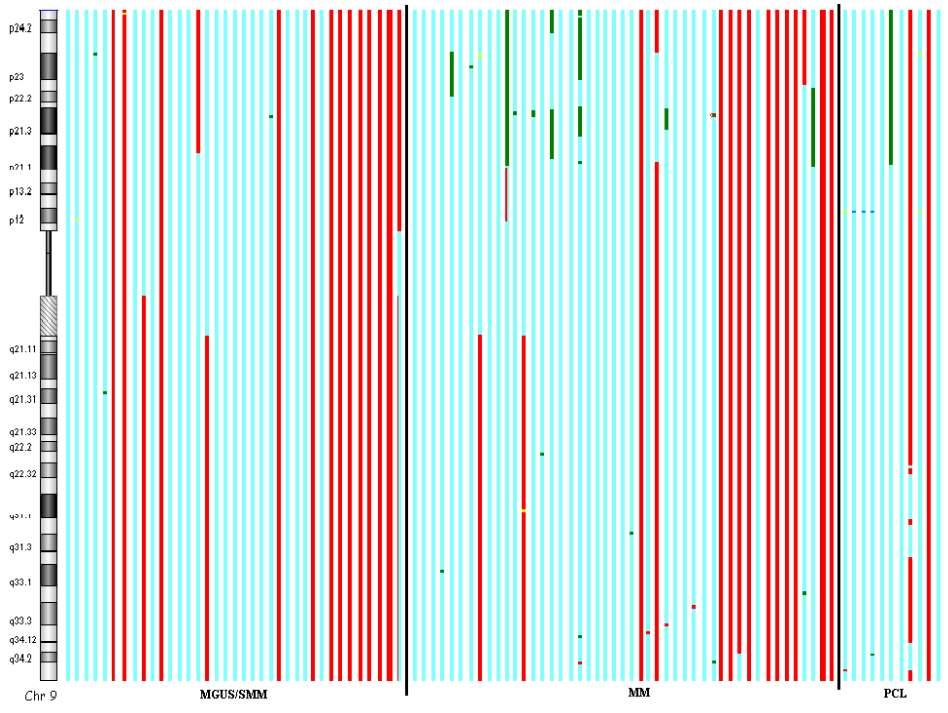

Chromosome 10

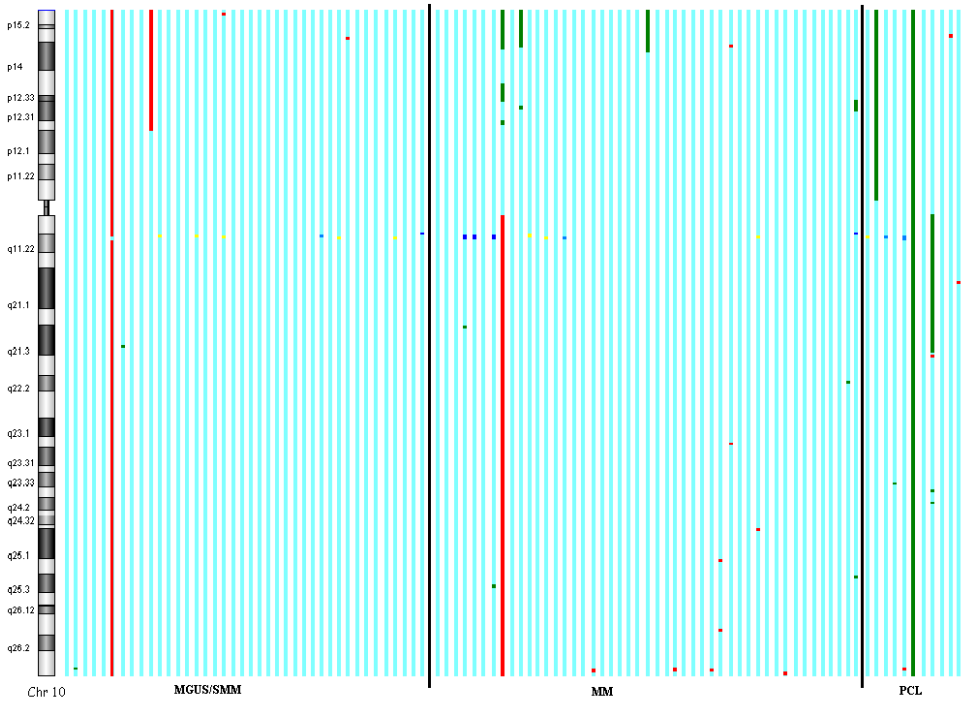

Chromosome 11

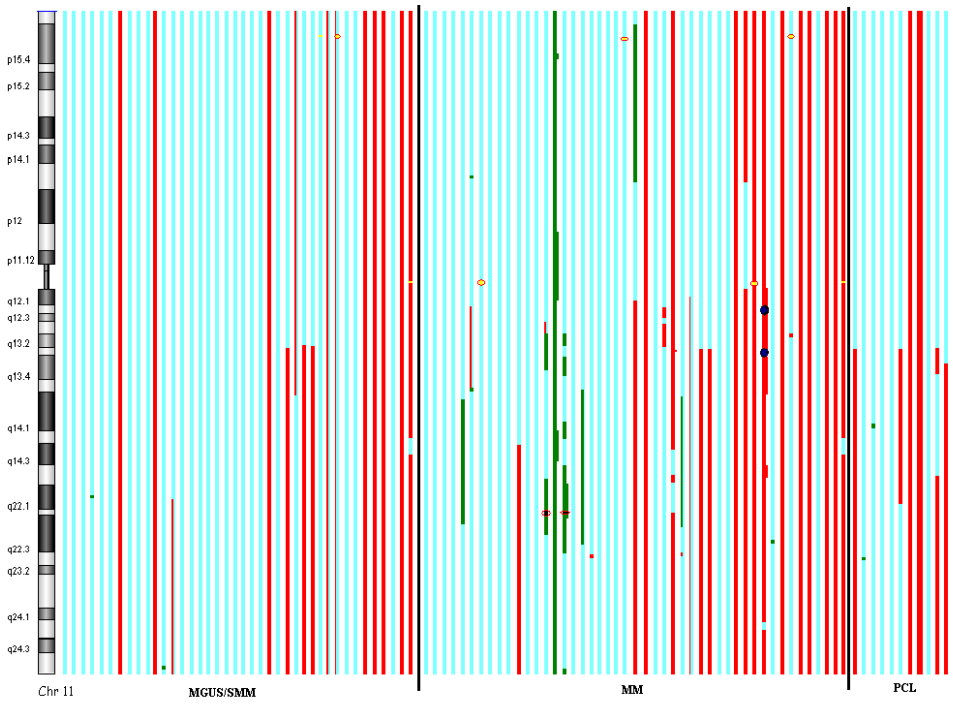

Chromosome 12

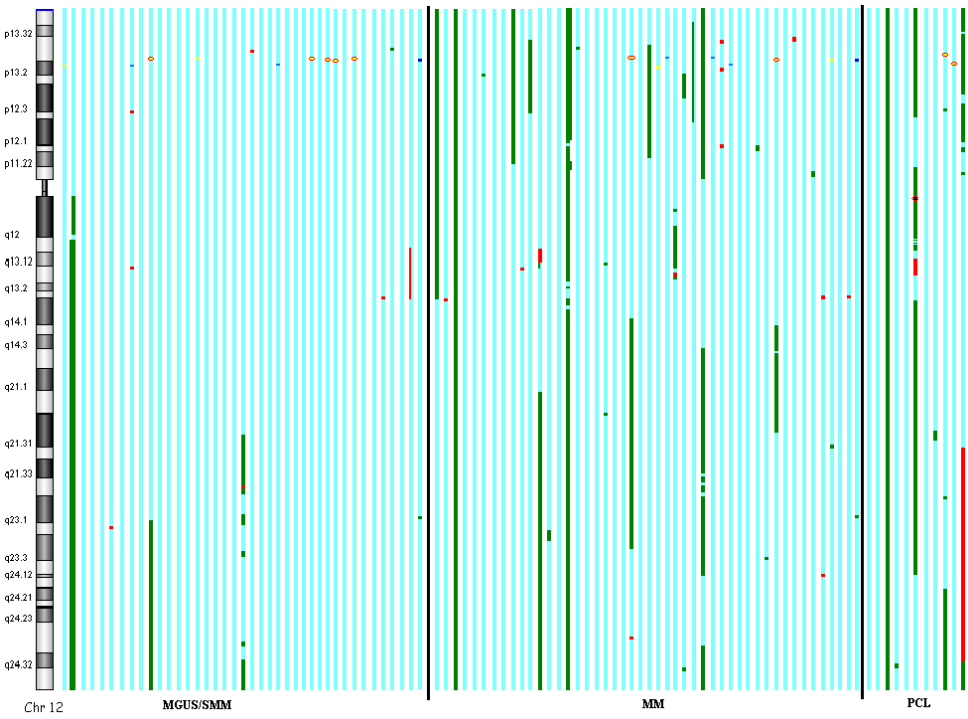

Chromosome 13

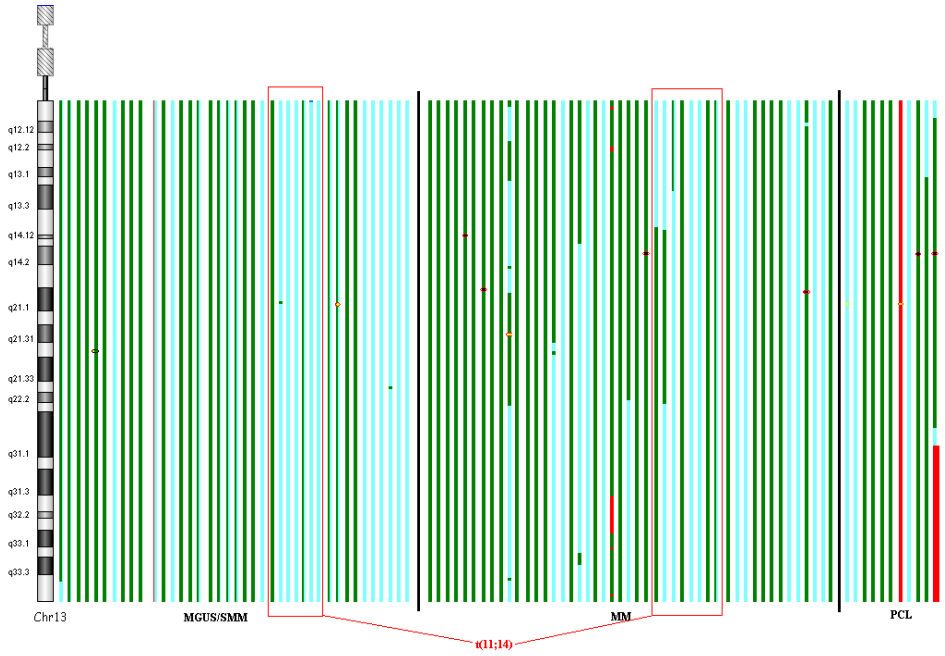

Chromosome 14

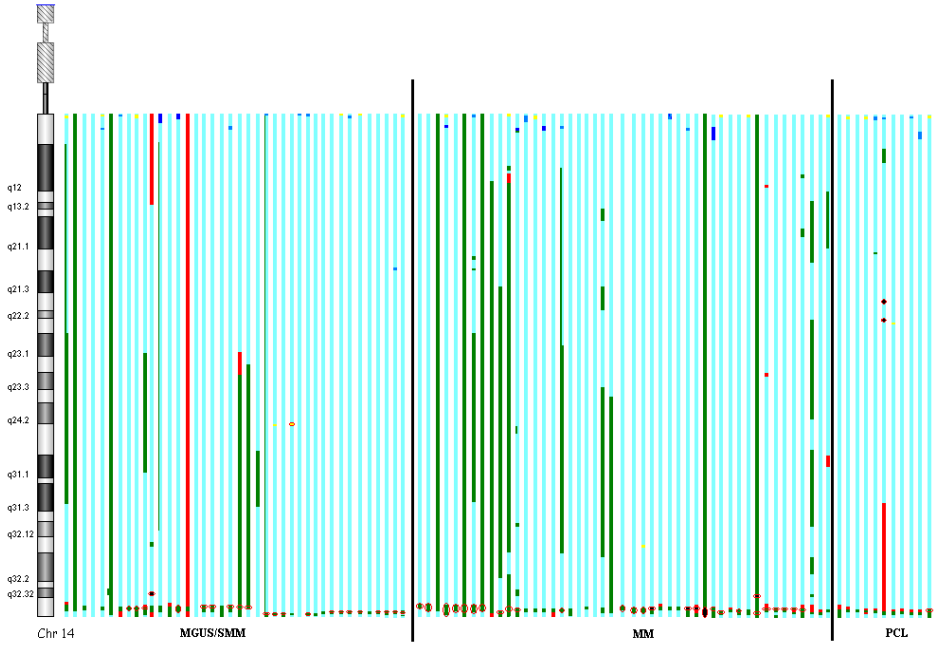

Chromosome 15

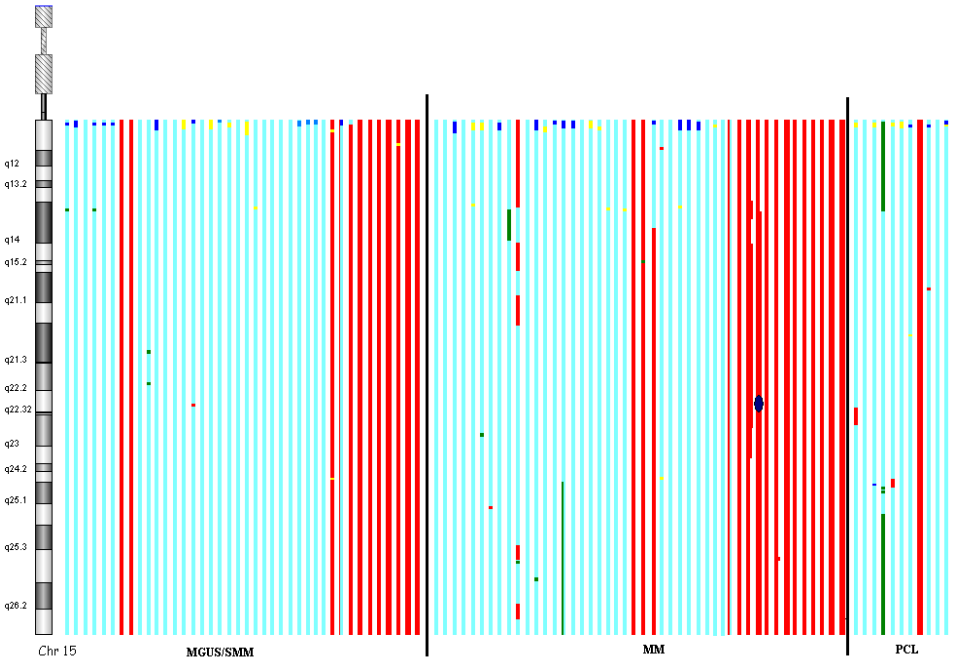

Chromosome 16

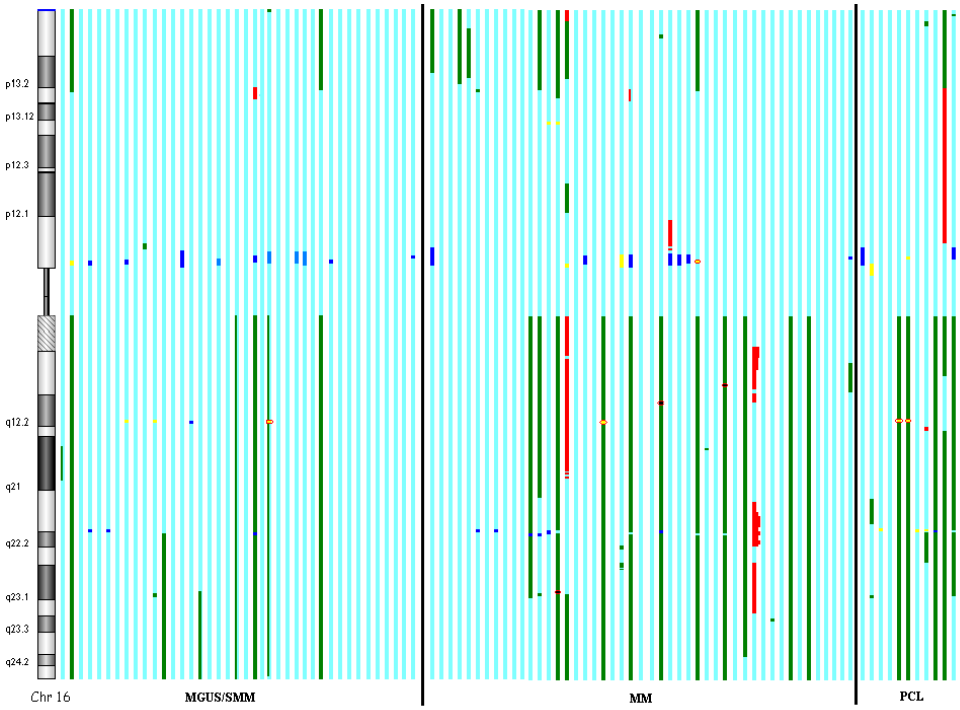

Chromosome 17

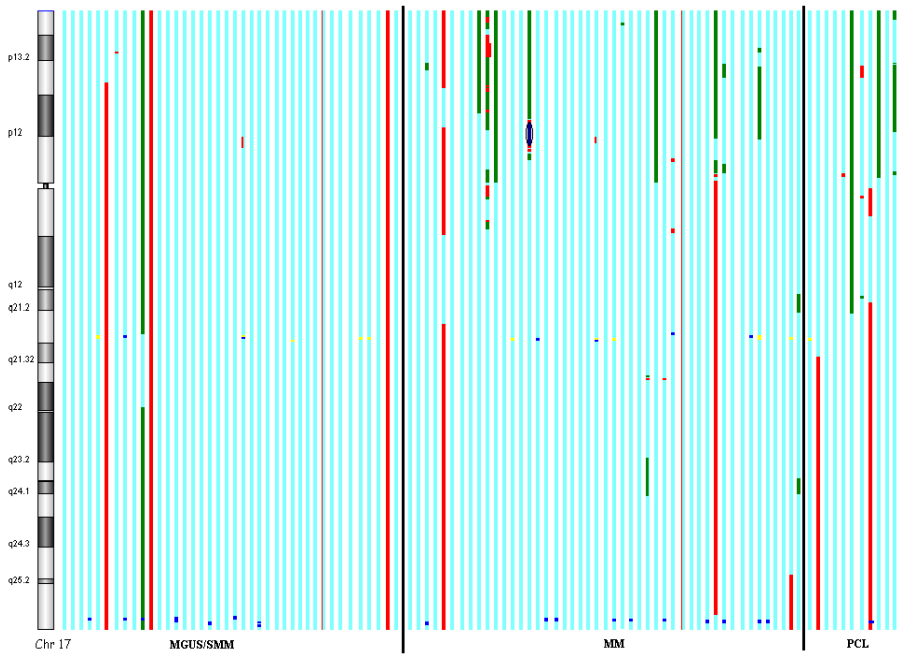

Chromosome 18

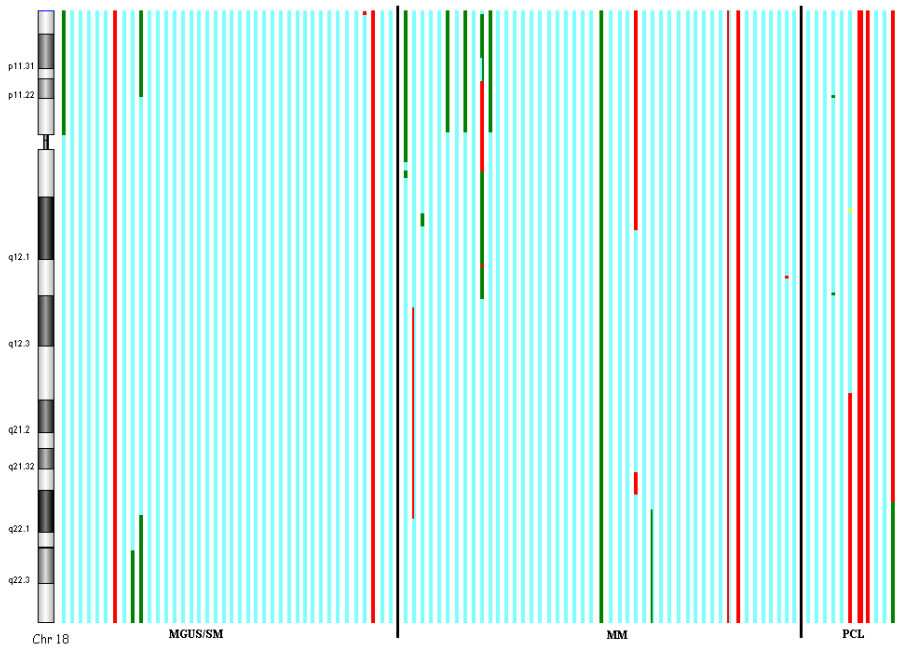

Chromosome 19

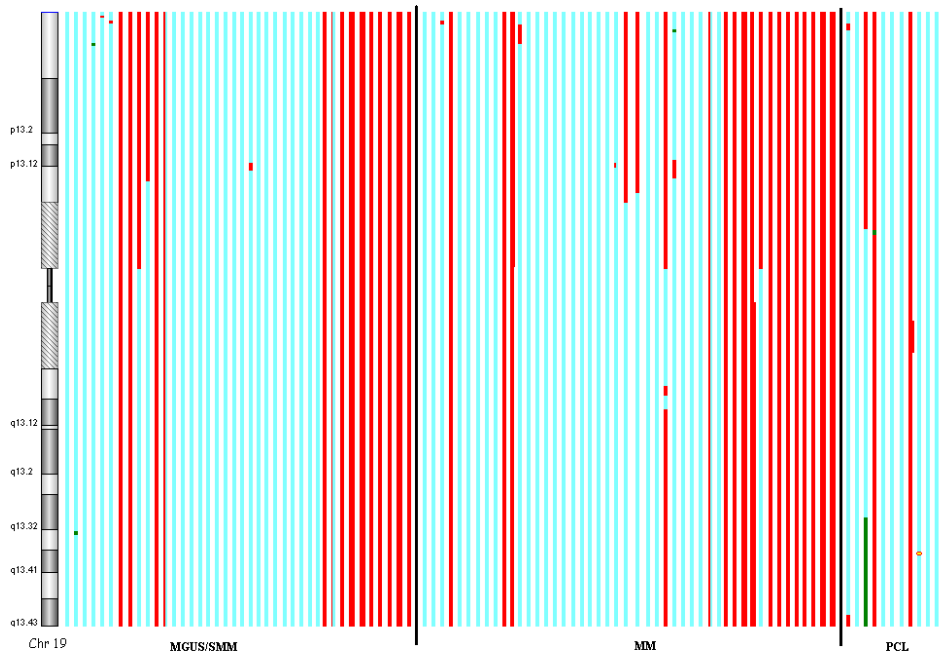

Chromosome 20

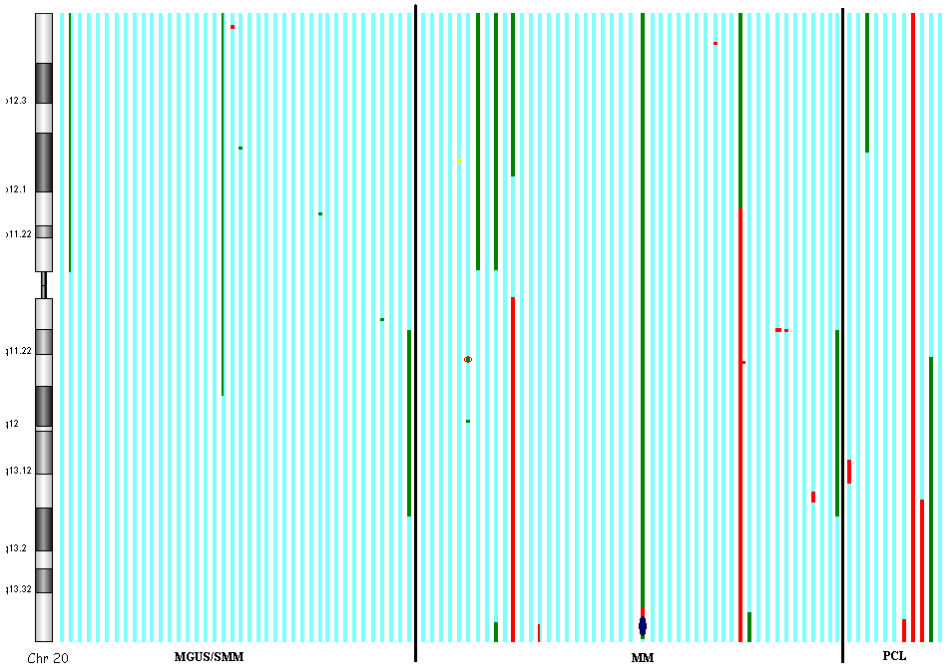

Chromosome 21

Chromosome 22

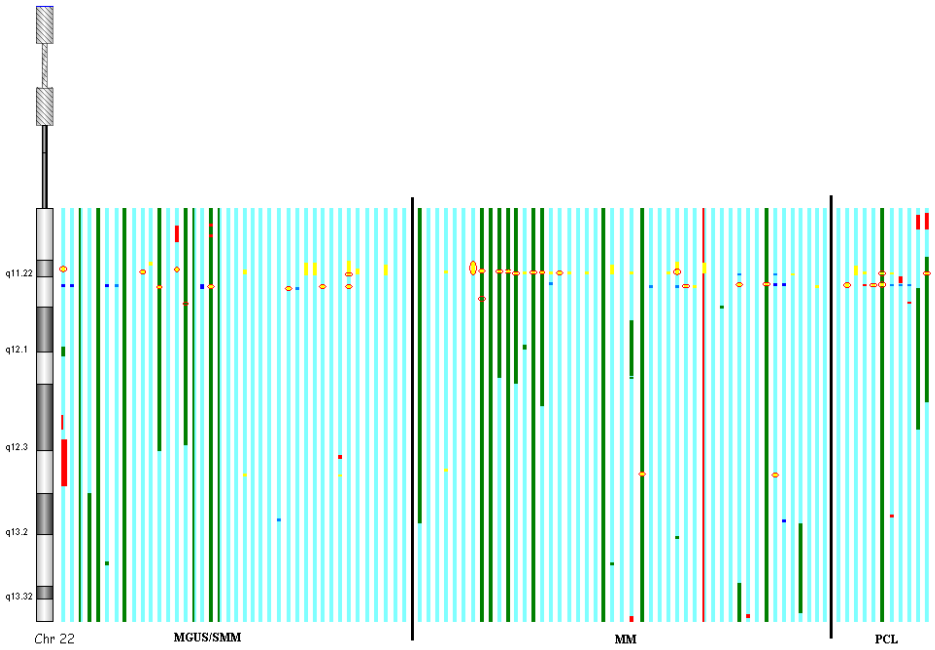

Chromosome X

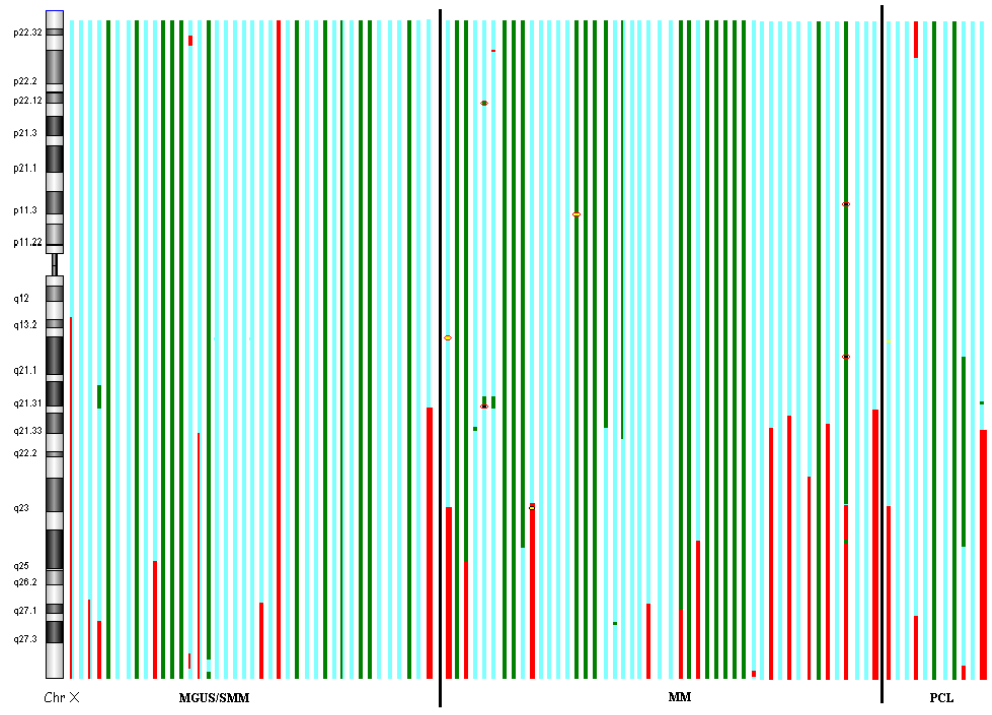

Appendix 10: Karyotype description of the cytogenetically abnormal MM patients with t(14;20)

RegID	Karyotype
320	49,XY,dic(1;15)(q10;q10),+3,+9,-13,der(14)t(14;20)(q32;q11),+17,der(20)t(14;20)(q32;q11)t(1;14)(q11;q32.3),+mar[cp8]/46,XY[45]
656	53,XY,add(1)(p13),+3,+5,der(6)t(1;6)(p22;q13),+9,+11,+15,+19,+21[5]/53,idem,der(6)t(1;6)t(1;3)(p32;p21),add(12)(p10),inc[6]/46,XY[30]
716	56,X,-Y,+der(2)t(2;16)(q32;?q11)t(1;16)(?;?),+der(3)t(3;4)(p13;q13)t(2;4)(?q33;q35),der(4)t(3;4)(p13;q13),del(5)(q12),+der(5)t(5;6)(q11;p2?1),der(6)t(5;6)(q11;p21)t(4;5)(q32;q35),+rea(6)del(6)(?),+7,+dic(9;15)(q34;p11),+del(11)(p?12p?14),+der(15)t(1;15)(q21;q21),der(16)t(5;16)(?;?),+del(19)(?p13),der(20)t(15;20)(q?;q12),+der(22)t(1;22)(?;p11),+mar[cp6]/46,XY[12]
839	44,X,-Y,del(1)(p13p34),del(13)(q12q32),t(14;20)(q32;q13),der(16)t(1;16)(q12;q23)[2]/46,XY[6]
1045	52,XY,der(1)del(1)(p32p34)t(1;20)(p34;q13),der(3)t(3;6)(p25;q22)t(3;17)(q27;q21),+5,der(6)t(3;6),+7,+9,+11,-13,+15,der(16)t(1;16)(q21;q24),der(17)t(3;17)(q27;q21),+19,+19,der(20)t(1;20)[6]/53,idem,+15[29]/46,XY[34]
1127	43,X,-X,+1,dic(1;5)(q10;q35),-13,t(14;20)(q32;q11),-20[25]/46,XX[21]
1183	44,XX,dic(1;12)(1qter->1p12::10q21-10q24::12q21.32->12pter),t(8;22)(q24;q11),del(10)(q11q26.1),-13,t(14;20)(q32;q11),der(16)t(1;16)(q12;q12),der(18)t(1;18)(p22.3;p11),+21,der(21;22)(q10;q10)[39]/45,idem,+dic(1;12)[26]/88,idemx2[18]/90,idemx2,+dic(1;12)x2[17]/46,XX[3]
1267	50,X,-Y,add(2)(p1?),+4,+?5,der(6)t(1;6)(q12;q15),+9,-13,t(14;20)(q32;q12),+18,+19,+21,add(22)(q1?3)[4]/46,XY[78]
1404	44,XY,dup(1)(q44q32),der(7)t(7;14)(p15;q13)t(14;20)(q32;q12),-13,der(17)t(17;20)(q23;p12),-20,del(22)(q1)[7]/83,idemx2[cp3]/46,XY[29]
1415	45,XX,+der(1;19)(q10;q10),-13,t(14;20)(q32;q12),add(16)(p13.3),-22[3]/45,idem,del(7)(q31q34)[2]/46,XX[31]
1548	43,XY,t(1;12)(q21;q2?3),der(1)del(1)(p13p32)t(1;5)(q21;q31),der(2)t(1;2)(q12;q37),add(7)(p11),-8,del(9)(p13p24),der(12)t(7;12)(p11;q15),-13,t(14;20)(q32;q11),dic(15;17)(q10;q10),add(16)(p13),der(16)t(15;16)(q11;q11),-20,dic(21;21)(p11;p11),-22,+3mar[6]/41,idem,-4,t(6;11)(q?15;q23),-9[1]/43,idem,+21,-mar[1]/42,idem,-der(12)t(7;12),-dic(15;17),+add(15)(p1),+17,-18[1]/43,idem,del(17)(q21)[1]/46,XY[12]
1648	55,X,-X,+del(3)(p14),+7,der(8)t(1;8)(q12;q24),+9,+add(9)(q22),add(12)(q24),der(13)t(1;13)(q12;q14),t(14;20)(q32;q12),+15,+18,+19,+21,+21,+21[13] /56,idem,+11[4]/46,XX[14]
1651	42,X,-X,-1,add(1)(p13),add(3)(q13),add(3)(q13),der(4)t(4;17)(p16;q11),del(6)(q11),dic(7;?20)(p13;q12),add(9)(p?),-12,?del(14)(q24),?add(17)(q23),del(17)(p11),-19,+mar,inc[1]/46,XX[93]
1849	~90,XXY,t(2;22)(p11;q13),-13,t(14;20)(q32;q12)inc[1]/46,XY[117]
1890	46,XX,t(2;8)(p11;q24),t(14;20)(q32;q12)[13]
2314	87,XX,-X,-X,del(1)(p1p3?2)x2,t(1;8)(p1;q22)x2,del(2)(q3?1q3?3)x2,inv(2)(p1?3q3?7)x2,+3,+3,der(6)t(3;6)(q12;q12)x2,-13,-13,t(14;20)(q32;q12)x2,-16,?add(16)(q21),-20,+mar[4]/46,XX[16]
2951	43,X,-X,add(1)(p3?6),?del(1)(p1),add(2)(q?3),add(6)(q?1),-10,-13,-14,add(14)(q32),-17,-18,-21,+4mar,inc[1]/46,XX[53]
3137	48,X,-Y,+6,+7,add(8)(q24),der(9)t(1;9)(q11;p2?2),-13,t(14;20)(q32;q1),+15,der(16)t(1;16)(q;q),+21,del(22)(q13)[1]/46,XY[4]

Appendix 11: Characteristics of PCL patients

RegID	Age	Sex	Prior MM	WBC	Hb	Plts	Ca	Albumin	β2M	PP type	BM PC %	Status	OS
Indice/ Normal values	*Years*			*5-10 x 10^9/L*	*120-150 g/L*	*150-400 x 10^9/L*	*2.15-2.55 nmol/L*	*32-47 g/L*	*1.2-2.4 mg/L*				*Months*
325	52	F	No	20.0	61.0	165	3.4	32.0	47.5	IgGk	89	Dead	1
3210	78	F	No	33.2	86.0	18	4.3	36.0	1.9	IgGk	nr	Dead	5
1576	79	M	No	11.8	82.0	168	2.7	28.0	7.4	IgA	85	Dead	6
3272	59	M	No	64.0	12.5	112	3.0	'normal'	nr	nr	high	Dead	12
742	84	F	No	5.7	94.0	340	2.2	26.0	8.0	IgAk	80	Dead	1
165	73	F	No	38.0	nr	107	2.5	34.0	5.2	IgGλ	100	Dead	1
3125	23	M	No	31.4	11.0	212	2.0	25.0	nr	IgGλ	42	Alive	13†
3343	83	F	No	nr	71.0	nr	2.2	25.0	nr	IgGk	47	Alive	3†
2359	50	M	No	14.6	61.0	23	3.4	19.0	9.6	IgAλ	55	Dead	0
128	78	M	No	2.5	84.0	122	2.4	32.0	14.5	IgGk	nr	Dead	0
1188	62	F	Yes	15.0	nr	221	3.5	27.0	2.8	IgGλ	98	Alive	20†
3342	72	F	Yes	42.0	7.7	162	1.89	35.0	nr	IgGk	nr	Dead	1

(RegID, patient identification; F, female; M, male; PP, paraprotein; MM, myeloma; OS, overall survival; nr, non reported; †, still alive at the time of the study)

Appendix 12: Primers for the eight genes included in the common minimally deleted region at 5q33.1

		Primers	
Gene	**Primer location & product size**	**Fwd**	**Rew**
SPINK5L2	Primers in exons 2 & 4; product: 206bp	5'-CTGTTTCAGGCCCTAGACACTG	5'-CAAGCTCTCAACACACAGAATGC
SPINK6	Primers in exons 1 & 4; product: 248bp	5'-ATGTTTCTGCTCCTCTCTCTGG	5'-GCATTTTCCAGGATGCTTTAGG
SPINK5L3	Primers in exons 3 & 4; product: 180bp	5'-CGTGACTTCACTAGGTGGCCTAAG	5'-CACTCATTCTGGAAAGTGTGGC
SPINK7	Primers in exons 1 & 3; product: 163bp	5'-CCTTCTGCTCTGTACAGTGG	5'-GTGACATTCATTCCCATAGG
SPINK9	Primers in exons 1 & 3; PCR product: 153bp	5'-TACTCTTGGCTCTGACACTTGC	5'-TGCCATCAGATCCACAAATTG
FBXO38	Primers in exons 14 & 16; two PCR products: 150bp & 850bp	5'-GTGGATTTATCTGCTGTCCGCTTC	5'-ACGGTACTCGGCGTTACTCTGAAC
HTR4	Primers in exons 6 & 7; product: 328bp	5'-CGCATCTATGTCACAGCTAAGG	5'-ACAGGGGAACAGCCACTTAGTA
ADRB2	One exon; PCR product: 380bp	5'-CGGTCACCAACTACTTCATCAC	5'-GTCACAGCAGGTCTCATTGG

Appendix 13: Primers for all exons of the *FBXO38* gene at 5q33.1

Exon	Fwd (5' to 3')	Rev (5' to 3')
1	GGATGACAACACTCCGGAAATA	CCTAGAAGGCCAGGAACTACAAA
2	ATGATACCTCTGCTTGTGTGTG	CCAGCCTACAAGGTGACTTAGATT
3	GTATGACCGTATGTGTGGTAGCTT	GTGACCCAAGAAACATGTACTCAC
4/5	GTGGAGTTTCTGACTCATTTCCTC	TTGTCCTATACACCGTGTCCACTA
6	GTGGAGTTTCTGACTCATTTCCTC	AAGGGAGATTAAGGAAGCCAAC
7	CAAGAACCTGATTTCAGAGAGC	GCTCATGGTTACTTACTGTCCATC
8	CAGATGCCATCAGTGTCTTTGC	TGGAGACAATGGTCCTGAGAGG
9	GTCAGCAGCATAGAAACGGACTAA	TCAAGACGTGAGAGCACCTAAGAT
10	ACCTGAACCCAATGATAAGCAG	TACACTTCTAGGCAGAGAACGTCA
11	CCAGGCCATTTAGTTCTCACA	AAGTCCGACTGTAACACCGTAAAG
12	CAGATCTCTTCTCCTTGCATGACT	TCACCTACTCCCTCATGTTCCTTA
13	AGGCCTAGTAATCAGCGGGACTG	CAGAATGATGAATGTGGGATGG
14	GCATCTCTGTTGATTCCAGATCC	CCCAAGTTGTCATATTAAGGCCAAG
15	TGAGGTTTGAAGGCATAGCTAAGGAG	GAAACAAGTTCATGCCTTTCTGC
16	TGAATGTGCTTGAGGGAAAGA	GGAACTGGGCTAGACTGTGATAAAGG
17	TCACAGTCTAGCCCAGTTCCTAA	GGCGGAACTAAAGATAACCCAACA
18	CCAAAGATGATATGTACGGAGCTTAC	ACTGTAGGTTGGGCAAGTGAATGA
19	CGGAGAGAGATTTCTAAGGCATTC	GAGTCCCTGCTATGAGAAATGA
20	GATGGTTCCTTCCTACCCGACAC	CTACATTTGGGTTACTGCTTGCTG
21	CCCACGCCAGTTAGCAATGTTAC	CACTGCACTGCTCCTAACTCACAA
22	GGACCAGCTTATCAGTGATTTTCT	CTGGATGGCCCTACTTGCTTTCT

Appendix 14: Primers for all exons of the *PPP2R2A* and *CDCA2* genes at 8p21.2

PPP2R2A

Exon	Fwd (5' to 3')	Rev (5' to 3')
1	CTGCCGGAGAAAGAGCACGA	ACCCTACTCCCTCAAACCCGA
2	TGTGTGGGCAGAACTAGGCTG	TCGGCTTCAAGGAAATCCTCC
3	GTTCTGAAACTAGTGAGTCGGG	TCCTCTGATGAGATTCTCCAGTGC
4	TGCAGGGTCCTTTGGAATTG	CCTGCCCAAGATTACGAGACTG
5	CATGGAATTTATGAGTGCCACC	GCTCTGCTCAGGATTTGGGCT
6	GCTTGGCATGTCTTTCAAGC	ATGGGCACAACATGCCTTCTT
7	GGCTGCAGTGAGCCGAGATTG	CAAGTGGCTCTGGACACACGGG
8	GAAGCTTTCAGGAGAATTCTAGCC	GGTGAACAAACACCATACAGG
9	GTACCTCCCTGAAGGGCTTGT	GACGAAGTTAGGACCTGGAATG
10	GCTTCCTATGGTTTAATTGCCG	CAATGTGTTGTCGAATGGCAC

CDCA2

Exon	Fwd (5' to 3')	Rev (5' to 3')
1	CGGAGTTAAAGCGCTAAGAGAAG	GCCGAACAAAGTGCCTAGAAAT
2	GATCGAATCACGTTCATCTTGC	TCCTGAAACGGACGACATATTG
3	GCCTCCTTGTGAAGTTGAAGGT	GCAAGTTTGCAGAGTAGGCAAT
4	CTCAGGCTGGTACATCACGAGT	GCTTCATTAACGGAATTCACGAC
5	TTGGATTCAATGGCTGTAGGC	AACCATGCGGAAATGTAGGATT
6	GCTGAAATCGCACCATTGTAC	CCAACAACTTCATTTTCCTATGC
7	GAAGGTGACTGATTGAACATCAG	GGCAACTGGCCATGTACTAAGA
8	GACGTTACTGCCCAATCAGGTT	CGGTAAGACGAGTAAGACATTTCC
9	CTGCAGTTGACAGAGAATTTCA	ACCAATTCTGAGGCTCTCCAAG
10	CTTGGAGAGCCTCAGAATTGGT	TTATTGCTCATGCAAAGCAGGT
11	TGGGCACATTATGTATTCACTGC	AGCTTCATGTCAGCTTCCCAAT
12	CACAGTGTTTCCAAAGGAAGATG	TACGTTGTGCCAAACACAAACA
13	TTGCTTGTGCTTTACGGTATCC	TCTTGGTCCAAAGTCAACTGGA
14	GTTGCAGTGAGCTGAGATTGTG	TGTCAGGATACCTGAACCCAG
15	GAGGAGGAGGAGGATGACAGAA	AGCATTTACTCTCTGGCGGAAG

Appendix 15: Excel sheet describing MLPA results for the PCL patient 3210

	PEAK AREA																																								
Probe location		**Control**	**Sample**	1	9	19	3	8	1	19	2	1	19	1	14	19	19	3	19	15	1	19	1	1	17	19	1	1	1	1	1	8	19	1	5	1	1	19	11	1	14	12	1	13	1
CDKN2C exon 2	108	554		0	0	0	0	0	0	0	0	0	0	0	0	0	0	0	0	0	0	0	0	0	0	0	0	0	0	0	0	0	0	0	0	0	0	0	0	0	0	0	0	0	0
CDKN2C exon 3	111	253		0	0	0	0	0	0	0	0	0	0	0	0	0	0	0	0	0	0	0	0	0	0	0	0	0	0	0	0	0	0	0	0	0	0	0	0	0	0	0	0	0	0
centromeric of CDKN2C	114	444		0	0	0	0	0	0	0	0	0	0	0	0	0	0	0	0	0	0	0	0	0	0	0	0	0	0	0	0	0	0	0	0	0	0	0	0	0	0	0	0	0	0
FAF1 intron 1-2 distal	117	517	735	1.121	0.621	0.561	0.721	0.543	1.079	0.617	0.699	0.59	0.485	0.622	0.555	0.637	0.496	0.615	0.62	0.647	1.098	0.538	1.102	0.958	0.94	0.537	0.558	0.592	0.505	0.99	0.604	0.64	0.42	0.549	0.428	0.644	0.435	0.567	0.615	0.679	0.974	0.545	1.043	0.975	0.927
FAF1 intron 1-2 prox	120	557	714	1.01	0.56	0.506	0.65	0.49	0.973	0.556	0.63	0.532	0.438	0.561	0.5	0.574	0.447	0.554	0.559	0.583	0.99	0.485	0.994	0.864	0.848	0.484	0.503	0.533	0.455	0.893	0.545	0.577	0.378	0.495	0.386	0.581	0.393	0.511	0.555	0.612	0.878	0.492	0.94	0.879	0.836
Between FAF1 & CDKN2C	124	363		0	0	0	0	0	0	0	0	0	0	0	0	0	0	0	0	0	0	0	0	0	0	0	0	0	0	0	0	0	0	0	0	0	0	0	0	0	0	0	0	0	0
NOTCH2 1p11.2	130	748	949	1	0.554	0.501	0.643	0.485	0.963	0.55	0.624	0.527	0.433	0.555	0.495	0.568	0.442	0.548	0.553	0.577	0.98	0.48	0.983	0.855	0.839	0.479	0.498	0.528	0.48	0.883	0.539	0.571	0.375	0.49	0.382	0.575	0.389	0.506	0.549	0.606	0.869	0.487	0.93	0.87	0.827
con 9q21	136	442	1012	1.805	1	0.903	1.16	0.875	1.737	0.993	1.126	0.95	0.782	1.001	0.894	1.025	0.798	0.99	0.998	1.042	1.768	0.866	1.775	1.543	1.515	0.865	0.899	0.953	0.813	1.594	0.973	1.031	0.676	0.884	0.689	1.037	0.701	0.913	0.991	1.093	1.569	0.878	1.679	1.57	1.493
SMARCA4 19p13.3	142	550	1394	1.998	1.107	1	1.285	0.969	1.923	1.099	1.247	1.052	0.865	1.108	0.989	1.135	0.884	1.096	1.105	1.153	1.957	0.959	1.965	1.708	1.677	0.958	0.995	1.055	0.9	1.765	1.077	1.141	0.748	0.979	0.763	1.148	0.776	1.011	1.097	1.21	1.737	0.972	1.859	1.738	1.653
con 3q29	148	557	1099	1.555	0.862	0.778	1	0.754	1.497	0.856	0.97	0.819	0.674	0.863	0.77	0.884	0.688	0.853	0.86	0.898	1.523	0.747	1.529	1.33	1.305	0.745	0.775	0.821	0.7	1.374	0.839	0.889	0.582	0.762	0.594	0.894	0.604	0.787	0.854	0.942	1.352	0.757	1.447	1.353	1.286
con 8q24	154	396	1036	2.062	1.143	1.032	1.326	1	1.985	1.135	1.287	1.086	0.893	1.144	1.021	1.172	0.912	1.131	1.141	1.19	2.02	0.99	2.028	1.763	1.731	0.988	1.027	1.089	0.929	1.822	1.112	1.178	0.772	1.01	0.788	1.185	0.801	1.043	1.132	1.249	1.793	1.004	1.919	1.794	1.706
PPAP2B 1p32	160	456	601	1.039	0.576	0.52	0.668	0.504	1	0.572	0.648	0.547	0.45	0.576	0.514	0.59	0.46	0.57	0.575	0.6	1.018	0.499	1.022	0.888	0.872	0.498	0.517	0.548	0.468	0.918	0.56	0.594	0.389	0.509	0.397	0.597	0.404	0.525	0.57	0.629	0.903	0.506	0.967	0.904	0.859
CCNE1 19q12	166	471	1086	1.817	1.007	0.91	1.169	0.881	1.749	1	1.134	0.957	0.787	1.008	0.9	1.033	0.804	0.997	1.005	1.049	1.78	0.872	1.767	1.554	1.525	0.871	0.905	0.959	0.818	1.605	0.98	1.038	0.681	0.89	0.694	1.045	0.706	0.919	0.998	1.101	1.58	0.885	1.691	1.581	1.503
con 2p16	171	632	1285	1.603	0.888	0.802	1.03	0.777	1.543	0.882	1	0.844	0.694	0.889	0.794	0.911	0.709	0.879	0.887	0.925	1.57	0.769	1.576	1.37	1.345	0.768	0.798	0.846	0.722	1.416	0.864	0.916	0.6	0.785	0.612	0.921	0.625	0.811	0.88	0.971	1.393	0.78	1.491	1.394	1.326
GNB1 1p36.33	178	457	1101	1.899	1.052	0.951	1.221	0.921	1.828	1.045	1.185	1	0.822	1.053	0.94	1.079	0.84	1.042	1.051	1.096	1.86	0.912	1.867	1.624	1.594	0.91	0.946	1.002	0.855	1.677	1.024	1.085	0.711	0.93	0.725	1.091	0.738	0.961	1.042	1.151	1.651	0.924	1.767	1.652	1.571
PDCD5 19q13.12	184	368	1078	2.309	1.279	1.156	1.485	1.12	2.223	1.27	1.441	1.216	1	1.281	1.143	1.312	1.021	1.266	1.277	1.333	2.262	1.108	2.271	1.974	1.938	1.107	1.15	1.219	1.04	2.04	1.245	1.319	0.865	1.131	0.882	1.327	0.897	1.168	1.268	1.399	2.007	1.124	2.148	2.008	1.91
TNNT2 1q32.1	190	561	1283	1.803	0.999	0.902	1.159	0.874	1.735	0.992	1.125	0.949	0.781	1	0.893	1.024	0.797	0.989	0.997	1.04	1.766	0.865	1.773	1.541	1.513	0.864	0.898	0.952	0.812	1.592	0.972	1.03	0.675	0.883	0.688	1.036	0.701	0.912	0.99	1.092	1.567	0.877	1.677	1.568	1.491
con 14q24	202	265	679	2.02	1.119	1.011	1.299	0.979	1.944	1.111	1.26	1.064	0.875	1.12	1	1.147	0.893	1.108	1.117	1.166	1.978	0.969	1.986	1.727	1.695	0.968	1.006	1.066	0.909	1.784	1.089	1.154	0.756	0.989	0.771	1.161	0.785	1.022	1.109	1.224	1.756	0.983	1.879	1.757	1.671
LDLR 19p13.3	211	528	1179	1.76	0.975	0.881	1.132	0.854	1.694	0.968	1.098	0.927	0.762	0.976	0.871	1	0.779	0.965	0.974	1.016	1.724	0.845	1.731	1.505	1.477	0.844	0.877	0.929	0.793	1.555	0.949	1.006	0.659	0.862	0.672	1.012	0.684	0.89	0.966	1.066	1.53	0.857	1.639	1.531	1.456
PPP1R15A 19q13.2	220	455	1305	2.261	1.253	1.132	1.454	1.096	2.176	1.244	1.411	1.19	0.979	1.254	1.119	1.284	1	1.24	1.251	1.305	2.214	1.085	2.223	1.933	1.897	1.084	1.126	1.193	1.018	1.997	1.219	1.292	0.847	1.107	0.863	1.299	0.879	1.144	1.241	1.37	1.966	1.1	2.103	1.966	1.87
con 3p25	229	281	650	1.823	1.01	0.913	1.172	0.884	1.755	1.003	1.138	0.96	0.79	1.011	0.903	1.036	0.807	1	1.009	1.052	1.786	0.875	1.793	1.559	1.53	0.874	0.908	0.963	0.821	1.611	0.983	1.042	0.683	0.893	0.696	1.048	0.709	0.922	1.001	1.105	1.585	0.887	1.696	1.586	1.508
UPK1A 19q13.13	238	283	649	1.808	1.002	0.905	1.162	0.877	1.74	0.995	1.128	0.952	0.783	1.003	0.895	1.027	0.8	0.991	1	1.043	1.771	0.868	1.778	1.546	1.517	0.866	0.9	0.954	0.814	1.597	0.975	1.033	0.677	0.885	0.69	1.039	0.702	0.914	0.992	1.095	1.572	0.88	1.682	1.572	1.495
con 15q21	247	409	899	1.732	0.96	0.867	1.114	0.84	1.668	0.953	1.081	0.912	0.75	0.961	0.858	0.984	0.766	0.95	0.958	1	1.697	0.832	1.704	1.481	1.454	0.83	0.863	0.915	0.78	1.53	0.934	0.99	0.649	0.849	0.662	0.996	0.673	0.876	0.951	1.05	1.506	0.843	1.612	1.507	1.433
GTF2B 1p22.2	256	359	465	1.021	0.566	0.511	0.656	0.495	0.983	0.562	0.637	0.538	0.442	0.566	0.506	0.58	0.452	0.56	0.565	0.589	1	0.49	1.004	0.873	0.857	0.489	0.509	0.539	0.46	0.902	0.551	0.583	0.382	0.5	0.39	0.587	0.397	0.516	0.56	0.619	0.888	0.497	0.95	0.888	0.845
BC-2 19q13.4	266	367	970	2.083	1.154	1.043	1.34	1.01	2.005	1.146	1.3	1.097	0.902	1.156	1.032	1.184	0.922	1.143	1.153	1.202	2.041	1	2.049	1.781	1.748	0.999	1.038	1.1	0.938	1.84	1.123	1.19	0.78	1.02	0.796	1.197	0.81	1.054	1.144	1.262	1.811	1.014	1.938	1.812	1.723
LPHN2 1p31.1	274	293	378	1.017	0.563	0.509	0.654	0.493	0.979	0.56	0.635	0.535	0.44	0.564	0.504	0.578	0.45	0.558	0.563	0.587	0.996	0.488	1	0.869	0.853	0.487	0.507	0.537	0.458	0.898	0.548	0.581	0.381	0.498	0.388	0.584	0.395	0.514	0.558	0.616	0.884	0.495	0.946	0.884	0.841
FAF1 1p32.3	**283**	**246**	**365**	**1.169**	0.648	0.585	**0.752**	0.567	**1.126**	0.644	**0.73**	0.616	0.507	0.649	0.579	0.664	0.517	0.641	0.647	0.675	**1.146**	0.561	**1.15**	1	**0.982**	0.561	0.583	0.617	0.527	**1.033**	0.631	0.668	0.438	0.573	0.447	0.572	0.454	0.592	0.642	**0.709**	**1.017**	0.569	**1.088**	**1.017**	**0.967**
con 17q11	292	385	582	1.192	0.66	0.596	0.766	0.578	1.147	0.656	0.743	0.627	0.516	0.661	0.59	0.677	0.527	0.654	0.659	0.688	1.167	0.572	1.172	1.019	1	0.571	0.594	0.629	0.537	1.053	0.643	0.681	0.446	0.584	0.455	0.685	0.463	0.603	0.654	0.722	1.036	0.58	1.109	1.036	0.986
BAX 19q13.3	301	300	794	2.086	1.156	1.044	1.341	1.012	2.008	1.148	1.302	1.099	0.904	1.157	1.033	1.185	0.923	1.144	1.154	1.204	2.043	1.001	2.052	1.784	1.751	1	1.039	1.101	0.939	1.843	1.125	1.192	0.781	1.022	0.797	1.199	0.811	1.055	1.145	1.264	1.814	1.015	1.941	1.814	1.726
LMNA 1q21.2	310	298	759	2.008	1.112	1.005	1.291	0.974	1.932	1.105	1.253	1.057	0.869	1.114	0.994	1.141	0.888	1.101	1.111	1.159	1.966	0.964	1.974	1.717	1.685	0.962	1	1.06	0.904	1.773	1.083	1.147	0.752	0.983	0.767	1.154	0.78	1.016	1.102	1.216	1.745	0.977	1.868	1.746	1.661
PTAFR 1p35.3	320	310	745	1.894	1.05	0.948	1.218	0.919	1.823	1.042	1.182	0.998	0.82	1.051	0.938	1.076	0.838	1.039	1.048	1.093	1.855	0.909	1.863	1.62	1.59	0.908	0.944	1	0.853	1.673	1.021	1.082	0.709	0.928	0.723	1.089	0.736	0.958	1.04	1.148	1.647	0.922	1.762	1.648	1.567
TP73 1p36.3	328	312	879	2.221	1.23	1.112	1.428	1.077	2.138	1.222	1.386	1.169	0.962	1.232	1.1	1.262	0.982	1.218	1.229	1.282	2.175	1.066	2.184	1.899	1.864	1.064	1.106	1.172	1	1.962	1.197	1.269	0.832	1.088	0.848	1.276	0.863	1.123	1.219	1.345	1.931	1.081	2.066	1.931	1.837
CYP2J2 1p32.1	337	149	214	1.132	0.627	0.567	0.728	0.549	1.09	0.623	0.706	0.596	0.49	0.628	0.561	0.643	0.501	0.621	0.626	0.653	1.109	0.543	1.113	0.968	0.95	0.543	0.564	0.598	0.51	1	0.61	0.647	0.424	0.554	0.432	0.651	0.44	0.573	0.621	0.686	0.984	0.551	1.053	0.985	0.936
TNFRSF14 1p36.33	346	465	1094	1.854	1.028	0.928	1.192	0.899	1.785	1.02	1.157	0.977	0.803	1.029	0.918	1.054	0.82	1.017	1.026	1.07	1.816	0.89	1.824	1.586	1.556	0.889	0.924	0.979	0.835	1.638	1	1.06	0.694	0.908	0.708	1.066	0.721	0.938	1.018	1.124	1.612	0.903	1.725	1.613	1.534
con 8q13	355	467	1037	1.75	0.97	0.876	1.125	0.849	1.685	0.963	1.092	0.922	0.758	0.971	0.867	0.994	0.774	0.96	0.968	1.01	1.714	0.84	1.721	1.497	1.469	0.839	0.872	0.924	0.788	1.546	0.944	1	0.655	0.857	0.668	1.006	0.68	0.885	0.961	1.06	1.522	0.852	1.628	1.522	1.448
TGFB1 19q13.31	364	178	603	2.67	1.48	1.337	1.717	1.295	2.57	1.469	1.666	1.406	1.156	1.481	1.322	1.517	1.181	1.465	1.477	1.541	2.615	1.282	2.626	2.283	2.241	1.28	1.33	1.41	1.202	2.359	1.44	1.526	1	1.308	1.02	1.535	1.038	1.351	1.466	1.618	2.322	1.3	2.484	2.322	2.209
DPYD 1p21.3	373	183	474	2.042	1.131	1.022	1.313	0.99	1.965	1.123	1.274	1.075	0.884	1.133	1.011	1.16	0.903	1.12	1.129	1.178	2	0.98	2.008	1.746	1.713	0.979	1.017	1.078	0.919	1.803	1.101	1.166	0.765	1	0.78	1.173	0.793	1.033	1.121	1.237	1.775	0.994	1.899	1.776	1.689
con 5q22	382	115	382	2.618	1.451	1.311	1.684	1.27	2.52	1.441	1.634	1.379	1.134	1.452	1.296	1.488	1.158	1.436	1.448	1.511	2.565	1.257	2.575	2.239	2.197	1.255	1.304	1.382	1.179	2.313	1.412	1.496	0.981	1.282	1	1.505	1.017	1.324	1.437	1.586	2.276	1.274	2.436	2.277	2.166
TNFRSF4 1p36.33	391	188	415	1.74	0.964	0.871	1.119	0.844	1.675	0.957	1.086	0.916	0.754	0.965	0.862	0.989	0.77	0.954	0.963	1.004	1.704	0.835	1.711	1.488	1.46	0.834	0.867	0.919	0.784	1.537	0.938	0.994	0.652	0.852	0.665	1	0.676	0.88	0.955	1.054	1.513	0.847	1.619	1.513	1.439
MFN2 1p36.22	400	136	444	2.573	1.428	1.288	1.655	1.248	2.477	1.416	1.606	1.355	1.114	1.428	1.274	1.462	1.138	1.411	1.424	1.485	2.52	1.235	2.531	2.2	2.16	1.234	1.282	1.358	1.159	2.273	1.388	1.47	0.964	1.26	0.983	1.479	1	1.302	1.413	1.559	2.237	1.252	2.394	2.238	2.129
ZNF342 19q13.3	409	248	622	1.977	1.095	0.99	1.271	0.959	1.903	1.088	1.234	1.041	0.856	1.097	0.979	1.123	0.874	1.084	1.094	1.141	1.936	0.949	1.944	1.69	1.659	0.948	0.985	1.044	0.89	1.746	1.066	1.129	0.74	0.968	0.755	1.136	0.768	1	1.085	1.198	1.719	0.962	1.839	1.719	1.635
con 11q23	418	315	728	1.822	1.009	0.912	1.171	0.883	1.754	1.002	1.137	0.959	0.789	1.011	0.902	1.135	0.806	0.999	1.008	1.051	1.784	0.874	1.791	1.558	1.529	0.873	0.907	0.962	0.82	1.609	0.982	1.041	0.682	0.892	0.696	1.047	0.708	0.921	1	1.104	1.584	0.887	1.695	1.584	1.507
CRB1 1q31.3	427	245	513	1.65	0.915	0.826	1.061	0.8	1.589	0.908	1.03	0.869	0.715	0.916	0.817	0.938	0.73	0.905	0.913	0.953	1.617	0.792	1.623	1.411	1.385	0.791	0.822	0.871	0.743	1.458	0.89	0.943	0.618	0.808	0.63	0.949	0.641	0.835	0.906	1	1.435	0.803	1.536	1.435	1.365
con 14q22	436	233	340	1.15	0.637	0.576	0.74	0.558	1.107	0.633	0.718	0.606	0.498	0.638	0.57	0.653	0.509	0.631	0.636	0.664	1.127	0.552	1.131	0.983	0.965	0.551	0.573	0.607	0.518	1.016	0.62	0.657	0.431	0.563	0.439	0.661	0.447	0.582	0.631	0.697	1	0.56	1.07	1	0.951
con 12p13	445	211	550	2.055	1.138	1.028	1.321	0.996	1.978	1.131	1.282	1.082	0.89	1.14	1.017	1.167	0.909	1.127	1.137	1.186	2.012	0.986	2.02	1.757	1.724	0.985	1.023	1.085	0.925	1.815	1.108	1.174	0.769	1.006	0.785	1.181	0.798	1.039	1.128	1.245	1.786	1	1.912	1.787	1.7
PARK7 1p36.2	454	198	270	1.075	0.596	0.538	0.691	0.521	1.035	0.591	0.671	0.566	0.466	0.596	0.532	0.611	0.475	0.59	0.595	0.62	1.053	0.516	1.057	0.919	0.902	0.515	0.535	0.567	0.484	0.949	0.58	0.614	0.403	0.526	0.411	0.618	0.418	0.544	0.59	0.651	0.934	0.523	1	0.935	0.889
con 13q14	463	242	353	1.15	0.637	0.576	0.739	0.558	1.107	0.633	0.717	0.605	0.498	0.638	0.569	0.653	0.509	0.631	0.636	0.664	1.126	0.552	1.131	0.983	0.965	0.551	0.573	0.607	0.518	1.016	0.62	0.657	0.431	0.563	0.439	0.661	0.447	0.582	0.631	0.697	1	0.56	1.07	1	0.951
NRAS 1p13.2	472	163	250	1.209	0.67	0.605	0.777	0.586	1.164	0.665	0.754	0.637	0.524	0.671	0.599	0.687	0.535	0.663	0.669	0.696	1.184	0.58	1.189	1.034	1.015	0.579	0.602	0.638	0.544	1.068	0.652	0.691	0.453	0.592	0.462	0.695	0.47	0.612	0.664	0.732	1.051	0.588	1.125	1.051	1

Peak height ratios below 0.7 or above 1.3 are regarded as indicative of a heterozygous deletion or duplication, respectively. Cells highlighted in yellow are those indicating probes on chromosome 1p. All MLPA results were compared with array CGH results and no discrepancies were found. Four probes on 1p showed a peak height ratio of '0' indicative of a HD. These probes involved *CDKN2C*, the region between *FAF1* and *CDKN2C* but not *FAF1*.

Appendix 16: Level of *MYC* expression in the seven PCL and 19 MM patients relative to *BCR* and *GUSB*

	Ratio compared to calibrator sample Pfaffl [a]		*MYC* abnormalities	
Sample RegID	***BCR*** **(control gene)**	***GUSB*** **(control gene)**	**FISH**	**Array CGH**
Calibrator				
MDS case	1.00	1.00	N	-
Cell line				
HL60	16.92	17.99	Amp (DM)	-
PCL				
325	8.75	7.91	Amp (DM) [b]	High level gain
3210	20.01	5.53	*MYC* split	N
1576	9.02	10.43	Gain of one copy (tandem duplication)	Interstitial gain involving *MYC* & *TMEM75*
742	6.23	11.49	Gain of two copies	Gain of whole 8q, further gain involving *MYC* & *TMEM75*
2359	1.11	0.84	N	Normal
1188	19.48	24.25	N	Deletion telomeric to *TMEM75*
3342	7.33	4.96	N	N
MM				
1037	3.46	3.90	Unbalanced t(8;14)	Loss 8pter–q24.21 (centromeric to *MYC*)
1426	2.77	2.83	Unbalanced t(8;14)	-
1247	17.70	5.13	Four intrachromosomal extra-copies in ring chromosome	-
1524	95.71	159.84	Two to five intrachromosomal extra copies in marker chromosome	High level gain
290	2.66	3.01	Gain of one copy (tandem duplication)	-
1213	5.69	1.80	t(8;14)	-
1148	0.72	0.73	N	N
2204	0.12	0.08	N	-
296	0.57	0.75	N	-
628	4.16	4.30	N	-
2859	2.79	2.90	N	-
832	1.19	0.85	N	-
938	0.29	0.64	N	-
1679	0.46	1.18	N	-
993	1.73	4.54	N	-
777	0.85	1.16	N	-
1623	6.94	15.08	N	-
571	1.98	4.28	N	-
667	5.66	1.89	N	-

MDS, myelodisplastic; N, normal; Amp, amplification; DM, double minute

[a] Ratio compared with the myelodisplastic sample

[b] Amplification in form of DM was only present in 10% PC

REFERENCES

1. Albertson DG, Collins C, McCormick F and Gray JW. Chromosome aberrations in solid tumors. NatGenet. 2003;34:369-376.

2. Vogelstein B and Kinzler KW. Cancer genes and the pathways they control. NatMed. 2004;10:789-799.

3. Strachan T and Read AP. Human Molecular Genetics 3; chapter 17: 'Cancer genetics'. Garland Science. pp 487-504; 2004.

4. Santarosa M and Ashworth A. Haploinsufficiency for tumour suppressor genes: when you don't need to go all the way. BiochimBiophysActa. 2004;1654:105-122.

5. Nowell P and Hungerford DA. A minute chromosome in chronic granulocytic leukemia. Science. 1960;132:1497.

6. Rowley JD. Letter: A new consistent chromosomal abnormality in chronic myelogenous leukaemia identified by quinacrine fluorescence and Giemsa staining. Nature. 1973;243:290-293.

7. Heisterkamp N, Stam K, Groffen J, de KA and Grosveld G. Structural organization of the bcr gene and its role in the Ph' translocation. Nature. 1985;315:758-761.

8. Deininger MW, Goldman JM and Melo JV. The molecular biology of chronic myeloid leukemia. Blood. 2000;96:3343-3356.

9. Schlegel J, Stumm G, Scherthan H, Bocker T, Zirngibl H, Ruschoff J and Hofstadter F. Comparative genomic in situ hybridization of colon carcinomas with replication error. Cancer Res. 1995;55:6002-6005.

10. Weissman IL. Stem cells: units of development, units of regeneration, and units in evolution. Cell. 2000;100:157-168.

11. Lemischka I. Stem cell dogmas in the genomics era. RevClinExpHematol. 2001;5:15-25.

12. Kondo M, Weissman IL and Akashi K. Identification of clonogenic common lymphoid progenitors in mouse bone marrow. Cell. 1997;91:661-672.

13. Akashi K, Traver D, Miyamoto T and Weissman IL. A clonogenic common myeloid progenitor that gives rise to all myeloid lineages. Nature. 2000;404:193-197.

14. Orkin SH and Zon LI. Hematopoiesis and stem cells: plasticity versus developmental heterogeneity. NatImmunol. 2002;3:323-328.

15. Rolink AG, Schaniel C, Andersson J and Melchers F. Selection events operating at various stages in B cell development. CurrOpinImmunol. 2001;13:202-207.

16. Ghia P, ten BE, Rolink AG and Melchers F. B-cell development: a comparison between mouse and man. ImmunolToday. 1998;19:480-485.

17. Shapiro-Shelef M and Calame K. Regulation of plasma-cell development. NatRevImmunol. 2005;5:230-242.

18. Kuppers R, Klein U, Hansmann ML and Rajewsky K. Cellular origin of human B-cell lymphomas. N Engl J Med. 1999;341:1520-1529.

19. Roitt I BJMD. Immunology (Sixth Edition). Mosby. Antibodies. pp 65-85; 2001.

20. Bross L, Fukita Y, McBlane F, Demolliere C, Rajewsky K and Jacobs H. DNA double-strand breaks in immunoglobulin genes undergoing somatic hypermutation. Immunity. 2000;13:589-597.

21. Papavasiliou FN and Schatz DG. Cell-cycle-regulated DNA double-stranded breaks in somatic hypermutation of immunoglobulin genes. Nature. 2000;408:216-221.

22. Kuppers R and Dalla-Favera R. Mechanisms of chromosomal translocations in B cell lymphomas. Oncogene. 2001;20:5580-5594.

23. Harris NL, Stein H, Coupland SE, Hummel M, Favera RD, Pasqualucci L and Chan WC. New approaches to lymphoma diagnosis. HematologyAmSocHematolEducProgram. 2001:194-220.

24. Dalla-Favera R and Gaidano G. Molecular Biology of Lymphomas. In: De Vita VTJ, Hellman S, Rosenberg SA. Principles and Prectise of Oncology. Philadelphia, Lippincott Williams & Wilkins. pp2215-2235; 2001.

25. Rubnitz JE and Pui CH. Recent advances in the treatment and understanding of childhood acute lymphoblastic leukaemia. Cancer Treat Rev. 2003;29:31-44.

26. van Gent DC, Hoeijmakers JH and Kanaar R. Chromosomal stability and the DNA double-stranded break connection. Nat Rev Genet. 2001;2:196-206.

27. Tsujimoto Y, Cossman J, Jaffe E and Croce CM. Involvement of the bcl-2 gene in human follicular lymphoma. Science. 1985;228:1440-1443.

28. Tsujimoto Y, Louie E, Bashir MM and Croce CM. The reciprocal partners of both the t(14; 18) and the t(11; 14) translocations involved in B-cell neoplasms are rearranged by the same mechanism. Oncogene. 1988;2:347-351.

29. Pelicci PG, Knowles DM, 2nd, Magrath I and Dalla-Favera R. Chromosomal breakpoints and structural alterations of the c-myc locus differ in endemic and sporadic forms of Burkitt lymphoma. Proc Natl Acad Sci U S A. 1986;83:2984-2988.

30. Rabbitts TH, Forster A, Baer R and Hamlyn PH. Transcription enhancer identified near the human C mu immunoglobulin heavy chain gene is unavailable to the translocated c-myc gene in a Burkitt lymphoma. Nature. 1983;306:806-809.

31. Gelmann EP, Psallidopoulos MC, Papas TS and Dalla-Favera R. Identification of reciprocal translocation sites within the c-myc oncogene and immunoglobulin mu locus in a Burkitt lymphoma. Nature. 1983;306:799-803.

32. Kuipers J, Vaandrager JW, Weghuis DO, Pearson PL, Scheres J, Lokhorst HM, Clevers H and Bast BJ. Fluorescence in situ hybridization analysis shows the frequent occurrence of 14q32.3 rearrangements with involvement of immunoglobulin switch regions in myeloma cell lines. Cancer Genet Cytogenet. 1999;109:99-107.

33. Pasqualucci L, Neumeister P, Goossens T, Nanjangud G, Chaganti RS, Kuppers R and la-Favera R. Hypermutation of multiple proto-oncogenes in B-cell diffuse large-cell lymphomas. Nature. 2001;412:341-346.

34. Kuehl WM and Bergsagel PL. Multiple myeloma: evolving genetic events and host interactions. NatRevCancer. 2002;2:175-187.

35. Criteria for the classification of monoclonal gammopathies, multiple myeloma and related disorders: a report of the International Myeloma Working Group. BrJHaematol. 2003;121:749-757.

36. Swerdlow SH, Campo E, Harris NL, Jaffe ES, Pileri SA, Stein H, Thiele J and Vardiman JW. WHO Classification of Tumours of Haematopoietic and Lymphoid Tissues; 2008.

37. Durie BG, Harousseau JL, Miguel JS, Blade J, Barlogie B, Anderson K, Gertz M, Dimopoulos M, Westin J, Sonneveld P, Ludwig H, Gahrton G, Beksac M, Crowley J, Belch A, Boccadaro M, Cavo M, Turesson I, Joshua D, Vesole D, Kyle R, Alexanian R, Tricot G, Attal M, Merlini G, Powles R, Richardson P, Shimizu K, Tosi P, Morgan G and Rajkumar SV. International uniform response criteria for multiple myeloma. Leukemia. 2006;20:1467-1473.

38. Smith A, Wisloff F and Samson D. Guidelines on the diagnosis and management of multiple myeloma 2005. BrJHaematol. 2006;132:410-451.

39. Kyle RA, Remstein ED, Therneau TM, Dispenzieri A, Kurtin PJ, Hodnefield JM, Larson DR, Plevak MF, Jelinek DF, Fonseca R, Melton LJ, III and Rajkumar SV. Clinical course and prognosis of smoldering (asymptomatic) multiple myeloma. NEnglJMed. 2007;356:2582-2590.

40. Kyle RA, Therneau TM, Rajkumar SV, Offord JR, Larson DR, Plevak MF and Melton LJ, III. A long-term study of prognosis in monoclonal gammopathy of undetermined significance. NEnglJMed. 2002;346:564-569.

41. Weber DM, Dimopoulos MA, Moulopoulos LA, Delasalle KB, Smith T and Alexanian R. Prognostic features of asymptomatic multiple myeloma. BrJHaematol. 1997;97:810-814.

42. Kyle RA, Therneau TM, Rajkumar SV, Larson DR, Plevak MF, Offord JR, Dispenzieri A, Katzmann JA and Melton LJ, III. Prevalence of monoclonal gammopathy of undetermined significance. NEnglJMed. 2006;354:1362-1369.

43. Cohen HJ, Crawford J, Rao MK, Pieper CF and Currie MS. Racial differences in the prevalence of monoclonal gammopathy in a community-based sample of the elderly. AmJMed. 1998;104:439-444.

44. Fonseca R, Bailey RJ, Ahmann GJ, Rajkumar SV, Hoyer JD, Lust JA, Kyle RA, Gertz MA, Greipp PR and Dewald GW. Genomic abnormalities in monoclonal gammopathy of undetermined significance. Blood. 2002;100:1417-1424.

45. Drach J, Angerler J, Schuster J, Rothermundt C, Thalhammer R, Haas OA, Jager U, Fiegl M, Geissler K, Ludwig H and Huber H. Interphase fluorescence in situ hybridization identifies chromosomal abnormalities in plasma cells from patients with monoclonal gammopathy of undetermined significance. Blood. 1995;86:3915-3921.

46. Fonseca R, Barlogie B, Bataille R, Bastard C, Bergsagel PL, Chesi M, Davies FE, Drach J, Greipp PR, Kirsch IR, Kuehl WM, Hernandez JM, Minvielle S, Pilarski LM, Shaughnessy JD, Jr., Stewart AK and vet-Loiseau H. Genetics and cytogenetics of multiple myeloma: a workshop report. Cancer Res. 2004;64:1546-1558.

47. Kyle RA. 'Benign' monoclonal gammopathy--after 20 to 35 years of follow-up. Mayo ClinProc. 1993;68:26-36.

48. Rajkumar SV, Lacy MQ and Kyle RA. Monoclonal gammopathy of undetermined significance and smoldering multiple myeloma. Blood Rev. 2007;21:255-265.

49. Cesana C, Klersy C, Barbarano L, Nosari AM, Crugnola M, Pungolino E, Gargantini L, Granata S, Valentini M and Morra E. Prognostic factors for malignant transformation in monoclonal gammopathy of undetermined significance and smoldering multiple myeloma. JClinOncol. 2002;20:1625-1634.

50. Rosinol L, Cibeira MT, Montoto S, Rozman M, Esteve J, Filella X and Blade J. Monoclonal gammopathy of undetermined significance: predictors of malignant transformation and recognition of an evolving type characterized by a progressive increase in M protein size. Mayo Clin Proc. 2007;82:428-434.

51. Gregersen H, Mellemkjaer L, Ibsen JS, Dahlerup JF, Thomassen L and Sorensen HT. The impact of M-component type and immunoglobulin concentration on the risk of malignant transformation in patients with monoclonal gammopathy of undetermined significance. Haematologica. 2001;86:1172-1179.

52. Blade J, Lopez-Guillermo A, Rozman C, Cervantes F, Salgado C, Aguilar JL, Vives-Corrons JL and Montserrat E. Malignant transformation and life expectancy in monoclonal gammopathy of undetermined significance. Br J Haematol. 1992;81:391-394.

53. Kyle RA and Greipp PR. Smoldering multiple myeloma. NEnglJMed. 1980;302:1347-1349.

54. Rosinol L, Blade J, Esteve J, Aymerich M, Rozman M, Montoto S, Gine E, Nadal E, Filella X, Queralt R, Carrio A and Montserrat E. Smoldering multiple myeloma: natural history and recognition of an evolving type. BrJHaematol. 2003;123:631-636.

55. Blade J, Rosinol L, Cibeira MT and de Larrea CF. Pathogenesis and progression of monoclonal gammopathy of undetermined significance. Leukemia. 2008;22:1651-1657.

56. Dimopoulos MA, Kastritis E and Anagnostopoulos A. Hematological malignancies: myeloma. AnnOncol. 2006;17 Suppl 10:x137-x143.

57. Klein B, Zhang XG, Lu ZY and Bataille R. Interleukin-6 in human multiple myeloma. Blood. 1995;85:863-872.

58. Rajkumar SV, Fonseca R, Dewald GW, Therneau TM, Lacy MQ, Kyle RA, Greipp PR and Gertz MA. Cytogenetic abnormalities correlate with the plasma cell labeling index and extent of bone marrow involvement in myeloma. Cancer GenetCytogenet. 1999;113:73-77.

59. Greipp PR, San MJ, Durie BG, Crowley JJ, Barlogie B, Blade J, Boccadoro M, Child JA, vet-Loiseau H, Kyle RA, Lahuerta JJ, Ludwig H, Morgan G, Powles R, Shimizu K, Shustik C, Sonneveld P, Tosi P, Turesson I and Westin J. International staging system for multiple myeloma. JClinOncol. 2005;23:3412-3420.

60. Kyle RA and Rajkumar SV. Multiple myeloma. N Engl J Med. 2004;351:1860-1873.

61. Sirohi B and Powles R. Multiple myeloma. Lancet. 2004;363:875-887.

62. Barlogie B, Shaughnessy J, Tricot G, Jacobson J, Zangari M, Anaissie E, Walker R and Crowley J. Treatment of multiple myeloma. Blood. 2004;103:20-32.

63. Kyle RA, Maldonado JE and Bayrd ED. Plasma cell leukemia. Report on 17 cases. ArchInternMed. 1974;133:813-818.

64. Saccaro S, Fonseca R, Veillon DM, Cotelingam J, Nordberg ML, Bredeson C, Glass J and Munker R. Primary plasma cell leukemia: report of 17 new cases treated with autologous or allogeneic stem-cell transplantation and review of the literature. AmJHematol. 2005;78:288-294.

65. Chang H, Sloan S, Li D and Patterson B. Genomic aberrations in plasma cell leukemia shown by interphase fluorescence in situ hybridization. Cancer GenetCytogenet. 2005;156:150-153.

66. Noel P and Kyle RA. Plasma cell leukemia: an evaluation of response to therapy. AmJMed. 1987;83:1062-1068.

67. Dimopoulos MA, Palumbo A, Delasalle KB and Alexanian R. Primary plasma cell leukaemia. BrJHaematol. 1994;88:754-759.

68. Ruiz-Arguelles GJ and San Miguel JF. Cell surface markers in multiple myeloma. Mayo ClinProc. 1994;69:684-690.

69. Van CB, Durie BG, Spier C, De WM, Van RI, Vela E, Frutiger Y, Richter L and Grogan TM. Plasma cells in multiple myeloma express a natural killer cell-associated antigen: CD56 (NKH-1; Leu-19). Blood. 1990;76:377-382.

70. Pellat-Deceunynck C, Bataille R, Robillard N, Harousseau JL, Rapp MJ, Juge-Morineau N, Wijdenes J and Amiot M. Expression of CD28 and CD40 in human myeloma cells: a comparative study with normal plasma cells. Blood. 1994;84:2597-2603.

71. Garcia-Sanz R, Orfao A, Gonzalez M, Tabernero MD, Blade J, Moro MJ, Fernandez-Calvo J, Sanz MA, Perez-Simon JA, Rasillo A and Miguel JF. Primary plasma cell leukemia: clinical, immunophenotypic, DNA ploidy, and cytogenetic characteristics. Blood. 1999;93:1032-1037.

72. Dimopoulos MA, Moulopoulos LA, Maniatis A and Alexanian R. Solitary plasmacytoma of bone and asymptomatic multiple myeloma. Blood. 2000;96:2037-2044.

73. Dimopoulos MA, Kiamouris C and Moulopoulos LA. Solitary plasmacytoma of bone and extramedullary plasmacytoma. HematolOncolClinNorth Am. 1999;13:1249-1257.

74. Landgren O, Kyle RA, Pfeiffer RM, Katzmann JA, Caporaso NE, Hayes RB, Dispenzieri A, Kumar S, Clark RJ, Baris D, Hoover R and Rajkumar SV. Monoclonal gammopathy of undetermined significance (MGUS) consistently precedes multiple myeloma: a prospective study. Blood. 2009;113:5412-5417.

75. Weiss BM, Abadie J, Verma P, Howard RS and Kuehl WM. A monoclonal gammopathy precedes multiple myeloma in most patients. Blood. 2009;113:5418-5422.

76. Pratt G. Molecular aspects of multiple myeloma. MolPathol. 2002;55:273-283.

77. Jego G, Bataille R, Geffroy-Luseau A, Descamps G and Pellat-Deceunynck C. Pathogen-associated molecular patterns are growth and survival factors for human myeloma cells through Toll-like receptors. Leukemia. 2006;20:1130-1137.

78. Bohnhorst J, Rasmussen T, Moen SH, Flottum M, Knudsen L, Borset M, Espevik T and Sundan A. Toll-like receptors mediate proliferation and survival of multiple myeloma cells. Leukemia. 2006;20:1138-1144.

79. Mantovani A and Garlanda C. Inflammation and multiple myeloma: the Toll connection. Leukemia. 2006;20:937-938.

80. Vacca A and Ribatti D. Bone marrow angiogenesis in multiple myeloma. Leukemia. 2006;20:193-199.

81. Sawyer JR, Waldron JA, Jagannath S and Barlogie B. Cytogenetic findings in 200 patients with multiple myeloma. Cancer GenetCytogenet. 1995;82:41-49.

82. Tricot G, Barlogie B, Jagannath S, Bracy D, Mattox S, Vesole DH, Naucke S and Sawyer JR. Poor prognosis in multiple myeloma is associated only with partial or complete deletions of chromosome 13 or abnormalities involving 11q and not with other karyotype abnormalities. Blood. 1995;86:4250-4256.

83. Facon T, Lai JL, Nataf E, Preudhomme C, Zandecki M, Hammad M, Wattel E, Jouet JP and Bauters F. Improved cytogenetic analysis of bone marrow plasma cells after cytokine stimulation in multiple myeloma: a report on 46 patients. BrJHaematol. 1993;84:743-745.

84. Smadja NV, Louvet C, Isnard F, Dutel JL, Grange MJ, Varette C and Krulik M. Cytogenetic study in multiple myeloma at diagnosis: comparison of two techniques. BrJHaematol. 1995;90:619-624.

85. Avet-Loiseau H, Facon T, Daviet A, Godon C, Rapp MJ, Harousseau JL, Grosbois B and Bataille R. 14q32 translocations and monosomy 13 observed in monoclonal gammopathy of undetermined significance delineate a multistep process for the oncogenesis of multiple myeloma. Intergroupe Francophone du Myelome. Cancer Res. 1999;59:4546-4550.

86. Flactif M, Zandecki M, Lai JL, Bernardi F, Obein V, Bauters F and Facon T. Interphase fluorescence in situ hybridization (FISH) as a powerful tool for the detection of aneuploidy in multiple myeloma. Leukemia. 1995;9:2109-2114.

87. Chiecchio L, Protheroe RK, Ibrahim AH, Cheung KL, Rudduck C, Dagrada GP, Cabanas ED, Parker T, Nightingale M, Wechalekar A, Orchard KH, Harrison CJ, Cross NC, Morgan GJ and Ross FM. Deletion of chromosome 13 detected by conventional cytogenetics is a critical prognostic factor in myeloma. Leukemia. 2006;20:1610-1617.

88. Arzoumanian V, Hoering A, Sawyer J, van RF, Bailey C, Gurley J, Shaughnessy JD, Jr., Anaissie E, Crowley J and Barlogie B. Suppression of abnormal karyotype predicts superior survival in multiple myeloma. Leukemia. 2008;22:850-855.

89. Chng WJ, Glebov O, Bergsagel PL and Kuehl WM. Genetic events in the pathogenesis of multiple myeloma. BestPractResClinHaematol. 2007;20:571-596.

90. Bergsagel PL and Kuehl WM. Molecular pathogenesis and a consequent classification of multiple myeloma. JClinOncol. 2005;23:6333-6338.

91. Drach J, Schuster J, Nowotny H, Angerler J, Rosenthal F, Fiegl M, Rothermundt C, Gsur A, Jager U and Heinz R. Multiple myeloma: high incidence of chromosomal aneuploidy as detected by interphase fluorescence in situ hybridization. Cancer Res. 1995;55:3854-3859.

92. Smadja NV, Bastard C, Brigaudeau C, Leroux D and Fruchart C. Hypodiploidy is a major prognostic factor in multiple myeloma. Blood. 2001;98:2229-2238.

93. Smadja NV, Fruchart C, Isnard F, Louvet C, Dutel JL, Cheron N, Grange MJ, Monconduit M and Bastard C. Chromosomal analysis in multiple myeloma: cytogenetic evidence of two different diseases. Leukemia. 1998;12:960-969.

94. bes-Marun CS, Dewald GW, Bryant S, Picken E, Santana-Davila R, Gonzalez-Paz N, Winkler JM, Kyle RA, Gertz MA, Witzig TE, Dispenzieri A, Lacy MQ, Rajkumar SV, Lust JA, Greipp PR and Fonseca R. Chromosome abnormalities clustering and its implications for pathogenesis and prognosis in myeloma. Leukemia. 2003;17:427-436.

95. Zandecki M, Lai JL, Genevieve F, Bernardi F, Volle-Remy H, Blanchet O, Francois M, Cosson A, Bauters F and Facon T. Several cytogenetic subclones may be identified within plasma cells from patients with monoclonal gammopathy of undetermined significance, both at diagnosis and during the indolent course of this condition. Blood. 1997;90:3682-3690.

96. Barlogie B, Drewinko B, Schumann J, Gohde W, Dosik G, Latreille J, Johnston DA and Freireich EJ. Cellular DNA content as a marker of neoplasia in man. Am J Med. 1980;69:195-203.

97. Avet-Loiseau H, Daviet A, Brigaudeau C, Callet-Bauchu E, Terre C, Lafage-Pochitaloff M, Desangles F, Ramond S, Talmant P and Bataille R. Cytogenetic, interphase, and multicolor fluorescence in situ hybridization analyses in primary plasma cell leukemia: a study of 40 patients at diagnosis, on behalf of the Intergroupe Francophone du Myelome and the Groupe Francais de Cytogenetique Hematologique. Blood. 2001;97:822-825.

98. Avet-Louseau H, Daviet A, Sauner S and Bataille R. Chromosome 13 abnormalities in multiple myeloma are mostly monosomy 13. BrJHaematol. 2000;111:1116-1117.

99. Fonseca R, Oken MM, Harrington D, Bailey RJ, Van Wier SA, Henderson KJ, Kay NE, Van NB, Greipp PR and Dewald GW. Deletions of chromosome 13 in multiple myeloma identified by interphase FISH usually denote large deletions of the q arm or monosomy. Leukemia. 2001;15:981-986.

100. Shaughnessy J, Tian E, Sawyer J, Bumm K, Landes R, Badros A, Morris C, Tricot G, Epstein J and Barlogie B. High incidence of chromosome 13 deletion in multiple myeloma detected by multiprobe interphase FISH. Blood. 2000;96:1505-1511.

101. Hanahan D and Weinberg RA. The hallmarks of cancer. Cell. 2000;100:57-70.

102. Shaughnessy J, Jacobson J, Sawyer J, McCoy J, Fassas A, Zhan F, Bumm K, Epstein J, Anaissie E, Jagannath S, Vesole D, Siegel D, Desikan R, Munshi N, Badros A, Tian E, Zangari M, Tricot G, Crowley J and Barlogie B. Continuous absence of metaphase-defined cytogenetic abnormalities, especially of chromosome 13 and hypodiploidy, ensures long-term survival in multiple myeloma treated with Total Therapy I: interpretation in the context of global gene expression. Blood. 2003;101:3849-3856.

103. Konigsberg R, Ackermann J, Kaufmann H, Zojer N, Urbauer E, Kromer E, Jager U, Gisslinger H, Schreiber S, Heinz R, Ludwig H, Huber H and Drach J. Deletions of chromosome 13q in monoclonal gammopathy of undetermined significance. Leukemia. 2000;14:1975-1979.

104. Brousseau M, Leleu X, Gerard J, Gastinne T, Godon A, Genevieve F, Dib M, Lai JL, Facon T and Zandecki M. Hyperdiploidy is a common finding in monoclonal gammopathy of undetermined significance and monosomy 13 is restricted to these hyperdiploid patients. ClinCancer Res. 2007;13:6026-6031.

105. Gutierrez NC, Castellanos MV, Martin ML, Mateos MV, Hernandez JM, Fernandez M, Carrera D, Rosinol L, Ribera JM, Ojanguren JM, Palomera L, Gardella S, Escoda L, Hernandez-Boluda JC, Bello JL, de la RJ, Lahuerta JJ and San Miguel JF. Prognostic and biological implications of genetic abnormalities in multiple myeloma undergoing autologous stem cell transplantation: t(4;14) is the most relevant adverse prognostic factor, whereas RB deletion as a unique abnormality is not associated with adverse prognosis. Leukemia. 2007;21:143-150.

106. Gabrea A, Leif BP and Michael KW. Distinguishing primary and secondary translocations in multiple myeloma. DNA Repair (Amst). 2006;5:1225-1233.

107. Bergsagel PL and Kuehl WM. Chromosome translocations in multiple myeloma. Oncogene. 2001;20:5611-5622.

108. Fonseca R, Blood E, Rue M, Harrington D, Oken MM, Kyle RA, Dewald GW, Van NB, Van Wier SA, Henderson KJ, Bailey RJ and Greipp PR. Clinical and biologic implications of recurrent genomic aberrations in myeloma. Blood. 2003;101:4569-4575.

109. Avet-Loiseau H, Facon T, Grosbois B, Magrangeas F, Rapp MJ, Harousseau JL, Minvielle S and Bataille R. Oncogenesis of multiple myeloma: 14q32 and 13q chromosomal abnormalities are not randomly distributed, but correlate with natural history, immunological features, and clinical presentation. Blood. 2002;99:2185-2191.

110. Fabris S, Storlazzi CT, Baldini L, Nobili L, Lombardi L, Maiolo AT, Rocchi M and Neri A. Heterogeneous pattern of chromosomal breakpoints involving the MYC locus in multiple myeloma. Genes ChromosomesCancer. 2003;37:261-269.

111. Avet-Loiseau H, Gerson F, Magrangeas F, Minvielle S, Harousseau JL and Bataille R. Rearrangements of the c-myc oncogene are present in 15% of primary human multiple myeloma tumors. Blood. 2001;98:3082-3086.

112. Shou Y, Martelli ML, Gabrea A, Qi Y, Brents LA, Roschke A, Dewald G, Kirsch IR, Bergsagel PL and Kuehl WM. Diverse karyotypic abnormalities of the c-myc locus associated with c-myc dysregulation and tumor progression in multiple myeloma. Proc Natl Acad Sci U S A. 2000;97:228-233.

113. Chesi M, Bergsagel PL, Brents LA, Smith CM, Gerhard DS and Kuehl WM. Dysregulation of cyclin D1 by translocation into an IgH gamma switch region in two multiple myeloma cell lines. Blood. 1996;88:674-681.

114. Chesi M, Bergsagel PL, Shonukan OO, Martelli ML, Brents LA, Chen T, Schrock E, Ried T and Kuehl WM. Frequent dysregulation of the c-maf proto-oncogene at 16q23 by translocation to an Ig locus in multiple myeloma. Blood. 1998;91:4457-4463.

115. Chesi M, Nardini E, Lim RS, Smith KD, Kuehl WM and Bergsagel PL. The t(4;14) translocation in myeloma dysregulates both FGFR3 and a novel gene, MMSET, resulting in IgH/MMSET hybrid transcripts. Blood. 1998;92:3025-3034.

116. Chesi M, Nardini E, Brents LA, Schrock E, Ried T, Kuehl WM and Bergsagel PL. Frequent translocation t(4;14)(p16.3;q32.3) in multiple myeloma is associated with increased expression and activating mutations of fibroblast growth factor receptor 3. NatGenet. 1997;16:260-264.

117. Shaughnessy J, Jr., Gabrea A, Qi Y, Brents L, Zhan F, Tian E, Sawyer J, Barlogie B, Bergsagel PL and Kuehl M. Cyclin D3 at 6p21 is dysregulated by recurrent chromosomal translocations to immunoglobulin loci in multiple myeloma. Blood. 2001;98:217-223.

118. Hanamura I, Iida S, Akano Y, Hayami Y, Kato M, Miura K, Harada S, Banno S, Wakita A, Kiyoi H, Naoe T, Shimizu S, Sonta SI, Nitta M, Taniwaki M and Ueda R. Ectopic expression of MAFB gene in human myeloma cells carrying (14;20)(q32;q11) chromosomal translocations. JpnJCancer Res. 2001;92:638-644.

119. Keats JJ, Reiman T, Belch AR and Pilarski LM. Ten years and counting: so what do we know about t(4;14)(p16;q32) multiple myeloma. LeukLymphoma. 2006;47:2289-2300.

120. Peters K, Ornitz D, Werner S and Williams L. Unique expression pattern of the FGF receptor 3 gene during mouse organogenesis. DevBiol. 1993;155:423-430.

121. Kanai M, Goke M, Tsunekawa S and Podolsky DK. Signal transduction pathway of human fibroblast growth factor receptor 3. Identification of a novel 66-kDa phosphoprotein. JBiolChem. 1997;272:6621-6628.

122. Chesi M, Brents LA, Ely SA, Bais C, Robbiani DF, Mesri EA, Kuehl WM and Bergsagel PL. Activated fibroblast growth factor receptor 3 is an oncogene that contributes to tumor progression in multiple myeloma. Blood. 2001;97:729-736.

123. Keats JJ, Reiman T, Maxwell CA, Taylor BJ, Larratt LM, Mant MJ, Belch AR and Pilarski LM. In multiple myeloma, t(4;14)(p16;q32) is an adverse prognostic factor irrespective of FGFR3 expression. Blood. 2003;101:1520-1529.

124. Zhan F, Huang Y, Colla S, Stewart JP, Hanamura I, Gupta S, Epstein J, Yaccoby S, Sawyer J, Burington B, Anaissie E, Hollmig K, Pineda-Roman M, Tricot G, van RF, Walker R, Zangari M, Crowley J, Barlogie B and Shaughnessy JD, Jr. The molecular classification of multiple myeloma. Blood. 2006;108:2020-2028.

125. Mateos MV, Hernandez JM, Hernandez MT, Gutierrez NC, Palomera L, Fuertes M, az-Mediavilla J, Lahuerta JJ, de la RJ, Terol MJ, Sureda A, Bargay J, Ribas P, de AF, Alegre A, Oriol A, Carrera D, Garcia-Larana J, Garcia-Sanz R, Blade J, Prosper F, Mateo G, Esseltine DL, van dV and San Miguel JF. Bortezomib plus melphalan and prednisone in elderly untreated patients with multiple myeloma: results of a multicenter phase 1/2 study. Blood. 2006;108:2165-2172.

126. Shaughnessy JD, Zhou Y, Haessler J, van Rhee F, Anaissie E, Nair B, Waheed S, Alsayed Y, Epstein J, Crowley J and Barlogie B. TP53 deletion is not an adverse feature in multiple myeloma treated with total therapy 3. Br J Haematol. 2009;147:347-351.

127. Fonseca R, Blood EA, Oken MM, Kyle RA, Dewald GW, Bailey RJ, Van Wier SA, Henderson KJ, Hoyer JD, Harrington D, Kay NE, Van NB and Greipp PR. Myeloma and the t(11;14)(q13;q32); evidence for a biologically defined unique subset of patients. Blood. 2002;99:3735-3741.

128. Hayman SR, Bailey RJ, Jalal SM, Ahmann GJ, Dispenzieri A, Gertz MA, Greipp PR, Kyle RA, Lacy MQ, Rajkumar SV, Witzig TE, Lust JA and Fonseca R. Translocations involving the immunoglobulin heavy-chain locus are possible early genetic events in patients with primary systemic amyloidosis. Blood. 2001;98:2266-2268.

129. Cicatiello L, Addeo R, Sasso A, Altucci L, Petrizzi VB, Borgo R, Cancemi M, Caporali S, Caristi S, Scafoglio C, Teti D, Bresciani F, Perillo B and Weisz A. Estrogens and progesterone promote persistent CCND1 gene activation during G1 by inducing transcriptional derepression via c-Jun/c-Fos/estrogen receptor (progesterone receptor) complex assembly to a distal regulatory element and recruitment of cyclin D1 to its own gene promoter. Mol Cell Biol. 2004;24:7260-7274.

130. Moreno-Bueno G, Rodriguez-Perales S, Sanchez-Estevez C, Hardisson D, Sarrio D, Prat J, Cigudosa JC, Matias-Guiu X and Palacios J. Cyclin D1 gene (CCND1) mutations in endometrial cancer. Oncogene. 2003;22:6115-6118.

131. Freier K, Joos S, Flechtenmacher C, Devens F, Benner A, Bosch FX, Lichter P and Hofele C. Tissue microarray analysis reveals site-specific prevalence of oncogene amplifications in head and neck squamous cell carcinoma. Cancer Res. 2003;63:1179-1182.

132. Janssen JW, Vaandrager JW, Heuser T, Jauch A, Kluin PM, Geelen E, Bergsagel PL, Kuehl WM, Drexler HG, Otsuki T, Bartram CR and Schuuring E. Concurrent activation of a novel putative transforming gene, myeov, and cyclin D1 in a subset of multiple myeloma cell lines with t(11;14)(q13;q32). Blood. 2000;95:2691-2698.

133. Natkunam Y, Tedoldi S, Paterson JC, Zhao S, Rodriguez-Justo M, Beck AH, Siebert R, Mason DY and Marafioti T. Characterization of c-Maf transcription factor in normal and neoplastic hematolymphoid tissue and its relevance in plasma cell neoplasia. Am J Clin Pathol. 2009;132:361-371.

134. Paige AJ, Taylor KJ, Taylor C, Hillier SG, Farrington S, Scott D, Porteous DJ, Smyth JF, Gabra H and Watson JE. WWOX: a candidate tumor suppressor gene involved in multiple tumor types. ProcNatlAcadSciUSA. 2001;98:11417-11422.

135. Ried K, Finnis M, Hobson L, Mangelsdorf M, Dayan S, Nancarrow JK, Woollatt E, Kremmidiotis G, Gardner A, Venter D, Baker E and Richards RI. Common chromosomal fragile site FRA16D sequence: identification of the FOR gene spanning FRA16D and homozygous deletions and translocation breakpoints in cancer cells. HumMolGenet. 2000;9:1651-1663.

136. Hurt EM, Wiestner A, Rosenwald A, Shaffer AL, Campo E, Grogan T, Bergsagel PL, Kuehl WM and Staudt LM. Overexpression of c-maf is a frequent oncogenic event in multiple myeloma that promotes proliferation and pathological interactions with bone marrow stroma. Cancer Cell. 2004;5:191-199.

137. Malgeri U, Baldini L, Perfetti V, Fabris S, Vignarelli MC, Colombo G, Lotti V, Compasso S, Bogni S, Lombardi L, Maiolo AT and Neri A. Detection of t(4;14)(p16.3;q32) chromosomal translocation in multiple myeloma by reverse transcription-polymerase chain reaction analysis of IGH-MMSET fusion transcripts. Cancer Res. 2000;60:4058-4061.

138. Van Wier SA, Ahmann G, Henderson K, Greipp P, Rajkumar SV, Larson D, Dispenzieri A, Gertz M, Kyle R and Fonseca R. The t(4;14) is present in patients with early stage plasma cell proliferative disorders including MGUS and smouldering multiple myeloma (SMM). Blood. 2005;ASH Annual Meeting Abstracts 2005;106: Abstract 1545.

139. Fabris S, Agnelli L, Mattioli M, Baldini L, Ronchetti D, Morabito F, Verdelli D, Nobili L, Intini D, Callea V, Stelitano C, Lombardi L and Neri A. Characterization of oncogene dysregulation in multiple myeloma by combined FISH and DNA microarray analyses. Genes ChromosomesCancer. 2005;42:117-127.

140. Kataoka K, Fujiwara KT, Noda M and Nishizawa M. MafB, a new Maf family transcription activator that can associate with Maf and Fos but not with Jun. MolCell Biol. 1994;14:7581-7591.

141. Adhikary S and Eilers M. Transcriptional regulation and transformation by Myc proteins. Nat Rev Mol Cell Biol. 2005;6:635-645.

142. Wanzel M, Herold S and Eilers M. Transcriptional repression by Myc. Trends Cell Biol. 2003;13:146-150.

143. Avet-Loiseau H, Attal M, Moreau P, Charbonnel C, Garban F, Hulin C, Leyvraz S, Michallet M, Yakoub-Agha I, Garderet L, Marit G, Michaux L, Voillat L, Renaud M, Grosbois B, Guillerm G, Benboubker L, Monconduit M, Thieblemont C, Casassus P, Caillot D, Stoppa AM, Sotto JJ, Wetterwald M, Dumontet C, Fuzibet JG, Azais I, Dorvaux V, Zandecki M, Bataille R, Minvielle S, Harousseau JL, Facon T and Mathiot C. Genetic abnormalities and survival in multiple myeloma: the experience of the Intergroupe Francophone du Myelome. Blood. 2007;109:3489-3495.

144. Fonseca R, Harrington D, Oken MM, Dewald GW, Bailey RJ, Van Wier SA, Henderson KJ, Blood EA, Rajkumar SV, Kay NE, Van Ness B and Greipp PR. Biological and prognostic significance of interphase fluorescence in situ hybridization detection of chromosome 13 abnormalities (delta13) in multiple myeloma: an eastern cooperative oncology group study. Cancer Res. 2002;62:715-720.

145. Drach J, Ackermann J, Fritz E, Kromer E, Schuster R, Gisslinger H, DeSantis M, Zojer N, Fiegl M, Roka S, Schuster J, Heinz R, Ludwig H and Huber H. Presence of a p53 gene deletion in patients with multiple myeloma predicts for short survival after conventional-dose chemotherapy. Blood. 1998;92:802-809.

146. Chng WJ, Price-Troska T, Gonzalez-Paz N, Van Wier S, Jacobus S, Blood E, Henderson K, Oken M, Van Ness B, Greipp P, Rajkumar SV and Fonseca R. Clinical significance of TP53 mutation in myeloma. Leukemia. 2007;21:582-584.

147. Xiong W, Zhan F, Huang Y, Barlogie B and Shaughnessy J. TP53 Gene expression, correlated with 17p13 deletion, is a significant and independent adverse prognostic factor in multiple myeloma treated with high-dose therapy and auto-transplants. ASH Annual Meeting Abstracts 2006;108:3394. 2006.

148. Neri A, Baldini L, Trecca D, Cro L, Polli E and Maiolo AT. p53 gene mutations in multiple myeloma are associated with advanced forms of malignancy. Blood. 1993;81:128-135.

149. Corradini P, Inghirami G, Astolfi M, Ladetto M, Voena C, Ballerini P, Gu W, Nilsson K, Knowles DM, Boccadoro M and et al. Inactivation of tumor suppressor genes, p53 and Rb1, in plasma cell dyscrasias. Leukemia. 1994;8:758-767.

150. Preudhomme C, Facon T, Zandecki M, Vanrumbeke M, Lai JL, Nataf E, Loucheux-Lefebvre MH, Kerckaert JP and Fenaux P. Rare occurrence of P53 gene mutations in multiple myeloma. Br J Haematol. 1992;81:440-443.

151. Avet-Loiseau H, ndree-Ashley LE, Moore D, Mellerin MP, Feusner J, Bataille R and Pallavicini MG. Molecular cytogenetic abnormalities in multiple myeloma and plasma cell leukemia measured using comparative genomic hybridization. Genes ChromosomesCancer. 1997;19:124-133.

152. Sawyer JR, Tricot G, Mattox S, Jagannath S and Barlogie B. Jumping translocations of chromosome 1q in multiple myeloma: evidence for a mechanism involving decondensation of pericentromeric heterochromatin. Blood. 1998;91:1732-1741.

153. Gutierrez NC, Hernandez JM, Garcia JL, Canizo MC, Gonzalez M, Hernandez J, Gonzalez MB, Garcia-Marcos MA and San Miguel JF. Differences in genetic changes between multiple myeloma and plasma cell leukemia demonstrated by comparative genomic hybridization. Leukemia. 2001;15:840-845.

154. Shaughnessy JD, Jr., Zhan F, Burington BE, Huang Y, Colla S, Hanamura I, Stewart JP, Kordsmeier B, Randolph C, Williams DR, Xiao Y, Xu H, Epstein J, Anaissie E, Krishna SG, Cottler-Fox M, Hollmig K, Mohiuddin A, Pineda-Roman M, Tricot G, van RF, Sawyer J, Alsayed Y, Walker R, Zangari M, Crowley J and Barlogie B. A validated gene expression model of high-risk multiple myeloma is defined by deregulated expression of genes mapping to chromosome 1. Blood. 2007;109:2276-2284.

155. Walker BA, Leone PE, Jenner MW, Li C, Gonzalez D, Johnson DC, Ross FM, Davies FE and Morgan GJ. Integration of global SNP-based mapping and expression arrays reveals key regions, mechanisms, and genes important in the pathogenesis of multiple myeloma. Blood. 2006;108:1733-1743.

156. Inoue J, Otsuki T, Hirasawa A, Imoto I, Matsuo Y, Shimizu S, Taniwaki M and Inazawa J. Overexpression of PDZK1 within the 1q12-q22 amplicon is likely to be associated with drug-resistance phenotype in multiple myeloma. AmJPathol. 2004;165:71-81.

157. Shaughnessy J. Amplification and overexpression of CKS1B at chromosome band 1q21 is associated with reduced levels of p27Kip1 and an aggressive clinical course in multiple myeloma. Hematology. 2005;10 Suppl 1:117-126.

158. Fabris S, Ronchetti D, Agnelli L, Baldini L, Morabito F, Bicciato S, Basso D, Todoerti K, Lombardi L, Lambertenghi-Deliliers G and Neri A. Transcriptional features of multiple myeloma patients with chromosome 1q gain. Leukemia. 2007;21:1113-1116.

159. Zhan F, Colla S, Wu X, Chen B, Stewart JP, Kuehl WM, Barlogie B and Shaughnessy JD, Jr. CKS1B, overexpressed in aggressive disease, regulates multiple myeloma growth and survival through. Blood. 2007;109:4995-5001.

160. Le BP, Leroux D, Dascalescu C, Duley S, Marais D, Esmenjaud E, Sotto JJ and Callanan M. Novel evidence of a role for chromosome 1 pericentric heterochromatin in the pathogenesis of B-cell lymphoma and multiple myeloma. Genes ChromosomesCancer. 2001;32:250-264.

161. Sawyer JR, Tricot G, Lukacs JL, Binz RL, Tian E, Barlogie B and Shaughnessy J, Jr. Genomic instability in multiple myeloma: evidence for jumping segmental duplications of chromosome arm 1q. Genes ChromosomesCancer. 2005;42:95-106.

162. Hanamura I, Stewart JP, Huang Y, Zhan F, Santra M, Sawyer JR, Hollmig K, Zangarri M, Pineda-Roman M, van RF, Cavallo F, Burington B, Crowley J, Tricot G, Barlogie B and Shaughnessy JD, Jr. Frequent gain of chromosome band 1q21 in plasma-cell dyscrasias detected by fluorescence in situ hybridization: incidence increases from MGUS to relapsed myeloma and is related to prognosis and disease progression following tandem stem-cell transplantation. Blood. 2006;108:1724-1732.

163. Chang H, Yeung J, Xu W, Ning Y and Patterson B. Significant increase of CKS1B amplification from monoclonal gammopathy of undetermined significance to multiple myeloma and plasma cell leukaemia as demonstrated by interphase fluorescence in situ hybridisation. BrJHaematol. 2006;134:613-615.

164. Rosinol L, Carrio A, Blade J, Queralt R, Aymerich M, Cibeira MT, Esteve J, Rozman M, Campo E and Montserrat E. Comparative genomic hybridisation identifies two variants of smoldering multiple myeloma. BrJHaematol. 2005;130:729-732.

165. Fonseca R, Van Wier SA, Chng WJ, Ketterling R, Lacy MQ, Dispenzieri A, Bergsagel PL, Rajkumar SV, Greipp PR, Litzow MR, Price-Troska T, Henderson KJ, Ahmann GJ and Gertz MA. Prognostic value of chromosome 1q21 gain by fluorescent in situ hybridization and increase CKS1B expression in myeloma. Leukemia. 2006;20:2034-2040.

166. Avet-Loiseau H, Attal M, Moreau P, Charbonnel C, Garban F, Harousseau J, Facon T and Mathiot C. A comprehensive analysis of cytogenetics abnormalities in myeloma: results of the FISH analysis of 1000 patients enrolled in the IFM99 Trials. Blood (ASH Annual Meeting Abstracts). 2005;106.

167. Avet-Loiseau H, Li C, Magrangeas F, Gouraud W, Charbonnel C, Harousseau JL, Attal M, Marit G, Mathiot C, Facon T, Moreau P, Anderson KC, Campion L, Munshi NC and Minvielle S. Prognostic Significance of Copy-Number Alterations in Multiple Myeloma. J Clin Oncol. 2009.

168. Bergsagel PL, Kuehl WM, Zhan F, Sawyer J, Barlogie B and Shaughnessy J, Jr. Cyclin D dysregulation: an early and unifying pathogenic event in multiple myeloma. Blood. 2005;106:296-303.

169. Decaux O, Lode L, Magrangeas F, Charbonnel C, Gouraud W, Jezequel P, Attal M, Harousseau JL, Moreau P, Bataille R, Campion L, vet-Loiseau H and Minvielle S. Prediction of Survival in Multiple Myeloma Based on Gene Expression Profiles Reveals Cell Cycle and Chromosomal Instability Signatures in High-Risk Patients and Hyperdiploid Signatures in Low-Risk Patients: A Study of the Intergroupe Francophone du Myelome. JClinOncol. 2008.

170. Zhan F, Tian E, Bumm K, Smith R, Barlogie B and Shaughnessy J, Jr. Gene expression profiling of human plasma cell differentiation and classification of multiple myeloma based on similarities to distinct stages of late-stage B-cell development. Blood. 2003;101:1128-1140.

171. Davies FE, Dring AM, Li C, Rawstron AC, Shammas MA, O'Connor SM, Fenton JA, Hideshima T, Chauhan D, Tai IT, Robinson E, Auclair D, Rees K, Gonzalez D, Ashcroft AJ, Dasgupta R, Mitsiades C, Mitsiades N, Chen LB, Wong WH, Munshi NC, Morgan GJ and Anderson KC. Insights into the multistep transformation of MGUS to myeloma using microarray expression analysis. Blood. 2003;102:4504-4511.

172. Zhan F, Barlogie B, Arzoumanian V, Huang Y, Williams DR, Hollmig K, Pineda-Roman M, Tricot G, van RF, Zangari M, Dhodapkar M and Shaughnessy JD, Jr. Gene-expression signature of benign monoclonal gammopathy evident in multiple myeloma is linked to good prognosis. Blood. 2007;109:1692-1700.

173. Chng WJ, Chesi M, Price-Troska T, Ahmann G, Henderson K, Greipp P, Kyle R, Rajkumar SV, Gertz M, Fonseca R and Bergsagel L. Activation of MYC pathway is a unifying pathological event in the progression from monoclonal gammopathy of undetermined significance (MGUS) to myeloma (MM). ASH Annual Meeting Abstracts 2007;110:241. 2007.

174. Anguiano A, Tuchman SA, Acharya C, Salter K, Gasparetto C, Zhan F, Dhodapkar M, Nevins J, Barlogie B, Shaughnessy JD, Jr. and Potti A. Gene expression profiles of tumor biology provide a novel approach to prognosis and may guide the selection of therapeutic targets in multiple myeloma. J Clin Oncol. 2009;27:4197-4203.

175. Kallioniemi A, Kallioniemi OP, Sudar D, Rutovitz D, Gray JW, Waldman F and Pinkel D. Comparative genomic hybridization for molecular cytogenetic analysis of solid tumors. Science. 1992;258:818-821.

176. Solinas-Toldo S, Durst M and Lichter P. Specific chromosomal imbalances in human papillomavirus-transfected cells during progression toward immortality. Proc Natl Acad Sci U S A. 1997;94:3854-3859.

177. Pinkel D, Segraves R, Sudar D, Clark S, Poole I, Kowbel D, Collins C, Kuo WL, Chen C, Zhai Y, Dairkee SH, Ljung BM, Gray JW and Albertson DG. High resolution analysis of DNA copy number variation using comparative genomic hybridization to microarrays. Nat Genet. 1998;20:207-211.

178. Carrasco DR, Tonon G, Huang Y, Zhang Y, Sinha R, Feng B, Stewart JP, Zhan F, Khatry D, Protopopova M, Protopopov A, Sukhdeo K, Hanamura I, Stephens O, Barlogie B, Anderson KC, Chin L, Shaughnessy JD, Jr., Brennan C and Depinho RA. High-resolution genomic profiles define distinct clinico-pathogenetic subgroups of multiple myeloma patients. Cancer Cell. 2006;9:313-325.

179. Largo C, Saez B, Alvarez S, Suela J, Ferreira B, Blesa D, Prosper F, Calasanz MJ and Cigudosa JC. Multiple myeloma primary cells show a highly rearranged unbalanced genome with amplifications and homozygous deletions irrespective of the presence of immunoglobulin-related chromosome translocations. Haematologica. 2007;92:795-802.

180. Largo C, Alvarez S, Saez B, Blesa D, Martin-Subero JI, Gonzalez-Garcia I, Brieva JA, Dopazo J, Siebert R, Calasanz MJ and Cigudosa JC. Identification of overexpressed genes in frequently gained/amplified chromosome regions in multiple myeloma. Haematologica. 2006;91:184-191.

181. Keats JJ, Fonseca R, Chesi M, Schop R, Baker A, Chng WJ, Van WS, Tiedemann R, Shi CX, Sebag M, Braggio E, Henry T, Zhu YX, Fogle H, Price-Troska T, Ahmann G, Mancini C, Brents LA, Kumar S, Greipp P, Dispenzieri A, Bryant B, Mulligan G, Bruhn L, Barrett M, Valdez R, Trent J, Stewart AK, Carpten J and Bergsagel PL. Promiscuous mutations activate the noncanonical NF-kappaB pathway in multiple myeloma. Cancer Cell. 2007;12:131-144.

182. Annunziata CM, Davis RE, Demchenko Y, Bellamy W, Gabrea A, Zhan F, Lenz G, Hanamura I, Wright G, Xiao W, Dave S, Hurt EM, Tan B, Zhao H, Stephens O, Santra M, Williams DR, Dang L, Barlogie B, Shaughnessy JD, Jr., Kuehl WM and Staudt LM. Frequent engagement of the classical and alternative NF-kappaB pathways by diverse genetic abnormalities in multiple myeloma. Cancer Cell. 2007;12:115-130.

183. Cheng SH, Ng MH, Lau KM, Liu HS, Chan JC, Hui AB, Lo KW, Jiang H, Hou J, Chu RW, Wong WS, Chan NP and Ng HK. 4q loss is potentially an important genetic event in MM tumorigenesis: identification of a tumor suppressor gene regulated by promoter methylation at 4q13.3, platelet factor 4. Blood. 2007;109:2089-2099.

184. Durie BG. Staging and kinetics of multiple myeloma. SeminOncol. 1986;13:300-309.

185. Rajkumar SV, Dispenzieri A and Kyle RA. Monoclonal gammopathy of undetermined significance, Waldenstrom macroglobulinemia, AL amyloidosis, and related plasma cell disorders: diagnosis and treatment. Mayo Clin Proc. 2006;81:693-703.

186. Plowright EE, Li Z, Bergsagel PL, Chesi M, Barber DL, Branch DR, Hawley RG and Stewart AK. Ectopic expression of fibroblast growth factor receptor 3 promotes myeloma cell proliferation and prevents apoptosis. Blood. 2000;95:992-998.

187. Shaffer LG and Tommerup N. An International System for Human Cytogenetic Nomenclature. 2005.

188. Langer-Safer PR, Levine M and Ward DC. Immunological method for mapping genes on Drosophila polytene chromosomes. Proc Natl Acad Sci U S A. 1982;79:4381-4385.

189. Van Prooijen-Knegt AC, Van Hoek JF, Bauman JG, Van Duijn P, Wool IG and Van der Ploeg M. In situ hybridization of DNA sequences in human metaphase chromosomes visualized by an indirect fluorescent immunocytochemical procedure. Exp Cell Res. 1982;141:397-407.

190. Landegent JE, Jansen in de Wal N, van Ommen GJ, Baas F, de Vijlder JJ, van Duijn P and Van der Ploeg M. Chromosomal localization of a unique gene by non-autoradiographic in situ hybridization. Nature. 1985;317:175-177.

191. Ross FM, Ibrahim AH, Vilain-Holmes A, Winfield MO, Chiecchio L, Protheroe RK, Strike P, Gunasekera JL, Jones A, Harrison CJ, Morgan GJ and Cross NC. Age has a profound effect on the incidence and significance of chromosome abnormalities in myeloma. Leukemia. 2005;19:1634-1642.

192. Collins J and Hohn B. Cosmids: a type of plasmid gene-cloning vector that is packageable in vitro in bacteriophage lambda heads. Proc Natl Acad Sci U S A. 1978;75:4242-4246.

193. Burke DT, Carle GF and Olson MV. Cloning of large segments of exogenous DNA into yeast by means of artificial chromosome vectors. Science. 1987;236:806-812.

194. Ioannou PA, Amemiya CT, Garnes J, Kroisel PM, Shizuya H, Chen C, Batzer MA and de Jong PJ. A new bacteriophage P1-derived vector for the propagation of large human DNA fragments. Nat Genet. 1994;6:84-89.

195. Shizuya H, Birren B, Kim UJ, Mancino V, Slepak T, Tachiiri Y and Simon M. Cloning and stable maintenance of 300-kilobase-pair fragments of human DNA in Escherichia coli using an F-factor-based vector. Proc Natl Acad Sci U S A. 1992;89:8794-8797.

196. Kim UJ, Shizuya H, de Jong PJ, Birren B and Simon MI. Stable propagation of cosmid sized human DNA inserts in an F factor based vector. Nucleic Acids Res. 1992;20:1083-1085.

197. Lizardi PM, Huang X, Zhu Z, Bray-Ward P, Thomas DC and Ward DC. Mutation detection and single-molecule counting using isothermal rolling-circle amplification. Nat Genet. 1998;19:225-232.

198. Dean FB, Nelson JR, Giesler TL and Lasken RS. Rapid amplification of plasmid and phage DNA using Phi 29 DNA polymerase and multiply-primed rolling circle amplification. Genome Res. 2001;11:1095-1099.

199. Pinkel D and Albertson DG. Array comparative genomic hybridization and its applications in cancer. NatGenet. 2005;37 Suppl:S11-S17.

200. Pinkel D and Albertson DG. Comparative genomic hybridization. AnnuRevGenomics HumGenet. 2005;6:331-354.

201. Pollack JR, Perou CM, Alizadeh AA, Eisen MB, Pergamenschikov A, Williams CF, Jeffrey SS, Botstein D and Brown PO. Genome-wide analysis of DNA copy-number changes using cDNA microarrays. NatGenet. 1999;23:41-46.

202. Ishkanian AS, Malloff CA, Watson SK, DeLeeuw RJ, Chi B, Coe BP, Snijders A, Albertson DG, Pinkel D, Marra MA, Ling V, MacAulay C and Lam WL. A tiling resolution DNA microarray with complete coverage of the human genome. NatGenet. 2004;36:299-303.

203. Kallioniemi A, Visakorpi T, Karhu R, Pinkel D and Kallioniemi OP. Gene Copy Number Analysis by Fluorescence in Situ Hybridization and Comparative Genomic Hybridization. Methods. 1996;9:113-121.

204. Gorringe KL and Campbell IG. High-resolution copy number arrays in cancer and the problem of normal genome copy number variation. Genes ChromosomesCancer. 2008;47:933-938.

205. Nowell PC and Hungerford DA. Chromosome studies on normal and leukemic human leukocytes. JNatlCancer Inst. 1960;25:85-109.

206. Mullis KB. Target amplification for DNA analysis by the polymerase chain reaction. AnnBiolClin(Paris). 1990;48:579-582.

207. De Vos J, Thykjaer T, Tarte K, Ensslen M, Raynaud P, Requirand G, Pellet F, Pantesco V, Reme T, Jourdan M, Rossi JF, Orntoft T and Klein B. Comparison of gene expression profiling between malignant and normal plasma cells with oligonucleotide arrays. Oncogene. 2002;21:6848-6857.

208. Birnie GD. The HL60 cell line: a model system for studying human myeloid cell differentiation. BrJCancer Suppl. 1988;9:41-45.

209. Kunz F, Shalaby T, Lang D, von BA, Hainfellner JA, Slavc I, Tabatabai G and Grotzer MA. Quantitative mRNA expression analysis of neurotrophin-receptor TrkC and oncogene c-MYC from formalin-fixed, paraffin-embedded primitive neuroectodermal tumor samples. Neuropathology. 2006;26:393-399.

210. Gabert J, Beillard E, van dVV, Bi W, Grimwade D, Pallisgaard N, Barbany G, Cazzaniga G, Cayuela JM, Cave H, Pane F, Aerts JL, De MD, Thirion X, Pradel V, Gonzalez M, Viehmann S, Malec

M, Saglio G and van Dongen JJ. Standardization and quality control studies of 'real-time' quantitative reverse transcriptase polymerase chain reaction of fusion gene transcripts for residual disease detection in leukemia - a Europe Against Cancer program. Leukemia. 2003;17:2318-2357.

211. Branford S, Hughes TP and Rudzki Z. Monitoring chronic myeloid leukaemia therapy by real-time quantitative PCR in blood is a reliable alternative to bone marrow cytogenetics. BrJHaematol. 1999;107:587-599.

212. Pfaffl MW. A new mathematical model for relative quantification in real-time RT-PCR. Nucleic Acids Res. 2001;29:e45.

213. Schouten JP, McElgunn CJ, Waaijer R, Zwijnenburg D, Diepvens F and Pals G. Relative quantification of 40 nucleic acid sequences by multiplex ligation-dependent probe amplification. Nucleic Acids Res. 2002;30:e57.

214. Avet-Loiseau H, Li JY, Facon T, Brigaudeau C, Morineau N, Maloisel F, Rapp MJ, Talmant P, Trimoreau F, Jaccard A, Harousseau JL and Bataille R. High incidence of translocations t(11;14)(q13;q32) and t(4;14)(p16;q32) in patients with plasma cell malignancies. Cancer Res. 1998;58:5640-5645.

215. Chng WJ, Van Wier SA, Ahmann GJ, Winkler JM, Jalal SM, Bergsagel PL, Chesi M, Trendle MC, Oken MM, Blood E, Henderson K, Santana-Davila R, Kyle RA, Gertz MA, Lacy MQ, Dispenzieri A, Greipp PR and Fonseca R. A validated FISH trisomy index demonstrates the hyperdiploid and nonhyperdiploid dichotomy in MGUS. Blood. 2005;106:2156-2161.

216. Wuilleme S, Robillard N, Lode L, Magrangeas F, Beris H, Harousseau JL, Proffitt J, Minvielle S and vet-Loiseau H. Ploidy, as detected by fluorescence in situ hybridization, defines different subgroups in multiple myeloma. Leukemia. 2005;19:275-278.

217. Bochtler T, Hegenbart U, Cremer FW, Heiss C, Benner A, Hose D, Moos M, Bila J, Bartram CR, Ho AD, Goldschmidt H, Jauch A and Schonland SO. Evaluation of the cytogenetic aberration pattern in amyloid light chain amyloidosis as compared with monoclonal gammopathy of undetermined significance reveals common pathways of karyotypic instability. Blood. 2008;111:4700-4705.

218. Avet-Loiseau H. Role of genetics in prognostication in myeloma. BestPractResClinHaematol. 2007;20:625-635.

219. Nilsson T, Lenhoff S, Rylander L, Hoglund M, Turesson I, Mitelman F, Westin J and Johansson B. High frequencies of chromosomal aberrations in multiple myeloma and monoclonal gammopathy of undetermined significance in direct chromosome preparation. Br J Haematol. 2004;126:487-494.

220. Sawyer JR, Lukacs JL, Munshi N, Desikan KR, Singhal S, Mehta J, Siegel D, Shaughnessy J and Barlogie B. Identification of new nonrandom translocations in multiple myeloma with multicolor spectral karyotyping. Blood. 1998;92:4269-4278.

221. van Dongen JJ, Langerak AW, Bruggemann M, Evans PA, Hummel M, Lavender FL, Delabesse E, Davi F, Schuuring E, Garcia-Sanz R, van Krieken JH, Droese J, Gonzalez D, Bastard C, White HE, Spaargaren M, Gonzalez M, Parreira A, Smith JL, Morgan GJ, Kneba M and Macintyre EA. Design and standardization of PCR primers and protocols for detection of clonal immunoglobulin and T-cell receptor gene recombinations in suspect lymphoproliferations: report of the BIOMED-2 Concerted Action BMH4-CT98-3936. Leukemia. 2003;17:2257-2317.

222. Dean FB, Hosono S, Fang L, Wu X, Faruqi AF, Bray-Ward P, Sun Z, Zong Q, Du Y, Du J, Driscoll M, Song W, Kingsmore SF, Egholm M and Lasken RS. Comprehensive human genome amplification using multiple displacement amplification. ProcNatlAcadSciUSA. 2002;99:5261-5266.

223. Masciullo V, Ferrandina G, Pucci B, Fanfani F, Lovergine S, Palazzo J, Zannoni G, Mancuso S, Scambia G and Giordano A. p27Kip1 expression is associated with clinical outcome in advanced epithelial ovarian cancer: multivariate analysis. Clin Cancer Res. 2000;6:4816-4822.

224. Catzavelos C, Bhattacharya N, Ung YC, Wilson JA, Roncari L, Sandhu C, Shaw P, Yeger H, Morava-Protzner I, Kapusta L, Franssen E, Pritchard KI and Slingerland JM. Decreased levels of the cell-cycle inhibitor p27Kip1 protein: prognostic implications in primary breast cancer. Nat Med. 1997;3:227-230.

225. Fabris S, Todoerti K, Mosca L, Agnelli L, Intini D, Lionetti M, Guerneri S, Lambertenghi-Deliliers G, Bertoni F and Neri A. Molecular and transcriptional characterization of the novel 17p11.2-p12 amplicon in multiple myeloma. Genes ChromosomesCancer. 2007;46:1109-1118.

226. Dib A, Peterson TR, Raducha-Grace L, Zingone A, Zhan F, Hanamura I, Barlogie B, Shaughnessy J, Jr. and Kuehl WM. Paradoxical expression of INK4c in proliferative multiple myeloma tumors: bi-allelic deletion vs increased expression. Cell Div. 2006;1:23.

227. Kulkarni MS, Daggett JL, Bender TP, Kuehl WM, Bergsagel PL and Williams ME. Frequent inactivation of the cyclin-dependent kinase inhibitor p18 by homozygous deletion in multiple myeloma cell lines: ectopic p18 expression inhibits growth and induces apoptosis. Leukemia. 2002;16:127-134.

228. Chang H, Qi X, Jiang A, Xu W, Young T and Reece D. 1p21 deletions are strongly associated with 1q21 gains and are an independent adverse prognostic factor for the outcome of high-dose chemotherapy in patients with multiple myeloma. Bone Marrow Transplantation. 2010;45:5.

229. Filipits M, Pohl G, Stranzl T, Kaufmann H, Ackermann J, Gisslinger H, Greinix H, Chott A and Drach J. Low p27Kip1 expression is an independent adverse prognostic factor in patients with multiple myeloma. Clin Cancer Res. 2003;9:820-826.

230. Slingerland J and Pagano M. Regulation of the cdk inhibitor p27 and its deregulation in cancer. J Cell Physiol. 2000;183:10-17.

231. Zhang SL, DuBois W, Ramsay ES, Bliskovski V, Morse HC, III, Taddesse-Heath L, Vass WC, Depinho RA and Mock BA. Efficiency alleles of the Pctr1 modifier locus for plasmacytoma susceptibility. MolCell Biol. 2001;21:310-318.

232. Uchida T, Kinoshita T, Ohno T, Ohashi H, Nagai H and Saito H. Hypermethylation of p16INK4A gene promoter during the progression of plasma cell dyscrasia. Leukemia. 2001;15:157-165.

233. Gonzalez-Paz N, Chng WJ, McClure RF, Blood E, Oken MM, Van NB, James CD, Kurtin PJ, Henderson K, Ahmann GJ, Gertz M, Lacy M, Dispenzieri A, Greipp PR and Fonseca R. Tumor suppressor p16 methylation in multiple myeloma: biological and clinical implications. Blood. 2007;109:1228-1232.

234. Sarasquete ME, Garcia-Sanz R, Armellini A, Fuertes M, Martin-Jimenez P, Sierra M, Del Carmen Chillon M, Alcoceba M, Balanzategui A, Ortega F, Hernandez JM, Sureda A, Palomera L, Gonzalez M and San Miguel JF. The association of increased p14ARF/p16INK4a and p15INK4a gene expression with proliferative activity and the clinical course of multiple myeloma. Haematologica. 2006;91:1551-1554.

235. O'Connor BP, Raman VS, Erickson LD, Cook WJ, Weaver LK, Ahonen C, Lin LL, Mantchev GT, Bram RJ and Noelle RJ. BCMA is essential for the survival of long-lived bone marrow plasma cells. JExpMed. 2004;199:91-98.

236. Moreaux J, Cremer FW, Reme T, Raab M, Mahtouk K, Kaukel P, Pantesco V, De VJ, Jourdan E, Jauch A, Legouffe E, Moos M, Fiol G, Goldschmidt H, Rossi JF, Hose D and Klein B. The level of TACI gene expression in myeloma cells is associated with a signature of microenvironment dependence versus a plasmablastic signature. Blood. 2005;106:1021-1030.

237. Hideshima T, Chauhan D, Richardson P, Mitsiades C, Mitsiades N, Hayashi T, Munshi N, Dang L, Castro A, Palombella V, Adams J and Anderson KC. NF-kappa B as a therapeutic target in multiple myeloma. JBiolChem. 2002;277:16639-16647.

238. Hideshima T, Neri P, Tassone P, Yasui H, Ishitsuka K, Raje N, Chauhan D, Podar K, Mitsiades C, Dang L, Munshi N, Richardson P, Schenkein D and Anderson KC. MLN120B, a novel IkappaB kinase beta inhibitor, blocks multiple myeloma cell growth in vitro and in vivo. ClinCancer Res. 2006;12:5887-5894.

239. Ghosh S and Karin M. Missing pieces in the NF-kappaB puzzle. Cell. 2002;109 Suppl:S81-96.

240. Zarnegar BJ, Wang Y, Mahoney DJ, Dempsey PW, Cheung HH, He J, Shiba T, Yang X, Yeh WC, Mak TW, Korneluk RG and Cheng G. Noncanonical NF-kappaB activation requires coordinated assembly of a regulatory complex of the adaptors cIAP1, cIAP2, TRAF2 and TRAF3 and the kinase NIK. Nat Immunol. 2008;9:1371-1378.

241. Vallabhapurapu S, Matsuzawa A, Zhang W, Tseng PH, Keats JJ, Wang H, Vignali DA, Bergsagel PL and Karin M. Nonredundant and complementary functions of TRAF2 and TRAF3 in a

ubiquitination cascade that activates NIK-dependent alternative NF-kappaB signaling. Nat Immunol. 2008;9:1364-1370.

242. Gilmore TD. Introduction to NF-kappaB: players, pathways, perspectives. Oncogene. 2006;25:6680-6684.

243. Basseres DS and Baldwin AS. Nuclear factor-kappaB and inhibitor of kappaB kinase pathways in oncogenic initiation and progression. Oncogene. 2006;25:6817-6830.

244. Fracchiolla NS, Lombardi L, Salina M, Migliazza A, Baldini L, Berti E, Cro L, Polli E, Maiolo AT and Neri A. Structural alterations of the NF-kappa B transcription factor lyt-10 in lymphoid malignancies. Oncogene. 1993;8:2839-2845.

245. Demchenko YN, Glebov OK, Zingone A, Keats JJ, Bergsagel PL and Kuehl WM. Classical and/or alternative NF{kappa}B pathway activation in multiple myeloma. Blood.

246. De VJ, Couderc G, Tarte K, Jourdan M, Requirand G, Delteil MC, Rossi JF, Mechti N and Klein B. Identifying intercellular signaling genes expressed in malignant plasma cells by using complementary DNA arrays. Blood. 2001;98:771-780.

247. Mandai K, Nakanishi H, Satoh A, Obaishi H, Wada M, Nishioka H, Itoh M, Mizoguchi A, Aoki T, Fujimoto T, Matsuda Y, Tsukita S and Takai Y. Afadin: A novel actin filament-binding protein with one PDZ domain localized at cadherin-based cell-to-cell adherens junction. JCell Biol. 1997;139:517-528.

248. Jenner MW, Leone PE, Walker BA, Ross FM, Johnson DC, Gonzalez D, Chiecchio L, Dachs CE, Dagrada GP, Nightingale M, Protheroe RK, Stockley D, Else M, Dickens NJ, Cross NC, Davies FE and Morgan GJ. Gene mapping and expression analysis of 16q loss of heterozygosity identifies WWOX and CYLD as being important in determining clinical outcome in multiple myeloma. Blood. 2007;110:3291-3300.

249. Azar GM, Gogineni SK, Hyde P and Verma RS. Highly complex chromosomal abnormalities in plasma cell leukemia as detected by FISH technique. Leukemia. 1997;11:772-774.

250. Johnson MR, Del Carpio-Jayo D, Lin P, Giralt S, Anderlini P, Champlin RE, Khouri IF, Vadhan-Raj S, Medeiros LJ and Bueso-Ramos CE. Primary plasma cell leukemia: morphologic, immunophenotypic, and cytogenetic features of 4 cases treated with chemotherapy and stem cell transplantation. AnnDiagnPathol. 2006;10:263-268.

251. Knutsen T, Vakulchuk A, Mosijczuk AD, Gabrea A, Ried T and Tretyak N. Complex rearrangements involving der(8)t(8;20) and der(14)t(8;14)t(11;14), CCND1, and duplication of IgH constant region in acute plasmablastic leukemia. Cancer GenetCytogenet. 2006;164:137-141.

252. Tiedemann RE, Gonzalez-Paz N, Kyle RA, Santana-Davila R, Price-Troska T, Van Wier SA, Chng WJ, Ketterling RP, Gertz MA, Henderson K, Greipp PR, Dispenzieri A, Lacy MQ, Rajkumar SV, Bergsagel PL, Stewart AK and Fonseca R. Genetic aberrations and survival in plasma cell leukemia. Leukemia. 2008;22:1044-1052.

253. Kujawski L, Ouillette P, Erba H, Saddler C, Jakubowiak A, Kaminski M, Shedden K and Malek SN. Genomic complexity identifies patients with aggressive chronic lymphocytic leukemia. Blood. 2008;112:1993-2003.

254. Smadja NV, Leroux D, Soulier J, Dumont S, Arnould C, Taviaux S, Taillemite JL and Bastard C. Further cytogenetic characterization of multiple myeloma confirms that 14q32 translocations are a very rare event in hyperdiploid cases. Genes ChromosomesCancer. 2003;38:234-239.

255. Nilsson T, Nilsson L, Lenhoff S, Rylander L, strand-Grundstrom I, Strombeck B, Hoglund M, Turesson I, Westin J, Mitelman F, Jacobsen SE and Johansson B. MDS/AML-associated cytogenetic abnormalities in multiple myeloma and monoclonal gammopathy of undetermined significance: evidence for frequent de novo occurrence and multipotent stem cell involvement of del(20q). Genes ChromosomesCancer. 2004;41:223-231.

256. Chang H, Qi X, Yeung J, Reece D, Xu W and Patterson B. Genetic aberrations including chromosome 1 abnormalities and clinical features of plasma cell leukemia. LeukRes. 2008.

257. Smaldone S, Laub F, Else C, Dragomir C and Ramirez F. Identification of MoKA, a novel F-box protein that modulates Kruppel-like transcription factor 7 activity. Mol Cell Biol. 2004;24:1058-1069.

258. Smaldone S and Ramirez F. Multiple pathways regulate intracellular shuttling of MoKA, a co-activator of transcription factor KLF7. Nucleic Acids Res. 2006;34:5060-5068.

259. Laub F, Aldabe R, Friedrich V, Jr., Ohnishi S, Yoshida T and Ramirez F. Developmental expression of mouse Kruppel-like transcription factor KLF7 suggests a potential role in neurogenesis. Dev Biol. 2001;233:305-318.

260. Bryant B, Danaee H, Lichter D, Shaughnessy J, Bergsagel L, Sonneveld P, Anderson K, Boral A, Trepicchio WL and Mulligan G. High-resolution assessment of chromosomal gains and losses in multiple myeloma tumours from bortezomib clinical trial, Journal of Clinical Oncology, 2008 ASCO Annual Meeting Proceedings. Vol 26, No 15S (May 20 Supplement): 8570.

261. Jin Y, Mertens F, Kullendorff CM and Panagopoulos I. Fusion of the tumor-suppressor gene CHEK2 and the gene for the regulatory subunit B of protein phosphatase 2 PPP2R2A in childhood teratoma. Neoplasia. 2006;8:413-418.

262. Liu W, Xie CC, Zhu Y, Li T, Sun J, Cheng Y, Ewing CM, Dalrymple S, Turner AR, Isascs JT, Chang BL, Zheng SL, Isaacs WB and Xu J. Homozygous deletions and recurrent amplifications implicate new genes involved in prostate cancer. Neoplasia. 2008;10:897-907.

263. Dib A, Gabrea A, Glebov O, Bergsagel L and Kuehl M. Characterization of MYC Translocations in Multiple Myeloma Cell Lines. Journal of the National Cancer Institute Monographs. 2008;39:25-31.

264. Gabrea A, Martelli ML, Qi Y, Roschke A, Barlogie B, Shaughnessy JD, Jr., Sawyer JR and Kuehl WM. Secondary genomic rearrangements involving immunoglobulin or MYC loci show similar prevalences in hyperdiploid and nonhyperdiploid myeloma tumors. Genes ChromosomesCancer. 2008;47:573-590.

265. He TC, Sparks AB, Rago C, Hermeking H, Zawel L, da Costa LT, Morin PJ, Vogelstein B and Kinzler KW. Identification of c-MYC as a target of the APC pathway. Science. 1998;281:1509-1512.

266. Fonseca R, Bergsagel PL, Drach J, Shaughnessy J, Gutierrez N, Stewart AK, Morgan G, Van Ness B, Chesi M, Minvielle S, Neri A, Barlogie B, Kuehl WM, Liebisch P, Davies F, Chen-Kiang S, Durie BG, Carrasco R, Sezer O, Reiman T, Pilarski L and Avet-Loiseau H. International Myeloma Working Group molecular classification of multiple myeloma: spotlight review. Leukemia. 2009;23:2210-2221.

267. Eymin B, Gazzeri S, Brambilla C and Brambilla E. Mdm2 overexpression and p14(ARF) inactivation are two mutually exclusive events in primary human lung tumors. Oncogene. 2002;21:2750-2761.

268. Stott FJ, Bates S, James MC, McConnell BB, Starborg M, Brookes S, Palmero I, Ryan K, Hara E, Vousden KH and Peters G. The alternative product from the human CDKN2A locus, p14(ARF), participates in a regulatory feedback loop with p53 and MDM2. EMBO J. 1998;17:5001-5014.

269. Chang H, Qi X, Trieu Y, Xu W, Reader JC, Ning Y and Reece D. Multiple myeloma patients with CKS1B gene amplification have a shorter progression-free survival post-autologous stem cell transplantation. BrJHaematol. 2006;135:486-491.

270. Debes-Marun CS, Dewald GW, Bryant S, Picken E, Santana-Davila R, Gonzalez-Paz N, Winkler JM, Kyle RA, Gertz MA, Witzig TE, Dispenzieri A, Lacy MQ, Rajkumar SV, Lust JA, Greipp PR and Fonseca R. Chromosome abnormalities clustering and its implications for pathogenesis and prognosis in myeloma. Leukemia. 2003;17:427-436.

271. Leone PE, Walker BA, Jenner MW, Chiecchio L, Dagrada G, Protheroe RK, Johnson DC, Dickens NJ, Brito JL, Else M, Gonzalez D, Ross FM, Chen-Kiang S, Davies FE and Morgan GJ. Deletions of CDKN2C in multiple myeloma: biological and clinical implications. ClinCancer Res. 2008;14:6033-6041.

272. Nilsson JA and Cleveland JL. Myc pathways provoking cell suicide and cancer. Oncogene. 2003;22:9007-9021.

273. Dalla-Favera R, Martinotti S, Gallo RC, Erikson J and Croce CM. Translocation and rearrangements of the c-myc oncogene locus in human undifferentiated B-cell lymphomas. Science. 1983;219:963-967.

274. Shen-Ong GL, Keath EJ, Piccoli SP and Cole MD. Novel myc oncogene RNA from abortive immunoglobulin-gene recombination in mouse plasmacytomas. Cell. 1982;31:443-452.

275. Pear WS, Wahlstrom G, Nelson SF, Axelson H, Szeles A, Wiener F, Bazin H, Klein G and Sumegi J. 6;7 chromosomal translocation in spontaneously arising rat immunocytomas: evidence for c-myc breakpoint clustering and correlation between isotypic expression and the c-myc target. Mol Cell Biol. 1988;8:441-451.

276. Chesi M, Robbiani DF, Sebag M, Chng WJ, Affer M, Tiedemann R, Valdez R, Palmer SE, Haas SS, Stewart AK, Fonseca R, Kremer R, Cattoretti G and Bergsagel PL. AID-dependent activation of a MYC transgene induces multiple myeloma in a conditional mouse model of post-germinal center malignancies. Cancer Cell. 2008;13:167-180.

277. Okazaki IM, Kotani A and Honjo T. Role of AID in tumorigenesis. Adv Immunol. 2007;94:245-273.

278. van den Akker TW, de Glopper-van der Veer E, Radl J and Benner R. The influence of genetic factors associated with the immunoglobulin heavy chain locus on the development of benign monoclonal gammapathy in ageing IgH-congenic mice. Immunology. 1988;65:31-35.

279. Chng WJ, Huang G, Bergsagel L and Fonseca R. Identification of Cellular Pathways Mediating Progression of Monoclonal Gammopathy (MGUS) to Multiple Myeloma (MM) Using Gene Expression Profiling (GEP). Blood (ASH Annual Meeting Abstracts)

2008;112.

280. Chng WJ, Huang G, Ng SB, Chesi M, Bergsagel L and Fonseca R. MYC Activation Is a Common Transformation Event in Myeloma and Associated with Poor Prognosis. Blood (ASH Annual Meeting Abstracts). 2009;114.

281. Basso K, Margolin AA, Stolovitzky G, Klein U, Dalla-Favera R and Califano A. Reverse engineering of regulatory networks in human B cells. Nat Genet. 2005;37:382-390.

282. Rasmussen T, Kuehl M, Lodahl M, Johnsen HE and Dahl IM. Possible roles for activating RAS mutations in the MGUS to MM transition and in the intramedullary to extramedullary transition in some plasma cell tumors. Blood. 2005;105:317-323.

283. Jost PJ and Ruland J. Aberrant NF-kappaB signaling in lymphoma: mechanisms, consequences, and therapeutic implications. Blood. 2007;109:2700-2707.

284. Keller U, Nilsson JA, Maclean KH, Old JB and Cleveland JL. Nfkb 1 is dispensable for Myc-induced lymphomagenesis. Oncogene. 2005;24:6231-6240.

285. Dave SS, Fu K, Wright GW, Lam LT, Kluin P, Boerma EJ, Greiner TC, Weisenburger DD, Rosenwald A, Ott G, Muller-Hermelink HK, Gascoyne RD, Delabie J, Rimsza LM, Braziel RM, Grogan TM, Campo E, Jaffe ES, Dave BJ, Sanger W, Bast M, Vose JM, Armitage JO, Connors JM, Smeland EB, Kvaloy S, Holte H, Fisher RI, Miller TP, Montserrat E, Wilson WH, Bahl M, Zhao H, Yang L, Powell J, Simon R, Chan WC and Staudt LM. Molecular diagnosis of Burkitt's lymphoma. N Engl J Med. 2006;354:2431-2442.

286. Hummel M, Bentink S, Berger H, Klapper W, Wessendorf S, Barth TF, Bernd HW, Cogliatti SB, Dierlamm J, Feller AC, Hansmann ML, Haralambieva E, Harder L, Hasenclever D, Kuhn M, Lenze D, Lichter P, Martin-Subero JI, Moller P, Muller-Hermelink HK, Ott G, Parwaresch RM, Pott C, Rosenwald A, Rosolowski M, Schwaenen C, Sturzenhofecker B, Szczepanowski M, Trautmann H, Wacker HH, Spang R, Loeffler M, Trumper L, Stein H and Siebert R. A biologic definition of Burkitt's lymphoma from transcriptional and genomic profiling. N Engl J Med. 2006;354:2419-2430.

287. Klapproth K, Sander S, Marinkovic D, Baumann B and Wirth T. The IKK2/NF-{kappa}B pathway suppresses MYC-induced lymphomagenesis. Blood. 2009;114:2448-2458.